

Tesis Doctoral

Sistemas para el control eficaz y sostenible de enfermedades fúngicas de la madera en planta joven de vid

Autora

Natalia Langa Lomba

Directores

Dr. D. Pablo Martín Ramos
Dr. D. Vicente González García

Universidad de Zaragoza - Escuela de Doctorado
2023

TESIS DOCTORAL

**SISTEMAS PARA EL CONTROL EFICAZ Y SOSTENIBLE DE
ENFERMEDADES FÚNGICAS DE LA MADERA EN PLANTA
JOVEN DE VID**

Memoria presentada por

Natalia Langa Lomba

para optar el Grado de Doctora por la Universidad de Zaragoza

Directores:

Dr. D. Pablo Martín Ramos
Dr. D. Vicente González García

Tutor Académico:

Dr. D. José Casanova Gascón

Huesca, agosto de 2023

Escuela Politécnica Superior
Departamento de Ciencias Agrarias y del Medio Natural
Universidad de Zaragoza



**Universidad
Zaragoza**



**Universidad
Zaragoza**

D. Pablo Martín Ramos, Profesor Titular en el Departamento de Ingeniería Agroforestal de la Universidad de Valladolid, y D. Vicente González García, Investigador en el Departamento de Sistemas Agrícolas, Forestales y Medio Ambiente del Centro de Investigación y Tecnología Agroalimentaria de Aragón (CITA).

CERTIFICAN:

Que la presente memoria, titulada **“SISTEMAS PARA EL CONTROL EFICAZ Y SOSTENIBLE DE ENFERMEDADES FÚNGICAS DE LA MADERA EN PLANTA JOVEN DE VID”** correspondiente al plan de investigación aprobado por la Comisión de Doctorado del Departamento de Ciencias Agrarias y del Medio Natural y presentada para optar al grado de Doctora por la Universidad de Zaragoza, ha sido realizada bajo nuestra dirección por **D^a. Natalia Langa Lomba** en la Escuela Politécnica Superior de la Universidad de Zaragoza y el Centro de Investigación y Tecnología Agroalimentaria de Aragón (CITA), autorizando su presentación como compendio de publicaciones para proseguir los trámites oportunos y proceder a su calificación por el tribunal correspondiente.

Y para que así conste, firman el presente certificado en Huesca, a 17 de agosto de 2023.


Firmado
digitalmente por
MARTIN RAMOS
PABLO - 71128357Y

Firmado por GONZALEZ GARCIA
VICENTE - DNI ***0433** el día
12/09/2023 con un certificado
emitido por AC Sector Público

Fdo.: Dr. Pablo Martín Ramos

Fdo.: Dr. Vicente González García

INFORME SOBRE LAS PUBLICACIONES DE LA TESIS DOCTORAL

Esta Tesis doctoral es un compendio de trabajos previamente publicados. Se compone de once artículos, publicados en revistas científicas indexadas en Web of Science (WOS) – Journal Citation Reports (JCR), ocho de ellas en primer cuartil (Q1) y tres en segundo cuartil (Q2). Natalia Langa ha sido primera firmante en siete publicaciones, segunda firmante en tres y tercera en una. Las referencias completas de los artículos que constituyen el cuerpo de la Tesis Doctoral son:

1. Buzón-Durán, L.; Langa-Lomba, N.; González-García, V.; Casanova-Gascón, J.; Martín-Gil, J.; Pérez-Lebeña, E.; Martín-Ramos, P. On the applicability of chitosan oligomers-amino acid conjugate complexes as eco-friendly fungicides against grapevine trunk pathogens. *Agronomy*, 2021, 11(2), 324; <https://doi.org/10.3390/agronomy11020324>; Q1. JIF₂₀₂₁ = 3,949.
2. Langa-Lomba, N.; Buzón-Durán, L.; Martín-Ramos, P.; Casanova-Gascón, J.; Martín-Gil, J.; Sánchez-Hernández, E.; González-García, V. Assessment of conjugate complexes of chitosan and *Urtica dioica* or *Equisetum arvense* extracts for the control of grapevine trunk pathogens. *Agronomy*, 2021, 11(5), 976; <https://doi.org/10.3390/agronomy11050976>; Q1. JIF₂₀₂₁ = 3,949.
3. Langa-Lomba, N.; Buzón-Durán, L.; Sánchez-Hernández, E.; Martín-Ramos, P.; Casanova-Gascón, J.; Martín-Gil, J.; González-García, V. Antifungal activity against *Botryosphaeriaceae* fungi of the hydro-methanolic extract of *Silybum marianum* capitula conjugated with stevioside. *Plants*, 2021, 10(7), 1363; <https://doi.org/10.3390/plants10071363>; Q1. JIF₂₀₂₁ = 4,658.
4. Buzón-Durán, L., Langa-Lomba, N., González-García, V., Casanova-Gascón, J., Sánchez-Hernández, E., Martín-Gil, J., Martín Ramos, P. Rutin-stevioside and related conjugates for potential control of grapevine trunk diseases. *Phytopathologia Mediterranea*, 2022, 61 (1), 65; <https://doi.org/10.36253/phyto-13108>; Q2. JIF₂₀₂₂ = 2,4.
5. Langa-Lomba, N.; Sánchez-Hernández, E.; Buzón-Durán, L.; González-García, V.; Casanova-Gascón, J.; Martín-Gil, J.; Martín-Ramos, P. Activity of anthracenediones and flavoring phenols in hydromethanolic extracts of *Rubia tinctorum* against grapevine phytopathogenic fungi. *Plants*, 2021, 10(8), 1527; <https://doi.org/10.3390/plants10081527>; Q1. JIF₂₀₂₁ = 4,658.
6. Sánchez-Hernández, E.; Langa-Lomba, N.; González-García, V.; Casanova-Gascón, J.; Martín-Gil, J.; Santiago-Aliste, A.; Torres-Sánchez, S.; Martín-Ramos, P. Lignin-chitosan nanocarriers for the delivery of bioactive natural products against wood-decay phytopathogens. *Agronomy*, 2022, 12(2), 461; <https://doi.org/10.3390/agronomy12020461>; Q1. JIF₂₀₂₂ = 3,7.
7. Santiago-Aliste, A.; Sánchez-Hernández, E.; Langa-Lomba, N.; González-García, V.; Casanova-Gascón, J.; Martín-Gil, J.; Martín-Ramos, P. Multifunctional nanocarriers based on chitosan oligomers and graphitic carbon nitride assembly. *Materials* 2022; 15(24), 8981; <https://doi.org/10.3390/ma15248981>; Q2. JIF₂₀₂₂ = 3,4.
8. Langa-Lomba, N.; Martín-Ramos, P.; Casanova-Gascón, J.; Julián-Lagunas, C.; González-García, V. Potential of native *Trichoderma* strains as antagonists for the control of fungal wood pathologies in young grapevine plants. *Agronomy*, 2022, 12(2), 336; <https://doi.org/10.3390/agronomy12020336>; Q1. JIF₂₀₂₂ = 3,7.
9. Langa-Lomba, N.; González-García, V.; Venturini-Crespo, M.E.; Casanova-Gascón, J.; Barriuso-Vargas, J.J.; Martín-Ramos, P. Comparison of the efficacy of *Trichoderma* and *Bacillus* strains and commercial biocontrol products against grapevine *Botryosphaeria* dieback pathogens. *Agronomy*, 2023, 13(2), 533; <https://doi.org/10.3390/agronomy13020533>; Q1. JIF₂₀₂₂ = 3,7.
10. Langa-Lomba, N., González-García, V., Martín-Ramos, P.; Casanova-Gascón, J. Screening of *Vitis vinifera* cultivars from the Grapevine Germplasm Bank of Aragon for susceptibility to *Botryosphaeria* dieback fungi. *Journal of Plant Diseases and Protection*, 2023, 130, 999-1006; <https://doi.org/10.1007/s41348-023-00741-9>; Q2. JIF₂₀₂₂ = 2,0

11. Langa-Lomba, N.; Grimplet, J.; Sánchez-Hernández, E.; Martín-Ramos, P.; Casanova-Gascón, J.; Julián-Lagunas, C.; González-García, V. Metagenomic study of fungal microbial communities in two PDO Somontano vineyards (Huesca, Spain): Effects of age, plant genotype, and initial phytosanitary status on the priming and selection of their associated microorganisms. *Plants*, 2023, 12(12), 2251; <https://doi.org/10.3390/plants12122251>; Q1. JIF₂₀₂₂ = 4,5.

Los artículos nº 1, nº 2, y nº 6 han sido seleccionados como “*Editor’s Choice*”. El artículo nº 1 también ha sido destacado como “*Feature Paper*”.

El artículo nº 7 ha sido seleccionado como “*most notable article*” de la revista *Materials* en el periodo noviembre 2022-enero 2023 en la categoría de biomateriales.

El artículo nº 5 ha sido re-publicado en forma de capítulo del libro “*Advances in Alternative Measures in Plant Protection*” (Špela Mechora and Dragana Šunjka, Eds.), con ISBN 978-3-0365-7396-0, <https://doi.org/10.3390/books978-3-0365-7397-7>, Mayo 2023.

Así mismo, durante el periodo de realización de la Tesis Doctoral, Natalia Langa también ha co-autorado como tercera firmante el artículo Q1 (no centrado en enfermedades de la madera de la vid, sino en el manzano, y excluido del compendio de publicaciones): “*Characterization and antimicrobial activity of a halophyte from the Asturian coast (Spain): *Limonium binervosum* (G.E.Sm.) C.E.Salmon*” *Plants*, 2021, 10(9), 1852; <https://doi.org/10.3390/plants10091852>; Q1. JIF₂₀₂₁ = 4,658.

Las investigaciones presentadas han sido financiadas a través del proyecto “*Nuevas composiciones bioactivas para aplicaciones fitosanitarias en Viticultura*”, premiado a nivel nacional en la IV Convocatoria de Ayudas de la Cátedra AgroBank para la transferencia del conocimiento al sector agroalimentario; el proyecto “*Sistemas para el control eficaz y sostenible de enfermedades fúngicas de la madera en planta joven de vid*” (JIUZ-2020-TEC-06), en la Convocatoria Fundación Ibercaja-Universidad de Zaragoza de proyectos de investigación, desarrollo e innovación para jóvenes investigadores; el proyecto “*Síntesis y caracterización de nuevas composiciones antifúngicas para aplicaciones fitosanitarias (NEWPHYTOSAN)*” (UZ2019-TEC-07), de la Convocatoria de Proyectos de Investigación (proyectos “puente”) 2019 de la Universidad de Zaragoza; y el proyecto “*Síntesis y validación de nuevos antifúngicos de origen natural con aplicaciones en viticultura: Estrategias de lucha contra la yesca en la D.O. Ribera del Duero*” (VA258P18) de la Convocatoria de subvenciones del programa de apoyo a proyectos de investigación cofinanciadas por el Fondo Europeo de Desarrollo Regional (ORDEN EDU/1255/2018, de 20 de noviembre) de la Junta de Castilla y León.



**Universidad
Zaragoza**



UNIÓN EUROPEA
Fondo Europeo de
Desarrollo Regional

AGRADECIMIENTOS

Ante todo, me gustaría expresar mi agradecimiento a mis directores, Pablo Martín Ramos y Vicente González García, y a mi tutor académico, José Casanova Gascón, por su profesionalidad, su dedicación durante la realización de esta investigación y por encontrar el modo de compatibilizarla con mi oposición. Sin ellos, esta Tesis no hubiera sido posible.

Pablo, gracias por confiar en mí, por impulsarme a comenzar esta Tesis, por luchar por una beca para mi doctorado, por convertirte en un pilar fundamental de las últimas decisiones para encaminar mi vida. Es admirable tu fuerza de voluntad, tu gran capacidad de trabajo, tu pasión por enseñar y ayudar al alumnado.

Vicente, gracias por formarme durante cuatro años, por transmitirme tu pasión por la investigación, por enseñarme a trabajar de manera ordenada en el laboratorio. No habrá día que me deje de sorprender tu amplitud de conocimientos. Gracias por enseñarme tanto.

José, agradezco de corazón todo el tiempo y esfuerzo que has dedicado a esta Tesis, tu constante ayuda y guía, y tu infinita paciencia. No puede haber mejor profesor que tú.

A Carmen Julián Lagunas, auxiliar del Laboratorio de Micología de la Unidad de Protección Vegetal del CITA, por su excelente disposición para ayudarme y enseñarme en el laboratorio.

A Esther López, Joaquín Lanuza, Begoña Portaña y Jaime Arranz, técnicos del invernadero de la Escuela Politécnica Superior, cuya ayuda ha sido clave para llevar a buen puerto muchos de los experimentos.

A la bodega Viñas del Vero S.A., en especial a Sergio Torres Sánchez y Adrián Jarné Casasús, por poner a mi disposición sus parcelas para llevar a cabo los ensayos y por mostrarme una visión realista del sector vitivinícola.

Al Centro de Sanidad y Certificación Vegetal, en especial a Raúl Langa Lomba y Pedro Mingote Ballestín, por facilitarme los datos sobre las enfermedades de la vid en Aragón. Su colaboración ha enriquecido el estudio a nivel de nuestra Comunidad Autónoma.

Al Centro de Investigación y Tecnología Agroalimentaria (CITA) y a la Escuela Politécnica Superior de la Universidad de Zaragoza, por el acceso a las instalaciones y a todos los medios necesarios para llevar a cabo la investigación.

Al Centro de Transferencia Agroalimentaria (CTA) de Aragón, por facilitarme el material vegetal empleado en el estudio de variedades.

Al Prof. Jesús Martín Gil, del Laboratorio de Materiales Avanzados de la E.T.S. de Ingeniería Agrarias de la Universidad de Valladolid, por hacerme sentir siempre bienvenida en mis estancias en su laboratorio e iniciarme en la Ciencia de Materiales.

A Luis Buetas, por la disponibilidad para ayudarme, por su paciencia y apoyo.

A mis padres, por inculcarme el valor del trabajo y el esfuerzo desde pequeña.

A mi hermano, Raúl Langa, por impulsarme a comenzar la Tesis, por formarme, por enseñarme la realidad de la vida y la justicia, por estar siempre presente en todas las decisiones.

RESUMEN

Las enfermedades fúngicas de la madera de la vid (EMV) se han convertido en un importante desafío para la viticultura en las últimas 2-3 décadas, al generar graves pérdidas económicas en las plantaciones. Esto se debe a la falta de medidas completamente efectivas para su control. La adopción de estándares fitosanitarios más respetuosos con el medio ambiente en la Unión Europea y otras zonas productoras mundiales, con la prohibición de productos fitosanitarios efectivos, y la generalización de nuevos sistemas de manejo más intensivos y exigentes desde el punto de vista de la biología de la planta, han contribuido al aumento de su incidencia en los últimos años. Uno de los impactos socioeconómicos más destacados de estas enfermedades son las pérdidas económicas y problemas asociados a la producción y establecimiento de material vegetal de nueva plantación. La presente Tesis Doctoral se centra en la búsqueda y desarrollo de alternativas de control novedosas y respetuosas con el medio ambiente, conforme a los principios de la Gestión Integrada de Plagas. Con esta visión, se ha evaluado la eficacia de extractos naturales obtenidos de diversas especies vegetales, formulados para potenciar su efecto y capacidad antimicrobiana, y el potencial de microorganismos endofíticos (hongos y bacterias) nativos de la planta de la vid como antagonistas microbianos y/o promotores del crecimiento frente a patógenos responsables de las EMVs, especialmente aquellos que afectan a plantas jóvenes. Estos objetivos se han abordado mediante la realización de ensayos tanto *in vitro* como *in vivo*. Los resultados obtenidos en los tratamientos basados en complejos conjugados con oligómeros de quitosano y esteviósido, en el caso del control mediante extractos vegetales, y los observados con un aislado de *Bacillus velezensis*, en el caso de abordaje mediante el empleo de antagonistas microbianos, sugieren que pueden ser una opción prometedora para reducir la dependencia de fitosanitarios de síntesis química en el control de las EMV. Además, la encapsulación de estos agentes terapéuticos en nanotransportadores y su liberación controlada, ensayada mediante endoterapia en parcelas de la D.O.P. Somontano infectadas de forma natural con este tipo de patógenos, ha conducido a resultados que indican la necesidad de ampliar las investigaciones sobre el tipo de nanotransportador empleado y la época fenológica de aplicación. Manteniendo un marco conceptual de Gestión Integrada de Plagas, estas investigaciones se han complementado con un cribado de fuentes de resistencia natural a patógenos en genotipos de vid del Banco de Germoplasma de la Vid de Aragón. También se ha llevado a cabo un estudio comparativo de las comunidades microbianas fúngicas en dos viñedos situados en la misma unidad biogeográfica de la D.O.P. Somontano, empleando tanto secuenciación de alto rendimiento como métodos microbiológicos clásicos. En el primer caso, los resultados sugieren que las fuentes y genes de resistencia natural a este tipo de fitopatógenos no son muy abundantes y que esta resistencia es de carácter cuantitativo en virtud del comportamiento observado en los genotipos ensayados. En lo que respecta al estudio comparativo de las comunidades microbianas, los resultados han demostrado la utilidad de combinar ambos tipos de metodología para obtener una caracterización más completa de la diversidad microbiana y para tomar decisiones informadas sobre los tratamientos de control según el estado fitosanitario de cada viñedo en particular.

Palabras clave: agentes de biocontrol, enfermedades de la madera de la vid, esteviósido, extractos vegetales, metagenómica, nanotransportadores, resistencia varietal, quitosano, vid.

ABSTRACT

Grapevine trunk diseases (GTDs) have become a major challenge for viticulture in the last 2-3 decades, generating serious economic losses in plantations. This is due to the lack of fully effective measures for their control. The adoption of more environmentally friendly phytosanitary standards in the European Union and other producing areas worldwide, with the prohibition of effective phytosanitary products, and the generalization of new, more intensive, and demanding management systems from the point of view of plant biology, have contributed to the increase in GTDs' incidence in recent years. Some of the most important socioeconomic impacts of these diseases are the economic losses and problems associated with the production and establishment of new planting material. This PhD Thesis focuses on the search for and development of novel and environmentally friendly control alternatives, under the principles of Integrated Pest Management (IPM). With this vision, the efficacy of natural extracts obtained from various plant species, formulated to enhance their effect and antimicrobial capacity, and the potential of endophytic microorganisms (fungi and bacteria) native to the grapevine plant as microbial antagonists and/or growth promoters against pathogens responsible for GTDs, especially those affecting young plants, have been evaluated. These objectives have been addressed by performing both *in vitro* and *in vivo* assays. The results obtained with treatments based on conjugate complexes with chitosan oligomers and stevioside, in the case of control strategies involving plant extracts, and those observed with an isolate of *Bacillus velezensis*, in the case of the approach based on microbial antagonists, suggest that they may be promising options for reducing dependence on chemically synthesized pesticides in the control of GTDs. Moreover, the encapsulation of these therapeutic agents in nanocarriers and their controlled release, tested employing endotherapy in Somontano PDO plots naturally infected with this type of pathogens, has led to results that indicate the need for further research on the type of nanocarrier used and the phenological time of application. Maintaining a conceptual framework of IPM, these investigations have been complemented with a screening of sources of natural resistance to pathogens in grapevine genotypes from the Grapevine Germplasm Bank of Aragon. A comparative study of fungal microbial communities in two vineyards located in the same biogeographical unit of the Somontano PDO has also been carried out, using both high-throughput sequencing and classical microbiological methods. In the first case, the results suggest that the sources and genes of natural resistance to this type of phytopathogens are not very abundant and that this resistance is quantitative in nature by virtue of the behavior observed in the genotypes tested. Regarding the comparative study of microbial communities, the results have demonstrated the usefulness of combining both types of methodology to obtain a more complete characterization of microbial diversity and to make informed decisions on control treatments according to the phytosanitary status of each particular vineyard.

Keywords: biocontrol agents, grapevine trunk diseases, stevioside, plant extracts, metagenomics, nanocarriers, varietal resistance, chitosan, grapevine.

ÍNDICE

1. INTRODUCCIÓN	1
1.1. Marco de referencia.....	1
1.1.1. <i>Situación actual del cultivo de la vid</i>	1
1.1.2. <i>Impacto de las enfermedades de la madera de la vid</i>	2
1.2. Enfermedades de la madera de la vid	4
1.2.1. <i>Enfermedades de madera que afectan a plantas jóvenes</i>	4
1.2.2. <i>Enfermedades de madera que afectan a plantas adultas</i>	5
1.3. Medidas de control de las enfermedades de la madera.....	6
1.3.1. <i>Prácticas de gestión fitosanitaria en viveros</i>	7
1.3.2. <i>Manejo cultural</i>	7
1.3.3. <i>Control biológico</i>	9
1.3.4. <i>Productos naturales con capacidad antifúngica</i>	11
1.3.5. <i>Estudio de la microbiota mediante secuenciación masiva</i>	11
1.3.6. <i>Resistencias naturales</i>	12
1.4. Objetivos de la Tesis Doctoral	12
1.4.1. <i>Hipótesis de trabajo</i>	12
1.4.2. <i>Objetivos generales</i>	13
1.4.3. <i>Objetivos específicos</i>	13
1.5. Justificación de la unidad temática de los artículos.....	13
1.6. Metodología general	14
1.7. Referencias.....	15
2. COMPENDIO DE PUBLICACIONES	25
3. DISCUSIÓN GLOBAL	211
3.1. Productos naturales.....	211
3.2. Agentes de biocontrol	215
3.3. Resistencias.....	215
3.4. Análisis de comunidades microbianas	216
4. CONCLUSIONES	219
APÉNDICE	221

1. INTRODUCCIÓN

1.1. Marco de referencia

1.1.1. Situación actual del cultivo de la vid

La vid es el cultivo frutícola más extendido a nivel mundial, especialmente en la cuenca mediterránea. El informe de la Organización Internacional de la Viña y el Vino (OIV) titulado “*Actualidad de la coyuntura del sector vitivinícola mundial en 2021*” [1] resume los datos más relevantes sobre el cultivo en 2021. En ese año, la superficie total de viñedo en el mundo fue de 7,3 millones de ha (incluidas las vides jóvenes que aún no producen), una cifra ligeramente inferior a la registrada en 2020 (-0,3%). La Unión Europea cuenta con 3,3 millones de ha, destacando España como el país con mayor extensión vitícola del mundo, con 964.000 ha, habiendo aumentado un 0,4% respecto a 2020. Francia ocupa el segundo lugar, con 798.000 ha; seguida de China, con 783.000 ha; Italia, con 718.000 ha; Turquía, con 419.000 ha; y Estados Unidos, con 400.000 ha.

La producción de uva en 2021 alcanzó los 74,8 millones de toneladas a nivel mundial. La producción de vino (excluidos zumos y mostos) se estima en 260 millones de hectolitros para ese año, que representan una ligera disminución de casi 3 millones de hectolitros (-1%) en comparación con 2020. De esta producción vinícola, la Unión Europea aportó 153,7 millones de hectolitros, registrando una disminución del 8% con respecto a 2020. Italia lidera la producción, con 50,2 millones de hectolitros; seguida de Francia, con 37,6 millones de hectolitros; y España, con 35,5 millones de hectolitros, que en conjunto representan el 47% de la producción mundial de vino en 2021. Estados Unidos se posiciona como el cuarto productor, con 24,1 millones de hectolitros.

De acuerdo con el informe “*Perspectivas de la producción mundial del vino*” de la OIV [2], la producción mundial de vino (excluidos zumos y mostos) se estima en 259,9 millones de hectolitros en 2022, producción similar a la del año anterior. No obstante, no se disponen actualmente de datos de China y Rusia. La producción de la Unión Europea se espera que alcance los 157 millones de hectolitros, con un aumento anual de 3,5 millones de hectolitros respecto a 2021. Italia se mantiene como el mayor productor (50,3 millones de hectolitros), seguido de Francia (44,2 millones de hectolitros), y España (33 millones de hectolitros, por los efectos de la sequía y la falta de recursos hídricos en numerosas regiones). Estados Unidos ocupa de nuevo el cuarto lugar en producción, con 23,1 millones de hectolitros.

El consumo mundial de vino en 2021 se estimó en 236 millones de hectolitros, siendo EE.UU. el principal consumidor (33 millones de hectolitros), seguido de Francia (25,2 millones de hectolitros), Italia (24,2 millones de hectolitros), Alemania (19,8 millones de hectolitros), Reino Unido (13,4 millones de hectolitros), y España (10,5 millones de hectolitros) [1].

La actividad vitivinícola, que abarca desde la viticultura hasta la elaboración del vino y su comercialización, genera un valor añadido bruto superior a los 23.700 millones de euros en España, equivalente al 2,2% del PIB total del país. Esto demuestra claramente el impacto económico de este sector.

Según la “*Encuesta sobre Superficies y Rendimientos de Cultivos (ESYRE) de 2022*” del Ministerio de Agricultura, Pesca y Alimentación (MAPA) [3], la superficie española dedicada al cultivo de la vid fue de 948.024 ha en 2022, con una disminución a lo largo de los años de un -1,03% respecto al 2004. Este cultivo se concentra en tierras de secano, con 550.572 ha (58,1%) frente a 397.452 ha en regadío (41,9%). Prácticamente la totalidad de la superficie (98,3%) se dedica a la uva de transformación, correspondiendo el resto a la uva de mesa. La comunidad autónoma con mayor superficie dedicada al cultivo de la vid es Castilla-La Mancha (48,1%), seguida de Extremadura

(8,7%), y Castilla y León (7,9%). Aragón ocupa la séptima posición nacional, con un 3,8% del total, abarcando 35.734 ha, de las cuales 23.516 ha se cultivan en secano (65,8%) y 12.218 ha en regadío (34,19%). Gran parte de la superficie se encuentra en la provincia de Zaragoza (80,0%), seguida de Huesca (15,0%) y Teruel (5,0%). El destino de la superficie de uva aragonesa es para la transformación (en este caso, para vinificación) y tan solo 2 ha de secano se dedican a uva de mesa (0,6% del total de superficie en 2021).

Según el informe de “*Avance de datos de Viñedo de 2021*” del MAPA [4], la producción total nacional en 2021 fue de 6.086.025 toneladas, destinadas principalmente a vinificación (94,9%). El rendimiento medio nacional en regadío fue de 11.676 kg/ha y de 4.659 kg/ha en secano en uva de vinificación. En Aragón los rendimientos fueron menores, con 6.073 kg/ha en regadío y 2.775 kg/ha en secano respectivamente.

De acuerdo con el informe del Gobierno de Aragón “*Avance de macromagnitudes del sector agrario aragonés 2021*” [5], la producción aragonesa fue de 139.811 toneladas en 2021, con un aumento de un 5,2% respecto al año anterior. Esta producción corresponde a 48.248.776 € de producción final agraria (PFA), decreciendo un 1,8% respecto a 2020. Se encuentra en la quinta posición de PFA del subsector agrícola (2,5%), después de los cereales, frutas, forrajes, y hortalizas.

Las áreas con mayor concentración de superficie de viñedo coinciden con aquellas delimitadas por las diferentes figuras de calidad diferenciada, es decir, Denominaciones de Origen Protegidas (DOP) e Indicaciones Geográficas Protegidas (IGP). En estas zonas, la vitivinicultura se ha convertido en un motor de desarrollo y un freno a la despoblación rural.

El territorio aragonés posee en la actualidad seis DOPs: DOP Cariñena, DOP Campo de Borja, DOP Calatayud, DOP Somontano, DOP Aylés (Vinos de Pago), y DOP Cava (con ámbito territorial supraautonómico). Además, cuenta con seis IGP denominadas Vinos de la Tierra: IGP Bajo Aragón, IGP Ribera del Jiloca, IGP Ribera del Gállego-Cinco Villas, IGP Valdejalón, IGP Valle del Cinca, e IGP Ribera del Queiles.

1.1.2. Impacto de las enfermedades de la madera de la vid

Las enfermedades de la madera de la vid (EMV) son patologías causadas por diversas especies de hongos patógenos que dañan la madera, produciendo un decaimiento general de la planta, afectando al rendimiento y calidad del producto, e incluso pudiendo llegar a la muerte de la planta [6-8]. Los síntomas típicos que causan en las vides son necrosis sectoriales o vasculares en la madera, podredumbres en las raíces, decoloración y desecación en las hojas, y retraso del crecimiento [9,10].

Entre las EMV más frecuentes asociadas a la viña joven (menos de 8 años) se encuentran la enfermedad de Petri, el pie negro, el “brazo muerto” o decaimiento por *Botryosphaeria*, y la excoriosis o decaimiento por *Diaporthe*. En los últimos años, se ha detectado además un incremento en la incidencia de la podredumbre basal causada por *Rhizoctonia solani* J.G. Kühn en plantas-injerto provenientes de vivero. En cuanto a la planta adulta (más de 8 años), las enfermedades más comunes son la yesca, la eutipiosis, y el decaimiento por *Botryosphaeria*.

Existen diferentes modos de infección de las vides en función de la biología de los patógenos implicados. El pie negro penetra en la vid por heridas en las raíces o en la base del patrón. En cambio, el “brazo muerto”, la yesca, la eutipiosis, y la excoriosis habitualmente infectan heridas de poda. La enfermedad de Petri puede entrar tanto a través de heridas en raíces como por las heridas de poda. En las infecciones a través de esporas, éstas se producen y liberan en los cuerpos fructíferos y se transmiten y desplazan por el agua, el viento, insectos, o las herramientas de poda [10,11].

En las últimas tres décadas, las EMV están consideradas como uno de los desafíos más importantes para los viticultores por su capacidad destructiva [10], que compromete la rentabilidad económica del cultivo con unos costes de replantación de más de 1500 M\$ al año a nivel mundial [12]. Estos hongos se han convertido en una de las principales temáticas de investigación relacionadas con el sector vitivinícola [7].

Una publicación reciente de la Organización Internacional de la Viña y el Vino (OIV) recoge que la incidencia de enfermedades de madera en la vid es del 10% en España, el 13% en Francia y de entre un 8% y un 19% en Italia, y que las pérdidas en California superan los 260 M\$/año [6]. Según el artículo de Martínez-Diz *et al.* [13], el coste anual de replantar el cultivar ‘Tempranillo’ afectado por EMV en DOP Rioja se estima en 7,16 M€ anuales (estimación basada en el 1% de muerte de cepas de viñedo) [13].

Los datos proporcionados por el Centro de Sanidad y Certificación Vegetal (CSCV) del Gobierno de Aragón ofrecen una visión más precisa de la importancia de las EMV en la región aragonesa. Durante el período comprendido entre el 15/04/2020 y el 10/02/2023, se realizaron 469 consultas al Laboratorio Regional de Análisis del mencionado CSCV para la identificación de plagas y enfermedades en vides enfermas. Del total de peticiones de análisis efectuadas, el 48,0% correspondió a bacterias (*Xylella fastidiosa* Wells et al., 1987 (96,9%); *Agrobacterium tumefaciens* (Smith & Townsend, 1907) Conn, 1942 (1,3%); *Phytoplasma* sp. (0,9%); *Rhizobium vitis* (Ophel & Kerr) Young, Kuykendall, Martínez-Romero, Kerr & Sawada (0,4%); y *Agrobacterium* sp. (0,4%)), el 21,7% a virus (Grapevine fleck virus (25,5%), Grapevine fanleaf virus (20,6%), Grapevine leafroll-associated virus 1 (19,6%), Arabis mosaic virus (17,6%), y Grapevine leafroll-associated virus 3 (16,7%)), el 16,8% a hongos (brazo muerto (62,3%), pie negro (16,4%), eutiposis (8,2%), *Rhizoctonia solani* (4,9%), enfermedad de Petri (4,9%), y *Phomopsis* o excoriosis (3,3%)), el 3,6% a plagas (*Aethes margarotana* (17,6%), *Anacridium aegyptium* (11,8%), *Phaneroptera nana* (11,8%), *Aethes margaritona* (5,9%), *Agrotis* sp. (5,9%), *Lobesia brotana* (5,9%), *Tetranychus* sp. (5,9%), *Tropinota squalida* (5,9%), *Xylotrechus arvicola* (5,9%), *Sitochroa verticalis* (5,9%), *Aphanus rolandri* (5,9%), *Crusptoblabs gnidiella* (5,9%), y roedores (5,9%)) y el 0,9% a fisiopatías (exceso de humedad (50%), fisiopatía (25%), y fitotoxicidad (25%)).

El 13% de las consultas totales relacionadas con la vid fueron de EMV, y el 77,2% de las consultas de vid de hongos fueron EMV (Tabla 1), con alta prevalencia de *Neofusicoccum parvum*.

Tabla 1. Consultas relativas a hongos que afectan a la vid en el Centro de Sanidad y Certificación Vegetal (Gobierno de Aragón).

Patógeno	Enfermedad de la madera de la vid u otro hongo	Nº consultas
<i>Neofusicoccum parvum</i>	Brazo muerto	25
<i>Diplodia</i> spp.	Brazo muerto	9
<i>Botryosphaeriaceae</i>	Brazo muerto	3
<i>Diplodia mutila</i>	Brazo muerto	1
<i>Cylindrocarpon</i> spp.	Pie negro	10
<i>Eutypa</i> sp.	Eutiposis	3
<i>Eutypa lata</i>	Eutiposis	2
<i>Phaeoacremonium</i> spp.	Enfermedad de Petri	3
<i>Rhizoctonia</i> spp.	Podredumbre basal	3
<i>Diaporthe</i> spp.	Excoriosis o <i>Phomopsis</i>	1
<i>Phomopsis viticola</i>	Excoriosis o <i>Phomopsis</i>	1
<i>Phoma</i> sp.	Otro hongo	5
<i>Penicillium</i> sp.	Otro hongo	4
<i>Armillaria mellea</i>	Podredumbre blanca de raíz	2
<i>Alternaria</i> sp.	Otro hongo	1
<i>Armillaria</i> sp.	Otro hongo	1

El incremento reciente de este tipo de patologías puede ser atribuido a la interacción simultánea de varios factores fundamentales [14]. En primer lugar, la prohibición de numerosos productos fitosanitarios como el arsenito de sodio, el benomilo, la carbendazima, los benzimidazoles [6], y el bromuro de metilo, que eran eficaces contra ciertos patógenos de las EMV, debido a su toxicidad para los viticultores y el medio ambiente [7]. En segundo lugar, desde los años noventa se ha producido un aumento en la demanda de plantas en viveros, lo que ha afectado negativamente el estado fitosanitario del material vegetal de propagación [15], incrementando la mortalidad de plantas jóvenes de vid en los 1–3 años posteriores a su plantación. Por último, los nuevos manejos más intensivos del cultivo de la vid, como el aumento de densidad de plantación, el sistema de formación en espaldera, la poda mecánica, escasa protección de heridas de poda, riego y fertilización [14], también han favorecido el desarrollo de estos hongos.

En la actualidad, no existe un método eficaz para la erradicación completa de estos patógenos fúngicos [14,16]. Por lo tanto, es imprescindible la búsqueda e implementación de nuevas soluciones preventivas y de control en un marco de Gestión Integrada de Plagas (GIP).

1.2. Enfermedades de la madera de la vid

1.2.1. Enfermedades de madera que afectan a plantas jóvenes

1.2.1.1. Pie negro (“Black Foot Disease”)

El pie negro se reconoce por la presencia de lesiones necróticas en las raíces y una decoloración marrón rojiza en la base del portainjerto de las vides afectadas [14]. La planta muestra una reducción de la biomasa radicular, un menor vigor, tallos poco gruesos, acortamiento de los entrenudos, desigualdad en la lignificación de la madera, escaso follaje y hojas pequeñas con clorosis y necrosis internervial [10,17]. Esta enfermedad provoca generalmente la muerte rápida de la vid joven en la misma campaña o en siguientes [18].

Está asociada a especies de los géneros *Campylocarpon*, *Cylindrocarpon*, *Cylindrocladiella*, *Dactylonectria*, *Ilyonectria*, *Thelonectria*, *Neonectria*, y *Pleiocarpon* [14,19-22]. Estas especies infectan los patrones durante el proceso de enraizamiento en la producción de planta injertada en vivero [23,24]. En España, la especie más frecuente causante de pie negro es *Dactylonectria torresensis* (A. Cabral, Rego & P.W. Crous) L. Lombard & P.W. Crous [25].

1.2.1.2. Enfermedad de Petri

Los síntomas de la enfermedad de Petri son una vegetación débil, hojas pequeñas cloróticas con necrosis, entrenudos cortos, un tronco de tamaño escaso y un sistema radicular pobre, pudiendo llevar a la muerte de la planta [10,18]. Al realizar un corte transversal de la madera afectada, se observa un oscurecimiento de los elementos vasculares centrales que forman un anillo alrededor de la médula que puede producir una exudación gomosa negra llamada “black goo” [26,27].

Las especies fúngicas que la causan son *Phaeoconiella chlamydospora* (W. Gams, Crous, M. J. Wingf. & L. Mugnai) Crous & W. Gams, hasta 29 especies de *Phaeoacremonium* (siendo la más frecuente *Phaeoacremonium minimum* (Tulasne & C. Tulasne) D. Gramaje, L. Mostert & Crous), *Pleurostoma richardsiae* (Nannf.) Réblová & Jaklitsch., y seis especies de *Cadophora* (siendo la más común *Cadophora luteo-olivacea* (J.F.H. Beyma) T.C. Harr. & McNew) [14]. Los propágulos infectivos (esporas) de estas especies se dispersan generalmente a través de lluvia y viento.

1.2.1.3. Decaimiento por *Botryosphaeriaceae* o brazo muerto (“*Black Dead Arm*”)

El decaimiento por *Botryosphaeriaceae* es una de las enfermedades de madera más perjudiciales, emergentes y extendidas que afectan en la actualidad a los viñedos [28,29].

Las vides afectadas presentan brazos secos y muertos, y fuertemente defoliados [18]. En ocasiones, se pueden observar hojas con clorosis o deformaciones [27]. En una sección transversal de la madera se puede observar la presencia de necrosis oscuras duras en forma de cuña o “V”, síntomas parecidos a los causados por *Eutypa lata* (Pers.) Tul. & C. Tul. y otros hongos de la familia *Diatrypaceae*. Los patógenos infectan la planta a través de heridas, mayormente heridas de poda, y las esporas se propagan a través de la lluvia y el viento [30].

Las especies asociadas al brazo muerto pertenecen a los géneros *Botryosphaeria*, *Neofusicoccum*, *Neoscytalidium*, *Phaeobotryosphaeria*, *Diplodia*, *Lasiodiplodia*, *Dothiorella*, *Spencermartinsia* y *Sphaeropsis* [14,30]. Destaca entre todas ellas *Neofusicoccum parvum* (Pennycook & Samuels) Crous, Slippers & A.J.L. Phillips, un patógeno polífago muy virulento y que infecta rápidamente la madera [31-33].

1.2.1.4. Podredumbre basal por *Rhizoctonia solani*

Los principales síntomas causados por el basidomiceto *Rhizoctonia solani* son la podredumbre basal de la raíz y la base del tallo de las plantas-injerto o barbados, causando una reducción de la biomasa de las raíces, un menor desarrollo de la planta y su muerte en los primeros años de la plantación [34,35]. Las hojas pueden presentar un cambio de color de amarillo a permaneciendo en la vid después de que la planta se muera [36].

Este patógeno clásico y cosmopolita aparece como un problema emergente en el suelo de los viveros donde se produce el material de propagación de la vid. *Rhizoctonia solani* cada vez se aísla más en plantas injertadas provenientes de vivero en las distintas DO de Aragón.

1.2.1.5. Excoriosis o decaimiento por *Diaporthe* (“*Phomopsis cane and leaf spot*”)

El decaimiento por *Diaporthe* puede afectar a plantas jóvenes, adultas y al material de propagación [18]. En las hojas aparecen manchas oscuras de color marrón-negro, que pueden deformarse y finalmente caer [24]. Los brotes jóvenes y sarmientos presentan necrosis y chancros oscuros con grietas superficiales en la corteza y presencia de estructuras de reproducción asexual (picnidios) [18]. En las ramas, puede observarse un estrangulamiento en la base que puede provocar la rotura debido al viento o al peso de los racimos de uva. Además, los frutos se vuelven marrones y se marchitan [10], disminuyendo el rendimiento y la calidad de la fruta [37]. En la madera, *Diaporthe* puede estar también asociado a necrosis sectoriales duras de color marrón oscuro [18].

La infección se produce a través de heridas abiertas, mayormente causadas por la poda [11], siendo más grave en la regiones productoras de vino con un clima templado-húmedo [10].

Las especies patógenas asociadas a esta enfermedad pertenecen al género *Diaporthe*, siendo la especie más virulenta *Diaporthe ampelina* (Berk. & M.A. Curtis) R.R. Gomes, Glienke & Crous (= *Phomopsis viticola* (Sacc.) Sacc.) [11,38].

1.2.2. Enfermedades de madera que afectan a plantas adultas

1.2.2.1. Yesca

Los síntomas externos de la yesca se clasifican en dos modelos, según sea su evolución lenta o rápida (conocida como apopléjica) [18]. En la forma lenta, las zonas internerviales de las hojas presentan un color amarillo en las variedades blancas y rojo en las tintas [18]. Las hojas tienen un aspecto atigrado característico [9], finalmente se necrosan y caen [39]. Los racimos pueden llegar

a pasificarse prematuramente, por lo que el rendimiento disminuye [18,40]. Estos síntomas suelen presentarse de forma intermitente a lo largo de la vida del viñedo, pudiendo ser muy graves un año y leves al siguiente [18]. En la forma rápida, que se suele producir en verano y en climas secos o en situaciones severas de estrés hídrico, se produce la muerte repentina de la planta [39]. Empieza con una pérdida de turgencia de las hojas y una coloración verde-grisácea [41], perdiendo su capacidad fotosintética [42]. La madera afectada se vuelve blanda, esponjosa y amarillenta [39].

En el interior de la madera se pueden observar estrías y “punteaduras” necróticas, a veces rodeadas por una decoloración rosa-marrón. En estadios finales en plantas añosas, aparece la podredumbre seca, esponjosa y blanda en las zonas centrales del tronco y/o brazos, como consecuencia de la degradación de los materiales lignocelulósicos del leño de la planta [18].

Los patógenos que provocan la yesca incluyen los basidiomicetos *Fomitiporia mediterranea* M. Fischer, *Inonotus hispidus* (Bull.) P. Karst., y, en menor medida, *Stereum hirsutum* (Willd.) Pers., junto a los hongos ascomicetos (*Phaeomoniella chlamydospora* y *Phaeoacremonium* spp.), causantes de la enfermedad de Petri anteriormente mencionada [10]. Todos estos patógenos generalmente penetran en la vid a través de heridas de poda y más raramente a través del suelo.

1.2.2.2. Eutipiosis

Los síntomas foliares de esta patología incluyen clorosis con márgenes necróticos, desecación y deformación de las hojas [14,39]. Los entrenudos en plantas afectadas son cortos [24]. Los racimos maduran de forma desigual y son pequeños, llegando incluso a marchitarse. En el tronco, el corte transversal presenta podredumbres de la madera en forma de cuña o “V” de color marrón y aspecto seco [39,43]. Los patógenos reducen el crecimiento vegetativo (“raquitismo”) y, finalmente, conducen a la muerte de la vid [44].

El principal agente causal pertenece al género *Eutypa* (*E. lata*), siendo el más perjudicial y el responsable de los síntomas foliares [45,46]. Además, aparecen otros géneros como *Eutypella*, *Diatrype*, *Diatrypella*, *Cryptosphaeria*, *Cryptovalsa*, *Anthostoma*, y *Peroneutypa* [11]. Las infecciones se producen por la entrada de las esporas de estos patógenos en la madera, principalmente en heridas de poda o asociadas a heladas, granizo o recolección mecánica [39].

1.3. Medidas de control de las enfermedades de la madera

En la actualidad no existen medidas de control curativas eficaces para las enfermedades fúngicas de madera. Hoy en día, se están aplicando métodos y tratamientos preventivos, siendo clave la producción y comercialización de planta libre de estos patógenos. Por ello, es imprescindible seguir investigando en alternativas de control que permitan mejorar la calidad fitosanitaria del material de plantación.

Además, es esencial el desarrollo de nuevas tecnologías que permitan detectar de forma fácil y precisa los patógenos causantes de las enfermedades de la madera de la vid, permitiendo así elegir entre la aplicación de medidas fitosanitarias o la eliminación de las plantas enfermas, mejorando así la gestión de las plantaciones. Las nuevas prácticas y métodos de detección, identificación y cuantificación del material enfermo también mejorarían el control en los viveros y las exportaciones, disminuyendo el movimiento de vides infectadas y evitando una mayor extensión en las regiones productoras [11].

En lo que respecta al manejo, se recomienda evitar métodos intensivos de cultivo en tanto conducen a un mayor desarrollo de enfermedades (al aumentar las situaciones de estrés en las plantas), dando importancia al sistema de formación (de cordón simple), la recolección mecánica

(que puede causar defoliación y heridas), y la simplificación excesiva del sistema de conducción a través de métodos de poda y vendimia mecanizados, analizados más adelante.

1.3.1. Prácticas de gestión fitosanitaria en viveros

Como ya se ha indicado, el material vegetal es una vía de propagación y entrada de las EMV por las zonas vitivinícolas.

En vivero, el tratamiento más habitual frente a estas patologías es la termoterapia, sometiendo los materiales de propagación a baños con agua caliente a 50 °C durante 30 minutos, siendo un método eficaz para desinfectar el material de propagación y la planta injerto [47-49] de ciertos patógenos de las EMV como la enfermedad de pie negro y la enfermedad de Petri, aunque se ha mostrado menos efectivo frente a otros [14,30,50]. En España, se ha demostrado que el tratamiento a 53 °C durante 30 min mejora significativamente la eficacia contra los patógenos de EMV, generalmente sin efectos perjudiciales para la planta [14,51,52]. Sin embargo, algunas variedades de vid resisten mal estos tratamientos [39,53].

También se ha ensayado el tratamiento con agua ácida electrolizada, con resultados preliminares prometedores frente a *Phaeoconiella chlamydospora* en un experimento de 3 años con estacas [54].

Otra alternativa es el uso de agua ozonizada. Según el ensayo de Pierron *et al.* [55], las propiedades fungicidas del agua ozonizada limitan la infección de la vid por *Phaeoacremonium aleophilum* W.Gams, Crous, M.J.Wingfield & Mugnai en los viveros. Los resultados concluyeron que el agua ozonizada suprimió totalmente la germinación de esporas *in vitro* y, a las 9 semanas posteriores a la inoculación, el desarrollo de hongos se redujo significativamente en un 50% en las plantas [55]. Asimismo, el estudio de Romeo-Olivan *et al.* [56] demostró que el agua ozonizada suprimió por completo la germinación de esporas de *Phaeoacremonium minimum* y *Phaeoconiella chlamydospora in vitro*, y en la planta también redujo el desarrollo fúngico. Además de sus propiedades antifúngicas, no tiene fitotoxicidad para la planta, lo que la convierte en una alternativa atractiva [56].

Una vía para mejorar la eficacia de estos tratamientos sería combinarlos con agentes de control biológico (analizados más abajo) y/o el uso de fungicidas, logrando así una mayor protección del material de propagación.

1.3.2. Manejo cultural

1.3.2.1. Medidas generales de lucha contra las EMV

La elección y aplicación de métodos culturales apropiados resultan esenciales para disminuir la propagación del inóculo de estos patógenos [10].

Antes de la plantación, se recomienda evitar el cultivo durante varios años (3–4 años), desinfectar el terreno o realizar una biofumigación con mostaza [57-60], colza [17], o coles, entre otras. Otro punto importante es un buen drenaje del suelo, para evitar la infección de patologías de suelo como el pie negro [61], favorecer el desarrollo en profundidad y evitar heridas en la planta durante la plantación.

Es importante partir de un material vegetal de calidad con buena distribución de raíces y libre de estos patógenos, siendo especialmente recomendable asegurarse mediante el envío de muestras a laboratorio para un análisis previo a la plantación. A este respecto, es preciso aclarar que la legislación española en materia de control y certificación de plantas de vid en vivero (Real Decreto 208/2003, de 21 de febrero; Figura 1) no recoge las principales enfermedades actuales de la madera de la vid. En algunos casos, las enfermedades se identifican incorrectamente a nivel taxonómico o están sin actualizar. A nivel Europeo, la Directiva de Ejecución 2020/177 de la

Comisión de 11 de febrero de 2020, que modifica las Directivas 66/401/CEE, 66/402/CEE, 68/193/CEE, 2002/55/CE, 2002/56/CE y 2002/57/CE del Consejo, así como las Directivas 93/49/CEE y 93/61/CEE, y las Directivas de Ejecución 2014/21/UE y 2014/98/UE de la Comisión, en lo que respecta a las plagas de los vegetales en semillas y otros materiales de reproducción vegetal, tampoco actualizan ni mencionan las nuevas enfermedades de madera.

ANEXO V

Organismos nocivos

a) Tratamiento en cultivo:

Deberán realizarse los tratamientos fitosanitarios periódicos necesarios, principalmente para el control de nematodos, ácaros, insectos, hongos y bacterias.

b) Plantas de vivero portadoras de plagas y enfermedades:

El material de multiplicación, así como las cepas madre, estarán libres de las siguientes plagas o enfermedades:

Nematodos: «Xiphinema sp»; «Longidorus sp».

Ácaros: «Phyllocoptes vitis», «Panonychus ulmi 7 eotetranychus carpini».

Cochinillas: «Pseudococcus citri» y «quadraspidiotus perniciosus».

Podredumbres: «Armillariella mellea» y «Rosellinia necatrix».

Excoriosis: «Phomosis sp».

Eutioplosis: «Eutypa armeniaca».

Yesca: «Estereum sp».

Bacteriosis: «Xanthomonas ampelina».

Se admitirá la presencia de ligeras infestaciones de las plagas y enfermedades citadas en el apartado a), siempre que se hubieran realizado los oportunos tratamientos.

c) Virosis:

1. Entrenudo corto (GFLV).

2. Enrollado, razas 1 y 3 (GLRaV1, GLRaV3).

3. Jaspeado (GFkV).

Figura 1. Anexo V del Real Decreto 208/2003, de 21 de febrero, por el que se aprueba el Reglamento técnico de control y certificación de plantas de vivero de vid.

1.3.2.2. Poda y conducción

Se ha demostrado que las heridas de poda son la principal vía de entrada de la mayoría de enfermedades de madera [62], y que la dinámica de la infección difiere en función del hongo [63]. Por lo tanto, la poda debe realizarse en el momento óptimo, cuando haya menos humedad en el ambiente, mayor capacidad de cicatrización de la herida y una menor cantidad de inóculo en el ambiente, siendo variable entre regiones productoras y años. Se recomendaba la poda estación de reposo vegetativo, porque las heridas cicatrizan más rápidamente que con mayores temperaturas [10]. Sin embargo, otras investigaciones en España sugieren que la tasa de infección natural de las heridas de poda fue menor tras la poda temprana (otoño) [14,64,65].

Se han desarrollado unas ecuaciones para describir la dinámica de dispersión de propágulos infectivos de *P. chlamydospora* que podrían usarse para construir modelos que puedan predecir períodos de alto riesgo de dispersión de este patógeno, pero deben validarse antes de su uso [66]. Estos modelos serían ventajosos para evitar la poda si hay alto riesgo de infección [18].

Se recomienda asimismo disminuir el tamaño de los cortes y dejar unos centímetros de madera de protección para mejorar el flujo de savia de la planta. Además, las herramientas de poda también son un medio de propagación de estos patógenos [67], por lo que se deben desinfectar con soluciones de hipoclorito sódico, alcohol o peróxido de hidrógeno antes del uso entre plantas.

Finalmente, es interesante la protección de las heridas de poda con pinturas, masillas y pastas, que son los protectores de heridas más fiables, especialmente cuando se complementan con

fungicidas o formulaciones a base de agentes de control biológico [14,68-71], creando así una barrera física que impide la entrada de esporas del patógeno en las heridas.

En España, los productos de protección de heridas de poda autorizados incluyen al menos tres basados en un agente de control biológico con antagonistas del género *Trichoderma* y uno basado en materias activas fungicidas: Esquive® (*Trichoderma atroviride* P. Karst. 1892 cepa I-1237), Vintec® (*T. atroviride* cepa SC1), Blindar® (*Trichoderma asperellum* Samuels, Lieckf. & Nirenberg cepa ICC012 + *Trichoderma gamsii* Samuels & Druzhin. cepa ICC080) y Tessior® (polímero líquido, piraclostrobin 0,5% y boscalid 1%) [18]. Sin embargo, el mayor inconveniente de la pintura y la pasta es que su aplicación debe realizarse manualmente, lo que encarece de dos a cuatro veces el coste de la aplicación con un pulverizador [72]. Por este motivo, se buscan productos líquidos de recubrimiento de heridas susceptibles de aplicación con pulverizador.

1.3.2.3. Renovación del tronco y saneamiento del cultivo

La renovación del tronco o brazos se realiza a través de los chupones sanos de la base de la planta, eliminando y cauterizando la madera dañada por el hongo [10]. Se recomienda cortar toda la madera infectada, junto con 20 centímetros adicionales como margen de seguridad, para asegurar una eliminación del patógeno más completa [14,73]. Esta técnica es costosa, pero es rentable si se compara con el coste de replantar un viñedo [14,72]. Además, se recomienda destruir la madera enferma de los restos de poda, aumentando la eficacia de esta medida si se aplica en toda la zona productora de uva [14].

1.3.3. Control biológico

Los agentes de control biológico (BCA por sus siglas en inglés, *BioControl Agents*) constituyen una estrategia preventiva eficaz y medioambientalmente sostenible frente a las enfermedades de la madera de la vid, pero en campo aún no han alcanzado resultados consistentes.

Las especies del género *Trichoderma* se encuentran entre los microorganismos más utilizados en gestión de plagas y son habitualmente empleadas en numerosos preparados comerciales. La mayoría de miembros de *Trichoderma* poseen varios mecanismos y estrategias autoecológicas de interés para el control de enfermedades, como su comportamiento hiperparasitario activo, la producción de enzimas líticas, sustancias antimicrobianas y otros metabolitos secundarios con acción germicida [74]. Además, promueven el crecimiento de la planta [75] y las enzimas que producen provocan la liberación de oligosacáridos de bajo peso molecular que inducen resistencia [76]. Diferentes especies de *Trichoderma* han sido evaluadas contra patógenos de la madera de la vid como *Eutypa lata*, *Phaeoconiella chlamydospora*, *Phaeacremonium* spp., *Phomopsis viticola*, y diferentes especies de la familia *Botryosphaeriaceae* [76-79]. Por ejemplo, *Trichoderma atroviride* resultó eficaz al disminuir la infección por hongos asociados a la enfermedad de Petri durante la fase de hidratación en vivero [74]. Se ha observado que varias cepas de *Trichoderma atroviride* y *T. harzianum* Rifai reducen las infecciones de *Botryosphaeriaceae* (como *Neofusicoccum parvum* y *Diplodia seriata* De Not.) [75,80-84], aunque con resultados variables en términos de eficacia.

La mayoría de los productos basados en cepas de diversas especies de *Trichoderma* se aplican mediante pulverización para la protección de heridas poco después de la poda, en el momento de la parada vegetativa de la vid y el sangrado. El mayor obstáculo para la extensión y adopción masiva de este tipo de tratamientos ha sido su eficacia variable en condiciones de campo, atribuible a diversos factores, como la edad del viñedo, la variedad, el estado fenológico en el que se realiza el tratamiento, el modo de aplicación, el intervalo de tiempo entre la poda y el tratamiento, las condiciones climáticas y ambientales durante y después de la aplicación, el nivel de incidencia de las EMV en el viñedo tratado o el origen geográfico y el huésped de procedencia de la cepa fúngica utilizada [85]. Se ha tratado de mejorar la eficacia de *Trichoderma* mediante su

encapsulación, pudiendo aumentar así su viabilidad hasta alcanzar los 14 meses [86]. En particular, al encapsular *Trichoderma reesei* E.G. Simmons IBWF 034-05 en nanocapsulas de lignina y entrar éstas en contacto con la yesca, el patógeno degrada la lignina y libera las esporas de *Trichoderma*, logrando un tratamiento de tipo curativo [87].

Por otra parte, los hongos micorrícicos arbusculares (MA) aumentan el crecimiento y la nutrición de la vid, y la protegen de estreses bióticos (activando la respuesta defensiva frente a patologías radiculares) y abióticos (sequía, asfixia radicular, salinidad, y clorosis férrica) [88]. Por ejemplo, en presencia del hongo MA *Glomus intraradices* N.C.Schenck & G.S.Sm., la vid desarrolla menos síntomas de la enfermedad de pie negro causada por *Cylindrocarpon macrodidymum* Schroers, Halleen & Crous en hojas y raíces en comparación con plantas sin micorrizar, tanto en vivero como en viñedo [89]. También se ha demostrado que otras dos especies de hongos MA, *Acaulospora laevis* Gerd. & Trappe y *Funneliformis mosseae* (T.H.Nicolson & Gerd.) Gerd. & Trappe aumentan la tolerancia de los portainjertos de vid a la enfermedad del pie negro causada por *Ilyonectria* spp. [90]. Por el contrario, el artículo de Holland *et al.* [91] pone en duda la aplicabilidad general de los hongos micorrícicos como protectores contra patógenos de las raíces, al constatar que la colonización por estos hongos no suprimió la presencia de *Ilyonectria*.

También se ha sugerido que otras especies de ascomicetos mitosporicos como *Cladosporium herbarum* (Pers.) Link y *Fusarium lateritium* Nees pueden proporcionar un buen control de *E. lata* en vid [92-95].

Respecto al uso de bacterias, las especies de *Bacillus* producen y secretan moléculas beneficiosas (precursores de fitohormonas, sideróforos, y lipopolisacáridos) que inducen o provocan las defensas de las plantas frente a patógenos [83]. Por ejemplo, se ha reportado que *Bacillus subtilis* (Ehrenberg 1835) Cohn 1872 reduce las infecciones por especies de *Botryosphaeriaceae* [80,83,96]. Las sustancias antagónicas producidas por *Bacillus subtilis* AG1 también redujeron el crecimiento de *Phaeoconiella chlamydospora* y *Phaeoacremonium minimum*, además de mostrar actividad antifúngica contra *Verticillium dahliae* Kleb. y *Botryosphaeria rhodina* (Berk. and Curtis) Arx en ensayos *in vitro* [97].

Otra de las bacterias filamentosas (actinomicetos) más ensayadas es *Streptomyces* spp., que disminuye significativamente la infección por pie negro (*Dactylonectria* sp. y *Ilyonectria* sp.) y por enfermedad de Petri (*P. chlamydospora* y *P. minimum*) en planta injerto en vivero [98].

Pythium oligandrum Drechsler, que coloniza naturalmente las raíces de la vid, estimula las defensas de las plantas y reduce significativamente las necrosis de la madera causadas por *Phaeoconiella chlamydospora*. Este oomiceto puede interactuar directamente con los patógenos (mediante micoparasitismo, antibiosis, o competencia por nutrientes) o indirectamente (a través de la estimulación de las defensas de las plantas) [99,100].

Sin embargo, la mayoría de los agentes de biocontrol comercializados en la actualidad, no son nativos de las plantas de vid, y los productos disponibles se desarrollaron para controlar diferentes patógenos en cultivos distintos a la vid. En el artículo de Pollard-Flamand *et al.* [75] se sugiere que la adopción de un producto de biocontrol procedente de otro clima o ecosistema puede dar problemas porque la eficacia de las formulaciones basadas en BCAs puede variar entre ensayos *in vitro* e *in vivo* realizados en diferentes hospedadores y bajo diferentes condiciones ambientales. Esto ha conducido a que, en la actualidad, exista un mayor interés en el denominado Control Biológico de Conservación [101], evaluando el potencial de BCAs endofíticos aislados localmente contra los patógenos de las EMV, debido a que podrían estar mejor adaptados al interior de las plantas-huésped a proteger. Además, se ha señalado que es esencial complementar el uso de BCAs con buenas prácticas de manejo en el viñedo (métodos de poda menos invasivos, restricción y eliminación de fuentes potenciales de inóculo, buen equilibrio nutricional de la vid, etc.).

1.3.4. *Productos naturales con capacidad antifúngica*

Los extractos naturales con capacidad antifúngica son una alternativa interesante y respetuosa con el medio ambiente para el manejo y control de los hongos asociados a las EMV.

Por otra parte, el quitosano, un polisacárido natural, promueve el crecimiento de las plantas, y activa mecanismos de defensa en los tejidos vegetales [102-104], mejorando su resistencia contra estreses bióticos y abióticos. Se usa ampliamente como agente antimicrobiano por su biodegradabilidad, no toxicidad y propiedades antimicrobianas [105].

El quitosano ha sido estudiado *in vitro* e *in vivo* para el control de *Botryosphaeria* sp., *Phomopsis* sp., *Eutypa lata* sp., *Neonectria liriodendri* Halleen, Rego & Crous, *Phaeomoniella chlamydospora* y *Fomitiporia* sp. en vid, observándose su eficacia en términos de reducción del crecimiento micelial. Además, se apreció una mejora significativa del crecimiento de las plantas (tanto en altura como en número de raíces) y una disminución de la incidencia de enfermedades en comparación con las plantas no tratadas [103]. Otro estudio demostró *in vitro* que los oligosacáridos de quitosano en combinación con vainillina y extracto de ajo tenían una alta eficacia de inhibición del crecimiento de *Diplodia seriata* y *Phaeomoniella chlamydospora*. En ensayos de campo, se observó una disminución significativa de la mortalidad de las plantas tratadas en comparación con las no tratadas en heridas de poda [106]. Por otra parte, también se han ensayado nanopartículas de oleoil-quitosano, observándose una reducción del crecimiento del micelio de *Botryosphaeria dothidea* (Moug. ex Fr.) Ces. & De Not. [107]. Asimismo, se han probado *in vitro* compuestos de oligómeros de quitosano/propóleo/nanopartículas de plata contra *Diplodia seriata* [108] y de complejos conjugados de ϵ -polilisina con oligómeros de quitosano, mostrando actividad antifúngica frente a *Neofusicoccum parvum*, *Diplodia seriata*, y *Botryosphaeria dothidea* [109].

Junto al mencionado quitosano, se han estudiado otras sustancias naturales como método de control de agentes responsables de EMV en vid. Por ejemplo, una mezcla de cloruro de calcio, nitrato de magnesio y extracto de algas marinas (*Fucales*, *Phaeophyceae*) fue ensayada frente a plantas con yesca, reduciendo significativamente los síntomas foliares en las vides [110]. Otras, como el extracto de ajo y la lactoferrina, disminuyeron significativamente la infección de *Eutypa lata* en heridas de poda [111]. Finalmente, se ha demostrado que el aceite esencial de limón ejerce actividad antifúngica e inhibe el crecimiento *in vitro* de *Eutypa* sp., *Botryosphaeria dothidea*, y *Fomitiporia mediterranea* [112].

1.3.5. *Estudio de la microbiota mediante secuenciación masiva*

Las metodologías microbiológicas clásicas utilizadas para caracterizar las comunidades microbianas en los diferentes agroecosistemas presentan limitaciones, al reflejar sólo la diversidad microbiana cultivable, que suele representar una ínfima fracción del total de diversidad microbiana existente [113]. En respuesta a este inconveniente, durante la última década, la secuenciación de alto rendimiento ha cobrado gran importancia, al ofrecer una representación completa de la diversidad microbiana [114].

Actualmente, un nuevo enfoque considera que las plantas y sus microorganismos forman una unidad ecológica, llamado "holobionte" [115]. Así, la vid y sus comunidades microbianas forman un supraorganismo cuyo correcto funcionamiento y adaptabilidad y resiliencia frente a estreses abióticos y bióticos depende de las interacciones planta-microorganismo establecidas a lo largo de la vida de la planta [116].

El uso de técnicas de secuenciación de alto rendimiento ha permitido la caracterización de las comunidades microbianas asociadas al cultivo de la vid. Ciertas investigaciones se han enfocado en las relaciones entre el microbioma de la planta y su sanidad vegetal [116], o entre el microbioma y las prácticas de manejo del viñedo [117]. Otros estudios han comparado los microbiomas asociados a cultivos de diferentes edades [118], genotipos vegetales, estadios

fenológicos [119], o tejidos vegetales [120,121]. Los estudios metagenómicos de la diversidad microbiana asociada permiten también identificar especies fúngicas y bacterianas con potencial prometedor para el control biológico de patógenos asociados a las EMV [122,123].

1.3.6. Resistencias naturales

El reconocimiento y explotación de las fuentes de resistencia natural a las EMV puede ser una estrategia clave para disminuir el uso de fungicidas y los costes vinculados a la gestión de las enfermedades en los viñedos, al representar un enfoque ambientalmente respetuoso de control y manejo. No obstante, hasta la fecha no se han encontrado variedades de *Vitis* totalmente resistentes a los patógenos de la madera [71].

La información disponible sobre el grado de tolerancia/resistencia de las diferentes variedades y/o portainjertos más comúnmente utilizados es limitada [26]. Por ejemplo, se ha comprobado que el portainjerto '*Riparai Glorie*' es susceptible a la enfermedad del pie negro, mientras que el portainjerto 101-14 MGt presenta mayor tolerancia a esta enfermedad. Además, las variedades '*Garnacha tinta*', '*Cabernet Sauvignon*' y '*Syrah*' muestran una mayor incidencia de eutipiosis, mientras que '*Merlot*', '*Riesling*', '*Pinot noir*', '*Sauvignon blanc*', '*Chardonnay*', y '*Semillon*' son más tolerantes a la infección por *Eutypa lata*. Otros estudios también apuntan a que '*Merlot*', '*Malbec*', '*Petit verdot*', '*Pinot noir*', '*Chardonnay*', y '*Riesling*' mostrarían cierto grado de tolerancia frente a diversas enfermedades de la madera de la vid [29,124,125]. No obstante, las variedades blancas '*Sauvignon blanc*' y '*Riesling*' son más propensas a desarrollar síntomas foliares asociados a la yesca, mientras que la variedad '*Pinot blanc*' presenta menos síntomas. De entre las variedades tintas, '*Rebo*' es más susceptible, mientras que '*Syrah*' y '*Merlot*' presentan menos síntomas foliares asociados a este síndrome. A nivel de portainjertos, se ha reportado que las variedades injertadas sobre SO4 presentan una mayor incidencia de síntomas asociados a la yesca que las injertadas sobre 1103 P [26].

En cuanto a la tolerancia frente a las especies de *Botryosphaeriaceae*, hasta la fecha se han identificado algunas variedades y portainjertos más tolerantes a estos patógenos [28,29,124-130]. Por ejemplo, se ha demostrado que las variedades '*Bobal*', '*Monastrell*', '*Macabeo*', '*Moscatel serrano*', '*Caíño Longo*', '*Caíño Tinto*', '*Torrontés*', '*Treixadura*', y '*Dona Branca*' son más resistentes a *Neofusicoccum parvum* que otras variedades [18,28]. Según Sosnowski *et al.* [125], '*Traminer*', '*Sangiovese*', y '*Grüner Veltliner*' estarían entre las menos susceptibles a la colonización por *Diplodia seriata*.

1.4. Objetivos de la Tesis Doctoral

1.4.1. Hipótesis de trabajo

La Tesis Doctoral ha sido diseñada para abordar el reto de reducir la incidencia y severidad de las EMV en nuevas plantaciones de las diferentes zonas vitivinícolas de Aragón y en planta procedente de vivero. Esto solo puede conseguirse mediante estrategias de manejo integrado innovadoras y respetuosas con el medio ambiente, basadas en la selección de variedades y portainjertos con ciertos niveles de tolerancia, el conocimiento preciso del estado fitosanitario y la aptitud microbiológica de la planta, el uso de agentes de biocontrol o la aplicación de preparados antifúngicos novedosos a partir de productos naturales. Tal proposición constituye la hipótesis de partida de la Tesis Doctoral.

1.4.2. *Objetivos generales*

Esta Tesis Doctoral tiene como objetivos generales la mejora de la calidad sanitaria de las vides producidas en el vivero mediante el empleo de estrategias de manejo integrado, y la reducción en campo de las infecciones de las heridas de poda en el viñedo desde el momento de la plantación mediante la aplicación de productos alternativos.

1.4.3. *Objetivos específicos*

Los objetivos globales serán abordados mediante los siguientes de objetivos específicos:

- **Objetivo específico 1 (OE1).** Evidenciar la eficacia de tratamientos con productos alternativos de origen natural frente a determinadas patologías, incluyendo antagonistas microbianos y productos naturales.
- **Objetivo específico 2 (OE2).** Identificar y explotar las resistencias naturales en las distintas variedades empleadas en las Denominaciones Geográficas de calidad aragonesas mediante el reconocimiento de diferencias de comportamiento (susceptibilidad/tolerancia) en el germoplasma de variedades comerciales, locales, minoritarias, etc.
- **Objetivo específico (OE3).** Caracterizar, mediante técnicas de secuenciación masiva, la microbiota endosférica asociada a variedades de interés y su interacción con las EMV bajo condiciones de estrés biótico con el propósito de dilucidar el papel del microbioma asociado a la planta de vid en el comportamiento de ésta frente a dichos estreses.

1.5. Justificación de la unidad temática de los artículos

La Tesis Doctoral se compone de once artículos científicos, recogidos en la sección 2 de esta memoria.

La primera parte de la Tesis engloba los artículos del 1 al 9, teniendo en común la evaluación de la eficacia de nuevos materiales compuestos basados en productos naturales para el control de las EMV (OE1), con énfasis en patógenos como *Neofusicoccum parvum* y *Diplodia seriata*, pero abordando también su eficacia frente otros hongos como *Botryosphaeria dothidea*, *Rhizoctonia solani*, *Dothiorella iberica* A.J.L. Phillips, J. Luque & A. Alves, *Diplodia coryli* Fuckel, *Dothiorella sarmentorum* (Fr.) A.J.L. Phillips, Alves & Luque, *Dothiorella viticola* A.J.L. Phillips & J. Luque, y *Diplodia mutila*, además de dos bacterias patógenas de vid, *Xylophilus ampelinus* (Panagopoulos 1969) Willems et al. 1987 y *Pseudomonas syringae* van Hall 1902.

Orientados por los resultados obtenidos con los primeros materiales ensayados, basados en oligómeros de quitosano, COS (complejos COS–aminoácidos y COS–extractos de cola de caballo (*Equisetum arvense* L.), ortiga (*Urtica dioica* L.) y rubia (*Rubia tinctorum* L.); artículos #1, #2, #5) y en esteviósido (complejos esteviósido–extracto de cardo mariano (*Silybum marianum* (L.) Gaertn.) y esteviósido–rutina; artículos #3 y #4)), se continuó con el abordaje del diseño de nanotransportadores basados en COS para encapsular los extractos de las cuatro plantas mencionadas (artículo #6), y finalmente al desarrollo de un nanotransportador multifuncional para el encapsulado del producto que se mostró más activo, el extracto de *R. tinctorum* (artículo #7).

Alternativamente, se examinó la actividad de aislados de *Trichoderma harzianum* endofíticos nativos de vid (conforme a los principios del Control Biológico de Conservación) frente a *N. parvum* y *R. solani* (artículo #8). El más prometedor fue seleccionado para ensayos adicionales frente a *N. parvum* y *D. seriata*, comparando su eficacia con la de formulados comerciales de los

géneros *Bacillus* y *Trichoderma* y con la de una cepa de *Bacillus velezensis* Ruiz-Garcia et al. 2005 endofítica (artículo #9).

El desarrollo de las investigaciones se ha culminado con un análisis de resistencia de cultivares procedentes del Banco de Germoplasma de la Vid de Aragón (EO2, artículo #10) y un obligado estudio comparativo de las comunidades microbianas fúngicas asociadas a las plantas de vid en dos viñedos de diferentes edades y variedades, situados en la misma unidad biogeográfica de la D.O.P. Somontano, empleando tanto secuenciación de alto rendimiento como métodos microbiológicos clásicos (OE3, artículo #11).

1.6. Metodología general

En este estudio, la metodología empleada en los artículos publicados para la consecución de los anteriores objetivos fue la siguiente:

En relación con el OE1, se han realizado ensayos *in vitro*, *ex situ*, e *in vivo* utilizando los productos naturales previamente mencionados (aminoácidos, un glucósido flavonoide, o extractos de plantas en medio hidrometanólico). Con el fin de mejorar la solubilidad y biodisponibilidad, se combinaron con COS (artículos #1, #2, #5) o con glicósidos de esteviol (#3, #4 y #5), empleando técnicas de Química Verde como la ultrasonicación para la formación de complejos conjugados. Para facilitar su aplicación y lograr una liberación controlada, se recurrió a la encapsulación en nanotransportadores (*nanocarriers*) con capacidad de responder a estímulos externos (en este caso, al secretoma ligninolítico de los hongos responsables de las EMV). La síntesis de dichos nanotransportadores se realizó empleando agentes de entrecruzamiento para el ensamblaje de las distintas especies químicas (COS–lignina o COS–nitruro de carbono) y ultrasonicación.

Para determinar la capacidad antifúngica de los tratamientos, en los ensayos *in vitro* se ha evaluado la inhibición del crecimiento micelial mediante el método de dilución de agar (“*poisoned food method*”), de acuerdo con los procedimientos estándar de prueba de susceptibilidad antifúngica de EUCAST [131]. En el caso del artículo #7, en el que también se analizó la actividad antibacteriana, se utilizó el método de dilución de agar según el estándar CLSI M07-11 [132].

En los ensayos *ex situ* se han empleado estaquillas (artículo #5), mientras que en los ensayos *in vivo* se han utilizado generalmente plantas-injerto de 2–3 años. En cuanto a las variedades empleadas, se ha optado por emplear las más representativas de las diferentes D.O.P e I.G.P. aragonesas (*‘Tempranillo’*, *‘Garnacha’* y *‘Cabernet Sauvignon’*). Se han realizado diferentes tipos de inoculaciones según el producto y el patógeno en material vegetal de sanidad comprobada, cultivado en un sistema de sustrato o turba estéril en invernadero aproximadamente durante seis meses en el caso de los ensayos *in vivo*. La idoneidad de los tratamientos se ha evaluado mediante parámetros como longitud de las lesiones y necrosis vascular (traqueomicosis), comparando con plantas sanas e infectadas y no tratadas. La identificación de los aislados fúngicos (para satisfacer los postulados de Koch) se ha llevado a cabo con técnicas morfológicas, o mediante la amplificación por PCR convencional de fragmentos de genes específicos o, más generalmente, de la región ITS del ADN ribosomal. Uno de los tratamientos más prometedores se ha ensayado en campo, en parcelas de las bodegas de la D.O.P. Somontano, utilizando la técnica de endoterapia, inyectando el tratamiento en un brazo de la cepa y empleando el otro brazo como control (artículo #6).

En el caso de los agentes de biocontrol, para la evaluación del potencial de cepas del género *Trichoderma* como antagonistas microbianos frente a *N. parvum* y *R. solani* (artículo #8), se ha trabajado tanto *in vitro* (con enfrentamientos en placa) como *in vivo*, empleando tanto plantas injerto como plántulas obtenidas a partir de semilla, con inoculación simultánea o sucesiva de los

patógenos y antagonistas. La eficacia de los tratamientos se ha determinado tanto en términos de presencia y longitud de necrosis como en base al peso fresco y seco de biomasa, o el desarrollo radical y de la parte aérea de las plantas. En la posterior comparativa de eficacia de la cepa más prometedora (MYC-V102) con *Bacillus velezensis* (BUZ-14) y con los productos comerciales Trianium-P® (*T. harzianum*), Esquive® (*T. atroviride*), y Fungisei® (*B. subtilis*), se optó por evaluar la capacidad de protección de heridas de poda en plantas injerto frente a *N. parvum* y *D. seriata*, determinada a partir de las necrosis producidas.

Respecto al OE2, se han buscado fuentes de resistencia natural en 25 variedades del Banco de Germoplasma de Vid de Aragón (Movera, Zaragoza), tanto locales como comerciales, frente a dos de las especies fúngicas asociadas al decaimiento de la vid por *Botryosphaeriaceae* (*N. parvum* y *D. seriata*), inoculadas artificialmente en estaquillas enraizadas, plantadas en un campo de ensayo. Ocho meses tras la inoculación, se ha realizado la evaluación a partir de las necrosis, de forma análoga a la descrita para los ensayos *in vivo* del OE1.

En cuanto al OE3, el estudio se ha realizado en dos viñedos que pertenecen a la D.O.P. Somontano con el mismo régimen bioclimático que se diferencian principalmente en la combinación patrón/variedad empleada y el año de establecimiento de la plantación. Se han recogido muestras de plantas seleccionadas que presentaban síntomas asociados a las EMV para realizar el aislamiento de los hongos endófitos presentes mediante métodos microbiológicos clásicos y técnicas de secuenciación de alto rendimiento. Se ha realizado un análisis de alfa y beta diversidad de comunidades microbianas para detectar las diferencias en la estructura y composición taxonómica de las poblaciones.

1.7. Referencias

1. OIV. *State of the world vine and wine sector 2021*; OIV Publications: 2022.
2. OIV. *World Wine Production Outlook*; OIV Publications: 2022.
3. MAPA. *Encuesta sobre superficies y rendimientos de cultivos. Resultados provisionales nacionales y autonómicos. 2022*; Ministerio de Agricultura, Pesca y Alimentación: 2022.
4. MAPA. *Superficies y producciones anuales de cultivo de acuerdo con el Reglamento (CE) 543/2009. Avance de datos del Viñedo, 2021.*; Ministerio de Agricultura, Pesca y Alimentación: 2021.
5. Gobierno de Aragón. *Avance de macromagnitudes del sector agrario aragonés 2021*; Gobierno de Aragón. Departamento de Agricultura, Ganadería y Medio Ambiente: Zaragoza, Spain, 2022; pp. 56.
6. Mondello, V.; Songy, A.; Battison, E.; Pinto, C.; Coppin, C.; Trozel-Aziz, P.; Clement, C.; Mugnai, L.; Fontaine, F. Grapevine trunk diseases: A review of fifteen years of trials for their control with chemicals and biocontrol agents. *Plant Dis.* **2018**, *102*, 1189-1217, doi:10.1094/pdis-08-17-1181-fe.
7. Moretti, S.; Pacetti, A.; Pierron, R.; Kassemeyer, H.H.; Fischer, M.; Peros, J.P.; Perez-Gonzalez, G.; Bieler, E.; Schilling, M.; Di Marco, S.; Gelhaye, E.; Mugnai, L.; Bertsch, C.; Farine, S. *Fomitiporia mediterranea* M. Fisch., the historical Esca agent: a comprehensive review on the main grapevine wood rot agent in Europe. *Phytopathol. Mediterr.* **2021**, *60*, 351-379, doi:10.36253/phyto-13021.
8. Rezgui, A.; Vallance, J.; Ben Ghnaya-Chakroun, A.; Bruez, E.; Dridi, M.; Demasse, R.D.; Rey, P.; Sadfi-Zouaoui, N. Study of *Lasiodiplodia pseudotheobromae*, *Neofusicoccum parvum* and *Schizophyllum commune*, three pathogenic fungi associated with the grapevine trunk diseases in the North of Tunisia. *Eur. J. Plant Pathol.* **2018**, *152*, 127-142, doi:10.1007/s10658-018-1458-z.
9. Larignon, P.; Fontaine, F.; Farine, S.; Clement, C.; Bertsch, C. Esca and Black Dead Arm: two major actors of grapevine trunk diseases. *C. R. Biol.* **2009**, *332*, 765-783.

10. Fontaine, F.; Gramaje, D.; Armengol, J.; Smart, R.; Nagy, Z.A.; Borgo, M.; Rego, C.; Corio-Costet, M.-F. Grapevine trunk diseases: A review. OIV publications: 2016; p 25.
11. Azevedo-Nogueira, F.; Rego, C.; Gonçalves, H.M.R.; Fortes, A.M.; Gramaje, D.; Martins-Lopes, P. The road to molecular identification and detection of fungal grapevine trunk diseases. *Front. Plant Sci.* **2022**, *13*, 960289, doi:10.3389/fpls.2022.960289.
12. Hofstetter, V.; Buyck, B.; Croll, D.; Viret, O.; Couloux, A.; Gindro, K. What if Esca disease of grapevine were not a fungal disease? *Fungal Divers.* **2012**, *54*, 51-67, doi:10.1007/s13225-12-0171-z.
13. Martínez-Diz, M.D.; Díaz-Losada, E.; Barajas, E.; Ruano-Rosa, D.; Andrés-Sodupe, M.; Gramaje, D. Screening of Spanish *Vitis vinifera* germplasm for resistance to *Phaeomoniella chlamydospora*. *Sci. Hortic.* **2019**, *246*, 104-109, doi:10.1016/j.scienta.2018.10.049.
14. Gramaje, D.; Urbez-Torres, J.R.; Sosnowski, M.R. Managing grapevine trunk diseases with respect to etiology and epidemiology: Current strategies and future prospects. *Plant Dis.* **2018**, *102*, 12-39, doi:10.1094/PDIS-04-17-0512-FE.
15. Gramaje, D.; Armengol, J. Fungal trunk pathogens in the grapevine propagation process: Potential inoculum sources, detection, identification, and management strategies. *Plant Dis.* **2011**, *95*, 1040-1055, doi:10.1094/pdis-01-11-0025.
16. Úrbez-Torres, J.R.; Gubler, W.D. Susceptibility of grapevine pruning wounds to infection by *Lasiodiplodia theobromae* and *Neofusicoccum parvum*. *Plant Pathol.* **2011**, *60*, 261-270, doi:10.1111/j.1365-3059.2010.02381.x.
17. Carlos, A.-B.; Josep, A. Black-foot disease of grapevine: an update on taxonomy, epidemiology and management strategies. *Phytopathol. Mediterr.* **2013**, *52*, 245-261, doi:10.14601/Phytopathol_Mediterr-12662.
18. Gramaje, D.; Armengol, J.; Barajas, E.; Berbegal, M.; Chacón, J.L.; Cibrián Sabalza, J.F.; Díaz-Losada, E.; López-Manzanares, B.; Muñoz Gómez, R.; Martínez-Diz, M. *Guía sobre las enfermedades fúngicas de la madera de la vid*; Ministerio de Agricultura, Pesca y Alimentación: Madrid, Spain, 2020.
19. Lombard, L.; van der Merwe, N.; Groenewald, J.Z.; Crous, P. Lineages in *Nectriaceae*: Re-evaluating the generic status of *Ilyonectria* and allied genera. *Phytopathol. Mediterr.* **2014**, *53*, 340-357, doi:10.14601/Phytopathol_Mediterr-14976.
20. Aigoun-Mouhous, W.; Elena, G.; Cabral, A.; León, M.; Sabaou, N.; Armengol, J.; Chaouia, C.; Mahamedi, A.E.; Berraf-Tebbal, A. Characterization and pathogenicity of *Cylindrocarpon*-like asexual morphs associated with black foot disease in Algerian grapevine nurseries, with the description of *Pleioicarpum algeriense* sp. nov. *Eur. J. Plant Pathol.* **2019**, *154*, 887-901.
21. Lawrence, D.; Nouri, M.; Trouillas, F. Taxonomy and multi-locus phylogeny of *Cylindrocarpon*-like species associated with diseased roots of grapevine and other fruit and nut crops in California. *Fungal Syst. Evol.* **2019**, *4*, 59-75.
22. Berlanas, C.; Ojeda, S.; López-Manzanares, B.; Andrés-Sodupe, M.; Bujanda, R.; del Pilar Martínez-Diz, M.; Díaz-Losada, E.; Gramaje, D. Occurrence and diversity of black-foot disease fungi in symptomless grapevine nursery stock in Spain. *Plant Dis.* **2020**, *104*, 94-104.
23. González, V. Las enfermedades de la madera de vid: principales síndromes, estado actual de su conocimiento y perspectivas sobre su manejo y control. *Tierras de Castilla y León: Agricultura* **2012**, *192*, 74-82.
24. Muntean, M.D.; Dragulinescu, A.M.; Tomoiaga, L.L.; Comsa, M.; Racoare, H.S.; Sirbu, A.D.; Chedea, V.S. Fungal grapevine trunk diseases in romanian vineyards in the context of the international situation. *Pathogens* **2022**, *11*, 43, doi:10.3390/pathogens11091006.
25. Berlanas, C.; López-Manzanares, B.; Gramaje, D. Estimation of viable propagules of black-foot disease pathogens in grapevine cultivated soils and their relation to production systems and soil properties. *Plant Soil* **2017**, *417*, 467-479.
26. Maldonado-González, M.M.; Andrés Sodupe, M.; Berlanas Vicente, C.; Bujanda Muñoz, R.; Gramaje, D.; Martínez Diz, M.d.P.; Díaz Losada, E. Enfermedades fúngicas de la madera de

- la vid: líneas de investigación actuales y últimos avances para su control. *Cuaderno de campo* **2018**, 28-35.
27. Larignon, P. *Maladies cryptogamiques du bois de la vigne: symptomatologie et agents pathogènes*, 2 ed.; <http://www.vignevin.com>: 2012.
 28. Chacón, J.L.; Gramaje, D.; Izquierdo, P.M.; Martínez, J.; Mena, A. Evaluation of six red grapevine cultivars inoculated with *Neofusicoccum parvum*. *Eur. J. Plant Pathol.* **2020**, *158*, 811-815, doi:10.1007/s10658-020-02111-9.
 29. Chacon-Vozmediano, J.L.; Gramaje, D.; Leon, M.; Armengol, J.; Moral, J.; Izquierdo-Canas, P.M.; Martinez-Gascuena, J. Cultivar susceptibility to natural infections caused by fungal grapevine trunk pathogens in La Mancha Designation of Origin (Spain). *Plants-Basel* **2021**, *10*, 1171, doi:10.3390/plants10061171.
 30. Billones-Baaijens, R.; Savocchia, S. A review of *Botryosphaeriaceae* species associated with grapevine trunk diseases in Australia and New Zealand. *Australas. Plant Pathol.* **2019**, *48*, 3-18, doi:10.1007/s13313-018-0585-5.
 31. Laveau, C.; Letouze, A.; Louvet, G.; Bastien, S.; Guerin-Dubrana, L. Differential aggressiveness of fungi implicated in esca and associated diseases of grapevine in France. *Phytopathol. Mediterr.* **2009**, *48*, 32-46.
 32. Úrbez-Torres, J.; Leavitt, G.; Voegel, T.; Gubler, W. Identification and distribution of *Botryosphaeria* spp. associated with grapevine cankers in California. *Plant Dis.* **2006**, *90*, 1490-1503.
 33. Urbez-Torres, J.R. The status of *Botryosphaeriaceae* species infecting grapevines. *Phytopathol. Mediterr.* **2011**, *50*, S5-S45.
 34. Walker, G.E. Root rot of grapevine rootlings in South Australia caused by *Rhizoctonia solani*. *Australas. Plant Pathol.* **1992**, *21*, 58-60, doi:10.1071/APP9920058.
 35. Marais, P. Fungi associated with root rot in vineyards in the Western Cape. *Phytophylactica* **1979**, *11*, 65-68.
 36. Van Coller, G.J. An investigation of soilborne fungi associated with roots and crowns of nursery grapevines. Stellenbosch University, Stellenbosch, 2004.
 37. Nita, M.; Ellis, M.A.; Madden, L.V. Variation in disease incidence of phomopsis cane and leaf spot of grape in commercial vineyards in Ohio. *Plant Dis.* **2008**, *92*, 1053-1061, doi:10.1094/PDIS-92-7-1053.
 38. Hrycan, J.; Hart, M.; Bowen, P.; Forge, T.; Urbez-Torres, J.R. Grapevine trunk disease fungi: their roles as latent pathogens and stress factors that favour disease development and symptom expression. *Phytopathol. Mediterr.* **2020**, *59*, 395-424, doi:10.14601/Phyto-11275.
 39. Kenfaoui, J.; Radouane, N.; Mennani, M.; Tahiri, A.; El Ghadraoui, L.; Belabess, Z.; Fontaine, F.; El Hamss, H.; Amiri, S.; Lahlali, R.; Barka, E.A. A panoramic view on grapevine trunk diseases threats: Case of *Eutypa dieback*, *Botryosphaeria dieback*, and Esca disease. *J. Fungi* **2022**, *8*, 595, doi:10.3390/jof8060595.
 40. Barrios, G.; Coscolla, R.; Espadas, A.L.; Perez-de-Obanos, J.J.; Perez, J., L.; Toledo, J. *Los parásitos de la vid: estrategias de protección razonada*; Ministerio de Agricultura, Pesca y Alimentación: 2004.
 41. Letousey, P.; Baillieul, F.; Perrot, G.; Rabenoelina, F.; Boulay, M.; Vaillant-Gaveau, N.; Clément, C.; Fontaine, F. Early events prior to visual symptoms in the apoplectic form of grapevine Esca disease. *Phytopathology* **2010**, *100*, 424-431, doi:10.1094/phyto-100-5-0424.
 42. Lecomte, P.; Diarra, B.; Carbonneau, A.; Rey, P.; Chevrier, C. Esca of grapevine and training practices in France. *Phytopathol. Mediterr.* **2018**, *57*, 472-487.
 43. Marion, C.; Martin, N.; Florence, F.; Jacques, W. Current knowledge on grapevine trunk diseases with complex etiology: A systemic approach. *Phytopathol. Mediterr.* **2020**, *59*, 29-53, doi:10.14601/Phyto-11150.

44. Baranek, M.; Armengol, J.; Holleinová, V.; Pečenka, J.; Calzarano, F.; Peňázová, E.; Vachůn, M.; Eichmeier, A. Incidence of symptoms and fungal pathogens associated with grapevine trunk diseases in Czech vineyards. *Phytopathol. Mediterr.* **2018**, *57*, 449-458.
45. Trouillas, F.; Gubler, W. Pathogenicity of *Diatrypaceae* species in grapevines in California. *Plant Dis.* **2010**, *94*, 867-872.
46. Carter, M.V. *The status of Eutypa lata as a pathogen*; CAB International: 1991.
47. Crous, P.W.; Coertze, S.; Swart, L. The effect of hot-water treatment on fungi occurring in apparently healthy grapevine cuttings. *Phytopathol. Mediterr.* **2001**, *40*, 1000-1003.
48. Fourie, P.H.; Halleen, F. Proactive control of Petri disease of grapevine through treatment of propagation material. *Plant Dis.* **2004**, *88*, 1241-1245, doi:10.1094/PDIS.2004.88.11.1241.
49. May, P.; Waite, H. The effects of hot water treatment, hydration and order of nursery operations on cuttings of *Vitis vinifera* cultivars. *Phytopathol. Mediterr.* **2005**, *44*, 1000-1009.
50. Elena, G.; Di Bella, V.; Armengol, J.; Luque, J. Viability of *Botryosphaeriaceae* species pathogenic to grapevine after hot water treatment. *Phytopathol. Mediterr.* **2015**, *54*, 325-334.
51. Gramaje, D.; Alaniz, S.; Abad-Campos, P.; García-Jiménez, J.; Armengol, J. Effect of hot-water treatments in vitro on conidial germination and mycelial growth of grapevine trunk pathogens. *Ann. Appl. Biol.* **2010**, *156*, 231-241.
52. Gramaje, D.; Mañas, F.; Lerma, M.; Muñoz, R.; García-Jiménez, J.; Armengol, J. Effect of hot-water treatment on grapevine viability, yield components and composition of must. *Aust. J. Grape Wine Res.* **2014**, *20*, 144-148.
53. Bruez, E.; Larignon, P.; Compant, S.; Rey, P. Investigating the durable effect of the hot water treatment used in nurseries on pathogenic fungi inhabiting grapevine wood and involved in grapevine trunk diseases. *Crop Prot.* **2017**, *100*, 203-210, doi:10.1016/j.cropro.2017.07.001.
54. Di Marco, S.; Osti, F.; Bossio, D.; Nocentini, M.; Cinelli, T.; Calzarano, F.; Mugnai, L. Electrolyzed acid water: A clean technology active on fungal vascular pathogens in grapevine nurseries. *Crop Prot.* **2019**, *119*, 88-96, doi:10.1016/j.cropro.2019.01.005.
55. Pierron, R.J.G.; Pages, M.; Couderc, C.; Compant, S.; Jacques, A.; Violleau, F. *In vitro* and *in planta* fungicide properties of ozonated water against the esca-associated fungus *Phaeoacremonium aleophilum*. *Sci. Hortic.* **2015**, *189*, 184-191, doi:10.1016/j.scienta.2015.03.038.
56. Romeo-Olivan, A.; Pages, M.; Breton, C.; Lagarde, F.; Cros, H.; Yobregat, O.; Violleau, F.; Jacques, A. Ozone dissolved in water: An innovative tool for the production of young plants in grapevine nurseries? *Ozone: Sci. Eng.* **2021**, *44*, 521-535, doi:10.1080/01919512.2021.1984203.
57. Berlanas Vicente, C. New insights into the biology, ecology and control of black-foot disease in grapevine. Universidad de la Rioja, 2020.
58. Barbour, J.; Ridgway, H.J.; Jones, E.E. Influence of mustard biofumigation on growth, conidial germination and propagule recovery of *Ilyonectria macrodidyma*-complex species. *Phytopathol. Mediterr.* **2014**, *53*, 582.
59. Weckert, M.; Rahman, M.; Cappello, J.; Bartrop, K. Preliminary findings on the grapevine yield response to *Brassica* biofumigation soil. In Proceedings of 9th International Workshop on Grapevine Trunk Diseases, Adelaide, Australia; pp. 587-587.
60. Berlanas, C.; Andrés-Sodupe, M.; López-Manzanares, B.; Maldonado-González, M.M.; Gramaje, D. Effect of white mustard cover crop residue, soil chemical fumigation and *Trichoderma* spp. root treatment on black-foot disease control in grapevine. *Pest Manag. Sci.* **2018**, *74*, 2864-2873-2873, doi:10.1002/ps.5078.
61. Halleen, F.; Fourie, P.; Crous, P. Control of black foot disease in grapevine nurseries. *Plant Pathol.* **2007**, *56*, 637-645.

62. Díaz, G.A.; Latorre, B.A. Efficacy of paste and liquid fungicide formulations to protect pruning wounds against pathogens associated with grapevine trunk diseases in Chile. *Crop Prot.* **2013**, *46*, 106-112, doi:10.1016/j.cropro.2013.01.001.
63. Claverie, M.; Notaro, M.; Fontaine, F.; Wery, J. Current knowledge on grapevine trunk diseases with complex etiology: a systemic approach. *Phytopathol. Mediterr.* **2020**, *59*, 29-53, doi:10.36253/phyto-11150.
64. Elena, G.; Luque, J. Seasonal susceptibility of grapevine pruning wounds and cane colonization in Catalonia, Spain following artificial infection with *Diplodia seriata* and *Phaeoconiella chlamydospora*. *Plant Dis.* **2016**, *100*, 1651-1659.
65. Luque, J.; Elena, G.; Garcia-Figueres, F.; Reyes, J.; Barrios, G.; Legorburu, F. Natural infections of pruning wounds by fungal trunk pathogens in mature grapevines in Catalonia (Northeast Spain). *Aust. J. Grape Wine Res.* **2014**, *20*, 134-143.
66. González-Domínguez, E.; Berlanas, C.; Gramaje, D.; Armengol, J.; Rossi, V.; Berbegal, M. Temporal dispersal patterns of *Phaeoconiella chlamydospora*, causal agent of Petri disease and Esca, in vineyards. *Phytopathology* **2020**, *110*, 1216-1225, doi:10.1094/phyto-10-19-0400-r.
67. Agustí-Brisach, C.; León, M.; García-Jiménez, J.; Armengol, J. Detection of grapevine fungal trunk pathogens on pruning shears and evaluation of their potential for spread of infection. *Plant Dis.* **2015**, *99*, 976-981, doi:10.1094/pdis-12-14-1283-re.
68. Sosnowski, M.; Creaser, M.; Wicks, T.; Lardner, R.; Scott, E. Protection of grapevine pruning wounds from infection by *Eutypa lata*. *Aust. J. Grape Wine Res.* **2008**, *14*, 134-142.
69. Rolshausen, P.E.; Úrbez-Torres, J.R.; Rooney-Latham, S.; Eskalen, A.; Smith, R.J.; Gubler, W.D. Evaluation of pruning wound susceptibility and protection against fungi associated with grapevine trunk diseases. *Am. J. Enol. Vitic.* **2010**, *61*, 113-119.
70. Sosnowski, M.R.; Loschiavo, A.P.; Wicks, T.J.; Scott, E.S. Evaluating treatments and spray application for the protection of grapevine pruning wounds from infection by *Eutypa lata*. *Plant Dis.* **2013**, *97*, 1599-1604.
71. Bertsch, C.; Ramírez-Suero, M.; Magnin-Robert, M.; Larignon, P.; Chong, J.; Abou-Mansour, E.; Spagnolo, A.; Clément, C.; Fontaine, F. Grapevine trunk diseases: Complex and still poorly understood. *Plant Pathol.* **2013**, *62*, 243-265.
72. Sosnowski, M.; McCarthy, G. Economic impact of grapevine trunk disease management in Sauvignon Blanc vineyards of New Zealand. *Wine Vitic. J.* **2017**, *32*, 42.
73. Sosnowski, M.R.; Wicks, T.J.; Scott, E.S. Control of *Eutypa* dieback in grapevines using remedial surgery. *Phytopathol. Mediterr.* **2011**, *50*, S277-S284.
74. Pertot, I.; Prodorutti, D.; Colombini, A.; Pasini, L. *Trichoderma atroviride* SC1 prevents *Phaeoconiella chlamydospora* and *Phaeoacremonium aleophilum* infection of grapevine plants during the grafting process in nurseries. *BioControl* **2016**, *61*, 257-267, doi:10.1007/s10526-016-9723-6.
75. Pollard-Flamand, J.; Boule, J.; Hart, M.; Urbez-Torres, J.R. Biocontrol activity of *Trichoderma* species isolated from grapevines in British Columbia against *Botryosphaeria* dieback fungal pathogens. *J. Fungi* **2022**, *8*, 409, doi:10.3390/jof8040409.
76. Compant, S.; Mathieu, F. *Biocontrol of major grapevine diseases: leading research*; CABI International: Wallingford, UK, 2016; pp. 256.
77. Wallis, C.M. Nutritional niche overlap analysis as a method to identify potential biocontrol fungi against trunk pathogens. *Biocontrol* **2021**, *66*, 559-571, doi:10.1007/s10526-021-10091-w.
78. Silva-Valderrama, I.; Toapanta, D.; Miccono, M.d.l.A.; Lolas, M.; Díaz, G.A.; Cantu, D.; Castro, A. Biocontrol potential of grapevine endophytic and rhizospheric fungi against trunk pathogens. *Front. Microbiol.* **2021**, *11*, 614620.
79. Fourie, P.H.; Halleen, F.; van der Vyver, J.; Schreuder, W. Effect of *Trichoderma* treatments on the occurrence of decline pathogens in the roots and rootstocks of nursery grapevines. *Phytopathol. Mediterr.* **2001**, *40*, S473-S478.

80. Kotze, C.; Van Niekerk, J.; Mostert, L.; Halleen, F.; Fourie, P.H. Evaluation of biocontrol agents for grapevine pruning wound protection against trunk pathogen infection. *Phytopathol. Mediterr.* **2011**, *50*, S247-S263.
81. Urbez-Torres, J.R.; Tomaselli, E.; Pollard-Flamand, J.; Boule, J.; Gerin, D.; Pollastro, S. Characterization of *Trichoderma* isolates from southern Italy, and their potential biocontrol activity against grapevine trunk disease fungi. *Phytopathol. Mediterr.* **2020**, *59*, 425-439, doi:10.14601/Phyto-11273.
82. Blundell, R.; Eskalen, A. Biological and chemical pruning wound protectants reduce infection of grapevine trunk disease pathogens. *Calif. Agric.* **2021**, *75*, 128-134, doi:10.3733/ca.2021a0018.
83. Leal, C.; Richet, N.; Guise, J.F.; Gramaje, D.; Armengol, J.; Fontaine, F.; Trotel-Aziz, P. Cultivar contributes to the beneficial effects of *Bacillus subtilis* PTA-271 and *Trichoderma atroviride* SC1 to protect grapevine against *Neofusicoccum parvum*. *Front. Microbiol.* **2021**, *12*, 726132, doi:10.3389/fmicb.2021.726132.
84. Martinez-Diz, M.D.; Diaz-Losada, E.; Diaz-Fernandez, A.; Bouzas-Cid, Y.; Gramaje, D. Protection of grapevine pruning wounds against *Phaeoemoniella chlamydospora* and *Diplodia seriata* by commercial biological and chemical methods. *Crop Prot.* **2021**, *143*, 105465, doi:10.1016/j.cropro.2020.105465.
85. Di Marco, S.; Osti, F.; Cesari, A. Experiments on the control of esca by *Trichoderma*. *Phytopathol. Mediterr.* **2004**, *43*, 108-115.
86. Locatelli, G.O.; dos Santos, G.F.; Botelho, P.S.; Finkler, C.L.L.; Bueno, L.A. Development of *Trichoderma* sp. formulations in encapsulated granules (CG) and evaluation of conidia shelf-life. *Biol. Control* **2018**, *117*, 21-29, doi:10.1016/j.biocontrol.2017.08.020.
87. Peil, S.; Beckers, S.J.; Fischer, J.; Wurm, F.R. Biodegradable, lignin-based encapsulation enables delivery of *Trichoderma reesei* with programmed enzymatic release against grapevine trunk diseases. *Mater Today Bio* **2020**, *7*, 100061, doi:10.1016/j.mtbio.2020.100061.
88. Trouvelot, S.; Bonneau, L.; Redecker, D.; van Tuinen, D.; Adrian, M.; Wipf, D. Arbuscular mycorrhiza symbiosis in viticulture: a review. *Agron. Sustain. Dev.* **2015**, *35*, 1449-1467, doi:10.1007/s13593-015-0329-7.
89. Petit, E.; Gubler, W.D. Influence of *Glomus intraradices* on black foot disease caused by *Cylindrocarpon macrodidymum* on *Vitis rupestris* under controlled conditions. *Plant Dis.* **2006**, *90*, 1481-1484, doi:10.1094/pd-90-1481.
90. Jones, E.E.; Hammond, S.E.; Blond, C.L.; Brown, D.S.; Ridgway, H.J. Interaction between arbuscular mycorrhizal fungi and rootstock cultivar on the susceptibility to infection by *Ilyonectria* species. *Phytopathol. Mediterr.* **2018**, *53*, 582-583.
91. Holland, T.; Bowen, P.; Kokkoris, V.; Urbez-Torres, J.R.; Hart, M. Does inoculation with arbuscular mycorrhizal fungi reduce trunk disease in grapevine rootstocks? *Horticulturae* **2019**, *5*, 61, doi:10.3390/horticulturae5030061.
92. Munkvold, G.; Marois, J. Efficacy of natural epiphytes and colonizers of grapevine pruning wounds for biological control of *Eutypa dieback*. *Phytopathology* **1993**, *83*, 624-629.
93. Rolshausen, P.E.; Gubler, W.D. Use of boron for the control of *Eutypa dieback* of grapevines. *Plant Dis.* **2005**, *89*, 734-738, doi:10.1094/PD-89-0734.
94. McMahan, G.; Yeh, W.; Marshall, M.N.; Olsen, M.; Sananikone, S.; Wu, J.Y.; Block, D.E.; VanderGheynst, J.S. Characterizing the production of a wild-type and benomyl-resistant *Fusarium lateritium* for biocontrol of *Eutypa lata* on grapevine. *J. Ind. Microbiol.* **2001**, *26*, 151-155, doi:10.1038/sj.jim.7000099.
95. John, S.; Wicks, T.J.; Hunt, J.S.; Lorimer, M.F.; Oakey, H.; Scott, E.S. Protection of grapevine pruning wounds from infection by *Eutypa lata* using *Trichoderma harzianum* and *Fusarium lateritium*. *Australas. Plant Pathol.* **2005**, *34*, 569-575, doi:10.1071/ap05075.

96. Rezgui, A.; Ben Ghnaya-Chakroun, A.; Vallance, J.; Bruez, E.; Hajlaoui, M.R.; Sadfi-Zouaoui, N.; Rey, P. Endophytic bacteria with antagonistic traits inhabit the wood tissues of grapevines from Tunisian vineyards. *Biol. Control* **2016**, *99*, 28-37, doi:10.1016/j.biocontrol.2016.04.005.
97. Alfonzo, A.; Conigliaro, G.; Torta, L.; Burruano, S.; Moschetti, G. Antagonism of *Bacillus subtilis* strain AG1 against vine wood fungal pathogens. *Phytopathol. Mediterr.* **2009**, *48*, 155-158.
98. Álvarez-Pérez, J.M.; González-García, S.; Cobos, R.; Olego, M.; Ibañez, A.; Díez-Galán, A.; Garzón-Jimeno, E.; Coque, J.J.R. Use of endophytic and rhizosphere actinobacteria from grapevine plants to reduce nursery fungal graft infections that lead to young grapevine decline. *Appl. Environ. Microbiol.* **2017**, *83*, e01564-01517, doi:10.1128/aem.01564-17.
99. Yacoub, A.; Gerbore, J.; Magnin, N.; Chambon, P.; Dufour, M.-C.; Corio-Costet, M.-F.; Guyoneaud, R.; Rey, P. Ability of *Pythium oligandrum* strains to protect *Vitis vinifera* L., by inducing plant resistance against *Phaeomoniella chlamydospora*, a pathogen involved in Esca, a grapevine trunk disease. *Biol. Control* **2016**, *92*, 7-16.
100. Gerbore, J. Lutte biologique contre un champignon pathogène impliqué dans l'esca de la vigne, par utilisation de l'oomycète *Pythium oligandrum*. Pau, 2013.
101. van Lenteren, J.C.; Bolckmans, K.; Köhl, J.; Ravensberg, W.J.; Urbaneja, A. Biological control using invertebrates and microorganisms: plenty of new opportunities. *Biocontrol* **2017**, *63*, 39-59, doi:10.1007/s10526-017-9801-4.
102. Li, K.; Xing, R.; Liu, S.; Li, P. Chitin and chitosan fragments responsible for plant elicitor and growth stimulator. *J. Agric. Food. Chem.* **2020**, *68*, 12203-12211, doi:10.1021/acs.jafc.0c05316.
103. Nascimento, T.; Rego, C.; Oliveira, H. Potential use of chitosan in the control of grapevine trunk diseases. *Phytopathol. Mediterr.* **2007**, *46*, 218-224.
104. Mukhtar Ahmed, K.B.; Khan, M.M.A.; Siddiqui, H.; Jahan, A. Chitosan and its oligosaccharides, a promising option for sustainable crop production-A review. *Carbohydr. Polym.* **2020**, *227*, 115331, doi:10.1016/j.carbpol.2019.115331.
105. Ma, Z.; Garrido-Maestu, A.; Jeong, K.C. Application, mode of action, and in vivo activity of chitosan and its micro- and nanoparticles as antimicrobial agents: A review. *Carbohydr. Polym.* **2017**, *176*, 257-265, doi:10.1016/j.carbpol.2017.08.082.
106. Cobos, R.; Mateos, R.M.; Álvarez-Pérez, J.M.; Olego, M.A.; Sevillano, S.; González-García, S.; Garzón-Jimeno, E.; Coque, J.J.R. Effectiveness of natural antifungal compounds in controlling infection by grapevine trunk disease pathogens through pruning wounds. *Appl. Environ. Microbiol.* **2015**, *81*, 6474-6483.
107. Xing, K.; Shen, X.; Zhu, X.; Ju, X.; Miao, X.; Tian, J.; Feng, Z.; Peng, X.; Jiang, J.; Qin, S. Synthesis and *in vitro* antifungal efficacy of oleoyl-chitosan nanoparticles against plant pathogenic fungi. *Int. J. Biol. Macromol.* **2016**, *82*, 830-836, doi:10.1016/j.ijbiomac.2015.09.074.
108. Matei, P.M.; Martín-Ramos, P.; Sánchez-Báscos, M.; Hernández-Navarro, S.; Correa-Guimaraes, A.; Navas-Gracia, L.M.; Rufino, C.A.; Ramos-Sánchez, M.C.; Martín-Gil, J. Synthesis of chitosan oligomers/propolis/silver nanoparticles composite systems and study of their activity against *Diplodia seriata*. *Int. J. Polym. Sci.* **2015**, *2015*, 864729, doi:10.1155/2015/864729.
109. Buzón-Durán, L.; Martín-Gil, J.; Pérez-Lebeña, E.; Ruano-Rosa, D.; Revuelta, J.L.; Casanova-Gascón, J.; Ramos-Sánchez, M.C.; Martín-Ramos, P. Antifungal agents based on chitosan oligomers, ϵ -polylysine and *Streptomyces* spp. secondary metabolites against three *Botryosphaeriaceae* species. *Antibiotics*, **2019**, *8*, 99. doi:10.3390/antibiotics8030099
110. Calzarano, F.; Di Marco, S.; D'Agostino, V.; Schiff, S.; Mugnai, L. Grapevine leaf stripe disease symptoms (Esca complex) are reduced by a nutrients and seaweed mixture. *Phytopathol. Mediterr.* **2014**, *53*, 543-558.

111. Ayres, M.; Wicks, T.; Scott, E.S.; Sosnowski, M. Developing pruning wound protection strategies for managing *Eutypa dieback*. *Aust. J. Grape Wine Res.* **2017**, *23*, 103-111.
112. Ammad, F.; Moumen, O.; Gasem, A.; Othmane, S.; Hisashi, K.-N.; Zebib, B.; Merah, O. The potency of lemon (*Citrus limon* L.) essential oil to control some fungal diseases of grapevine wood. *C. R. Biol.* **2018**, *341*, 97-101, doi:10.1016/j.crv.2018.01.003.
113. Hinsu, A.; Dumadiya, A.; Joshi, A.; Kotadiya, R.; Andharia, K.; Koringa, P.; Kothari, R. To culture or not to culture: a snapshot of culture-dependent and culture-independent bacterial diversity from peanut rhizosphere. *PeerJ* **2021**, *9*, e12035, doi:10.7717/peerj.12035.
114. Forbes, J.D.; Knox, N.C.; Ronholm, J.; Pagotto, F.; Reimer, A. Metagenomics: The next culture-independent game changer. *Front. Microbiol.* **2017**, *8*, 1069, doi:10.3389/fmicb.2017.01069.
115. Liu, H.; Brettell, L.E. Plant defense by VOC-induced microbial priming. *Trends Plant Sci.* **2019**, *24*, 187-189, doi:10.1016/j.tplants.2019.01.008.
116. Bettenfeld, P.; Canals, J.C.I.; Jacquens, L.; Fernandez, O.; Fontaine, F.; van Schaik, E.; Courty, P.E.; Trouvelot, S. The microbiota of the grapevine holobiont: A key component of plant health. *J. Adv. Res.* **2022**, *40*, 1-15, doi:10.1016/j.jare.2021.12.008.
117. Morgan, H.H.; du Toit, M.; Setati, M.E. The grapevine and wine microbiome: Insights from high-throughput amplicon sequencing. *Front. Microbiol.* **2017**, *8*, 820, doi:10.3389/fmicb.2017.00820.
118. Berlanas, C.; Berbegal, M.; Elena, G.; Laidani, M.; Cibriain, J.F.; Sagües, A.; Gramaje, D. The fungal and bacterial rhizosphere microbiome associated with grapevine rootstock genotypes in mature and young vineyards. *Front. Microbiol.* **2019**, *10*, 1142, doi:10.3389/fmicb.2019.01142.
119. Hamaoka, K.; Aoki, Y.; Takahashi, S.; Enoki, S.; Yamamoto, K.; Tanaka, K.; Suzuki, S. Diversity of endophytic bacterial microbiota in grapevine shoot xylems varies depending on wine grape-growing region, cultivar, and shoot growth stage. *Sci. Rep.* **2022**, *12*, 15772 doi:10.1038/s41598-022-20221-8.
120. Martínez-Diz, M.d.P.; Andrés-Sodupe, M.; Bujanda, R.; Díaz-Losada, E.; Eichmeier, A.; Gramaje, D. Soil-plant compartments affect fungal microbiome diversity and composition in grapevine. *Fungal Ecol.* **2019**, *41*, 234-244, doi:10.1016/j.funeco.2019.07.003.
121. Wei, Y.-j.; Wu, Y.; Yan, Y.-z.; Zou, W.; Xue, J.; Ma, W.-r.; Wang, W.; Tian, G.; Wang, L.-y. High-throughput sequencing of microbial community diversity in soil, grapes, leaves, grape juice and wine of grapevine from China. *PLoS One* **2018**, *13*, e0193097, doi:10.1371/journal.pone.0193097.
122. Niem, J.M.; Billones-Baaijens, R.; Stodart, B.; Savocchia, S. Diversity profiling of grapevine microbial endosphere and antagonistic potential of endophytic *Pseudomonas* against grapevine trunk diseases. *Front Microbiol* **2020**, *11*, 477, doi:10.3389/fmicb.2020.00477.
123. Cobos, R.; Ibañez, A.; Diez-Galán, A.; Calvo-Peña, C.; Ghorehshizadeh, S.; Coque, J.J.R. The grapevine microbiome to the rescue: Implications for the biocontrol of trunk diseases. *Plants* **2022**, *11*, 840, doi:10.3390/plants11070840.
124. Ramirez, M.; Perez, L.M.; Montealegre, J.R. Susceptibility of different grapevine (*Vitis vinifera* L.) cultivars to *Diplodia seriata* and *Diplodia mutila*. *Cienc Investig Agrar.* **2018**, *45*, 93-98, doi:10.7764/rcia.v45i1.1818.
125. Sosnowski, M.R.; Ayres, R.; McCarthy, G.; Scott, E.S. Winegrape cultivars (*Vitis vinifera*) vary in susceptibility to the grapevine trunk pathogens *Eutypa lata* and *Diplodia seriata*. *Aust. J. Grape Wine Res.* **2022**, *28*, 166-174, doi:10.1111/ajgw.12531.
126. Ramsing, C.K.; Gramaje, D.; Mocholi, S.; Agustí, J.; de Santa Maria, F.C.S.; Armengol, J.; Berbegal, M. Relationship between the xylem anatomy of grapevine rootstocks and their susceptibility to *Phaeoacremonium minimum* and *Phaeomoniella chlamydospora*. *Front. Plant Sci.* **2021**, *12*, 726461, doi:10.3389/fpls.2021.726461.

127. Travadon, R.; Rolshausen, P.E.; Gubler, W.D.; Cadle-Davidson, L.; Baumgartner, K. Susceptibility of cultivated and wild *Vitis* spp. to wood infection by fungal trunk pathogens. *Plant Dis.* **2013**, *97*, 1529-1536, doi:10.1094/pdis-05-13-0525-re.
128. Billones-Baaijens, R.; Jones, E.; Ridgway, H.; Jaspers, M. Susceptibility of common rootstock and scion varieties of grapevines to *Botryosphaeriaceae* species. *Australas. Plant Pathol.* **2014**, *43*, 25-31.
129. Serra, S.; Ligios, V.; Schianchi, N.; Prota, V.A.; Deidda, A.; Scanu, B. Incidence of grapevine trunk diseases on four cultivars in Sardinia, Southern Italy. *Vitis* **2021**, *60*, 35-42, doi:10.5073/vitis.2021.60.35-42.
130. Guan, X.; Essakhi, S.; Laloue, H.; Nick, P.; Bertsch, C.; Chong, J. Mining new resources for grape resistance against *Botryosphaeriaceae*: a focus on *Vitis vinifera* subsp. *sylvestris*. *Plant Pathol.* **2016**, *65*, 273-284, doi:10.1111/ppa.12405.
131. Arendrup, M.C.; Cuenca-Estrella, M.; Lass-Flörl, C.; Hope, W. EUCAST technical note on the EUCAST definitive document EDef 7.2: method for the determination of broth dilution minimum inhibitory concentrations of antifungal agents for yeasts EDef 7.2 (EUCAST-AFST). *Clin. Microbiol. Infect.* **2012**, *18*, E246-E247, doi:10.1111/j.1469-0691.2012.03880.x.
132. CLSI. *Methods for dilution antimicrobial susceptibility tests for bacteria that grow aerobically*. 11th Ed. CLSI standard M07; Clinical and Laboratory Standards Institute: Wayne, PA, USA, 2018; pp. 112.
133. Siameto, E.; Okoth, S.; Amugune, N.; Chege, N. Antagonism of *Trichoderma harzianum* isolates on soil borne plant pathogenic fungi from Embu District, Kenya. *J. Yeast Fungal Res.* **2010**, *1*, 47-54.
134. Mutawila, C.; Vinale, F.; Halleen, F.; Lorito, M.; Mostert, L. Isolation, production and in vitro effects of the major secondary metabolite produced by *Trichoderma* species used for the control of grapevine trunk diseases. *Plant Pathol.* **2016**, *65*, 104-113, doi:10.1111/ppa.12385.
135. Kotze, C.; Van Niekerk, J.; Halleen, F.; Mostert, L.; Fourie, P. Evaluation of biocontrol agents for grapevine pruning wound protection against trunk pathogen infection. *Phytopathol. Mediterr.* **2011**, *50*, 247-263, doi:10.14601/Phytopathol_Mediterr-8960.
136. John, S.; Scott, E.S.; Wicks, T.J.; Hunt, J.S. Interactions between *Eutypa lata* and *Trichoderma harzianum*. *Phytopathol. Mediterr.* **2004**, *43*, 95-104.
137. Halleen, F.; Fourie, P. An integrated strategy for the proactive management of grapevine trunk disease pathogen infections in grapevine nurseries. *South African J. Enol. Vitic.* **2016**, *37*, 104-114.
138. Calvo, H.; Gracia, A.; Venturini Crespo, M.; Roudet, J.; Fermaud, M. Comparison of efficacy and modes of action of two high-potential biocontrol *Bacillus* strains and commercial biocontrol products against *Botrytis cinerea* in table grapes. *OENO One* **2021**, *55*, 4688, doi:10.20870/oeno-one.2021.55.3.4688.
139. Calvo, H.; Mendiara, I.; Arias, E.; Blanco, D.; Venturini, M. The role of iturin A from *B. amyloliquifaciens* BUZ-14 in the inhibition of the most common postharvest fruit rots. *Food Microbiol.* **2019**, *82*, 62-69.
140. Halleen, F.; Fourie, P.H.; Lombard, P.J. Protection of grapevine pruning wounds against *Eutypa lata* by biological and chemical methods. *Enol. Vitic.* **2010**, *31*, 125-132.
141. Trotel-Aziz, P.; Abou-Mansour, E.; Courteaux, B.; Rabenoelina, F.; Clement, C.; Fontaine, F.; Aziz, A. *Bacillus subtilis* PTA-271 counteracts *Botryosphaeria dieback* in grapevine, triggering immune responses and detoxification of fungal phytotoxins. *Front. Plant Sci.* **2019**, *10*, 25, doi:10.3389/fpls.2019.00025.
142. Sebestyen, D.; Perez-Gonzalez, G.; Goodell, B. Antioxidants and iron chelators inhibit oxygen radical generation in fungal cultures of plant pathogenic fungi. *Fungal Biol.* **2022**, *126*, 480-487, doi:10.1016/j.funbio.2022.04.002.

143. Gramaje, D.; Eichmeier, A.; Spetik, M.; Carbone, M.J.; Bujanda, R.; Vallance, J.; Rey, P. Exploring the temporal dynamics of the fungal microbiome in rootstocks, the lesser-known half of the grapevine crop. *J. Fungi* **2022**, *8*, 421, doi:10.3390/jof8050421.
144. Del Frari, G.; Gobbi, A.; Aggerbeck, M.R.; Oliveira, H.; Hansen, L.H.; Ferreira, R.B. Characterization of the wood mycobiome of *Vitis vinifera* in a vineyard affected by Esca. Spatial distribution of fungal communities and their putative relation with leaf symptoms. *Front. Plant Sci.* **2019**, *10*, 910, doi:10.3389/fpls.2019.00910.
145. Lade, S.B.; Štraus, D.; Oliva, J. Variation in fungal community in grapevine (*Vitis vinifera*) nursery stock depends on nursery, variety and rootstock. *Journal of Fungi* **2022**, *8*, 47, doi:10.3390/jof8010047.
146. Knapp, D.G.; Lázár, A.; Molnár, A.; Vajna, B.; Karácsony, Z.; Váczy, K.Z.; Kovács, G.M. Above-ground parts of white grapevine *Vitis vinifera* cv. *Furmint* share core members of the fungal microbiome. *Environ. Microbiol. Rep.* **2021**, *13*, 509-520, doi:10.1111/1758-2229.12950.
147. Bruez, E.; Vallance, J.; Gautier, A.; Laval, V.; Compant, S.; Maurer, W.; Sessitsch, A.; Lebrun, M.H.; Rey, P. Major changes in grapevine wood microbiota are associated with the onset of Esca, a devastating trunk disease. *Environ. Microbiol.* **2020**, *22*, 5189-5206, doi:10.1111/1462-2920.15180.
148. Dissanayake, A.J.; Purahong, W.; Wubet, T.; Hyde, K.D.; Zhang, W.; Xu, H.; Zhang, G.; Fu, C.; Liu, M.; Xing, Q. Direct comparison of culture-dependent and culture-independent molecular approaches reveal the diversity of fungal endophytic communities in stems of grapevine (*Vitis vinifera*). *Fungal Divers.* **2018**, *90*, 85-107.
149. Jayawardena, R.S.; Purahong, W.; Zhang, W.; Wubet, T.; Li, X.; Liu, M.; Zhao, W.; Hyde, K.D.; Liu, J.; Yan, J. Biodiversity of fungi on *Vitis vinifera* L. revealed by traditional and high-resolution culture-independent approaches. *Fungal Divers.* **2018**, *90*, 1-84, doi:10.1007/s13225-018-0398-4.

2. COMPENDIO DE PUBLICACIONES

ARTÍCULO 1: "On the applicability of chitosan oligomers-amino acid conjugate complexes as eco-friendly fungicides against grapevine trunk pathogens" *Agronomy*, 2021, 11(2), 324; <https://doi.org/10.3390/agronomy11020324>; Q1 (JCR, Science Edition – AGRONOMY). JIF₂₀₂₁ = 3,949. 11 citas recibidas (WOS).



agronomy

an Open Access Journal by MDPI

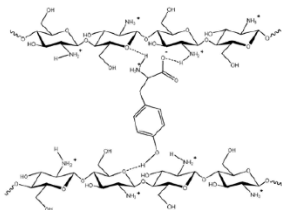


On the Applicability of Chitosan Oligomers-Amino Acid Conjugate Complexes as Eco-Friendly Fungicides against Grapevine Trunk Pathogens

Laura Buzón-Durán; Natalia Langa-Lomba; Vicente González-García; José Casanova-Gascón; Jesús Martín-Gil; Eduardo Pérez-Lebeña; Pablo Martín-Ramos

Agronomy 2021, Volume 11, Issue 2, 324

**Chitosan oligomers
+
amino acids**



In vitro tests



+



In planta bioassays



**Eco-friendly
control of GTDs**

- *N. parvum*
- *D. seriata*
- *B. dothidea*



Article

On the Applicability of Chitosan Oligomers-Amino Acid Conjugate Complexes as Eco-Friendly Fungicides against Grapevine Trunk Pathogens

Laura Buzón-Durán ¹, Natalia Langa-Lomba ^{2,3}, Vicente González-García ³, José Casanova-Gascón ^{2,*},
Jesús Martín-Gil ¹, Eduardo Pérez-Lebeña ¹ and Pablo Martín-Ramos ²

- ¹ Department of Agricultural and Forestry Engineering, ETSIIAA, Universidad de Valladolid, 34004 Palencia, Spain; laura.buzon@uva.es (L.B.-D.); mgil@iaf.uva.es (J.M.-G.); eplebena@gmail.com (E.P.-L.)
- ² Instituto Universitario de Investigación en Ciencias Ambientales de Aragón (IUCA), EPS, Universidad de Zaragoza, Carretera de Cuarte, s/n, 22071 Huesca, Spain; natalialangalomba@gmail.com (N.L.-L.); pmr@unizar.es (P.M.-R.)
- ³ Plant Protection Unit, Agrifood Research and Technology Centre of Aragón, Instituto Agroalimentario de Aragón—IA2 (CITA-Universidad de Zaragoza), Avda. Montañana 930, 50059 Zaragoza, Spain; vgonzalezg@aragon.es
- * Correspondence: jcasan@unizar.es; Tel.: +34-974239339



Citation: Buzón-Durán, L.; Langa-Lomba, N.; González-García, V.; Casanova-Gascón, J.; Martín-Gil, J.; Pérez-Lebeña, E.; Martín-Ramos, P. On the Applicability of Chitosan Oligomers-Amino Acid Conjugate Complexes as Eco-Friendly Fungicides against Grapevine Trunk Pathogens. *Agronomy* **2021**, *11*, 324. <https://doi.org/10.3390/agronomy11020324>

Academic Editor: Thorsten Kraska
Received: 29 December 2020
Accepted: 7 February 2021
Published: 12 February 2021

Publisher's Note: MDPI stays neutral with regard to jurisdictional claims in published maps and institutional affiliations.



Copyright: © 2021 by the authors. Licensee MDPI, Basel, Switzerland. This article is an open access article distributed under the terms and conditions of the Creative Commons Attribution (CC BY) license (<https://creativecommons.org/licenses/by/4.0/>).

Abstract: In a context in which the incidence and severity of grapevine fungal diseases is increasing as a result of both climate change and modern management culture practices, reducing the excessive use of phytosanitary products in viticulture represents a major challenge. Specifically, grapevine trunk diseases (GTDs), caused by several complexes of wood decay or xylem-inhabiting fungi, pose a major challenge to vineyard sustainability. In this study, the efficacy of chitosan oligomers (COS)–amino acid conjugate complexes against three fungal species belonging to the *Botryosphaeriaceae* family (*Neofusicoccum parvum*, *Diplodia seriata*, and *Botryosphaeria dothidea*) was investigated both in vitro and in planta. In vitro tests led to EC₅₀ and EC₉₀ effective concentrations in the 254.6–448.5 and 672.1–1498.5 µg·mL⁻¹ range, respectively, depending on the amino acid involved in the conjugate complex (viz. cysteine, glycine, proline or tyrosine) and on the pathogen assayed. A synergistic effect between COS and the amino acids was observed against *D. seriata* and *B. dothidea* (synergy factors of up to 2.5 and 2.8, respectively, according to Wadley's method). The formulations based on COS and on the conjugate complex that showed the best inhibition rates, COS–tyrosine, were further investigated in a greenhouse trial on grafted vines of two varieties (“Tempranillo” on 775P and “Garnacha” on 110R rootstock), artificially inoculated with the mentioned three *Botryosphaeriaceae* species. The in planta bioassay revealed that the chosen formulations induced a significant decrease in disease severity against *N. parvum* and *B. dothidea*. In summary, the reported conjugate complexes may be promising enough to be worthy of additional examination in larger field trials.

Keywords: *Botryosphaeriaceae*; chitosan; fungicide; GTD; IPM; tyrosine; *Vitis vinifera*

1. Introduction

The so-called grapevine trunk diseases (GTDs) represent one of the greatest threats to vineyards in the last 20–25 years, as a consequence of changes in the management and intensification of the crop, the increase in the production of propagating plant material, the banning of chemicals or the existence of a climate change scenario. The International Organization of Vine and Wine (OIV) has estimated that the incidence rate of GTDs is approximately 10, 13 and 13.5% of Spanish, French and Italian vineyards, respectively [1]. At a global level, economic losses caused by GTDs exceed US\$1.5 billion/year [2].

Among these, ascomycetous taxa belonging to the family *Botryosphaeriaceae* are responsible for large losses due to their incidence, especially in young grapevine plants coming

from nurseries. Pathogenicity studies have shown that grapevine-associated species belonging to the genera *Botryosphaeria*, *Lasiodiplodia* and *Neofusicoccum* are among the fastest colonizing wood fungi and are therefore considered the most virulent cause of wood diseases [3]. External symptoms produced by this pathogenic complex include death of the cordons, canes, shoots and buds, stunting, bud necrosis, bleached canes, reduced bunch set and bunch rots, while internal symptoms like brown wood streaking and wedge-shaped discolorations are very frequent [4,5]. Together with these disease symptoms, these and other related GTD fungi are known to produce toxic metabolites [6], some of them well characterized by chemical methods, whose toxicity has been proven on different organs and tissues of several *Vitis vinifera* L. cultivars [7].

A comprehensive overview of the current state-of-the-art concerning chemicals (including inorganic, synthetic organic, natural, and elicitor compounds), biocontrol agents (BCAs) or preventive and post-infection management practices that have been examined against GTDs may be found in the review papers by Vincenzo, et al. [8], Gramaje, Urbez-Torres and Sosnowski [3] and Mondello, Songy, Battiston, Pinto, Coppin, Trotel-Aziz, Clement, Mugnai and Fontaine [1]. However, it is necessary to clarify that at present there are no last-generation chemical methods or alternative treatments with proven efficacy [9], which explains why preventive cultural measures are generally used [10].

In order to comply with the European legislation currently in force (Article 14 in European Directive 2009/128/EC), the implementation of integrated pest management (IPM) methods has become a priority objective in plant disease control worldwide. The efforts oriented towards the selection and/or development of rootstocks and varieties with certain levels of tolerance against different trunk mycoses have not been successful to date [11–16], and the use of strategies involving endophytic microorganisms as microbial antagonists (BCAs) obtains a certain degree of protection, but no single BCA application has been able to control GTDs at similar rates to those shown by chemical fungicides, which are now banned [17]. Hence, other alternative/complementary strategies have to be explored and improved, such as the application of substances of natural origin that are safe, effective and sustainable from an environmental point of view [18].

As regards this latter option, polysaccharide-amino acid conjugates are drawing much attention due to their biocompatibility, design flexibility, adjustable degradability, and similarity—in terms of structure—to natural glycoproteins [19].

It is worth noting that plant host defense peptides (HDPs) or antimicrobial peptides (AMPs), generally cysteine-rich (nodule-specific cysteine-rich peptides, NCRs), are considered one of the main barriers developed by plants to fight infective agents [20–22], and are now being studied as antimicrobial agents against drug-resistant bacteria and other biomedical applications [23,24]. Amongst the different types of HDPs, the Snakin class is particularly interesting, as it encompasses the principal cysteine-rich peptides and given that the Snakin/GASA gene family has been identified in the grapevine [25]. As noted by Álvarez, et al. [26], cysteine is a keystone metabolite in the immune response pathways of plants, functioning as a precursor for many defense compounds (for example, phytoalexins, thionins, glucosinolates, etc.), and is associated with high resistance rates to both bio- and necrotrophic phytopathogens. In a recent study by Roblin, et al. [27], it was reported that cysteine may be able to control fungal diseases either by acting directly on fungal development and/or functioning as an early signal that elicits the plant's host reaction. In relation to GTDs, the same group also chose cysteine as a one of the chemicals in their experimental model aimed at the elaboration of preventive and/or curative treatments of esca syndrome [28].

Regarding polysaccharides, chitosan, a well-known compound with proven control properties, has been assayed against GTDs in different formulations: e.g., chitosan oligomers can protect pruning wounds inoculated with *Phaeoconiella chlamydospora* (W. Gams, Crous, M.J. Wingf. & Mugnai) Crous & W. Gams and *Diplodia seriata* de Not. in field trials [29]; high molecular weight chitosan reduced mycelial growth of *Botryosphaeria* sp., *Phomopsis* sp., *Eutypa lata* (Pers.) Tul. & C. Tul., *Neonectria liriodendri* Halleen, Rego & Crous, 2006, *P. chlamydospora*

and *Fomitiporia* sp. [30]; oleoyl-chitosan nanoparticles reduced the mycelium growth of *Botryosphaeria dothidea* (Moug. ex Fr.) Ces. & De Not. [31]; chitosan oligomers/propolis/silver nanoparticles composites have been tested against *D. seriata* [32]; and ϵ -polylysine:chitosan oligomers conjugates showed antifungal activity against *Neofusicoccum parvum* (Pennycook & Samuels) Crous, Slippers & A.J.L. Phillips, *Diplodia seriata*, and *B. dothidea* [33].

In connection with polysaccharide-amino acid conjugates, several examples for medical applications have been recently reported [34–36], but applications in the field of agronomy are still at a very early stage of development. To the best of the authors' knowledge, there is only one recent study on chitosan oligomers–amino acid conjugates against *Fusarium culmorum* (Wm.G. Sm.) Sacc., in spelt (*Triticum spelta* L.) by some of the co-authors of this work [37].

The aim of this study was to assess both the *in vitro* and *in vivo* antifungal efficacy of chitosan oligomers and amino acid conjugate complexes to control three of the most prevalent fungal pathogens associated with GTDs, especially in young plants: *N. parvum*, *D. seriata*, and *B. dothidea*.

2. Materials and Methods

2.1. Fungal Isolates

The three fungal isolates under study, viz. *N. parvum* (ITACYL_F111), *D. seriata* (ITACYL_F079) and *B. dothidea* (ITACYL_F141), were all isolated from diseased grapevine plants from D.O. Ribera de Duero and supplied as lyophilized vials (later reconstituted and refreshed as PDA subcultures) by the Agricultural Technological Institute of Castilla and Leon (ITACYL, Valladolid, Spain) [38].

2.2. Reagents and Preparation of Chitosan Oligomers and Bioactive Formulations

Chitosan (CAS 9012-76-4; high MW: 310,000–375,000 Da) was supplied by Hangzhou Simit Chem. & Tech. Co. (Hangzhou, China). The four amino acids (cysteine, CAS 52-90-4; glycine, CAS 56-40-6; proline, CAS 147-75-3; and tyrosine, CAS 60-8-4) were purchased from Panreac (Barcelona, Spain). Citric acid (CAS 77-92-9), sodium alginate (CAS 9005-38-3) and calcium carbonate (CAS 471-34-1) were purchased from Sigma-Aldrich Química (Madrid, Spain). NeutrasedTM 0.8 L enzyme was supplied by Novozymes A/S (Bagsværd, Denmark). Potato dextrose agar (PDA) was purchased from Becton Dickinson (Bergen County, NJ, USA).

Chitosan oligomers (COS) were prepared according to the procedure previously reported in [33]. Cysteine (Cys), glycine (Gly), proline (Pro) and tyrosine (Tyr) solutions were obtained by dissolution of the amino acids (with 99% purity) in sterile double distilled water at an initial concentration of 3000 $\mu\text{g}\cdot\text{mL}^{-1}$. The COS–amino acid conjugate complexes were obtained by mixing of the respective solutions in a 1:1 (*v/v*) ratio. The mixture was then sonicated for 15 min in five 3-min periods (so that the temperature did not exceed 60 °C) using a probe-type ultrasonicator (model UIP1000hdT; Hielscher Ultrasonics, Teltow, Germany).

2.3. In Vitro Tests of Mycelial Growth Inhibition

The fungicidal potential of the different compounds was determined employing an agar dilution method [39]; briefly, aliquots of stock solutions were incorporated onto the PDA medium to obtain the usual concentrations defined in the EUCAST standard antifungal susceptibility testing procedures [40]. Then, mycelial plugs ($\varnothing = 5$ mm) of each pathogen coming from the margin of 7-day-old PDA cultures were transferred to plates incorporating the above mentioned concentrations for each compound (3 plates per treatment/concentration, with 2 replicates) and incubated 7 days at 25 °C in the dark. Control plates consisted of PDA medium without any amendment.

Mycelial growth rates were determined by calculating the average diameter of 2 perpendicular colony axes for each replicate. Growth inhibition of each treatment and concentration was calculated at the end of the incubating period according to the formula:

$$((d_c - d_t) / d_c) \times 100, \quad (1)$$

where d_c represents the average diameter of the fungal colony of the control and d_t is the average diameter of the treated fungal colony.

Results were also expressed as both EC₅₀ and 90% effective concentrations, estimated by means of PROBIT analysis in IBM SPSS Statistics v.25 (IBM; Armonk, NY, USA) software.

Synergy factors were determined according to Wadley's method to quantify the level of interaction [41].

2.4. Greenhouse Bioassays in Grafted Plants

Together with the experiments of fungal pathogens growth inhibition *in vitro*, bioassays with the mentioned natural products and formulations were performed in grapevine plants in order to scale the protective capabilities of these compounds against three *Botryosphaeriaceae* species responsible of GTDs on young grapevine plants. Thus, plant material consisted of 48 plants each of varieties "Tempranillo" (CL. 32 clone) (2-years old) and "Garnacha" (VCR3 clone) (one year old) grafted on 775P and 110R rootstocks, respectively. Plants were planted on 3.5 L plastic pots with a mixed substrate of peat and autoclaved natural soil (75:25), incorporating slow release fertilizer when needed. Plants were maintained in the greenhouse with drip irrigation and anti-weed ground cover for six months (June-December) (Figure 1a). One week after placing them in the greenhouse, grafted plants were inoculated with three pathogens and either COS or COS-Tyr treatments. Five repetitions were arranged for each pathogen/control product and grapevine plant combination (cultivar/rootstock), together with 4 repetitions per pathogen and variety as positive control plus 3 repetitions of negative controls (inoculating only the bioactive product) for each treatment (Table S1).

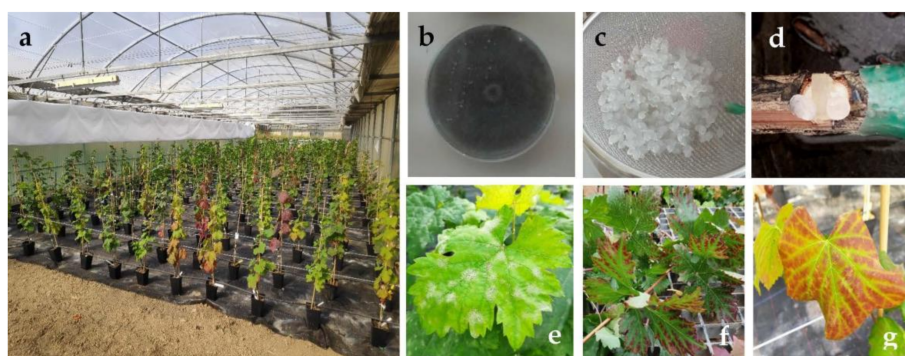


Figure 1. Bioassays in the greenhouse with grafted grapevine plants. (a): Bioassay overview; (b): fresh culture of *Neofusicoccum parvum* on PDA plate; (c): calcium alginate beads including control product; (d): inoculation method; (e): leaves infected with powdery mildew; (f,g): presence of foliar symptoms in grapevine plants.

For the fungal inocula, pure cultures of *N. parvum*, *D. seriata* and *B. dothidea* were maintained as fresh colonies in 9 cm Ø Petri dishes with PDA medium at 25 °C in the dark (Figure 1b). When necessary, the strains were subcultured in the aforementioned medium to keep them fresh and viable before use. Inoculations of both pathogens and control products were carried out on the trunk of the living plants at two sites per individual (separated at least 5 cm among them) below the grafting point and not reaching the root crown. In the case of fungal strains, agar plugs from fresh PDA cultures of each fungus in question were used as fungal inoculum. In the defined points of each grapevine plant, slits (with a scalpel) of approx. 3 mm in diameter and 0.5 cm deep were done. After this,

0.5 cm diameter agar plugs were inoculated and placed in such a way that the mycelium was in contact with the incision of the stem. Two calcium alginate beads (Figure 1c) including the different control products assayed were placed at both sides of the agar plug (Figure 1d). For this, beads were prepared as follows; each biological compound was added to a 3% sodium alginate solution in a 2:8 ratio (20 mL treatment/80 mL sodium alginate). Then, the solution incorporating each treatment was dispensed drop by drop onto a 3% calcium carbonate solution to spherify (polymerize) the beads containing the mentioned treatments. Finally, both discs and beads were covered with cotton soaked in sterile double distilled water and sealed with Parafilm™ tape. During the culturing period, application of copper to control powdery mildew (Figure 1e) was performed in mid-July, together with a first sprouting (followed by periodic sprouting). In addition, releasing of *Amblyseius (Typhlodromips) swirskii* Athias-Henriot for biological control of whitefly, thrips and spider mite, *Encarsia formosa* Gahan/*Eretmocerus eremicus* Rose & Zolnerowich for whitefly and *Aphelinus abdominalis* Dalman for aphids at the end of July (Biobest Group NV, Almeria, Spain) were also performed.

Potted grapevine plants were examined weekly during the whole assay period by taking photographs (Figure 1f,g) in cases where different foliar symptoms including internervial necroses were observed. Six months after inoculation, plants were removed and two sections of the inoculated stems between the grafting point and the root crown were prepared, opened longitudinally and the length of the vascular necroses (tracheomycosis) caused by the different pathogens was evaluated. For this, the length of the vascular necroses was measured longitudinally on upper and lower directions from the inoculation point for both halves of the longitudinal cut, and the measures of these were statistically analyzed and compared depending on the type of pathogen and product formulation employed. All the data were compared with controls.

At the beginning of the assay, some of the grapevine plants did not sprout or died in the first month after transplantation. These were removed and examined to verify the presence of pre-existing root rot in the plant material related to this circumstance, and analyzed in the laboratory to isolate the possible responsible fungal species. The rest of the plants removed and measured at the end of the assay were finally processed to re-isolate the different pathogenic taxa previously inoculated. Thus, in order to fulfill Koch's postulates, wood fragments approximately 0.5 cm long surrounding the different vascular necroses (1–2 cm around the wounds) were washed, surface sterilized, placed in PDA plates amended with streptomycin sulphate (to avoid bacterial contamination) and incubated at 26 °C in the dark in a culture chamber for 2–3 days.

2.5. Statistical Analyses

Differences in the in vitro mycelial growth inhibition results were assessed by analysis of variance (ANOVA) followed by post hoc comparison of means through Tukey's test at $p < 0.05$ (provided that the homogeneity and homoscedasticity requirements were satisfied, according to the Shapiro–Wilk and Levene tests [42]). In the case of in planta results, the Johnson transformation [43,44] was first used to transform the data to follow a normal distribution, and then descriptive statistics, ANOVA and Tukey's tests of the necrosis lengths were performed. The SPSS Statistics v.25 software was used (IBM; Armonk, NY, USA).

3. Results

Below are shown the results of the assays carried out to test the antifungal capacity of a series of conjugates based on chitosan polymers and certain amino acids, for the control, both in vitro and in plant, of some taxa of the *Botryosphaeriaceae* family involved in the so-called wood diseases in young grapevine plants.

3.1. Mycelial Growth Inhibition Tests

The results of the growth inhibition tests are presented in Figure 2. The performances of the amino acid-only treatments were much lower than those of the treatments based on

COS, either alone or in combination with them (Figures S1–S3). Concerning the dosage of the compounds assayed, higher inhibition was obtained upon increase of the concentration for all treatments.

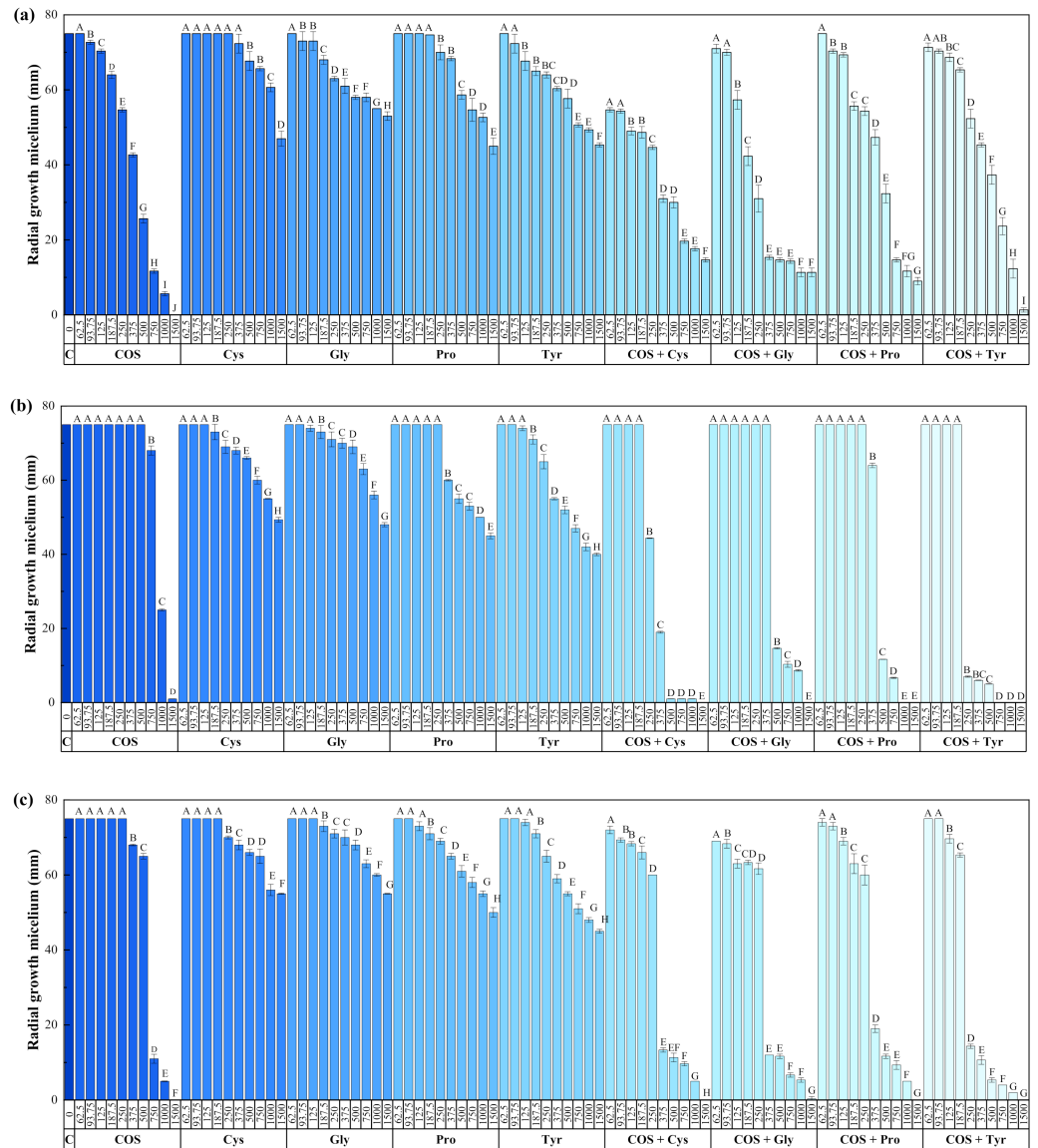


Figure 2. Colony growth values of (a) *N. parvum*, (b) *D. seriata* and (c) *B. dothidea* strains when cultured in PDA plates containing several control products, i.e., chitosan oligomers (COS), cysteine (Cys), glycine (Gly), proline (Pro), tyrosine (Tyr), and the respective COS–amino acid (1:1 *v/v*) conjugate compounds. The same letters above concentrations mean that they are not significantly different at $p < 0.05$. Error bars represent standard deviations.

The effective *in vitro* concentrations are summarized in Table 1 for comparison purposes (effective concentrations for amino acids alone are not presented, provided that full inhibition was not attained even at the highest assayed concentration, so a reliable fitting could not be obtained). In the case of *N. parvum*, a synergistic effect was only observed for COS–Cys and COS–Tyr in the EC_{50} values. Conversely, for *D. seriata* and *B. dothidea*, a synergistic effect was observed for all the COS–amino acid conjugate complexes, particularly evident for COS–Tyr, with estimated synergy factors (SF) of 2.03 and 2.29 in the EC_{50} values and SF of 2.48 and 2.84 in the EC_{90} values, respectively.

Table 1. EC₅₀ and EC₉₀ effective concentrations, expressed in µg·mL⁻¹.

Pathogen	Effective Concentration	COS	COS-Cys	COS-Gly	COS-Pro	COS-Tyr
<i>N. parvum</i>	EC ₅₀	320.9	208.8	417.8	402.9	258.9
	EC ₉₀	967.4	1347.0	1498.5	1439.0	1021.4
<i>D. seriata</i>	EC ₅₀	448.1	297.8	448.5	398.7	254.6
	EC ₉₀	1360.6	774.6	1286.7	1086.5	672.1
<i>B. dothidea</i>	EC ₅₀	425.8	306.2	291.1	316.0	255.1
	EC ₉₀	1339.2	897.9	887.9	907.4	707.7

COS = chitosan oligomers; Cys = cysteine; Gly = glycine; Pro = proline; Tyr = tyrosine.

3.2. In Vivo Tests

After removing, cutting and measuring vascular necroses present in the different treated grafted plants, it was primarily observed that no statistically significant differences were obtained among neither between plant combination (cultivar/rootstock) nor between upper and lower wounds (Figure S4). In fact, in this latter case, the Pearson correlation coefficient was 0.738.

Upon comparison of necrosis lengths in the negative controls (i.e., plants whose wounds were only treated with the bioactive product, with no pathogen inoculation) and positive controls (i.e., plants inoculated only with pathogens), significant differences between pathogens in terms of their aggressiveness were only observed for the lower wound (Table S2). The most aggressive fungus was *N. parvum*, while *D. seriata* showed an intermediate virulence, and *B. dothidea* induced the least necrosis. This can be ascribed to both differences in the wood decay enzymatic activities and in the ability of these fungi to metabolize major grapevine phytoalexins [45,46].

When the effect of the treatments on the infection rates of the three pathogens was studied, significant differences were found between the treated plants and the positive control in the case of *N. parvum* and *B. dothidea* (Table 2). On the other hand, the synergistic behavior between COS and tyrosine observed in vitro (particularly evident for *B. dothidea*) was not reflected in statistically significant differences (compared with single COS treatment) in the plant bioassay at the greenhouse scale.

Table 2. Analysis of variance (ANOVA) of the lengths of vascular necroses for *N. parvum* (left), *B. dothidea* (center) and *D. seriata* (right).

<i>N. parvum</i>	Upper Wound	Lower Wound	<i>B. dothidea</i>	Upper Wound	Lower Wound	<i>D. seriata</i>	Upper Wound	Lower Wound
Positive control	0.848 a	0.895 a	Positive control	0.529 a	0.397 a	Positive control	0.609 a	0.486 a
COS	0.258 b	0.351 b	COS-Tyr	-0.121 b	-0.196 b	COS	0.145 b	0.412 a
COS-Tyr	0.257 b	0.217 b	COS	-0.136 b	-0.236 b	COS + tyr	0.332 ab	0.279 a
Negative control	-1.444 c	-1.210 c	Negative control	-1.444 c	-1.210 c	Negative control	-1.444 c	-1.210 b
Pr > F	<0.0001	<0.0001	Pr > F	<0.0001	<0.0001	Pr > F	<0.0001	<0.0001
Significant	Yes	Yes	Significant	Yes	Yes	Significant	Yes	Yes

Treatments/controls labelled with the same letters are not significantly different at $p < 0.05$.

Finally, in the case of *D. seriata*, significant differences were only observed in the upper wounds, with a better performance of the treatment based solely on COS, an unexpected result on the basis of the effective concentration values reported in Table 1. In the lower wounds, no significant differences were seen, but the COS-Tyr treatment seemed to show a better performance than that based solely on COS, in line with the results of the in vitro tests.

Plants prematurely removed from the bioassay displayed basal rots (due to *Rhizoctonia solani* J.G. Kühn and *Neonectria* spp.) already present in the starting material. Moreover, the rest of the plants of the assay were submitted to Koch' postulates, isolating the previously inoculated pathogens in most (80%) of them.

As previously mentioned, together with the vascular necrosis, during the whole assay period it was observed that many of the grapevine plants exhibited certain foliar symptoms (Figure 1f,g), probably due to a long-dispersal action of phytotoxins produced by the inoculated pathogens. The production of such type of secondary metabolites by these and other GTD-related fungi is well known [7,47–49]. Among these, low molecular weight lipophilic phytotoxins (for example, naphthalenone pentaketides, melleins and polyphenols) produced by the different *Bot* taxa could be responsible for the observed symptoms (i.e., moderate to severe withering and necrotic spots). When analyzing such symptoms, no correlations were observed among either the plants inoculated exclusively with the pathogens and the controls without any fungus or the treated plants, probably due to the basal phytosanitary status of the propagation material, which could also influence the appearance of these foliar symptoms, regardless the treatment assayed.

4. Discussion

4.1. Comparison of the Efficacy of the Treatments

Regarding chitosan only-based treatments, chitosan oligosaccharides (molecular weight < 3000 Da) at a concentration of 1000 $\mu\text{g}\cdot\text{mL}^{-1}$ were reported to completely inhibit the mycelial growth of *D. seriata* and *B. dothidea* when performing in vitro assays [29]. These values are of the same order of magnitude as the EC_{90} values presented herein, so differences may be attributed to the isolate-dependency of the susceptibility profile.

For the same strains of *N. parvum* and *D. seriata*, EC_{90} values of 1270 and 1120.7 $\mu\text{g}\cdot\text{mL}^{-1}$ were attained for COS with molecular weight < 2000 Da in [33]. In this case, differences may be tentatively ascribed to slight differences in the molecular weight, polymerization degree or deacetylation degree of COS, which are known to influence its efficacy against phytopathogenic fungi [50,51].

In relation to non-in vitro bioassays with chitosan, Cobos, Mateos, Alvarez-Perez, Olego, Sevillano, Gonzalez-Garcia, Garzon-Jimeno and Coque [29] reported that 96.8% growth inhibition of *D. seriata* was attained in autoclaved vine shoots using chitosan oligosaccharides, although at a much higher concentration (25 $\text{mg}\cdot\text{mL}^{-1}$). In artificially inoculated plants, the same authors found a significant reduction in the incidence of *D. seriata* when the pruning wounds were treated with chitosan oligosaccharides and other natural compounds, decreasing lipid peroxidation levels and guaiacol peroxidase (GPX) activity (a recognized stress marker). Albeit for different GTD pathogens, Nascimento, Rego and Oliveira [30]—in greenhouse experiments carried on potted grapevine plants (cultivar "Castelão") growing in a substrate artificially infested with *Phaeoconiella chlamydospora* or *Neonectria liriodendri*—observed that foliar sprays of chitosan oligosaccharin (<3 kDa) only reduced the disease incidence of *P. chlamydospora*, but had an effect against *N. liriodendri* similar to that of some selected fungicides (tebuconazole, cyprodinil + fludioxonil and carbendazim + flusilazole).

Concerning aminoacids, cysteine has been reported to have an inhibitory effect on the in vitro mycelial growth of *P. chlamydospora* and *Phaeoacremonium minimum*; at a concentration of 10 mM (that is, 1216 $\mu\text{g}\cdot\text{mL}^{-1}$), an inhibition of 77% for *P. chlamydospora* and 58% for *P. minimum* was attained. The respective EC_{100} values were 15 and 20 mM (1824 and 2432 $\mu\text{g}\cdot\text{mL}^{-1}$) [28]. At a 10 mM concentration, it exhibited a strong inhibition (79–100%) against various strains of *E. lata*, while lower efficacies were observed against other fungal species associated with other grapevine diseases (*P. chlamydospora* and *Phaeoacremonium aleophilum*, *Botryosphaeria parva* and *B. obtusa*, that were inhibited by 63%, 40%, 54% and 40%, respectively) [52].

Regarding analogous polysaccharide-peptide based formulations, little information is available in the literature. The EC_{90} values attained with a COS- ϵ -polylysine conjugate

(507.5, 580.2 and 497.4 $\mu\text{g}\cdot\text{mL}^{-1}$ for *N. parvum*, *D. seriata* and *B. dothidea*, respectively [33]) were better than those attained in this work for the COS–Tyr conjugate (1021.4, 672.1 and 707.7 $\mu\text{g}\cdot\text{mL}^{-1}$, respectively), but—from an economic perspective—the latter formulation would be much more viable (given that the price of ϵ -polylysine is much higher than that of tyrosine: 245 €/100 mg vs. 58 €/100 g). An additional advantage of the COS–Tyr formulation could be its versatility as a crop protection product: EC₅₀ and EC₉₀ values against *Fusarium culmorum* (320 and 1107 $\mu\text{g}\cdot\text{mL}^{-1}$, respectively) were of the same order of magnitude as those reported herein [37].

If the EC₅₀ values for COS and the COS–amino acid conjugate complexes are compared with those reported for chemical fungicides used in GTDs control, it may be observed that the efficacies would be comparable: for example, Pitt, et al. [53] found values in the 360–440, 530–620 and 450 $\mu\text{g}\cdot\text{mL}^{-1}$ range for *N. parvum*, *D. seriata* and *B. dothidea*, respectively, taking data pooled across fungicides (viz. carbendazim, fluazinam, fludioxonil, flusilazole, iprodione, myclobutanil, penconazole, procymidone, pyraclostrobin and tebuconazole) to estimate average EC₅₀ values for isolate sensitivity. Nonetheless, if one considers the excellent EC₅₀ values reported by Olmo, et al. [54] against *N. parvum* and *D. seriata* for tebuconazole (90 and 150 $\mu\text{g}\cdot\text{mL}^{-1}$, respectively) and pyraclostrobin (100 and 250 $\mu\text{g}\cdot\text{mL}^{-1}$, respectively), it becomes apparent that there is still room for improvement in the efficacy of the natural composites.

4.2. Mechanism of Action

A panorama of the molecular mechanisms behind chitosan interactions with plants and fungi has been recently presented in the review paper by Lopez-Moya, et al. [55]. With regard to its role as an antimicrobial agent, it is well established that it can permeabilize fungal plasmatic membranes (triggering intracellular production of ROS and cell death), arrest germination and growth by deprivation of nutrients (which leads to cell wall architecture modification), alter gene expression (e.g., affecting oxidoreductase activity, respiration and transport gene ontology functions), etc.

Regarding the precise function of amino acids in the response of plants to pathogens, it is not well established: on one hand, they are required for growth and metabolism in microorganisms, and on the other hand, careful optimization of composition and concentration can produce antimicrobial effects [56]. Besides this, changes in the contents of amino acids appear to be a common characteristic of plant response to GTDs. For instance, in a recent study of the wood metabolomic responses of wild (*Vitis vinifera* subsp. *sylvestris*) and cultivated grapevine (*V. v.* subsp. *vinifera*) to infection with *N. parvum*, Labois, et al. [57] found that the metabolic response of the former to the infection featured a faster and more intense alteration in primary metabolites in comparison to the latter, accompanied by a higher induction of various resveratrol oligomer contents. Infection by *N. parvum* caused an increase in alanine, β -alanine and glycine, and a decrease in aspartic acid, asparagine and serine.

To the best of the authors' knowledge, no data on the role of tyrosine on GTDs has been published to date. Nonetheless, cysteine has been reported to be involved in signaling, plant resistance and antifungal development [27]. Like other amino acids, cysteine can be transported along the vascular tissues of vines over long distances, and it can induce dramatic alterations in the structural organization of the mycelium (nucleus, mitochondria, vacuoles and cell wall), causing the death of the hyphae [52]. Octave, Amborabé, Luini, Ferreira, Fleurat-Lessard and Roblin [52] hypothesized that the action of cysteine may be based on its ability to interfere with a certain metabolic pathway and also by triggering the secretion of ergosterol, which presents properties of an elicitor.

As regards the mode of action of the conjugate complex, it may be the result of an enhanced additive fungicidal effect per se, and/or via a concurrent action on diverse fungal metabolic sites. In a previous work [37], we also hypothesized that conjugation of COS and Tyr increases the cationic surface charge of COS, enhancing the linkage (through

electrostatic interactions) to the negatively charged site-specific binding receptors on the fungal membrane.

4.3. Significance of the Reported Findings

The three fungal species tested in the present study belong to the *Botryosphaeriaceae* family, a group of polyphagous ascomycetous taxa associated not only with grapevine diseases, but also pathogenic on a vast range of woody plants, specially forestry species [58], stone and pome fruits (i.e., almond, peach, apple, apricot, etc.) [59], and even on woody crops of recent implantation and extension in Spain such as pistachio [60,61]. Furthermore, *D. seriata* and *B. dothidea* have been cited as phytopathogens on apple [62], while *N. parvum* causes avocado dieback [63], *B. dothidea* causes Botryosphaeria blights and cankers on olive trees [64], and as mentioned, the three of them are commonly related to branch cankers on almond trees [54]. Therefore, the findings obtained in the present study may also be applied and extended to other basic Mediterranean crops that usually share these types of pathogens. In fact, many authors have verified that many of the pathogens of crops such as olive, stone fruit or grapevine, share plant hosts during some phase of their life cycle and are isolated repeatedly from adjacent crops [65], resulting in an even higher ecological and economic impact. Thus, any type of research in the control of global and aggressive pathogens such as *B. dothidea* [66] or *N. parvum* [67] is relevant, since the incidence and economic importance of the losses caused by both fungi has been increasing in recent years, especially in grapevine crop due to damage to young plants coming from the nursery. Both taxa tend to have a prolonged latent or endophytic phase [68], which makes their detection very difficult, especially in quarantine inspection surveys, since their symptoms occasionally appear in situations of stress of the plant host. Furthermore, in the nurseries that produce young grafted vine plants in Spain, *N. parvum* is considered one of the main mycoses associated with propagation material [69], being ultimately responsible for the uprooting of thousands of hectares of grapevine plants in the first years after their plantation.

4.4. Limitations of the Study and Further Research

A clear limiting factor in the *in planta* bioassays was the choice of calcium alginate as a dispersion medium to protect the pruning wounds, given that it limited the amount of the bioactive solution that could be incorporated to the matrix to approximately 20% (otherwise gelation was not attained). Considering that the initial concentration of the bioactive solutions was $3000 \mu\text{g}\cdot\text{mL}^{-1}$, the formulations were tested at a concentration of *ca.* $600 \mu\text{g}\cdot\text{mL}^{-1}$, that is, at values closer in many cases to the EC_{50} value than to the EC_{90} one. This would explain why, even though significant differences were observed, a higher degree of protection was not attained. The use of other thickener agents (e.g., pectin, vegetable gums, starches, or haloxyite, which are cheaper than alginate) should be assayed in future studies. Alternatively, more advanced delivery methods, such as the use of lignin nanocarriers (analogous to those recently reported by Wurm's group [70,71] for azoxystrobin, pyraclostrobin, tebuconazole, and boscalid delivery) could overcome the aforementioned limitation.

Since the results obtained here refer only to the reduction of vascular necrosis in artificially inoculated grapevine plants, complementary tests will be required in future multiyear assays to correlate these levels of protection with the intensity and incidence of foliar symptoms, harvest yield, etc., to have a more complete view of the effect of this type of alternative substances.

Another particularly interesting aspect to be considered in follow-up studies would be the inclusion of synthetic chemicals as additional treatments, provided that this would allow direct comparisons with the natural products both in terms of efficacy and cost-effectiveness.

5. Conclusions

Conjugate complexes of chitosan oligomers (with MW < 2 kDa) and amino acids, inspired in plant HDPs, were assayed for their control effects against three *Botryosphaeriaceae* fungi responsible for some of the GTDs. In vitro growth inhibition tests revealed a synergistic effect between COS and the amino acids against two of the pathogens, viz. *D. seriata* and *B. dothidea*, which was not present (or was very weak) in the case of *N. parvum*. The lowest EC₅₀ and EC₉₀ effective concentrations, comparable to those reported for conventional synthetic fungicides used in the control of these mycoses, were obtained for the COS–tyrosine conjugate complex. Hence, this formulation and the one based on COS alone were further assayed for wound protection applications in a greenhouse bioassay conducted on potted grapevines of two varieties (“Tempranillo” on 775P and “Garnacha” on 110R rootstock), which were artificially inoculated with the mentioned pathogenic species. A significant decrease in vascular necrosis severity was observed for *N. parvum* and *B. dothidea*, while the efficacy against *D. seriata* was only statistically significant for the upper wounds. Taking into consideration that the incidence and economic importance of the losses caused by the former two fungi has been increasing in recent years, and that they affect many other woody plants (not only grapevine), the reported formulations may pose a promising alternative to synthetic chemical pesticides for the protection of trunk diseases of woody crops.

6. Patents

The work reported in this manuscript is related to Spanish patents P201931118 and P201831106.

Supplementary Materials: The following are available online at <https://www.mdpi.com/2073-4395/11/2/324/s1>, Figures S1–S3: Sensitivity tests for *N. parvum*, *D. seriata* and *B. dothidea*; Figure S4: Box-plot of the lengths of the vascular necroses in the upper and lower wounds; Table S1: Repetitions for each of the plant/treatment combinations in the greenhouse bioassay; Table S2: ANOVA of lengths of the vascular necroses in the positive and negative controls for the three fungi under study.

Author Contributions: Conceptualization, E.P.-L., J.M.-G. and V.G.-G.; methodology, J.M.-G., J.C.-G. and V.G.-G.; validation, J.C.-G., V.G.-G. and P.M.-R.; formal analysis, J.C.-G., V.G.-G. and P.M.-R.; investigation, L.B.-D., N.L.-L., V.G.-G., J.C.-G., J.M.-G. and P.M.-R.; resources, J.M.-G. and P.M.-R.; data curation, J.C.-G.; writing—original draft preparation, L.B.-D., N.L.-L., V.G.-G., J.C.-G., J.M.-G. and P.M.-R.; writing—review and editing, V.G.-G. and P.M.-R.; visualization, L.B.-D. and N.L.-L.; supervision, V.G.-G. and P.M.-R.; project administration, V.G.-G., J.M.-G. and P.M.-R.; funding acquisition, J.M.-G. and P.M.-R. All authors have read and agreed to the published version of the manuscript.

Funding: This research was funded by Junta de Castilla y León under project VA258P18, with FEDER co-funding, and by Universidad de Zaragoza under project UZ2019-TEC-07.

Informed Consent Statement: Not applicable.

Data Availability Statement: The data presented in this study are available on request from the corresponding author. The data are not publicly available due to their relevance as part of an ongoing PhD Thesis.

Acknowledgments: V.G.-G thanks C. Julián (Plant Protection Unit, CITA) for her technical assistance. L.B.-D. gratefully acknowledges the support of Gregorio Michu in the in vitro tests.

Conflicts of Interest: The authors declare no conflict of interest. The funders had no role in the design of the study; in the collection, analyses, or interpretation of data; in the writing of the manuscript, or in the decision to publish the results.

References

1. Mondello, V.; Songy, A.; Battiston, E.; Pinto, C.; Coppin, C.; Trotel-Aziz, P.; Clement, C.; Mugnai, L.; Fontaine, F. Grapevine Trunk Diseases: A Review of Fifteen Years of Trials for Their Control with Chemicals and Biocontrol Agents. *Plant Dis.* **2018**, *102*, 1189–1217. [[CrossRef](#)]
2. Peil, S.; Beckers, S.J.; Fischer, J.; Wurm, F.R. Biodegradable, lignin-based encapsulation enables delivery of *Trichoderma reesei* with programmed enzymatic release against grapevine trunk diseases. *Mater Today Bio* **2020**, *7*, 100061. [[CrossRef](#)]

3. Gramaje, D.; Urbez-Torres, J.R.; Sosnowski, M.R. Managing Grapevine Trunk Diseases With Respect to Etiology and Epidemiology: Current Strategies and Future Prospects. *Plant Dis.* **2018**, *102*, 12–39. [[CrossRef](#)]
4. Phillips, A.J.L. Botryosphaeria species associated with diseases of grapevines in Portugal. *Phytopathol. Mediterr.* **2002**, *41*, 3–18. [[CrossRef](#)]
5. Taylor, A.; St, J.; Hardy, G.E.; Wood, P.; Burgess, T. Identification and pathogenicity of Botryosphaeria species associated with grapevine decline in Western Australia. *Australas. Plant. Pathology* **2005**, *34*, 34. [[CrossRef](#)]
6. Martos, S.; Andolfi, A.; Luque, J.; Mugnai, L.; Surico, G.; Evidente, A. Production of phytotoxic metabolites by five species of Botryosphaeriaceae causing decline on grapevines, with special interest in the species *Neofusicoccum luteum* and *N. parvum*. *Eur. J. Plant Pathol.* **2008**, *121*, 451–461. [[CrossRef](#)]
7. Andolfi, A.; Mugnai, L.; Luque, J.; Surico, G.; Cimmino, A.; Evidente, A. Phytotoxins Produced by Fungi Associated with Grapevine Trunk Diseases. *Toxins* **2011**, *3*, 1569–1605. [[CrossRef](#)] [[PubMed](#)]
8. Vincenzo, M.; Philippe, L.; Josep, A.; Andreas, K.; Kalman, V.; Fanny, P.; Eric, S.; Cecilia, R.; Laura, M.; Florence, F. Management of grapevine trunk diseases: Knowledge transfer, current strategies and innovative strategies adopted in Europe. *Phytopathol. Mediterr.* **2018**, *57*. [[CrossRef](#)]
9. Del Frari, G.; Gobbi, A.; Aggerbeck, M.R.; Oliveira, H.; Hansen, L.H.; Ferreira, R.B. Fungicides and the Grapevine Wood Mycobiome: A Case Study on Tracheomycotic Ascomycete *Phaeoconiella chlamydospora* Reveals Potential for Two Novel Control Strategies. *Front. Plant. Science* **2019**, *10*. [[CrossRef](#)] [[PubMed](#)]
10. Grozić, K.; Bubola, M.; Poljuha, D. Symptoms and management of grapevine trunk diseases. *J. Cent. Eur. Agric.* **2019**, *20*, 876–890. [[CrossRef](#)]
11. Chacón, J.L.; Gramaje, D.; Izquierdo, P.M.; Martínez, J.; Mena, A. Evaluation of six red grapevine cultivars inoculated with *Neofusicoccum parvum*. *Eur. J. Plant Pathol.* **2020**, *158*, 811–815. [[CrossRef](#)]
12. Martínez-Diz, M.d.P.; Diaz-Losada, E.; Barajas, E.; Ruano-Rosa, D.; Andres-Sodupe, M.; Gramaje, D. Screening of Spanish *Vitis vinifera* germplasm for resistance to *Phaeoconiella chlamydospora*. *Sci. Hortic.* **2019**, *246*, 104–109. [[CrossRef](#)]
13. Gramaje, D.; Alaniz, S.; Abad-Campos, P.; Garcia-Jimenez, J.; Armengol, J. Evaluation of grapevine rootstocks against soilborne pathogens associated with trunk diseases. *Acta Hortic.* **2016**, *1136*, 245–249. [[CrossRef](#)]
14. Guan, X.; Essakhi, S.; Laloue, H.; Nick, P.; Bertsch, C.; Chong, J. Mining new resources for grape resistance against *Botryosphaeriaceae*: A focus on *Vitis vinifera* subsp. *sylvestris*. *Plant Pathol.* **2016**, *65*, 273–284. [[CrossRef](#)]
15. Murolo, S.; Romanazzi, G. Effects of grapevine cultivar, rootstock and clone on esca disease. *Australas. Plant. Pathology* **2014**, *43*, 215–221. [[CrossRef](#)]
16. Travadon, R.; Rolshausen, P.E.; Gubler, W.D.; Cadle-Davidson, L.; Baumgartner, K. Susceptibility of Cultivated and Wild *Vitis* spp. to Wood Infection by Fungal Trunk Pathogens. *Plant Dis.* **2013**, *97*, 1529–1536. [[CrossRef](#)]
17. Martínez-Diz, M.d.P.; Diaz-Losada, E.; Andres-Sodupe, M.; Bujanda, R.; Maldonado-Gonzalez, M.M.; Ojeda, S.; Yacoub, A.; Rey, P.; Gramaje, D. Field evaluation of biocontrol agents against black-foot and Petri diseases of grapevine. *Pest. Manag. Sci.* **2020**. [[CrossRef](#)]
18. Pertot, I.; Caffi, T.; Rossi, V.; Mugnai, L.; Hoffmann, C.; Grando, M.S.; Gary, C.; Lafond, D.; Duso, C.; Thiery, D.; et al. A critical review of plant protection tools for reducing pesticide use on grapevine and new perspectives for the implementation of IPM in viticulture. *Crop. Protect.* **2017**, *97*, 70–84. [[CrossRef](#)]
19. Song, H.-Q.; Fan, Y.; Hu, Y.; Cheng, G.; Xu, F.-J. Polysaccharide-Peptide Conjugates: A Versatile Material Platform for Biomedical Applications. *Adv. Funct. Mater.* **2020**. [[CrossRef](#)]
20. Dos Santos-Silva, C.A.; Zupin, L.; Oliveira-Lima, M.; Vilela, L.M.B.; Bezerra-Neto, J.P.; Ferreira-Neto, J.R.; Ferreira, J.D.C.; de Oliveira-Silva, R.L.; Pires, C.d.J.; Aburjaile, F.F.; et al. Plant Antimicrobial Peptides: State of the Art, In Silico Prediction and Perspectives in the Omics Era. *Bioinf. Biol. Insights* **2020**, *14*. [[CrossRef](#)]
21. Sathoff, A.E.; Samac, D.A. Antibacterial Activity of Plant Defensins. *Mol. Plant-Microbe Interact.* **2019**, *32*, 507–514. [[CrossRef](#)]
22. Su, T.; Han, M.; Cao, D.; Xu, M. Molecular and Biological Properties of Snakins: The Foremost Cysteine-Rich Plant Host Defense Peptides. *J. Fungi* **2020**, *6*, 220. [[CrossRef](#)]
23. Kundu, R. Cationic Amphiphilic Peptides: Synthetic Antimicrobial Agents Inspired by Nature. *Chemmedchem* **2020**, *15*, 1887–1896. [[CrossRef](#)]
24. Srivastava, S.; Dashora, K.; Ameta, K.L.; Singh, N.P.; El-Enshasy, H.A.; Pagano, M.C.; Hesham, A.E.-L.; Sharma, G.D.; Sharma, M.; Bhargava, A. Cysteine-rich antimicrobial peptides from plants: The future of antimicrobial therapy. *Phytother. Res.* **2020**. [[CrossRef](#)] [[PubMed](#)]
25. Ahmad, B.; Yao, J.; Zhang, S.; Li, X.; Zhang, X.; Yadav, V.; Wang, X. Genome-Wide Characterization and Expression Profiling of GASA Genes during Different Stages of Seed Development in Grapevine (*Vitis vinifera* L.) Predict Their Involvement in Seed Development. *Int. J. Mol. Sci.* **2020**, *21*, 1088. [[CrossRef](#)] [[PubMed](#)]
26. Álvarez, C.; Ángeles Bermúdez, M.; Romero, L.C.; Gotor, C.; García, I. Cysteine homeostasis plays an essential role in plant immunity. *New Phytol.* **2012**, *193*, 165–177. [[CrossRef](#)] [[PubMed](#)]
27. Roblin, G.; Octave, S.; Faucher, M.; Fleurat-Lessard, P.; Berjeaud, J.-M. Cysteine: A multifaceted amino acid involved in signaling, plant resistance and antifungal development. *Plant Physiol. Biochem.* **2018**, *129*, 77–89. [[CrossRef](#)] [[PubMed](#)]

28. Roblin, G.; Luini, E.; Fleurat-Lessard, P.; Larignon, P.; Berjeaud, J.-M. Towards a preventive and/or curative treatment of esca in grapevine trunk disease: General basis in the elaboration of treatments to control plant pathogen attacks. *Crop Protect.* **2019**, *116*, 156–169. [[CrossRef](#)]
29. Cobos, R.; Mateos, R.M.; Alvarez-Perez, J.M.; Olego, M.A.; Sevillano, S.; Gonzalez-Garcia, S.; Garzon-Jimeno, E.; Coque, J.J. Effectiveness of Natural Antifungal Compounds in Controlling Infection by Grapevine Trunk Disease Pathogens through Pruning Wounds. *Appl. Environ. Microbiol.* **2015**, *81*, 6474–6483. [[CrossRef](#)]
30. Nascimento, T.; Rego, C.; Oliveira, H. Potential use of chitosan in the control of grapevine trunk diseases. *Phytopathol. Mediterr.* **2007**, *46*, 218–224.
31. Xing, K.; Shen, X.; Zhu, X.; Ju, X.; Miao, X.; Tian, J.; Feng, Z.; Peng, X.; Jiang, J.; Qin, S. Synthesis and *in vitro* antifungal efficacy of oleoyl-chitosan nanoparticles against plant pathogenic fungi. *Int. J. Biol. Macromol.* **2016**, *82*, 830–836. [[CrossRef](#)] [[PubMed](#)]
32. Matei, P.M.; Martín-Ramos, P.; Sánchez-Báscones, M.; Hernández-Navarro, S.; Correa-Guimaraes, A.; Navas-Gracia, L.M.; Rufino, C.A.; Ramos-Sánchez, M.C.; Martín-Gil, J. Synthesis of chitosan oligomers/propolis/silver nanoparticles composite systems and study of their activity against *Diplodia seriata*. *Int. J. Polym. Sci.* **2015**, *2015*, 1–11. [[CrossRef](#)]
33. Buzón-Durán, L.; Martín-Gil, J.; Pérez-Lebeña, E.; Ruano-Rosa, D.; Revuelta, J.L.; Casanova-Gascón, J.; Ramos-Sánchez, M.C.; Martín-Ramos, P. Antifungal agents based on chitosan oligomers, ϵ -polylysine and *Streptomyces* spp. secondary metabolites against three *Botryosphaeriaceae* species. *Antibiotics* **2019**, *8*, 99. [[CrossRef](#)] [[PubMed](#)]
34. Monteiro, C.; Fernandes, H.; Oliveira, D.; Vale, N.; Barbosa, M.; Gomes, P.; Martins, M.C.L. AMP-Chitosan Coating with Bactericidal Activity in the Presence of Human Plasma Proteins. *Molecules* **2020**, *25*, 3046. [[CrossRef](#)]
35. Song, J.; Feng, H.; Wu, M.; Chen, L.; Xia, W.; Zhang, W. Preparation and characterization of arginine-modified chitosan/hydroxypropyl methylcellulose antibacterial film. *Int. J. Biol. Macromol.* **2020**, *145*, 750–758. [[CrossRef](#)]
36. Thappeta, K.R.V.; Vikhe, Y.S.; Yong, A.M.H.; Chan-Park, M.B.; Kline, K.A. Combined Efficacy of an Antimicrobial Cationic Peptide Polymer with Conventional Antibiotics to Combat Multidrug-Resistant Pathogens. *ACS Infectious Diseases* **2020**, *6*, 1228–1237. [[CrossRef](#)]
37. Buzón-Durán, L.; Martín-Gil, J.; Marcos-Robles, J.L.; Fombellida-Villafruela, Á.; Pérez-Lebeña, E.; Martín-Ramos, P. Antifungal Activity of Chitosan Oligomers–Amino Acid Conjugate Complexes against *Fusarium culmorum* in Spelt (*Triticum spelta* L.). *Agronomy* **2020**, *10*, 1427. [[CrossRef](#)]
38. Martín, M.T.; Cobos, R. Identification of Fungi Associated with Grapevine Decline in Castilla y León (Spain). *Phytopathol. Mediterr.* **2007**, *46*, 18–25.
39. Balouiri, M.; Sadiki, M.; Ibsouda, S.K. Methods for *in vitro* evaluating antimicrobial activity: A review. *J. Pharm. Anal.* **2016**, *6*, 71–79. [[CrossRef](#)]
40. Arendrup, M.C.; Cuenca-Estrella, M.; Lass-Flörl, C.; Hope, W. EUCAST technical note on the EUCAST definitive document EDef 7.2: Method for the determination of broth dilution minimum inhibitory concentrations of antifungal agents for yeasts EDef 7.2 (EUCAST-AFST)*. *Clin. Microbiol. Infect.* **2012**, *18*, E246–E247. [[CrossRef](#)]
41. Wadley, F.M. *The evidence required to show synergistic action of insecticides and a short cut in analysis*; U.S. Government Printing Office: Washington, DC, USA, 1945.
42. Glaz, B.; Yeater, K.M. *Applied statistics in agricultural, biological, and environmental sciences*; American Society of Agronomy, Soil Science Society of America, Crop Science Society of America: Madison, WI, USA, 2018. [[CrossRef](#)]
43. Yeo, I.K.; Johnson, R.A. A new family of power transformations to improve normality or symmetry. *Biometrika* **2000**, *87*, 954–959. [[CrossRef](#)]
44. Piepho, H.-P. Data Transformation in Statistical Analysis of Field Trials with Changing Treatment Variance. *Agron. J.* **2009**, *101*, 865–869. [[CrossRef](#)]
45. Sarrocco, S.; Stempien, E.; Goddard, M.-L.; Wilhelm, K.; Tarnus, C.; Bertsch, C.; Chong, J. Grapevine *Botryosphaeria dieback* fungi have specific aggressiveness factor repertory involved in wood decay and stilbene metabolization. *PLoS ONE* **2017**, *12*. [[CrossRef](#)]
46. Bénard-Gellon, M.; Farine, S.; Goddard, M.L.; Schmitt, M.; Stempien, E.; Pensec, F.; Laloue, H.; Mazet-Kieffer, F.; Fontaine, F.; Larignon, P.; et al. Toxicity of extracellular proteins from *Diplodia seriata* and *Neofusicoccum parvum* involved in grapevine *Botryosphaeria dieback*. *Protoplasma* **2014**, *252*, 679–687. [[CrossRef](#)]
47. Reveglia, P.; Savocchia, S.; Billones-Baaijens, R.; Masi, M.; Cimmino, A.; Evidente, A. Phytotoxic metabolites by nine species of *Botryosphaeriaceae* involved in grapevine dieback in Australia and identification of those produced by *Diplodia mutila*, *Diplodia seriata*, *Neofusicoccum australe* and *Neofusicoccum luteum*. *Nat. Prod. Res.* **2018**, *33*, 2223–2229. [[CrossRef](#)]
48. Reveglia, P.; Savocchia, S.; Billones-Baaijens, R.; Masi, M.; Evidente, A. Spencertoxin and spencer acid, new phytotoxic derivatives of diacrylic acid and dipyrindinbutan-1,4-diol produced by *Spencermartinsia viticola*, a causal agent of grapevine *Botryosphaeria dieback* in Australia. *Arabian J. Chem.* **2020**, *13*, 1803–1808. [[CrossRef](#)]
49. Abou-Mansour, E.; Débieux, J.-L.; Ramírez-Suero, M.; Bénard-Gellon, M.; Magnin-Robert, M.; Spagnolo, A.; Chong, J.; Farine, S.; Bertsch, C.; L’Haridon, F.; et al. Phytotoxic metabolites from *Neofusicoccum parvum*, a pathogen of *Botryosphaeria dieback* of grapevine. *Phytochemistry* **2015**, *115*, 207–215. [[CrossRef](#)] [[PubMed](#)]
50. Rahman, M.H.; Hjeljord, L.G.; Aam, B.B.; Sørli, M.; Tronsmo, A. Antifungal effect of chito-oligosaccharides with different degrees of polymerization. *Eur. J. Plant Pathol.* **2014**, *141*, 147–158. [[CrossRef](#)]
51. Younes, I.; Sellimi, S.; Rinaudo, M.; Jellouli, K.; Nasri, M. Influence of acetylation degree and molecular weight of homogeneous chitosans on antibacterial and antifungal activities. *Int. J. Food Microbiol.* **2014**, *185*, 57–63. [[CrossRef](#)] [[PubMed](#)]

52. Octave, S.; Amborabé, B.-E.; Luini, E.; Ferreira, T.; Fleurat-Lessard, P.; Roblin, G. Antifungal effects of cysteine towards *Eutypa lata*, a pathogen of vineyards. *Plant Physiol. Biochem.* **2005**, *43*, 1006–1013. [[CrossRef](#)] [[PubMed](#)]
53. Pitt, W.M.; Sosnowski, M.R.; Huang, R.; Qiu, Y.; Steel, C.C.; Savocchia, S. Evaluation of fungicides for the management of Botryosphaeria canker of grapevines. *Plant Dis.* **2012**, *96*, 1303–1308. [[CrossRef](#)]
54. Olmo, D.; Gramaje, D.; Armengol, J. Evaluation of fungicides to protect pruning wounds from *Botryosphaeriaceae* species infections on almond trees. *Phytopathol. Mediterr.* **2017**, *56*, 77–86.
55. Lopez-Moya, F.; Suarez-Fernandez, M.; Vicente Lopez-Llorca, L. Molecular Mechanisms of Chitosan Interactions with Fungi and Plants. *Int. J. Mol. Sci.* **2019**, *20*, 332. [[CrossRef](#)]
56. Idrees, M.; Mohammad, A.R.; Karodia, N.; Rahman, A. Multimodal Role of Amino Acids in Microbial Control and Drug Development. *Antibiotics* **2020**, *9*, 330. [[CrossRef](#)] [[PubMed](#)]
57. Labois, C.; Wilhelm, K.; Laloue, H.; Tarnus, C.; Bertsch, C.; Goddard, M.-L.; Chong, J. Wood Metabolomic Responses of Wild and Cultivated Grapevine to Infection with *Neofusicoccum parvum*, a Trunk Disease Pathogen. *Metabolites* **2020**, *10*, 232. [[CrossRef](#)] [[PubMed](#)]
58. Batista, E.; Lopes, A.; Alves, A. *Botryosphaeriaceae* species on forest trees in Portugal: Diversity, distribution and pathogenicity. *Eur. J. Plant Pathol.* **2020**, *158*, 693–720. [[CrossRef](#)]
59. Damm, U.; Crous, P.W.; Fourie, P.H. Botryosphaeriaceae as potential pathogens of *Prunus* species in South Africa, with descriptions of *Diplodia africana* and *Lasiodiplodia plurivora* sp. nov. *Mycologia* **2007**, *99*, 664–680. [[CrossRef](#)]
60. Sohrabi, M.; Mohammadi, H.; León, M.; Armengol, J.; Banihashemi, Z. Fungal pathogens associated with branch and trunk cankers of nut crops in Iran. *Eur. J. Plant Pathol.* **2020**, *157*, 327–351. [[CrossRef](#)]
61. Moral, J.; Morgan, D.; Trapero, A.; Michailides, T.J. Ecology and Epidemiology of Diseases of Nut Crops and Olives Caused by *Botryosphaeriaceae* Fungi in California and Spain. *Plant Dis.* **2019**, *103*, 1809–1827. [[CrossRef](#)]
62. Ahmad, H.; K, V.; K, R.; Bhat, A.; Shah, A. Study of bio-fabrication of iron nanoparticles and their fungicidal property against phytopathogens of apple orchards. *IET Nanobiotechnol.* **2016**, *11*, 230–235. [[CrossRef](#)]
63. Arjona-Girona, I.; Ruano-Rosa, D.; López-Herrera, C.J. Identification, pathogenicity and distribution of the causal agents of dieback in avocado orchards in Spain. *Span. J. Agric. Res.* **2019**, *17*, e1003. [[CrossRef](#)]
64. Moral, J.; Agustí-Brisach, C.; Pérez-Rodríguez, M.; Xaviér, C.; Raya, M.C.; Rhouma, A.; Trapero, A. Identification of fungal species associated with branch dieback of olive and resistance of table cultivars to *Neofusicoccum mediterraneum* and *Botryosphaeria dothidea*. *Plant Dis.* **2017**, *101*, 306–316. [[CrossRef](#)] [[PubMed](#)]
65. Gramaje, D.; Agustí-Brisach, C.; Pérez-Sierra, A.; Moralejo, E.; Olmo, D.; Mostert, L.; Damm, U.; Armengol, J. Fungal trunk pathogens associated with wood decay of almond trees on Mallorca (Spain). *Persoonia Mol. Phylogeny Evol. Fungi* **2012**, *28*, 1–13. [[CrossRef](#)] [[PubMed](#)]
66. Marsberg, A.; Kemler, M.; Jami, F.; Nagel, J.H.; Postma-Smidt, A.; Naidoo, S.; Wingfield, M.J.; Crous, P.W.; Spatafora, J.W.; Hesse, C.N.; et al. Botryosphaeria dothidea: A latent pathogen of global importance to woody plant health. *Mol. Plant Pathol.* **2017**, *18*, 477–488. [[CrossRef](#)] [[PubMed](#)]
67. Urbez-Torres, J.R. The status of *Botryosphaeriaceae* species infecting grapevines. In *Phytopathologia Mediterranea*; University of Florence: Florence, Italy, 2011; Volume 50, pp. 5–45.
68. Slippers, B.; Wingfield, M.J. *Botryosphaeriaceae* as endophytes and latent pathogens of woody plants: Diversity, ecology and impact. *Fungal Biol. Rev.* **2007**, *21*, 90–106. [[CrossRef](#)]
69. Gramaje, D.; Armengol, J. Fungal Trunk Pathogens in the Grapevine Propagation Process: Potential Inoculum Sources, Detection, Identification, and Management Strategies. *Plant Dis.* **2011**, *95*, 1040–1055. [[CrossRef](#)] [[PubMed](#)]
70. Fischer, J.; Beckers, S.J.; Yiamsawas, D.; Thines, E.; Landfester, K.; Wurm, F.R. Targeted Drug Delivery in Plants: Enzyme-Responsive Lignin Nanocarriers for the Curative Treatment of the Worldwide Grapevine Trunk Disease Esca. *Adv. Sci.* **2019**, *6*. [[CrossRef](#)]
71. Machado, T.O.; Beckers, S.J.; Fischer, J.; Müller, B.; Sayer, C.; de Araújo, P.H.H.; Landfester, K.; Wurm, F.R. Bio-Based Lignin Nanocarriers Loaded with Fungicides as a Versatile Platform for Drug Delivery in Plants. *Biomacromolecules* **2020**, *21*, 2755–2763. [[CrossRef](#)] [[PubMed](#)]

ARTÍCULO 2: “Assessment of conjugate complexes of chitosan and *Urtica dioica* or *Equisetum arvense* extracts for the control of grapevine trunk pathogens” *Agronomy*, 2021, 11(5), 976; <https://doi.org/10.3390/agronomy11050976>; Q1 (JCR, Science Edition – AGRONOMY). JIF₂₀₂₁ = 3,949. 16 citas recibidas (CrossRef), 14 citas recibidas (WOS).



agronomy

an Open Access Journal by MDPI



Assessment of Conjugate Complexes of Chitosan and *Urtica dioica* or *Equisetum arvense* Extracts for the Control of Grapevine Trunk Pathogens

Natalia Langa-Lomba; Laura Buzón-Durán; Pablo Martín-Ramos; José Casanova-Gascón; Jesús Martín-Gil; Eva Sánchez-Hernández; Vicente González-García

Agronomy 2021, Volume 11, Issue 5, 976

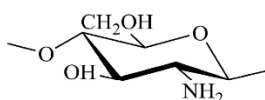
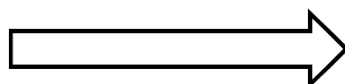
Horsetail
(*Equisetum arvense*)



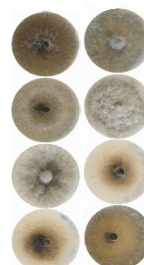
Nettle
(*Urtica dioica*)



Efficacy of their **conjugate complexes with chitosan oligomers** for the eco-friendly control of **8 Botryosphaeriaceae taxa**



D. seriata
N. parvum
B. dothidea
D. iberica
D. coryli
D. sarmentorum
D. viticola
D. mutila



Article

Assessment of Conjugate Complexes of Chitosan and *Urtica dioica* or *Equisetum arvense* Extracts for the Control of Grapevine Trunk Pathogens

Natalia Langa-Lomba^{1,2}, Laura Buzón-Durán³, Pablo Martín-Ramos¹ , José Casanova-Gascón^{1,*} , Jesús Martín-Gil³ , Eva Sánchez-Hernández³ and Vicente González-García²

¹ Instituto Universitario de Investigación en Ciencias Ambientales de Aragón (IUCA), EPS, Universidad de Zaragoza, Carretera de Cuarte s/n, 22071 Huesca, Spain; natalialangalomba@gmail.com (N.L.-L.); pmr@unizar.es (P.M.-R.)

² Plant Protection Unit, Agrifood Research and Technology Centre of Aragón, Instituto Agroalimentario de Aragón—IA2 (CITA-Universidad de Zaragoza), Avda. Montañana 930, 50059 Zaragoza, Spain; vgonzalezg@aragon.es

³ Department of Agricultural and Forestry Engineering, ETSIIAA, Universidad de Valladolid, Avenida de Madrid 44, 34004 Palencia, Spain; laura.buzon@uva.es (L.B.-D.); mgil@iaf.uva.es (J.M.-G.); eva.sanchez.hernandez@uva.es (E.S.-H.)

* Correspondence: jcasan@unizar.es; Tel.: +34-9742-39339



Citation: Langa-Lomba, N.; Buzón-Durán, L.; Martín-Ramos, P.; Casanova-Gascón, J.; Martín-Gil, J.; Sánchez-Hernández, E.; González-García, V. Assessment of Conjugate Complexes of Chitosan and *Urtica dioica* or *Equisetum arvense* Extracts for the Control of Grapevine Trunk Pathogens. *Agronomy* **2021**, *11*, 976. <https://doi.org/10.3390/agronomy11050976>

Academic Editors: Beatriz Gámiz and Essaid Ait Barka

Received: 27 March 2021

Accepted: 12 May 2021

Published: 14 May 2021

Publisher's Note: MDPI stays neutral with regard to jurisdictional claims in published maps and institutional affiliations.



Copyright: © 2021 by the authors. Licensee MDPI, Basel, Switzerland. This article is an open access article distributed under the terms and conditions of the Creative Commons Attribution (CC BY) license (<https://creativecommons.org/licenses/by/4.0/>).

Abstract: In the work presented herein, we analyze the efficacy of three basic substances that comply with European Regulation (EC) No 1107/2009, namely chitosan, horsetail (*Equisetum arvense* L.) and nettle (*Urtica dioica* L.), for the control of grapevine trunk diseases (GTDs) in organic farming. The *E. arvense* and *U. dioica* aqueous extracts, prepared according to SANCO/12386/2013 and SANTE/11809/2016, have been studied by gas chromatography–mass spectrometry (GC-MS), identifying their main active constituents. The three basic substances, either alone or in combination (forming conjugate complexes), have been tested in vitro against eight *Botryosphaeriaceae* species, and in vivo, in grafted plants artificially inoculated with *Neofusicoccum parvum* and *Diplodia seriata*. A clear synergistic behavior between chitosan and the two plant extracts has been observed in the mycelial growth inhibition tests (resulting in EC₉₀ values as low as 208 µg·mL⁻¹ for some of the isolates), and statistically significant differences have been found in terms of vascular necroses lengths between treated and non-treated plants, providing further evidence of aforementioned synergism in the case of *D. seriata*. The reported data supports the possibility of extending the applications of these three basic substances in Viticulture beyond the treatment of mildew.

Keywords: basic substances; *Botryosphaeriaceae*; chitosan; fungicide; GTDs; horsetail; nettle; *Vitis vinifera*

1. Introduction

Phytofungicides are receiving increasing attention as an alternative to synthetic fungicides for the management of many fungal plant diseases [1,2], due to their advantages in terms of safety, easy biodegradability, environmental friendliness and low toxicity.

In the European Union, some of the active substances allowed in organic production (viz. bio-sourced and traditional botanical extracts, light supports/aids and plant defense enhancers), have been approved as ‘basic substances’ under the EU plant protection products regulation (Article 23 of (EC) No 1107/2009) [3]. These basic substances are listed in Part C of the Annex to Regulation 540/2011, and include *Equisetum arvense* L., chitosan hydrochloride, *Urtica* spp., *Salix* spp. cortex, mustard seeds powder and *Allium cepa* L. bulb extract, among others.

Chitosan exhibits antimicrobial properties, but also functions as an elicitor, stimulating natural defense mechanisms [4]. The accepted and potential mechanisms of action behind its antimicrobial properties are thoroughly discussed in the review paper by Ma, et al. [5].

According to SANCO/12388/2013, it can be used in water solution for application on various crops, including 'fruit berries and small fruit'.

Horsetail (*E. arvense*) was the first approved basic substance, in 2014. A complex mixture of biologically-active carbohydrates [6], flavonoids [7] and antioxidants [8] can be obtained from its dried aerial parts. Silicic, tartaric, protocatechuic and caffeic acids, as well as apigenin, kaempferol and isoquercitrin have been found in its extracts [9–11]. Horsetail can be used in accordance with SANCO/12386/2013. In the particular case of *Vitis vinifera* L., discussed in this work, Appendix II includes its use as a fungicide for the control of downy (*Plasmopara viticola* (Berk. & M.A.Curtis) Berl. & De Toni) and powdery (*Erysiphe necator* (Schwein.) Burrill) mildews by foliar application, but extensions of its use against other fungal diseases on vegetable crops and horticulture are being analyzed [12].

More recently, Commission Implementing Regulation (EU) 2017/419 approved *Urtica* spp. as a basic substance. Its biological activity has been referred to its content in acetic, chlorogenic and formic acids, rutin, lecithin and L-prunasin [13]. Review report SANTE/11809/2016 contemplates its use in grapevine to control downy mildew by foliar spraying.

Regarding the applicability of these three basic substances as natural antifungal products for crop-protection, that of chitosan is well-established, as discussed in a recent review by Mukhtar Ahmed, et al. [14]. There are also studies on the antimicrobial properties of extracts from *E. arvense* [15,16] and other *Equisetum* spp. [10,17–19], and *Urtica* spp. extracts [20–24].

Nonetheless, to the best of the authors' knowledge, while chitosan has been tested against grapevine trunk diseases (GTDs) in various studies [25–27], the other two basic substances have not (the application of *E. arvense* extracts against fungal pathogens in relation to grapevine has been limited to assays against *P. viticola* [28] and ochratoxigenic moulds [29]). Taking into consideration that an enhanced antifungal activity generally results from the formation of conjugate complexes between chitosan and other substances of natural origin [30–32], and that the legal framework would place no obstacles to a combined use of already approved basic substances, this possibility deserves to be explored, since it can be instrumental in controlling GTDs, which are among the main challenges facing modern Viticulture [33].

Even though some of GTDs-associated problems have been described for at least a century, from the 1990s there has been a notable advance in unraveling the etiology and epidemiology of a series of complex syndromes first collectively known as grapevine esca [34]. Despite the numerous advances made in the generation of knowledge about this type of pathologies, in the last 25–30 years the incidence and economic losses in the sector due to these mycoses have not stopped increasing [35]. At present, it is commonly accepted that there are several factors that are influencing the advance of this type of phytopathological problems in the vineyard, highlighting above all the changes in cultural practices, the prohibition of certain fungicidal substances and the high demand for propagation material. Concerning current approaches employed to prevent and control these pathologies, Mondello, et al. [33] summarized, in an extensive revision, the different trials and strategies assayed in the last 25 years to find and make available to the market different GTD control strategies, based on a wide-range of organic and inorganic compounds, both synthetic and natural, and on biocontrol agents (BCAs). Some of these approaches have included natural compounds, just in the same way as the ones assayed in the present work.

The aim of the study presented herein has been to explore the effectiveness of aforementioned three basic substances and their conjugate complexes against certain GTDs, with a view to providing scientific evidence to support their extension to other applications in Viticulture beyond the treatment of diseases that affect the green organs.

2. Materials and Methods

2.1. Fungal Isolates

The eight fungal isolates employed in the study represented some of the main *Botryosphaeriaceae* taxa associated with the so-called Botryosphaeria dieback/Black Dead Arm disease in Spain (Table 1) and were supplied as lyophilized vials (later reconstituted and refreshed as PDA subcultures) by the Agricultural Technological Institute of Castilla and Leon (ITACYL, Valladolid, Spain).

Table 1. Fungal isolates used in the study.

Code	Isolate	Binomial Nomenclature	Geographical Origin	Host/Date
ITACYL_F098	Y-084-01-01a	<i>Diplodia seriata</i> De Not.	Spain (DO Toro)	Grapevine (Tempranillo) 2004
ITACYL_F111	Y-091-03-01c	<i>Neofusicoccum parvum</i> (Pennycook & Samuels) Crous, Slippers & A.J.L.Phillips	Spain (Navarra, nursery)	Grapevine (Verdejo) 2006
ITACYL_F141	Y-127-02-01	<i>Botryosphaeria dothidea</i> (Moug.) Ces. & De Not.	Spain (Galicia)	Grapevine 2005
ITACYL_F066	T-046-05-3B	<i>Dothiorella iberica</i> A.J.L.Phillips, J.Luque & A.Alves	Spain	Grapevine (Tempranillo) 2009
ITACYL_F187	Y-291-24-01	<i>Diplodia coryli</i> Fuckel	Spain (Gordoncillo, León)	Grapevine (Prieto Picudo) 2010
ITACYL_F081	Y-051-04-03a	<i>Dothiorella sarmentorum</i> (Fr.) A.J.L.Phillips, A.Alves & J.Luque	Spain (DO Tierra de León)	Grapevine (Prieto Picudo) 2004
ITACYL_F118	Y-103-08-01	<i>Dothiorella viticola</i> A.J.L.Phillips & J.Luque	Spain (Extremadura)	Grapevine 2004
ITACYL_F080	Y-050-05-01c	<i>Diplodia mutila</i> (Fr.) Mont.	Spain (DO Ribera de Duero)	Grapevine 2004

2.2. Reagents and Preparation of Chitosan Oligomers and Bioactive Formulations

Chitosan (CAS 9012-76-4; high MW: 310,000–375,000 Da) was supplied by Hangzhou Simit Chem. & Tech. Co. (Hangzhou, China). Citric acid (CAS 77-92-9), sodium alginate (CAS 9005-38-3) and calcium carbonate (CAS 471-34-1) were purchased from Sigma-Aldrich Química (Madrid, Spain). Neutrase™ 0.8 L enzyme was supplied by Novozymes A/S (Bagsværd, Denmark). Potato dextrose agar (PDA) was purchased from Becton Dickinson (Bergen County, NJ, USA). For the preparation of the *E. arvense* and *U. dioica* extracts, European Pharmacopoeia certified dry plants were purchased from El Antiguo Herbolario (Alicante, Spain).

Chitosan oligomers (COS) were prepared according to the procedure previously reported in [31]. The obtaining of the *E. arvense* and *U. dioica* extracts was conducted according to Appendix I in SANCO/12386/2013 and SANTE/11809/2016, respectively. In short, horsetail extract was obtained by water decoction: 200 g of dry plant were macerated in 10 L of water for 30 min (soaking) and then boiled for 45 min. After cooling down, the decoction was filtrated and further diluted 10-fold with water, to obtain a final concentration of 2000 µg/mL. In the case of nettle extract, dry nettle leaves (15 g/L) were macerated 3 to 4 days at 20 °C, followed by filtering and dilution of the filtrate to obtain a final concentration of 2000 µg/mL.

The COS–nettle extract and COS–horsetail extract complexes were obtained by mixing of the respective solutions in a 1:1 (*v/v*) ratio. The mixture was then sonicated for 15 min in five 3-min pulses (so that the temperature did not exceed 60 °C) using a probe-type ultrasonicator (model UIP1000hdT; Hielscher Ultrasonics, Teltow, Germany; 1000 W, 20 kHz).

Infrared spectroscopy was used to confirm the formation of the conjugate complexes (see supporting information).

2.3. Horsetail and Nettle Extracts Characterization

Taking into consideration that materials of plant origin are usually characterized by a high variability of phytochemical composition, resulting from both genetic and environmental variability (due to the influence of weather and soil fertility on the content of active substances), and that extraction procedures also influence the content of bioactive compounds, the aqueous plant extracts were characterized by gas chromatography-mass spectrometry (GC-MS) at the Research Support Services (STI) at Universidad de Alicante (Alicante, Spain). A gas chromatograph model 7890A coupled to a quadrupole mass spectrometer model 5975C (both from Agilent Technologies, Santa Clara, CA, USA) was used. The chromatographic conditions were: injection volume = 1 μ L; injector temperature = 280 $^{\circ}$ C, in splitless mode; initial oven temperature = 60 $^{\circ}$ C, 2 min, followed by ramp of 10 $^{\circ}$ C/min up to a final temperature of 300 $^{\circ}$ C, 15 min. The chromatographic column used for the separation of the compounds was an Agilent Technologies HP-5MS UI of 30 m length, 0.250 mm diameter and 0.25 μ m film. The mass spectrometer conditions were: temperature of the electron impact source of the mass spectrometer = 230 $^{\circ}$ C and of the quadrupole = 150 $^{\circ}$ C; ionization energy = 70 eV. NIST11 library was used for compound identification.

2.4. In Vitro Tests of Mycelial Growth Inhibition

The fungicidal potential of the different compounds was determined employing an agar dilution method [36]; briefly, aliquots of stock solutions of each product combination were incorporated onto the PDA medium to concentrations in the 62.5–1500 μ g·mL⁻¹ range. Then, mycelial plugs (5 mm in diam.) of each pathogen coming from the margin of 7-day-old PDA cultures were transferred to plates incorporating the above-mentioned concentrations for each compound (3 plates per treatment/concentration, with 2 replicates) and incubated for 6 days (in the case of *N. parvum* and *D. seriata*) or 7 days (for the other six fungi) at 25 $^{\circ}$ C in the dark, which was the amount of time needed for the isolates to reach the Petri dish border in the control plates (which consisted of PDA medium without any amendment). Thus, a total of 2400 plates were scored and analyzed as a result of having tested five treatments (COS, *E. arvense* extract, *U. dioica* extract, COS-*E. arvense* conjugate complex and COS-*U. dioica* conjugate complex) at 10 concentrations per treatment against eight fungal pathogens.

Mycelial growth rates were determined by calculating the average diameter of 2 perpendicular colony axes for each replicate. Growth inhibition of each treatment and concentration was calculated and compared with controls at the end of the incubating period according to the formula:

$$((d_c - d_t))/d_c \times 100 \quad (1)$$

where d_c and d_t represent the average diameters of the fungal colony of the control and the treated fungal colony, respectively.

Results were also expressed as both EC₅₀ and EC₉₀ effective concentrations, estimated by means of PROBIT analysis in R statistical software [37].

2.5. Greenhouse Bioassays in Grafted Plants

Together with the experiments of mycelial growth inhibition in vitro, bioassays with the mentioned basic substances and their conjugate complexes (which comply with EU regulation) were performed in living young grapevine plants in order to scale the protective capabilities of these compounds against two *Botryosphaeriaceae* species responsible for grapevine trunk diseases (GTDs). *Neofusicoccum parvum* and *D. seriata* were then selected on the basis of their prevalence/frequency of isolation in Spain and adjacent areas [38], especially in young grapevine plants coming from nurseries [39]. In summary, potted plants were artificially infected with the two mentioned pathogens, treated simultane-

ously with the different conjugate complexes and, finally, protection effects were analyzed from the comparison of the vascular lesions produced after the different treatments tested with the different controls. Briefly, plant material consisted of 47 plants each of cultivars “Tempranillo” (CL. 32 clone) (2-years old) and “Garnacha” (VCR3 clone) (one year old) grafted on 775P and 110R rootstocks, respectively. Plants were grown on 3.5 L plastic pots containing a mixed substrate of moss peat and sterilized natural soil (75:25), incorporating slow release fertilizer when needed. Plants were maintained in the greenhouse with drip irrigation and anti-weed ground cover for six months (June–December 2020). One week after placing them in the greenhouse, grapevine plants were inoculated with the mentioned two *Botryosphaeriaceae* taxa together with either COS, COS-nettle or COS-horsetail treatments simultaneously. Five repetitions were arranged for each pathogen/control product and plant combination (cultivar/rootstock), together with 4 positive controls per pathogen and cultivar plus 3 negative controls (incorporating only the bioactive product) for each treatment (Table S1). Inoculations of both pathogens and control products were carried out directly on the trunk of the living plants at two sites per plant stand (separated a minimum of 5 cm among them) below the grafting point and not reaching the root crown. For the pathogens, agar plugs coming from 5-days-old fresh PDA cultures of each species were used as fungal inoculum. In the mentioned two inoculation points of each grapevine plant, slits (made up with a scalpel) of approx. 3 mm in diameter and 0.5 cm deep were done. After this, 0.5 cm diameter agar plugs were inoculated and placed in such a way that the mycelium was in contact with vascular tissue in the stem. Calcium alginate beads served as dispersal matrix, including the different control products and conjugates assayed, and beads were placed at both sides of the agar plug. For this, beads were prepared as follows; each control product was added to a 3% sodium alginate solution in a 2:8 ratio (20 mL compound/80 mL sodium alginate). Then, this solution was dispensed drop by drop onto a 3% calcium carbonate solution to spherify (polymerize) in beads of 0.4–0.6 cm diameter containing the different control treatments. Finally, both agar plugs and beads were covered with cotton soaked in sterile bi-distilled water and sealed with Parafilm™ tape. During the assay period, application of copper (cuprous oxide 75%, Cobre Nordox™ 75 WG) to control downy mildew outbreaks was performed in mid-July, together with a first sprouting (followed by periodic sprouting). Grapevine plants were visually examined weekly during the whole assay period for the presence foliar symptoms including both inter-nerval and nerval necroses. After six months in the greenhouse, plants were removed and two sections of the inoculated stems between the grafting point and the root crown were prepared, sectioned longitudinally and the length of the vascular necroses (tracheomycosis) caused by the different pathogens evaluated. Thus, the length of the vascular necroses was measured longitudinally on upper and lower directions from the inoculation point for both halves of the longitudinal cut, and the average measures of these statistically analyzed and compared depending on the type of pathogen and product formulation employed. All the data were compared with controls. Finally, grapevine plants removed and measured at the end of the assay were also processed to re-isolate the different pathogenic taxa previously inoculated. Thus, in order to fulfill Koch’s postulates, 0.5 cm long wood chips exhibiting vascular necroses (1–2 cm around the wounds) were washed, surface sterilized, placed in PDA plates amended with streptomycin sulphate (to prevent bacterial contamination) and incubated at 26 °C in the dark in a culture chamber for 2–3 days.

2.6. Statistical Analyses

Data obtained in the in vitro mycelial growth inhibition tests were assessed by analysis of variance (ANOVA) followed by post hoc comparison of means through Tukey’s test at $p < 0.05$ (provided that the homogeneity and homoscedasticity requirements were satisfied, according to the Shapiro–Wilk and Levene tests). In the case of greenhouse assay results, since the normality and homoscedasticity requirements were not met, the

Kruskal-Wallis non-parametric test was used instead, with Conover-Iman test for post hoc multiple pairwise comparisons. R statistical software was used [37].

3. Results

3.1. Horsetail and Nettle Extracts

The spectra of the aqueous extracts for the two plant species are presented in Figure 1.

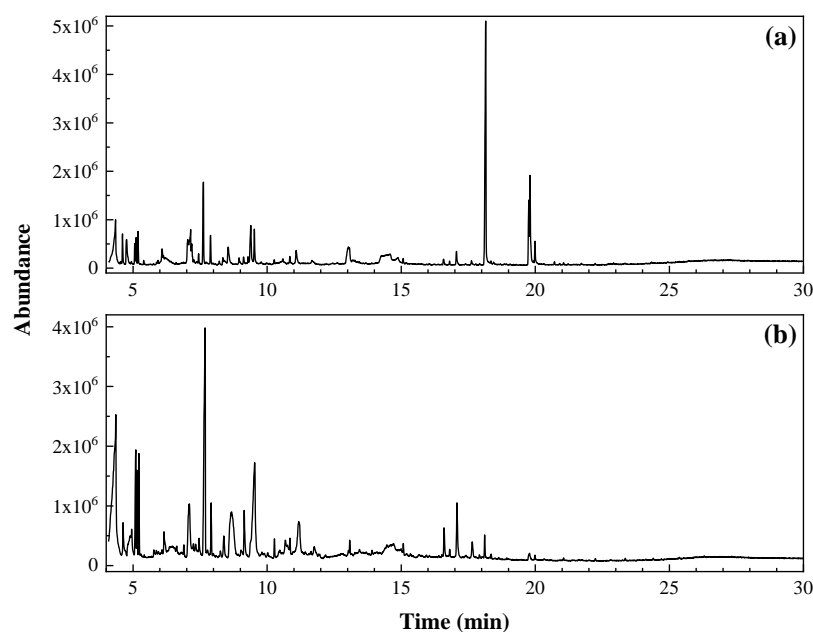


Figure 1. GC/MS spectra of (a) *E. arvensis* and (b) *U. dioica* aqueous extracts.

The main constituents of *E. arvensis* aqueous extract were: *n*-hexadecanoic acid or palmitic acid (18.3%), 2-furanmethanol or α -furylcarbinol (9.1%), oleic acid (5.9%), cyclopropyl carbinol (5.0%), 1,6-anhydro- β -D-glucopyranose or levoglucosan (4.1%), 4-oxo-pentanoic acid or levulinic acid (3.9%), 1-bromo-7-(tetrahydro-2-pyraniloxy)heptane (3.8%), (*Z,Z*)-9,12-octadecadienoic acid or *cis*-linoleic acid (3.7%), 3-deoxy-d-mannonic lactone (3.6%), dihydroxyacetone (2.8%), 2-ethyl-5-methyl-tetrahydrofuran (2.7%), 5-hydroxymethylfurfural (2.3%) and dihydro-4-hydroxy-2(3H)-furanone (2.2%).

Regarding *U. dioica* aqueous extract, the main phytoconstituents were found to be: 2-furanmethanol (16.7%), *N*-methyl-1,3-propanediamine (10.1%), thiazole (8.9%), dihydro-4-hydroxy-2(3H)-furanone (6.4%), tetrahydro-2H-pyran-2-methanol (4.1%), 4,5-dihydro-2-methyl-1H-imidazole (2.9%), (*S*)-2-hydroxy-2-methyl-butanedioic acid or L-citramalic acid (2.3%), 3-deoxy-d-mannonic lactone (2.2%), 2-hydroxy-2-cyclopenten-1-one (2.0%) and *N*-[2-(4-morpholinyl)ethyl]- α -oxo-1H-indole-3-acetamide (2.0%).

A more detailed analysis of their chemical composition is presented in Tables S2 and S3, together with a comparison with other phytochemical analyses reported in the literature for the extracts from these two plants.

3.2. In Vitro Efficacy

Fungal growth tests for *E. arvensis* and *U. dioica* extracts-alone (data not shown) led to very low inhibition percentages (below 25% in all cases). More promising results of growth inhibition were observed in tests employing treatments based on COS, either alone or in combination with the plant aqueous extracts (Figure 2, Figures S3–S5). In these tests, it was observed that, concerning the amount of bioactive compound, the higher the dosage assayed, the higher the growth inhibition obtained for all treatments, with significant differences among concentrations. Together with this, a synergistic effect was observed when conjugate complexes were employed instead of the stand-alone basic substances: while full inhibition was observed for all pathogens for COS at a concentration of

1500 $\mu\text{g}\cdot\text{mL}^{-1}$ (except for *D. mutila*, for which full inhibition was reached at 1000 $\mu\text{g}\cdot\text{mL}^{-1}$), complete fungal growth inhibition was attained at noticeably lower concentrations (ranging from 250 to 1500 $\mu\text{g}\cdot\text{mL}^{-1}$, depending on the treatment and isolate) for the COS-plant extracts conjugate complexes. Moreover, the results showed that pathogens such as *D. viticola* or *D. mutila* were much more sensitive to the action of the conjugate complexes than the rest of the species tested: for these two taxa, noticeable reductions in mycelial growth were detected at doses of around 250 $\mu\text{g}\cdot\text{mL}^{-1}$. On the other hand, differences were also observed in the ability to control fungal growth between the two types of conjugates, at least for some of the pathogens: species such as *D. iberica* or *D. coryli* were found to be more sensitive to the action of the COS-*E. arvense* conjugate than to the COS-*U. dioica* treatment, both in terms of the level of reduction of growth rates at the same concentrations and in terms of the lethal dose.

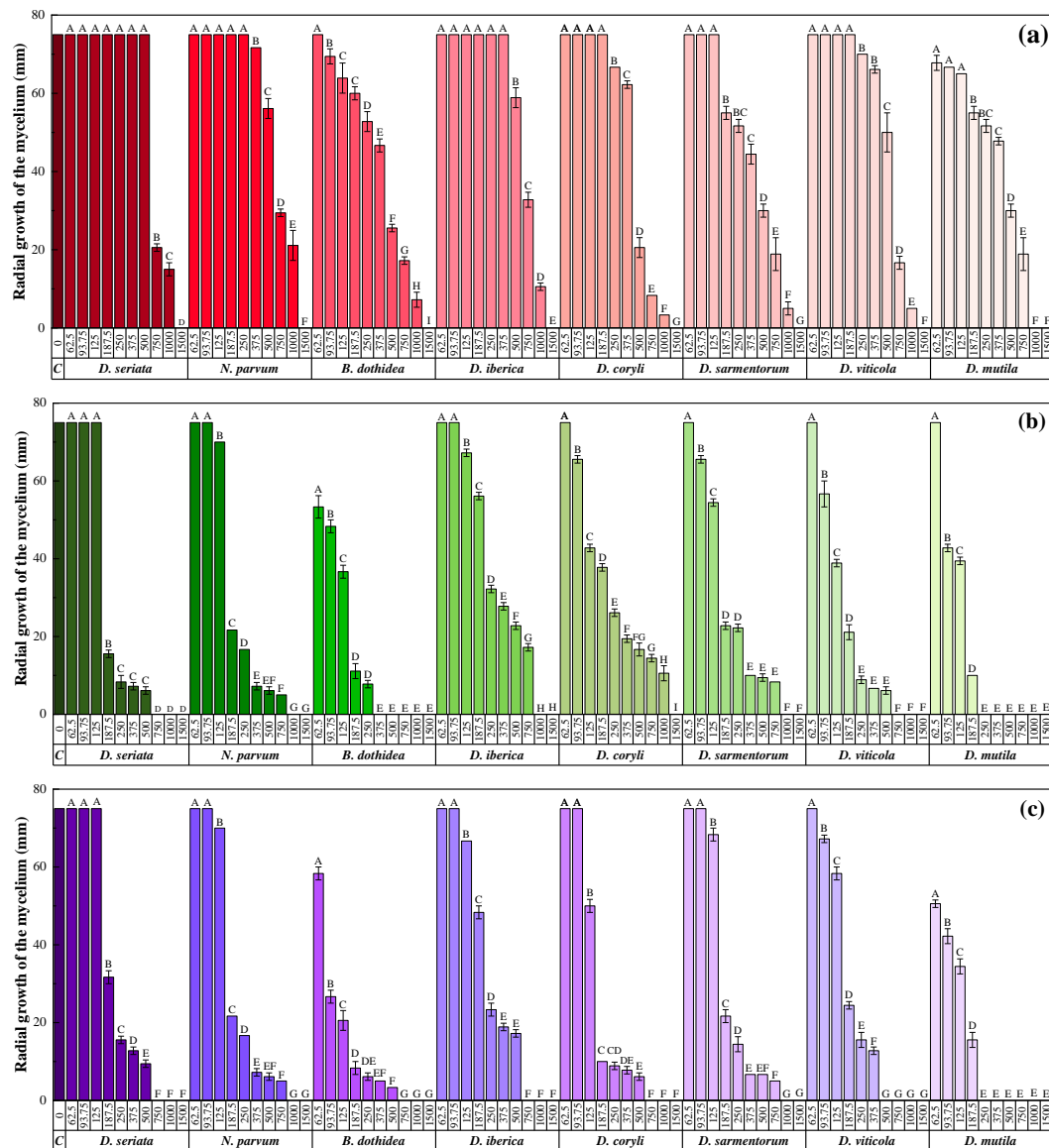


Figure 2. Radial growth of the mycelium for the eight *Botryosphaeriaceae* species under study obtained in in vitro tests conducted in PDA medium with different concentrations (62.5, 93.75, 125, 187.5, 250, 375, 500, 750, 1000 and 1500 $\mu\text{g}\cdot\text{mL}^{-1}$) of: (a) chitosan oligomers (COS); (b) COS-*U. dioica* extracts conjugate complex; and (c) COS-*E. arvense* extracts conjugate complex. The same letters above concentrations mean that they are not significantly different at $p < 0.05$. Error bars represent standard deviations. 'C' in the leftmost column refers to the control (PDA-only, without any amendment) plates. Only one control plate is plotted for the sake of readability, although there was one control plate per isolate (as shown in the bottom row of Figures S3–S5).

To facilitate comparisons between treatments, the effective in vitro concentrations are summarized in Table 2 (effective concentrations for the *E. arvense* and *U. dioica* extracts alone are not presented, provided that—as mentioned above—full inhibition was not attained even at the highest assayed concentration, so a reliable fitting could not be obtained). In line with the observations made upon comparison of the series of compound dosages (Figure 2), a clear synergistic effect was observed for the two COS-plant extract conjugate complexes in all cases, except for *D. coryli*, in which the EC₉₀ for COS alone was lower than that of COS-*E. arvense* formulation. The efficacy for the COS-horsetail and COS-nettle extract treatments were similar in most cases (except against *D. coryli*, in which the performance of COS-nettle extract was noticeably better).

Table 2. EC₅₀ and EC₉₀ effective concentrations for the different treatments, expressed in µg·mL⁻¹.

Treatment		<i>D. seriata</i>	<i>N. parvum</i>	<i>B. dothidea</i>	<i>D. iberica</i>	<i>D. coryli</i>	<i>D. sarmentorum</i>	<i>D. viticola</i>	<i>D. mutila</i>
COS	EC ₅₀	744.4	680.2	362.8	706.6	472.2	398.7	554.3	343.7
	EC ₉₀	1179.9	1326.6	1191.6	1196.4	972.4	1075.9	1138.7	1196.8
COS- <i>E. arvense</i>	EC ₅₀	173.9	214.1	109.4	304.1	155.3	198.2	148.2	118.6
	EC ₉₀	429.0	637.1	267.1	817.3	999.0	669.0	351.1	208.3
COS- <i>U. dioica</i>	EC ₅₀	211.5	215.2	72.6	253.0	162.9	203.0	175.3	100.3
	EC ₉₀	483.5	650.2	334.4	625.8	411.6	533.0	379.7	227.1

3.3. In Planta Assays

Statistically significant differences were found in terms of the lengths of the vascular necroses between treated and non-treated plants for both fungal pathogens. In addition, visual comparison of the lengths observed after sectioning grapevine plants between treated plants and controls (those plants inoculated only with the pathogens or with the control products, respectively) corroborated statistical results (Figure 3). As regards differences among treatments, in the case of *N. parvum* the performance of the three assayed formulations (and unlike what was observed in in vitro tests) was found to be similar (Table 3), while in the case of *D. seriata* the synergistic behavior observed in the in vitro tests was evidenced (Table 4), with a higher efficacy of the treatments based on conjugate complexes than that of COS alone, which was not significantly different from the control. It was also observed that, in general terms, treatments based on conjugate complexes were slightly more effective when used against *D. seriata*.

Table 3. Kruskal-Wallis test and multiple pairwise comparisons using the Conover-Iman procedure for the lengths of the vascular necroses for *N. parvum*.

Sample	Frequency	Sum of Ranks	Mean of Ranks	Groups
COS negative control	48	3366.000	70.125	A
COS- <i>U. dioica</i> negative control	48	3458.500	72.052	A
COS- <i>E. arvense</i> negative control	40	3444.500	86.113	A
COS- <i>E. arvense</i>	64	15017.000	234.641	B
COS- <i>U. dioica</i>	72	17119.500	237.771	B
COS	64	16600.000	259.375	B
Positive control	64	21194.500	331.164	C

Treatments/controls labelled with the same letters are not significantly different at $p < 0.05$.

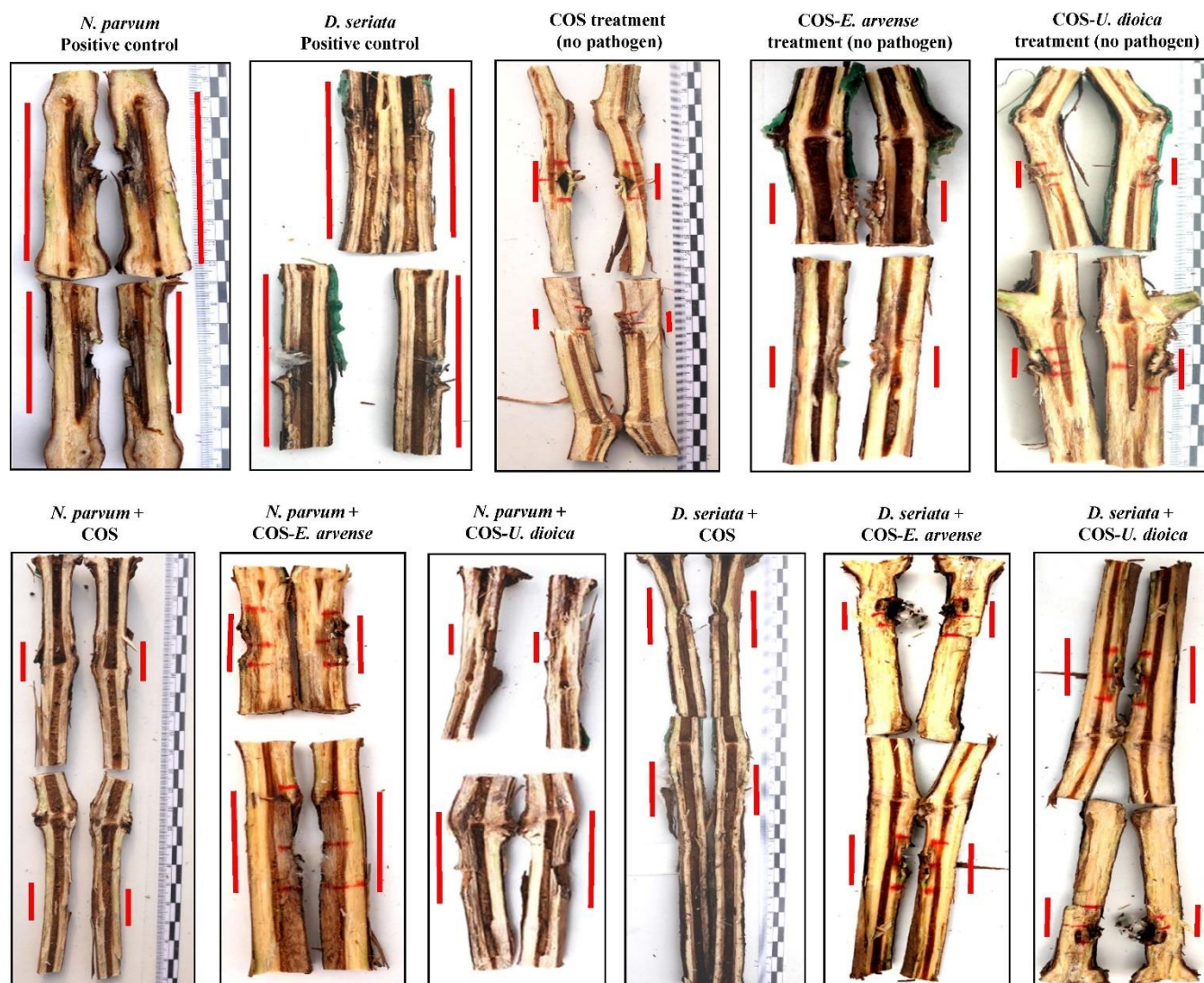


Figure 3. Vascular necroses observed after removal and sectioning of grapevine plants artificially inoculated with both pathogens and control products. Top row, from left to right: vascular necroses produced by *N. parvum*, *D. seriata*, COS treatment, COS-*E. arvensis* extract and COS-*U. dioica* extract; Bottom row, from left to right: vascular necroses produced by *N. parvum* + COS, *N. parvum* + COS-*E. arvensis* extract, *N. parvum* + COS-*U. dioica* extract, *D. seriata* + COS, *D. seriata* + COS-*E. arvensis* extract and *D. seriata* + COS-*U. dioica* extract, respectively. Red lines delimit the extent of lesions.

Table 4. Kruskal-Wallis test and multiple pairwise comparisons using the Conover-Iman procedure for the lengths of the vascular necroses for *D. seriata*.

Sample	Frequency	Sum of Ranks	Mean of Ranks	Groups
COS- <i>U. dioica</i> negative control	48	4216.500	87.844	A
COS negative control	48	4255.000	88.646	A
COS- <i>E. arvensis</i> negative control	40	4504.500	112.613	A
COS- <i>E. arvensis</i>	80	16097.000	201.213	B
COS- <i>U. dioica</i>	80	18098.500	226.231	B
COS	64	20311.000	317.359	C
Positive control	56	19253.500	343.813	C

Treatments/controls labelled with the same letters are not significantly different at $p < 0.05$.

4. Discussion

4.1. Efficacy Comparisons

Regarding chitosan oligosaccharides-based treatments, Cobos, et al. [25] found a complete inhibition of *D. seriata* and *B. dothidea* at 1000 $\mu\text{g}\cdot\text{mL}^{-1}$; and EC_{90} values in the 967–1270 $\mu\text{g}\cdot\text{mL}^{-1}$ range for *N. parvum*, in the 1121–1360 $\mu\text{g}\cdot\text{mL}^{-1}$ range for *D. seriata* and of 1339 $\mu\text{g}\cdot\text{mL}^{-1}$ for *B. dothidea* were obtained for the same strains in [30,31] (vs. 1326, 1180, 1192 $\mu\text{g}\cdot\text{mL}^{-1}$ in this work, respectively). Differences in the inhibitory concentrations may be ascribed to the existence of different isolate-dependent susceptibility profiles or to slight variances in the molecular weight or deacetylation degree of COS, which influence its efficacy.

In connection with *E. arvense* and *U. dioica* extracts, a summary of their effectiveness against various polyphagous phytopathogenic fungi (*Phytophthora infestans*, *Fusarium* spp., *Aspergillus* spp., *Alternaria* spp., etc.), including grapevine pathogens (*Botrytis cinerea*, *Plasmopara viticola*) and wood decay fungi (*Phanerochaete chrysosporium*, *Ceriporiopsis subvermispora*, *Gloeophyllum trabeum*, *Trametes versicolor*, *Oligoporus placenta*, *Pleurotus ostreatus* and *Coniophora puteana*) is presented in Table S4. It is worth noting that, although 100% inhibition has been attained against some fungal pathogens by using concentrations of *E. arvense* extract of 3% [40,41] and of *U. dioica* extract of 0.9% [23], such concentrations exceed the limit allowed by the European Union (0.2%). In the studies in which this latter concentration was tested, the inhibition was moderate: for instance, for *E. arvense* extract, La Torre, et al. [28] reported a 32.4% effectiveness against *P. viticola*, and Sen and Yalcin [24] found inhibitions of 25% against *P. chrysosporium*, *G. trabeum*, *P. ostreatus* and *C. puteana* for *U. dioica* extracts. These results are comparable to the inhibition found in the present study (<25%).

Concerning COS-based conjugate complexes, EC_{90} values of 507.5, 580.2 and 497.4 $\mu\text{g}\cdot\text{mL}^{-1}$ were obtained in previous studies for *N. parvum*, *D. seriata* and *B. dothidea*, respectively, with a COS- ϵ -polylysine conjugate [31]. When COS-tyrosine conjugate was used instead, EC_{90} values of 1021.4, 672.1 and 707.7 $\mu\text{g}\cdot\text{mL}^{-1}$, respectively, were reported [30]. For the COS-*E. arvense* extract and COS-*U. dioica* extract conjugates discussed herein, EC_{90} values of 637–650, 429–483 and 267–334 $\mu\text{g}\cdot\text{mL}^{-1}$ were registered. While the efficacy against *N. parvum* would be slightly lower than that of COS- ϵ -polylysine conjugate complex, those against *D. seriata* and *B. dothidea* would be higher, with the additional advantage of using legally-accepted basic substances.

As regards a comparison with the EC_{50} values of technical-grade commercial fungicides (Table S5), the values obtained for the conjugate complexes (173.9–211.5, 214.1–215.2, 72.6–109.4 and 100.3–118.6 $\mu\text{g}\cdot\text{mL}^{-1}$ against *D. seriata*, *N. parvum*, *B. dothidea* and *D. mutila*, respectively) would be in the same order of magnitude of the less effective conventional fungicides (e.g., boscalid, metalaxyl or copper oxychloride), but would exhibit a substantially lower effectiveness than fungicides such as flusilazole, tebuconazole, carbendazim or fludioxonil.

With respect to plant bioassays, comparisons of lengths of vascular necroses measured after the application of the different treatments (COS alone and conjugate complexes) showed that, regardless the pathogen considered, the average lengths of necroses were reduced with the different treatments and that these lengths were statistically different from both those produced in control plants inoculated only with the pathogens and from lesions observed when only control products were incorporated to the artificial wounds (Tables 3 and 4). Visual estimations of this protective effect can be also observed in Figure 3: vascular necroses were clearly lower in treated plants (for the three treatments), at both sides of inoculation points, in comparison with positive controls. In this sense, the statistical analyses indicated that the application of control products in the absence of any pathogen produced very low values of vascular discoloration length, which were similar in the three compounds, probably due to a hypersensitivity reaction restricted to the area occupied by the artificially inflicted wounds (Figure 3). In general terms, the median lengths of vascular necrosis obtained after the application of the control products in the case of *N. parvum* were further away from the values recorded in the case of *D. seriata*. Moreover, the treatment of this latter pathogen with COS did not result in a significant

reduction of vascular necrosis, being in the same range as the pathogen control. The control of these two and other *Botryosphaeriaceae* taxa has been extensively studied in vine plants through the use of fungicidal substances, biocontrol agents or natural products. Rusin, et al. [42], in a study on the control of *Lasiodiplodia theobromae* employing a combined set of BCAs, synthetic fungicides and natural products, found different protection levels depending on the product applied, but in the case of plant extracts (garlic and clove), these authors obtained average length values higher than those obtained with the assayed synthetic fungicides and BCAs. Amponsah, et al. [43] evaluated the sensitivity of certain *Botryosphaeriaceae* taxa (*N. luteum*, *N. australe* and *D. mutila*) against several technical-grade commercial fungicides in potted grapevines treated with chemicals, and reported dieback lesion lengths for *N. luteum* noticeably lower than the ones obtained in our study. Other studies on the control of these botryosphaeriaceous fungi dealing with BCAs [44] or conventional fungicides [45] have shown that, with some exceptions, the degree of protection tends to be higher when conventional fungicidal substances are used instead of microbial antagonists.

4.2. Mechanism of Action

Liu, et al. [46] suggested that fatty acids might be applicable to the integrated control of phytopathogens. They tested fatty acids against *Alternaria solani*, *Fusarium oxysporum* f. sp. *cucumerinum*, *F. oxysporum* f. sp. *lycopersici* and *Colletotrichum lagenarium*, finding that they had an inhibitory effect both on the mycelial growth and spore germination. The extent of inhibition varied depending upon both the type of fatty acids and the fungal species tested. They concluded that saturated fatty acids, i.e., palmitic acid (found in *E. arvense* extract at high concentrations, see above), showed stronger antifungal activity than unsaturated fatty acids. The main molecular mechanism by which fatty acids are thought to act is through their direct insertion into the fungal plasma membrane, resulting in increased fluidity, deregulation of membrane proteins and altered hydrostatic turgor pressure within the cell, leading to cytoplasmic disorder and ultimately to cell death [47]. According to Pohl, et al. [48], palmitic acid should result in an enhanced antifungal efficiency, which has been demonstrated against *Aspergillus niger*, *A. terreus* and *Emericella nidulans* by Altieri, et al. [49].

With regard to other active substances present in *E. arvense*, dihydroxyacetone (Figure S2) has been reported to exhibit fungicidal activity in medical contexts [50], and 3-deoxy-d-mannonic lactone (present, for instance, in garlic) also has antimicrobial activity [51].

Concerning carbinols, it is recognized that 2-furylcarbinols serve as versatile building blocks in the synthesis of highly oxygenated natural products, via the oxidative conversion of 2-furylcarbinols to pyranones [52]. Pyranone and furanone derivatives, present in both plant extracts discussed herein, have been shown to possess antifungal activity [53].

Imidazoles, such as 4,5-dihydro-2-methylimidazole present in *U. dioica* extract, block ergosterol synthesis, and thereby fungal growth, by binding in the active site of 14 α -demethylase enzyme [54]: the key interaction in the active site is the amidine nitrogen atom (N-3), which is believed to bind to the heme iron of the enzyme. This molecular reaction has led to an extensive use of triazoles (conazoles or imidazoles) as systemic fungicides, e.g., triadimefon, triadimenol, difenoconazole, propiconazole, cyproconazole and tebuconazole [55].

In connection with the observed synergistic behavior for the chitosan oligomers-plant extract conjugate complexes, the enhanced efficacy observed for COS-*U. dioica* may be tentatively explained taking into consideration changes in the unsaturated/saturated fatty acids ratio mediated by the imidazoles. On the one hand, it is well-established—on the basis of fatty acid analyses—that plasma membranes of chitosan-sensitive fungi have lower levels of unsaturated fatty acids than chitosan-resistant fungi [56]; and, on the other hand, it has been reported that imidazole antifungal agents at concentrations able to inhibit ergosterol biosynthesis (0.1 μ M) decrease the ratio of unsaturated to saturated fatty acids [57]. Hence, the presence of 4,5-dihydro-2-methylimidazole in the conjugate complex would increase the sensitivity of the fungal membrane to COS. This hypothesis would be

supported by a recent study by Lo, et al. [58], who found a synergistic antifungal activity of chitosan with fluconazole against *Candida* spp.

With reference to the synergism observed for COS-E. *arvense*, it may be hypothesized that it would be related to the high content in saturated fatty acids (and particularly palmitic acid) in *E. arvense* extract, which would unbalance the unsaturated/saturated ratio, promoting a higher sensitivity of the fungal membrane to COS. Moreover, palmitic acid would also act as a facilitating factor of the interaction, conferring higher solubility to COS: it has been shown that amphiphilic chitosan derivatives synthesized through grafting of palmitic acid onto chitosan can dissolve in water at concentrations up to 0.35% giving colorless solutions, whereas chitosan is insoluble in water at neutral pH [59].

However, further research is needed to understand the exact mechanism of action and to confirm (or discard) the proposed hypotheses.

4.3. Significance of the Reported Findings, Limitations of the Study and Further Research

The present study deals with the potential of certain phytochemicals or basic substances to control the development of one of the most important fungal group involved in the so-called grapevine trunk diseases, and more specifically one of these mycoses, the so-called “Black Dead Arm” or “Botryosphaeria dieback” [60,61]. At least 20 taxa of this group of ascomycetous fungi have been found to cause wood symptoms in grapevine [61], although some of them have a higher incidence in young grapevine plants coming from nursery [62]. Those include taxa like *N. parvum*, *D. seriata*, *L. theobromae*, *B. dothidea* or *D. mutila*, most of them included in the present study. Some of these species have been associated not only with *Vitis vinifera*, but also with many other plant hosts [63–65], where they can induce cankers, diebacks and fruit rots. Furthermore, one of these taxa studied here, viz. *N. parvum*, is considered nowadays as one of the main mycoses associated with propagation material in Spain, being directly involved in a large percentage of the basal infections observed in grafted plants (from their natural infection in rootstock mother fields [62]) and being ultimately responsible for the failure of young grafted plants, 2–5 years after their plantation. Moreover, this group of *Botryosphaeriaceae* species represents a potential threat to numerous crops in the Mediterranean environment, being linked to woody species that usually share habitat and bioclimatic conditions in large areas of the Mediterranean basin. Taking into consideration that in recent years there has been a drastic reduction in the number of legal active ingredients available for the treatment of these wood pathologies (current legislation recommends the universal adoption of the use of alternative methods and substances for disease control), the testing and evaluation of the protective capacities of certain simple compounds or phytochemicals of natural origin constitute a promising approach for the integrated management of this type of crops.

One clear limiting factor found in the in planta control bioassay deals with the fact that, although the vine plants were artificially infected with two pathogens of economic importance and relevance in the nursery, *N. parvum* and *D. seriata*, these were acquired with a significant baseline level of pre-existing pathologies in the commercial material. Thus, a first phytopathological analysis of some plants that did not sprout in the first days of the trial revealed the presence of previous wood pathologies such as vascular rot present both above the grafting point and in the environment of the root crown, and attributed to species such as *Ilyonectria liriodendri*, *Dactylonectria macrodidyma*, *Rhizoctonia solani* or *N. parvum* itself. Later and at the end of the trial, the processing of the plants that completed the entire bioassay evidenced the presence of these previous pathologies in a large percentage of them. Due to this and related to a second limiting factor in our investigation that had to do with the lack of correlation between foliar symptoms and vascular symptoms, some of the control plants of the trial exhibited symptoms (intra and inter-nerval foliar necrosis or decay of young shoots) not expected based on the absence of pathogenic inoculation. Other aspects susceptible to improvement would be associated with the dispersion medium (calcium alginate) chosen for the in planta assays, that – due to the type of polymerization reaction required for the formulation of the hydrogel beads –

restricts the amount of active ingredient in the bioactive solution that can be incorporated to the matrix to <20%. Furthermore, subsequent experimental designs for testing the germicidal potential of these and other bioactive compounds should include different genotypes for each tested pathogen, to take into account the presumed dose/response variability when establishing sensitivity profiles for each species [66].

Given the speed at which the different fungicidal substances of chemical origin are being banned or withdrawn from their use against this type of wood pathologies, research on the potentialities offered by a wide range of alternative products is increasingly urgent and necessary. All these investigations to be carried out in the coming years must necessarily be based on the discovery, optimization and commercialization of a series of products and formulations based either on the use of substances of natural origin, alone or in combinations of several of them, or on antagonistic microbial agents, all in combination with a less intensive and stressful management of the crop.

5. Conclusions

The antifungal activity of the phytochemicals identified in the extracts of *E. arvense* and *U. dioica*, which may be referred to both their shared constituents (carbinols and other building blocks) and their specific phytochemicals (saturated fatty acids in the case of *E. arvense* and imidazoles in the case of *U. dioica*), was found to be modest in the absence of chitosan oligomers. Nonetheless, for the conjugate complexes of COS with the extracts of the two plants, a clear synergistic behavior was observed, both in vitro—against eight *Botryosphaeriaceae* fungi, with EC₉₀ values in the 208–999 µg/mL range—and in vivo—with statistically significant differences in the vascular necroses caused by *N. parvum* and *D. seriata* in artificially inoculated grapevine plants. Such synergism may be ascribed to the contribution of saturated fatty acids to an enhanced sensitivity of the fungal membrane to chitosan, either directly—in the case of *E. arvense* extract—or mediated by imidazoles—in the case of *U. dioica*. Even though larger scale field trials are needed to further confirm the results presented herein, a combined use of these basic substances may be put forward as a promising treatment against GTDs either in organic Viticulture or as a substitute for treatments based on chemical synthesis fungicides in conventional management.

Supplementary Materials: The following are available online at <https://www.mdpi.com/article/10.3390/agronomy11050976/s1>, Table S1: Repetitions for each of the plant/treatment combinations in the greenhouse bioassay. Each grafted plant was inoculated at two sites below grafting point; Table S2: GC-MS analysis of *E. arvense* aqueous extract; Table S3. GC-MS analysis of *U. dioica* aqueous extract; Table S4: Examples of application of *E. arvense* and *U. dioica* extracts against phytopathogenic fungi reported in the literature; Table S5: In vitro EC₅₀ sensitivity values of some *Botryosphaeriaceae* species to technical-grade fungicides; . FTIR spectra of COS, *E. arvense* and *U. dioica* extract and COS-*E. arvense* and COS-*U. dioica* conjugate complexes; Figure S2. Chemical structures of phytochemicals with potential antifungal activity identified by GC-MS in *E. arvense* and *U. dioica* aqueous extracts; Figure S3. Growth inhibition for the eight *Botryosphaeriaceae* species under study with the chitosan oligomers (COS) treatment; Figure S4. Growth inhibition for the eight *Botryosphaeriaceae* species under study with the COS-*E. arvense* extract conjugate complex treatment; Figure S5. Growth inhibition for the eight *Botryosphaeriaceae* species under study with the COS-*U. dioica* extract conjugate complex treatment.

Author Contributions: Conceptualization, J.M.-G., P.M.-R. and V.G.-G.; methodology, J.M.-G., J.C.-G. and V.G.-G.; validation, J.C.-G., V.G.-G. and P.M.-R.; formal analysis, J.C.-G., V.G.-G. and P.M.-R.; investigation, L.B.-D., N.L.-L., V.G.-G., J.C.-G., J.M.-G., E.S.-H. and P.M.-R.; resources, J.M.-G. and P.M.-R.; data curation, J.C.-G.; writing—original draft preparation, L.B.-D., N.L.-L., V.G.-G., J.C.-G., J.M.-G., E.S.-H. and P.M.-R.; writing—review and editing, V.G.-G. and P.M.-R.; visualization, L.B.-D. and N.L.-L.; supervision, V.G.-G. and P.M.-R.; project administration, V.G.-G., J.M.-G. and P.M.-R.; funding acquisition, J.M.-G. and P.M.-R. All authors have read and agreed to the published version of the manuscript.

Funding: This research was funded by Junta de Castilla y León under project VA258P18, with FEDER co-funding; by Cátedra Agrobank under “IV Convocatoria de Ayudas de la Cátedra AgroBank para la transferencia del conocimiento al sector agroalimentario” program; and by Fundación Ibercaja-Universidad de Zaragoza under “Convocatoria Fundación Ibercaja-Universidad de Zaragoza de proyectos de investigación, desarrollo e innovación para jóvenes investigadores” program.

Institutional Review Board Statement: Not applicable.

Informed Consent Statement: Not applicable.

Data Availability Statement: The data presented in this study are available on request from the corresponding author. The data are not publicly available due to their relevance to be part of an ongoing Ph.D. Thesis.

Acknowledgments: V.G.-G thanks C. Julián (Plant Protection Unit, CITA) for her technical assistance. The authors gratefully acknowledge the support of Pilar Blasco and Pablo Candela at the Servicios Técnicos de Investigación, Universidad de Alicante, for conducting the GC-MS analyses.

Conflicts of Interest: The authors declare no conflict of interest. The funders had no role in the design of the study; in the collection, analyses, or interpretation of data; in the writing of the manuscript, or in the decision to publish the results.

References

1. Damalas, C.A.; Koutroubas, S.D. Botanical Pesticides for Eco-Friendly Pest Management. In *Pesticides in Crop Production*; Srivastava, P.K., Singh, V.P., Singh, A., Tripathi, D.K.S., Samiksha, Prasad, S.M., Chauhan, D.K., Eds.; Wiley: Chichester, UK, 2020; pp. 181–193.
2. Marrone, P.G. Pesticidal natural products—Status and future potential. *Pest Manag. Sci.* **2019**. [CrossRef] [PubMed]
3. Marchand, P.A. Basic Substances under EU Pesticide Regulation: An Opportunity for Organic Production? *Org. Farming* **2017**, *3*. [CrossRef]
4. Li, K.; Xing, R.; Liu, S.; Li, P. Chitin and Chitosan Fragments Responsible for Plant Elicitor and Growth Stimulator. *J. Agric. Food Chem.* **2020**, *68*, 12203–12211. [CrossRef]
5. Ma, Z.; Garrido-Maestu, A.; Jeong, K.C. Application, mode of action, and in vivo activity of chitosan and its micro- and nanoparticles as antimicrobial agents: A review. *Carbohydr. Polym.* **2017**, *176*, 257–265. [CrossRef] [PubMed]
6. Patova, O.A.; Smirnov, V.V.; Golovchenko, V.V.; Vityazev, F.V.; Shashkov, A.S.; Popov, S.V. Structural, rheological and antioxidant properties of pectins from *Equisetum arvense* L. and *Equisetum sylvaticum* L. *Carbohydr. Polym.* **2019**, *209*, 239–249. [CrossRef]
7. Francescato, L.N.; Debenedetti, S.L.; Schwanz, T.G.; Bassani, V.L.; Henriques, A.T. Identification of phenolic compounds in *Equisetum giganteum* by LC-ESI-MS/MS and a new approach to total flavonoid quantification. *Talanta* **2013**, *105*, 192–203. [CrossRef]
8. Stajner, D.; Popović, B.M.; Čanadanović-Brunet, J.; Anačkov, G. Exploring *Equisetum arvense* L., *Equisetum ramosissimum* L. and *Equisetum telmateia* L. as sources of natural antioxidants. *Phytother. Res.* **2009**, *23*, 546–550. [CrossRef] [PubMed]
9. Committee on Herbal Medicinal Products. European Union Herbal Monograph on *Equisetum arvense* L., Herba. EMA/HMPC/278091/2015. Available online: <https://www.ema.europa.eu/en/medicines/herbal/equiseti-herba> (accessed on 12 May 2021).
10. Milovanović, V.; Radulović, N.; Todorović, Z.; Stanković, M.; Stojanović, G. Antioxidant, Antimicrobial and Genotoxicity Screening of Hydro-alcoholic Extracts of Five Serbian *Equisetum* Species. *Plant Foods Hum. Nutr.* **2007**, *62*, 113–119. [CrossRef] [PubMed]
11. Mimica-Dukic, N.; Simin, N.; Cvejic, J.; Jovin, E.; Orcic, D.; Bozin, B. Phenolic Compounds in Field Horsetail (*Equisetum arvense* L.) as Natural Antioxidants. *Molecules* **2008**, *13*, 1455–1464. [CrossRef]
12. EFSA (European Food Safety Authority). Technical report on the outcome of the consultation with Member States and EFSA on the basic substance application for approval of *Equisetum arvense* L. for the extension of use in plant protection against fungal diseases on horticulture and vegetable crops. *Efsa Support. Publ.* **2020**, *17*, 42. [CrossRef]
13. EFSA (European Food Safety Authority). Technical report on the outcome of the consultation with Member States and EFSA on the basic substance applications for *Urtica* spp. for use in plant protection as insecticide, acaricide and fungicide. *Efsa Support. Publ.* **2016**, *13*. [CrossRef]
14. Mukhtar Ahmed, K.B.; Khan, M.M.A.; Siddiqui, H.; Jahan, A. Chitosan and its oligosaccharides, a promising option for sustainable crop production—A review. *Carbohydr. Polym.* **2020**, *227*. [CrossRef] [PubMed]
15. Radulovic, N.; Stojanovic, G.; Palic, R. Composition and antimicrobial activity of *Equisetum arvense* L. essential oil. *Phytother. Res.* **2006**, *20*, 85–88. [CrossRef]
16. Čanadanović-Brunet, J.M.; Četković, G.S.; Djilas, S.M.; Tumbas, V.T.; Savatović, S.S.; Mandić, A.I.; Markov, S.L.; Cvetković, D.D. Radical scavenging and antimicrobial activity of horsetail (*Equisetum arvense* L.) extracts. *Int. J. Food Sci. Technol.* **2009**, *44*, 269–278. [CrossRef]

17. Nagai, T.; Myoda, T.; Nagashima, T. Antioxidative activities of water extract and ethanol extract from field horsetail (*tsukushi*) *Equisetum arvense* L. *Food Chem.* **2005**, *91*, 389–394. [[CrossRef](#)]
18. Radojevic, I.D.; Stankovic, M.S.; Stefanovic, O.D.; Topuzovic, M.D.; Comic, L.R.; Ostojic, A.M. Great horsetail (*Equisetum telmateia* Ehrh.): Active substances content and biological effects. *Excli J.* **2012**, *11*, 59–67.
19. Rogozhin, E.A.; Tepkeeva, I.I.; Zaitsev, D.V.; Demushkin, V.P.; Smirnov, A.N. Biological activity of peptide extracts of medicinal plants against phytopathogenic fungi and oomycetes. *Russ. Agric. Sci.* **2011**, *37*, 314–317. [[CrossRef](#)]
20. Sehari, M.; Kouadria, M.; Amirat, M.; Sehari, N.; Hassani, A. Phytochemistry and antifungal activity of plant extracts from Nettle (*Urtica dioica* L.). *Ukr. J. Ecol.* **2020**, *10*, 1–6. [[CrossRef](#)]
21. Torun, B.; Biyik, H.H.; Ercin, Z.; Coban, E.P. Antifungal activities of *Urtica dioica* L., *Sinapis arvensis* L. and *Apium graveolens* Mill. leaves on *Botrytis cinerea* Pers. *Ann. Phytomed.-Int. J.* **2018**, *7*, 94–97. [[CrossRef](#)]
22. Romanazzi, G.; Feliziani, E.; Santini, M.; Landi, L. Effectiveness of postharvest treatment with chitosan and other resistance inducers in the control of storage decay of strawberry. *Postharvest Biol. Technol.* **2013**, *75*, 24–27. [[CrossRef](#)]
23. Hadizadeh, I.; Peivastegan, B.; Kolahi, M. Antifungal activity of nettle (*Urtica dioica* L.), colocynth (*Citrullus colocynthis* L. Schrad), oleander (*Nerium oleander* L.) and konar (*Ziziphus spina-christi* L.) extracts on plants pathogenic fungi. *Pak. J. Biol. Sci. Pjbs* **2009**, *12*, 58–63. [[CrossRef](#)]
24. Sen, S.; Yalcin, M. Activity of commercial still waters from volatile oils production against wood decay fungi. *Maderas-Cienc. Y Technol.* **2010**, *12*, 127–133. [[CrossRef](#)]
25. Cobos, R.; Mateos, R.M.; Alvarez-Perez, J.M.; Olego, M.A.; Sevillano, S.; Gonzalez-Garcia, S.; Garzon-Jimeno, E.; Coque, J.J. Effectiveness of natural antifungal compounds in controlling infection by grapevine trunk disease pathogens through pruning wounds. *Appl. Environ. Microbiol.* **2015**, *81*, 6474–6483. [[CrossRef](#)]
26. Nascimento, T.; Rego, C.; Oliveira, H. Potential use of chitosan in the control of grapevine trunk diseases. *Phytopathol. Mediterr.* **2007**, *46*, 218–224.
27. Matei, P.M.; Martín-Ramos, P.; Sánchez-Báscones, M.; Hernández-Navarro, S.; Correa-Guimaraes, A.; Navas-Gracia, L.M.; Rufino, C.A.; Ramos-Sánchez, M.C.; Martín-Gil, J. Synthesis of chitosan oligomers/propolis/silver nanoparticles composite systems and study of their activity against *Diplodia seriata*. *Int. J. Polym. Sci.* **2015**, *2015*, 1–11. [[CrossRef](#)]
28. La Torre, A.; Righi, L.; Iovino, V.; Battaglia, V. Evaluation of copper alternative products to control grape downy mildew in organic farming. *J. Plant. Pathol.* **2019**, *101*, 1005–1012. [[CrossRef](#)]
29. Garcia-Cela, E.; Ramos, A.J.; Sanchis, V.; Marin, S. Ochratoxigenic moulds and effectiveness of grape field antifungals in a climatic change scenario. *J. Sci. Food Agric.* **2012**, *92*, 1455–1461. [[CrossRef](#)]
30. Buzón-Durán, L.; Langa-Lomba, N.; González-García, V.; Casanova-Gascón, J.; Martín-Gil, J.; Pérez-Lebeña, E.; Martín-Ramos, P. On the applicability of chitosan oligomers-amino acid conjugate complexes as eco-friendly fungicides against grapevine trunk pathogens. *Agronomy* **2021**, *11*, 324. [[CrossRef](#)]
31. Buzón-Durán, L.; Martín-Gil, J.; Pérez-Lebeña, E.; Ruano-Rosa, D.; Revuelta, J.L.; Casanova-Gascón, J.; Ramos-Sánchez, M.C.; Martín-Ramos, P. Antifungal agents based on chitosan oligomers, ϵ -polylysine and *Streptomyces* spp. secondary metabolites against three *Botryosphaeriaceae* species. *Antibiotics* **2019**, *8*, 99. [[CrossRef](#)] [[PubMed](#)]
32. Buzón-Durán, L.; Martín-Gil, J.; Marcos-Robles, J.L.; Fombellida-Villafruela, Á.; Pérez-Lebeña, E.; Martín-Ramos, P. Antifungal Activity of Chitosan Oligomers–Amino Acid Conjugate Complexes against *Fusarium culmorum* in Spelt (*Triticum spelta* L.). *Agronomy* **2020**, *10*, 1427. [[CrossRef](#)]
33. Mondello, V.; Songy, A.; Battiston, E.; Pinto, C.; Coppin, C.; Trotel-Aziz, P.; Clement, C.; Mugnai, L.; Fontaine, F. Grapevine trunk diseases: A review of fifteen years of trials for their control with chemicals and biocontrol agents. *Plant Dis.* **2018**, *102*, 1189–1217. [[CrossRef](#)]
34. Gramaje, D.; Urbez-Torres, J.R.; Sosnowski, M.R. Managing Grapevine Trunk Diseases With Respect to Etiology and Epidemiology: Current Strategies and Future Prospects. *Plant. Dis.* **2018**, *102*, 12–39. [[CrossRef](#)]
35. Fontaine, F.; Gramaje, D.; Armengol, J.; Smart, R.; Nagy, Z.A.; Borgo, M.; Rego, C.; Corio-Costet, M.-F. *Grapevine trunk diseases. A review*; OIV publications: Paris, France, 2016; p. 25.
36. Balouiri, M.; Sadiki, M.; Ibsouda, S.K. Methods for in vitro evaluating antimicrobial activity: A review. *J. Pharm. Anal.* **2016**, *6*, 71–79. [[CrossRef](#)] [[PubMed](#)]
37. R Core Team. *R: A Language and Environment for Statistical Computing*; R Foundation for Statistical Computing: Vienna, Austria, 2020.
38. Luque, J.; Elena, G.; Garcia-Figueres, F.; Reyes, J.; Barrios, G.; Legorburu, F.J. Natural infections of pruning wounds by fungal trunk pathogens in mature grapevines in Catalonia (Northeast Spain). *Aust. J. Grape Wine Res.* **2014**, *20*, 134–143. [[CrossRef](#)]
39. Aroca, Á.; Gramaje, D.; Armengol, J.; García-Jiménez, J.; Raposo, R. Evaluation of the grapevine nursery propagation process as a source of *Phaeoacremonium* spp. and *Phaeomoniella chlamydospora* and occurrence of trunk disease pathogens in rootstock mother vines in Spain. *Eur. J. Plant. Pathol.* **2010**, *126*, 165–174. [[CrossRef](#)]
40. Garcia, D.; Garcia-Cela, E.; Ramos, A.J.; Sanchis, V.; Marin, S. Mould growth and mycotoxin production as affected by *Equisetum arvense* and *Stevia rebaudiana* extracts. *Food Control.* **2011**, *22*, 1378–1384. [[CrossRef](#)]
41. Garcia, D.; Ramos, A.J.; Sanchis, V.; Marin, S. Effect of *Equisetum arvense* and *Stevia rebaudiana* extracts on growth and mycotoxin production by *Aspergillus flavus* and *Fusarium verticillioides* in maize seeds as affected by water activity. *Int. J. Food Microbiol.* **2012**, *153*, 21–27. [[CrossRef](#)] [[PubMed](#)]

42. Rusin, C.; Cavalcanti, F.R.; Lima, P.C.G.d.; Faria, C.M.D.R.; Almança, M.A.K.; Botelho, R.V. Control of the fungi *Lasioidiplodia theobromae*, the causal agent of dieback, in cv. syrah grapevines. *Acta Sci. Agron.* **2020**, *43*. [[CrossRef](#)]
43. Amponsah, N.T.; Jones, E.; Ridgway, H.J.; Jaspers, M.V. Evaluation of fungicides for the management of *Botryosphaeria dieback* diseases of grapevines. *Pest. Manag. Sci.* **2012**, *68*, 676–683. [[CrossRef](#)]
44. Kotze, C.; Van Niekerk, J.; Halleen, F.; Mostert, L.; Fourie, P. Evaluation of biocontrol agents for grapevine pruning wound protection against trunk pathogen infection. *Phytopathol. Mediterr.* **2011**, *50*, 247–263. [[CrossRef](#)]
45. Díaz, G.A.; Latorre, B.A. Efficacy of paste and liquid fungicide formulations to protect pruning wounds against pathogens associated with grapevine trunk diseases in Chile. *Crop Prot.* **2013**, *46*, 106–112. [[CrossRef](#)]
46. Liu, S.; Ruan, W.; Li, J.; Xu, H.; Wang, J.; Gao, Y.; Wang, J. Biological Control of Phytopathogenic Fungi by Fatty Acids. *Mycopathologia* **2008**, *166*, 93–102. [[CrossRef](#)] [[PubMed](#)]
47. Clitherow, K.H.; Binaljadm, T.M.; Hansen, J.; Spain, S.G.; Hatton, P.V.; Murdoch, C. Medium-Chain Fatty Acids Released from Polymeric Electrospun Patches Inhibit *Candida albicans* Growth and Reduce the Biofilm Viability. *Acs Biomater. Sci. Eng.* **2020**, *6*, 4087–4095. [[CrossRef](#)]
48. Pohl, C.H.; Kock, J.L.; Thibane, V.S. Antifungal free fatty acids: A review. *Sci. Against Microb. Pathog. Commun. Curr. Res. Technol. Adv.* **2011**, *3*, 61–71.
49. Altieri, C.; Cardillo, D.; Bevilacqua, A.; Sinigaglia, M. Inhibition of *Aspergillus* spp. and *Penicillium* spp. by Fatty Acids and Their Monoglycerides. *J. Food Prot.* **2007**, *70*, 1206–1212. [[CrossRef](#)]
50. Stopiglia, C.D.O.; Vieira, F.J.; Mondadori, A.G.; Oppe, T.P.; Scroferneker, M.L. In Vitro Antifungal Activity of Dihydroxyacetone Against Causative Agents of Dermatofungal Mycosis. *Mycopathologia* **2010**, *171*, 267–271. [[CrossRef](#)] [[PubMed](#)]
51. Shobana, S.; Vidhya, V.; Ramya, M. Antibacterial activity of garlic varieties (*ophioscordon* and *sativum*) on enteric pathogens. *Curr. Res. J. Biol. Sci.* **2009**, *1*, 123–126.
52. Honda, T. Investigation of Innovative Synthesis of Biologically Active Compounds on the Basis of Newly Developed Reactions. *Chem. Pharm. Bull.* **2012**, *60*, 687–705. [[CrossRef](#)] [[PubMed](#)]
53. Komai, S.-i.; Hosoe, T.; Nozawa, K.; Okada, K.; de Campos Takaki, G.M.; Fukushima, K.; Miyaji, M.; Horie, Y.; Kawai, K.-i. Antifungal activity of pyranone and furanone derivatives, isolated from *Aspergillus* sp. IFM51759, against *Aspergillus fumigatus*. *Mycotoxins* **2003**, *53*, 11–18. [[CrossRef](#)]
54. Xiao, L.; Madison, V.; Chau, A.S.; Loebenberg, D.; Palermo, R.E.; McNicholas, P.M. Three-Dimensional Models of Wild-Type and Mutated Forms of Cytochrome P450 14 α -Sterol Demethylases from *Aspergillus fumigatus* and *Candida albicans* Provide Insights into Posaconazole Binding. *Antimicrob. Agents Chemother.* **2004**, *48*, 568–574. [[CrossRef](#)] [[PubMed](#)]
55. Agrios, G.N. Control of Plant Diseases. *Plant Pathol.* **2005**, 293–353. [[CrossRef](#)]
56. Xing, K.; Shen, X.; Zhu, X.; Ju, X.; Miao, X.; Tian, J.; Feng, Z.; Peng, X.; Jiang, J.; Qin, S. Synthesis and in vitro antifungal efficacy of oleoyl-chitosan nanoparticles against plant pathogenic fungi. *Int. J. Biol. Macromol.* **2016**, *82*, 830–836. [[CrossRef](#)] [[PubMed](#)]
57. Georgopadakou, N.H.; Dix, B.A.; Smith, S.A.; Freudenberger, J.; Funke, P.T. Effect of antifungal agents on lipid biosynthesis and membrane integrity in *Candida albicans*. *Antimicrob. Agents Chemother.* **1987**, *31*, 46–51. [[CrossRef](#)]
58. Lo, W.-H.; Deng, F.-S.; Chang, C.-J.; Lin, C.-H. Synergistic Antifungal Activity of Chitosan with Fluconazole against *Candida albicans*, *Candida tropicalis*, and Fluconazole-Resistant Strains. *Molecules* **2020**, *25*, 5114. [[CrossRef](#)] [[PubMed](#)]
59. Kolesnyk, I.; Konovalova, V.; Kharchenko, K.; Burban, A.; Kujawa, J.; Kujawski, W. Enhanced transport and antifouling properties of polyethersulfone membranes modified with α -amylase incorporated in chitosan-based polymeric micelles. *J. Membr. Sci.* **2020**, 595. [[CrossRef](#)]
60. Laignon, P.; Dubos, B. Le Black Dead Arm: Maladie nouvelle à ne pas confondre avec l'esca. *Phytoma-La Défense Des Végétaux* **2001**, *538*, 26–29.
61. Urbez-Torres, J.R. The status of *Botryosphaeriaceae* species infecting grapevines. In *Phytopathologia Mediterranea*; University of Florence: Florence, Italy, 2011; Volume 50, pp. 5–45.
62. Gramaje, D.; Armengol, J. Fungal Trunk Pathogens in the Grapevine Propagation Process: Potential Inoculum Sources, Detection, Identification, and Management Strategies. *Plant Dis.* **2011**, *95*, 1040–1055. [[CrossRef](#)]
63. Marsberg, A.; Kemler, M.; Jami, F.; Nagel, J.H.; Postma-Smidt, A.; Naidoo, S.; Wingfield, M.J.; Crous, P.W.; Spatafora, J.W.; Hesse, C.N.; et al. *Botryosphaeria dothidea*: A latent pathogen of global importance to woody plant health. *Mol. Plant Pathol.* **2017**, *18*, 477–488. [[CrossRef](#)]
64. Moral, J.; Agustí-Brisach, C.; Pérez-Rodríguez, M.; Xaviér, C.; Raya, M.C.; Rhouma, A.; Trapero, A. Identification of fungal species associated with branch dieback of olive and resistance of table cultivars to *Neofusicoccum mediterraneum* and *Botryosphaeria dothidea*. *Plant Dis.* **2017**, *101*, 306–316. [[CrossRef](#)]
65. Olmo, D.; Gramaje, D.; Armengol, J. Evaluation of fungicides to protect pruning wounds from *Botryosphaeriaceae* species infections on almond trees. *Phytopathol. Mediterr.* **2017**, *56*, 77–86.
66. Fan, K.; Wang, J.; Fu, L.; Li, X.; Zhang, Y.; Zhang, X.; Zhai, H.; Qu, J. Sensitivity of *Botryosphaeria dothidea* from apple to tebuconazole in China. *Crop Prot.* **2016**, *87*, 1–5. [[CrossRef](#)]

ARTÍCULO 3: “Antifungal activity against *Botryosphaeriaceae* fungi of the hydro-methanolic extract of *Silybum marianum* capitula conjugated with stevioside” *Plants*, 2021, 10(7), 1363; <https://doi.org/10.3390/plants10071363>; Q1 (JCR, Science Edition – PLANT SCIENCES). JIF₂₀₂₁ = 4,658. 5 citas recibidas (WOS).



plants

an Open Access Journal by MDPI



Antifungal Activity against *Botryosphaeriaceae* Fungi of the Hydro-Methanolic Extract of *Silybum marianum* Capitula Conjugated with Stevioside

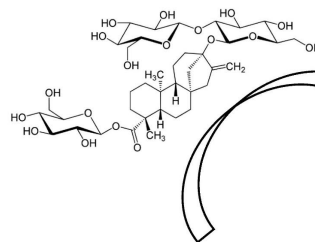
Natalia Langa-Lomba; Laura Buzón-Durán; Eva Sánchez-Hernández; Pablo Martín-Ramos; José Casanova-Gascón; Jesús Martín-Gil; Vicente González-García

Plants 2021, Volume 10, Issue 7, 1363

Milk thistle
(*Silybum marianum*)
capitula

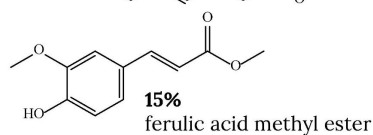
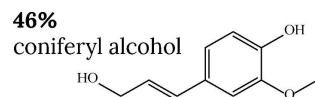


Flowering phenological
stage (stage 67)



Conjugation with stevioside

Hydromethanolic extract



Enhanced antifungal activity
(*in vitro* + *in vivo*) against fungi
responsible for *Botryosphaeria*
dieback of grapevine:

- *Neofusicoccum parvum*
- *Dothiorella viticola*
- *Diplodia seriata*



Article

Antifungal Activity against *Botryosphaeriaceae* Fungi of the Hydro-Methanolic Extract of *Silybum marianum* Capitula Conjugated with Stevioside

Natalia Langa-Lomba ^{1,2}, Laura Buzón-Durán ³, Eva Sánchez-Hernández ³ , Pablo Martín-Ramos ^{1,*} , José Casanova-Gascón ¹ , Jesús Martín-Gil ³ and Vicente González-García ²

¹ Instituto Universitario de Investigación en Ciencias Ambientales de Aragón (IUCA), EPS, Universidad de Zaragoza, Carretera de Cuarte, s/n, 22071 Huesca, Spain; natalialangalomba@gmail.com (N.L.-L.); jcasan@unizar.es (J.C.-G.)

² Plant Protection Unit, Agrifood Research and Technology Centre of Aragón, Instituto Agroalimentario de Aragón—IA2 (CITA-Universidad de Zaragoza), Avda. Montañana 930, 50059 Zaragoza, Spain; vgonzalezg@aragon.es

³ Agriculture and Forestry Engineering Department, ETSIIAA, Universidad de Valladolid, Avenida de Madrid 44, 34004 Palencia, Spain; laura.buzon@uva.es (L.B.-D.); eva.sanchez.hernandez@uva.es (E.S.-H.); jesus.martin.gil@uva.es (J.M.-G.)

* Correspondence: pmr@unizar.es



Citation: Langa-Lomba, N.; Buzón-Durán, L.; Sánchez-Hernández, E.; Martín-Ramos, P.; Casanova-Gascón, J.; Martín-Gil, J.; González-García, V. Antifungal Activity against *Botryosphaeriaceae* Fungi of the Hydro-Methanolic Extract of *Silybum marianum* Capitula Conjugated with Stevioside. *Plants* **2021**, *10*, 1363. <https://doi.org/10.3390/plants10071363>

Academic Editor: Adam Stebel

Received: 17 June 2021

Accepted: 30 June 2021

Published: 3 July 2021

Publisher's Note: MDPI stays neutral with regard to jurisdictional claims in published maps and institutional affiliations.



Copyright: © 2021 by the authors. Licensee MDPI, Basel, Switzerland. This article is an open access article distributed under the terms and conditions of the Creative Commons Attribution (CC BY) license (<https://creativecommons.org/licenses/by/4.0/>).

Abstract: *Silybum marianum* (L.) Gaertn, viz. milk thistle, has been the focus of research efforts in the past few years, albeit almost exclusively restricted to the medicinal properties of its fruits (achenes). Given that other milk thistle plant organs and tissues have been scarcely investigated for the presence of bioactive compounds, in this study, we present a phytochemical analysis of the extracts of *S. marianum* capitula during the flowering phenological stage (stage 67). Gas chromatography–mass spectroscopy results evidenced the presence of high contents of coniferyl alcohol (47.4%), and secondarily of ferulic acid ester, opening a new valorization strategy of this plant based on the former high-added-value component. Moreover, the application of the hydro-methanolic extracts as an antifungal agent has been also explored. Specifically, their activity against three fungal species responsible for the so-called *Botryosphaeria* dieback of grapevine (*Neofusicoccum parvum*, *Dothiorella viticola* and *Diplodia seriata*) has been assayed both in vitro and in vivo. From the mycelial growth inhibition assays, the best results (EC₉₀ values of 303, 366, and 355 µg·mL⁻¹ for *N. parvum*, *D. viticola*, and *D. seriata*, respectively) were not obtained for the hydroalcoholic extract alone, but after its conjugation with stevioside, which resulted in a strong synergistic behavior. Greenhouse experiments confirmed the efficacy of the conjugated complexes, pointing to the potential of the combination of milk thistle extracts with stevioside as a promising plant protection product in organic Viticulture.

Keywords: coniferyl alcohol; ferulic acid; grapevine trunk diseases; milk thistle; stevioside

1. Introduction

Silybum marianum (L.) Gaertn (syn. *Carduus marianus* L.), commonly known as milk thistle, St. Mary's Thistle, or wild artichoke, is an herbaceous plant of the *Asteraceae* family. Native to the Mediterranean area, it is nowadays grown in many countries as a medicinal plant, due to the variety of biological activities—mostly linked to the hepatoprotective properties and anti-carcinogenic capacity—associated with the main pharmacological active ingredient extracted from its achenes (fruits): silymarin [1,2].

The standardized extract obtained from the dried fruits of *S. marianum* contains 70–80% of silymarin and 20–30% of polymeric and oxidized polyphenolic compounds [3]. Silymarin is a flavonolignan complex of polyphenolic molecules, which includes diastereoisomers silybin A and silybin B (whose mixture in a 1:1 ratio is named silibinin),

silydianin, silychristin, isosilychristin, isosilybin A and isosilybin B, and the taxifolin flavanone [4]. Biosynthesis of silybins from taxifolin and coniferyl alcohol is schematized in Figure S1 [5].

Most research has been focused on the study of silymarin, or its major compound silybin, instead of the plant as a whole. The concentration of silymarin is organ-dependent, and it is only localized in the outer portion of the fruit, which includes all the cell layers from the pericarp epidermis to the albumen, and embryos [6], accounting for 1.5–4.3% of the fruit weight [7]. Silymarin is not present in flowers, stems, or leaves, and it is not found in steps before the development of fruit [8,9], which explains why other milk thistle plant organs have been scarcely investigated for bioactive compounds: total polyphenol and flavonoid contents in leaves' extracts were studied by Saidi, et al. [10]; a phytochemical screening and gas chromatography–mass spectrometry (GC–MS) analysis of bioactive compounds present in ethanolic leaves extract was conducted by Mani, et al. [11]; and Sulas, et al. [12] studied the concentrations of crude protein, fat, total phenolics, and total flavonoids in leaves, heads, and stems.

A thorough search of the relevant literature yielded no analyses of the phytochemicals present in the capitula in the flowering stage, prior to seed maturation. Nonetheless, the existence of some precursors proposed in the bibliography, such as coniferyl alcohol or ferulic acid, may be expected (Figure S2) [5]. Coniferyl alcohol is one of the main monolignols of angiosperm dicotyledons [13], and it is distributed throughout the milk thistle plant [8]. It is associated with the defense mechanisms of trees and is known to have inhibitory activity against the growth of fungi [14,15]. Ferulic acid (4-hydroxy-3-methoxycinnamic acid) and its precursors, *p*-coumaric acid, and caffeic acid, are metabolites in the biosynthesis of lignins. These compounds are intermediates in the biosynthesis of some important natural products very often found in plants, such as *p*-coumaryl alcohol, curcumin, chlorogenic acid, diferulic acids, sinapic acid, synapyl alcohol, coniferyl alcohol, vanillin, etc. [16].

Regarding the antifungal activity of the above-cited compounds, the literature indicates that silymarin is effective against yeasts like *Candida* spp. (*C. albicans* (C.P. Robin) Berkhout, *C. krusei* (Castellani) Berkhout, and *C. glabrata* (H.W. Anderson) S.A. Mey. & Yarrow) [17,18], and that coniferyl derivatives are effective against *Cladosporium cucumerinum* Ellis & Arthur and *C. albicans* [19]. Ferulic acid has been reported as an inhibitor of the fungal growth of, for instance, *Pythium* spp. [20], *Fusarium* spp. [21,22], and *Aspergillus* spp. [23,24]. Esters of ferulic acid were found to be more potent antimicrobial agents than amides and anilides, according to Khatkar, et al. [25], and their high antimicrobial activity was evidenced by the results of Mahiwal, et al. [26].

Concerning the control of Botryosphaeriaceous fungi—which are recognized as aggressive plant pathogens on different types of hosts, from agricultural crops to ornamental and forest species—[27], ferulic acid has been assayed against taxa like *Diplodia seriata* and *Neofusicoccum parvum*, and against other grapevine trunk pathogens such as *Eutypa lata* (Pers.) Tul. & C.Tul., *Phaeoconiella chlamydospora* (W. Gams, Crous, M.J. Wingf. & Mugnai) Crous & W. Gams and *Phaeoacremonium minimum* (Tul. & C. Tul.) Gramaje, L. Mostert & Crous [28–30], but the activity of *S. marianum* extracts or coniferyl alcohol has not been assayed to date, in spite of the importance of these phytopathogens in economically important crops like Viticulture [31].

In this study, a phytochemical analysis of the extracts of *S. marianum* capitula during the flowering phenological stage (stage 67, when the head disk is covered by open florets (i.e., during the flowering stage and before the development of fruit)) is presented, with the aim of exploring the presence of high-added-value components and the potential application the hydro-methanolic extracts as antifungal agents against three *Botryosphaeriaceae* species that play a major role in the so-called grapevine trunk diseases (GTDs). To circumvent the bioavailability problems associated with the very low solubility in water of ferulic acid [32], coniferyl alcohol, and other constituents, inclusion compounds or conjugate complexes with terpene glycosides may be formed [33]. In this study, stevioside (the major

constituent of *Stevia rebaudiana* (Bertoni) Bertoni extract), which has antifungal properties, has been chosen to form such conjugate complexes, aiming at an enhancement of activity through synergism.

2. Material and Methods

2.1. Plant Material, Reagents, and Fungal Isolates

The specimens of *S. marianum* under study were collected in the banks of Carrión river as it passes through the town of Palencia (Spain) during stage 67 (or 6N7) according to the extended BBCH scale [34]. This stage was chosen because silybins precursors (Figure S1) should not have yet been consumed. The capitula of *S. marianum* were shade-dried and pulverized to fine powder in a mechanical grinder. Different specimens ($n = 25$) were thoroughly mixed to obtain a composite sample.

Chitosan (CAS 9012-76-4; high MW: 310,000–375,000 Da) was supplied by Hangzhou Simit Chem. and Tech. Co. (Hangzhou, China). Neutrase™ 0.8 L enzyme was supplied by Novozymes A/S (Bagsværd, Denmark). Stevioside (CAS 57817-89-7, 99%) was purchased from Wako Chemicals GmbH (Neuss, Germany). Coniferyl alcohol (CAS 458-35-5, 98%), ferulic acid (CAS 537-98-4, European Pharmacopoeia Reference Standard), sodium alginate (CAS 9005-38-3), calcium carbonate (CAS 471-34-1, $\geq 99.0\%$), and methanol (CAS 67-56-1, UHPLC, suitable for mass spectrometry) were acquired from Sigma-Aldrich Química (Madrid, Spain). PDA (potato dextrose agar) was supplied by Becton Dickinson (Bergen County, NJ, USA).

The three fungal pathogens (Table 1) were supplied as lyophilized vials (later reconstituted and refreshed as PDA subcultures) by the Agricultural Technological Institute of Castilla and Leon (ITACYL, Valladolid, Spain) [35].

Table 1. Fungal isolates used in the study.

Code	Isolate	Binomial Nomenclature	Geographical Origin	Host/Date
ITACYL_F111	Y-091-03-01c	<i>Neofusicoccum parvum</i> (Pennycook & Samuels) Crous, Slippers & A.J.L.Phillips	Spain (Navarra, nursery)	Grapevine ('Verdejo') 2006
ITACYL_F118	Y-103-08-01	<i>Dothiorella viticola</i> A.J.L.Phillips & J.Luque	Spain (Extremadura)	Grapevine 2004
ITACYL_F098	Y-084-01-01a	<i>Diplodia seriata</i> De Not.	Spain (DO Toro)	Grapevine ('Tempranillo') 2004

2.2. Preparation of Plant Extracts

Silybum marianum capitula samples were mixed (1:20, w/v) with a methanol/water solution (1:1 v/v) and heated in a water bath at 50 °C for 30 min, followed by sonication for 5 min in pulse mode with a 1 min stop for each 2.5 min, using a probe-type ultrasonicator model UIP1000hdT (Hielscher Ultrasonics, Teltow, Germany; 1000 W, 20 kHz). The solution was then centrifuged at 9000 rpm for 15 min and the supernatant was filtered through Whatman No. 1 paper. Finally, aliquots of the extract were lyophilized for infrared spectroscopy analyses.

2.3. Physicochemical Characterization of *S. marianum* Extracts

The infrared vibrational spectra were registered using a Thermo Scientific (Waltham, MA, USA) Nicolet iS50 Fourier-transform infrared spectrometer, equipped with an in-built diamond attenuated total reflection (ATR) system. The spectra were collected with a 1 cm^{-1} spectral resolution over the 400–4000 cm^{-1} range, taking the interferograms that resulted from co-adding 64 scans. The spectra were then corrected using the advanced ATR correction algorithm [36] available in OMNIC™ software suite.

The hydroalcoholic plant extracts were studied by gas chromatography–mass spectrometry (GC–MS) at the Research Support Services (STI) at Universidad de Alicante

(Alicante, Spain), using a gas chromatograph model 7890A coupled to a quadrupole mass spectrometer model 5975C (both from Agilent Technologies). The chromatographic conditions were: injection volume = 1 μL ; injector temperature = 280 $^{\circ}\text{C}$, in splitless mode; initial oven temperature = 60 $^{\circ}\text{C}$, 2 min, followed by ramp of 10 $^{\circ}\text{C}/\text{min}$ up to a final temperature of 300 $^{\circ}\text{C}$, 15 min. The chromatographic column used for the separation of the compounds was an Agilent Technologies HP-5MS UI of 30 m length, 0.250 mm diameter and 0.25 μm film. The mass spectrometer conditions were: temperature of the electron impact source of the mass spectrometer = 230 $^{\circ}\text{C}$ and of the quadrupole = 150 $^{\circ}\text{C}$; ionization energy = 70 eV. NIST11 library and Adams [37] were used for compound identification.

2.4. Preparation of Bioactive Formulations

The stevioside–*S. marianum*, stevioside–coniferyl alcohol, and stevioside–ferulic acid conjugate complexes were obtained by mixing of the respective solutions in a 1:1 (*v/v*) ratio. The mixture was then sonicated for 15 min in five 3-min periods (so that the temperature did not exceed 60 $^{\circ}\text{C}$) using a probe-type ultrasonicator [38].

2.5. Antifungal Activity Assessment

2.5.1. In Vitro Tests of Mycelial Growth Inhibition

The antifungal activity of the different treatments was determined using the agar dilution method according to EUCAST standard antifungal susceptibility testing procedures [39], by incorporating aliquots of stock solutions onto the PDA medium to obtain concentrations in the 62.5–1500 $\mu\text{g}\cdot\text{mL}^{-1}$ range. The solutions were added to the PDA after being sterilized in an autoclave, when the temperature of the medium was close to that of polymerization (over 60 $^{\circ}\text{C}$), in the same way that antibiotics are usually incorporated into these synthetic media. Mycelial plugs ($\varnothing = 5\text{ mm}$), from the margin of 1-week-old PDA cultures of *N. parvum*, *D. viticola* or *D. seriata*, were transferred to the center of plates incorporating the above-mentioned concentrations for each treatment (3 plates per treatment/concentration, with 2 replicates). Plates were then incubated at 25 $^{\circ}\text{C}$ in the dark for a week. PDA medium without any amendment was used as control. Mycelial growth inhibition was estimated according to the formula: $((d_c - d_t)/d_c) \times 100$, where d_c and d_t represent the average diameters of the fungal colony of the control and of the treated fungal colony, respectively. Effective concentrations (EC₅₀ and EC₉₀) were estimated using PROBIT analysis in IBM SPSS Statistics v.25 (IBM; Armonk, NY, USA) software. The level of interaction, i.e., synergy factors, were determined according to Wadley's method [40].

2.5.2. Greenhouse Bioassays on Grafted Plants

Together with the experiments of mycelial growth inhibition in vitro, bioassays with stevioside–*S. marianum* conjugate complexes were performed in living grapevine plants in order to scale the protective capabilities of these compounds against certain selected *Botryosphaeriaceae* species usually associated with GTD symptoms on young grapevine plants. Especially, *N. parvum*, *D. viticola*, and *D. seriata* were selected for the in vivo assay due to their significant presence as part of the contingent of fungi associated with decay problems in young vine plants [41] in Spain and other viticultural areas internationally. Plant material consisted of 30 plants each of cultivars 'Tempranillo' (CL. 32 clone) (2-years old) and 'Garnacha' (VCR3 clone) (one year old) grafted on 775P and 110R rootstocks, respectively (60 plants in total). Each grapevine plant was grown on a 3.5 L plastic pot containing a mixed substrate of moss peat and sterilized natural soil (75:25), incorporating slow release fertilizer when needed. Plants were kept in the greenhouse with drip irrigation and anti-weed ground cover for six months (June–December 2020). One week after placing them in the pots, grapevine plants were artificially inoculated with the mentioned three *Botryosphaeriaceae* taxa along with the stevioside–*S. marianum* treatment. Five repetitions were arranged for each pathogen/control product combination and variety ('Tempranillo' and 'Garnacha'), together with 8 positive controls (4 per grapevine variety) inoculated only with the pathogens, plus 6 negative controls (incorporating only the bioactive product), 3

for each variety (Table S1). Artificial inoculations of the pathogens and the control product were carried out directly on the trunk of the living plants at two sites per plant stand (separated a minimum of 5 cm among them) below the grafting point and not reaching the root crown. For the pathogens, agar plugs coming from 5-days-old fresh PDA cultures of each species were used as fungal inoculum. In the mentioned two inoculation points of each grapevine plant, slits (made up with a scalpel) of approx. 15 mm in diameter and 5 mm deep were done. After this, 5 mm diameter agar plugs were inoculated in contact with vascular tissues in the stem. Calcium alginate beads served as a dispersal matrix for the different control products and conjugates assayed, and were placed at both sides of the agar plug. For this, beads were prepared as follows: the control product was added to a 3% sodium alginate solution in a 2:8 ratio (20 mL compound/80 mL sodium alginate). Then, this solution was dispensed drop by drop onto a 3% calcium carbonate solution resulting in beads of 4–6 mm diameter containing the different control treatments. Finally, both agar plugs and beads were covered with cotton soaked in sterile bi-distilled water and sealed with Parafilm™ tape. During the assay period, application of copper to control powdery mildew outbreaks was performed in mid-July, together with a first sprouting (followed by periodic sprouting). Grapevine plants were visually examined weekly during the whole assay period, and the presence of foliar symptoms—including both internodal and nodal necroses—was scored to establish correlations between these and vascular symptoms at the end of bioassay. After six months in the greenhouse, plants were removed and two sections of the inoculated stems between the grafting point and the root crown were prepared, sectioned longitudinally, and the length of the vascular necroses caused by the different pathogens evaluated. Thus, the length of the vascular necroses was measured longitudinally on upper and lower directions from the inoculation point for both halves of the longitudinal cut, and the averages were statistically analyzed and compared depending on the type of pathogen and product formulation employed. All the data were compared with controls. Finally, grapevine plants removed and measured at the end of the assay were also processed (after taking measures) to re-isolate the different pathogens previously inoculated. Then, wood chips (0.5 cm long) exhibiting vascular necroses (1–2 cm around the wounds) were washed, surface sterilized, placed on PDA plates amended with streptomycin sulphate (to prevent bacterial contamination) and incubated at 26 °C in the dark in a culture chamber for 2–3 days to fulfil Koch's postulates.

2.6. Statistical Analyses

The results of the *in vitro* inhibition of mycelial growth of the three phytopathogens by the different concentrations of the treatments were statistically analyzed using one-way analysis of variance (ANOVA), followed by post hoc comparison of means through Tukey's test at $p < 0.05$ (provided that the homogeneity and homoscedasticity requirements were satisfied, according to the Shapiro–Wilk and Levene tests). In the case of the greenhouse assay results, since the normality and homoscedasticity requirements were not met, Kruskal–Wallis non-parametric test was used instead, with Conover–Iman test for post hoc multiple pairwise comparisons. R statistical software was used [42].

3. Results

3.1. Vibrational Characterization

The assignments of the major absorption IR bands in *S. marianum* extract spectrum (Figure S3) are presented in Table 2. The most prominent bands occurred at 3335, 1651–1602, 1457, 1313, 1242, and 1029 cm^{-1} . The band at 3335 cm^{-1} is attributed to phenolic (OH) vibrations; the multi-peak band at 1651 cm^{-1} to mixed (C=O) amide and (C=C) vibrations; the peak at 1515 cm^{-1} (typical of ferulic acid and vanillin) to $>\text{C}=\text{C}<$ aromatic; the peak at 1457 cm^{-1} to symmetric aromatic ring stretching vibration (C=C ring); and the peaks at 1030 cm^{-1} and 779 cm^{-1} to C–O stretching and C=C, respectively (both vanillin-related peaks).

Table 2. Main bands in the FTIR spectra of *S. marianum* lyophilized hydromethanolic extract, silymarin and ferulic acid. Band positions are expressed in cm^{-1} .

<i>Silybum marianum</i>	Silymarin	Ferulic Acid	Assignments
3335		3331	OH group in phenolic compounds
	3279		
3069			O–H stretching skeletal vibration due to aromatic C=C ring stretching and C=O stretching
2918	2932	2926	
1651			
1634		1649	
1602		1605	aromatic C=C stretching
1558			>C=C< aromatic
1515		1510	symmetric aromatic ring stretching vibration (C=C ring)
1457			olefinic C–H
1429	1458		
1313	1434		C–H vibration of the methyl group
		1329	Carboxylic acid C=O stretching
		1275	
1242	1257		in plane =C–H bending/C=C stretching
	1126		
1030	1076		C–O stretching/O–H out plane bending
	941		
779			C=C on the aromatic ring
			methylene rocking vibration
	721	693	

3.2. Gas Chromatography–Mass Spectrometry (GC-MS)

GC-MS analyses of the hydro-methanolic extract of *S. marianum* (Figure S4) allowed for the identification of 4-((1E)-3-hydroxy-1-propenyl)-2-methoxyphenol (also named coniferyl alcohol or γ -hydroxyisoeugenol); its analogue *trans*-isoeugenol; 2-propenoic acid, 3-(4-hydroxy-3-methoxyphenyl)-, methyl ester (known as ferulic acid methyl ester); 2-methoxyphenol; and 4-hydroxy-3-methylacetophenone as the main components (Table 3, Figure S5).

Table 3. Phytochemical compounds identified by GC-MS in the hydromethanolic extract of *S. marianum* capitula in phenological stage 67.

Peak	Rt (min)	Area (%)	Tentative Assignments
1	4.8755	2.67	methoxy-phenyl-oxime
2	6.0099	3.50	glycerin
3	7.3293	2.62	hexamethyl-cyclotrisiloxane; tris(tert-butyl)dimethylsilyloxy)arsane
4	7.6360	7.31	2-methoxy-phenol
5	9.4764	2.48	2,3-dihydro-benzofurane
6	9.6516	1.95	methenamine
7	10.8737	3.92	4-hydroxy-3-methylacetophenone
8	12.0275	1.64	vanillin
9	12.6653	1.51	<i>trans</i> -isoeugenol
10	13.0548	1.36	6-methoxy-3-methylbenzofuran
11	15.3139	1.69	4-((1E)-3-hydroxy-1-propenyl)-2-methoxyphenol (also named coniferol or γ -hydroxyisoeugenol)
12	15.5865	0.82	2-hydroxy-4-isopropyl-7-methoxytropone
13	15.9370	1.68	4-hydroxy-3-methoxybenzeneacetic acid, -, methyl ester
14	16.0636	45.64	4-((1E)-3-Hydroxy-1-propenyl)-2-methoxyphenol (also named coniferol or γ -hydroxyisoeugenol)
15	17.1153	14.99	2-propenoic acid, 3-(4-hydroxy-3-methoxyphenyl)-, methyl ester (also named ferulic acid methyl ester)

Table 3. Cont.

Peak	Rt (min)	Area (%)	Tentative Assignments
16	17.9234	0.49	ethyl (2E)-3-(4-hydroxy-3-methoxyphenyl)-2-propenoate
17	19.5447	0.67	9,15-octadecadienoic acid, methyl ester, (Z,Z)-
18	21.1027	2.93	2-(1,4,4-trimethyl-cyclohex-2-enyl)-ethanol
19	24.4377	2.13	9,12-octadecadienoic acid (Z,Z)-, 2,3-dihydroxypropyl ester

Peak = peak identification; Rt = retention time, expressed in minutes; Area = relative peak area percentage.

3.3. Antifungal Activity

3.3.1. In Vitro Growth Inhibition Tests

The results of the mycelial growth inhibition tests are summarized in Figure 1. When tested alone, a higher efficacy of coniferyl alcohol as compared to ferulic acid could be observed: full inhibition was only reached for the former in the case of *N. parvum* and *D. viticola*. In the case of *D. seriata*, for which both treatments resulted in full inhibition, it was attained at a lower dose for coniferyl alcohol (1000 vs. 1500 $\mu\text{g}\cdot\text{mL}^{-1}$). Hence, the antifungal efficacy found for the extracts should be mostly ascribed to its main constituent. On the other hand, upon conjugation with stevioside, a clear enhancement in terms of efficacy was found in all cases, which was particularly evident in the case of the extracts, for which even higher inhibition than that of the coniferyl alcohol conjugates was attained at almost all concentrations against the three pathogens.

If effective concentrations are compared (Table 4), differences in the efficacy of the treatments as a function of the pathogen could be observed for some of the treatments more clearly: for instance, a slightly higher efficacy of stevioside and stevioside–*S. marianum* conjugate complex was found against *N. parvum*, and *D. seriata* seemed to be particularly sensitive to ferulic acid and its conjugate. On the other hand, the response of the three fungi to the coniferyl alcohol-based treatments was very similar.

Table 4. Estimated EC₅₀ and EC₉₀ effective concentrations. Values are expressed in $\mu\text{g}\cdot\text{mL}^{-1}$, and are followed by the standard errors of the fit.

Pathogen	EC	Stevioside	<i>S. marianum</i>	Stevioside– <i>S. marianum</i>	Coniferyl Alcohol	Stevioside–Coniferyl Alcohol	Ferulic Acid	Stevioside–Ferulic Acid
<i>N. parvum</i>	EC ₅₀	152.2 ± 13.4	677.2 ± 47.0	89.2 ± 15.3	214.3 ± 26.2	157.8 ± 16.6	1394.5 ± 63.0	465.9 ± 27.51
	EC ₉₀	824.1 ± 56.7	2938.3 ± 286.6	262.1 ± 19.2	1005.1 ± 71.3	384.9 ± 22.8	2948.6 ± 268.1	1132.7 ± 127.3
<i>D. viticola</i>	EC ₅₀	271.4 ± 26.6	1088.4 ± 93.8	148.3 ± 11.7	361.1 ± 38.8	156.5 ± 8.3	1387.2 ± 134.3	544.5 ± 24.4
	EC ₉₀	1017.0 ± 74.3	9943.2 ± 1038.6	360.7 ± 39.0	988.5 ± 88.6	368.2 ± 26.6	3921.3 ± 438.6	1183.2 ± 111.0
<i>D. seriata</i>	EC ₅₀	230.1 ± 15.3	703.0 ± 26.6	127.1 ± 15.5	370.3 ± 10.4	191.6 ± 12.6	433.0 ± 31.5	209.0 ± 18.1
	EC ₉₀	840.5 ± 62.3	1461.1 ± 111.8	355.4 ± 38.1	913.2 ± 65.6	360.5 ± 29.6	903.4 ± 74.4	465.9 ± 33.2

N. parvum = *Neofusicoccum parvum*; *D. viticola* = *Dothiorella viticola*; *D. seriata* = *Diplodia seriata*; *S. marianum* = *Silybum marianum*; EC = effective concentration; EC₅₀ and EC₉₀ = 50% and 90% effective concentrations, respectively.

In concordance with the above statements, the calculation of synergy factors (Table 5) indicated a strong synergistic behavior for the stevioside–*S. marianum* conjugate, with SF values in the 2.7–5.1 range.

Table 5. Synergy factors for the stevioside–*S. marianum* conjugate complex against the three *Botryosphaeriaceae* taxa.

Effective Concentration	<i>N. parvum</i>	<i>D. viticola</i>	<i>D. seriata</i>
EC ₅₀	2.8	2.9	2.7
EC ₉₀	4.9	5.1	3.0

N. parvum = *Neofusicoccum parvum*; *D. viticola* = *Dothiorella viticola*; *D. seriata* = *Diplodia seriata*; *S. marianum* = *Silybum marianum*; EC₅₀ and EC₉₀ = 50% and 90% effective concentrations, respectively. Synergy factors are expressed as absolute values.

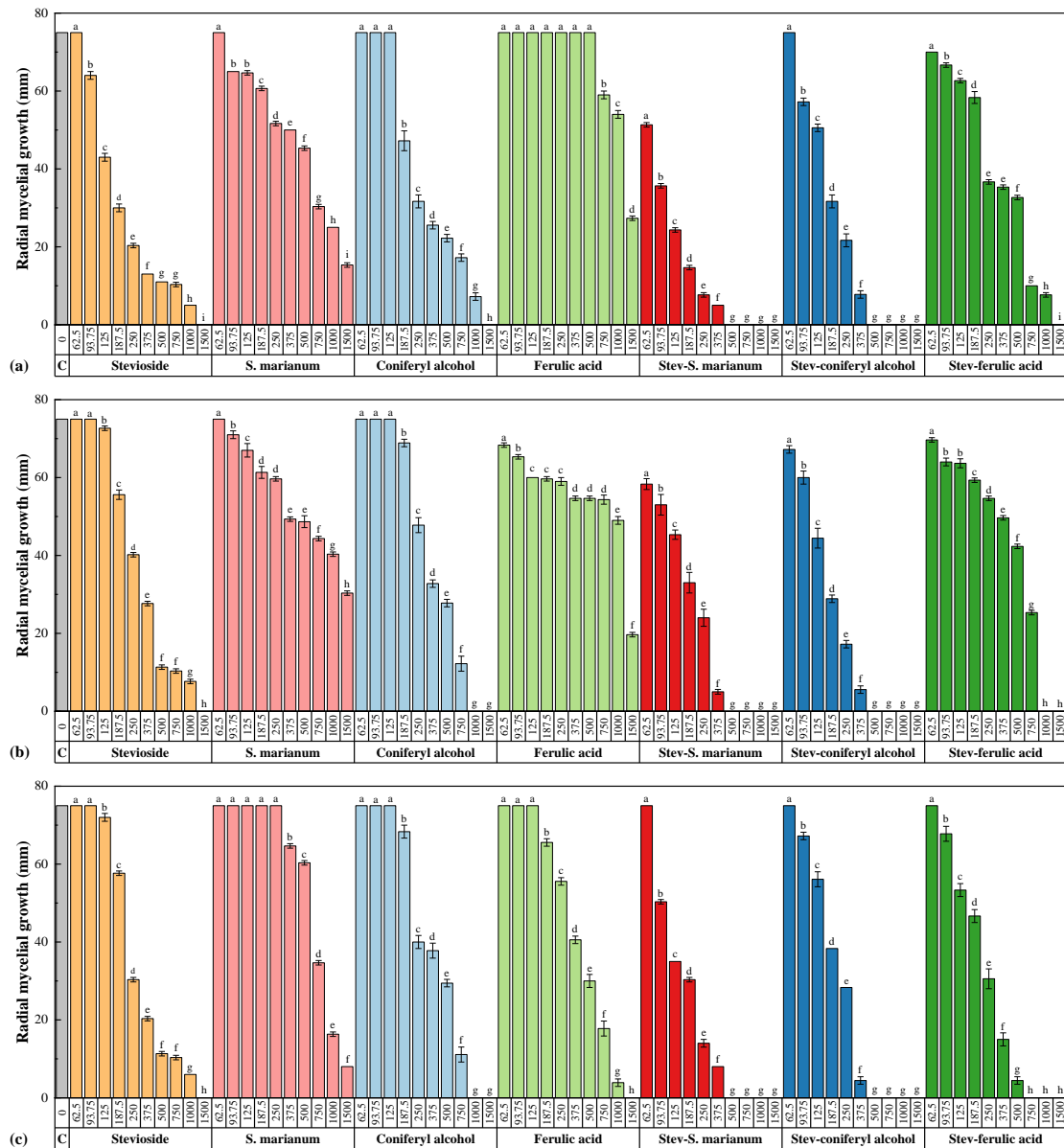


Figure 1. Colony growth measures of (a) *N. parvum*, (b) *D. viticola*, and (c) *D. seriata* strains when cultured in PDA plates containing the various control products (viz. stevioside, *S. marianum* hydromethanolic extract, coniferyl alcohol, ferulic acid, stevioside–*S. marianum*, stevioside–coniferyl alcohol and stevioside–ferulic acid conjugate complexes) at concentrations in the 62.5–1500 µg·mL⁻¹ range. The same letters above concentrations indicate that they are not significantly different at $p < 0.05$. Error bars represent standard deviations.

3.3.2. Greenhouse Bioassays

Protective tests conducted on grafted plants with the stevioside–milk thistle treatment confirmed its efficacy in more realistic conditions (i.e., closer to field ones): the application of the conjugate complex resulted in statistically significant differences as compared to the positive (pathogen) controls in all cases (Table 6). It is worth noting that the median lengths of the vascular necroses were higher in the case of treated plants artificially inoculated with *N. parvum* than for treated plants artificially inoculated with the other two taxa (for which the effectiveness would be similar), which may be regarded as an unexpected result, provided that the associated EC₉₀ value was the lowest in the in vitro tests. This point was confirmed by including the fungus taxon in the statistical analysis as a second independent variable (Table S2). However, no statistically significant differences were observed among the three fungi in terms of necrosis lengths in the positive controls. Interestingly, in the

two-factor analysis, the lengths of the necroses for the treated plants artificially inoculated with *D. viticola* were not significantly different from those of the negative controls, pointing to a particularly high inhibition of this pathogen.

Table 6. Kruskal–Wallis test and multiple pairwise comparisons using the Conover–Iman procedure for the lengths of the vascular necroses for the three phytopathogen in greenhouse in vivo assays.

Pathogen	Sample	Frequency	Sum of Ranks	Mean of Ranks	Groups
<i>N. parvum</i>	Stevioside– <i>S. marianum</i> negative control	48	1275.500	26.573	A
	Stevioside– <i>S. marianum</i>	64	5911.000	92.359	B
	Positive control	64	8389.500	131.086	C
<i>D. viticola</i>	Stevioside– <i>S. marianum</i> negative control	48	2174.000	45.292	A
	Stevioside– <i>S. marianum</i>	64	4272.000	66.750	B
	Positive control	64	9130.000	142.656	C
<i>D. seriata</i>	Stevioside– <i>S. marianum</i> negative control	48	2062.500	42.969	A
	Stevioside– <i>S. marianum</i>	72	5641.500	78.354	B
	Positive control	56	7872.000	140.571	C

N. parvum = *Neofusicoccum parvum*; *D. viticola* = *Dothiorella viticola*; *D. seriata* = *Diplodia seriata*; *S. marianum* = *Silybum marianum*. Treatments/controls labelled with the same letters are not significantly different at $p < 0.05$.

4. Discussion

4.1. Valorization of Coniferyl Alcohol and Ferulic Acid

As expected from the phenological stage in which the plants were collected (flowering, before fruit ripening) and taking into consideration that the entire capitula were used for the extraction (not only the fruits), the panel of extracted components was different from those present in the commercially available milk thistle seed extract: instead of silybin (A and B) and isosilybin (A and B), coniferyl alcohol and other eugenol analogues were identified; and instead of vanillin, the quantitative presence of its precursor (ferulic acid methyl ester) was evidenced.

Coniferyl alcohol is a valuable chemical, which reaches 350 USD·g⁻¹ when bought from commercial suppliers such as Sigma-Aldrich. Current approaches to obtain coniferyl alcohol are either inefficient, harmful (*Penicillium simplicissimum* (Oudemans) Thom vanillyl alcohol oxidase (PsVAO) can be used to produce it, but it intrinsically produces harmful byproduct H₂O₂), or expensive (its synthesis involves expensive substrates and catalyst and harsh reaction conditions) [43,44]. These limitations can be overcome with the ultrasonic-assisted hydro-methanolic extraction of the capitula, reported in this paper, which may allow for the obtainment of the phenylpropanoid coniferyl alcohol with a yield of 50–80%. Alternative extractive approaches, such as the use of ionic liquid analogs (deep eutectic solvents) as extractive solvents [45], microwave-assisted extraction, dynamic maceration process [46], negative pressure cavitation-assisted extraction with macroporous resin enrichment [47], etc., should nonetheless be explored in order to optimize the yield.

In the case that the production of silymarin-based drugs is desired, the biotransformation of eugenol and coniferyl alcohol to silybin and isosilybin can be efficiently attained by the oxidation of the precursors by milk thistle ascorbate peroxidase (APX1), as shown in Figure 2a.

In the same way, the finding of a 10:1 ratio for the ferulic acid–vanillin pair confirms that, for *S. marianum* capitula during the flowering phenological stage in a hydro-methanolic medium, the presence of the ferulic acid precursor is enhanced. Should vanillin be the desired chemical to obtain, the quantitative conversion of ferulic acid into vanillic acid could be feasible in presence of *Pseudomonas* spp. [48] (Figure 2b). The polypore

species *Pycnoporus cinnabarinus* (Jacq.) P. Karst. has also been proposed for the production of vanillin from ferulic acid [49], although the vanillin produced is either rapidly converted to other products or utilized by the fungus as a source of carbon and energy. Genetic engineering has been applied to produce vanillin from ferulic acid using metabolically engineered *Escherichia coli* (Migula, 1895) Castellani and Chalmers, 1919 [50,51]. Another alternative would be the use of packed bed-stirred fermenters using *Bacillus subtilis* (Ehrenberg, 1835) Cohn, 1872 [52].

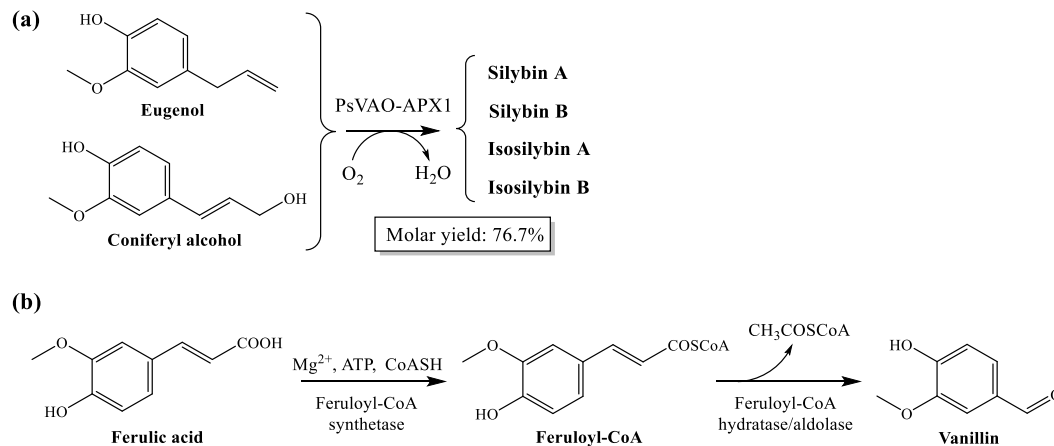


Figure 2. (a) Highly efficient enzymatic cascade engineered for biotransformation of eugenol to silybin and isosilybin. Adapted from [44]. (b) Schematic representation of the non- β -oxidative pathway for conversion of ferulic acid into vanillin, according to [51].

It should be noted that the extraction of coniferyl alcohol and ferulic acid would not preclude the valorization of the rest of the biomass as a feedstock for bioenergy production [53–55].

4.2. Efficacy of the Treatments

Stevioside, a terpene glycoside obtained from *Stevia rebaudiana* (Bertoni) Bertoni, showed a high inhibitory activity, comparable to that of coniferyl alcohol. Since—to the best of the authors' knowledge—this is the first time that this compound is assayed against *Botryosphaeriaceae* fungi, no comparisons with similar taxa in terms of MIC values are available. However, the detected antifungal activity would be in good agreement with the results presented by other authors, who reported an inhibitory effect against other fungi (*Alternaria solani* Sorauer, *Helminthosporium solani* Durieu & Montagne, *Aspergillus* spp., *Fusarium* spp., *Penicillium chrysogenum* Thom, or *Botrytis cinerea* Pers., among others) [56–60], with MIC values varying over a wide range (from 250 to 3000 $\mu\text{g}\cdot\text{mL}^{-1}$).

With regard to the activity of *S. marianum*-derived phytochemicals, the antifungal activity of silymarin/silibinin against *Candida* spp. and its underlying mechanism has been studied by Yun and Lee [18,61] and Janeczko and Kochanowicz [62]. Fernández, et al. [63] found significant inhibition against *Fusarium graminearum* Schwabe for four flower defensins from milk thistle. Safarpour, et al. [64] reported moderate antifungal activities of ethanolic extracts of milk thistle against *C. albicans* and *Aspergillus oryzae* (Ahlb.) Cohn. Some antifungal activity was also reported for leaf and flower ethanolic extracts by Keskin, et al. [65] against *C. albicans*. Nonetheless, in these two latter studies no details were provided about the phenological stage in which the plants were collected, and effective concentrations were not reported.

Concerning the antifungal action of coniferyl alcohol, no data against GTD-related fungi is available in the literature, but—according to Kuc [66]—it has strong antifungal properties. For instance, coniferyl alcohol and its derivatives have been shown to be effective against *Colletotrichum lagenarium* (Pass.) Ellis & Halst., *C. cucumerinum*, *Melampsora lini* Ehrenb.) Lév., and *C. albicans* [19,67,68].

In relation to ferulic acid, it has been assayed against GTDs, and, according to Lambert, et al. [28], it is the phenolic acid with the strongest activity against *D. seriata*, *N. parvum*, *E. lata*, and *P. chlamydospora*. The same group, in a different study, found inhibition percentages in the 23–35% range for ferulic acid at a concentration of 500 μM ($97 \mu\text{g}\cdot\text{mL}^{-1}$) against different *N. parvum* isolates [69]. Gómez, et al. [29] reported half maximal effective concentrations of 3530 and 4740 $\mu\text{g}\cdot\text{mL}^{-1}$ against *Botryosphaeriaceae* sp. and *P. minimum*, and Dekker, et al. [30] found an EC_{50} value of 15 mM ($2913 \mu\text{g}\cdot\text{mL}^{-1}$) against *Botryosphaeria* sp. Srivastava, et al. [70] found that ferulic acid at 25 mM ($4855 \mu\text{g}\cdot\text{mL}^{-1}$) resulted in ca. 80% and ca. 70% mycelium growth inhibition of *B. rhodina* (Berk. & M.A. Curtis) Arx and *B. ribis* Grossenbacher & Duggar, respectively; and 100% inhibition was attained at 20 mM ($3885 \mu\text{g}\cdot\text{mL}^{-1}$) in the case of *B. obtusa* (Schwein.) Shoemaker. Such concentrations are close to the EC_{90} values against *N. parvum* and *D. viticola* reported in this work.

Regarding the conjugate complexes with stevioside, no data is available against GTDs. The most similar assayed product would be the stevioside:silymarin conjugate complexes (in a 1:1 molar ratio) tested against *Fusarium culmorum* (Wm.G. Sm.) Sacc., for which an EC_{90} value of 160 $\mu\text{g}\cdot\text{mL}^{-1}$ and a synergy factor of 1.43 were reported [71]. No antifungal efficacy data is available for stevioside–coniferyl alcohol conjugate complexes, but stevioside–ferulic acid inclusion compounds (with different molar ratios to the one assayed herein, and involving a more complex preparation procedure) have been tested against *F. culmorum* and *Phytophthora cinnamomi* de Bary. In the former case, composites based on stevioside:ferulic acid inclusion compounds (in a 5:1 molar ratio), combined with chitosan oligomers in hydroalcoholic solution or in choline chloride:urea deep eutectic solvent media, led to EC_{90} values in the 377–713 $\mu\text{g}\cdot\text{mL}^{-1}$ range against *F. culmorum* [72], depending on the dispersion medium. In the case of *P. cinnamomi*, inclusion compounds from stevioside and ferulic acid in 6:1 ratio, dispersed in a hydroalcoholic solution of chitosan oligomers, resulted in EC_{90} values of 446–450 $\mu\text{g}\cdot\text{mL}^{-1}$ (depending on the presence/absence of silver nanoparticles) [73,74].

5. Conclusions

In the hydromethanolic extract of *Silybum marianum* capitula, during the flowering stage, high contents of coniferyl alcohol derivatives and ferulic acid esters were found, instead of other chemical species such as the silymarin complex or vanillin. Given the high price of coniferyl alcohol, this may pose an alternative valorization strategy for this weed, compatible with a subsequent valorization for bioenergy purposes. Concerning the antifungal activity of the hydroalcoholic extract, the EC_{50} and EC_{90} values obtained against the three studied Botryosphaeriaceous grapevine pathogens (*N. parvum*, *D. viticola* and *D. seriata*) were in the 557–1088 and 1461–9942 $\mu\text{g}\cdot\text{mL}^{-1}$ range, respectively. However, a significant efficacy enhancement (with EC_{50} and EC_{90} values in the 87–148 and 303–596 $\mu\text{g}\cdot\text{mL}^{-1}$, respectively) was obtained by formation of conjugate complexes of the hydromethanolic extract of *S. marianum* with stevioside, evidencing a clear synergistic behavior (with synergy factor values of up to 5.1) as a result of the solubility and bioavailability improvement. The efficacy of the stevioside–milk thistle conjugate complexes was further assessed in artificially inoculated grafted plants, obtaining significant differences in the vascular necroses lengths vs. the positive controls in all cases. The presented results support the possibility of extending the applications of milk thistle to agriculture as an antifungal agent, in particular for the protection of grapevines against certain fungal trunk diseases.

Supplementary Materials: The following are available online at <https://www.mdpi.com/article/10.3390/plants10071363/s1>, Table S1. Repetitions for each of the plant/treatment/pathogen combinations in the greenhouse bioassay; Table S2. Kruskal-Wallis test and multiple pairwise comparisons using the Conover-Iman procedure for the lengths of the vascular necroses in greenhouse in vivo assays considering two independent variables (treatment and taxa); Figure S1. Biosynthesis of silybins from taxifolin and coniferyl alcohol; Figure S2. Formation of coniferyl alcohol; Figure S3. Infrared spectrum of *S. marianum* extract (after lyophilization); Figure S4. GC–MS spectrum of *S. marianum*

hydromethanolic extract; Figure S5. Chemical structures of some of the phytochemicals identified by GC-MS in the hydro-methanolic extract of *S. marianum*.

Author Contributions: Conceptualization, J.M.-G., P.M.-R. and V.G.-G.; methodology, J.M.-G., J.C.-G. and V.G.-G.; validation, J.C.-G., V.G.-G. and P.M.-R.; formal analysis, J.C.-G., V.G.-G. and P.M.-R.; investigation, L.B.-D., N.L.-L., V.G.-G., J.C.-G., J.M.-G., E.S.-H. and P.M.-R.; resources, J.M.-G. and P.M.-R.; data curation, J.C.-G.; writing—original draft preparation, L.B.-D., N.L.-L., V.G.-G., J.C.-G., J.M.-G., E.S.-H. and P.M.-R.; writing—review and editing, V.G.-G. and P.M.-R.; visualization, L.B.-D. and N.L.-L.; supervision, V.G.-G. and P.M.-R.; project administration, V.G.-G., J.M.-G. and P.M.-R.; funding acquisition, J.M.-G. and P.M.-R. All authors have read and agreed to the published version of the manuscript.

Funding: This research was funded by Junta de Castilla y León under project VA258P18, with FEDER co-funding; by Cátedra Agrobank under “IV Convocatoria de Ayudas de la Cátedra AgroBank para la transferencia del conocimiento al sector agroalimentario” program; and by Fundación Ibercaja-Universidad de Zaragoza under “Convocatoria Fundación Ibercaja-Universidad de Zaragoza de proyectos de investigación, desarrollo e innovación para jóvenes investigadores” program.

Institutional Review Board Statement: Not applicable.

Informed Consent Statement: Not applicable.

Data Availability Statement: The data presented in this study are available on request from the corresponding author. The data are not publicly available due to their relevance to be part of an ongoing Ph.D. Thesis.

Acknowledgments: V.G.-G thanks C. Julián (Plant Protection Unit, CITA) for her technical assistance. The authors gratefully acknowledge the support of Pilar Blasco and Pablo Candela at the Servicios Técnicos de Investigación, Universidad de Alicante, for conducting the GC-MS analyses.

Conflicts of Interest: The authors declare no conflict of interest. The funders had no role in the design of the study; in the collection, analyses, or interpretation of data; in the writing of the manuscript, or in the decision to publish the results.

References

1. Das, S.K.; Mukherjee, S.; Vasudevan, D. Medicinal properties of milk thistle with special reference to silymarin—An overview. *Nat. Prod. Radianc* **2008**, *7*, 182–192.
2. Gazak, R.; Walterova, D.; Kren, V. Silybin and silymarin—New and emerging applications in medicine. *Curr. Med. Chem.* **2007**, *14*, 315–338. [[CrossRef](#)]
3. Šimánek, V.; Kren, V.; Ulrichová, J.; Vicar, J.; Cvak, L. Silymarin: What is in the name . . . ? An appeal for a change of editorial policy. *Hepatology* **2000**, *32*, 442–444. [[CrossRef](#)]
4. ElSayed, A.I.; El-hamahmy, M.A.M.; Rafudeen, M.S.; Mohamed, A.H.; Omar, A.A. The impact of drought stress on antioxidant responses and accumulation of flavonolignans in milk thistle (*Silybum marianum* (L.) Gaertn.). *Plants* **2019**, *8*, 611. [[CrossRef](#)] [[PubMed](#)]
5. AbouZid, S.; Ahmed, O.M. Silymarin flavonolignans: Structure–activity relationship and biosynthesis. In *Studies in Natural Products Chemistry*; Atta-ur-Rahman, F.R.S., Ed.; Elsevier: Amsterdam, The Netherlands, 2013; Volume 40, pp. 469–484.
6. AbouZid, S.F.; Chen, S.-N.; McAlpine, J.B.; Friesen, J.B.; Pauli, G.F. *Silybum marianum* pericarp yields enhanced silymarin products. *Fitoterapia* **2016**, *112*, 136–143. [[CrossRef](#)] [[PubMed](#)]
7. Habán, M.; Otepka, P.; Kobida, L.; Habánová, M. Production and quality of milk thistle (*Silybum marianum* [L.] Gaertn.) cultivated in cultural conditions of warm agri-climatic macroregion. *Hortic. Sci.* **2009**, *36*, 69–74. [[CrossRef](#)]
8. Lv, Y.; Gao, S.; Xu, S.; Du, G.; Zhou, J.; Chen, J. Spatial organization of silybin biosynthesis in milk thistle [*Silybum marianum* (L.) Gaertn.]. *Plant J.* **2017**, *92*, 995–1004. [[CrossRef](#)] [[PubMed](#)]
9. Drouet, S.; Tungmunnithum, D.; Lainé, É.; Hano, C. Gene expression analysis and metabolite profiling of silymarin biosynthesis during milk thistle (*Silybum marianum* (L.) Gaertn.) fruit ripening. *Int. J. Mol. Sci.* **2020**, *21*, 4730. [[CrossRef](#)] [[PubMed](#)]
10. Saidi, I.; Bessam, H.M.; Benchaachoua, A. Effects of different extraction methods and solvents on the phenolic composition and antioxidant activity of *Silybum marianum* leaves extracts. *Int. J. Med. Sci. Clin. Invent.* **2018**, *5*, 3641–3647. [[CrossRef](#)]
11. Mani, P.; Senthilkumar, S.; Sasikala, P.; Azhagumadhavan, S.; Jayaseelan, T.; Ganesan, S.; Padma, M. Phytochemical screening and GC-MS analysis of bioactive compounds present in ethanolic leaves extract of *Silybum marianum* (L.). *J. Drug Deliv. Ther.* **2019**, *9*, 85–89. [[CrossRef](#)]
12. Sulas, L.; Re, G.A.; Bullitta, S.; Piluzza, G. Chemical and productive properties of two Sardinian milk thistle (*Silybum marianum* (L.) Gaertn.) populations as sources of nutrients and antioxidants. *Genet. Resour. Crop. Evol.* **2015**, *63*, 315–326. [[CrossRef](#)]

13. Vanholme, R.; Demedts, B.; Morreel, K.; Ralph, J.; Boerjan, W. Lignin biosynthesis and structure. *Plant Physiol.* **2010**, *153*, 895–905. [[CrossRef](#)]
14. Daurade-Le Vagueresse, M.H.; Romiti, C.; Grosclaude, C.; Bounias, M. Coevolutionary toxicity as suggested by differential coniferyl alcohol inhibition of ceratocystis species growth. *Toxicon* **2001**, *39*, 203–208. [[CrossRef](#)]
15. Kalinova, J.; Triska, J.; Vrchotova, N. Occurrence of eugenol, coniferyl alcohol and 3,4,5-trimethoxyphenol in common buck-wheat (*Fagopyrum esculentum* Moench) and their biological activity. *Acta Physiol. Plant.* **2011**, *33*, 1679–1685. [[CrossRef](#)]
16. de Oliveira Silva, E.; Batista, R. Ferulic acid and naturally occurring compounds bearing a feruloyl moiety: A review on their structures, occurrence, and potential health benefits. *Compr. Rev. Food Sci. Food Saf.* **2017**, *16*, 580–616. [[CrossRef](#)] [[PubMed](#)]
17. Mohammed, F.S.; Pehlivan, M.; Sevindik, M. Antioxidant, antibacterial and antifungal activities of different extracts of *Silybum marianum* collected from Duhok (Iraq). *Int. J. Second. Metab.* **2019**, 317–322. [[CrossRef](#)]
18. Yun, D.G.; Lee, D.G. Silymarin exerts antifungal effects via membrane-targeted mode of action by increasing permeability and inducing oxidative stress. *Biochim. Biophys. Acta Biomembr.* **2017**, *1859*, 467–474. [[CrossRef](#)] [[PubMed](#)]
19. Fuzzati, N. Phenylpropane derivatives from roots of *Cosmos caudatus*. *Phytochemistry* **1995**, *39*, 409–412. [[CrossRef](#)]
20. Tawata, S.; Taira, S.; Kobamoto, N.; Zhu, J.; Ishihara, M.; Toyama, S. Synthesis and antifungal activity of cinnamic acid esters. *Biosci. Biotechnol. Biochem.* **2014**, *60*, 909–910. [[CrossRef](#)]
21. Wu, H.-s.; Luo, J.; Raza, W.; Liu, Y.-x.; Gu, M.; Chen, G.; Hu, X.-f.; Wang, J.-h.; Mao, Z.-s.; Shen, Q.-r. Effect of exogenously added ferulic acid on in vitro *Fusarium oxysporum* f. sp. *niveum*. *Sci. Hortic.* **2010**, *124*, 448–453. [[CrossRef](#)]
22. Barral, B.; Chillet, M.; Minier, J.; Léchaudel, M.; Schorr-Galindo, S. Evaluating the response to *Fusarium ananatum* inoculation and antifungal activity of phenolic acids in pineapple. *Fungal Biol.* **2017**, *121*, 1045–1053. [[CrossRef](#)]
23. Ribes, S.; Fuentes, A.; Talens, P.; Barat, J.M. Combination of different antifungal agents in oil-in-water emulsions to control strawberry jam spoilage. *Food Chem.* **2018**, *239*, 704–711. [[CrossRef](#)]
24. Liu, H.; Zhao, H.; Lyu, L.; Huang, Z.; Fan, S.; Wu, W.; Li, W. Synergistic effect of natural antifungal agents for postharvest diseases of blackberry fruits. *J. Sci. Food Agric.* **2019**, *99*, 3343–3349. [[CrossRef](#)]
25. Khatkar, A.; Nanda, A.; Kumar, P.; Narasimhan, B. Synthesis and antimicrobial evaluation of ferulic acid derivatives. *Res. Chem. Intermed.* **2013**, *41*, 299–309. [[CrossRef](#)]
26. Mahiwal, K.; Kumar, P.; Narasimhan, B. Synthesis, antimicrobial evaluation, ot-QSAR and mt-QSAR studies of 2-amino benzoic acid derivatives. *Med. Chem. Res.* **2010**, *21*, 293–307. [[CrossRef](#)]
27. Batista, E.; Lopes, A.; Alves, A. What do we know about Botryosphaeriaceae? An overview of a worldwide cured dataset. *Forests* **2021**, *12*, 313. [[CrossRef](#)]
28. Lambert, C.; Bisson, J.; Waffo-Teguo, P.; Papastamoulis, Y.; Richard, T.; Corio-Costet, M.F.; Merillon, J.M.; Cluzet, S. Phenolics and their antifungal role in grapevine wood decay: Focus on the Botryosphaeriaceae family. *J. Agric. Food. Chem.* **2012**, *60*, 11859–11868. [[CrossRef](#)]
29. Gómez, P.; Báidez, A.G.; Ortuño, A.; del Río, J.A. Grapevine xylem response to fungi involved in trunk diseases. *Ann. Appl. Biol.* **2016**, *169*, 116–124. [[CrossRef](#)]
30. Dekker, R.F.H.; Barbosa, A.M.; Sargent, K. The effect of lignin-related compounds on the growth and production of laccases by the ascomycete, *Botryosphaeria* sp. *Enzym. Microb. Technol.* **2002**, *30*, 374–380. [[CrossRef](#)]
31. Mondello, V.; Songy, A.; Battiston, E.; Pinto, C.; Coppin, C.; Trotel-Aziz, P.; Clement, C.; Mugnai, L.; Fontaine, F. Grapevine trunk diseases: A review of fifteen years of trials for their control with chemicals and biocontrol agents. *Plant Dis.* **2018**, *102*, 1189–1217. [[CrossRef](#)]
32. Shakeel, F.; Salem-Bekhit, M.M.; Haq, N.; Siddiqui, N.A. Solubility and thermodynamics of ferulic acid in different neat sol-vents: Measurement, correlation and molecular interactions. *J. Mol. Liq.* **2017**, *236*, 144–150. [[CrossRef](#)]
33. Nguyen, T.T.H.; Si, J.; Kang, C.; Chung, B.; Chung, D.; Kim, D. Facile preparation of water soluble curcuminoids extracted from turmeric (*Curcuma longa* L.) powder by using steviol glucosides. *Food Chem.* **2017**, *214*, 366–373. [[CrossRef](#)]
34. Martinelli, T.; Andrzejewska, J.; Salis, M.; Sulas, L. Phenological growth stages of *Silybum marianum* according to the extended BBCH scale. *Ann. Appl. Biol.* **2015**, *166*, 53–66. [[CrossRef](#)]
35. Martín, M.T.; Cobos, R. Identification of fungi associated with grapevine decline in Castilla y León (Spain). *Phytopathol. Mediterr.* **2007**, *46*, 18–25.
36. Nunn, S.; Nishikida, K. *Advanced ATR Correction Algorithm—Application Note 50581*; ThermoScientific: Madison, WI, USA, 2008; p. 4.
37. Adams, R.P. *Identification of Essential Oil Components by Gas Chromatography/Mass Spectroscopy*, 4th ed.; Allured Publishing Corporation: Carol Stream, IL, USA, 2007; p. 804.
38. Buzón-Durán, L.; Martín-Gil, J.; Pérez-Lebeña, E.; Ruano-Rosa, D.; Revuelta, J.L.; Casanova-Gascón, J.; Ramos-Sánchez, M.C.; Martín-Ramos, P. Antifungal agents based on chitosan oligomers, ϵ -polylysine and *Streptomyces* spp. secondary metabolites against three Botryosphaeriaceae species. *Antibiotics* **2019**, *8*, 99. [[CrossRef](#)]
39. Arendrup, M.C.; Cuenca-Estrella, M.; Lass-Flörl, C.; Hope, W. EUCAST technical note on the EUCAST definitive document EDef 7.2: Method for the determination of broth dilution minimum inhibitory concentrations of antifungal agents for yeasts EDef 7.2 (EUCAST-AFST). *Clin. Microbiol. Infect.* **2012**, *18*, E246–E247. [[CrossRef](#)] [[PubMed](#)]
40. Levy, Y.; Benderly, M.; Cohen, Y.; Gisi, U.; Bassand, D. The joint action of fungicides in mixtures: Comparison of two methods for synergy calculation. *EPPO Bull.* **1986**, *16*, 651–657. [[CrossRef](#)]

41. Aroca, Á.; Gramaje, D.; Armengol, J.; García-Jiménez, J.; Raposo, R. Evaluation of the grapevine nursery propagation process as a source of *Phaeoacremonium* spp. and *Phaeomoniella chlamydospora* and occurrence of trunk disease pathogens in root-stock mother vines in Spain. *Eur. J. Plant Pathol.* **2010**, *126*, 165–174. [[CrossRef](#)]
42. R Core Team. *R: A Language and Environment for Statistical Computing*; R Foundation for Statistical Computing: Vienna, Austria, 2020.
43. Lv, Y.; Cheng, X.; Wu, D.; Du, G.; Zhou, J.; Chen, J. Improving bioconversion of eugenol to coniferyl alcohol by in situ eliminating harmful H₂O₂. *Bioresour. Technol.* **2018**, *267*, 578–583. [[CrossRef](#)] [[PubMed](#)]
44. Lv, Y.; Xu, S.; Lyu, Y.; Zhou, S.; Du, G.; Chen, J.; Zhou, J. Engineering enzymatic cascades for the efficient biotransformation of eugenol and taxifolin to silybin and isosilybin. *Green Chem.* **2019**, *21*, 1660–1667. [[CrossRef](#)]
45. Zainal-Abidin, M.H.; Hayyan, M.; Hayyan, A.; Jayakumar, N.S. New horizons in the extraction of bioactive compounds using deep eutectic solvents: A review. *Anal. Chim. Acta* **2017**, *979*, 1–23. [[CrossRef](#)] [[PubMed](#)]
46. Pereira, S.V.; Reis, R.A.S.P.; Garbuio, D.C.; de Freitas, L.A.P. Dynamic maceration of *Matricaria chamomilla* inflorescences: Optimal conditions for flavonoids and antioxidant activity. *Rev. Bras. Farmacogn.* **2018**, *28*, 111–117. [[CrossRef](#)]
47. Qi, X.-L.; Peng, X.; Huang, Y.-Y.; Li, L.; Wei, Z.-F.; Zu, Y.-G.; Fu, Y.-J. Green and efficient extraction of bioactive flavonoids from *Equisetum palustre* L. by deep eutectic solvents-based negative pressure cavitation method combined with macroporous resin enrichment. *Ind. Crop. Prod.* **2015**, *70*, 142–148. [[CrossRef](#)]
48. Civolani, C.; Barghini, P.; Roncetti, A.R.; Ruzzi, M.; Schiesser, A. Bioconversion of ferulic acid into vanillic acid by means of a vanillate-negative mutant of *Pseudomonas fluorescens* strain BF13. *Appl. Environ. Microbiol.* **2000**, *66*, 2311–2317. [[CrossRef](#)]
49. Oddou, J.; Stentelaire, C.; Lesage-Meessen, L.; Asther, M.; Colonna Ceccaldi, B. Improvement of ferulic acid bioconversion into vanillin by use of high-density cultures of *Pycnoporus cinnabarinus*. *Appl. Microbiol. Biotechnol.* **1999**, *53*, 1–6. [[CrossRef](#)]
50. Barghini, P.; di Gioia, D.; Fava, F.; Ruzzi, M. Vanillin production using metabolically engineered *Escherichia coli* under non-growing conditions. *Microb. Cell Factories* **2007**, *6*. [[CrossRef](#)] [[PubMed](#)]
51. Luziatelli, F.; Brunetti, L.; Ficca, A.G.; Ruzzi, M. Maximizing the efficiency of vanillin production by biocatalyst enhancement and process optimization. *Front. Bioeng. Biotechnol.* **2019**, *7*, 279. [[CrossRef](#)] [[PubMed](#)]
52. Yan, L.; Chen, P.; Zhang, S.; Li, S.; Yan, X.; Wang, N.; Liang, N.; Li, H. Biotransformation of ferulic acid to vanillin in the packed bed-stirred fermentors. *Sci. Rep.* **2016**, *6*. [[CrossRef](#)]
53. Sulas, L.; Ventura, A.; Murgia, L. Phytomass production from *Silybum marianum* for bioenergy. In *Sustainable Mediterranean Grasslands and Their Multi-Functions*; Porqueddu, C., Tavares de Sousa, M.M., Eds.; Mediterranean Agronomic Institute of Zaragoza: Zaragoza, Spain, 2008; Volume 79, pp. 487–490.
54. Domínguez, M.T.; Madejón, P.; Madejón, E.; Diaz, M.J. Novel energy crops for Mediterranean contaminated lands: Valorization of *Dittrichia viscosa* and *Silybum marianum* biomass by pyrolysis. *Chemosphere* **2017**, *186*, 968–976. [[CrossRef](#)] [[PubMed](#)]
55. Hunce, S.Y.; Clemente, R.; Bernal, M.P. Energy production potential of phytoremediation plant biomass: *Helianthus annuus* and *Silybum marianum*. *Ind. Crop. Prod.* **2019**, *135*, 206–216. [[CrossRef](#)]
56. Ghosh, S.; Subudhi, E.; Nayak, S. Antimicrobial assay of *Stevia rebaudiana* Bertoni leaf extracts against 10 pathogens. *Int. J. Integr. Biol.* **2008**, *2*, 27–31.
57. Abou-Arab, E.; Abu-Salem, F. Evaluation of bioactive compounds of *Stevia rebaudiana* leaves and callus. *J. Food Dairy Sci.* **2010**, *1*, 209–224. [[CrossRef](#)]
58. Arya, A.; Kumar, S.; Kasana, M. In vitro regeneration of *Stevia* and evaluation of antimicrobial and antiprotozoal properties of regenerated calli and plants. *Electron. J. Plant Breed.* **2012**, *3*, 916–924.
59. Shukla, S.; Mehta, A.; Bajpai, V.K. Phytochemical screening and anthelmintic and antifungal activities of leaf extracts of *Stevia rebaudiana*. *J. Biol. Act. Prod. Nat.* **2013**, *3*, 56–63. [[CrossRef](#)]
60. Guerra Ramírez, P.; Guerra Ramírez, D.; Zavaleta Mejía, E.; Aranda Ocampo, S.; Nava Díaz, C.; Rojas Martínez, R.I. Extracts of *Stevia rebaudiana* against *Fusarium oxysporum* associated with tomato cultivation. *Sci. Hort.* **2020**, *259*, 108683. [[CrossRef](#)]
61. Yun, D.G.; Lee, D.G. Assessment of silibinin as a potential antifungal agent and investigation of its mechanism of action. *IUBMB Life* **2017**, *69*, 631–637. [[CrossRef](#)]
62. Janeczko, M.; Kochanowicz, E. Silymarin, a popular dietary supplement shows anti-*Candida* activity. *Antibiotics* **2019**, *8*, 206. [[CrossRef](#)]
63. Fernández, A.; Colombo, M.L.; Curto, L.M.; Gómez, G.E.; Delfino, J.M.; Guzmán, F.; Bakás, L.; Malbrán, I.; Vairo-Cavalli, S.E. Peptides derived from the α -core and γ -core regions of a putative *Silybum marianum* flower defensin show antifungal activity against *Fusarium graminearum*. *Front. Microbiol.* **2021**, *12*, 632008. [[CrossRef](#)]
64. Safarpour, M.; Ghaedi, M.; Asfaram, A.; Yousefi-Nejad, M.; Javadian, H.; Zare Khafri, H.; Bagherinasab, M. Ultra-sound-assisted extraction of antimicrobial compounds from *Thymus daenensis* and *Silybum marianum*: Antimicrobial activity with and without the presence of natural silver nanoparticles. *Ultrason. Sonochem.* **2018**, *42*, 76–83. [[CrossRef](#)]
65. Keskin, D.; Oskay, D.; Oskay, M. Antimicrobial activity of selected plant spices marketed in the West Anatolia. *Int. J. Agric. Biol.* **2010**, *12*, 916–920.
66. Kuc, J. Induced systemic resistance in plants to diseases caused by fungi and bacteria. In *The Dynamics of Host Defence*; Bailey, J., Deverall, B., Eds.; Academic Press: New York, NY, USA, 1983; pp. 191–221.
67. Hammerschmidt, R.; Kuč, J. Lignification as a mechanism for induced systemic resistance in cucumber. *Physiol. Plant Pathol.* **1982**, *20*, 61–71. [[CrossRef](#)]

68. Keen, N.T.; Littlefield, L.J. The possible association of phytoalexins with resistance gene expression in flax to *Melampsora lini*. *Physiol. Plant Pathol.* **1979**, *14*, 265–280. [[CrossRef](#)]
69. Lambert, C.; Papastamoulis, Y.; Waffo-Tégou, P.; Mérillon, J.; Cluzet, S. Effects of phenolic compounds towards grapevine wood decay fungi. Proceedings of Oeno2011: Actes de colloques du 9e symposium international d’oenologie de Bordeaux, Bordeaux, France, 15–17 June 2011; pp. 90–94.
70. Srivastava, P.; Andersen, P.C.; Marois, J.J.; Wright, D.L.; Srivastava, M.; Harmon, P.F. Effect of phenolic compounds on growth and ligninolytic enzyme production in *Botryosphaeria* isolates. *Crop Prot.* **2013**, *43*, 146–156. [[CrossRef](#)]
71. Buzón-Durán, L.; Martín-Gil, J.; Ramos-Sánchez, M.d.C.; Pérez-Lebeña, E.; Marcos-Robles, J.L.; Fombellida-Villafruela, Á.; Martín-Ramos, P. Antifungal activity against *Fusarium culmorum* of stevioside, *Silybum marianum* seed extracts, and their conjugate complexes. *Antibiotics* **2020**, *9*, 440. [[CrossRef](#)] [[PubMed](#)]
72. Matei, P.; Iacomì, B.; Martín-Gil, J.; Pérez-Lebeña, E.; Ramos-Sánchez, M.; Barrio-Arredondo, M.; Martín-Ramos, P. In vitro antifungal activity of composites of AgNPs and polyphenol inclusion compounds against *Fusarium culmorum* in different dispersion media. *Agronomy* **2018**, *8*, 239. [[CrossRef](#)]
73. Matei, P.; Martín-Gil, J.; Michaela Iacomì, B.; Pérez-Lebeña, E.; Barrio-Arredondo, M.; Martín-Ramos, P. Silver nanoparticles and polyphenol inclusion compounds composites for *Phytophthora cinnamomi* mycelial growth inhibition. *Antibiotics* **2018**, *7*, 76. [[CrossRef](#)]
74. Matei, P.M.; Buzón-Durán, L.; Pérez-Lebeña, E.; Martín-Gil, J.; Iacomì, B.M.; Ramos-Sánchez, M.C.; Martín-Ramos, P. In vitro antifungal activity of chitosan-polyphenol conjugates against *Phytophthora cinnamomi*. *AgriEngineering* **2020**, *2*, 72–77. [[CrossRef](#)]

ARTÍCULO 4: "Rutin-stevioside and related conjugates for potential control of grapevine trunk diseases" *Phytopathologia Mediterranea*, 2022, 61 (1), 65; <https://doi.org/10.36253/phyto-13108>; Q2 (JCR, Science Edition – AGRONOMY; PLANT SCIENCES). JIF₂₀₂₂ = 2,4. 1 cita recibida (CrossRef).

PHYTOPATHOLOGIA MEDITERRANEA

ABOUT THE JOURNAL ▾

ONLINEFIRST ARTICLES

CURRENT ISSUE

ALL ISSUES ▾

OUR POLICIES ▾

Vol. 61 No. 1 (2022)

ARTICLES

Rutin-stevioside and related conjugates for potential control of grapevine trunk diseases

 Laura Buzón-Durán,  Natalia Langa-Lomba, Vicente González-García,  José Casanova-Gascón,  Eva Sánchez-Hernández,  Jesús Martín-Gil,  Pablo Martín Ramos



Citation: L. Buzón-Durán, N. Langa-Lomba, V. González-García, J. Casanova-Gascón, E. Sánchez-Hernández, J. Martín-Gil, P. Martín-Ramos (2022) Rutin-stevioside and related conjugates for potential control of grapevine trunk diseases. *Phytopathologia Mediterranea* 61(1): 65-77. doi: 10.36253/phyto-13108

Accepted: November 9, 2021

Published: March 25, 2022

Copyright: © 2022 L. Buzón-Durán, N. Langa-Lomba, V. González-García, J. Casanova-Gascón, E. Sánchez-Hernández, J. Martín-Gil, P. Martín-Ramos. This is an open access, peer-reviewed article published by Firenze University Press (<http://www.fupress.com/pm>) and distributed under the terms of the Creative Commons Attribution License, which permits unrestricted use, distribution, and reproduction in any medium, provided the original author and source are credited.

Data Availability Statement: All relevant data are within the paper and its Supporting Information files.

Competing Interests: The Author(s) declare(s) no conflict of interest.

Editor: José R. Úrbez Torres, Agriculture and Agri-Food Canada, Summerland, British Columbia, Canada.

Research Papers

Rutin-stevioside and related conjugates for potential control of grapevine trunk diseases

LAURA BUZÓN-DURÁN¹, NATALIA LANGA-LOMBA^{2,3}, VICENTE GONZÁLEZ-GARCÍA^{3,*}, JOSÉ CASANOVA-GASCÓN², EVA SÁNCHEZ-HERNÁNDEZ¹, JESÚS MARTÍN-GIL¹, PABLO MARTÍN-RAMOS²

¹ Department of Agricultural and Forestry Engineering, ETSIIAA, Universidad de Valladolid, Avda. Madrid 44, 34004 Palencia, Spain

² Instituto Universitario de Investigación en Ciencias Ambientales de Aragón (IUCA), EPS, Universidad de Zaragoza, Carretera de Cuarte s/n, 22071 Huesca, Spain

³ Plant Protection Unit, Agrifood Research and Technology Centre of Aragón, Instituto Agroalimentario de Aragón—IA2 (CITA-Universidad de Zaragoza), Avda. Montañana 930, 50059 Zaragoza, Spain

* Corresponding author. E-mail: vgonzalezg@aragon.es

Summary. Flavonoids and phenolic acids play roles in grapevine defence against pathogens causing grapevine trunk diseases (GTDs). Rutin is a major flavonoid in vegetative organs of the grapevines, and this compound, unlike other flavonoids, is non-toxic and non-oxidizable. Rutin was assayed *in vitro* and *in vivo* against two *Botryosphaeriaceae* taxa. The limited bioavailability of this compound was circumvented by conjugation with stevioside, a glycoside obtained from *Stevia rebaudiana*. Clear synergistic effects were observed for the stevioside-rutin adduct, resulting in EC₅₀ and EC₉₀ values of 306.0 and 714.9 µg·mL⁻¹ against *Neofusicoccum parvum* and 241.6 and 457.8 µg·mL⁻¹ against *Dothiorella viticola*. In greenhouse experiments, moderate inhibition of *N. parvum* growth and complete inhibition of *D. viticola* were observed. These inhibitory effects were greater than those of ferulic acid, which has been considered the most effective phenolic acid against GTDs. Conjugation with stevioside provided solubility enhancement of rutin, paving the way to the design of glycopesticides based on rutin-rich plant extracts as promising antifungals against GTDs.

Keywords. Antifungal, *Botryosphaeria dieback*, candyleaf, GTDs, rutoside.

INTRODUCTION

Grapevine (*Vitis vinifera* L.) cultivars can be severely affected by many pathogens, including fungi, bacteria, oomycetes, and viruses. Grapevine trunk diseases (GTDs) have long been responsible for significant economic losses, with some of these diseases being well-known for more than 100 years. The interest of the viticulture sector in this group of diseases has increased in the last three decades, due to, firstly, increased mortality of young nursery-produced grapevine plants, especially 1–3 years after planting in the field, and secondly, the progressive suspension of the use of chemical

fungicides, which has resulted in progressive increases in the incidence and losses due to these diseases.

Current agricultural policies are provoking interest in the development of alternative, naturally-derived antifungal products for the sustainable management of grapevine diseases. However, there are other factors directly or indirectly involved in the expansion of GTDs, in young and mature vineyards. Some factors are related to changes in cultural practices, such as reduced protection of pruning wounds or reductions in sanitary control measures in certified propagation material (Graniti *et al.*, 2000). It is also commonly accepted that a correlation exists between the increase in the incidence of decay of young grapevine plants and increased demand for new plantings or replacements in the different world production areas. This has led to the advocacy of a system where infected propagation material from nurseries is considered the primary source of inoculum causing young vine decline. Numerous studies (see Surico (2001) and Fourie and Halleen (2004)) have correlated the presence of particular fungi causing propagation material decay in nurseries with the death of grapevine plants in the very first years after vineyard planting.

Natural compounds that have been tested against the three main GTDs (*Botryosphaeria dieback*, *Esca* complex, and *Eutypa dieback*) include chitosan, garlic extract, tea tree (*Melaleuca alternifolia* (Maiden & Betche) Cheel) oil, green coffee extract, lemon peel extract, honey, propolis, seaweed extract, and saponins (Mondello *et al.*, 2018). Nonetheless, few studies have focused on the specific bioactive phytochemicals associated with these natural extracts and compounds, which could provide increased efficacy for products with variable phytochemical composition, resulting from genetic variability, and/or environmental variability influenced by weather or soil fertility.

Phytoalexins, which in grapevines are phenolic compounds including tannins, phenolic acids, flavonoids, and stilbenes, are involved in grapevine defence, increasing host resistance to pathogens (Del Río *et al.*, 2004). The progression of fungal pathogens along grapevine wood is inhibited by polyphenol-rich reaction zones (Fontaine *et al.*, 2016). The possible roles of phenolics in defence against GTD casual agents were studied by Lambert *et al.* (2012a), who analysed the *in vitro* effects of 24 grapevine compounds (eight phenolic acids, three flavan-3-ols, two flavonols, and 11 stilbenoids) on six *Botryosphaeriaceae* taxa. They showed that these pathogens were differentially susceptible to phenolics, and concluded that ferulic acid (*trans*-4-hydroxy-3-methoxycinnamic acid) was one of the

most active compounds, causing an inhibition comparable to that from the stilbenoids ϵ -viniferin, vitisin A and B, or *trans*-pterostilbene. However, Lambert *et al.* (2012a) detected no inhibitory activity on any wood disease fungi for flavonols (kaempferol and quercetin) and flavan-3-ols [(+)-catechin, (-)-epicatechin, and epicatechin-3-*O*-gallate]. In some cases, these compounds enhanced the growth of some of the assayed fungi. In contrast, other authors have reported that catechin inhibited fungi involved in Petri disease, and other GTDs (caused by *Phaeoconiella chlamydospora* (W. Gams, Crous, M.J. Wingf. & Mugnai) Crous & W. Gams, *Phaeoacremonium aleophilum* W. Gams, Crous, M.J. Wingf. & L. Mugnai, *Eutypa lata* (Pers.) Tul & C. Tul, and *Stereum hirsutum* (Willd.) Pers.) (Del Río *et al.*, 2004). Furthermore, the antifungal efficacy of flavonoids is well-recognised (Jin, 2019; Al Aboody and Mickymaray, 2020). To gain further insight into these conflicting results, the present study compared the effectiveness of the flavonoid-3-*O*-glycoside rutin (also known as rutoside, phytomelin, or quercetin 3-*O*-rutinoside) with that of ferulic acid. Rutin is one of the most abundant polyphenols (excluding stilbenes) in the vegetative organs of grapevine plants, found at mean concentrations of 257 mg·kg⁻¹ (Goufo *et al.*, 2020), and has significant antimicrobial activity (Ganeshpurkar and Saluja, 2017). The use of rutin is advantageous compared with other flavonoids as it is non-toxic and non-oxidizable (Sharma *et al.*, 2013).

Low water-solubility of phenolic acids, e.g., ferulic acid (Shakeel *et al.*, 2017) and flavonoids (Chebil *et al.*, 2007), can limit their bioavailability and applicability (Hussain *et al.*, 2017). This may be circumvented through the formation of inclusion compounds or conjugate complexes with terpene glycosides (Nguyen *et al.*, 2017). Stevioside (the major constituent of *Stevia rebaudiana* (Bertoni) Bertoni extract) may be a suitable option to form conjugate complexes, resulting in enhanced antifungal activity. Clear synergistic effects have been reported from the conjugation of phenolic acids with stevioside against *Fusarium culmorum* (Wm.G.Sm.) Sacc. (Buzón-Durán *et al.*, 2020) and *Phytophthora cinnamomi* Rands (Matei *et al.*, 2018b).

The goal of the present study was to assess the *in vitro* and *in vivo* antifungal activities of rutin against the two most important *Botryosphaeriaceae* taxa that cause GTDs, especially of young grapevines. Rutin was assessed alone and in a conjugate complex with stevioside, and was compared with ferulic acid as a reference substance. This information should be useful for selecting promising plant sources of natural antifungal products for use in organic or integrative viticulture.

MATERIALS AND METHODS

Reagents

Rutin hydrate (CAS 207671-50-9, $\geq 94\%$), ferulic acid (CAS 537-98-4, European Pharmacopoeia reference standard), sodium alginate (CAS 9005-38-3), calcium carbonate (CAS 471-34-1, $\geq 99.0\%$), and methanol (CAS 67-56-1, UHPLC, suitable for MS) were supplied by Sigma-Aldrich/Merck KGaA (Darmstadt, Germany). Stevioside (CAS 57817-89-7, 99%) was purchased from Wako Chemicals GmbH (Neuss, Germany). Potato dextrose agar (PDA) was supplied by Becton, Dickinson & Company (Franklin Lakes, NJ, USA).

Fungal isolates

Neofusicoccum parvum (Pennycook & Samuels) Crous, Slippers & A.J.L. Phillips (code ITACYL_F111; isolate Y-091-03-01c; isolated from 'Verdejo' cultivar grapevines in a nursery in Navarra, Spain, in 2006) and *Dothiorella viticola* A.J.L. Phillips & J. Luque (code ITACYL_F118; isolate Y-103-08-01; isolated from grapevines in Extremadura, Spain, in 2004) were supplied as lyophilized vial cultures (later reconstituted and refreshed as PDA subcultures) by the Agricultural Technological Institute of Castilla and Leon (ITACYL, Valladolid, Spain) (Martin and Cobos, 2007).

Preparation of bioactive formulations

Treatments based on pure stevioside, rutin, or ferulic acid were prepared by dissolving the respective compounds in Milli-Q water (stevioside) or methanol (for rutin and ferulic acid), without further purification.

Ultrasonication-assisted aqueous biphasic system separation was used to prepare the stevioside-polyphenol conjugate complexes in a 1:1 molar ratio. 50 mL of an aqueous solution of stevioside (126 mg, MW = 804.87 g·mol⁻¹, 0.156 mM) were mixed with a 50 mL methanol solution of either ferulic acid (95.2 mg, MW = 610.517 g·mol⁻¹, 0.156 mM) or rutin (75.3 mg, MW = 482.44 g·mol⁻¹, 0.156 mM). The solutions were sonicated with a probe-type UIP1000hdT ultrasonicator (Hielscher, Teltow, Germany; 1000 W, 20 kHz) for 15 min, keeping the temperature below 60°C.

For *in vivo* experiments, the conjugate complexes were dispersed in a calcium alginate matrix, in the form of hydrogel beads. The beads were prepared as follows: each bioactive product was added to a 3% sodium alginate solution in a 2:8 ratio (20 mL bioactive product:80 mL sodium alginate), and this solution was then dispensed

drop by drop onto a 3% calcium carbonate solution to spherify (polymerize) the solution. Beads of $\varnothing = 0.4\text{--}0.6$ cm containing the different treatments were obtained.

In vitro tests of mycelium growth inhibition

The biological activity of the different treatments was determined using the agar dilution method, incorporating aliquots of stock solutions into PDA medium to provide final concentrations of 62.5, 93.75, 125, 187.5, 250, 375, 500, 750, 1000, and 1500 $\mu\text{g}\cdot\text{mL}^{-1}$. Mycelium plugs ($\varnothing = 5$ mm) of each pathogen from the edges of 7-day-old cultures were transferred to plates filled with amended media (three plates per treatment and concentration). Plates containing only PDA without amendment were used as experimental controls. The experiment was carried out twice.

Radial mycelium growth was determined by calculating the average of two perpendicular colony diameters for each replicate. Mycelium growth inhibition, after 7 days of incubation at 25°C in the dark for each treatment and concentration, was calculated according to the formula: $((d_c - d_i)/d_c) \times 100$, where d_c is the average fungal colony diameter in the experimental control and d_i is the average colony diameter treated with composite.

Fitting the radial growth inhibition values (%) with a DoseResp function, using an orthogonal distance regression (ODR) algorithm, allowed expression of the results as 50% (EC₅₀) and 90% (EC₉₀) effective concentrations.

For treatment interactions, synergy factors (SF) were estimated using Wadley's method (Levy *et al.*, 1986). This method assumes that one component of a mixture can substitute at a constant proportion for the other component. The expected effectiveness of the mixture is then directly predictable from the effectiveness of the constituents if the relative proportions are known (as in this case). The synergy factor (SF) was estimated as:

$$\text{SF} = \frac{ED(\text{exp})}{ED(\text{obs})} = \frac{\left(\frac{a + b}{\frac{a}{ED_A} + \frac{b}{ED_B}} \right)}{ED(\text{obs})}$$

where a and b are the proportions of the products A and B in the mixture and $a + b = 1$, ED_A and ED_B are their equally effective doses, $ED(\text{exp})$ is the expected equally effective dose and $ED(\text{obs})$ is the equally effective dose observed in the experiment.

If SF = 1, the hypothesis of similar joint action (i.e., additivity) can be accepted; if SF > 1, there is synergistic action; and if SF < 1, there is antagonistic action between the two fungicide products.

Greenhouse bioassays on grafted plants

The protective capabilities of the most promising formulations and dosages, as indicated from the *in vitro* mycelium growth inhibition experiments, were further assayed in grafted plants against the two selected *Botryosphaeriaceae*, using the method described by Buzón-Durán *et al.* (2021). Briefly, 68 plants were used, half of which were 2-year-old ‘Tempranillo’ vines (CL. 32 clone) grafted on 775P rootstock, and the rest were 1-year-old ‘Garnacha’ vines (VCR3 clone) grafted on 110R rootstock. The two cultivars were tested to assess potential differences in their sensitivity to the pathogens under study. The cultivar choice was guided by the relevance of ‘Tempranillo’ and ‘Garnacha’ in the protected designations of origin in Aragón, Spain.

Plants were grown on 3.5 L capacity plastic pots containing a mixed substrate of moss peat and sterilized natural soil (75:25), to which a slow-release fertilizer was incorporated when needed. The plants were kept in a greenhouse with drip irrigation and anti-weed ground cover for 6 months (from June to December 2020).

One week after placing in the greenhouse, the grapevine plants were artificially inoculated with the two pathogens (*N. parvum* and *D. viticola*) and simultaneously treated with either the stevioside–rutin or the stevioside–ferulic acid treatment. Inoculations of both pathogens and bioactive products were carried out directly on the trunks of the living plants at two sites on each plant, at least 5 cm apart from each other, and below the grafting point (and not reaching the root crown). For the pathogens, agar plugs from 5-day-old fresh PDA cultures of each species were used as the fungal inoculum. At the two inoculation points, slits ($\varnothing \approx 15$ mm, 5 mm deep) were made with a scalpel. Agar plugs ($\varnothing = 5$ mm) were then placed so that the mycelium was in contact with the stem vascular tissue. The beads containing the bioactive product were then placed at both sides of the agar plug, and the agar plug and beads were covered with cotton soaked in sterile double distilled water and sealed with Parafilm™ tape.

Five repetitions were arranged for each pathogen/bioactive product and plant (cultivar/rootstock) combination. Four positive controls/(pathogen*cultivar) and three negative controls (only the bioactive product) for each treatment were used (Table 1).

During the assay period, cuprous oxide (75%) was applied in mid-July to control downy mildew outbreaks, together with a first sprouting (followed by periodic sprouting). *Amblyseius (Typhlodromips) swirskii* Athias-Henriot was used for the biological control of whitefly, thrips, and spider mite; *Encarsia formosa* Gahan/*Eret-*

mocerus eremicus Rose & Zolnerowich for whitefly; and *Aphelinus abdominalis* Dalman for aphids at the end of July (Biobest Group NV, Almería, Spain). The grapevine plants were visually examined each week throughout the assay period for the presence of foliar symptoms (including interveinal and veinal necroses).

At the end of the experiment, plants were removed and two transversal sections of each inoculated stem, between the grafting point and the root crown, were prepared and sectioned longitudinally. The effects of the inoculated fungi were evaluated by measuring the lengths of longitudinal vascular necroses in each direction from the inoculation point.

Samples from the assayed plants were further processed to re-isolate the previously inoculated fungi, and to fulfill Koch’s postulates. Wood chips (length = 5 mm) exhibiting vascular necroses (1–2 cm around the wounds) were washed, surface sterilized, and placed in PDA plates amended with streptomycin sulphate (to avoid bacterial contamination). The plates were incubated at 26°C in the dark for 2–3 days in a culture chamber. Emerging colonies were identified based on their morphological characters. A selection of the isolates recovered from vascular lesions was identified by comparing ribosomal ITS sequences with those from the inoculated isolates.

Table 1. Details of plant/treatment combinations for the greenhouse bioassay. Each grafted plant was inoculated at two sites below the grafting point.

Plant	Treatment	Pathogen	Number of replicates
‘Tempranillo’ (CL. 32 clone) on 775P rootstock	Stevioside- ferulic acid	<i>N. parvum</i>	5
		<i>D. viticola</i>	5
		Nil (negative control)	3
	Stevioside- rutin	<i>N. parvum</i>	5
		<i>D. viticola</i>	5
		Nil (negative control)	3
	Nil (positive control)	<i>N. parvum</i>	4
		<i>D. viticola</i>	4
	‘Garnacha’ (VCR3 clone) on 110R rootstock	Stevioside- ferulic acid	<i>N. parvum</i>
<i>D. viticola</i>			5
Nil (negative control)			3
Stevioside- rutin		<i>N. parvum</i>	5
		<i>D. viticola</i>	5
		Nil (negative control)	3
Nil (positive control)		<i>N. parvum</i>	4
		<i>D. viticola</i>	4

Statistical analyses

Given that the homogeneity and homoscedasticity requirements were satisfied, according to Shapiro–Wilk and Levene tests, the results of the *in vitro* mycelium growth inhibition experiments were statistically analyzed using one-way analysis of variance (ANOVA), followed by *post hoc* comparison of means through Tukey's test at $P < 0.05$. For the greenhouse assays, since normality and homoscedasticity requirements were not met, Kruskal-Wallis non-parametric test was used, with Conover-Iman test for *post hoc* multiple pairwise comparisons. R statistical software was used for all the statistical analyses (R Core Team, 2020).

RESULTS

In vitro tests of mycelium growth inhibition

From *in vitro* tests (Figure 1 and Figure S1), greater antifungal activity was recorded from stevioside or rutin alone than for ferulic acid against both *Botryosphaeriaceae* taxa, especially against *N. parvum* (Table S1). Statistically significant increases in antifungal activity were observed for the stevioside-rutin and stevioside-ferulic acid conjugate complexes. For stevioside-rutin, almost complete inhibition of *N. parvum* occurred at $1000 \mu\text{g}\cdot\text{mL}^{-1}$, and for *D. viticola* complete inhibition was observed at $750 \mu\text{g}\cdot\text{mL}^{-1}$, compared with $1500 \mu\text{g}\cdot\text{mL}^{-1}$ for the non-conjugated compounds against both fungi. For the ferulic acid adduct, efficacy was also slightly lower than that of the rutin adduct: concentrations of 1500

and $1000 \mu\text{g}\cdot\text{mL}^{-1}$ were required for complete inhibition of *N. parvum* and *D. viticola*, respectively. Inhibition of 64% for *N. parvum* and 74% for *D. viticola* resulted from the $1500 \mu\text{g}\cdot\text{mL}^{-1}$ ferulic acid treatment.

Comparison of EC_{50} s and EC_{90} s (Table 2) for colony diameter measurements corroborated the lower EC values for rutin than for ferulic acid, especially against *D. viticola*. On the basis of the EC_{90} values, synergism was observed for the two complexes, with SF values close to 1.45 for *N. parvum*, and ranging from 1.6 to 2.2 for *D. viticola*.

Greenhouse bioassays with grafted plants

After removing, cutting, and measuring vascular necroses present in the different treated plants, no statistically significant differences were detected between cultivar/rootstock combinations, as shown in Table S2.

Statistically significant differences were detected for mean lengths of vascular necroses between treated and non-treated plants for both pathogens. Against *N. parvum* (Figure 2), the two assayed formulations gave similar results (Table 3). Against *D. viticola*, the stevioside-rutin treatments gave a greater reduction in lesion lengths than the stevioside-ferulic acid treatment, as it occurred in the *in vitro* tests (Table 4). Mean lengths of necroses for the treated plants were not significantly different from those of the negative controls (i.e., those from plants treated with conjugate complexes without pathogens), indicating strong inhibition of *D. viticola*. Lesions from the two negative controls were similar.

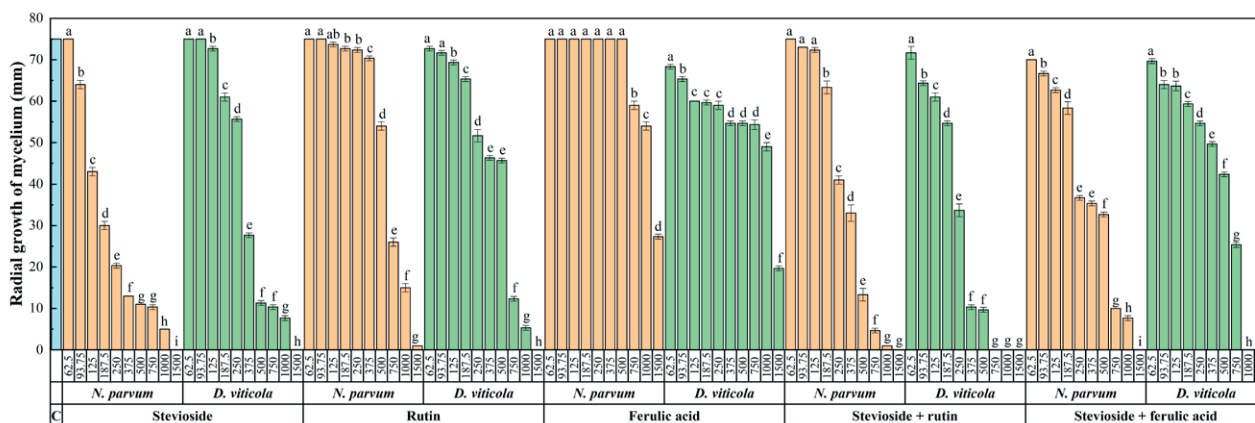


Figure 1. Mean colony radial diameters for *Neofusicoccum parvum* and *Dothiorella viticola* strains when cultured in PDA plates containing the different treatments) at concentrations ranging from 62.5 to $1500 \mu\text{g}\cdot\text{mL}^{-1}$. Means accompanied by the same letters are not significantly different ($P < 0.05$), and bars indicate standard deviations.

Table 2. Mean EC_{50} s and EC_{90} s ($\mu\text{g}\cdot\text{mL}^{-1}$; \pm standard errors), and calculated synergy factors (S.F.).

Pathogen	Effective Concentration	Stevioside	Rutin	Ferulic acid	Stevioside-rutin	S.F.	Stevioside-ferulic acid	S.F.
<i>N. parvum</i>	EC_{50}	154.9 \pm 13.5	656.9 \pm 25.4	1394.4 \pm 63.0	306.0 \pm 23.6	0.82	435.6 \pm 66.8	0.64
	EC_{90}	923.8 \pm 56.7	1156.5 \pm 72.2	4121.3 \pm 313.5	714.9 \pm 31.9	1.44	1032.2 \pm 43.1	1.46
<i>D. viticola</i>	EC_{50}	309.6 \pm 16.6	575.1 \pm 34.9	1287.2 \pm 51.3	241.6 \pm 12.8	1.67	574.4 \pm 46.3	0.87
	EC_{90}	1007.1 \pm 66.0	981.1 \pm 58.6	2948.6 \pm 168.0	457.8 \pm 21.7	2.17	921.8 \pm 72.5	1.63



Figure 2. Foliar symptoms and vascular necroses observed in grapevine plants artificially inoculated with *Neofusicoccum parvum* and treated with two conjugate complexes of natural products. Top row, left to right; general aspect of plants treated with *N. parvum* (positive control), stevioside-ferulic acid, stevioside-rutin, *N. parvum* + stevioside-ferulic acid and *N. parvum* + stevioside-rutin. Bottom row; vascular lesions after sectioning the stems of the grapevine plants in the top row.

Table 3. Mean lengths of the vascular necroses in grapevine plants after inoculations with *Neofusicoccum parvum*. Mean of rank values accompanied by the same letters are not significantly different ($P < 0.05$; Kruskal-Wallis test, and multiple pairwise comparisons using the Conover-Iman procedure).

Treatment	Mean of ranks	Groups
Stevioside-rutin negative control	42.573	A
Stevioside-ferulic acid negative control	48.188	A
Stevioside-rutin	145.656	B
Stevioside-ferulic acid	155.638	B
Positive control	183.313	C

Table 4. Mean lengths of vascular necroses in grapevine plants after inoculations with *Dothiorella viticola*. Mean of rank values accompanied by the same letters are not significantly different ($P < 0.05$; Kruskal-Wallis test, and multiple pairwise comparisons using the Conover-Iman procedure).

Treatment	Mean of ranks	Groups
Stevioside-rutin	90.472	A
Stevioside-rutin negative control	110.813	A B
Stevioside-ferulic acid negative control	123.713	B C
Stevioside-ferulic acid	145.632	C
Positive control	260.766	D

DISCUSSION

Comparison with reported antifungal efficacies for bioactive substances

When comparing results of sensitivity of fungal pathogens to exposure to fungicidal compounds, susceptibility profiles in these microorganisms are usually species, and isolate-dependent, so comparisons of effective concentrations discussed below should be taken with caution.

Previous research has advocated ferulic acid as the phenolic acid having the strongest anti-fungal activity (Lambert *et al.*, 2012a; Sabel *et al.*, 2017; Zabka and Pavela, 2013). In assessments of the efficacy of ferulic acid against GTDs, Lambert *et al.* (2012b) assayed a concentration of 500 μM (97 $\mu\text{g}\cdot\text{mL}^{-1}$), and measured *in vitro* growth inhibitions of 23% against *N. parvum* strain PER20 and 35% against *N. parvum* strain Bp0014. However, these authors did not report MIC or EC values for ferulic acid against these fungi. Gómez *et al.* (2016) reported EC_{50} values of 3530 $\mu\text{g}\cdot\text{mL}^{-1}$ for ferulic acid against several *Botryosphaeriaceae* species and 4740 $\mu\text{g}\cdot\text{mL}^{-1}$ against *Phaeoacremonium minimum* (Tul. & C. Tul.) Gramaje, L. Mostert & Crous. Dekker *et al.*

(2002) reported 62% inhibition for ferulic acid against *Botryosphaeria* Ces. & de Not. species at 25 mM (4855 $\mu\text{g}\cdot\text{mL}^{-1}$), with an EC_{50} value of 15 mM (2913 $\mu\text{g}\cdot\text{mL}^{-1}$). In general terms, EC_{50} s in these reports were 2 to 3 times greater than those recorded in the present study (1340 and 1454 $\mu\text{g}\cdot\text{mL}^{-1}$). Srivastava *et al.* (2013) tested ten naturally occurring phenolic compounds from plants against isolates from different *Botryosphaeriaceae* genera (viz. *Lasiodiplodia theobromae* (Pat.) Griffon & Maubl., *B. obtusa* (Schwein.) Shoemaker, and *Neofusicoccum ribis* (Slippers, Crous & M.J. Wingf.) Crous, Slippers & A.J.L. Phillips). They reported that ferulic acid at 25 mM (4855 $\mu\text{g}\cdot\text{mL}^{-1}$) gave ca. 80% mycelium growth inhibition of *L. theobromae* and ca. 70% inhibition of *N. ribis*, while 100% inhibition was attained at 20 mM (3885 $\mu\text{g}\cdot\text{mL}^{-1}$) for *B. obtusa*. These concentrations are similar to the EC_{90} values obtained in the present study against *N. parvum* (3230 $\mu\text{g}\cdot\text{mL}^{-1}$) and *D. viticola* (3921 $\mu\text{g}\cdot\text{mL}^{-1}$).

Zabka and Pavela (2013) assessed the efficacy of 21 phenolic components of essential oils and plant substances against several toxicogenic filamentous fungi. They reported MIC values >1000 $\mu\text{g}\cdot\text{mL}^{-1}$ for ferulic acid against *Fusarium oxysporum* Schltdl., *F. verticillioides* (Sacc.) Nirenberg, *Penicillium brevicompactum* Dierckx, *P. expansum* Link, *Aspergillus flavus* Link, and *A. fumigatus* Fresen. EC_{50} values ranged from 411 (*P. expansum*) to 895 $\mu\text{g}\cdot\text{mL}^{-1}$ (*A. flavus*). Wu *et al.* (2010) found that ferulic acid inhibited conidium germination of the watermelon soil-borne pathogen *F. oxysporum* f. sp. *niveum* (E.F. Sm.) W.C. Snyder & H.N. Hansen at concentrations of 800 $\mu\text{g}\cdot\text{mL}^{-1}$. Asiegbu *et al.* (1996) reported that ferulic acid at 5000 $\mu\text{g}\cdot\text{mL}^{-1}$ severely repressed growth of the lignocellulolytic fungi *Trichoderma harzianum* Rifai, *Chaetomium cellulolyticum* Chahal & D. Hawksw., *Phanerochaete chrysosporium* Burds., *Trametes versicolor* (L.) Lloyd and *Pleurotus sajor-caju* (Fr.) Singer. Ferulic acid or ferulic acid-rich extracts have also been suggested as natural alternatives for reducing post-harvest fruit losses. Hernández *et al.* (2021) reported almost 100% inhibition of *Monilinia fructicola* (G. Winter) Honey at a dose of 2 mM (390 $\mu\text{g}\cdot\text{mL}^{-1}$), and 90% inhibition of *Alternaria alternata* (Fr.) Keissl. at 3 mM (583 $\mu\text{g}\cdot\text{mL}^{-1}$), and of *Botrytis cinerea* Pers. at 7.5 mM (1457 $\mu\text{g}\cdot\text{mL}^{-1}$).

There have been no previous reports of the antifungal activity of rutin against GTDs. To date, more than 70 plant species have been shown to contain rutin (Gullón *et al.*, 2017), and different plant extracts with high contents of this compound have shown inhibitory effects on the growth of fungi. Devi *et al.* (2007) found significant growth inhibition from extracts of *Eupatorium birmanicum* DC [*Eupatorium cannabinum* subsp. *cannabinum*]

against *F. oxysporum* (at 1000 ppm), *Curvularia lunata* Boedijn (at 500 ppm), and *Trichoderma viride* Pers. (at 100 ppm). Salvador *et al.* (2004) showed that ethanolic extracts from *Alternanthera maritima* (Mart.) St. Hil gave moderate inhibition of *Candida albicans* (C.P. Robin) Berkhout, *C. tropicalis* (Castell.) Berkhout, *C. glabrata* (H.W. Anderson) S.A. Mey. & Yarrow, *C. parapsilosis* (Ashford) Langeron & Talice, *Trichophyton mentagrophytes* C.P. Robin R. Blanch. and *T. rubrum* (Castell.) Sabour. Pure rutin against the same fungi gave MIC values of 500 $\mu\text{g}\cdot\text{mL}^{-1}$.

Parvu *et al.* (2015) found rutin contents of 130 $\mu\text{g}\cdot\text{mL}^{-1}$ in flower extracts of *Hedera helix* L. (ivy), and 170 $\mu\text{g}\cdot\text{mL}^{-1}$ in fruit extracts of the same plant, and assayed these against *Aspergillus niger* Tiegh., *B. cinerea*, *F. oxysporum* f. sp. *tulipae* Apt., *Penicillium gladioli* L. McCulloch & Thom, and *Sclerotinia sclerotiorum* (Lib.) Korf & Dumont. Full inhibition of mycelium growth of these fungi was attained at concentrations of 8 to 12% for flower extracts, and of 10 to 14% for fruit extracts.

Elansary *et al.* (2020a) assayed the stem extracts of six *Ferocactus* species (*F. gracilis*, *F. pottsii*, *F. herrerae*, *F. horridus*, *F. glaucescens*, and *F. emoryi*), with rutin contents of up to 108 mg per 100 g DW, against several bacteria and fungi. They found strong antifungal effects against *A. flavus*, *A. ochraceus*, *A. niger*, *C. albicans*, *Penicillium funiculosum*, and *P. ochrochloron* (with MICs from 100 to 730 $\mu\text{g}\cdot\text{mL}^{-1}$). They found slightly greater rutin concentrations (139 mg/100 g DW) in *Ocimum basilicum* L. (basil), giving MIC values from 290 to 560 $\mu\text{g}\cdot\text{mL}^{-1}$ against these fungal pathogens (Elansary *et al.*, 2020d). Much greater rutin concentrations (1533 and 1010 mg/100 g DW) were found in leaves of *Acacia saligna* L. and *Ruta graveolens* L. leaves by Elansary *et al.* (2020b; 2020c). In the associated *in vitro* assays, conducted for the leaf methanolic extracts and several pure bioactive compounds detected by high-performance liquid chromatography–diode array detection (HPLC-DAD), these authors found MIC values against the different fungi ranging from 180 to 300 $\mu\text{g}\cdot\text{mL}^{-1}$ for pure rutin, from 300 to 580 $\mu\text{g}\cdot\text{mL}^{-1}$ for *A. saligna* extract, and from 330 to 780 $\mu\text{g}\cdot\text{mL}^{-1}$ for *R. graveolens* extract.

Concerning the antifungal activity of stevioside (*Stevia rebaudiana* extracts), Ghosh *et al.* (2008) and Abou-Arab and Abu-Salem (2010) reported growth inhibition effects against *A. solani*, *Helminthosporium solani*, *A. niger*, *A. ochraceus* K. Wilh., *A. parasiticus* Speare, *A. flavus*, and *Penicillium chrysogenum* Thom, but MIC values were not determined in these studies. Arya *et al.* (2012) also demonstrated the antifungal activity of stevioside (at 50000 $\mu\text{g}\cdot\text{mL}^{-1}$) against *A. flavus*, *A. fumigatus*, *A. niger*, and *Fusarium oxysporum*. Abdel-Fatt *et*

al. (2018) measured MIC values of 250 to 300 $\mu\text{g}\cdot\text{mL}^{-1}$ for stevioside against *A. flavus*, *A. ochraceus*, *A. niger*, and *Fusarium moniliforme* Sheldon. Shukla *et al.* (2013) reported stevioside MIC values of 3 $\text{mg}\cdot\text{mL}^{-1}$ against *B. cinerea* and 2 $\text{mg}\cdot\text{mL}^{-1}$ against *F. oxysporum*, and Guerra Ramírez *et al.* (2020) found that the hexane extract of stevioside at 833 ppm inhibited mycelium growth of *F. oxysporum* by up to 50%.

No data are available on the antifungal activity of stevioside-polyphenol conjugate complexes against fungi associated with GTDs. Buzón-Durán *et al.* (2020) reported an EC_{50} of 123 $\mu\text{g}\cdot\text{mL}^{-1}$ and an EC_{90} of 160 $\mu\text{g}\cdot\text{mL}^{-1}$ against *F. culmorum* for conjugate complexes based on a 1:1 mixture of stevioside with polyphenols present in milk thistle seeds (*Silybum marianum* (L.) Gaertn). Composites based on stevioside:ferulic acid inclusion compounds (in a 5:1 molar ratio), combined with chitosan oligomers in hydroalcoholic solution or in choline chloride:urea deep eutectic solvent media, were assayed against *F. culmorum* by Matei *et al.* (2018a), obtaining EC_{50} s ranging from 175 to 292 $\mu\text{g}\cdot\text{mL}^{-1}$ and EC_{90} s in the 377 to 713 $\mu\text{g}\cdot\text{mL}^{-1}$ interval, depending on the dispersion medium. Inclusion compounds from stevioside and ferulic acid in 6:1 ratio, dispersed in a hydroalcoholic solution of chitosan oligomers, were also assayed against *P. cinnamomi* by Matei *et al.* (2018b) and Matei *et al.* (2020), obtaining EC_{50} s of 171 to 229 $\mu\text{g}\cdot\text{mL}^{-1}$ and EC_{90} s of 446 to 450 $\mu\text{g}\cdot\text{mL}^{-1}$, depending on the presence or absence of silver nanoparticles.

Mechanisms of action

The antimicrobial activity of ferulic acid can involve different modes of action, mainly related to the destabilization and permeabilization of cytoplasmatic membranes and to enzyme inhibition by the oxidized products (Borges *et al.*, 2013). Phenolic acids also affect the physicochemical surface properties of microbial cells, given that these compounds are electrophilic and change hydrophobicity. Due to their partially lipophilic character, it is assumed that ferulic acid crosses cell membrane by passive diffusion in undissociated form, disturbing cell membrane structure by localized hyperacidification, and possibly acidifying the cytoplasm and causing protein denaturation. The alteration of cell membrane potential makes it more permeable and causes leakage of cell constituents, including proteins and nucleic acids. Additionally, ferulic acid (like p-coumaric acid and caffeic acid) affects the cell membrane structure and rigidity, and alters phospholipid chain dynamics (Ota *et al.*, 2011). Shi *et al.* (2016) also noted that ferulic acid causes changes in intracellular ATP concentrations.

The antifungal mechanism of action of flavonoids was comprehensively reviewed by Al Aboody and Mickymaray (2020). Flavonoids inhibit fungal growth via various underlying mechanisms, including disruption of plasma membranes, induction of mitochondrial dysfunction, and inhibition of efflux mediated pumping, cell division, cell wall formation, and protein and RNA syntheses. For rutin, the mechanisms of pharmacological action were summarized by Koval'skii *et al.* (2014), who also noted that this compound can interact with various structures at molecular levels (including free radicals, protein systems, and enzymes).

In addition to direct effects, which cause reductions of fungal growth by altering hyphal morphology, grapevine phenolic compounds also exert their actions against GTD fungi through indirect effects, via inhibition of the extracellular fungal manganese peroxidase (MnP) involved in lignin degradation (Gómez *et al.*, 2016). A decrease of laccase production and pectinase activity of *Botryosphaeria* isolates resulting from phenolic compounds was also reported by Srivastava *et al.* (2013).

Khan *et al.* (2017) suggested that the antimycotic activity of phytoglycosides is mediated through different and multiple targets that are not fully understood. However, there is a consensus that the main antimycotic mechanism is related to their ability to complex with sterols of fungal membranes. This produces spore-like structures that cause pore formations in membranes, losses in membrane integrity, and even membrane rupture, leading to fungal cell death.

Solubility and synergistic behaviour

A major disadvantage associated with rutin is its poor bioavailability, mainly caused by its low aqueous solubility and poor stability. Gullón *et al.* (2017) indicated that this hinders the *in vivo* biological effects of rutin, although the compound may have detectable bioactivity in different *in vitro* systems. Common approaches used to enhance rutin bioavailability include particle diminution to the submicron range and complex formation with cyclodextrins and various metals. Also, various carrier systems have been proposed for rutin delivery, including micro- and nano-emulsions, nanocrystals and nanosuspensions (Sharma *et al.*, 2013).

An alternative approach is to use steviol glycosides as natural solubilizers, an approach that has been successfully tested for several natural phenols, such as curcumin (a diarylheptanoid) (Zhang *et al.*, 2011; Nguyen *et al.*, 2017), liquiritin (the 4'-*O*-glucoside of the flavanone liquiritigenin) (Nguyen *et al.*, 2014), and betulinic acid (a pentacyclic triterpenoid) (Zhang *et al.*, 2016). For rutin,

Ko *et al.* (2016) optimized its solubility by the Box-Behnken design with the aid of microwave treatment (instead of ultrasonic treatment, as in the present study). Nguyen *et al.* (2015) attained similar results for quercetin, by complexation with rubusoside and rebaudioside, finding that as the glycoside concentration increased, the solubility of quercetin in water increased, without reducing its biological functions. Solubility optimization could be responsible for synergistic effects of conjugates of the two glycodrugs against GTD pathogens. The same rationale may be applied to tentatively explain the synergy observed for ferulic acid (although this was weaker than that attained for rutin).

Opportunities for future GTDs treatments

Levels of phenolic compounds have been reported to increase in the discoloured wood of Esca-affected grapevines (Agrelli *et al.*, 2009; Amalfitano *et al.*, 2011), while phenolic compounds have also been shown to limit fungal development in grapevine vascular tissues (Lambert *et al.*, 2012a; Lima *et al.*, 2011). Spagnolo *et al.* (2014) found the greatest levels of total phenolics in the brown striped wood of three grapevine cultivars infected with *N. parvum* and *Diplodia seriata* De Not. Martin *et al.* (2009) showed that stilbene polyphenols such as resveratrol and ϵ -viniferin increased in the wood of vines artificially inoculated with *Phaeoconiella chlamydospora*. Quercetin-3-*O*-glucoside and *trans*-caffeoyltartaric acid (analogous to rutin and ferulic acid studied here) were associated with resistance to *Plasmopara viticola* (Berk. & M.A. Curtis) Berl. & De Toni in grapevine leaves (Ali *et al.*, 2012), and increases in quercetin-3-*O*-galactoside and kaempferol-3-*O*-glucoside have been found in asymptomatic leaves of plants infected with the Bois noir phytoplasma (Rusjan *et al.*, 2012).

The approach presented here, based on mimicking the grapevine response via intrinsic phenolic compounds, along with solubility and bioavailability enhancements, is a "natural" and effective way to control the development of particular GTD pathogens. Although pure reagents were assayed in this study, the results attained indicate that selection of natural antifungal compounds could show promise. In the case of rutin, extracts from *Echinodorus grandiflorus* (Cham. & Schltld.) Micheli, *Sambucus nigra* L., *Drimys winteri* J.R.Forst. or *Taraxacum officinale* Weber ex Wiggins (Meinhart *et al.*, 2020) may deserve further attention for large-scale field experiments. If plants rich in rutin and ferulic were preferred, the activity of the extracts from sea buckthorn (*Hippophae Rhamnoides* L.) (Criste *et al.*, 2020), *Rhinacanthus nasutus* (L.) Kurz (Huang *et al.*, 2015), *Artemisia absinthium* L., *Achil-*

lea millefolium L., *Sambucus nigra* L. or *Salvia officinalis* L. (Bljajić *et al.*, 2021) could be explored.

CONCLUSIONS

In an attempt to mimic grapevine defence responses against GTDs, the anti-fungal efficacy of rutin, either alone or in conjugate complexes with stevioside, was assayed against two *Botryosphaeriaceae* taxa. While the *in vitro* performance of the pure flavonoid-3-*O*-glycoside was moderate, with EC₉₀s of 1157 µg·mL⁻¹ against *N. parvum* and 981 µg·mL⁻¹ against *D. viticola*, considerable increases in activity (EC₉₀s of 715 and 458 µg·mL⁻¹, respectively) were attained for stevioside-rutin. The synergistic behaviour (with SFs of 1.44 and 2.17) may be due to solubility and bioavailability optimization. Testing of the formulations in greenhouse *in vivo* conditions showed moderate inhibition of *N. parvum* and full inhibition against *D. viticola* for the stevioside-rutin treatments. These EC₉₀s and *in vivo* results were consistently better than those found for ferulic acid and stevioside-ferulic acid, used as references. The promising results attained with this approach provide guidance for the selection of new plant extracts that could be utilized as antifungal agents in organic viticulture.

ACKNOWLEDGMENTS

V.G.-G thanks C. Julián (Plant Protection Unit, CITA) for technical assistance. The financial support for this study was provided by Junta de Castilla y León under project VA258P18, with FEDER co-funding; by Cátedra Agrobank under the “IV Convocatoria de Ayudas de la Cátedra AgroBank para la transferencia del conocimiento al sector agroalimentario” programme, and by Fundación Ibercaja-Universidad de Zaragoza under “Convocatoria Fundación Ibercaja-Universidad de Zaragoza de proyectos de investigación, desarrollo e innovación para jóvenes investigadores”.

LITERATURE CITED

- Abdel-Fatt, S. M., Badr, A. N., Abu Seif, F. A.-H., Mohamed Al, S., and Ahmed Hass, R., 2018. Anti-fungal and anti-mycotoxigenic impact of eco-friendly extracts of wild Stevia. *Journal of Biological Sciences* 18: 488–499.
- Abou-Arab, E., and Abu-Salem, F., 2010. Evaluation of bioactive compounds of *Stevia rebaudiana* leaves and callus. *Journal of Food and Dairy Sciences* 1: 209–224.
- Agrelli, D., Amalfitano, C., Conte, P., and Mugnai, L., 2009. Chemical and spectroscopic characteristics of the wood of *Vitis vinifera* cv. Sangiovese affected by esca disease. *Journal of Agricultural and Food Chemistry* 57: 11469–11475.
- Al Aboody, M. S., and Mickymaray, S., 2020. Anti-fungal efficacy and mechanisms of flavonoids. *Antibiotics* 9: 45.
- Ali, K., Maltese, F., Figueiredo, A., Rex, M., Fortes, A. M., Zyprian, E., ... Choi, Y. H., 2012. Alterations in grapevine leaf metabolism upon inoculation with *Plasmopara viticola* in different time-points. *Plant Science* 191: 100–107.
- Amalfitano, C., Agrelli, D., Arrigo, A., Mugnai, L., Surico, G., and Evidente, A., 2011. Stilbene polyphenols in the brown red wood of *Vitis vinifera* cv. Sangiovese affected by “esca proper”. *Phytopathologia Mediterranea* 50: S224-S235.
- Arya, A., Kumar, S., and Kasana, M., 2012. In vitro regeneration of Stevia and evaluation of antimicrobial and antiprotozoal properties of regenerated calli and plants. *Electronic Journal of Plant Breeding* 3: 916–924.
- Asiegbu, F. O., Paterson, A., and Smith, J. E., 1996. Inhibition of cellulose saccharification and glycolignin-attacking enzymes of five lignocellulose-degrading fungi by ferulic acid. *World Journal of Microbiology and Biotechnology* 12: 16–21.
- Bljajić, K., Brajković, A., Čačić, A., Vujić, L., Jablan, J., Saraiva de Carvalho, I., and Zovko Končić, M., 2021. Chemical composition, antioxidant, and α-glucosidase-inhibiting activity of aqueous and hydroethanolic extracts of traditional antidiabetics from Croatian ethnomedicine. *Horticulturae* 7: 15.
- Borges, A., Ferreira, C., Saavedra, M. J., and Simões, M., 2013. Antibacterial activity and mode of action of ferulic and gallic acids against pathogenic bacteria. *Microbial Drug Resistance* 19: 256–265.
- Buzón-Durán, L., Martín-Gil, J., Ramos-Sánchez, M. d. C., Pérez-Lebeña, E., Marcos-Robles, J. L., Fombellida-Villafruela, Á., and Martín-Ramos, P., 2020. Anti-fungal activity against *Fusarium culmorum* of stevioside, *Silybum marianum* seed extracts, and their conjugate complexes. *Antibiotics* 9(8): 440.
- Buzón-Durán, L., Langa-Lomba, N., González-García, V., Casanova-Gascón, J., Martín-Gil, J., Pérez-Lebeña, E., and Martín-Ramos, P., 2021. On the applicability of chitosan oligomers-amino acid conjugate complexes as eco-friendly fungicides against grapevine trunk pathogens. *Agronomy* 11(2): 324.
- Chebil, L., Humeau, C., Anthoni, J., Dehez, F., Engasser, J.-M., and Ghoul, M., 2007. Solubility of flavonoids in

- organic solvents. *Journal of Chemical & Engineering Data* 52: 1552–1556.
- Criste, A., Urcan, A. C., Bunea, A., Pripon Furtuna, F. R., Olah, N. K., Madden, R. H., and Corcionivoschi, N., 2020. Phytochemical composition and biological activity of berries and leaves from four Romanian sea buckthorn (*Hippophae rhamnoides* L.) varieties. *Molecules* 25: 1170.
- Dekker, R. F. H., Barbosa, A. M., and Sargent, K., 2002. The effect of lignin-related compounds on the growth and production of laccases by the ascomycete, *Botryosphaeria* sp. *Enzyme and Microbial Technology* 30: 374–380.
- Del Río, J. A., Gómez, P., Báidez, A., Fuster, M. D., Ortuño, A., and Frías, V., 2004. Phenolic compounds have a role in the defence mechanism protecting grapevine against the fungi involved in Petri disease. *Phytopathologia Mediterranea* 43: 87–94.
- Devi, L. R., Singh, T. S., and Laitonjam, W. S., 2007. Antifungal and phytochemical studies of *Eupatorium birmanicum* DC. *Indian Journal of Chemistry Section B-Organic Chemistry Including Medicinal Chemistry* 46: 1868–1872.
- Elansary, H. O., Szopa, A., Klimek-Szczykutowicz, M., Ekiert, H., Barakat, A. A., and Al-Mana, F. A., 2020a. Antiproliferative, antimicrobial, and antifungal activities of polyphenol extracts from *Ferocactus* species. *Processes* 8: 138.
- Elansary, H. O., Szopa, A., Kubica, P., Ekiert, H., Al-Mana, F. A., and Al-Yafarsi, M. A., 2020b. Antioxidant and biological activities of *Acacia saligna* and *Lawsonia inermis* natural populations. *Plants* 9: 908.
- Elansary, H. O., Szopa, A., Kubica, P., Ekiert, H., El-Ansary, D. O., Al-Mana, F. A., and Mahmoud, E. A., 2020c. Polyphenol content and biological activities of *Ruta graveolens* L. and *Artemisia abrotanum* L. in Northern Saudi Arabia. *Processes* 8: 531.
- Elansary, H. O., Szopa, A., Kubica, P., Ekiert, H., El-Ansary, D. O., Al-Mana, F. A., and Mahmoud, E. A., 2020d. Saudi *Rosmarinus officinalis* and *Ocimum basilicum* L. polyphenols and biological activities. *Processes* 8: 446.
- Fontaine, F., Pinto, C., Vallet, J., Clement, C., Gomes, A. C., and Spagnolo, A., 2016. The effects of grapevine trunk diseases (GTDs) on vine physiology. *European Journal of Plant Pathology* 144: 707–721.
- Fourie, P. H., and Halleen, F., 2004. Proactive Control of Petri Disease of Grapevine Through Treatment of Propagation Material. *Plant Disease* 88: 1241–1245.
- Ganeshpurkar, A., and Saluja, A. K., 2017. The pharmacological potential of rutin. *Saudi Pharmaceutical Journal* 25: 149–164.
- Ghosh, S., Subudhi, E., and Nayak, S., 2008. Antimicrobial assay of *Stevia rebaudiana* Bertoni leaf extracts against 10 pathogens. *International Journal of Integrative Biology* 2: 27–31.
- Gómez, P., Báidez, A. G., Ortuño, A., and Del Río, J. A., 2016. Grapevine xylem response to fungi involved in trunk diseases. *Annals of Applied Biology* 169: 116–124.
- Goufo, P., Singh, R. K., and Cortez, I., 2020. A reference list of phenolic compounds (including stilbenes) in grapevine (*Vitis vinifera* L.) roots, woods, canes, stems, and leaves. *Antioxidants* 9: 398.
- Graniti, A., Surico, G., and Mugnai, L., 2000. Esca of grapevine a disease complex or a complex of diseases? *Phytopathologia Mediterranea* 39: 16–20.
- Guerra Ramírez, P., Guerra Ramírez, D., Zavaleta Mejía, E., Aranda Ocampo, S., Nava Díaz, C., and Rojas Martínez, R. I., 2020. Extracts of *Stevia rebaudiana* against *Fusarium oxysporum* associated with tomato cultivation. *Scientia Horticulturae* 259: 108683.
- Gullón, B., Lú-Chau, T. A., Moreira, M. T., Lema, J. M., and Eibes, G., 2017. Rutin: A review on extraction, identification and purification methods, biological activities and approaches to enhance its bioavailability. *Trends in Food Science & Technology* 67: 220–235.
- Hernández, A., Ruiz-Moyano, S., Galván, A. I., Merchán, A. V., Pérez Nevado, F., Aranda, E., ... Martín, A., 2021. Anti-fungal activity of phenolic sweet orange peel extract for controlling fungi responsible for post-harvest fruit decay. *Fungal Biology* 125: 143–152.
- Huang, R. T., Lu, Y. F., Inbaraj, B. S., and Chen, B. H., 2015. Determination of phenolic acids and flavonoids in *Rhinacanthus nasutus* (L.) Kurz by high-performance-liquid-chromatography with photodiode-array detection and tandem mass spectrometry. *Journal of Functional Foods* 12: 498–508.
- Hussain, Z., Thu, H. E., Amjad, M. W., Hussain, F., Ahmed, T. A., and Khan, S., 2017. Exploring recent developments to improve antioxidant, anti-inflammatory and antimicrobial efficacy of curcumin: A review of new trends and future perspectives. *Materials Science and Engineering C* 77: 1316–1326.
- Jin, Y. S., 2019. Recent advances in natural antifungal flavonoids and their derivatives. *Bioorganic & Medicinal Chemistry Letters* 29: 126589.
- Khan, H., Khan, Z., Amin, S., Mabkhot, Y. N., Mubarak, M. S., Hadda, T. B., and Maione, F., 2017. Plant bioactive molecules bearing glycosides as lead compounds for the treatment of fungal infection: A review. *Biomedicine & Pharmacotherapy* 93: 498–509.
- Ko, J.-A., Nam, S.-H., and Kim, Y., 2016. Optimization of soluble rutin using stevioside as a natural solubilizer. *Journal of Chitin and Chitosan* 21: 181–187.

- Koval'skii, I. V., Krasnyuk, I. I., Krasnyuk, I. I., Nikulina, O. I., Belyatskaya, A. V., Kharitonov, Y. Y., ... Lutsenko, S. V., 2014. Mechanisms of rutin pharmacological action. *Pharmaceutical Chemistry Journal* 48: 73–76.
- Lambert, C., Bisson, J., Waffo-Téguo, P., Papastamoulis, Y., Richard, T., Corio-Costet, M.-F., ... Cluzet, S., 2012a. Phenolics and their antifungal role in grapevine wood decay: Focus on the Botryosphaeriaceae family. *Journal of Agricultural and Food Chemistry* 60: 11859–11868.
- Lambert, C., Papastamoulis, Y., Waffo-Téguo, P., Mérillon, J., and Cluzet, S., 2012b. Effects of phenolic compounds towards grapevine wood decay fungi. In *Oeno2011: Actes de colloques du 9e symposium international d'oenologie de Bordeaux*, Dunod, Bordeaux, France, 90–94.
- Levy, Y., Benderly, M., Cohen, Y., Gisi, U., and Bassand, D., 1986. The joint action of fungicides in mixtures: comparison of two methods for synergy calculation. *EPPO Bulletin* 16: 651–657.
- Lima, M. R. M., Ferreres, F., and Dias, A. C. P., 2011. Response of *Vitis vinifera* cell cultures to *Phaeomoniliella chlamydospora*: changes in phenolic production, oxidative state and expression of defence-related genes. *European Journal of Plant Pathology* 132: 133–146.
- Martin, M. T., and Cobos, R., 2007. Identification of fungi associated with grapevine decline in Castilla y León (Spain). *Phytopathologia Mediterranea* 46: 18–25.
- Martin, N., Vesentini, D., Rego, C., Monteiro, S., Oliveira, H., and Ferreira, R. B., 2009. *Phaeomoniliella chlamydospora* infection induces changes in phenolic compounds content in *Vitis vinifera*. *Phytopathologia Mediterranea* 48: 101–116.
- Matei, P., Iacomì, B., Martín-Gil, J., Pérez-Lebeña, E., Ramos-Sánchez, M., Barrio-Arredondo, M., and Martín-Ramos, P., 2018a. *In vitro* antifungal activity of composites of AgNPs and polyphenol inclusion compounds against *Fusarium culmorum* in different dispersion media. *Agronomy* 8(11): 239.
- Matei, P., Martín-Gil, J., Michaela Iacomì, B., Pérez-Lebeña, E., Barrio-Arredondo, M., and Martín-Ramos, P., 2018b. Silver nanoparticles and polyphenol inclusion compounds composites for *Phytophthora cinnamomi* mycelial growth inhibition. *Antibiotics* 7(3): 76.
- Matei, P. M., Buzón-Durán, L., Pérez-Lebeña, E., Martín-Gil, J., Iacomì, B. M., Ramos-Sánchez, M. C., and Martín-Ramos, P., 2020. *In vitro* antifungal activity of chitosan-polyphenol conjugates against *Phytophthora cinnamomi*. *AgriEngineering* 2(1): 72–77.
- Meinhart, A. D., Damin, F. M., Caldeirão, L., Teixeira-Filho, J., and Godoy, H. T., 2020. Rutin in herbs and infusions: screening of new sources and consumption estimation. *Food Science and Technology* 40: 113–120.
- Mondello, V., Songy, A., Battiston, E., Pinto, C., Coppin, C., Trotel-Aziz, P., ... Fontaine, F., 2018. Grapevine trunk diseases: A review of fifteen years of trials for their control with chemicals and biocontrol agents. *Plant Disease* 102: 1189–1217.
- Nguyen, T. T. H., Jung, S.-J., Kang, H.-K., Kim, Y.-M., Moon, Y.-H., Kim, M., and Kim, D., 2014. Production of rubusoside from stevioside by using a thermostable lactase from *Thermus thermophilus* and solubility enhancement of liquiritin and teniposide. *Enzyme and Microbial Technology* 64–65: 38–43.
- Nguyen, T. T. H., Yu, S.-H., Kim, J., An, E., Hwang, K., Park, J.-S., and Kim, D., 2015. Enhancement of quercetin water solubility with steviol glucosides and the studies of biological properties. *Functional Foods in Health and Disease* 5: 437.
- Nguyen, T. T. H., Si, J., Kang, C., Chung, B., Chung, D., and Kim, D., 2017. Facile preparation of water soluble curcuminoids extracted from turmeric (*Curcuma longa* L.) powder by using steviol glucosides. *Food Chemistry* 214: 366–373.
- Ota, A., Abramovič, H., Abram, V., and Poklar Ulrih, N., 2011. Interactions of p-coumaric, caffeic and ferulic acids and their styrenes with model lipid membranes. *Food Chemistry* 125: 1256–1261.
- Parvu, M., Vlase, L., Parvu, A. E., Rosca-Casian, O., Gheldiu, A. M., and Parvu, O., 2015. Phenolic compounds and antifungal activity of *Hedera helix* L. (ivy) flowers and fruits. *Notulae Botanicae Horti Agrobotanici Cluj-Napoca* 43: 53–58.
- R Core Team, 2020. R: A language and environment for statistical computing, R Foundation for Statistical Computing, Vienna, Austria.
- Rusjan, D., Halbwrith, H., Stich, K., Mikulič-Petkovšek, M., and Veberič, R., 2012. Biochemical response of grapevine variety 'Chardonnay' (*Vitis vinifera* L.) to infection with grapevine yellows (Bois noir). *European Journal of Plant Pathology* 134: 231–237.
- Sabel, A., Bredefeld, S., Schlandler, M., and Claus, H., 2017. Wine phenolic compounds: antimicrobial properties against yeasts, lactic acid and acetic acid bacteria. *Beverages* 3: 29.
- Salvador, M. J., Zucchi, O., Candido, R. C., Ito, I. Y., and Dias, D. A., 2004. *In vitro* antimicrobial activity of crude extracts and isolated constituents of *Alternanthera maritima*. *Pharmaceutical Biology* 42: 138–148.
- Shakeel, F., Salem-Bekhit, M. M., Haq, N., and Siddiqui, N. A., 2017. Solubility and thermodynamics of ferulic acid in different neat solvents: Measurement, correla-

- tion and molecular interactions. *Journal of Molecular Liquids* 236: 144–150.
- Sharma, S., Ali, A., Ali, J., Sahni, J. K., and Baboota, S., 2013. Rutin: therapeutic potential and recent advances in drug delivery. *Expert Opinion on Investigational Drugs* 22: 1063–1079.
- Shi, C., Zhang, X., Sun, Y., Yang, M., Song, K., Zheng, Z., ... Xia, X., 2016. Antimicrobial activity of ferulic acid against *Cronobacter sakazakii* and possible mechanism of action. *Foodborne Pathogens and Disease* 13: 196–204.
- Shukla, S., Mehta, A., and Bajpai, V. K., 2013. Phytochemical screening and anthelmintic and antifungal activities of leaf extracts of *Stevia rebaudiana*. *Journal of Biologically Active Products from Nature* 3: 56–63.
- Spagnolo, A., Larignon, P., Magnin-Robert, M., Hovasse, A., Cilindre, C., Van Dorsselaer, A., ... Fontaine, F., 2014. Flowering as the most highly sensitive period of grapevine (*Vitis vinifera* L. cv Mourvèdre) to the Botryosphaeria dieback agents *Neofusicoccum parvum* and *Diplodia seriata* infection. *International Journal of Molecular Sciences* 15: 9644–9669.
- Srivastava, P., Andersen, P. C., Marois, J. J., Wright, D. L., Srivastava, M., and Harmon, P. F., 2013. Effect of phenolic compounds on growth and ligninolytic enzyme production in *Botryosphaeria* isolates. *Crop Protection* 43: 146–156.
- Surico, G., 2001. Towards commonly agreed answers to some basic questions on esca. *Phytopathologia Mediterranea* 40: S487-S490.
- Wu, H.-s., Luo, J., Raza, W., Liu, Y.-x., Gu, M., Chen, G., ... Shen, Q.-r., 2010. Effect of exogenously added ferulic acid on in vitro *Fusarium oxysporum* f. sp. *niveum*. *Scientia Horticulturae* 124: 448–453.
- Zabka, M., and Pavela, R., 2013. Antifungal efficacy of some natural phenolic compounds against significant pathogenic and toxinogenic filamentous fungi. *Chemosphere* 93: 1051–1056.
- Zhang, F., Koh, G. Y., Jeansonne, D. P., Hollingsworth, J., Russo, P. S., Vicente, G., ... Liu, Z., 2011. A novel solubility-enhanced curcumin formulation showing stability and maintenance of anticancer activity. *Journal of Pharmaceutical Sciences* 100: 2778–2789.
- Zhang, J., Chou, G., Liu, Z., and Liu, M., 2016. Employing rubusoside to improve the solubility and permeability of antitumor compound betulonic acid. *Nanomedicine* 11: 2829–2844.

ARTÍCULO 5: “Activity of anthracenediones and flavoring phenols in hydromethanolic extracts of *Rubia tinctorum* against grapevine phytopathogenic fungi” *Plants*, 2021, 10(8), 1527; <https://doi.org/10.3390/plants10081527>; Q1 (JCR, Science Edition – PLANT SCIENCES). JIF₂₀₂₁ = 4,658. 11 citas recibidas (WOS)



plants

an Open Access Journal by MDPI

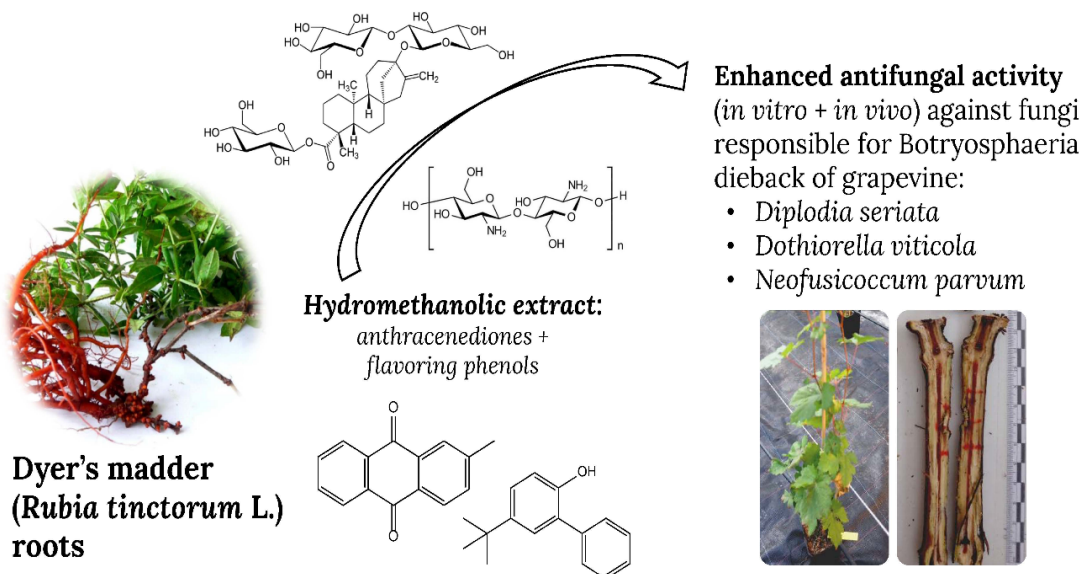


Activity of Anthracenediones and Flavoring Phenols in Hydromethanolic Extracts of *Rubia tinctorum* against Grapevine Phytopathogenic Fungi

Natalia Langa-Lomba; Eva Sánchez-Hernández; Laura Buzón-Durán; Vicente González-García; José Casanova-Gascón; Jesús Martín-Gil; Pablo Martín-Ramos

Plants 2021, Volume 10, Issue 8, 1527

Conjugation with chitosan oligomers or stevioside



Article

Activity of Anthracenediones and Flavoring Phenols in Hydromethanolic Extracts of *Rubia tinctorum* against Grapevine Phytopathogenic Fungi

Natalia Langa-Lomba ^{1,2}, Eva Sánchez-Hernández ³, Laura Buzón-Durán ³, Vicente González-García ², José Casanova-Gascón ¹, Jesús Martín-Gil ³ and Pablo Martín-Ramos ^{1,*}

¹ Instituto Universitario de Investigación en Ciencias Ambientales de Aragón (IUCA), EPS, Universidad de Zaragoza, Carretera de Cuarte, s/n, 22071 Huesca, Spain; natalialangalomba@gmail.com (N.L.-L.); jcasan@unizar.es (J.C.-G.)

² Agrifood Research and Technology Centre of Aragón, Plant Protection Unit, Instituto Agroalimentario de Aragón—IA2 (CITA-Universidad de Zaragoza), Avda. Montañana 930, 50059 Zaragoza, Spain; vgonzalezg@aragon.es

³ Department of Agricultural and Forestry Engineering, ETSIIAA, Universidad de Valladolid, 34004 Palencia, Spain; eva.sanchez.hernandez@uva.es (E.S.-H.); laura.buzon@uva.es (L.B.-D.); mgil@iaf.uva.es (J.M.-G.)

* Correspondence: pmr@unizar.es



Citation: Langa-Lomba, N.; Sánchez-Hernández, E.; Buzón-Durán, L.; González-García, V.; Casanova-Gascón, J.; Martín-Gil, J.; Martín-Ramos, P. Activity of Anthracenediones and Flavoring Phenols in Hydromethanolic Extracts of *Rubia tinctorum* against Grapevine Phytopathogenic Fungi. *Plants* **2021**, *10*, 1527. <https://doi.org/10.3390/plants10081527>

Academic Editors: Dragana Šunjka and Špela Mechora

Received: 8 July 2021

Accepted: 23 July 2021

Published: 26 July 2021

Publisher's Note: MDPI stays neutral with regard to jurisdictional claims in published maps and institutional affiliations.



Copyright: © 2021 by the authors. Licensee MDPI, Basel, Switzerland. This article is an open access article distributed under the terms and conditions of the Creative Commons Attribution (CC BY) license (<https://creativecommons.org/licenses/by/4.0/>).

Abstract: In this work, the chemical composition of *Rubia tinctorum* root hydromethanolic extract was analyzed by GC–MS, and over 50 constituents were identified. The main phytochemicals were alizarin-related anthraquinones and flavoring phenol compounds. The antifungal activity of this extract, alone and in combination with chitosan oligomers (COS) or with stevioside, was evaluated against the pathogenic taxa *Diplodia seriata*, *Dothiorella viticola* and *Neofusicoccum parvum*, responsible for the so-called Botryosphaeria dieback of grapevine. In vitro mycelial growth inhibition tests showed remarkable activity for the pure extract, with EC₅₀ and EC₉₀ values as low as 66 and 88 µg·mL⁻¹, respectively. Nonetheless, enhanced activity was attained upon the formation of conjugate complexes with COS or with stevioside, with synergy factors of up to 5.4 and 3.3, respectively, resulting in EC₅₀ and EC₉₀ values as low as 22 and 56 µg·mL⁻¹, respectively. The conjugate with the best performance (COS-*R. tinctorum* extract) was then assayed ex situ on autoclaved grapevine wood against *D. seriata*, confirming its antifungal behavior on this plant material. Finally, the same conjugate was evaluated in greenhouse assays on grafted grapevine plants artificially inoculated with the three aforementioned fungal species, resulting in a significant reduction in the infection rate in all cases. This natural antifungal compound represents a promising alternative for developing sustainable control methods against grapevine trunk diseases.

Keywords: antifungal; *Botryosphaeriaceae*; chitosan; GTDs; madder; stevioside; *Vitis vinifera*

1. Introduction

The joint presence of compounds of quinone and phenol categories in plant extracts and, specifically, the differential content of anthracenediones and 4-*tert*-butyl-2-phenyl-phenol, which might be responsible for the chromatic aberration of teak (difference between heartwood and sapwood), has been the object of attention in the bibliography [1].

Anthracenediones are a class of molecules based on the 9,10-anthracenedione parent (Figure 1a), which—among others—include purpurin (Figure 1a) and those synthesized by the American Cyanamid Laboratories in the late 1970s [2]. Although mitoxantrone, which has a dihydroxyanthraquinone central chromophore with two symmetrical aminoalkyl side chains (Figure 1a), is considered the biologically most active anthracenedione [3], other anthracenediones have also been reported to have antimicrobial activities: for instance, anthraquinone aglycones have been found to have a remarkable in vitro activity

against clinical strains of dermatophytes [4]; anthraquinone derivatives exhibit antifungal activity against *Candida albicans* (C.P. Robin) Berkhout, *Cryptococcus neoformans* (San Felice) Vuill., *Trichophyton mentagrophytes* (C.P. Robin) R. Blanch., *Aspergillus fumigatus* Fresen. and *Sporothrix schenckii* Hektoen and C.F. Perkins [5,6]; purpurin possesses remarkable antifungal activity against *Candida* spp. [7]; and alizarin or 1,2-dihydroxyanthraquinone (Figure 1b) show antifungal behavior against *Aspergillus niger* Tieghem and *A. ochraceus* K. Wilhelm [8].

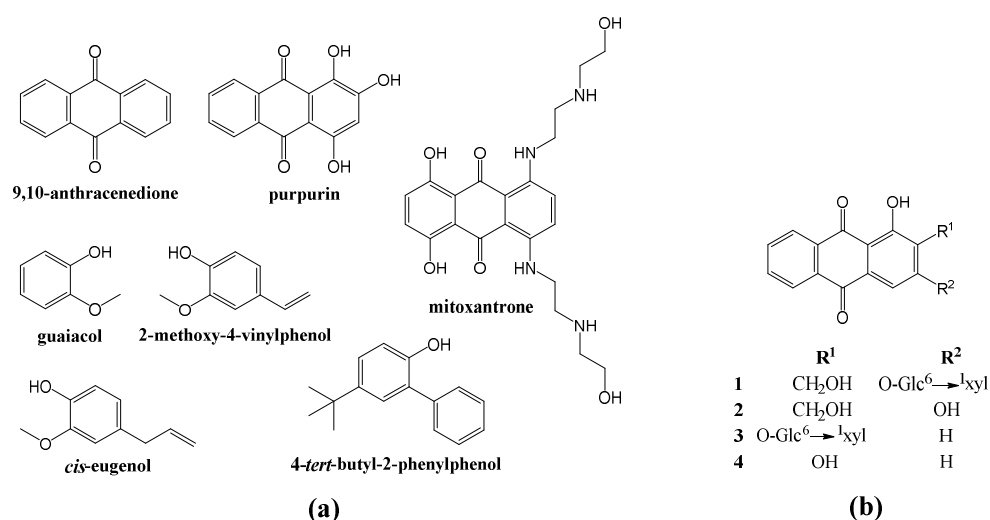


Figure 1. (a) Structures of different anthracenediones and phenols; (b) structures of alizarin-3-*O*- β -primeveroside, 3; lucidin-3-*O*- β -primeveroside, 1; and their aglycons (alizarin, 4; lucidin, 2). Glc, D-glucose; xyl, D-xylose.

Flavoring phenols is a category that includes small free phenolic compounds (Figure 1a), such as 2-methoxy-phenol (or guaiacol), 2-methoxy-4-vinylphenol (or 4-vinyl-guaiacol), *cis*-2-methoxy-4-(1-propenyl)-phenol (or *cis*-eugenol) and 4-*tert*-butyl-2-phenyl-phenol, which participate in the aroma of wine. Guaiacol and eugenol are characterized by spice, clove, and smoke notes (guaiacol provides a roasted aroma and eugenol confers a clove aroma); and 4-vinyl-guaiacol has an odor reminiscent of carnation (*Dianthus* flowers). 4-((1*E*)-3-hydroxy-1-propenyl)-2-methoxyphenol (or coniferyl alcohol) is a precursor of grape and wine volatiles [9]. All of them are present in oak, but 4-*tert*-butyl-2-phenyl-phenol has been referred as a constituent of *Rubia cordifolia* L. essential oil [10,11]. Regarding their antifungal activities, a strong antifungal activity against *Botrytis cinerea* Pers. has been referred for eugenol [12], and guaiacol has been found to be effective against sap-staining fungi (*Ophiostoma* spp.) [13].

In this paper, the possibility of a joint presence of both anthracenediones and flavoring phenols in *Rubia tinctorum* L. (*Rubiaceae*) has been explored, given that the presence of 9,10-anthraquinones and other biologically active compounds has been reported for other members of the genus *Rubia*, mainly for *R. cordifolia*, as summarized in the review paper by Singh, et al. [14].

R. tinctorum is widely distributed in southern and southeastern Europe, in the Mediterranean area, and in central Asia. Its reddish roots contain hydroxyanthraquinones, such as alizarin (used for the dyeing of textiles [15] and in the treatment of kidney and bladder stones), purpurin (1,2,4-trihydroxyanthraquinone), and lucidin (Figure 1b.4) [16,17]; and flavoring phenols such as 4-vinyl-guaiacol [18].

The interest in the joint presence of anthracenediones and phenols (as 2-methoxyphenols and 4-*tert*-butyl-2-phenyl-phenol) lies in the possibility of synergies that enhance their microbiological activity. In particular, this work focuses on their potential application for the control of grapevine trunk diseases (GTDs), currently considered one of the most relevant challenges in Viticulture, as these pathologies cause significant economic losses in

grape growing areas all over the world. Under this generic concept, a series of mycoses are grouped, which affect the wood of grapevine throughout its entire life cycle [19,20]. Among them, those that affect young plants coming from the nursery and in the first years after planting are especially important from the economic point of view, being responsible for numerous losses derived from the removal and replacement of plants in hundreds of thousands of hectares around the world [21]. Some of these include the so-called "Black Foot" disease, caused by different species belonging to soil-borne genera like *Ilyonectria*, *Campylocarpon*, *Cylindrocladiella*, *Dactylonectria*, etc.; the etiological agents responsible for Petri disease (mainly species of the genus *Phaeoacremonium*, and *Phaeomoniella chlamydospora* (W. Gams, Crous, M.J. Wingf. and Mugnai) Crous and W. Gams) that for many authors would be part of the first stages of the complex esca syndrome; or some species of the ascomycete family *Botryosphaeriaceae*, especially certain aggressive taxa in the early years of the plant such as *Neofusicoccum parvum* (included in the present study). In addition to these pathologies, other complex syndromes have been described, such as the aforementioned esca (attributable to certain species of lignicolous basidiomycetes), Eutypiosis (caused in Europe by *Eutypa lata* (Pers.) Tul. and C. Tul.), or the so-called Botryosphaeria decay of grapevine plants (also known as "Black Dead Arm" disease) caused by various genera and species of this family such as the aforementioned *N. parvum*, *Diplodia* spp., *Dothiorella* spp., *Lasiodiplodia* spp. or *Botryosphaeria* spp.

Given that the prohibition of active ingredients such as sodium arsenite and benzimidazoles, which were used to control GTDs, has worsened the impact of these diseases, they have become the subject of intense research efforts. Unfortunately, due to the breadth and complexity of the problem, no single effective control measure against these mycoses has been developed to date. Current strategies and future prospects for the management of GTDs are thoroughly discussed in the review papers by Fontaine, et al. [22], Bertsch, et al. [20], Mondello, et al. [23] and Gramaje, et al. [24], but the use of active ingredients of natural origin, instead of conventional chemicals, poses an especially interesting approach, aligned with the criteria of European legislation currently in force (Article 14 in European Directive 2009/128/EC).

Taking into consideration that many phytochemicals have solubility and bioavailability problems, in this work the bioactivity of the hydromethanolic extracts of *R. tinctorum* against GTDs has also been assayed after the formation of conjugate complexes, either with chitosan oligomers (COS) or with stevioside [a terpene glycoside obtained from *Stevia rebaudiana* (Bertoni) Bertoni extract], which also have antifungal properties and which may lead to a synergistic fungicide behaviour [25,26].

2. Material and Methods

2.1. Plant Material and Chemicals

The specimens of *Rubia tinctorum* under study were collected on the banks of the Carrión river as it passes through the town of Palencia (Spain). The roots were shade-dried and pulverized to fine powder in a mechanical grinder. Samples from different specimens ($n = 25$) were thoroughly mixed to obtain composite samples.

Chitosan (CAS 9012-76-4; high MW: 310,000–375,000 Da) was supplied by Hangzhou Simit Chem. & Tech. Co. (Hangzhou, China). NeutrasedTM 0.8 L enzyme was supplied by Novozymes A/S (Bagsværd, Denmark). Stevioside (CAS 57817-89-7, 99%) was purchased from Wako Chemicals GmbH (Neuss, Germany). Quantities of 4-*tert*-butyl-2-phenylphenol (CAS 98-27-1, 97%), 1,2-dihydroxyanthraquinone (CAS 72-48-0, 97%), sodium alginate (CAS 9005-38-3), calcium carbonate (CAS 471-34-1, $\geq 99.0\%$) and methanol (CAS 67-56-1, UHPLC, suitable for mass spectrometry) were acquired from Sigma-Aldrich Química (Madrid, Spain). Agar (CAS 9002-18-0) and PDA (potato dextrose agar) were supplied by Becton Dickinson (Bergen County, NJ, USA).

2.2. Preparation and Physicochemical Characterization of the of *R. tinctorum* Extracts

Rubia tinctorum samples were mixed (1:20, *w/v*) with a methanol/water solution (1:1 *v/v*) and heated in a water bath at 50 °C for 30 min, followed by sonication for 5 min in pulse mode with a 1 min stop for each 2.5 min, using a 1000 W probe-type ultrasonicator operated at 20 kHz (model UIP1000hdT, Hielscher Ultrasonics, Teltow, Germany). The solution was then centrifuged at 9000 rpm for 15 min and the supernatant was filtered through Whatman No. 1 paper. Aliquots were lyophilized for the vibrational spectroscopy analysis.

The infrared vibrational spectra of both dried and ground roots and the lyophilized extract were registered using a Thermo Scientific (Waltham, MA, USA) Nicolet iS50 Fourier-transform infrared spectrometer, equipped with an in-built diamond attenuated total reflection (ATR) system. The spectra were collected with a 1 cm⁻¹ spectral resolution over the 400–4000 cm⁻¹ range, taking the interferograms that resulted from co-adding 64 scans. The spectra were then corrected using the advanced ATR correction algorithm [27] available in OMNIC™ software suite.

The hydroalcoholic plant extract was studied by gas chromatography–mass spectrometry (GC–MS) at the Research Support Services (STI) at Universidad de Alicante (Alicante, Spain), using a gas chromatograph model 7890A coupled to a quadrupole mass spectrometer model 5975C (both from Agilent Technologies). The chromatographic conditions were: 3 injections/vial, injection volume = 1 µL; injector temperature = 280 °C, in splitless mode; initial oven temperature = 60 °C, 2 min, followed by ramp-up of 10 °C/min to a final temperature of 300 °C, 15 min. The chromatographic column used for the separation of the compounds was an Agilent Technologies HP-5MS UI of 30 m length, 0.250 mm diameter and 0.25 µm film. The mass spectrometer conditions were: temperature of the electron impact source of the mass spectrometer = 230 °C and of the quadrupole = 150 °C; ionization energy = 70 eV. Test mixture 2 for apolar capillary columns according to Grob (Supelco 86501) and PFTBA tuning standards were used for equipment calibration. NIST11 library and the monograph by Adams [28] were used for compound identification.

2.3. Preparation of Chitosan Oligomers and Bioactive Formulations

Chitosan oligomers (COS) were prepared according to the procedure reported by Santos-Moriano, et al. [29], with the modifications indicated in [30], obtaining oligomers with a molecular weight <2000 Da.

The COS-*R. tinctorum* and stevioside-*R. tinctorum* conjugate complexes were obtained by mixing the respective solutions in a 1:1 (*v/v*) ratio. The mixtures were then sonicated for 15 min in five 3-minute periods (so that the temperature did not exceed 60 °C) using a probe-type ultrasonicator.

For the assays carried out on autoclaved wood, the conjugate complex was dispersed in an agar matrix (15 g/L in Milli-Q water), using a procedure analogous to the one described below for the in vitro tests.

For the in vivo assays, the bioactive product was dispersed in a calcium alginate matrix. Hydrogel beads were prepared as follows: the control product was added to a 3% sodium alginate solution in a 2:8 ratio (20 mL compound/80 mL sodium alginate). Subsequently, this solution was dispensed drop by drop onto a 3% calcium carbonate solution to polymerize (30 min curing), obtaining beads with diameters in the 4–6 mm range.

2.4. Fungal Isolates

The three fungal isolates used (Table 1) were supplied as lyophilized vials (later reconstituted and refreshed as PDA subcultures) by the Agricultural Technological Institute of Castilla and Leon (ITACYL, Valladolid, Spain) [31].

Table 1. Fungal isolates used in the study.

Code	Isolate	Binomial Nomenclature	Geographical Origin	Host/Date
ITACYL_F098	Y-084-01-01a	<i>Diplodia seriata</i> De Not.	Spain (DO Toro)	Grapevine (‘Tempranillo’) 2004
ITACYL_F118	Y-103-08-01	<i>Dothiorella viticola</i> A.J.L.Phillips and J.Luque	Spain (Extremadura)	Grapevine 2004
ITACYL_F111	Y-091-03-01c	<i>Neofusicoccum parvum</i> (Pennycook and Samuels) Crous, Slippers and A.J.L.Phillips	Spain (Navarra, nursery)	Grapevine (‘Verdejo’) 2006

2.5. Antifungal Activity Assessment

2.5.1. In vitro Tests of Mycelial Growth Inhibition

The antifungal activity of the different treatments was determined using the agar dilution method according to EUCAST standard antifungal susceptibility testing procedures [32], by incorporating aliquots of stock solutions onto the PDA medium to obtain concentrations in the 15.62–1500 $\mu\text{g}\cdot\text{mL}^{-1}$ range. Mycelial plugs ($\varnothing = 5$ mm) from the margin of 1-week-old PDA cultures of *D. seriata*, *D. viticola* or *N. parvum* were transferred to plates incorporating the above-mentioned concentrations for each treatment (3 plates per treatment/concentration, with 2 replicates each). Plates were then incubated at 25 °C in the dark for a week. PDA medium without any amendment was used as control. Mycelial growth inhibition was estimated according to the formula: $((d_c - d_t)/d_c) \times 100$, where d_c and d_t represent the average diameters of the fungal colony of the control and of the treated fungal colony, respectively. Effective concentrations (EC₅₀ and EC₉₀) were estimated using PROBIT analysis in IBM SPSS Statistics v.25 (IBM; Armonk, NY, USA) software. The level of interaction (i.e., synergy factors) was determined according to Wadley’s method [33].

2.5.2. Assays on Autoclaved Grape Wood

The formulation (COS-R. *tinctorum* conjugate) that showed the best performance in the in vitro assays was then tested on autoclaved grapevine wood to assess its behaviour on plant material against the least sensitive fungus in the previous plate tests. One-year-old dormant canes (*Vitis vinifera* L. cv. ‘Tempranillo’) were cut into 16 cm (length) and 0.8–1 cm (diameter) segments and autoclaved twice at 121 °C (20 min) to eliminate any microbial contamination. Inoculation was performed by first making two approximately 3 mm deep slits with a scalpel (without reaching the medullary tissue) per shoot, 8–10 cm apart and located in the internodes. A 3 mm diameter plug of PDA agar coming from the margin of a 10-day colony of the pathogen (*D. seriata*) was placed in each slit, flanked by 2 plugs ($\varnothing = 3$ mm) of bacteriological agar that contained the tested conjugate complex. After this, the wounds were covered with autoclaved cotton moistened with sterile bi-distilled water and sealed with Parafilm™ tape. Inoculated shoots were placed in transparent culture boxes on a bed of sterile filter paper, periodically moistened (with sterile double distilled water), and incubated for 21 days in a climatic chamber at 26 °C, with 70% RH and a 12/12 h photoperiod. A total of 5 boxes with 3 replicates/box each were arranged, together with a positive control inoculated only with *D. seriata* (1 box with 3 replicates) and a negative control without pathogen, inoculated only with the conjugate (also 1 box with 3 replicates).

After the incubation period, segments were recovered from the boxes, and each of them was divided into two halves of approximately 8 cm, before longitudinal cuts were made in each half. Finally, the length of the vascular necroses produced was measured longitudinally on upper and lower directions from the inoculation point for both halves, and compared with those of controls.

2.5.3. Greenhouse Bioassays on Grafted Plants

Bioassays with COS (chosen as a reference) and COS-R. *tinctorum* conjugate complexes were performed in living plants in order to scale the protective capabilities of these compounds against the three selected *Botryosphaeriaceae* species in young grapevine plants. As summarized in Table S1, plant material consisted of 30 plants of 'Tempranillo' (CL. 32 clone) (2 year old) cultivar and 30 plants of 'Garnacha' (VCR3 clone) (1 year old) cultivar, grafted on 775P and 110R rootstocks, respectively. Each plant was cultured on a 3.5 L plastic pot containing a mixed substrate of moss peat and sterilized natural soil (75:25), incorporating slow release fertilizer when needed along the culture cycle. Plants were maintained in the greenhouse with drip irrigation and anti-weed ground cover from June to December 2020 (6 months). One week after placing them in pots, young, grafted plants were artificially inoculated with the pathogens and the COS-R. *tinctorum* treatment. Five repetitions (plants) were arranged for each pathogen*cultivar combination, together with 4 positive controls/(pathogen*cultivar) plus 3 negative controls (incorporating only the bioactive product) for each cultivar. Inoculations of both pathogens and the control product were carried out directly on the trunk of the living plants at two sites per stem (separated >5 cm) below the grafting point and not reaching the root crown. For the different fungi, agar plugs from the margin of 5 day old fresh PDA cultures of each species were used as fungal inoculum. In the aforementioned two inoculation points of each grapevine plant, slits of approx. 15 mm in diameter and 5 mm deep were made with a scalpel. Subsequently, 5 mm diameter agar plugs were placed directly into contact with vascular tissue in the stem; simultaneously, calcium alginate hydrogel beads containing the bioactive product were placed at both sides of the agar plug; and the whole set was covered with cotton soaked in sterile bi-distilled water and sealed with Parafilm™ tape. During the culture period, application of copper (cuprous oxide 75%, Cobre Nordox™ 75 WG) to control downy mildew outbreaks was performed in mid-July, accompanied with a first sprouting (followed by periodic sprouting). Plants were visually examined weekly for the presence of foliar symptoms. After six months in the greenhouse, the plants were removed, two sections of the inoculated stems between the grafting point and the root crown were prepared and sectioned longitudinally. The length of the vascular necroses was scored longitudinally on upper and lower directions from the inoculation point for both halves of the longitudinal cut, and the average measures of these were statistically analysed and compared depending on the type of pathogen. All the data were compared with positive and negative controls. Finally, grapevine plants removed and measured at the end of the assay were also processed to re-isolate the different pathogenic taxa previously inoculated. Thus, 5 mm long wood chips exhibiting vascular necroses (1–2 cm around the wounds) were washed, their surface sterilized, then placed in PDA plates amended with streptomycin sulphate (to avoid bacterial contamination) and incubated in a culture chamber at 26 °C in the dark for 2–3 days.

2.6. Statistical Analyses

The results of the in vitro inhibition of mycelial growth were statistically analyzed using one-way analysis of variance (ANOVA), followed by post hoc comparison of means through Tukey's test at $p < 0.05$ (provided that the homogeneity and homoscedasticity requirements were satisfied, according to the Shapiro–Wilk and Levene tests). In the case of autoclaved grapevine wood and greenhouse assay results, since the normality and homoscedasticity requirements were not met, the Kruskal–Wallis non-parametric test was used instead, with the Conover–Iman test for post hoc multiple pairwise comparisons. R statistical software was used for all the statistical analyses [34].

3. Results

3.1. Vibrational Characterization

The assignment of the main absorption bands in the infrared spectra of the *R. tinctorum* root powder and root extracts is shown in Table 2. The most prominent band, attributed to

the benzene ring in aromatic compounds, occurs at ca. 1500 cm^{-1} . The bands at 1592 cm^{-1} and 1676 cm^{-1} can be assigned to the in-phase C=O and symmetrical C=C vibrations from anthraquinone.

Table 2. Main bands in the infrared spectra of root and lyophilized *R. tinctorum* extract and of two of its main constituents.

<i>R. tinctorum</i> Root Powder	<i>R. tinctorum</i> Extract	Anthraquinone	4-tert-butyl-2-phenylphenol	Assignment
3334	3335			Bonded O–H stretching (cellulose)
2920	2920	2964 2925		sp^3 C–H =C–H groups of aromatic rings
		2856		aliphatic C–H asymmetrical stretching
		2724		β -OH, typical of α -hydroxy anthraquinone
1727	1733			C=O from esters
		1704		ester C=O
		1676		C=O in anthraquinones
1639	1620	1633		C=O in anthraquinones
1602	1605	1592	1585	phenyl ring (aromatic skeletal vibration) >C=C< in anthraquinones
1552			1545	carboxylate stretches/C=C aromatic
	1511		1480	methylene C–H bend
		1461	1470	methyl C–H asymmetrical
	1435		1430	=C–H in plane bending
1414	1416		1420	vinyl C–H in plane bending
1370	1406 1370	1377 1366	1385	C–C asymmetrical stretching phenolic hydroxyl groups
			1355	C–O stretching/methylene C–H bending
		1333 1329	1325	C–H in-plane deformation methylene C–H bending
1316	1316	1306		vinylidene C–H in plane bending
1255	1255	1287	1270	C–O stretching/C=C symmetric stretching
		1207	1215	C–O stretching/C–H in plane bending
		1171	1180	–C–O–C– stretching
	1142	1153	1135	
	1100	1099		
		1087	1080	
1020			1025	C–C stretching
	951	969		C–H out-of-plane bending

3.2. Gas Chromatography–Mass Spectrometry Analysis of the Extract

In *R. tinctorum* root hydromethanolic extracts, the main analyzed components (Table 3) were: the anthraquinone family (19.4%) consisting of 2-methyl-9,10-anthracenedione (or β -methylantraquinone) (15.5%), 1,2-dihydroxyanthraquinone (or alizarin), 1,8-dihydroxy-3-methylantraquinone, 1-hydroxy-9,10-anthracenedione (or α -hydroxyanthraquinone) and 1-hydroxy-4-methylantraquinone; cyclopentenones (2.3%), such as 2-hydroxy-2-cyclopenten-

1-one and 4-cyclopentene-1,3-dione; and the phenol category (7.5%), constituted by *cis*-2-methoxy-4-(1-propenyl)-phenol (or *cis*-eugenol), 2-methoxy-phenol (or guaiacol), 2-methoxy-4-vinylphenol (or 4-vinyl-guaiacol), 4-*tert*-butyl-2-phenylphenol, and coniferyl alcohol. Other phytochemicals of interest were 4-methoxy-4',5'-methylenedioxybiphenyl-2-carboxylic acid (8.6%), 1,4-diacetyl-3-acetoxymethyl-2,5-methylene-1-rhamnitol (8.3%) and guanosine (5.8%).

Table 3. Phytochemicals identified in *R. tinctorum* root hydromethanolic extract by GC-MS.

Peak	R _t (min)	Area (%)	Assignments
1	4.6369	1.99	4-pentenoic acid, ethyl ester
2	4.7440	0.26	l-gala-l-ido-octose
3	4.8414	0.52	4-cyclopentene-1,3-dione
4	5.0021	1.09	oxime-, methoxy-phenyl-
5	5.1968	0.46	1-(2-furanyl)-ethanone
6	5.2942	1.36	2,5-diethenyltetrahydro-2-methyl-furan
7	5.3770	1.82	2-hydroxy-2-cyclopenten-1-one
8	6.0781	0.70	2,4-dihydroxy-2,5-dimethyl-3(2H)-furan-3-one
9	6.3312	2.91	2-hydroxy- γ -butyrolactone
10	6.6331	2.47	glycerin
11	6.7694	1.93	1,2-cyclopentanedione, 3-methyl-
12	6.9690	1.19	2-acetamido-2-deoxy- α -D-glucopyranose
13	7.1345	0.76	butyronitrile, 4-ethoxy-3-hydroxy-
14	7.2952	1.55	2,5-dimethyl-4-hydroxy-3(2H)-furanone
15	7.4267	0.77	trimethyl(tetrahydrofuran-2-ylperoxy)silane
16	7.6798	1.01	2-methoxy-phenol (or guaiacol)
17	7.7869	2.20	L-alanine, methyl ester
18	8.2008	2.65	dimethyl dl-malate
19	8.3955	0.64	ethanamine, N-ethyl-N-nitroso-
20	8.5270	2.47	4H-pyran-4-one, 2,3-dihydro-3,5-dihydroxy-6-methyl-
21	9.1453	0.87	4H-pyran-4-one, 3,5-dihydroxy-2-methyl-
22	9.2865	0.97	catechol
23	9.4471	0.94	1,4:3,6-dianhydro- α -d-glucopyranose
24	9.6857	0.35	5-hydroxymethylfurfural
25	10.3965	0.31	2-acetoxy-5-hydroxyacetophenone
26	10.5718	0.50	p-cymen-7-ol
27	10.8882	2.80	2-methoxy-4-vinylphenol (or 4-vinylguaiacol)
28	11.2193	0.98	DL-arabinose
29	11.7451	1.09	DL-proline, 5-oxo-, methyl ester
30	12.0470	0.74	vanillin
31	12.6702	1.96	2-methoxy-4-(1-propenyl)-phenol (Z)- (or <i>cis</i> -isoeugenol)
32	13.1473	1.05	1-[4-(methylthio)phenyl]-ethanone
33	13.4492	0.86	butylated hydroxytoluene
34	13.6877	0.57	benzeneacetic acid, 4-hydroxy-3-methoxy-, methyl ester
35	13.9458	0.82	1,4-diacetyl-3-acetoxymethyl-2,5-methylene-1-rhamnitol
36	14.3693	2.44	α -methyl-l-sorboside
37	15.0461	5.78	guanosine
38	15.5865	8.31	1,4-diacetyl-3-acetoxymethyl-2,5-methylene-1-rhamnitol
39	16.0734	1.65	4-((1E)-3-hydroxy-1-propenyl)-2-methoxyphenol (or coniferyl alcohol)
40	17.4561	0.43	5-amino-1-(4-amino-furazan-3-yl)-1H-[1-3]triazole-4-carbonitrile
41	17.9088	1.18	hexadecanoic acid, methyl ester
42	18.2594	1.17	n-hexadecanoic acid
43	19.1552	0.76	5-(1,1-dimethylethyl)[1,1'-biphenyl]-2-ol (or 4- <i>tert</i> -butyl-2-phenylphenol)
45	19.4278	0.69	cyclopentadecane
46	19.6421	0.15	1-hydroxy-9,10-anthracenedione (or α -hydroxyanthraquinone)
47	19.8709	15.54	9,10-anthracenedione, 2-methyl- (or β -methylanthraquinone)
48	20.7278	1.43	1-hydroxy-4-methylanthraquinone
49	21.1659	1.75	1,2-dihydroxyanthraquinone (or alizarin)

Table 3. Cont.

Peak	R _t (min)	Area (%)	Assignments
50	21.8038	1.40	azacyclotridecan-2-one, 1-(3-aminopropyl)-
51	23.0550	0.81	glycerol 1-palmitate
52	23.3812	0.73	bis(2-ethylhexyl) phthalate
53	23.8973	0.24	1,8-dihydroxy-3-methyl-9,10-anthracenedione (or 1,8-dihydroxy-3-methyl anthraquinone)
54	24.2673	8.57	4-methoxy-4',5'-methylenedioxybiphenyl-2-carboxylic acid
55	24.4474	0.42	9-octadecenoic acid (Z)-,
56	25.4260	0.35	2-hydroxy-1-(hydroxymethyl)ethyl ester squalene
57	29.2333	0.62	octasiloxane,
58	29.9051	0.40	1,1,3,3,5,5,7,7,9,9,11,11,13,13,15,15-hexadecamethyl- γ-sitosterol

It is worth noting that the flavoring phenols found in the hydroalcoholic extracts from *R. tinctorum* (guaiacol, 4-vinyl-guaiacol and *cis*-eugenol) were the same present in oak, which are used to confer aroma to wine.

3.3. Antifungal Activity

3.3.1. In vitro Tests of Mycelial Growth Inhibition

The results of the mycelial growth inhibition tests for the hydromethanolic *R. tinctorum* root extract, alone or forming a conjugate complex with COS or stevioside, are presented in Figure 2 and Figures S2–S4. The antifungal activity of the extract was found to be much higher than those of COS and stevioside alone, reaching full inhibition at concentrations in the 93.8–250 µg·mL⁻¹ range, depending on the pathogen (vs. 1500 µg·mL⁻¹ for COS and stevioside). Upon conjugation with stevioside, some improvement in the germicide effect could be observed: for instance, the inhibition of *D. seriata* was higher at the 78.1 µg·mL⁻¹ concentration (76.3% vs. 45.9%), and the full inhibition of *D. viticola* and *N. parvum* was attained at a lower concentration (93.8 vs. 125 µg·mL⁻¹, and 125 vs. 250 µg·mL⁻¹, respectively). Nonetheless, the best results were obtained for the COS–*R. tinctorum* extracts, for which full inhibition was recorded at the lowest concentrations (in the 70.3–78.1 µg·mL⁻¹ range).

In order to provide a tentative explanation for the strong antifungal activity observed in the extracts, three of the presumably bioactive constituents were also assayed (an anthracenedione, a phenol and a purine nucleoside) separately. The results, presented in Figures S5–S8, showed that 4-*tert*-butyl-2-phenylphenol was the most active (full inhibition of the three fungi was attained at concentrations in the 78.1–93.8 µg·mL⁻¹ range), but 1,2,4-trihydroxyanthraquinone and guanosine were also effective (full inhibition was reached at concentrations in the 187.5–500 and 250–375 µg·mL⁻¹ ranges, respectively). Such values are comparable to those found for the whole *R. tinctorum* extract, suggesting that the activity cannot be ascribed to a single constituent, but rather to the combination of several of them.

To quantify the synergistic behavior observed for the conjugate complexes, effective concentrations were estimated (Table 4) and synergy factors (SF) were then calculated according to Wadley's method (Table 5). As expected, the synergism between COS and *R. tinctorum* extract was noticeably higher than the one observed between stevioside and *R. tinctorum* extract, with SF values in the 2.23–5.35 and 1.36–3.29 range, respectively.

3.3.2. Assays on Autoclaved Grapevine Wood

The results from the ex situ experiment conducted on autoclaved grapevine canes for the most promising treatment (COS-*R. tinctorum* conjugate complex) and the least sensitive fungus (*D. seriata*), presented in Table 6, showed that the application of the bioactive product led to statistically significant differences in terms of vascular necroses vs. the positive control. Nonetheless, it did not lead to full inhibition, given that there

were statistically significant differences in the length of vascular lesions compared with the negative control (shoots inoculated only with the bioactive compound). This could be tentatively attributed to the chosen dispersion medium (agar), which was replaced with calcium alginate in subsequent in vivo experiments.

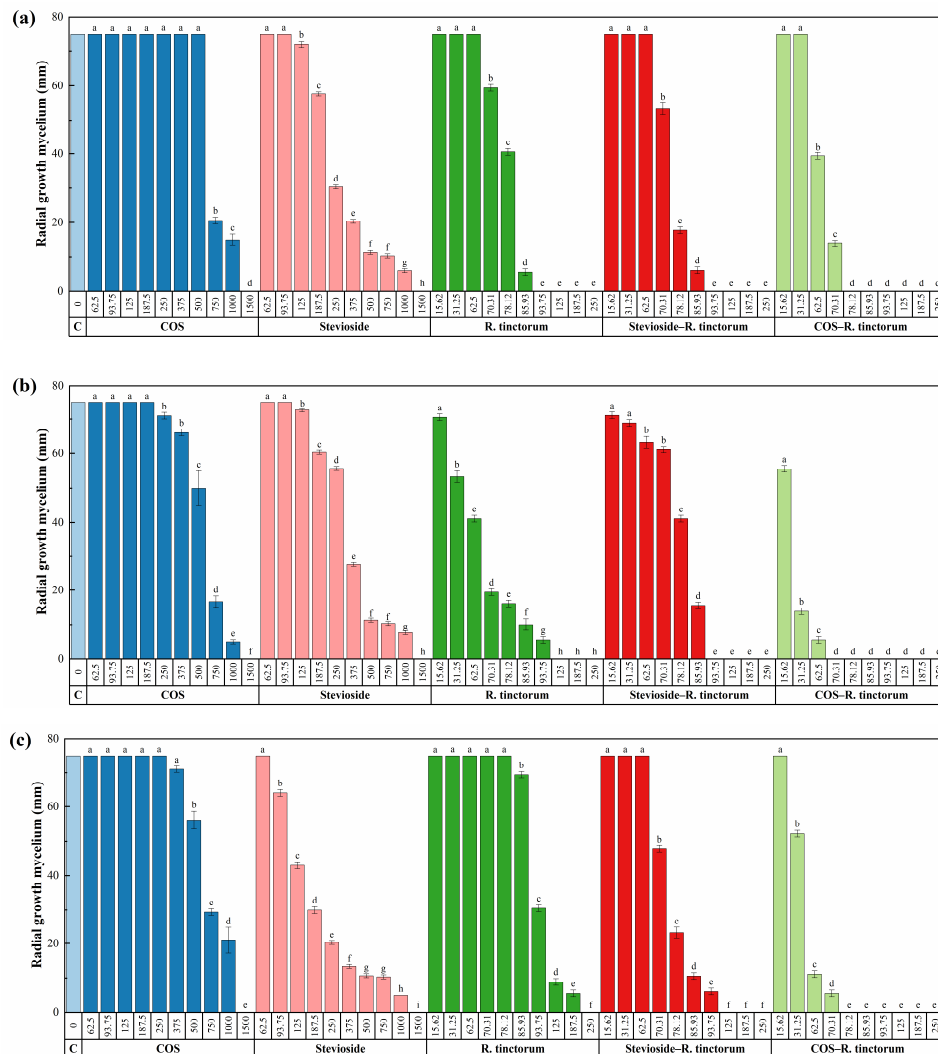


Figure 2. Colony growth measures of (a) *D. seriata*, (b) *D. viticola* and (c) *N. parvum* strains when cultured in PDA plates containing the various control products (viz. chitosan oligomers (COS), stevioside, *R. tinctorum* hydromethanolic extract, stevioside–*R. tinctorum* and COS–*R. tinctorum* conjugate complexes) at concentrations in the 62.5–1500 and 15.62–250 $\mu\text{g}\cdot\text{mL}^{-1}$ range ordered according to the least and the most active products, respectively. The same letters above concentrations indicate that they are not significantly different at $p < 0.05$. Error bars represent standard deviations.

Table 4. EC₅₀ and EC₉₀ effective concentrations. Values are expressed in $\mu\text{g}\cdot\text{mL}^{-1}$, and are followed by the standard errors of fit.

Pathogen	EC	COS	Stevioside	<i>R. tinctorum</i>	COS— <i>R. tinctorum</i>	Stevioside— <i>R. tinctorum</i>	4-tert ...	1,2,4-trihydro ...	Guanosine
<i>D. seriata</i>	EC ₅₀	744.4 ± 43.9	288.1 ± 15.3	78.0 ± 0.8	63.1 ± 0.3	73.6 ± 0.3	53.0 ± 2.1	45.4 ± 3.4	130.4 ± 12.8
	EC ₉₀	1179.9 ± 58.2	840.5 ± 62.3	87.8 ± 1.9	73.4 ± 0.9	82.4 ± 0.7	73.2 ± 2.3	171.4 ± 18.7	249.9 ± 28.5
<i>D. viticola</i>	EC ₅₀	554.3 ± 27.4	306.9 ± 26.6	66.2 ± 2.9	22.1 ± 1.4	80.0 ± 0.7	25.7 ± 3.6	37.2 *	182.7 ± 7.7
	EC ₉₀	1138.7 ± 75.0	917.0 ± 74.3	90.2 ± 8.7	55.5 ± 4.6	90.7 ± 1.5	71.2 ± 9.0	74.9 *	308.1 ± 23.7
<i>N. parvum</i>	EC ₅₀	680.2 ± 43.1	194.8 ± 13.4	92.3 ± 0.5	38.2 ± 1.4	75.1 ± 0.8	62.2 ± 0.7	72.0 ± 14.8	95.1 ± 22.6
	EC ₉₀	1326.6 ± 83.2	723.8 ± 56.7	184.0 ± 1.1	66.3 ± 4.2	89.2 ± 1.9	70.6 ± 2.2	338.4 ± 37.9	317.8 ± 33.9

* Could not be reliably calculated (lack of points).

Table 5. Synergy factors, estimated according to Wadley's method.

Pathogen	EC	Synergy Factor	
		COS- <i>R. tinctorum</i>	Stevioside— <i>R. tinctorum</i>
<i>D. seriata</i>	EC ₅₀	2.24	1.67
	EC ₉₀	2.23	1.93
<i>D. viticola</i>	EC ₅₀	5.35	1.36
	EC ₉₀	3.01	1.81
<i>N. parvum</i>	EC ₅₀	4.26	1.67
	EC ₉₀	4.87	3.29

Table 6. Kruskal–Wallis test and multiple pairwise comparisons using the Conover–Iman procedure for the lengths of the vascular necroses scored for *D. seriata* in the ex situ autoclaved grapevine canes assay.

Sample	Frequency	Sum of Ranks	Mean of Ranks	Groups
COS- <i>R. tinctorum</i> negative control	24	300.000	12.500	A
COS- <i>R. tinctorum</i> - <i>D. seriata</i>	120	10,193.000	84.942	B
Positive control	24	3703.000	154.292	C

Treatments/controls labelled with the different letters are significantly different at $p < 0.05$.

3.3.3. Greenhouse Bioassays on Grafted Plants

When the best treatment (COS-*R. tinctorum* conjugate complex) was further assayed in vivo, significant differences were found against the positive controls in all cases (Table 7), confirming its antifungal behavior on the plant material. Nonetheless, complete inhibition was not reached against any of the three pathogens for the assayed dose (100 $\mu\text{g}\cdot\text{mL}^{-1}$) comparing with non-infected controls, suggesting that a higher concentration than the EC₉₀ values found in the in vitro tests (and/or a different dispersion medium) should be assayed when the treatment is used in future field trials.

Table 7. Kruskal–Wallis test and multiple pairwise comparisons using the Conover–Iman procedure for the lengths of the vascular necroses for the three phytopathogen in greenhouse in vivo assays.

Pathogen	Sample	Frequency	Sum of Ranks	Mean of Ranks	Groups
<i>D. seriata</i>	COS- <i>R. tinctorum</i> negative control	32	725.500	22.672	A
	COS- <i>R. tinctorum</i> - <i>D. seriata</i>	72	6124.000	85.056	B
	Positive control	56	6030.500	107.688	C
<i>D. viticola</i>	COS- <i>R. tinctorum</i> negative control	32	1295.000	40.469	A
	COS- <i>R. tinctorum</i> - <i>D. viticola</i>	72	4885.000	67.847	B
	Positive control	64	8016.000	125.250	C
<i>N. parvum</i>	COS- <i>R. tinctorum</i> negative control	32	572.000	17.875	A
	COS- <i>R. tinctorum</i> - <i>N. parvum</i>	48	3695.000	76.979	B
	Positive control	64	6173.000	96.453	C

Treatments/controls labelled with the different letters are significantly different at $p < 0.05$.

4. Discussion

4.1. On the Constituents of *R. tinctorum* Extracts

The composition here reported was different from that found by Derksen and Van Beek [35] (using LC–DAD and HPLC–MS(/MS) with ESI or APCI), where lucidin primeveroside and ruberythric acid were the major anthraquinone components in an ethanolic-water extract, and from the one reported by Jalil [18] for a methanolic extract, which was rich in 9,12-octadecadienoic acid (29.75%), 9-octadecenoic acid hexadecyl ester (26.1%) and 2-ethyl-2-(hydroxymethyl)-1,3-propanediol, (10.1%), but poor in anthracenediones (4.0%) and 2-methoxy-4-vinylphenol (0.5%).

Significant differences in composition were also observed in comparison with the *Rubia cordifolia* essential oil characterized by GC–MS, in which mollugin (rubimaillin or methyl 6-hydroxy-2,2-dimethylbenzo[h]chromene-5-carboxylate) was found to be the major component, followed by 3-methyl-2-cyclopenten-1-one, eugenol, anethole and 4-*tert*-butyl-2-phenylphenol [10,11].

Although the geographical location, time of year and age of the plant are known to influence the composition [15], the observed differences should be mainly ascribed to differences in both the extractive chemicals and in the extraction process (nature of the alcoholic solvent, alcohol:water ratio and mechanical enhancers such as sonication [36,37]), and to the characterization technique, provided that previous studies on *R. tinctorum* extracts [36,38–41] were conducted by HPLC and LC–HRMS (instead of GC–MS) and generally focused only on anthraquinones, anthraquinone glycosides and aglycones.

4.2. On the Combined Effect of Anthraquinones and Phenols

It is known that increasing the activity of a parent molecule can be pursued either by testing multiple substituent changes on the base core (the impact of the number, nature, and location of substituents on the anthraquinone moiety on its inhibitory potency against pathogenic fungi has been studied in [42]), or by testing the effect of coexistence with other molecules with which synergistic behavior may occur. In general, anthraquinone per se is a relatively inert compound, but in the presence of glucose, anthrahydroquinone units (formed by reduction of anthraquinone) reduce the quinone–methide units (issued by dehydration of phenolic β -O-4 lignin) mainly by electron transfer leading to guaiaicol [43]. Thus, the presence of 4-vinyl-guaiaicol, *cis*-eugenol, coniferyl alcohol or 4-*tert*-butyl-2-phenylphenol phytochemicals in the *R. tinctorum* hydromethanolic extract should be referred to the same origin. As regards a subsequent interaction of these phenols with anthraquinones, it cannot be excluded: Maurino et al. [44] have demonstrated that quinonoid compounds excited by sunlight react with phenols, transforming them into tetrasubstituted dihydroxybiphenyls and phenoxyphenols. Nevertheless, in the absence of induced sunlight, no reaction between anthraquinones and methoxy- and phenyl-phenols has been described in the literature (to the best of the authors' knowledge), so at this point it is not possible to establish whether the activity of *R. tinctorum* extracts may be referred to an additive effect of both families of components or to a synergistic one.

4.3. Comparison with Efficacies Reported in the Literature

An overview of the antimicrobial activities reported for *R. tinctorum* in the literature is presented in Table S2. Concerning its antifungal behavior, full inhibition of *Aspergillus flavus* Link and *Fusarium oxysporum* Schldl. at a concentration of 100 $\mu\text{g}\cdot\text{mL}^{-1}$ has been reported by Kalyoncu, et al. [45], and inhibition percentages in the 18–43% range were reported against *Trichoderma viride* Pers., *Doratomyces stemonitis* (Pers.) Nees, *Aspergillus niger*, *Penicillium verrucosum* Dierckx, *Alternaria alternata* (Fr.) Keissl., *Aureobasidium pullulans* (de Bary) G. Arnaud and *Mucor mucedo* L. by Manojlovic et al. [46], although the assayed concentration was not reported. Activity against other fungi (e.g., *Penicillium expansum* Link, *Geotrichum candidum* Link, *Fusarium solani* (Mart.) Sacc., *Postia placenta* (Fr.) M.J. Larsen and Lombard, *Trametes versicolor* (L.) Lloyd) has also been reported, albeit not in a quantitative manner [47,48].

The contribution of anthraquinones to antifungal activity is well-established, given that anthracenediones from other plants have proven to be effective against a wide variety of phytopathogenic fungi. For instance, anthraquinones isolated from *Cassia tora* L., *Coccoloba mollis* Casar., *Rheum palmatum* L., *Morinda lucida* Benth. or *Aegle marmelos* (L.) Corrêa, to name a few, showed antifungal behavior against phytopathogenic fungi such as *Botrytis cinerea*, *Blumeria graminis* (DC.) Speer, *Phytophthora infestans* (Mont.) de Bary, *Puccinia recondita* Roberge ex Desm., *Pycularia grisea* Sacc., *Rhizoctonia solani* J.G. Kühn, *Botryosphaeria ribis* Grossenbacher and Duggar, *B. rhodina* (Berk. and M.A. Curtis) Arx, *Lasioidiplodia theobromae* (Pat.) Griffon and Maubl., *Fusarium* sp., *Fusarium graminearum*

Schwabe, *Mycosphaerella melonis* (Pass.) W.F. Chiu and J.C. Walker, *Fusarium oxysporum* f. sp. *vasinfectum* (G.F. Atk.) W.C. Snyder and H.N. Hansen, *Phyllosticta zae* Stout, *Sclerotinia sclerotiorum* (Lib.) de Bary, *Cladosporium cucumerinum* Ellis and Arthur and *Aspergillus* spp. [49–53]. The underlying mechanism of action has been studied, for example, for purpurin against *Candida* spp., finding that it elevates intracellular ROS levels, depolarizes the mitochondrial membrane potential, downregulates of the expression of hypha-specific genes and the central morphogenetic regulator Ras1p and degrades DNA [54,55].

On the other hand, the antifungal activities of 2-methoxy- and 2-*tert*-butyl-substituted phenols against phytopathogens have been less studied, although a strong antifungal activity of 2-methoxy-4-(1-propenyl)-phenol against *Botrytis cinerea* was reported by Wang et al. [12]; against *B. rhodina*, *Rhizoctonia* sp. and *Alternaria* sp. by de Oliveira Pereira et al. [56]; and against *A. alternata* (Fr.) Keissl., *Sarocladium oryzae* (Sawada) W. Gams and D. Hawksw., *F. graminearum*, *F. equiseti* (Corda) Sacc. and *F. verticillioides* (Sacc.) Nirenberg by Pilar Santamarina et al. [57]. Likewise, 2-methoxy-phenol was effective against sap-staining fungi (*Ophiostoma* spp.), according to Velmurugan et al. [13]. Regarding their mechanism of action, it has been proposed that, for instance, eugenol acts on cell membrane by a mechanism that seems to involve the inhibition of ergosterol biosynthesis, and the lower ergosterol content interferes with the integrity and functionality of the cell membrane [56]. It has also been suggested that, taking into consideration that it induced the generation of H₂O₂ and increased free Ca²⁺ in the cytoplasm, its activity may also be referred to membrane binding and permeability alteration, leading to the destabilization and disruption of the plasma membrane [12].

4.4. On the Synergistic Behaviour of *R. tinctorum* Extracts with COS and Stevioside

To date, it has been verified that chitosan acts as an elicitor on *R. tinctorum*, stimulating anthraquinone synthesis [58]; chitosan/poly (lactic acid) nanoparticles have been evaluated as a novel carrier for the delivery of anthraquinone [59]; and chitosan-based hydrogels have been studied for the adsorption of anthraquinone dyes [60]. Nonetheless, after a thorough bibliographical survey, no previous examples of the use of chitosan or stevioside for the formation of conjugate complexes with anthraquinones could be found.

On the other hand, examples of synergistic behaviour have been reported, for instance, for chitosan combined with *Cinnamomum zeylanicum* Blume essential oils, rich in eugenol [61]. These authors hypothesized that eugenol alters the surface and structure of the fungal cell wall, and COS acts as a potentiator by reducing cell wall synthesis and facilitating death in an energy-dependent manner. In this regard, the accepted and potential mechanisms of action behind the antimicrobial properties of chitosan have been thoroughly discussed in the review paper by Ma et al. [62]. Those of stevioside have been discussed in [63], and are related to the uncoupling of mitochondrial oxidative phosphorylation and the permeabilization of the cell membrane.

Nonetheless, taking into consideration that the antifungal activity of both COS and stevioside alone was substantially lower than that of the *R. tinctorum* extract, and given that the use of most free anthraquinones in pharmaceutical industries is limited by their poor water solubility and low bioavailability [64], the observed strong synergistic behavior with COS and stevioside should probably be referred to a solubility and bioavailability enhancement through the formation of inclusion compounds or conjugate complexes (discussed, in the case of chitosan, in the recent review paper by Detsi et al. [65] and, for steviol glycosides, in the works by Nguyen et al. [66,67]). Examples of antifungal activity enhancement via the formation of conjugate complexes against GTDs have been previously reported in [25,26,68], albeit with worse EC₅₀ and EC₉₀ values than those reported in this work.

5. Conclusions

The GC–MS analysis of *R. tinctorum* hydroalcoholic extracts revealed that, apart from members of the anthraquinone family (19.4%), flavoring phenols similar to those found in

oak (used to confer aroma to wine) and guanosine were also present. *R. tinctorum* extract, alone and forming conjugate complexes with COS and stevioside, along with three of its constituents, were assayed in vitro against three *Botryosphaeriaceae* taxa. *R. tinctorum* extract led to a strong mycelial growth inhibitory effect in all cases, with EC₉₀ values as low as 88 µg·mL⁻¹. Although 4-*tert*-butyl-2-phenylphenol was its most active constituent, 1,2,4-trihydroxyanthraquinone and guanosine were also effective, suggesting the activity cannot be ascribed to a single constituent, but rather to the combination of several of them. As regards the strong synergistic behavior observed upon conjugation with COS, which resulted in EC₉₀ values in the 56–73 µg·mL⁻¹ range, it may be ascribed to solubility and bioavailability enhancement, rather than to the antifungal activity of chitosan (which is much weaker than that of *R. tinctorum*). The treatment for which the best results were attained in plate tests (COS-*R. tinctorum* conjugate complex) was then tested ex situ on autoclaved grapevine twigs and in young, grafted plants in greenhouse assays. A significant reduction in the infection rate was found in all cases. Hence, this natural antifungal compound may deserve further examination in larger field trials, as it may hold promise for the sustainable control of GTDs.

Supplementary Materials: The following are available online at <https://www.mdpi.com/article/10.3390/plants10081527/s1>, Table S1. Repetitions for each of the plant/treatment combinations in the greenhouse bioassay. Each grafted plant was inoculated at two sites below grafting point; Table S2. Examples of application of *R. tinctorum* extracts against microorganisms reported in the literature; Figure S1. GC-MS spectrum of *R. tinctorum* root hydromethanolic extract; Figures S2–S4. Mycelial growth inhibition of *D. seriata*/*D. viticola*/*N. parvum* upon treatment with: chitosan oligomers, stevioside, *R. tinctorum* hydromethanolic extract, stevioside-*R. tinctorum* conjugate complex, and COS-*R. tinctorum* conjugate complex at different concentrations; Figure S5. Colony growth measures of *D. seriata*, *D. viticola* and *N. parvum* strains when cultured in PDA plates containing the main phytochemicals found in *R. tinctorum* hydromethanolic extracts at concentrations in the 62.5–1500 and 15.62–250 µg·mL⁻¹ range for the least and the most active products, respectively; Figures S6–S8. Mycelial growth inhibition of *D. seriata*/*D. viticola*/*N. parvum* upon treatment with the main phytochemicals found in *R. tinctorum* hydromethanolic extracts: purpurin, guanosine, and 4-*tert*-butyl-2-phenylphenol, at different concentrations.

Author Contributions: Conceptualization, J.M.-G., P.M.-R. and V.G.-G.; methodology, J.M.-G., J.C.-G. and V.G.-G.; validation, J.C.-G., V.G.-G. and P.M.-R.; formal analysis, J.C.-G., V.G.-G. and P.M.-R.; investigation, N.L.-L., E.S.-H., L.B.-D., V.G.-G., J.C.-G., J.M.-G. and P.M.-R.; resources, J.M.-G. and P.M.-R.; data curation, J.C.-G.; writing—original draft preparation, N.L.-L., E.S.-H., L.B.-D., V.G.-G., J.C.-G., J.M.-G. and P.M.-R.; writing—review and editing, V.G.-G. and P.M.-R.; visualization, N.L.-L. and E.S.-H.; supervision, V.G.-G. and P.M.-R.; project administration, V.G.-G., J.M.-G. and P.M.-R.; funding acquisition, J.M.-G. and P.M.-R. All authors have read and agreed to the published version of the manuscript.

Funding: This research was funded by Junta de Castilla y León under project VA258P18, with FEDER co-funding; by Cátedra Agrobank under the “IV Convocatoria de Ayudas de la Cátedra AgroBank para la transferencia del conocimiento al sector agroalimentario” program and by Fundación Ibercaja-Universidad de Zaragoza under the “Convocatoria Fundación Ibercaja-Universidad de Zaragoza de proyectos de investigación, desarrollo e innovación para jóvenes investigadores” program.

Data Availability Statement: The data presented in this study are available on request from the corresponding author. The data are not publicly available due to their relevance to an ongoing Ph.D. thesis.

Acknowledgments: V.G.-G thanks C. Julián (Plant Protection Unit, CITA) for her technical assistance. The authors gratefully acknowledge the support of Pilar Blasco and Pablo Candela at the Servicios Técnicos de Investigación, Universidad de Alicante, for conducting the GC-MS analyses.

Conflicts of Interest: The authors declare no conflict of interest. The funders had no role in the design of the study; in the collection, analyses, or interpretation of data; in the writing of the manuscript, or in the decision to publish the results.

References

1. Qiu, H.; Liu, R.; Long, L. Analysis of chemical composition of extractives by acetone and the chromatic aberration of teak (*Tectona Grandis* L.F.) from China. *Molecules* **2019**, *24*, 1989. [[CrossRef](#)] [[PubMed](#)]
2. Murdock, K.C.; Child, R.G.; Fabio, P.F.; Angier, R.D.; Wallace, R.E.; Durr, F.E.; Citarella, R.V. Antitumor agents. 1. 1,4-Bis[(aminoalkyl)amino]-9,10-anthracenediones. *J. Med. Chem.* **1979**, *22*, 1024–1030. [[CrossRef](#)] [[PubMed](#)]
3. Coufal, N.; Farnaes, L. Anthracyclines and anthracenediones. In *Cancer Management in Man: Chemotherapy, Biological Therapy, Hyperthermia and Supporting Measures*; Minev, B., Ed.; Springer: Dordrecht, The Netherlands, 2011; pp. 87–102. [[CrossRef](#)]
4. Wuthi-udomlert, M.; Kupittayanant, P.; Gritsanapan, W. In vitro evaluation of antifungal activity of anthraquinone derivatives of *Senna alata*. *J. Health Res.* **2010**, *24*, 117–122.
5. Agarwal, S.; Singh, S.S.; Verma, S.; Kumar, S. Antifungal activity of anthraquinone derivatives from *Rheum emodi*. *J. Ethnopharmacol.* **2000**, *72*, 43–46. [[CrossRef](#)]
6. Singh, D.; Verma, N.; Raghuvanshi, S.; Shukla, P.; Kulshreshtha, D. Antifungal anthraquinones from *Saprosma fragrans*. *Bioorg. Med. Chem. Lett.* **2006**, *16*, 4512–4514. [[CrossRef](#)]
7. Singh, J.; Hussain, Y.; Luqman, S.; Meena, A. Purpurin: A natural anthraquinone with multifaceted pharmacological activities. *Phytother. Res.* **2020**, *35*, 2418–2428. [[CrossRef](#)]
8. Essaidi, I.; Snoussi, A.; Koubaier, H.B.H.; Casabianca, H.; Bouzouita, N. Effect of acid hydrolysis on alizarin content, antioxidant and antimicrobial activities of *Rubia tinctorum* extracts. *Pigment. Resin Technol.* **2017**, *46*, 379–384. [[CrossRef](#)]
9. Ilc, T.; Werck-Reichhart, D.; Navrot, N. Meta-analysis of the core aroma components of grape and wine aroma. *Front. Plant Sci.* **2016**, *7*, 1472. [[CrossRef](#)]
10. Miyazawa, M.; Kawata, J. Identification of the key aroma compounds in dried roots of *Rubia cordifolia*. *J. Oleo Sci.* **2006**, *55*, 37–39. [[CrossRef](#)]
11. Li, W.-Q.; Quan, M.-P.; Li, Q. Chemical composition and antibacterial activity of the essential oil from Qiancao (*Rubia cordifolia* Linn.) roots against selected foodborne pathogens. *Asian J. Agric. Food Sci.* **2019**, *7*. [[CrossRef](#)]
12. Wang, C.; Zhang, J.; Chen, H.; Fan, Y.; Shi, Z. Antifungal activity of eugenol against *Botrytis cinerea*. *Trop. Plant Pathol.* **2010**, *35*, 137–143. [[CrossRef](#)]
13. Velmurugan, N.; Han, S.S.; Lee, Y.S. Antifungal activity of neutralized wood vinegar with water extracts of *Pinus densiflora* and *Quercus serrata* saw dusts. *Int. J. Environ. Res.* **2009**, *3*, 167–176. [[CrossRef](#)]
14. Singh, R.; Chauhan, S.M.S.G. 9,10-Anthraquinones and other biologically active compounds from the Genus *Rubia*. *Chem. Biodivers.* **2004**, *1*, 1241–1264. [[CrossRef](#)]
15. Angelini, L.G.; Pistelli, L.; Belloni, P.; Bertoli, A.; Panconesi, S. *Rubia tinctorum* a source of natural dyes: Agronomic evaluation, quantitative analysis of alizarin and industrial assays. *Ind. Crop. Prod.* **1997**, *6*, 303–311. [[CrossRef](#)]
16. Boldizsár, I.; Szücs, Z.; Füzfai, Z.; Molnár-Perl, I. Identification and quantification of the constituents of madder root by gas chromatography and high-performance liquid chromatography. *J. Chromatogr. A* **2006**, *1133*, 259–274. [[CrossRef](#)]
17. Nakanishi, F.; Nagasawa, Y.; Kabaya, Y.; Sekimoto, H.; Shimomura, K. Characterization of lucidin formation in *Rubia tinctorum* L. *Plant Physiol. Biochem.* **2005**, *43*, 921–928. [[CrossRef](#)]
18. Jalil, R.D.A. GC-MS analysis of extract of *Rubia tinctorum* having anticancer properties. *Int. J. Pharmacogn. Phytochem. Res.* **2017**, *9*, 286–292.
19. Úrbez-Torres, J.R.; Hrycan, J.; Hart, M.; Bowen, P.; Forge, T. Grapevine trunk disease fungi: Their roles as latent pathogens and stress factors that favour disease development and symptom expression. *Phytopathol. Mediterr.* **2020**, *59*, 395–424. [[CrossRef](#)]
20. Bertsch, C.; Ramírez-Suero, M.; Magninrobert, M.; Larignon, P.; Chong, J.; Mansour, E.A.; Spagnolo, A.; Clément, C.; Fontaine, F. Grapevine trunk diseases: Complex and still poorly understood. *Plant Pathol.* **2012**, *62*, 243–265. [[CrossRef](#)]
21. Gramaje, D.; Armengol, J. Fungal Trunk pathogens in the grapevine propagation process: Potential inoculum sources, detection, identification, and management strategies. *Plant Dis.* **2011**, *95*, 1040–1055. [[CrossRef](#)]
22. Fontaine, F.; Gramaje, D.; Armengol, J.; Smart, R.; Nagy, Z.A.; Borgo, M.; Rego, C.; Corio-Costet, M.-F. *Grapevine Trunk Diseases: A Review*; OIV Publications: Paris, France, 2016; p. 25.
23. Mondello, V.; Songy, A.; Battiston, E.; Pinto, C.; Coppin, C.; Trotel-Aziz, P.; Clément, C.; Mugnai, L.; Fontaine, F. Grapevine trunk diseases: A review of fifteen years of trials for their control with chemicals and biocontrol agents. *Plant Dis.* **2018**, *102*, 1189–1217. [[CrossRef](#)] [[PubMed](#)]
24. Gramaje, D.; Úrbez-Torres, J.R.; Sosnowski, M.R. Managing grapevine trunk diseases with respect to etiology and epidemiology: Current strategies and future prospects. *Plant Dis.* **2018**, *102*, 12–39. [[CrossRef](#)] [[PubMed](#)]
25. Langa-Lomba, N.; Buzón-Durán, L.; Sánchez-Hernández, E.; Martín-Ramos, P.; Casanova-Gascón, J.; Martín-Gil, J.; González-García, V. Antifungal activity against *Botryosphaeriaceae* fungi of the hydro-methanolic extract of *Silybum marianum* capitula conjugated with stevioside. *Plants* **2021**, *10*, 1363. [[CrossRef](#)]
26. Langa-Lomba, N.; Buzón-Durán, L.; Martín-Ramos, P.; Casanova-Gascón, J.; Martín-Gil, J.; Sánchez-Hernández, E.; González-García, V. Assessment of conjugate complexes of chitosan and *Urtica dioica* or *Equisetum arvense* extracts for the control of grapevine trunk pathogens. *Agronomy* **2021**, *11*, 976. [[CrossRef](#)]
27. Nunn, S.; Nishikida, K. *Advanced ATR Correction Algorithm—Application Note 50581*; ThermoScientific: Madison, WI, USA, 2008; p. 4.
28. Adams, R.P. *Identification of Essential Oil Components by Gas Chromatography/Mass Spectroscopy*, 4th ed.; Allured Publishing Corp.: Carol Stream, IL, USA, 2007; p. 804.

29. Santos-Moriano, P.; Fernandez-Arrojo, L.; Mengíbar, M.; Belmonte-Reche, E.; Peñalver, P.; Acosta, F.N.; Ballesteros, A.O.; Morales, J.C.; Kidibule, P.; Fernandez-Lobato, M.; et al. Enzymatic production of fully deacetylated chitoooligosaccharides and their neuroprotective and anti-inflammatory properties. *Biocatal. Biotransform.* **2017**, *36*, 57–67. [[CrossRef](#)]
30. Buzón-Durán, L.; Martín-Gil, J.; Pérez-Lebeña, E.; Ruano-Rosa, D.; Revuelta, J.L.; Casanova-Gascón, J.; Ramos-Sánchez, M.C.; Martín-Ramos, P. Antifungal agents based on chitosan oligomers, ϵ -polylysine and streptomyces spp. secondary metabolites against three botryosphaeriaceae species. *Antibiotics* **2019**, *8*, 99. [[CrossRef](#)]
31. Martín, M.T.; Cobos, R. Identification of fungi associated with grapevine decline in Castilla y León (Spain). *Phytopathol. Mediterr.* **2007**, *46*, 18–25. [[CrossRef](#)]
32. Arendrup, M.C.; Cuenca-Estrella, M.; Lass-Flörl, C.; Hope, W. EUCAST technical note on the EUCAST definitive document EDef 7.2: Method for the determination of broth dilution minimum inhibitory concentrations of antifungal agents for yeasts EDef 7.2 (EUCAST-AFST)*. *Clin. Microbiol. Infect.* **2012**, *18*, E246–E247. [[CrossRef](#)]
33. Levy, Y.; Benderly, M.; Cohen, Y.; Gisi, U.; Bassand, D. The joint action of fungicides in mixtures: Comparison of two methods for synergy calculation. *EPPO Bull.* **1986**, *16*, 651–657. [[CrossRef](#)]
34. R Core Team. *R: A Language and Environment for Statistical Computing*; R Foundation for Statistical Computing: Vienna, Austria, 2020.
35. Derksen, G.C.H.; Van Beek, T.A. Rubia tinctorum L. In *Studies in Natural Products Chemistry*; Ur-Rahman, A., Ed.; Elsevier: Amsterdam, The Netherlands, 2002; Volume 26, pp. 629–684.
36. DE Santis, D.; Moresi, M. Production of alizarin extracts from Rubia tinctorum and assessment of their dyeing properties. *Ind. Crop. Prod.* **2007**, *26*, 151–162. [[CrossRef](#)]
37. Dulo, B.; Phan, K.; Githaiga, J.; Raes, K.; De Meester, S. Natural quinone dyes: A review on structure, extraction techniques, analysis and application potential. *Waste Biomass Valoriz.* **2021**, 1–36. [[CrossRef](#)]
38. Derksen, G.; van Beek, T.A.; de Groot, A.; Capelle, A. High-performance liquid chromatographic method for the analysis of anthraquinone glycosides and aglycones in madder root (*Rubia tinctorum* L.). *J. Chromatogr. A* **1998**, *816*, 277–281. [[CrossRef](#)]
39. Derksen, G.C.H.; Lelyveld, G.P.; Van Beek, T.A.; Capelle, A. Two validated HPLC methods for the quantification of alizarin and other anthraquinones in *Rubia tinctorum* cultivars. *Phytochem. Anal.* **2004**, *15*, 397–406. [[CrossRef](#)]
40. Krizsán, K.; Szókán, G.; Tóth, Z.A.; Hollósy, F.; Laszlo, M.; Khlafula, A. HPLC Analysis of Anthraquinone Derivatives in Madder Root (*Rubia Tinctorum*) and Its Cell Cultures. *J. Liq. Chromatogr. Relat. Technol.* **1996**, *19*, 2295–2314. [[CrossRef](#)]
41. Eltamany, E.E.; Nafie, M.S.; Khodeer, D.M.; El-Tanahy, A.; Abdel-Kader, M.S.; Badr, J.M.; Abdelhameed, R.F.A. Rubia tinctorum root extracts: Chemical profile and management of type II diabetes mellitus. *RSC Adv.* **2020**, *10*, 24159–24168. [[CrossRef](#)]
42. Friedman, M.; Xu, A.; Lee, R.; Nguyen, D.N.; Phan, T.A.; Hamada, S.M.; Panchel, R.; Tam, C.C.; Kim, J.H.; Cheng, L.W.; et al. The inhibitory activity of anthraquinones against pathogenic protozoa, bacteria, and fungi and the relationship to structure. *Molecules* **2020**, *25*, 3101. [[CrossRef](#)]
43. Megiatto, J.J.D.; Cazeils, E.; Ham-Pichavant, F.; Grelier, S.; Gardrat, C.; Castellan, A. Styrene-spaced copolymers including anthraquinone and β -O-4 lignin model units: Synthesis, characterization and reactivity under alkaline pulping conditions. *Biomacromolecules* **2012**, *13*, 1652–1662. [[CrossRef](#)]
44. Maurino, V.; Borghesi, D.; Vione, D.; Minero, C. Transformation of phenolic compounds upon UVA irradiation of anthraquinone-2-sulfonate. *Photochem. Photobiol. Sci.* **2007**, *7*, 321–327. [[CrossRef](#)]
45. Kalyoncu, F.; Çetin, B.; Sağlam, H. Antimicrobial activity of common madder (*Rubia tinctorum* L.). *Phytother. Res.* **2006**, *20*, 490–492. [[CrossRef](#)]
46. Manojlovic, N.; Solujic, S.; Sukdolak, S.; Milosev, M. Antifungal activity of Rubia tinctorum, Rhamnus frangula and Caloplaca cerina. *Fitoterapia* **2005**, *76*, 244–246. [[CrossRef](#)]
47. Mehrabian, S.; Majd, A.; Majd, I. Antimicrobial effects of three plants (rubia tinctorum, carthamus tinctorius and juglans regia) on some airborne microorganisms. *Aerobiologia* **2000**, *16*, 455–458. [[CrossRef](#)]
48. Ozen, E.; Yeniocak, M.; Goktas, O.; Alma, M.H.; Yilmaz, F. Antimicrobial and antifungal properties of madder root (*Rubia tinctorum*) colorant used as an environmentally-friendly wood preservative. *Bioresources* **2014**, *9*, 1998–2009. [[CrossRef](#)]
49. Kim, Y.-M.; Lee, C.-H.; Kim, A.H.-G.; Lee, H.-S. Anthraquinones isolated from Cassiadora (Leguminosae) seed show an antifungal property against phytopathogenic fungi. *J. Agric. Food Chem.* **2004**, *52*, 6096–6100. [[CrossRef](#)]
50. De Barros, I.B.; Daniel, J.F.D.S.; Pinto, J.P.; Rezende, M.I.; Filho, R.B.; Ferreira, D.T. Phytochemical and antifungal activity of anthraquinones and root and leaf extracts of *Coccoloba mollis* on phytopathogens. *Braz. Arch. Biol. Technol.* **2011**, *54*, 535–541. [[CrossRef](#)]
51. Shang, X.-F.; Zhao, Z.-M.; Li, J.-C.; Yang, G.-Z.; Liu, Y.-Q.; Dai, L.-X.; Zhang, Z.-J.; Yang, Z.-G.; Miao, X.-L.; Yang, C.-J.; et al. Insecticidal and antifungal activities of *Rheum palmatum* L. anthraquinones and structurally related compounds. *Ind. Crop. Prod.* **2019**, *137*, 508–520. [[CrossRef](#)]
52. Rath, G.; Ndonzao, M.; Hostettmann, K. Antifungal anthraquinones from *Morinda lucida*. *Int. J. Pharmacogn.* **1995**, *33*, 107–114. [[CrossRef](#)]
53. Mishra, B.B.; Kishore, N.; Tiwari, V.K.; Singh, D.D.; Tripathi, V. A novel antifungal anthraquinone from seeds of *Aegle marmelos* Correa (family Rutaceae). *Fitoterapia* **2010**, *81*, 104–107. [[CrossRef](#)]
54. Tsang, P.W.-K.; Bandara, H.; Fong, W.-P. Purpurin suppresses candida albicans biofilm formation and hyphal development. *PLoS ONE* **2012**, *7*, e50866. [[CrossRef](#)]

55. Tsang, P.W.-K.; Wong, A.P.-K.; Yang, H.-P.; Li, N.-F. Purpurin triggers caspase-independent apoptosis in candida dubliniensis biofilms. *PLoS ONE* **2013**, *8*, e86032. [[CrossRef](#)]
56. Pereira, F.D.O.; Mendes, J.M.; Lima, E.D.O. Investigation on mechanism of antifungal activity of eugenol against *Trichophyton rubrum*. *Med. Mycol.* **2013**, *51*, 507–513. [[CrossRef](#)]
57. Santamarina, M.P.; Roselló, J.; Giménez, S.; Blázquez, M.A. Commercial *Laurus nobilis* L. and *Syzygium aromaticum* L. Merr. & Perry essential oils against post-harvest phytopathogenic fungi on rice. *LWT* **2016**, *65*, 325–332. [[CrossRef](#)]
58. Vasconsuelo, A.; Giulietti, A.M.; Boland, R. Signal transduction events mediating chitosan stimulation of anthraquinone synthesis in *Rubia tinctorum*. *Plant Sci.* **2004**, *166*, 405–413. [[CrossRef](#)]
59. Jeevitha, D.; Amarnath, K. Chitosan/PLA nanoparticles as a novel carrier for the delivery of anthraquinone: Synthesis, characterization and in vitro cytotoxicity evaluation. *Coll. Surf. B Biointerf.* **2013**, *101*, 126–134. [[CrossRef](#)] [[PubMed](#)]
60. Oladipo, A.A.; Gazi, M.; Yilmaz, E. Single and binary adsorption of azo and anthraquinone dyes by chitosan-based hydrogel: Selectivity factor and Box-Behnken process design. *Chem. Eng. Res. Des.* **2015**, *104*, 264–279. [[CrossRef](#)]
61. Mohammadi, A.; Hashemi, M.; Hosseini, S. The control of *Botrytis* fruit rot in strawberry using combined treatments of Chitosan with *Zataria multiflora* or *Cinnamomum zeylanicum* essential oil. *J. Food Sci. Technol.* **2015**, *52*, 7441–7448. [[CrossRef](#)]
62. Ma, Z.; Garrido-Maestu, A.; Jeong, K.C. Application, mode of action, and in vivo activity of chitosan and its micro- and nanoparticles as antimicrobial agents: A review. *Carbohydr. Polym.* **2017**, *176*, 257–265. [[CrossRef](#)]
63. Buzón-Durán, L.; Martín-Gil, J.; Ramos-Sánchez, M.D.C.; Pérez-Lebeña, E.; Marcos-Robles, J.L.; Fombellida-Villafuela, Á.; Martín-Ramos, P. Antifungal activity against *Fusarium culmorum* of stevioside, *Silybum marianum* seed extracts, and their conjugate complexes. *Antibiotics* **2020**, *9*, 440. [[CrossRef](#)]
64. Xu, H.; Lu, Y.; Zhang, T.; Liu, K.; Liu, L.; He, Z.; Xu, B.; Wu, X. Characterization of binding interactions of anthraquinones and bovine β -lactoglobulin. *Food Chem.* **2019**, *281*, 28–35. [[CrossRef](#)]
65. Detsi, A.; Kavetsou, E.; Kostopoulou, I.; Pitterou, I.; Pontillo, A.R.N.; Tzani, A.; Christodoulou, P.; Siliachli, A.; Zoumpoulakis, P. Nanosystems for the encapsulation of natural products: The case of chitosan biopolymer as a matrix. *Pharmaceutics* **2020**, *12*, 669. [[CrossRef](#)]
66. Nguyen, T.T.H.; Si, J.; Kang, C.; Chung, B.; Chung, D.; Kim, D. Facile preparation of water soluble curcuminoids extracted from turmeric (*Curcuma longa* L.) powder by using steviol glucosides. *Food Chem.* **2017**, *214*, 366–373. [[CrossRef](#)]
67. Nguyen, T.T.H.; Yu, S.-H.; Kim, J.; An, E.; Hwang, K.; Park, J.-S.; Kim, D. Enhancement of quercetin water solubility with steviol glucosides and the studies of biological properties. *Funct. Foods Health Dis.* **2015**, *5*, 437. [[CrossRef](#)]
68. Buzón-Durán, L.; Langa-Lomba, N.; González-García, V.; Casanova-Gascón, J.; Martín-Gil, J.; Pérez-Lebeña, E.; Martín-Ramos, P. On the applicability of chitosan oligomers-amino acid conjugate complexes as eco-friendly fungicides against grapevine trunk pathogens. *Agronomy* **2021**, *11*, 324. [[CrossRef](#)]

ARTÍCULO 6: “Lignin-chitosan nanocarriers for the delivery of bioactive natural products against wood-decay phytopathogens” *Agronomy*, 2022, 12(2), 461; <https://doi.org/10.3390/agronomy12020461>; Q1 (JCR, Science Edition – AGRONOMY). JIF₂₀₂₂ = 3,7. 15 citas recibidas (WOS).



agronomy

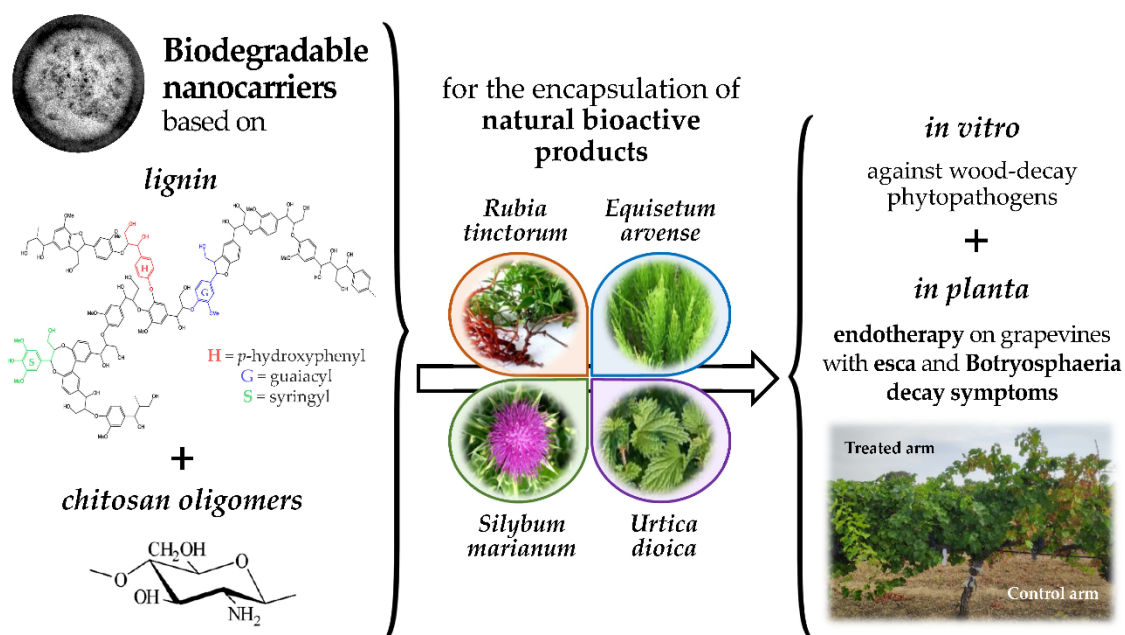
an Open Access Journal by MDPI



Lignin–Chitosan Nanocarriers for the Delivery of Bioactive Natural Products against Wood-Decay Phytopathogens

Eva Sánchez-Hernández; Natalia Langa-Lomba; Vicente González-García; José Casanova-Gascón; Jesús Martín-Gil; Alberto Santiago-Aliste; Sergio Torres-Sánchez; Pablo Martín-Ramos

Agronomy 2022, Volume 12, Issue 2, 461



Article

Lignin–Chitosan Nanocarriers for the Delivery of Bioactive Natural Products against Wood-Decay Phytopathogens

Eva Sánchez-Hernández ¹, Natalia Langa-Lomba ^{2,3}, Vicente González-García ³, José Casanova-Gascón ², Jesús Martín-Gil ^{1,*}, Alberto Santiago-Aliste ¹, Sergio Torres-Sánchez ⁴ and Pablo Martín-Ramos ²

¹ Department of Agricultural and Forestry Engineering, ETSIIAA, University of Valladolid, Avenida de Madrid 44, 34004 Palencia, Spain; eva.sanchez.hernandez@uva.es (E.S.-H.); alberto.santiago@alumnos.uva.es (A.S.-A.)

² Instituto Universitario de Investigación en Ciencias Ambientales de Aragón (IUCA), EPS, University of Zaragoza, Carretera de Cuarte s/n, 22071 Huesca, Spain; natalialangalomba@gmail.com (N.L.-L.); jcasan@unizar.es (J.C.-G.); pmr@unizar.es (P.M.-R.)

³ Plant Protection Unit, Instituto Agroalimentario de Aragón-IA2 (CITA-Universidad de Zaragoza), Avda. Montañana 930, 50059 Zaragoza, Spain; vgonzalezg@aragon.es

⁴ Viñas del Vero S.A., Carretera Nacional 123 (km 3.7), 22300 Barbastro, Spain; storres@vinasdelvero.es

* Correspondence: mgil@iaf.uva.es; Tel.: +34-(979)-108347

Abstract: The use of nanocarriers (NCs), i.e., nanomaterials capable of encapsulating drugs and releasing them selectively, is an emerging field in agriculture. In this study, the synthesis, characterization, and in vitro and in vivo testing of biodegradable NCs loaded with natural bioactive products was investigated for the control of certain phytopathogens responsible for wood degradation. In particular, NCs based on methacrylated lignin and chitosan oligomers, loaded with extracts from *Rubia tinctorum*, *Silybum marianum*, *Equisetum arvense*, and *Urtica dioica*, were first assayed in vitro against *Neofusicoccum parvum*, an aggressive fungus that causes cankers and diebacks in numerous woody hosts around the world. The in vitro antimicrobial activity of the most effective treatment was further explored against another fungal pathogen and two bacteria related to trunk diseases: *Diplodia seriata*, *Xylophilus ampelinus*, and *Pseudomonas syringae* pv. *syringae*, respectively. Subsequently, it was evaluated in field conditions, in which it was applied by endotherapy for the control of grapevine trunk diseases. In the in vitro mycelial growth inhibition tests, the NCs loaded with *R. tinctorum* resulted in EC₉₀ concentrations of 65.8 and 91.0 µg·mL⁻¹ against *N. parvum* and *D. seriata*, respectively. Concerning their antibacterial activity, a minimum inhibitory concentration of 37.5 µg·mL⁻¹ was obtained for this treatment against both phytopathogens. Upon application via endotherapy on 20-year-old grapevines with clear esca and Botryosphaeria decay symptoms, no phytotoxicity effects were observed (according to SPAD and chlorophyll fluorescence measurements) and the sugar content of the grape juice was not affected either. Nonetheless, the treatment led to a noticeable decrease in foliar symptoms as well as a higher yield in the treated arms as compared to the control arms (3177 vs. 1932 g/arm), suggestive of high efficacy. Given the advantages in terms of controlled release and antimicrobial product savings, these biodegradable NCs loaded with natural extracts may deserve further research in large-scale field tests.

Keywords: *Equisetum arvense*; grapevine trunk diseases; natural bioactive products; NCs; *Rubia tinctorum*; *Silybum marianum*; *Urtica dioica*



Citation: Sánchez-Hernández, E.; Langa-Lomba, N.; González-García, V.; Casanova-Gascón, J.; Martín-Gil, J.; Santiago-Aliste, A.; Torres-Sánchez, S.; Martín-Ramos, P. Lignin–Chitosan Nanocarriers for the Delivery of Bioactive Natural Products against Wood-Decay Phytopathogens. *Agronomy* **2022**, *12*, 461. <https://doi.org/10.3390/agronomy12020461>

Academic Editors: Alain Deloire and Ivo Toševski

Received: 29 December 2021

Accepted: 10 February 2022

Published: 12 February 2022

Publisher's Note: MDPI stays neutral with regard to jurisdictional claims in published maps and institutional affiliations.



Copyright: © 2022 by the authors. Licensee MDPI, Basel, Switzerland. This article is an open access article distributed under the terms and conditions of the Creative Commons Attribution (CC BY) license (<https://creativecommons.org/licenses/by/4.0/>).

1. Introduction

Diseases associated with phytopathogenic microorganisms are responsible for important economic losses, affecting both arable crops (cereals, leguminous plants, vegetables, etc.) and woody crops (olive groves, vineyards, stone fruit and citrus orchards, etc.).

In the particular case of woody crops, the control of phytopathogens that cause diseases such as dieback and canker on economically and ecologically relevant host plants

poses a major challenge. For instance, grapevine trunk diseases (GTDs) are a representative example of the difficulties faced by wine-growers to control these pathogens using conventional pesticide applications [1]. Once a plant is infected, the pathogens segregate lignin-degrading enzymes (e.g., laccases and peroxidases) [2], which lead to trunk wood decay and withering of the plant. The pathogens' location inside the grapevine trunk hampers a facile application of antifungal treatments, such as conventional spraying [3]. To date, commercially available treatments are based on preventive measures, including permanent disinfection of pruning tools, protection of wounds on the vine, and repetitive preventive spraying of fungicides in high doses [1]. For progressed infections, the entire grapevine generally needs to be replaced [4] and, to prevent further spreading, removal and burning of the infected materials are essential.

Many of the synthetic agrochemicals traditionally employed to control these diseases (e.g., sodium arsenite) have been banned or public pressure has increased to reduce their use. The lack of effective curative treatments against GTDs has become a big threat to the European wine industry, causing an estimated financial loss of USD 1.5 B/year [5]. Therefore, the implementation of integrated pest management (IPM) methods has become a priority, either through the search for biocontrol agents (BCAs) or with the application of substances of natural origin [6], which need to be vehiculated into the plant's xylem.

The work presented herein focuses on the synthesis of biodegradable nanocarriers (NCs), based on methacrylated lignin (ML) and chitosan oligomers (COS), aimed at the targeted delivery of biologically active compounds (including hydrophobic ones). By incorporating lignin in their composition, the NCs can respond to external stimuli (viz. to the lignocellulolytic enzymes secreted by bacteria and fungi associated with wood diseases) at the sites of infection, triggering a controlled release of the therapeutic agents.

It is worth noting that lignin has been previously investigated as a renewable, abundant, and inexpensive feedstock to develop sophisticated nanostructures [7–9]. Lignin-derived compounds are useful as biodegradable building blocks for nanomaterials, and, in the past few years, some studies have presented lignin-based NCs [10]. Other bibliographic precedents include the work by Pathania et al. [11] on the preparation of a chitosan-g-poly(acrylamide) nanocomposites by a simple method in the presence of microwaves; the study by Beckers et al. [12] on the synthesis of xylan NCs employing toluene diisocyanate as a cross-linking agent (in which NCs were loaded with a synthetic fungicide); the investigations by Ciftci et al. [13] on the synthesis of chitosan microcapsules containing glycidyl methacrylate terpolymer, maleic anhydride, and *N*-*tert*-butylacrylamide, and some other articles on the formation of lignin–chitosan films [14,15]. However, to the best of the authors' knowledge, there are no reports on the insertion of chitosan oligomers between lignins (Aradmehr and Javanbakht [16] described lignin–chitosan biocomposites, but the existence of covalent interactions between the groups was not evidenced).

Concerning the bioactive products encapsulated in the NCs, other works have used conventional fungicides of chemical origin such as azoxystrobin, pyraclostrobin, tebuconazole, or boscalid [9,17], or BCAs, such as *Trichoderma reesei* E.G. Simmons [18]. As an alternative, this work proposes the use of plant extracts for which inhibitory concentrations below 1000 ppm against *Botryosphaeriaceae* species have been previously reported by our group, such as *Rubia tinctorum* L., *Silybum marianum* (L.) Gaertn., *Urtica dioica* L., or *Equisetum arvense* L. [19–21], and which have proven effective for pruning wound protection applications. These products of natural origin would be suitable for use in organic or conventional agriculture (in fact, the latter two are 'basic substances' under the EU plant protection products regulation, Article 23 of (EC) No 1107/2009).

As regards the phytopathogens chosen to test the efficacy of the NCs under study, *Neofusicoccum parvum* (Pennycook & Samuels) Crous, Slippers & A.J.L. Phillips is responsible for grapevine symptoms, such as leaf spots, fruit rots, shoot dieback, bud necrosis, vascular discoloration of the wood, and perennial cankers, and is considered one of the most aggressive species of the *Botryosphaeriaceae* family [22], which is why it was selected for the initial screening. Another member of the same group, *Diplodia seriata* De Not., was

also tested, given that it is considered a primary and virulent pathogen of grapevines [23], but it also causes frog-eye leaf spot, black rot, and canker of apples [24,25]. To determine the potential antibacterial activity, *Xylophilus ampelinus* Willems et al. (syn. *Xanthomonas ampelina* and *Erwinia vitivora*) [26] and *Pseudomonas syringae* pv. *syringae* van Hall were selected. The former is the causal agent of bacterial necrosis of grapevines (the so-called “maladie d’Oléron” in France and “mal nero” in Italy), which severely affects grape crops, resulting in harvest losses as high as 70% of typical yield [23], and is categorized as a quarantine A2 organism by the European and Mediterranean Plant Protection Organization (EPPO). The latter is a Gammaproteobacterium distributed worldwide, which is responsible for bacterial canker on over a hundred different hosts, including the grapevine (in which it induces necrotic lesions in the leaf blades, veins, petioles, shoots, rachis, and tendrils) [27].

In this work, we show the versatility of the ML–COS platform for the encapsulation of natural products with antimicrobial properties to treat GTDs and other plant diseases associated with lignin-decomposing microorganisms. The efficacy of the ML–COS NCs is first demonstrated in vitro against the four aforementioned phytopathogens, and the treatments are then assayed in *Vitis vinifera* plants by injection, resulting in a reduction in GTDs leaf symptoms. This strategy for drug delivery may help to optimize fungicide application and efficacy.

2. Materials and Methods

2.1. Plant Material and Reagents

The specimens of *Rubia tinctorum* and *S. marianum* under study were collected on the banks of the Carrión River as it passes through the town of Palencia (Spain). The roots of *R. tinctorum* were shade-dried and pulverized to a fine powder in a mechanical grinder. Samples from different specimens ($n = 25$) were thoroughly mixed to obtain composite samples. In the case of *S. marianum*, the capitula were collected during stage 67 (or 6N7) according to the extended BBCH scale, in which silybins precursors should not have yet been consumed, as discussed in previous work [21]. The capitula were shade-dried and pulverized to a fine powder in a mechanical grinder. Again, different specimens ($n = 25$) were thoroughly mixed to obtain a composite sample. For the preparation of *E. arvense* and *U. dioica* extracts, dried plants certified by the European Pharmacopoeia were purchased from El Antiguo Herbolario (Alicante, Spain).

Chitosan (CAS 9012-76-4; high molecular weight: 310,000–375,000 Da) was supplied by Hangzhou Simit Chem. & Tech. Co. (Hangzhou, China). Neutrase™ 0.8 L enzyme was supplied by Novozymes A/S (Bagsværd, Denmark). Potato dextrose agar (PDA) was supplied by Becton Dickinson (Bergen County, NJ, USA). DMF (Dimethylformamide, CAS 68-12-2), isopropyl alcohol (CAS 67-63-0), alkali lignin (CAS 8068-05-1), lithium chloride (CAS 7447-41-8), methacrylic anhydride (CAS 760-93-0), methanol (UHPLC, suitable for mass spectrometry, CAS 67-56-1), triethylamine (CAS 121-44-8), TSA (tryptic soy agar, CAS 91079-40-2), and TSB (tryptic soy broth, CAS 8013-01-2) were acquired from Sigma-Aldrich Química (Madrid, Spain).

2.2. Fungal and Bacterial Isolates

The two fungal isolates under study, *Neofusicoccum parvum* (code ITACYL_F111, isolate Y-091-03-01c) and *Diplodia seriata* (code ITACYL_F098, isolate Y-084-01-01a) were isolated from diseased grapevine plants of the cultivar ‘Tempranillo’ from D.O. Toro (Spain) and supplied as lyophilized vials (later reconstituted and refreshed as PDA subcultures) by the Instituto Tecnológico Agrario de Castilla y León (ITACYL, Valladolid, Spain).

Regarding the two bacterial isolates, *Xylophilus ampelinus* was acquired by the Spanish Type Culture Collection (CECT), with CCUG 21,976 strain designation, and *Pseudomonas syringae* pv. *syringae* was supplied by Aldearrubia Regional Diagnosis Center (Junta de Castilla y León, Spain).

2.3. Preparation of Plant Extracts

Extracts of *R. tinctorum* and *S. marianum* were obtained in a methanol:water mixture (1:1 *v/v*) according to the previously reported procedure [20,21]. In short, the dried samples were mixed with the hydromethanolic medium in a 1:20 (*w/v*) ratio and heated in a water bath at 50 °C for 30 min, followed by 5 min of sonication. The solutions were centrifuged at 9000 rpm for 15 min and the supernatants were filtered through Whatman No. 1 filter paper.

To obtain the *E. arvense* and *U. dioica* extracts, the procedures established in the European regulations (SANCO/12386/2013 and SANTE/11809/2016, respectively) were followed. In brief, in the case of horsetail extract, 200 g of the dried plant were macerated in 10 L of water for 30 min (soaking) and then boiled for 45 min. After cooling, the decoction was filtered and diluted by a factor of 10 with water to obtain a final concentration of 2 mg·mL⁻¹. For the nettle extract, dried nettle leaves (15 g·L⁻¹) were macerated for 3–4 days at 20 °C, followed by filtering and dilution of the filtrate to obtain a final concentration of 2 mg·mL⁻¹ [19].

The bioactive constituents present in each of the extracts, characterized by gas chromatography-mass spectroscopy (GC-MS), have been reported in previous works [19–21].

2.4. Procedure for the Synthesis of the Biodegradable Nanocarriers

Methacrylated lignin (ML) was first synthesized following the protocol reported by Fischer et al. [9] with slight modifications. The methacrylation of lignin was performed by the addition of methacrylic anhydride, which modifies the hydroxyl groups of lignin to make them available for the encapsulation of bioactive compounds. In short, 2.6 g LiCl was dissolved in 60 mL DMF, alternating periods of stirring and sonication until complete dissolution. Next, 2 g of Kraft lignin (total hydroxyl group content: 6.2 mmol·g⁻¹ determined by ³¹P NMR) was added, the mixture was stirred and sonicated until complete dissolution, under Ar atmosphere at 90 °C. The sample was cooled to 40–50 °C, and 1 mL of triethylamine (10 mmol) was added, then the mixture was stirred for 10 min. Subsequently, 3 mL of methacrylic anhydride (20 mmol) was added dropwise. The mixture was stirred at 60 °C for 6 h. The mixture was precipitated into a large excess of isopropyl alcohol and isolated by centrifugation, and the precipitation extraction procedure was repeated two more times. The product was dried at room temperature in a vacuum oven.

Chitosan oligomers (COS) were prepared according to the procedure described in the work by Santos-Moriano et al. [28], with the modifications indicated in [29]. Commercial chitosan ($M_W = 310\text{--}375$ kDa) was dissolved in aqueous 1% (*w/w*) acetic acid, and, after filtration, the filtrate was neutralized with aqueous 4% (*w/w*) NaOH. The precipitate was collected and washed thoroughly with hot distilled water, ethanol, and acetone. The purified chitosan was obtained by drying. The degree of deacetylation (DD) was determined to be 90% according to Sannan et al. [30]. A total of 20 g of purified chitosan were dissolved in 1000 mL of Milli-Q water by adding 20 g de citric acid under constant stirring at 60 °C. Once dissolved, the commercial proteolytic preparation Neutrase 0.8 L (a protease from *Bacillus amyloliquefaciens*) was added to obtain a product enriched in deacetylated chitoooligosaccharides and to degrade the polymer chains. The mixture was sonicated for 3 min in 1 min of sonication/1 min without sonication cycles to keep the temperature in the 30–60 °C range. The molar mass of the COS samples was determined by measuring the viscosity, in agreement with Yang et al. [31] in a solvent of 0.20 mol·L⁻¹ NaCl + 0.1 mol·L⁻¹ CH₃COOH at 25 °C using an Ubbelohde capillary viscometer. Molar mass was determined using the Mark–Houwink equation $[\eta] = 1.81 \times 10^{-3} M^{0.93}$ [32]. At the end of the process, a solution with a pH in the four to six interval with oligomers of molecular weight < 2 kDa was obtained, with a polydispersity index of 1.6, within the usual range reported in the literature [33].

The formation of the new nanocarriers loaded with bioactive plant extracts was conducted in two steps: (i) reaction of the amine of the chitosan oligomer with the methyl group of the methacrylated lignin, leading to the formation of an inclusion complex via the Aza-Michael reaction; (ii) interaction of the free hydroxyl groups of the COS with at

least one functional group of the constituents of the bioactive plant extracts, forming weak hydrogen bonds or ionic bonds. In short, 500 mg of ML (2.75 mmol methacrylic groups) were added to an aqueous solution of 250 mg (ca. 1.375 mmol NH_2 groups, considering a degree of deacetylation of 90%) of COS to cross-link it (i.e., 2:1 ML: COS stoichiometric ratio, chosen after testing different ratios), and then 50 mL of aqueous or methanol:water (1:1 *v/v*) plant extract were added. The mixture was emulsified by sonication at 20 kHz, in periods of 2 min each, and for a total time of 20 min, avoiding letting the temperature exceed 50 °C. The resulting emulsion was stirred for 12 h at 40 °C. Then, the final volume was adjusted to 50 mL, obtaining a concentration of the encapsulated bioactive compound of 2 $\text{mg}\cdot\text{mL}^{-1}$.

Samples were purified by centrifugation at 10,000 rpm for 30 min. Next, the supernatant was frozen for 24 h and subsequently freeze-dried for study by attenuated total reflection Fourier-transform infrared spectroscopy (ATR-FTIR), thermal analysis, and transmission electron microscopy (TEM). Nanocarriers without active products were also freeze-dried for reference purposes.

An almost complete (over 95%) encapsulation efficiency was obtained for the four bioactive plant extracts tested. This encapsulation efficiency was determined using an indirect method, as in the work by Fischer et al. [9]. The sample was centrifuged at 10,000 rpm for 60 min and the supernatant containing the non-encapsulated plant extract was freeze-dried. The plant extract left was then dissolved in methanol:water (1:1, *v/v*), passed through a 0.2 μm filter and analyzed by high-pressure liquid chromatography (HPLC) with an Agilent 1200 series HPLC system (Agilent Technologies, Santa Clara, CA, USA) using methanol-5% acetic acid (pH 3) (70~30) as the mobile phase [34]. The injection volume was 10 μL and the column temperature was maintained at 20 °C. The analysis was conducted at a flow rate of 0.2 $\text{mL}\cdot\text{min}^{-1}$ with the G1315D detector operated at 250 nm. The encapsulation efficiency (EE) was determined according to the following equation:

$$EE(\%) = \frac{m(\text{bioactive product initial}) - m(\text{bioactive product supernatant})}{m(\text{bioactive product initial})} \times 100$$

2.5. Characterization of the Nanocarriers

To confirm the cross-linkage between ML and COS, ATR-FTIR was used. Infrared vibrational spectra were recorded using a Thermo Scientific (Waltham, MA, USA) Nicolet iS50 FTIR spectrometer equipped with an integrated diamond ATR system. The spectra were registered with a spectral resolution of 1 cm^{-1} in the range 400–4000 cm^{-1} , taking the interferograms that resulted from the co-addition of 64 scans. The spectra were then corrected using the advanced ATR correction algorithm available in the OMNIC™ software suite.

Thermal gravimetry (TGA) and differential scanning calorimetry (DSC) analyses were carried out using a simultaneous TG-DSC2 (Mettler Toledo; Columbus, OH, USA), in 'atmosphere of synthetic air' ($\text{N}_2:\text{O}_2$ in 4:1 ratio), with a heating ramp of 20 °C·min⁻¹. It should be clarified that the choice of the atmosphere would only influence the activation energy values [35].

Additional characterization of the NCs was carried out by dynamic light scattering (DLS), zeta potential (ZP), and transmission electron microscopy (TEM) at the Laboratory of Instrumental Techniques (LTI) of Universidad de Valladolid. The nanoparticle size distribution was evaluated by DLS using a Zetasizer Advance Pro Red Label apparatus (Malvern Panalytical Ltd., Malvern, UK), with a laser wavelength of 633 nm (He-Ne, 10 mW) and a 175° scattering angle. The zeta potential of nanoparticles was measured on a zeta potential analyzer (Brookhaven, GA, USA). For zeta potential measurements, samples were diluted with 0.1 mM KCl and measured in the automatic mode. DLS and ZP measurements were conducted in triplicate. TEM characterization was conducted using a JEOL (Akishima, Tokyo, Japan) JEM 1011 microscope. Operative conditions: 100 kV; 25,000–120,000× magnification. Micrographs have been obtained with a GATAN ES100W CCD camera (4000 × 2672 pixels).

2.6. In Vitro Antimicrobial Activity Assessment

The antifungal activity of the different treatments was determined by the agar dilution method according to the EUCAST antifungal susceptibility testing standard procedures [36], by incorporating aliquots of NCs, either empty or loaded with the different plant extracts, into PDA medium to obtain concentrations in the 6.25–150 $\mu\text{g}\cdot\text{mL}^{-1}$ range. Fungal mycelial plugs ($\phi = 5$ mm) from the margins of 1-week-old *N. parvum* and *D. seriata* colonies were transferred onto plates that incorporated the above concentrations for each treatment (3 plates per treatment/concentration, with 2 replicates each). Plates were then incubated at 25 °C in the dark for 1 week. PDA medium without any modification was used as a control. Mycelial growth inhibition was estimated according to the formula $(d_c - d_t)/d_c \times 100$, where d_c and d_t represent the mean diameters of the control and treated fungal colony, respectively. The effective concentrations at which mycelial growth was inhibited by 50 and 90% (EC₅₀ and EC₉₀, respectively) were estimated using PROBIT analysis in IBM SPSS Statistics v.25 software (IBM; Armonk, NY, USA).

The antibacterial activity was assessed according to CLSI standard M07–11 [37], using the agar dilution method to determine the minimum inhibitory concentration (MIC). In short, an isolated colony of *X. ampelinus* in a TSB liquid medium was incubated at 26 °C for 24 h. Serial dilutions were then conducted, starting from a 10^8 CFU·mL⁻¹ concentration, to obtain a final inoculum of $\sim 10^4$ CFU·mL⁻¹. Bacterial suspensions were then delivered to the surface of TSA plates, to which the treatments had previously been added at concentrations ranging from 6.25 to 150 $\mu\text{g}\cdot\text{mL}^{-1}$. Plates were incubated at 26 °C for 24 h. Readings were taken after 24 h. In the case of *P. syringae* pv. *syringae*, the same procedure was followed, albeit at 25 °C for 48 h. MICs were visually determined in the agar dilutions as the lowest concentrations of the bioactive products at which no bacterial growth was visible. All experiments were run in triplicate, with 3 plates per treatment/concentration.

2.7. In Planta Application of ML–COS NCs-Based Treatments

Bioassays with the ML–COS NCs treatment that showed the best performance at lab scale (viz. NCs loaded with *R. tinctorum* extract) were performed by injection (via endotherapy) in vines with clear symptoms of GTDs. A total of 20 grapevines of cultivar ‘Cabernet sauvignon’ grafted on SO4 rootstock, planted in 2000 on the ‘Clau’ estate of the Viñas del Vero winery (Somontano Designation of Origin Barbastro, Huesca, Spain) were used for the tests. Only plants in which both arms were clearly affected by GTDs (verified in previous years by the winery) were selected for this study (Figure 1).

In addition to the information provided by the winery, the phytosanitary status of the plot subjected to treatment was analyzed through the isolation and characterization of fungal pathogens associated with plants that showed the aforementioned symptoms compatible with the existence of GTDs, especially at the level of rot and decay of lignified tissues in arms. Briefly, these materials were fragmented, surface-sterilized (employing 70% ethanol, 5% commercial sodium hypochlorite, and sterile double distilled water), and incubated in Petri dishes containing PDA as nutritive medium and streptomycin sulfate to prevent bacterial contamination at 26 °C in the dark for 3–5 days. After this, the different emerging colonies were transferred to PDA plates as pure colonies and characterized both at the morphological level (through the microscope study of their morphological characters in culture) and by using molecular methods (through the obtaining and subsequent comparison of their ribosomal ITS sequences).



Figure 1. Upper row: examples of grapevine trunk diseases wood symptoms in the plants used for the in vivo study; lower row: inoculation point with a plug installed and injection of the treatment.

The treatment was injected into one of the arms (randomly chosen) of each symptomatic and diseased vine, using the other arm as a control. The arm site selected for the injection was first sprayed with 5% sodium hypochlorite to sterilize the wood surface. Subsequently, a 20 mm deep hole was drilled, in which a plug with a non-return valve was installed (Figure 1). The drill bit was sterilized with 70% ethanol before drilling the next plant. The injection system (ENDOkit Manual™, developed by ENDOTerapia Vegetal, Gerona, Spain) was then loaded with 5 mL of the corresponding nanocarrier ML-COS-*R. tinctorum* solution. It was not necessary to seal the wound with wax to avoid contamination due to the type of plug (ENDOplug™) used in the selected endotherapy system. The second injection application of the treatment was carried out a month later using the same injection site, so the same plug could be used (given that it had not been clogged with scar tissue yet). The monitoring of the plants lasted for 5 months.

Measurements of fast chlorophyll fluorescence induction kinetics were carried out using a continuous excitation chlorophyll fluorimeter (model Handy PEA+, Hansatech Instruments, Pentney, Norfolk, UK), on a bimonthly basis throughout the vegetative period (from late May till the beginning of September). Five measurements were taken on each arm of the twenty plants under study, to investigate subtle differences in the fluorescence signature of samples, which could be indicative of stress factors affecting the photosynthetic efficiency of the plant. The ratio of the variable fluorescence (F_v) over the maximum fluorescence value (F_m) was chosen as an indicator of the maximum quantum efficiency of Photosystem II, being a sensitive indication of plant photosynthetic performance. Presented as a ratio between 0 and 1, healthy samples typically achieve a maximum F_v/F_m value of approx. 0.85, while lower values suggest that the plant has been exposed to some type of biotic or abiotic stress factor. Leaf chlorophyll status was also monitored bimonthly throughout the entire vegetative period (May–September). A SPAD-502 m (Minolta, Osaka, Japan) was used. Five values were collected for each arm.

Upon grape harvest, the productivity of the treated and control arms was compared by recording both the number of bunches per arm and their fresh weight, provided that the pruning criterion was homogeneous in all the grapevines under study and that no cluster thinning was conducted. The approximate sugar content of the obtained grape

juice—a parameter used by the winery to determine the optimum time for harvesting—was analyzed using a PCE-032 refractometer (PCE Ibérica SL, Albacete, Spain) in order to investigate possible differences in the phenological state, relating berry maturity to the presence of disease in the arm that supported them.

2.8. Statistical Analysis

The results of in vitro mycelial growth inhibition were statistically analyzed by analysis of variance (ANOVA), followed by a post hoc comparison of means by Tukey's test (because the requirements of homogeneity and homoscedasticity were met, according to the Shapiro–Wilk and Levene tests). For the results of the field tests, non-parametric analyses were carried out with the Kruskal–Wallis test, accompanied by the comparison of pairs with the Dunn and Conover–Iman methods, applying the Bonferroni correction.

3. Results

3.1. Characterization by ATR-FTIR

Methacrylated lignin presents a weak band at 1397 cm^{-1} , which increased and split into two bands after the formation of the ML–COS NCs, with peaks at 1417 and 1396 cm^{-1} (Figure S1). With regard to the chitosan oligomers, they present two bands at 1062 and 1031 cm^{-1} that drastically decreased with the formation of the ML–COS NCs (with a concurrent shift towards 1107 and 1037 cm^{-1}). This corresponds to a decrease in the C=C bands of the vinyl groups due to their consumption during the Aza–Michael cross-linking polymerization, which was accompanied by the appearance of -NH bands at 1570 cm^{-1} [17]. Further, the increase in the vibrations of the ester bond at 1652 cm^{-1} (-C=O) and of the hydroxyl group (-OH) at 3377 cm^{-1} point to successful incorporation of COS into methacrylic groups of lignin.

On the other hand, in the spectra corresponding to ML–COS NCs loaded with *R. tinctorum* extracts (Figure S2) it was observed how the weak -NH band of the *R. tinctorum* extract at 1591 cm^{-1} overlapped with the 1570 cm^{-1} NH band of the ML–COS NCs to give rise to a very intense band at 1571 cm^{-1} .

3.2. Characterization by Thermal Analysis

The TGA curves for the ML–COS NCs (without encapsulated extracts), with a basic ML–COS–ML structure, showed high stability: below 200 °C a weight loss of 9% occurred and, from this temperature up to 750 °C , an additional 7% weight loss was registered. The maximum decomposition took place at 350 °C and was sensitized by the presence of an exotherm (Figure S3). The ML–COS–ML NC was, therefore, more stable than the lignin–diamine–lignin analogs reported to date [9,17]: the curves of ML–diamine–ML type NCs, presented in Figure S4, show that they experience weight losses of up to 37% at 350 °C due to lignin degradation (sensitized by an exotherm at 260 °C).

The curves for ML–COS NCs loaded with *R. tinctorum*, showed, upon heating up to 500 °C , three successive stages of decomposition with associated weight losses of 12, 30, and 10%, respectively. At higher temperatures, an exotherm was observed at 510 °C and, at the end of the process (at 750 °C), a 28% weight loss, in addition to the previous ones, was recorded (Figure S5). This thermal behavior was thus very different from that of the empty NCs and should be referred, fundamentally, to the presence of the *R. tinctorum* components inside the ML–COS–ML encapsulation.

3.3. Characterization by Transmission Electron Microscopy, Dynamic Light Scattering, and Zeta Potential

Figure 2 shows TEM micrographs of the nanocarriers. The addition of the plant extracts to the miniemulsion did not result in a significant change of the NCs size, compared to empty NCs, a result consistent with those reported by Fischer et al. [9].

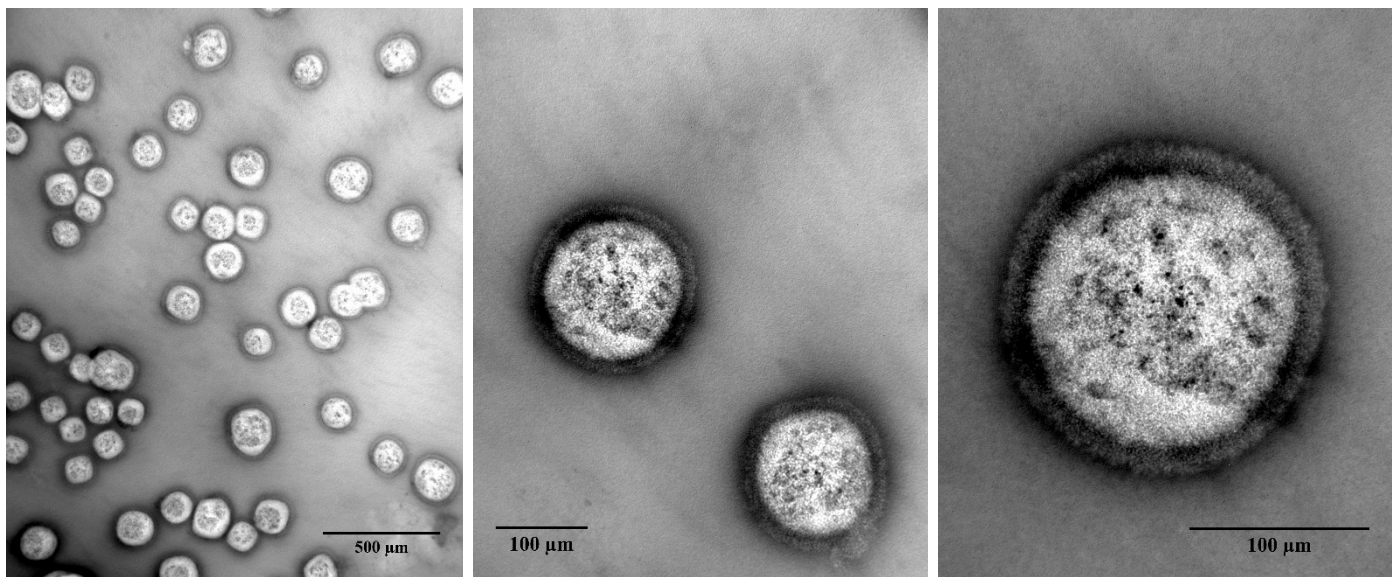


Figure 2. Transmission electron microscopy (TEM) images showing the ML-COS NCs loaded with *R. tinctorum* extract at different magnifications.

The average particle size ($D_p = 185$ nm; PDI = 0.35), determined by DLS, was on the lower end of the range reported by Machado et al. [17] (165–300 nm) and slightly smaller than those reported by Fischer et al. [9] (213–510 nm) for lignin NCs. The number distribution of ML-COS-*R. tinctorum* NCs showed that 99% of particles had sizes lesser than 200 nm, which included: 162.9 nm (19.29%), 185.7 nm (57.7%), and 209.1 nm (22.3%). The obtained PDI value, below 0.5, indicates that particles were monodispersed in nature, and suggests uniformity and stability of particles in suspension, according to Choudhary et al. [38].

Regarding the zeta potential, a +42 mV value was obtained, in the usual range for chitosan nanomaterials (+22 to +88 mV) [39] and above the 20 mV threshold required for colloidal stability [40].

3.4. In Vitro Antimicrobial Activity

3.4.1. Antifungal Activity

The visual results of the mycelial growth inhibition tests of *N. parvum* and *D. seriata* are shown in Figure S6.

Inhibition of *N. parvum* mycelial growth (Figure 3) was achieved at concentrations as low as 75 and 100 $\mu\text{g}\cdot\text{mL}^{-1}$ for the NCs loaded with the extracts of *R. tinctorum* and *S. marianum*, respectively, while the minimum inhibitory concentrations (MICs) for the encapsulated *E. arvense* and *U. dioica* extracts were higher (150 $\mu\text{g}\cdot\text{mL}^{-1}$ in both cases).

Due to the good results obtained with the NCs loaded with the *R. tinctorum* extract, these were further tested against another fungal pathogen of the *Botryosphaeriaceae* family, viz. *D. seriata* (Figure 4). In its case, the NCs loaded with *R. tinctorum* inhibited mycelial growth at a concentration of 100 $\mu\text{g}\cdot\text{mL}^{-1}$.

Regarding effective concentrations, Table 1 summarizes the EC_{50} and EC_{90} values obtained against *N. parvum* for NCs, either empty or loaded with the different bioactive compounds, together with the results obtained with unencapsulated extracts (for comparison purposes). A clear improvement in terms of activity was observed in all cases, with EC_{50} and EC_{90} as low as 41.2 and 65.8 $\mu\text{g}\cdot\text{mL}^{-1}$, respectively, for the NCs loaded with *R. tinctorum* extract.

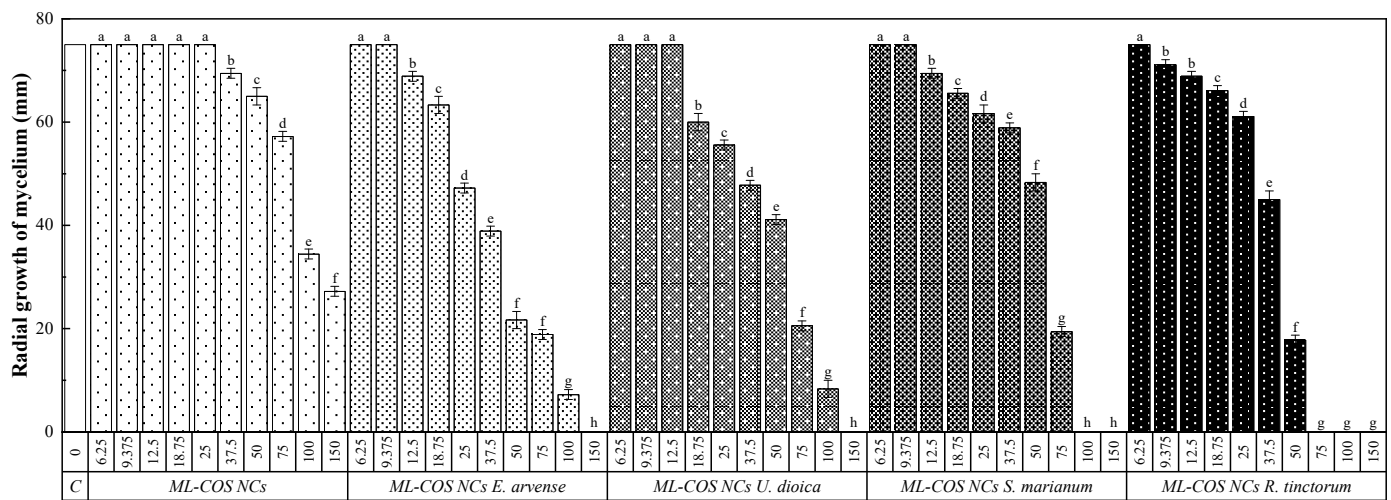


Figure 3. Diameter of *N. parvum* radial mycelial growth upon treatment with ML-COS NCs, either empty or loaded with four plant extracts at different concentrations (6.25; 9.375; 12.5; 18.75; 25; 37.5; 50; 75; 100; 150 $\mu\text{g}\cdot\text{mL}^{-1}$). Same letters above concentrations mean not significantly different at $p < 0.05$. Error bars represent standard deviations.

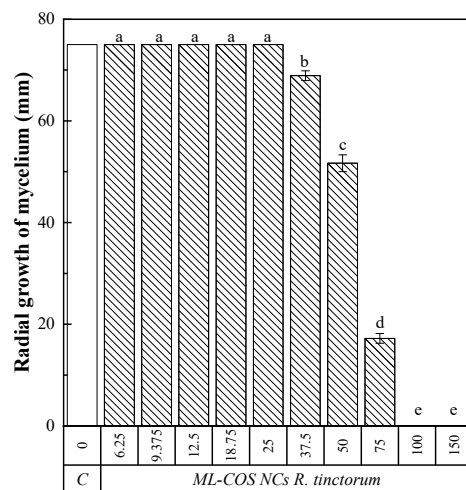


Figure 4. Diameter of *D. seriata* radial mycelial growth upon treatment with ML-COS NCs loaded with *R. tinctorum* extract at different concentrations (6.25; 9.375; 12.5; 18.75; 25; 37.5; 50; 75; 100; 150 $\mu\text{g}\cdot\text{mL}^{-1}$). Same letters above concentrations mean not significantly different at $p < 0.05$. Error bars represent standard deviations.

Table 1. EC₅₀ and EC₉₀ concentrations against *N. parvum* of the ML-COS NCs, with or without encapsulated bioactive products, expressed in $\mu\text{g}\cdot\text{L}^{-1}$. Effective concentrations of the non-encapsulated products are provided for comparison purposes.

Effective Concentration	ML-COS	NC-Based Treatments				COS	Non-Encapsulated Products [19–21]			
		ML-COS- <i>E. arvense</i>	ML-COS- <i>U. dioica</i>	ML-COS- <i>S. marianum</i>	ML-COS- <i>R. tinctorum</i>		<i>E. arvense</i>	<i>U. dioica</i>	<i>S. marianum</i>	<i>R. tinctorum</i>
EC ₅₀	82.7	66.5	50.2	60.9	41.2	680.2	*	*	557	92.3
EC ₉₀	243.2	105.2	113.0	90.6	65.8	1326.6	*	*	2938	184.0

* No inhibition of mycelial growth was observed at 1500 $\mu\text{g}\cdot\text{mL}^{-1}$, the highest concentration tested.

Regarding the EC₅₀ and EC₉₀ values obtained against *D. seriata* (Table 2), the *R. tinctorum* extract encapsulated in the NCs presented a lower EC₅₀ than that of the non-encapsulated extract, although the EC₉₀ value was similar in both cases.

Table 2. EC₅₀ and EC₉₀ concentrations against *D. seriata* of the ML–COS NCs loaded with *R. tinctorum* extract and of the non-encapsulated extract, expressed in $\mu\text{g}\cdot\text{L}^{-1}$.

Effective Concentration	Encapsulated Product ML–COS– <i>R. tinctorum</i>	Non-Encapsulated Product <i>R. tinctorum</i>
EC ₅₀	59.3	78.0
EC ₉₀	91.0	87.8

3.4.2. Antibacterial Activity

The efficacy of the most effective treatment in the antifungal in vitro tests, ML–COS–*R. tinctorum*, was assayed against two phytopathogenic bacteria, *P. syringae* pv. *syringae* and *X. ampelinus*, to investigate if these biodegradable NCs could have a wider spectrum of action against other microorganisms, not only restricted to eukaryotic plant pathogens. The inhibition attained against the two bacteria with the NCs loaded with *R. tinctorum* extract were similar, with a MIC value of $37.5 \mu\text{g}\cdot\text{mL}^{-1}$ (Table 3).

Table 3. Antibacterial activity of ML–COS–*R. tinctorum* treatment against the two phytopathogenic bacteria under study at different concentrations (expressed in $\mu\text{g}\cdot\text{mL}^{-1}$).

Pathogen	Concentration									
	6.25	9.75	12.5	18.75	25	37.5	50	75	100	150
<i>P. syringae</i> pv. <i>syringae</i>	+	+	+	+	+	–	–	–	–	–
<i>X. ampelinus</i>	+	+	+	+	+	–	–	–	–	–

“+” and “–” indicate the presence and absence of bacterial growth, respectively.

3.5. In Planta Application of ML–COS NCs Loaded with *R. tinctorum* Extract Treatment

After the morphological and molecular characterization of the isolates obtained from samples from symptomatic plants of the treated plot, the majority presence of species associated with GTDs such as the lignicolous basidiomycete species *Fomitiporia mediterranea* M. Fisch. or, with a greater frequency of appearance, certain *Botryosphaeriaceae* species such as *Diplodia seriata* or *Neofusicoccum parvum*, was verified.

When GTDs-associated foliar symptoms were monitored, most of the treated arms showed less interveinal chlorosis and necrosis than their respective control arms (Figure 5). Nonetheless, given that foliar symptoms associated with GTDs do not necessarily appear on the same diseased plant every year, other approaches were used to estimate the preliminary efficacy of the treatment.



Figure 5. Examples of decrease in foliar GTD symptoms in treated vs. non-treated grapevine arms.

Concerning SPAD and fluorometry measurements, always conducted on healthy leaves (not on leaves with chlorosis or necrosis symptoms), no statistically significant differences were detected between the treated and control arms, ruling out relevant phytotoxic effects of the treatment performed.

With regard to the yield measurements, significant differences (p -value = 0.047) were found in the number of clusters, with 39 ± 11.4 and 24.6 ± 9.1 clusters/arm in the treated vs. non-treated arms, respectively. This difference in the number of clusters did not lead to significant differences in the yield per arm (p -value = 0.117), although it was noticeably higher in the treated arms than in the control ones (3177 ± 1259 vs. 1932 ± 556 g/arm, respectively).

In relation to the probable sugar content of the grape juice, it was shown to be similar in both treated and control arms (22.0 ± 1.8 vs. 21.2 ± 1.6 °Bx), discarding differences in berry maturity.

4. Discussion

4.1. Comparison with Other NCs-Based Treatments

A summary of other research works reported in the literature in which NCs have been used to control diseases associated with wood-degrading fungi is presented in Table 4.

Table 4. Summary of NCs-based treatments reported in the literature against wood-degrading fungi.

Composition	Pathogen	Assays	Ref.
Kraft cationic lignin NCs loaded with <i>Trichoderma reesei</i> spores	Fungi associated with GTDs (esca)	Dual in vitro culture against <i>Phaeoconiella chlamydospora</i> and <i>Phaeoacremonium minimum</i> + in vitro NC degradation assays with culture filtrate of the two esca pathogens	[18]
Methacrylated Kraft lignin NCs loaded with pyraclostrobin	Fungi associated with GTDs (esca)	Field study with trunk injections in <i>V. vinifera</i> plants	[9]
Methacrylated Kraft lignin NCs loaded with different synthetic fungicides (pyraclostrobin, azoxystrobin, tebuconazole, boscalid)	Ligninase-producing microorganisms	In vitro antifungal activity against <i>P. chlamydospora</i> , <i>Neonectria ditissima</i> , <i>Phytophthora infestans</i> , <i>Magnaporthe oryzae</i> , <i>Botrytis cinerea</i> , <i>N. parvum</i> + in planta study through trunk injections in <i>V. vinifera</i> plants	[17]
Pyraclostrobin-loaded xylan NCs	Xylanase-producing fungi in viticulture and horticulture	In vitro assays against <i>Pyricularia oryzae</i> , <i>B. cinerea</i> , <i>P. chlamydospora</i> , <i>P. minimum</i> , and <i>N. ditissima</i>	[12]
Cellulose modified with undec-10-enoic acid NCs loaded with pyraclostrobin and captan	Cellulase segregating fungi in viticulture and apple trees	In vitro assays against <i>P. chlamydospora</i> , <i>N. ditissima</i> , <i>P. infestans</i> , <i>M. oryzae</i> , <i>B. cinerea</i> , and <i>N. parvum</i>	[41]

From a chemical perspective, the main difference between the NCs presented in this work and those based on lignin reported by other authors (e.g., the NCs protected by patent WO 2017/134308 A1 [42], tested in [9,17]) is that the latter are based on ML–diamine–ML networks (while the NCs reported herein are based on ML–COS–ML networks). In ML–diamine–ML networks, the space generated for the accommodation of the active compounds is of discrete dimensions and may not allow to stably accommodate large molecules, apart from the fact that the addition of the bioactive compounds would take place in a hydrophobic medium, which conditions bioavailability. Thus, the use of COS instead of diamines should facilitate the entry and encapsulation of large bioactive compounds such as flavonoids, di- and triterpenes, given that COS presents a large number of functional groups, such as hydroxyl and amino, and is considered a polycation with a high density of positive charges ideal for interacting with bioactive compounds. Hence, the formation of inclusion compounds between the ML–COS–ML shell and the encapsulated natural products shall not be excluded. Further, the NCs should also function more effectively as an antimicrobial upon the incorporation of chitosan, due to its non-specific mechanism of pathogen suppression (COS permeabilizes fungal plasma membranes and alters their gene expression), although it can be anticipated that the methacrylated COS used in the NCs will not have the same activity as free COS.

With regard to the efficacy of the treatments, the susceptibility profile is usually considered isolate-dependent, so comparisons of the effective concentrations below should be taken with caution. For instance, Machado et al. [17] reported MIC values against *N. parvum* of 5 and $>50 \mu\text{g}\cdot\text{mL}^{-1}$ for lignin NCs cross-linked with 2,2'-(ethylenedioxy)bis(ethylamine) (EDBEA) loaded with 30 wt% azoxystrobin or pyraclostrobin, and with boscalid or tebuconazole, respectively, similar to those attained for bulk fungicide formulations. For *P. chlamydospora*, MICs of $5 \mu\text{g}\cdot\text{mL}^{-1}$ were found in all cases. Comparable MICs $< 10 \mu\text{g}\cdot\text{mL}^{-1}$

against *P. chlamydospora* and *Phaeoacremonium aleophilum* were also reported by the same group for pyraclostrobin xylan-based nanocarriers [12]. When cellulose-based NCs loaded with pyraclostrobin (20–30 wt%) and captan (20–30 wt%) were used instead, MICs of 5 and $>50 \mu\text{g}\cdot\text{mL}^{-1}$ were obtained, respectively [41]. Hence, taking into consideration that the EC₉₀ value reported herein for the ML–COS NCs loaded with *R. tinctorum* extract against *N. parvum* was $65.8 \mu\text{g}\cdot\text{mL}^{-1}$, the efficacy would be worse than that of azoxystrobin or pyraclostrobin and higher than that of boscalid, tebuconazole or captan.

Concerning the antibacterial activity, no tests were conducted for any of the NCs presented in Table 4, but it is worth noting that the MIC value attained against *P. syringae* for the ML–COS NCs loaded with *R. tinctorum* extract ($37.5 \mu\text{g}\cdot\text{mL}^{-1}$) was substantially lower than, for instance, the one reported by Tang et al. [43] (MIC = $106.25 \mu\text{g}\cdot\text{mL}^{-1}$) for self-assembled nanoparticles based on polyhexa-methylene biguanide (PHMB) and fenhexamid (FHA) fungicide against *Pseudomonas syringae* pv. *lachrymans*.

In relation to in vivo studies, Fischer et al. [9] studied the effect of lignin NCs loaded with pyraclostrobin ($700 \mu\text{g}\cdot\text{mL}^{-1}$) on 43 grapevine plants. They observed a significant improvement in their conditions after 3 months and up to 4 years, occurring less or even no leaf symptoms, while treatment with non-encapsulated F500 pyraclostrobin-based commercial product (BASF) at a higher dose ($6000 \mu\text{g}\cdot\text{mL}^{-1}$) resulted in an initial improvement of the symptoms, but the symptom level increased again in the following years. In another study by the same group, Machado et al. [17] tested the long-term antifungal effect over a 4-year period on four *V. vinifera* cv. “Portugieser” plants treated with 5 mL of a 1 wt% dispersion of lignin NCs loaded with boscalid. Although the number of specimens was small, they observed almost no signs of esca in the boscalid NC treated plants, which was attributed to a slower degradation in planta or a possible depot effect that lasts for several years. In the study presented herein, the referred initial improvement was also observed, with a reduction of leaf symptoms, but the long-term efficacy has not been determined yet (the plants are still under observation for the next years).

The principle of operation would be similar in the three cases: the NCs are introduced by trunk injection, and transported along the plant, via xylem (upward movement) and phloem (downward movement), from the injection site to reach the infected tissues [9]. The lignin-based encapsulation inhibits the undesired premature release of the bioactive product (a synthetic fungicide in most cases, or *T. reesei* conidia in the work by Peil et al. [18]) and enables the application as an aqueous dispersion via trunk injection. When lignin-degrading fungi infect the plant, enzymatic degradation of the lignin-based shell occurs and the release of the fungicide is selectively triggered by the pathogenic fungi itself.

4.2. Limitations of the Study

Several limitations of the study should be brought to the reader’s attention. Firstly, the in vivo study was conducted in a single location over a single annual growth cycle. Hence, multi-year and multi-location tests would be needed to confirm the good performance of the treatment reported in this work. Optimization of the dispersion properties and dosage should also be addressed in future bioassays.

Secondly, the chosen application procedure by endotherapy would not be a suitable solution for all the GTDs-related scenarios that may be found in most wineries: (i) it requires that symptomatic plants have been previously identified, which implies that the GTDs may already be in an advanced state; (ii) the application is time-consuming (approximately 5 min/plant, considering the time required to drill the hole, insert the plug and inject the solution), so it may not be cost-effective unless the treated plants are used to produce quality wines (as it was the case in the chosen state); (iii) the plugs—which remain in the plant—cannot be reused for subsequent injections, as they are eventually clogged by the scar tissue; (iv) the depth of the drilling hole (20 mm) does not allow application of the treatments in young grapevine plants. It should be clarified that this latter point would not be an issue if the treatment was to be applied to trees.

5. Conclusions

In *in vitro* mycelial growth inhibition tests, the nanocarriers loaded with *R. tinctorum* extract were highly effective against *N. parvum*, with EC₅₀ and EC₉₀ concentrations of 41.2 and 65.8 µg·mL⁻¹, respectively (lower than those obtained for NCs loaded with *S. marianum*, 60.9 and 90.6 µg·mL⁻¹; *E. arvense*, 66.5 and 105.2 µg·mL⁻¹; and *U. dioica*, 50.2 and 113.0 µg·mL⁻¹, respectively). Hence, it was further assayed against other wood-degrading pathogens: EC₅₀ and EC₉₀ concentrations of 59.3 and 91.0 µg·mL⁻¹, respectively, were found against *D. seriata*, and a MIC of 37.5 µg·mL⁻¹ was obtained against *X. ampelinus* and *P. syringae* pv. *syringae*, respectively. Subsequently, it was evaluated in field conditions, in which it was applied by endotherapy to 20-year-old grapevines with clear GTD symptoms. SPAD and chlorophyll fluorescence measurements did not suggest any phytotoxicity effects associated with the treatment, and the sugar content of the grape juice was not affected either. Nonetheless, the NCs-based treatment led to a noticeable decrease in foliar symptoms, statistically significant differences in the number of bunches per arm, and a noticeably higher yield in the treated arms as compared to the control arms (3177 vs. 1932 g/arm), pointing to a high efficacy. Given the advantages of these ML-COS NCs over other systems for the delivery of bioactive compounds in phytosanitary applications due to the exclusive use of natural polymers (instead of synthetic cross-linking amines and organic solvents), together with a reduction in the amount of bioactive compound to be used and the feasibility of a controlled release, they hold promise for the effective and safe application of integrated control treatments against wood-degrading pathogens.

6. Patents

The work reported in this manuscript is related to the Spanish patent with application number P202131019 ('Compuesto reticulado de lignina metacrilada y oligómeros de quitosano capaz de actuar como nanotransportador de compuestos bioactivos, método de obtención y usos'; 'Cross-linked compound of methacrylated lignin and chitosan oligomers capable of acting as a nanocarrier of bioactive compounds, method of obtaining and uses' (tr.)), filed on 29 October 2021.

Supplementary Materials: The following are available online at <https://www.mdpi.com/article/10.3390/agronomy12020461/s1>, Figure S1: Comparison of the ATR-FTIR spectra of the ML-COS nanocarriers; lignin NCs with synthetic amine cross-linking prepared according to the procedure reported by Fischer et al.; enzymatically obtained chitosan oligomers. Figure S2: Comparison of the ATR-FTIR spectra of the ML-COS NCs loaded with *R. tinctorum* extract, ML-COS NCs with no encapsulated product, and the lyophilized *R. tinctorum* extract. Figure S3: Thermal analysis of the ML-COS nanocarriers. Figure S4. Thermal analysis of ML-diamine-ML nanocarriers prepared according to the procedure reported by Fischer et al. Figure S5. Thermal analysis of the ML-COS nanocarriers loaded with *R. tinctorum* extracts. Figure S6. Effect ML-COS NCs-based treatments at different concentrations on the mycelial growth of *N. parvum* and *D. seriata*, respectively.

Author Contributions: Conceptualization, J.M.-G., P.M.-R. and V.G.-G.; methodology, J.M.-G., J.C.-G., S.T.-S. and V.G.-G.; validation, J.C.-G., V.G.-G. and P.M.-R.; formal analysis, J.C.-G., V.G.-G. and P.M.-R.; investigation, E.S.-H., N.L.-L., V.G.-G., J.C.-G., J.M.-G., A.S.-A. and P.M.-R.; resources, J.M.-G., S.T.-S. and P.M.-R.; data curation, J.C.-G.; writing—original draft preparation, E.S.-H., N.L.-L., V.G.-G., J.C.-G., J.M.-G., S.T.-S. and P.M.-R.; writing—review and editing, E.S.-H., V.G.-G., J.M.-G., A.S.-A. and P.M.-R.; visualization, N.L.-L., E.S.-H. and A.S.-A.; supervision, V.G.-G. and P.M.-R.; project administration, J.M.-G. and P.M.-R.; funding acquisition, J.M.-G. and P.M.-R. All authors have read and agreed to the published version of the manuscript.

Funding: This research was funded by Junta de Castilla y León under project VA258P18, with FEDER co-funding by Cátedra Agrobank under the "IV Convocatoria de Ayudas de la Cátedra AgroBank para la transferencia del conocimiento al sector agroalimentario" program and by Fundación Ibercaja-Universidad de Zaragoza under the "Convocatoria Fundación Ibercaja-Universidad de Zaragoza de proyectos de investigación, desarrollo e innovación para jóvenes investigadores" program.

Institutional Review Board Statement: Not applicable.

Informed Consent Statement: Not applicable.

Data Availability Statement: The data presented in this study are available on request from the corresponding author. The data are not publicly available due to their relevance to an ongoing Ph.D. thesis.

Acknowledgments: To Fundación General de la Universidad de Valladolid, for funding the patent through the ‘Prometeo’ program. To José M. Ayuso-Rodríguez and Adrián Jarné-Casasús, from Viñas del Vero S.A. winery. The authors also gratefully acknowledge the support of Pilar Blasco and Pablo Candela at the Servicios Técnicos de Investigación, Universidad de Alicante, for conducting the GC-MS analyses, and wish to thank José Luis Palomo Gómez, from the Aldearrubia Regional Diagnostic Center (Junta de Castilla y León) for providing the *P. syringae* pv. *syringae* isolate used in the study.

Conflicts of Interest: The authors declare no conflict of interest.

References

1. Mondello, V.; Songy, A.; Battiston, E.; Pinto, C.; Coppin, C.; Trotel-Aziz, P.; Clément, C.; Mugnai, L.; Fontaine, F. Grapevine trunk diseases: A review of fifteen years of trials for their control with chemicals and biocontrol agents. *Plant Dis.* **2018**, *102*, 1189–1217. [[CrossRef](#)] [[PubMed](#)]
2. Wagschal, I.; Abou-Mansour, E.; Petit, A.-N. Wood diseases of grapevine: A review on eutypa dieback and esca. In *Plant-Microbe Interactions*; Ait Barka, E., Clément, C., Eds.; Research Signpost: Trivandrum, India, 2008; pp. 1–25.
3. Bertsch, C.; Ramírez-Suero, M.; Magnin-Robert, M.; Larignon, P.; Chong, J.; Abou-Mansour, E.; Spagnolo, A.; Clément, C.; Fontaine, F. Grapevine trunk diseases: Complex and still poorly understood. *Plant Pathol.* **2013**, *62*, 243–265. [[CrossRef](#)]
4. Gramaje, D.; Úrbez-Torres, J.R.; Sosnowski, M.R. Managing grapevine trunk diseases with respect to etiology and epidemiology: Current strategies and future prospects. *Plant Dis.* **2018**, *102*, 12–39. [[CrossRef](#)] [[PubMed](#)]
5. Hofstetter, V.; Buyck, B.; Croll, D.; Viret, O.; Couloux, A.; Gindro, K. What if esca disease of grapevine were not a fungal disease? *Fungal Divers.* **2012**, *54*, 51–67. [[CrossRef](#)]
6. Broda, M. Natural Compounds for Wood Protection against Fungi—A Review. *Molecules* **2020**, *25*, 3538. [[CrossRef](#)]
7. Yiamsawas, D.; Beckers, S.J.; Lu, H.; Landfester, K.; Wurm, F.R. Morphology-controlled synthesis of lignin nanocarriers for drug delivery and carbon materials. *ACS Biomater. Sci. Eng.* **2017**, *3*, 2375–2383. [[CrossRef](#)]
8. Yiamsawas, D.; Baier, G.; Thines, E.; Landfester, K.; Wurm, F.R. Biodegradable lignin nanocontainers. *RSC Adv.* **2014**, *4*, 11661–11663. [[CrossRef](#)]
9. Fischer, J.; Beckers, S.J.; Yiamsawas, D.; Thines, E.; Landfester, K.; Wurm, F.R. Targeted drug delivery in plants: Enzyme-responsive lignin nanocarriers for the curative treatment of the worldwide grapevine trunk disease Esca. *Adv. Sci.* **2019**, *6*, 1802315. [[CrossRef](#)]
10. Wurm, F.R.; Weiss, C.K. Nanoparticles from renewable polymers. *Front. Chem.* **2014**, *2*, 49. [[CrossRef](#)]
11. Pathania, D.; Gupta, D.; Agarwal, S.; Asif, M.; Gupta, V.K. Fabrication of chitosan-g-poly(acrylamide)/CuS nanocomposite for controlled drug delivery and antibacterial activity. *Mater. Sci. Eng. C* **2016**, *64*, 428–435. [[CrossRef](#)]
12. Beckers, S.J.; Wetherbee, L.; Fischer, J.; Wurm, F.R. Fungicide-loaded and biodegradable xylan-based nanocarriers. *Biopolymers* **2020**, *111*, e23413. [[CrossRef](#)] [[PubMed](#)]
13. Ciftci, N.; Sargin, I.; Arslan, G.; Arslan, U.; Okudan, A. Ascorbic acid adsorption-release performance and antibacterial activity of chitosan-ter(GMA-MA-NTBA) polymer microcapsules. *J. Polym. Environ.* **2020**, *28*, 2277–2288. [[CrossRef](#)]
14. Zou, T.; Sipponen, M.H.; Österberg, M. Natural shape-retaining microcapsules with shells made of chitosan-coated colloidal lignin particles. *Front. Chem.* **2019**, *7*, 370. [[CrossRef](#)] [[PubMed](#)]
15. Rosova, E.; Smirnova, N.; Dresvyanina, E.; Smirnova, V.; Vlasova, E.; Ivan'kova, E.; Sokolova, M.; Maslennikova, T.; Malafeev, K.; Kolbe, K.; et al. Biocomposite materials based on chitosan and lignin: Preparation and characterization. *Cosmetics* **2021**, *8*, 24. [[CrossRef](#)]
16. Aradmehr, A.; Javanbakht, V. A novel biofilm based on lignocellulosic compounds and chitosan modified with silver nanoparticles with multifunctional properties: Synthesis and characterization. *Colloids Surf. A Physicochem. Eng. Asp.* **2020**, *600*, 124952. [[CrossRef](#)]
17. Machado, T.O.; Beckers, S.J.; Fischer, J.; Müller, B.; Sayer, C.; de Araújo, P.H.H.; Landfester, K.; Wurm, F.R. Bio-based lignin nanocarriers loaded with fungicides as a versatile platform for drug delivery in plants. *Biomacromolecules* **2020**, *21*, 2755–2763. [[CrossRef](#)]
18. Peil, S.; Beckers, S.J.; Fischer, J.; Wurm, F.R. Biodegradable, lignin-based encapsulation enables delivery of *Trichoderma reesei* with programmed enzymatic release against grapevine trunk diseases. *Mater. Today Bio* **2020**, *7*, 100061. [[CrossRef](#)]
19. Langa-Lomba, N.; Buzón-Durán, L.; Martín-Ramos, P.; Casanova-Gascón, J.; Martín-Gil, J.; Sánchez-Hernández, E.; González-García, V. Assessment of conjugate complexes of chitosan and *Urtica dioica* or *Equisetum arvense* extracts for the control of grapevine trunk pathogens. *Agronomy* **2021**, *11*, 976. [[CrossRef](#)]

20. Langa-Lomba, N.; Sánchez-Hernández, E.; Buzón-Durán, L.; González-García, V.; Casanova-Gascón, J.; Martín-Gil, J.; Martín-Ramos, P. Activity of anthracenediones and flavoring phenols in hydromethanolic extracts of *Rubia tinctorum* against grapevine phytopathogenic fungi. *Plants* **2021**, *10*, 1527. [[CrossRef](#)]
21. Langa-Lomba, N.; Buzón-Durán, L.; Sánchez-Hernández, E.; Martín-Ramos, P.; Casanova-Gascón, J.; Martín-Gil, J.; González-García, V. Antifungal activity against Botryosphaeriaceae fungi of the hydro-methanolic extract of *Silybum marianum* capitula conjugated with stevioside. *Plants* **2021**, *10*, 1363. [[CrossRef](#)]
22. Leonardo, D.-C. *Botryosphaeriaceae* species associated with stem canker, die-back and fruit rot on apple in Uruguay. *Eur. J. Plant Pathol.* **2016**, *146*, 637–655. [[CrossRef](#)]
23. Szegedi, E.; Civerolo, E.L. Bacterial diseases of grapevine. *Int. J. Hortic. Sci.* **2011**, *17*, 45–49. [[CrossRef](#)]
24. Stevens, N.E. Two apple black rot fungi in the United States. *Mycologia* **2018**, *25*, 536–548. [[CrossRef](#)]
25. Brown-Rytlewski, D.E.; McManus, P.S. Virulence of *Botryosphaeria dothidea* and *Botryosphaeria obtusa* on apple and management of stem cankers with fungicides. *Plant Dis.* **2000**, *84*, 1031–1037. [[CrossRef](#)] [[PubMed](#)]
26. Willems, A.; Gillis, M.; Kersters, K.; Van Den Broecke, L.; De Ley, J. Transfer of *Xanthomonas ampelina* Panagopoulos 1969 to a new genus, *Xylophilus* gen. nov., as *Xylophilus ampelinus* (Panagopoulos 1969) comb. nov. *Int. J. Syst. Bacteriol.* **1987**, *37*, 422–430. [[CrossRef](#)]
27. Gerin, D.; Cariddi, C.; de Miccolis Angelini, R.M.; Rotolo, C.; Dongiovanni, C.; Faretra, F.; Pollastro, S. First report of *Pseudomonas* grapevine bunch rot caused by *Pseudomonas syringae* pv. *syringae*. *Plant Dis.* **2019**, *103*, 1954–1960. [[CrossRef](#)]
28. Santos-Moriano, P.; Fernandez-Arrojo, L.; Mengibar, M.; Belmonte-Reche, E.; Peñalver, P.; Acosta, F.N.; Ballesteros, A.O.; Morales, J.C.; Kidibule, P.; Fernandez-Lobato, M.; et al. Enzymatic production of fully deacetylated chitoooligosaccharides and their neuroprotective and anti-inflammatory properties. *Biocatal. Biotransform.* **2017**, *36*, 57–67. [[CrossRef](#)]
29. Buzón-Durán, L.; Martín-Gil, J.; Pérez-Lebeña, E.; Ruano-Rosa, D.; Revuelta, J.L.; Casanova-Gascón, J.; Ramos-Sánchez, M.C.; Martín-Ramos, P. Antifungal agents based on chitosan oligomers, ϵ -polylysine and *Streptomyces* spp. secondary metabolites against three *Botryosphaeriaceae* species. *Antibiotics* **2019**, *8*, 99. [[CrossRef](#)]
30. Sannan, T.; Kurita, K.; Iwakura, Y. Studies on chitin, 2. Effect of deacetylation on solubility. *Makromol. Chem.* **1976**, *177*, 3589–3600. [[CrossRef](#)]
31. Yang, Y.; Shu, R.; Shao, J.; Xu, G.; Gu, X. Radical scavenging activity of chitoooligosaccharide with different molecular weights. *Eur. Food Res. Technol.* **2005**, *222*, 36–40. [[CrossRef](#)]
32. Maghami, G.G.; Roberts, G.A.F. Evaluation of the viscometric constants for chitosan. *Makromol. Chem.* **1988**, *189*, 195–200. [[CrossRef](#)]
33. Tian, M.; Tan, H.; Li, H.; You, C. Molecular weight dependence of structure and properties of chitosan oligomers. *RSC Adv.* **2015**, *5*, 69445–69452. [[CrossRef](#)]
34. Krizsán, K.; Szókán, G.; Toth, Z.A.; Hollósy, F.; László, M.; Khlafulla, A. HPLC analysis of anthraquinone derivatives in madder root (*Rubia tinctorum*) and its cell cultures. *J. Liq. Chromatogr. Relat. Technol.* **2006**, *19*, 2295–2314. [[CrossRef](#)]
35. Cruz, G.; Crnkovic, P.M. Investigation into the kinetic behavior of biomass combustion under N₂/O₂ and CO₂/O₂ atmospheres. *J. Therm. Anal. Calorim.* **2015**, *123*, 1003–1011. [[CrossRef](#)]
36. Arendrup, M.C.; Cuenca-Estrella, M.; Lass-Flörl, C.; Hope, W. EUCAST technical note on the EUCAST definitive document EDef 7.2: Method for the determination of broth dilution minimum inhibitory concentrations of antifungal agents for yeasts EDef 7.2 (EUCAST-AFST). *Clin. Microbiol. Infect.* **2012**, *18*, E246–E247. [[CrossRef](#)]
37. CLSI. *Methods for Dilution Antimicrobial Susceptibility Tests for Bacteria That Grow Aerobically*, 11th ed.; CLSI standard M07; Clinical and Laboratory Standards Institute: Wayne, PA, USA, 2018.
38. Choudhary, R.C.; Kumari, S.; Kumaraswamy, R.V.; Pal, A.; Raliya, R.; Biswas, P.; Saharan, V. Characterization methods for chitosan-based nanomaterials. In *Plant Nanobionics*; Springer: Cham, Switzerland, 2019; pp. 103–116. [[CrossRef](#)]
39. Kumaraswamy, R.V.; Kumari, S.; Choudhary, R.C.; Pal, A.; Raliya, R.; Biswas, P.; Saharan, V. Engineered chitosan based nanomaterials: Bioactivities, mechanisms and perspectives in plant protection and growth. *Int. J. Biol. Macromol.* **2018**, *113*, 494–506. [[CrossRef](#)]
40. Bhattacharjee, S. DLS and zeta potential—What they are and what they are not? *J. Controll. Release* **2016**, *235*, 337–351. [[CrossRef](#)]
41. Machado, T.O.; Beckers, S.J.; Fischer, J.; Sayer, C.; de Araújo, P.H.H.; Landfester, K.; Wurm, F.R. Cellulose nanocarriers via miniemulsion allow pathogen-specific agrochemical delivery. *J. Colloid Interface Sci.* **2021**, *601*, 678–688. [[CrossRef](#)]
42. Wurm, F.; Landfester, K.; Yiamsawas, D.; Thines, E.; Fischer, J. Lignin Biomaterial as Agricultural Drug Carrier. U.S. Patent 2019/0037837 A1, 7 February 2019.
43. Tang, G.; Tian, Y.; Niu, J.; Tang, J.; Yang, J.; Gao, Y.; Chen, X.; Li, X.; Wang, H.; Cao, Y. Development of carrier-free self-assembled nanoparticles based on fenhexamid and polyhexamethylene biguanide for sustainable plant disease management. *Green Chem.* **2021**, *23*, 2531–2540. [[CrossRef](#)]

Artículo 7: “Multifunctional nanocarriers based on chitosan oligomers and graphitic carbon nitride assembly”. *Materials*, 2022; 15(24), 8981; <https://doi.org/10.3390/ma15248981>; Q2 (JCR, Science Edition – METALLURGY & METALLURGICAL ENGINEERING). JIF₂₀₂₂ = 3,4.



materials

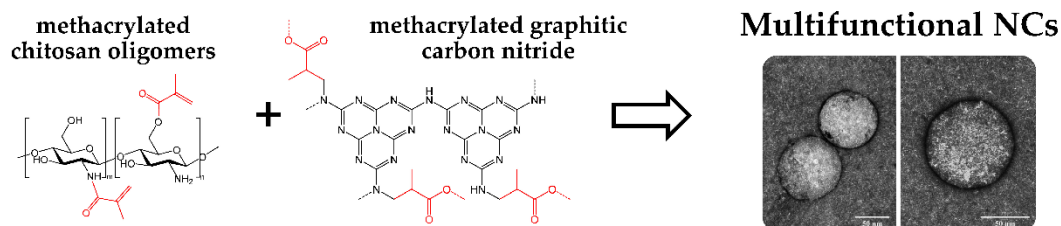
an Open Access Journal by MDPI



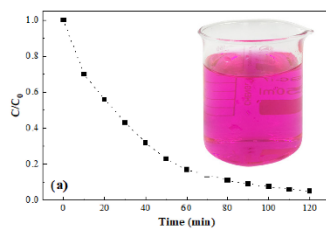
Multifunctional Nanocarriers Based on Chitosan Oligomers and Graphitic Carbon Nitride Assembly

Alberto Santiago-Aliste; Eva Sánchez-Hernández; Natalia Langa-Lomba; Vicente González-García; José Casanova-Gascón; Jesús Martín-Gil; Pablo Martín-Ramos

Materials 2022, Volume 15, Issue 24, 8981



Environmental remediation:
photocatalytic degradation of RhB
and photoreduction of U(VI)



Agrochemicals targeted delivery:
enhanced *in vitro* and *in vivo* activity
against grapevine phytopathogens of
R. tinctorum-loaded NCs

+



Article

Multifunctional Nanocarriers Based on Chitosan Oligomers and Graphitic Carbon Nitride Assembly

Alberto Santiago-Aliste ^{1,*}, Eva Sánchez-Hernández ^{1,*}, Natalia Langa-Lomba ^{2,3}, Vicente González-García ³, José Casanova-Gascón ², Jesús Martín-Gil ¹ and Pablo Martín-Ramos ^{1,2,*}

¹ Department of Agricultural and Forestry Engineering, ETSIIAA, University of Valladolid, Avenida de Madrid 44, 34004 Palencia, Spain

² Instituto Universitario de Investigación en Ciencias Ambientales de Aragón (IUCA), EPS, University of Zaragoza, Carretera de Cuarte s/n, 22071 Huesca, Spain

³ Plant Protection Unit, Instituto Agroalimentario de Aragón-IA2 (CITA-Universidad de Zaragoza), Avda. Montañana 930, 50059 Zaragoza, Spain

* Correspondence: eva.sanchez.hernandez@uva.es (E.S.-H.); pmr@uva.es (P.M.-R.)

Abstract: In this study, a graphitic carbon nitride and chitosan oligomers (g-C₃N₄-COS) nanocarrier assembly, which was obtained by cross-linking with methacrylic anhydride (MA), was synthesized and characterized. Its characterization was carried out using infrared spectroscopy, elemental and thermal analyses, and transmission electron microscopy. The new nanocarriers (NCs), with an average particle size of 85 nm in diameter and a 0.25 dispersity index, showed photocatalytic activity (associated with the g-C₃N₄ moiety), susceptibility to enzymatic degradation (due to the presence of the COS moiety), and high encapsulation and moderate-high release efficiencies (>95% and >74%, respectively). As a proof of concept, the visible-light-driven photocatalytic activity of the NCs was tested for rhodamine B degradation and the reduction of uranium(VI) to uranium(IV). Regarding the potential of the nanocarriers for the encapsulation and delivery of bioactive products for crop protection, NCs loaded with *Rubia tinctorum* extracts were investigated in vitro against three *Vitis vinifera* phytopathogens (viz. *Neofusicoccum parvum*, *Diplodia seriata*, and *Xylophilus ampelinus*), obtaining minimum inhibitory concentration values of 750, 250, and 187.5 µg·mL⁻¹, respectively. Their antifungal activity was further tested in vivo as a pruning wound protection product in young ‘Tempranillo’ grapevine plants that were artificially infected with the two aforementioned species of the family *Botryosphaeriaceae*, finding a significant reduction of the necrosis lengths in the inner woody tissues. Therefore, g-C₃N₄-MA-COS NCs may be put forward as a multifunctional platform for environmental and agrochemical delivery applications.

Keywords: chitosan oligomers; cross-linking; g-C₃N₄; grapevine phytopathogens; integrated pest management; methacrylic anhydride; photocatalytic degradation; photocatalytic reduction



Citation: Santiago-Aliste, A.; Sánchez-Hernández, E.; Langa-Lomba, N.; González-García, V.; Casanova-Gascón, J.; Martín-Gil, J.; Martín-Ramos, P. Multifunctional Nanocarriers Based on Chitosan Oligomers and Graphitic Carbon Nitride Assembly. *Materials* **2022**, *15*, 8981. <https://doi.org/10.3390/ma15248981>

Academic Editors: Feng Xu and Sheng Chen

Received: 20 October 2022

Accepted: 12 December 2022

Published: 15 December 2022

Publisher’s Note: MDPI stays neutral with regard to jurisdictional claims in published maps and institutional affiliations.



Copyright: © 2022 by the authors. Licensee MDPI, Basel, Switzerland. This article is an open access article distributed under the terms and conditions of the Creative Commons Attribution (CC BY) license (<https://creativecommons.org/licenses/by/4.0/>).

1. Introduction

Engineered nanocarriers (NCs) have substantially contributed to the development of precision medicine [1], and, more recently, they are also finding applications in agriculture as a promising route to increase crop production while reducing the environmental impact associated with food production and crop protection [2].

For agricultural purposes, the main characteristic of any nanocarrier is to exhibit controlled release properties and site-specific delivery, i.e., the release of the active ingredient should respond to the stimuli produced by the pest and/or the surrounding environment [3]. Nonetheless, other features are also highly desirable: good physical and chemical properties, stability in different media, a high adsorption capacity, ease of modification to tune the surface characteristics such as charge and permeability, biocompatibility, biodegradability, low toxicity, and competitive production costs [2].

The state-of-the-art of micro- and nanocarriers used for the encapsulation of agrochemicals have been covered in several recent review papers [3,4], which showed that naturally sourced polymers, such as chitosan (36%), alginate (23%), and plant-based proteins (16%); synthetic polymers (35%); and inorganic materials (e.g., metal-organic frameworks and calcium carbonate) are among the options that have been explored for the construction of NCs.

Concerning the preferred option (viz. chitosan), the agronanochemicals for crop protection based on this natural polymer would feature several attractive properties, as discussed in the review by Maluin and Hussein [5]. The encapsulation of the active ingredients in chitosan NCs shields the toxic effect of the free agrochemicals on the plant and minimizes the negative impacts on the environment and human health, it increases the uptake due to the enhanced penetration of the nanometer-sized particles on the plant cell wall and cuticle, and it minimizes the wastage and leaching of the active ingredients due to the controlled release properties and high bioavailability of the nanoformulations. Further, chitosan features amphiphilic and bioadhesive properties, enhances solubility and stability, and its use can result in synergistic effects. Chitosan may also be used for nutrient encapsulation, i.e., for the preparation of nanofertilizers [6], and it elicits immune-modulatory activity. In this regard, it should be clarified that chitin has a pathogen-associated molecular pattern, which can be detected by the LysM/CERK1 transmembrane chitin receptor in the plant cells, and its sensing triggers an intracellular defense immune response (involving the activation of kinases and up-regulation of defense-related genes, such as plant defensin PDF1.2) [2]. For environmental remediation purposes, chitosan can be used as a flocculant and coagulant, and as an adsorbent for the removal of pollutants such as heavy metals, pesticides, dyes, antibiotics, and biological contaminants from wastewater [7].

The development of cross-linked chitosan-based systems for drug delivery usually relies on tripolyphosphate (TPP), glutaraldehyde (GLA), ethylene glycol diglycidyl ether, epichlorohydrin, polyethyleneimine, and phenylalanine chemical cross-linkers [8], although some of them (e.g., GLA) are considered to be toxic and can inactivate macromolecular drugs [9], while the others (e.g., TPP) face aggregation and dissolution stability problems [10]. The aforementioned issues can be overcome by using anhydride methacrylate (MA) as an alternative cross-linker. MA has been commonly used to modify the chemical structure of various natural polymers and biomolecules—including polysaccharides—with a significant coupling efficiency under mild reaction conditions [11], without affecting the biocompatibility of the final product [12]. The carbon-carbon double bonds of the methacryl groups can react with hydroxyl- and amino-groups, leading to the covalent attachment of methacryloyl moieties, which can be used in subsequent cross-linkage reactions. Modification with MA has been reported to improve the encapsulation of the bioactive compounds [13] and to enhance the water solubility and the capacity of the gel and scaffold formation of chitosan [14]. Concerning NCs preparation, MA has been successfully used as a cross-linking agent in lignin-bio-based amine NCs [15] and lignin-chitosan oligomers-based NCs [16].

To exploit the susceptibility of MA to act as a link between the related chemical species, resulting in a ternary complex with transporter properties, and to broaden the profile of the analogous complexes, in this study, we have explored the feasibility of the synthesis and behavior of the graphene carbon nitride-methacrylate-chitosan oligomers ($g\text{-C}_3\text{N}_4\text{-MA-COS}$) system as a nanocarrier.

Regarding the inclusion of the $g\text{-C}_3\text{N}_4$ moiety in the $g\text{-C}_3\text{N}_4\text{-MA-COS}$ assembly, it should be noted that carbon nitride has gained extensive attention due to its excellent physicochemical properties, attractive electronic band structure, and low cost. Concerning the functions enabled by $g\text{-C}_3\text{N}_4$ toward the end applications of the multifunctional NCs, $g\text{-C}_3\text{N}_4$ nanosheets have been shown to be a suitable functional component for bioactive product delivery due to their low toxicity, excellent biocompatibility, high penetration into tissues ability, photosensitive and pH-sensitive properties, efficiency in drug encapsulation

(associated with their large surface area), and positive effect on the release of encapsulated compounds [17]. Regarding the environmental applications, g-C₃N₄-based photocatalysts are very efficient for pollutant degradation and bacterial disinfection [18,19].

The use of g-C₃N₄ in combination with chitosan has precedents in, for instance, the work by Gupta and Gupta [20] on chitosan hydrogels that were embedded with g-C₃N₄/ZnO nanoparticles for ciprofloxacin removal or in the chitosan films incorporated with curcumin-loaded hollow g-C₃N₄ nanoparticles (prepared using nanosized silica template) for bananas preservation that was reported by Ni et al. [21]. pH-sensitive NCs based on a composite of chitosan/agarose/g-C₃N₄ were also investigated by Rajabzadeh-Khosroshahi et al. [17] as a drug delivery system for anticancer curcumin release, in which glyoxal was used to cross-link chitosan and agarose (2:1, *w/w*). Likewise, a system based on Pd nanoparticles embedded in micro-sized chitosan-g-C₃N₄ hybrid spheres (0.9 mm in diameter) was reported by Yilmaz Baran et al. [22] for the treatment of environmental pollutants in the aqueous medium, although in this case the chitosan-g-C₃N₄ mixture spheres were obtained through a spherification process of chitosan (using GLA), in which g-C₃N₄ did not intervene. Hence, to the best of the authors' knowledge, the actual cross-linkage between chitosan and g-C₃N₄ to form NCs has not been explored to date.

In the work presented herein, we report the synthesis and characterization of multifunctional NCs based on the chemical cross-linkage of COS and g-C₃N₄ using MA. To assess the presumed versatility of these g-C₃N₄-MA-COS NCs, environmental remediation (with two paradigmatic pollutants, rhodamine B dye and uranium(VI)), and biorational-based antimicrobial delivery applications in agriculture (against three emerging grapevine pathogens) were also investigated.

2. Material and Methods

2.1. Reagents

High molecular weight chitosan (CAS No. 9012-76-4; MW: 310,000–375,000 Da) was supplied by Hangzhou Simit Chem. & Tech. Co. (Hangzhou, China). Melamine cyanurate (CAS No. 37640-57-6; >99.0%) was purchased from Nachmann S.r.l. (Milano, Italy). Neutrase™ 0.8 L enzyme was supplied by Novozymes A/S (Bagsværd, Denmark). Chitosanase from *Streptomyces griseus* (Krainisky) Waksman and Henrici (EC 3.2.1.132, CAS No. 51570-20-8), acetic acid (purum, 80% in H₂O; CAS No. 64-19-7), rhodamine B (analytical standard, CAS No. 81-88-9), methacrylic anhydride (CAS No. 760-93-0; ≥94%), Arsenazo III (CAS No. 1668-00-4), methanol (UHPLC, suitable for mass spectrometry, CAS 67-56-1), tetrahydrofuran (THF, CAS No. 109-99-9; ≥99.9%), tryptic soy agar (TSA, CAS No. 91079-40-2), and tryptic soy broth (TSB, CAS No. 8013-01-2) were supplied by Sigma–Aldrich Química (Madrid, Spain). Uranyl nitrate hexahydrate (CAS 13520-83-7, ACS grade, Honeywell Fluka) was supplied by Fisher Scientific SL (Madrid, Spain). Potato dextrose agar (PDA) was purchased from Becton Dickinson (Bergen County, NJ, USA).

2.2. Fungal and Bacterial Isolates

The two fungal isolates under study, *Neofusicoccum parvum* (Pennycook and Samuels) Crous, Slippers, and Phillips (code ITACYL F111, isolate Y-091-03-01c) and *Diplodia seriata* de Notaris (code ITACYL F098, isolate Y-084-01-01a) were kindly supplied by the Instituto Tecnológico Agrario de Castilla y León (ITACYL, Valladolid, Spain) as lyophilized vials, which were later reconstituted and refreshed as PDA subcultures. Regarding the bacterial isolate, *Xylophilus ampelinus* (Panagopoulos) Willems, Gillis, Kersters, van den Broeke, and De Ley was acquired by the Spanish Type Culture Collection (CECT), with a CCUG 21,976 strain designation.

2.3. Chitosan Oligomers and g-C₃N₄ Preparation

The chitosan oligomers (COS) were prepared according to the procedure described in the work by Santos-Moriano et al. [23] with the modifications indicated in [16] using the commercial proteolytic preparation Neutrase™ to degrade the chitosan polymer chains

and obtain a product enriched in deacetylated chitooligosaccharides. At the end of the process, a solution with a pH in the range from 4 to 6 with oligomers of a molecular weight of <2 kDa was obtained, with a polydispersity index of 1.6, which is within the usual range that has been reported in the literature [24].

High-purity nanosheets of g-C₃N₄ were obtained from the pyrolysis of melamine cyanurate in a capped crucible under an air atmosphere at 600 °C for 50 min according to the procedure previously reported by our group in [25].

2.4. Plant Material and Preparation of Extract

Rubia tinctorum L. specimens used for the preparation of the bioactive extract to be encapsulated were collected from the banks of the Carrión River as it passes through the town of Palencia (Spain). The details of the hydromethanolic extract preparation, its characterization using gas chromatography-mass spectroscopy (GC-MS), and its antimicrobial activity have been previously reported in [26].

'Tempranillo' grapevine plants used in the in vivo study were supplied by VCR Vivai Cooperativi Rauscedo (Italy), with supplier ID IT-06-1031. The clone was 'CL. 32' and the rootstock was '775P CFC 83/20'. The lot number was 'PN 001 19/1519507'.

2.5. Synthesis of the g-C₃N₄-MA-COS Nanocarriers

The preparation of the nanocarriers was carried out as described in patent P202230668 [27]. The synthesis of methacrylated chitosan was conducted according to the procedure proposed by Gupta and Gupta [20], but with modifications. In brief, the methacrylation of COS was performed by the addition of 420 mg of oligomers which were dispersed in a solution of methacrylic anhydride in tetrahydrofuran (THF), which was obtained by dispersing 0.5 mL of MA ($\rho = 1.035 \text{ g}\cdot\text{cm}^{-3}$) in 25 mL of THF. The mixture was sonicated for 5 min (distributed in 1 min periods) using a probe-type ultrasonicator (model UIP1000hdT; 1000 W, 20 kHz; Hielscher Ultrasonics, Teltow, Germany). The co-encapsulating chemical species was a porous form of g-C₃N₄ resulting from the attack of 210 mg of g-C₃N₄ with MA in THF (0.5 mL in 25 mL). The methacrylated g-C₃N₄ solution was then added dropwise to the methacrylated COS solution, which was followed by sonication for 5 min (distributed in 1 min periods) to obtain a g-C₃N₄:COS weight ratio of 0.5:1 (with an unknown MA proportion). It should be clarified that the other assayed weight ratios did not result in the formation of NCs or lead to non-monodisperse size distributions. The excess MA was removed by agitation and successive washings.

2.6. Encapsulation and Release of *R. tinctorum* Extract

For the agrochemical delivery tests, *R. tinctorum* extract was chosen as an example of a bioactive agent because it has previously shown high inhibitory efficacy against the aforementioned fungal and bacterial phytopathogens, which were both unencapsulated [26] and encapsulated in lignin–chitosan nanocarriers [16].

To prepare the nanocarriers with the encapsulated *R. tinctorum* extract, 105 mg of the lyophilized extract that was to be encapsulated was added to the g-C₃N₄-MA-COS solution to obtain a g-C₃N₄:COS:*R. tinctorum* 0.5:1:0.25 weight ratio. The mixture was subjected to sonication for 1 h, distributed in 5 min periods, while the temperature (which was always lower than 60 °C) and the pH (4–5) were controlled.

Concerning the plant extract encapsulation efficiency (EE), it was determined using the indirect method that was proposed by Fischer et al. [28]; the sample was centrifuged at 10,000 rpm (60 min), and the supernatant containing the non-encapsulated plant extract was first freeze-dried, then redissolved in methanol:water (1:1, v/v), passed through a 0.2 µm filter, and analyzed by high-pressure liquid chromatography (HPLC) using an Agilent 1200 series HPLC system (Agilent Technologies, Santa Clara, CA, USA). The operative conditions were [29]: methanol/5% acetic acid (pH 3) (70~30) mobile phase; 10 µL injection volume; 20 °C column temperature; 0.2 mL·min⁻¹ flow rate;

G1315D detector operated at 250 nm. The encapsulation efficiency was determined as $EE(\%) = (m(\text{extract initial}) - m(\text{extract supernatant})) / m(\text{extract initial}) \times 100$.

As for the release efficiency (RE), the release assays were performed by the addition of a weighted quantity of freeze-dried loaded NCs (obtained from the encapsulation efficiency test) and 2.5 U of chitosanase (EC 3.2.1.132) to a methanol:water (1:1, *v/v*) solution under light stirring (150 rpm) in the dark for 2 h. An aliquot was sampled, and the released *R. tinctorum* extract was assayed by the same method that was employed for the determination of residual (i.e., non-encapsulated) extract. The release efficiency was calculated from the amount of extract released as a percentage of the total amount of extract encapsulated in the NCs.

2.7. Characterization

The multi-elemental composition of the NCs, before and after encapsulation of *R. tinctorum* extract, was analyzed by scanning electron microscopy with energy-dispersive X-ray spectroscopy (SEM-EDX) using an EVO HD 25 (Carl Zeiss, Oberkochen, Germany) apparatus.

Infrared vibrational spectra were collected using a Thermo Scientific (Waltham, MA, USA) Nicolet iS50 FTIR spectrometer equipped with an integrated diamond attenuated total reflection (ATR) system. The spectra have been recorded with a spectral resolution of 1 cm^{-1} in the range of $400\text{--}4000 \text{ cm}^{-1}$, taking the interferograms resulting from the co-addition of 64 scans.

The Transmission Electron Microscopy (TEM) characterization was performed using a JEOL (Akishima, Tokyo, Japan) JEM 1011 HR microscope. The operating conditions were: 100 kV; $25,000\text{--}120,000\times$ magnification. Micrographs were obtained using a GATAN ES1000W CCD camera (4000×2672 pixels). Uranyl acetate (2%) was used for the negative staining of the samples.

The dispersity was calculated from the TEM data as $p = \sigma / R_{avg}$, where p is the dispersity, σ is the standard deviation of a radius in a batch of NCs, and R_{avg} is the average radius of the NCs [30].

The thermogravimetric/derivative thermogravimetric (TG/DTG) analyses were conducted using a TG-DSC2 (Mettler-Toledo, Columbus, OH, USA) thermal analyzer by heating the sample in a slow stream of N_2 ($20 \text{ mL}\cdot\text{min}^{-1}$) from room temperature up to $750 \text{ }^\circ\text{C}$ at a heating rate of $20 \text{ }^\circ\text{C}\cdot\text{min}^{-1}$.

2.8. Photocatalytic Activity

To evaluate the photocatalytic activity of the g- C_3N_4 -MA-COS NCs, rhodamine B (RhB) dye degradation tests were carried out under visible light irradiation ($\lambda > 420 \text{ nm}$) following the protocol described by Dong and Zhang [31], but with minor modifications. A 300 W xenon lamp with a 420 nm cutoff filter was chosen as a visible light source. The nanocarriers (0.1 g) were dispersed into 100 mL of $10 \text{ mg}\cdot\text{L}^{-1}$ RhB aqueous solution in a container with a cooling water jacket that was on the outside. To obtain an adsorption-desorption equilibrium between the assayed material and RhB, the solution was stirred in the dark for 2 h. During the irradiation, about 4 mL of the suspensions were taken from the reaction cell at 10 min intervals (over a 2 h period), and then, they were centrifuged to remove the nanoparticles. The RhB concentration was determined by taking absorbance measurements at 550 nm using a Multiskan GO Microplate spectrophotometer (Fisher Scientific). The reaction constant was calculated as $\ln(C/C_0) = -kt$, where C is the maximum peak of the absorption spectra of RhB for each irradiated time interval, and C_0 is the absorption of the starting concentration when the adsorption/desorption equilibrium was achieved.

Additional photocatalytic tests were conducted to investigate the ability of the NCs to reduce U(VI) to U(IV) under visible light following the methodology that is described in [32], but with modifications. In the catalytic process, 30 mg of g- C_3N_4 -MA-COS NCs was added into 60 mL of $3 \text{ mg}\cdot\text{L}^{-1}$ $\text{UO}_2(\text{NO}_3)_2$ solution (containing 3 mL methanol as the

electron sacrifice). The pH value was adjusted to 6.0. As in the RhB procedure described above, the visible light irradiation was obtained using a 300 W Xe lamp equipped with a 420 nm cutoff filter. Before irradiation, the reaction system was bubbled with N₂ in the dark for 2 h to reach the adsorption–desorption equilibrium and maintain the anaerobic conditions. After irradiation, 1 mL of suspension was pipetted out at a certain time and rapidly filtered. The U(VI) concentration was measured by UV-vis spectrophotometry at 652 nm using Arsenazo III. The photoreaction rate constant was calculated based on pseudo-first-order kinetics as $\ln(C/C_0) = -kt$, where C represents the concentration of uranium(VI) at a given time, and C_0 represents the initial concentration.

2.9. In Vitro Antimicrobial Activity

The g-C₃N₄-MA-COS nanocarriers, before and after encapsulation of *R. tinctorum* extract, were first assayed against *X. ampelinus*. The antibacterial activity was evaluated by determining the minimum inhibitory concentration (MIC). The agar dilution method was used according to CLSI standard M07-11 [33]. An isolated colony of *X. ampelinus* was cultured in TSB liquid medium at 26 °C for 18 h. Starting from a concentration of 10⁸ CFU·mL⁻¹, serial dilutions were made to obtain a final inoculum of ~10⁴ CFU·mL⁻¹. Subsequently, the bacterial suspension was applied to the surface of tryptic soy agar (TSA) plates that were amended with the treatments at concentrations ranging from 62.5 to 1500 µg·mL⁻¹. The plates were incubated at 26 °C for 24 h. The MICs were determined as the lowest concentrations at which no bacterial growth was observed in the agar dilutions. All of the experiments were performed in triplicate, and each replicate consisted of three plates per treatment/concentration.

Regarding the inhibition of mycelial growth, which was tested against *D. seriata* and *N. parvum*, it was determined by dilution in agar, according to the EUCAST antifungal susceptibility testing standard procedures [34], incorporating aliquots of stock solutions (of NCs, either empty or loaded with *R. tinctorum*) onto a potato dextrose agar (PDA) medium to obtain concentrations in the range of 62.5–1500 µg·mL⁻¹. Fungal mycelium plugs ($\varnothing = 5$ mm) were transferred from the margins of one-week-old *D. seriata* or *N. parvum* PDA cultures to plates incorporating the concentrations mentioned for each treatment (three plates per treatment/concentration with two replicates each). The plates were then incubated at 25 °C in the dark for one week. A PDA medium without any modification was used as control. The mycelial growth inhibition was estimated according to the formula: $((d_c - d_t)/d_c) \times 100$, where d_c and d_t represent the mean diameters of the control fungal colony and the treated fungal colony, respectively. The effective concentrations (EC₅₀ and EC₉₀) were estimated using the PROBIT analysis in IBM SPSS Statistics v.25 (IBM; Armonk, NY, USA).

2.10. In Planta Bioassays

To determine the in vivo protective activity, bioassays were carried out with the g-C₃N₄-MA-COS NCs loaded with the hydromethanolic extract of *R. tinctorum* in 2-year-old ‘Tempranillo’ grapevine plants that were artificially infected with the two selected Botryosphaeriaceous fungi. Each plant was grown in a 3.5 L plastic pot with a mixed substrate of peat and sterilized natural soil (75:25), incorporating slow-release fertilizer when it was necessary throughout the study period. One week after potting, the young grafted plants were ‘wounded’ on the trunk at two sites per stem (separated >5 cm), which were below the grafting point and without reaching the root crown. Thus, slits of approx. 15 mm diameter and 5 mm deep were made using a scalpel. The g-C₃N₄-MA-COS NCs loaded with a hydromethanolic extract of *R. tinctorum* (2 mL, at concentrations of 250 and 750 µg·mL⁻¹ against *D. seriata* and *N. parvum*, respectively) were then applied to each of the wounds using a pipette, and it was allowed to dry. Subsequently, a 5 mm diameter agar plug coming from the margin of a fresh 5day-old PDA culture of the fungal species (either *D. seriata* or *N. parvum*) was placed directly in contact with the vascular tissue in the stem at each wound, and the wound was covered with sterile cotton soaked in sterile

bi-distilled water and sealed with Parafilm™ tape. Twenty-eight replicates (plants) were set up for each pathogen, along with four positive controls per pathogen, plus four negative controls (incorporating only the treatment). The plants were kept in a greenhouse with drip irrigation and anti-weed mesh for five months. At the end of the experiment, the plants were removed and two transverse sections of each inoculated stem, between the grafting point and the root crown, were prepared and sectioned longitudinally. The effects of the inoculated fungi were evaluated by measuring the lengths of the longitudinal vascular necroses in each direction from the point of inoculation and comparing them with those observed in the controls. For each inoculation point, a single necrosis length value was obtained by averaging the four necrosis length measurements/wound (upper left, bottom left, upper right, and bottom right). Finally, the two mentioned fungi were re-isolated from the measured lesions and morphologically identified to fulfill Koch's postulates.

2.11. Statistical Analyses

The results of the in vitro mycelium growth inhibition assays were statistically analyzed using one-way analysis of variance (ANOVA), which was followed by a post hoc comparison of means using the Tukey test at $p < 0.05$ given that the homogeneity and homoscedasticity requirements were met according to the Shapiro–Wilk and Levene tests. For the in planta bioassays, in which the normality and homoscedasticity requirements were not met, the Kruskal–Wallis nonparametric test was used instead, with the Conover–Iman test for post hoc multiple pairwise comparisons. R statistical software was used for all of the statistical analyses [35].

3. Results

3.1. Nanocarriers Characterization

3.1.1. Elemental Analysis

Based on the results obtained from the elemental analysis (Table 1), the content of MA in the g-C₃N₄-MA-COS NCs would be in reasonable agreement with what may be expected for a 0.5:0.5:1 ratio. As for the changes in elemental composition after the encapsulation of the *R. tinctorum* extract, taking into consideration that its main phytoconstituents are members of the anthraquinone family, with a C₁₄H₈O₂ empirical formula, the amount of the extract may be close to 14 wt%.

Table 1. EDX elemental analysis results.

Samples	Elemental Composition (%)				Ref.
	C	H	N	O	
Methacrylic acid	55.7	7.0	-	37.3	-
COS	42.9	6.3	6.8	44.0	[36]
g-C ₃ N ₄ (g-C ₃ N ₄ – g-C ₃ N _{4,2} range)	39.4 (32.6–46.1)	10.1 (0–20.3)	50.4 (47.1–53.8)	-	[37]
Methacrylated COS	48.8 (45.5–52.1)	6.5 (5.2–7.8)	3.8 (1.1–6.5)	40.9 (39.0–42.8)	[36]
Methacrylated g-C ₃ N ₄	43.7	-	40.8	15.5	This work
g-C ₃ N ₄ -MA-COS assembly	47.1	-	16.1	36.8	This work
g-C ₃ N ₄ -MA-COS: <i>R. tinctorum</i>	52.1	-	16.1	31.8	This work

3.1.2. Vibrational Characterization

The infrared spectrum of the g-C₃N₄-MA-COS nanocarriers showed absorption bands at 3173, 3050, 2924, 2364, 1635, 1541, 1393, 1332, 1315, 1234, 1206, 1150, 1062, 1023, 891, 809, 702, 614, 522, and 452 cm⁻¹ (Figure 1). The band at 3170 cm⁻¹ corresponds to the amine groups, the band at 3050 cm⁻¹ is due to the C–H stretching vibration, the peak at 1393 cm⁻¹ represents the bending vibration for CH₃ groups, the band at 1062 cm⁻¹ can be assigned to CH₂ wagging from the CH₃ groups, and the band at 698 cm⁻¹ can be assigned to C–C bending. Characteristic absorption bands for chitosan appear at 2364 cm⁻¹ (C–N asymmetric band stretching) and at 1023 and 1150 cm⁻¹ (amine C–N stretching). Since

both the chitosan and methacrylate groups display alkyl C-H stretching at 2924 cm^{-1} , the increase in the intensity of this absorption band evidences the methacrylation [38]. The band at 1541 cm^{-1} arises from alkenyl C=C stretching, while the presence of the amide C=O stretching band at 1635 cm^{-1} supports methacrylation. The peaks at 1332, 1315, 1234, 1206, 891, and 809 cm^{-1} are characteristic of $g\text{-C}_3\text{N}_4$ [39], with the absorption bands at 1332 cm^{-1} and 1234 cm^{-1} being due to C–N stretching vibration [40], and those at 1315 and 809 cm^{-1} are due to triazine rings [41]. It should be noted that the infrared spectrum of the nanocarriers differs from that of the $g\text{-C}_3\text{N}_4\text{-MA}$ precursor by the loss of resolution of the bands, which the latter one exhibits at 1749 and 1719 cm^{-1} . Further, a comparison of FTIR spectra of the empty and *R. tinctorum*-loaded NCs exhibited no relevant spectral changes.

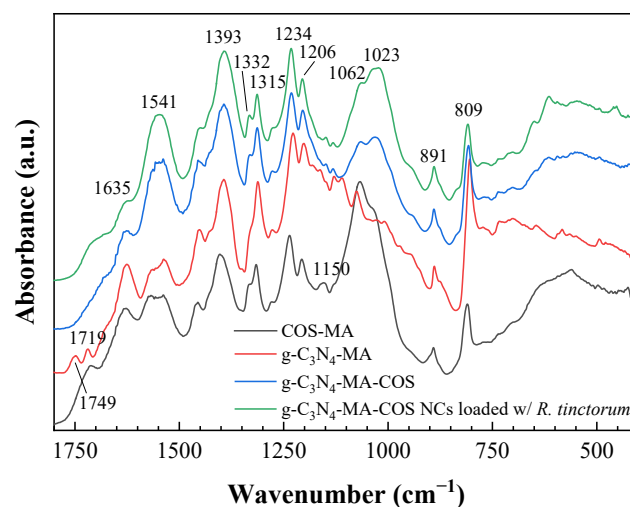


Figure 1. Fingerprint region of the infrared spectra of methacrylated chitosan oligomers (COS-MA), methacrylated graphitic carbon nitride ($g\text{-C}_3\text{N}_4\text{-MA}$), $g\text{-C}_3\text{N}_4\text{-MA-COS}$ nanocarriers, and $g\text{-C}_3\text{N}_4\text{-MA-COS}$ nanocarriers loaded with *R. tinctorum* extract.

3.1.3. Morphology

The transmission electron microscopy images of the nanocarriers showed spherical nanoparticles consisting of an outer assembly of $g\text{-C}_3\text{N}_4\text{-MA-COS}$ and a hollow space (Figure S1) where the phytochemicals can be accommodated, which in this case was the *R. tinctorum* extract (Figure 2). A histogram showing the size distribution is presented in Figure S2. The nanoparticles had a diameter of $85.5 \pm 21.3\text{ nm}$ (mean \pm SD), with a minimum size of 47 nm and a maximum size of 147 nm. The dispersity index value (0.25), which was lower than 0.3, and the existence of a single peak in the size distribution curve, suggest that the particles are monodisperse according to Sadeghi et al. [42].

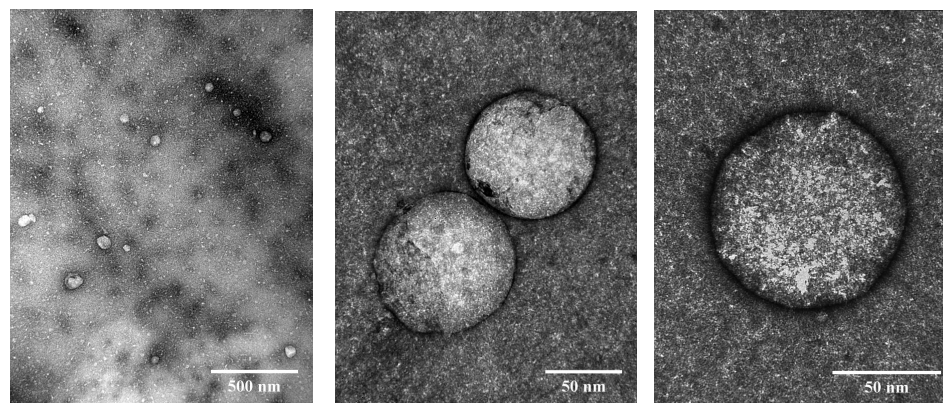


Figure 2. TEM micrographs of $g\text{-C}_3\text{N}_4\text{-MA-COS}$ nanocarriers loaded with *R. tinctorum* extract.

3.1.4. Thermal Analysis

The TG/DTG thermograms of the g-C₃N₄-MA-COS NCs, before and after encapsulation of *R. tinctorum* extract, are shown in Figure 3. Both of the samples showed three main effects at around 215, 346, and 570 °C. The former two effects can be attributed to the depolymerization of chitosan oligomers and decomposition of the substituted sites in the COS-MA moiety, respectively, while the third event may be ascribed to g-C₃N₄ deamination. The encapsulation of the *R. tinctorum* extract resulted in mass (%) differences that reached a maximum at ca. 500 °C, with a behavior similar to the one observed for lignin-MA-COS NCs loaded with the same extract [16]. Concerning the final residue at 750 °C, as expected, it was higher in the empty NCs (28.2%) than it was in the filled NCs (22.5%), and should be mainly attributed to char from COS [43].

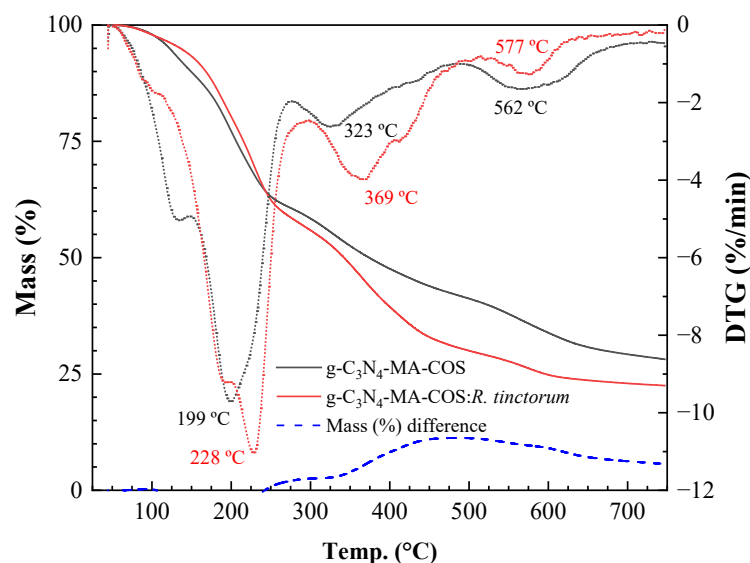


Figure 3. TG (left axis) and DTG (right axis) thermograms of g-C₃N₄-MA-COS NCs: empty NCs (black lines), NCs loaded with *R. tinctorum* extract (red lines).

3.2. Photocatalytic Activity

3.2.1. Rhodamine B Degradation

As expected from the presence of the g-C₃N₄ moiety, the g-C₃N₄-MA-COS nanoparticles exhibited photocatalytic activity under visible light irradiation, and they were able to degrade RhB (while its self-degradation, which is not shown in Figure 4a, was negligible). Under the experimental conditions (pH 6), the efficiency of RhB degradation reached 90% after 90 min of illumination. The dye degradation fitted to the pseudo-first-order kinetics had a calculated degradation constant (k) of 0.025 min⁻¹ ($R^2 = 0.9924$).

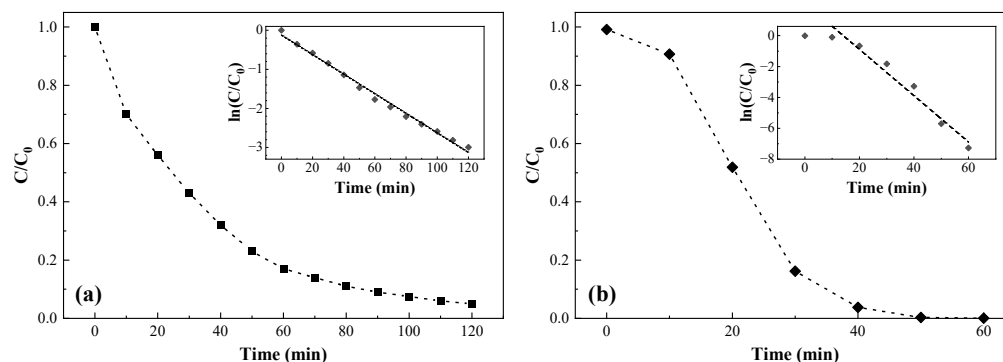


Figure 4. Photocatalytic activity for (a) RhB degradation and (b) U(VI) reduction with g-C₃N₄-MA-COS NCs at pH 6 under visible light irradiation.

3.2.2. Uranium(VI) Reduction

Firstly, the adsorption properties of the NCs for U(VI) were investigated in the dark, and a low removal rate (<5%) over a 24 h period was found. In contrast, a substantial reduction of U(VI) under visible light irradiation was observed, reaching complete removal after 50 min (Figure 4b), with a pseudo-first-order kinetics constant $k = 0.15 \text{ min}^{-1}$ ($R^2 = 0.964$).

3.3. Encapsulation and Release Efficiencies

An almost complete encapsulation (EE = 95–97%) of the *R. tinctorum* extract was achieved. However, the release efficiency upon the enzymatic degradation of the NCs using a commercial chitosanase (EC 3.2.1.132) was substantially lower, with RE values that were in the 74–81% range.

3.4. Antimicrobial Activity

3.4.1. Antibacterial Activity

The g-C₃N₄-MA-COS nanocarriers, in the absence of a bioactive compound inside, inhibited the growth of *X. ampelinus* (the causal agent of bacterial necrosis of grapevines) at a concentration of 1500 µg·mL⁻¹, i.e., at the highest concentration tested, while the NCs loaded with *R. tinctorum* extract presented over 10 times more germicide activity, fully inhibiting the phytopathogen at a dose as low as 125 µg·mL⁻¹ (Table 2).

Table 2. Antibacterial activity of the g-C₃N₄-MA-COS nanocarriers (NCs), before and after the encapsulation of *R. tinctorum* extract, against the phytopathogen *X. ampelinus*.

Treatment	Concentration (µg·mL ⁻¹)									
	62.5	93.75	125	187.5	250	375	500	750	1000	1500
Empty NCs	+	+	+	+	+	+	+	+	+	–
NCs loaded with <i>R. tinctorum</i>	+	+	–	–	–	–	–	–	–	–

“+” and “–” indicate the presence and absence of bacterial growth, respectively.

3.4.2. Antifungal Activity

Figure 5 shows the radial growth of the *D. seriata* and *N. parvum* colonies for the g-C₃N₄-MA-COS NCs, before and after the encapsulation of *R. tinctorum* extract. It could be observed that, in the absence of a bioactive compound, the NCs failed to fully inhibit mycelial growth in either of the phytopathogens studied. However, when they were loaded with an extract of *R. tinctorum*, the full inhibition of mycelial growth was achieved at a concentration of 250 and 750 µg·mL⁻¹ for *D. seriata* and *N. parvum*, respectively.

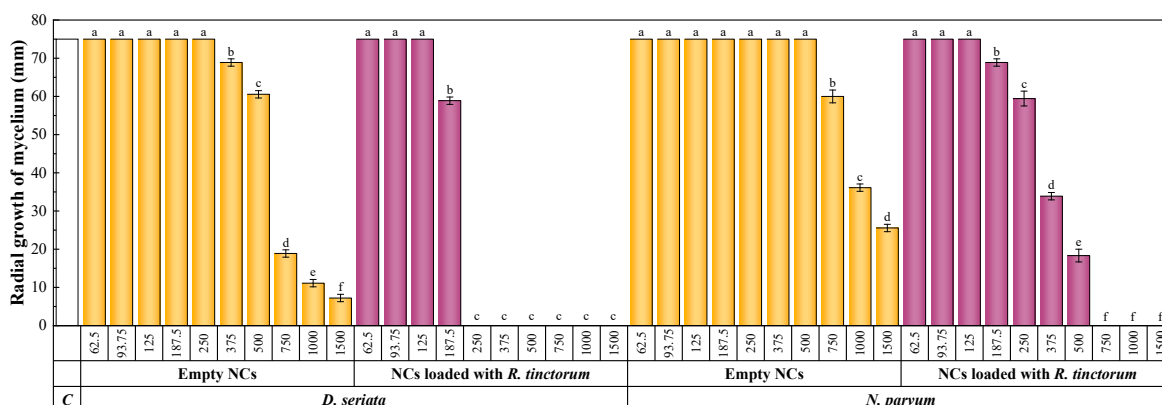


Figure 5. Diameter (in mm) of the mycelial growth of *D. seriata* and *N. parvum* for different concentrations of the g-C₃N₄-MA-COS nanocarriers, before and after the encapsulation of *R. tinctorum* extract. The letters above concentrations indicate that they are not significantly different at $p < 0.05$. ‘C’ and ‘NCs’ stand for control and nanocarriers, respectively.

3.4.3. In Planta Bioassays

As a first step towards field application, the NCs were assayed as a wound protection treatment against two fungal pathogens of the family *Botryosphaeriaceae* associated with grapevine black dead arm disease in greenhouse conditions (Figure 6). The MIC values determined in the previous section were chosen as the application dose (i.e., 250 and 750 $\mu\text{g}\cdot\text{mL}^{-1}$ for *D. seriata* and *N. parvum*, respectively). Statistically significant differences were found in the longitudinal vascular necroses between the plants that were treated with the g-C₃N₄-MA-COS NCs loaded with the *R. tinctorum* hydromethanolic extract and the positive controls (Table 3), confirming that they had some protective effect against both of the trunk pathogens. No phytotoxicity symptoms were observed in the negative controls.



Figure 6. (a) General view of the in planta assay; (b) application of the *R. tinctorum* extract-loaded NCs on one of the wounds made on a young ‘Tempranillo’ grapevine plant; (c) necrosis lengths in control plants; (d) necrosis lengths in treated plants. Bars = 1 cm. Necrosis lengths are indicated with arrows to facilitate identification.

Table 3. Results of the Kruskal–Wallis tests followed by multiple pairwise comparisons using the Conover–Iman procedure performed on the necrosis lengths caused by *D. seriata* and *N. parvum*. The mean of ranks values accompanied by the same letters are not significantly different (p -value (one-tailed) < 0.047 and 0.031 for *D. seriata* and *N. parvum*, respectively; $\alpha = 0.05$).

Treatment	<i>D. seriata</i>		<i>N. parvum</i>	
	Mean of Ranks	Groups	Mean of Ranks	Groups
NCs- <i>R. tinctorum</i>	30.750	A	30.607	A
Control	44.750	B	45.750	B

4. Discussion

4.1. On the Nanocarriers Structure and the Encapsulation Mechanism

The characterization results, in particular, the TEM micrographs, evidenced the g-C₃N₄-MA-COS assembly as being typical of nanocarriers. Nevertheless, the binding of their moieties remains an unsolved problem. It can be hypothesized that it is the result of grafting one of the moieties onto the other (Figure 7), but a polymeric scaffold cannot be ruled out.

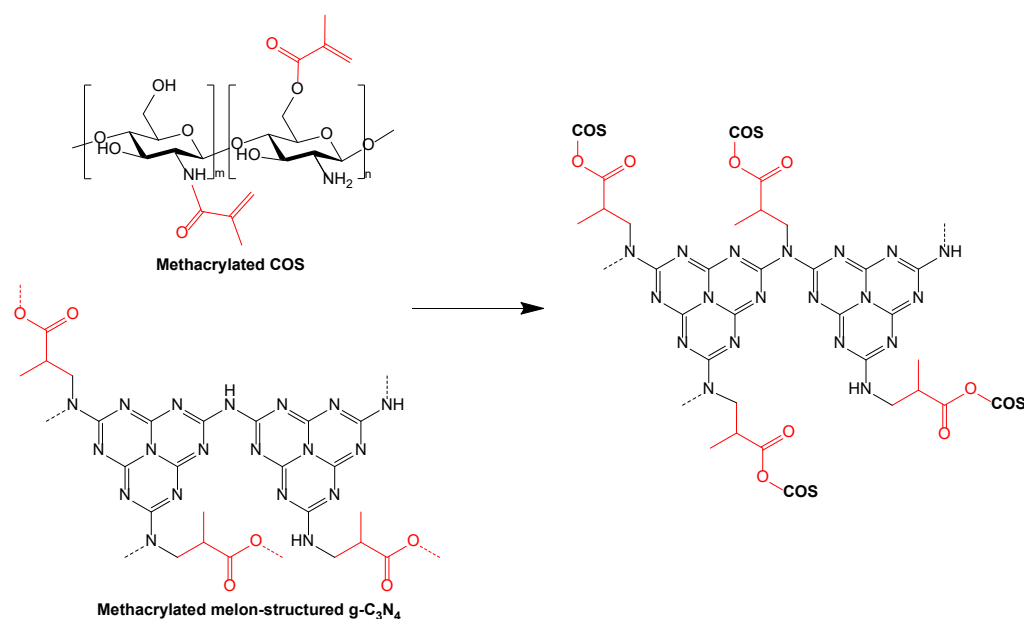


Figure 7. Hypothetical assembly of the methacrylated COS and methacrylated $g\text{-C}_3\text{N}_4$ moieties.

Concerning the nature of the encapsulation of *R. tinctorum* phytochemicals in $g\text{-C}_3\text{N}_4\text{-MA-COS}$ NCs, one would have to consider whether it would be based on physical or chemical entrapment. In the case of physical entrapment, no changes or minimal changes in the vibrational spectrum compared to the parent compounds would be expected, whereas in chemical entrapment, spectral changes might occur due to a possible chemical interaction between the extract components and the NCs [44]. Given that the encapsulation of *R. tinctorum* in the NCs resulted in no shifts of the characteristic bands of the FTIR spectra, thus suggesting that there was no modification or interaction between the ‘shell’ assembly and the phytochemicals, it may be safely assumed that the extract was physically entrapped (encapsulated) within the NCs, which is in agreement with other works [45,46].

4.2. Photocatalytic Activity

Concerning RhB degradation, the pseudo-first-order kinetics constant obtained in the experiment ($k = 0.025 \text{ min}^{-1}$) was about 3.8 times higher than that which was reported for the reduced graphene oxide/chitosan composite aerogels supported $g\text{-C}_3\text{N}_4$ photocatalyst ($k = 0.0065 \text{ min}^{-1}$) [47] and it was comparable to the value reported by Xu et al. [48] for a chitosan/ $\text{TiO}_2@g\text{-C}_3\text{N}_4$ nanocomposite membrane (0.0238 min^{-1}), although it should be noted that operative conditions were different ($30 \text{ mg}\cdot\text{L}^{-1}$ RhB, $\text{pH} = 2$, and a 30 W LED lamp in the former study, and $5 \text{ mg}\cdot\text{L}^{-1}$ RhB and 100 W LED lamp in the latter one), so comparisons should be made with caution. If a comparison with pristine (non-doped) $g\text{-C}_3\text{N}_4$ was made, the reported k value would be intermediate between those of $g\text{-C}_3\text{N}_4$ and high-surface-area porous $g\text{-C}_3\text{N}_4$ (0.014 and 0.131 min^{-1} , respectively) reported by Dong and Zhang [31]. It is worth noting that the indicated degradation rate would also be highly influenced by the pH value (six in our case for consistency reasons, provided that it is the usual choice in U(VI) reduction experiments) given that it substantially increases with the decrease in the pH values [49].

As for uranium(VI) reduction, no examples of composites consisting of $g\text{-C}_3\text{N}_4$ and chitosan have been reported in the literature, so a comparison with $g\text{-C}_3\text{N}_4$ -only experiments was provided instead. The removal rate ($k = 0.15 \text{ min}^{-1}$) was intermediate between those of the bulk pristine $g\text{-C}_3\text{N}_4$ ($0.04/0.06 \text{ min}^{-1}$) and the highly mesoporous $g\text{-C}_3\text{N}_4$ samples (0.27 min^{-1}) prepared using silica NPs ($\sim 12 \text{ nm}$) as a template [32,50] and it was comparable to other values obtained for pristine $g\text{-C}_3\text{N}_4$ and different $g\text{-C}_3\text{N}_4$ /co-catalyst systems, although k values in the $0.05\text{--}0.42 \text{ min}^{-1}$ range have been reported [51]. Again, although the pH was the same in all of the aforementioned studies, different initial concen-

trations of U(VI) and photocatalyst:U(VI) ratios were employed, so comparisons are made merely by way of guidance.

4.3. On the Antimicrobial Activity

With regard to the antibacterial activity, to the best of the authors' knowledge, no data on the efficacy of the *R. tinctorum* extract against *X. ampelinus* are available. Nonetheless, previous studies in which the bactericidal activity of COS has been evaluated against the same isolate showed that the bacterial growth was completely inhibited at $1500 \mu\text{g}\cdot\text{mL}^{-1}$ [52–55], which is a similar MIC to the one that was obtained in this work for the empty g-C₃N₄-MA-COS NCs.

As for the antifungal activity, a comparison of the EC₅₀ and EC₉₀ concentrations (i.e., the concentrations at which mycelial growth was inhibited by 50 and 90%, respectively) obtained for the *R. tinctorum*-loaded NCs versus those obtained for the unencapsulated *R. tinctorum* extract, which was previously reported in [26] against the same fungal isolates, is presented in Table 4. If the actual bioactive product weight is considered (ca. 14 wt%, according to elemental analysis results), the corrected EC₅₀ and EC₉₀ values would be noticeably lower than those that were obtained with the unencapsulated *R. tinctorum* extract. Although such a finding would support the hypothesis that the controlled release properties of the NCs would minimize wastage and leaching of the active ingredients, it should be taken as a first approximation given that the contribution of COS to the antifungal activity has been discarded (a simplification supported by its noticeably higher EC₉₀ values, viz. 1180 and $1327 \mu\text{g}\cdot\text{mL}^{-1}$ against *D. seriata* and *N. parvum*, respectively [56]).

Table 4. Comparison between the effective concentrations (EC₅₀ and EC₉₀, in $\mu\text{g}\cdot\text{mL}^{-1}$) against *D. seriata* and *N. parvum* of the g-C₃N₄-MA-COS nanocarriers loaded with *R. tinctorum* extract and those of the equivalent encapsulated and non-encapsulated *R. tinctorum* extracts.

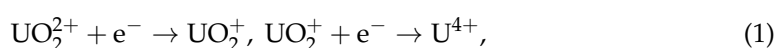
Pathogen	Effective Concentration	g-C ₃ N ₄ -MA-COS- <i>R. tinctorum</i>	Encapsulated <i>R. tinctorum</i> (ca. 14 wt%)	<i>R. tinctorum</i> Extract [26]
<i>D. seriata</i>	EC ₅₀	193.1	27.0	78.0
	EC ₉₀	241.0	33.7	87.8
<i>N. parvum</i>	EC ₅₀	362.7	50.8	92.3
	EC ₉₀	631.5	88.4	184.0

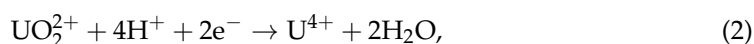
Regarding the in vivo results, it should be noted that the protective effect was limited by the assayed dose (i.e., the previously in vitro-determined MICs were 250 and $750 \mu\text{g}\cdot\text{mL}^{-1}$ for *D. seriata* and *N. parvum*, respectively), which suggests that a higher concentration would be needed to achieve full protection (in terms of reduction of vascular necrosis) in the field tests against the two pathogens.

4.4. Mechanism of Action

With regard to the photocatalytic activity, it should be only ascribed to the g-C₃N₄ moiety. In the case of RhB degradation, the photocatalytic pathway includes N-de-ethylation, chromophore structure cleavage, ring-opening, and mineralization processes [57]. Although hydroxyl radicals ($\bullet\text{OH}$) generated via the electron-induced multistep reduction of O₂ (induced by the light irradiation of g-C₃N₄) have generally been considered to be the main reactive oxidation species [58], more recent works have suggested that photogenerated superoxide (O₂ \bullet or HOO \bullet) species would play a major role in the photocatalytic process [57].

In relation to the U(VI) photocatalytic reduction mechanism, it is not fully understood, but Zhang et al. [51], based on a thorough review of the state-of-the-art, suggested two possible mechanisms:





with an associated redox potential (vs. NHE) that was in the +0.062 to +0.31 range in the case of Equation (1) (single photogenerated electron reduction process) and between +0.267 and +0.57 in the case of Equation (2) (in the presence of acidity and two photogenerated electrons).

Concerning the antimicrobial applications, it should be noted that antimicrobial activity has been reported for both g-C₃N₄ and COS. In the case of g-C₃N₄, it is ascribed to photocatalytic reactive oxygen species (ROS) generation [59], while in the case of COS, different mechanisms of action have been proposed [60], including the interaction of the positively charged COS with negatively charged phospholipid components (which results in increased membrane permeability and the leakage of cellular contents), the deprivation to fungi of trace elements that are essential for normal growth due to COS chelating action, and the inhibition of mRNA synthesis due to its binding to fungal DNA (which affects protein and enzyme production). However, as shown in the in vitro studies, the effectiveness of the empty NCs against the assayed pathogens would be very limited as they have high MIC values. Thus, the influence of the g-C₃N₄-MA-COS shell on the antimicrobial activity may be regarded as being negligible in comparison to that of the encapsulated product, and the role of the NCs in these potential applications would be mainly restricted to the targeted delivery of the bioactive products.

In this regard, in a similar fashion to previously reported lignin-based NCs, which successfully inhibited the growth of ligninolytic enzymes-producing microorganisms by releasing encapsulated fungicides [15], the presence of the COS moiety in the NCs studied herein may be useful to selectively release the encapsulated bioproducts (in this case, *R. tinctorum* extract) against bacterial and fungal pathogens. Such a release would be triggered upon the interaction with the chitosanase produced by the microorganisms, which would degrade the g-C₃N₄-MA-COS shell and selectively release its content. For instance, in the case of *N. parvum*, the chitosanolytic activity of the fungus is well established, and endo-chitosanase (GH75, R1GTL6) has been shown to have a central role in the host infection mechanism [61]. It should also be noted that, albeit they are less specific and have a lower efficiency, chitinases and cellulases also break down chitosan [62], and these enzymes are widely present in *Botryosphaeriaceae* and other wood-degrading fungi [63], suggesting that there is a wide applicability of the NC-based treatments.

Finally, concerning the *R. tinctorum* antimicrobial activity, it may be ascribed to a combined effect of both the anthraquinones and phenols present in the extract [26].

4.5. Limitations of the Study and Prospects of Nanocarriers for Agrochemical Delivery

The data presented herein support the rationale that the nanocarriers consisting of naturally or synthetically sourced polymers and inorganic materials can enhance the stability and performance of a broad range of active ingredients, which is in agreement with Pinto et al. [3]. However, despite their promising efficacy, the questions of economy and scalability must still be addressed in subsequent studies to determine whether these NCs may be scalable and transformable into economically viable solutions to solve present and future agricultural problems (i.e., technical constraints concerning the production of NCs for use in agriculture should be correlated with the economical boundaries which limit the production costs and configure the potential revenues for the producers [2]). Further, the issues related to safety assessment, evaluation standards, registration policies, and public concern should also be addressed, as noted by An et al. [64].

Concerning the NCs' prospective practical use, it is worth noting that the current level of knowledge does not yet allow a fair and unbiased assessment of the pros and cons that will arise from the use of nano-based systems for the encapsulation of bioactive products and their use in agriculture. Nonetheless, one may be optimistic about the applicability of NCs such as the ones presented in this work given that at the moment there are already over 200 products commercialized worldwide that can be classified as nano-based products

in agriculture and that the nanotechnology market in the agricultural sector is expected to grow at a compound annual growth rate of ca. 28% [4].

5. Conclusions

In this work, methacrylate anhydride was shown to be an efficient cross-linking agent to bind g-C₃N₄ and COS in a weight ratio of 0.5:1, leading to the formation of monodisperse nanocarriers with a mean size of 85.5 ± 21.3 nm. Regardless of whether the g-C₃N₄-MA-COS assembly is considered to be the result of grafting one of its moieties onto the other or a polymeric scaffold, the photocatalytic activity and the behavior as carriers for the targeted delivery of bioactive products have been demonstrated. Due to the presence of the g-C₃N₄ moiety, the nanocarriers were able to efficiently photodegrade RhB and photoreduce U(VI) with rate constants of 0.025 and 0.15 min⁻¹, respectively, which are higher than those of bulk pristine g-C₃N₄. In turn, the presence of the COS moiety allowed a selective release of encapsulated *R. tinctorum* extract against certain grapevine phytopathogens. The in vitro results supported the more efficient use of the bioactive product, with MIC values that are noticeably lower than those which were obtained with the unencapsulated extract. Moreover, the application of the extract-loaded NCs as a pruning wound protection product in young ‘Tempranillo’ grapevine plants that were artificially infected with *N. parvum* and *D. seriata* resulted in a significant reduction in the necrosis lengths. Therefore, g-C₃N₄-MA-COS nanocarriers may hold promise as a multifunctional platform as they are more versatile than conventional chitosan-based nanoparticles are for environmental and agrochemical delivery applications.

6. Patents

The work reported in this manuscript is related to the Spanish patent with application number P202230668 (‘Nanomaterial basado en el autoensamblaje de g-C₃N₄ y oligómeros de quitosano, proceso de obtención y usos’ which translates as ‘Nanomaterial based on self-assembly of g-C₃N₄ and chitosan oligomers, obtaining process and uses’ (tr.)), which was filed on 20 July 2022.

Supplementary Materials: The following supporting information can be downloaded at: <https://www.mdpi.com/article/10.3390/ma15248981/s1>, Figure S1. TEM micrographs of empty g-C₃N₄-MA-COS nanocarriers without negative staining (upper left) and with negative staining (other five images) at different magnifications; Figure S2. Histogram of the nanocarrier size distribution.

Author Contributions: Conceptualization, J.M.-G.; methodology, J.M.-G., V.G.-G. and J.C.-G.; validation, J.C.-G.; formal analysis, A.S.-A., E.S.-H., J.C.-G. and P.M.-R.; investigation, A.S.-A., E.S.-H., N.L.-L., V.G.-G., J.C.-G., J.M.-G. and P.M.-R.; resources, J.M.-G.; writing—original draft preparation, A.S.-A., E.S.-H., N.L.-L., V.G.-G., J.C.-G., J.M.-G. and P.M.-R.; writing—review and editing, A.S.-A., E.S.-H., V.G.-G. and P.M.-R.; visualization, A.S.-A. and E.S.-H.; supervision, P.M.-R.; project administration, J.M.-G.; funding acquisition, J.M.-G. All authors have read and agreed to the published version of the manuscript.

Funding: This research was funded by Junta de Castilla y León under project VA258P18, and FEDER co-funded it.

Institutional Review Board Statement: Not applicable.

Informed Consent Statement: Not applicable.

Data Availability Statement: The data presented in this study are available on request from the corresponding author. The data are not publicly available due to their relevance to an ongoing Ph.D. thesis.

Acknowledgments: The authors thank the Fundación General de la Universidad de Valladolid for funding the patent through the ‘Prometeo’ program. The authors would also like to thank to Advanced Microscopy Unit of the Science Park Foundation from the University of Valladolid for conducting the transmission electron microscope (TEM) characterization.

Conflicts of Interest: The authors declare no conflict of interest. The funder had no role in the design of the study; in the collection, analyses, or interpretation of data; in the writing of the manuscript, or in the decision to publish the results.

References

1. Shah, A.; Aftab, S.; Nisar, J.; Ashiq, M.N.; Iftikhar, F.J. Nanocarriers for targeted drug delivery. *J. Drug Deliv. Sci. Technol.* **2021**, *62*, 102426. [[CrossRef](#)]
2. Vega-Vásquez, P.; Mosier, N.S.; Irudayaraj, J. Nanoscale drug delivery systems: From Medicine to Agriculture. *Front. Bioeng. Biotechnol.* **2020**, *8*, 79. [[CrossRef](#)] [[PubMed](#)]
3. Pinto, T.V.; Silva, C.A.; Siquenique, S.; Learmonth, D.A. Micro- and nanocarriers for encapsulation of biological plant protection agents: A systematic literature review. *ACS Agric. Sci. Technol.* **2022**, *2*, 838–857. [[CrossRef](#)]
4. Machado, T.O.; Grabow, J.; Sayer, C.; de Araújo, P.H.H.; Ehrenhard, M.L.; Wurm, F.R. Biopolymer-based nanocarriers for sustained release of agrochemicals: A review on materials and social science perspectives for a sustainable future of agri- and horticulture. *Adv. Colloid Interface Sci.* **2022**, *303*, 102645. [[CrossRef](#)] [[PubMed](#)]
5. Maluin, F.N.; Hussein, M.Z. Chitosan-based agronanochemicals as a sustainable alternative in crop protection. *Molecules* **2020**, *25*, 1611. [[CrossRef](#)]
6. Jakhari, A.M.; Aziz, I.; Kaleri, A.R.; Hasnain, M.; Haider, G.; Ma, J.; Abideen, Z. Nano-fertilizers: A sustainable technology for improving crop nutrition and food security. *NanoImpact* **2022**, *27*, 100411. [[CrossRef](#)]
7. Pal, P.; Pal, A.; Nakashima, K.; Yadav, B.K. Applications of chitosan in environmental remediation: A review. *Chemosphere* **2021**, *266*, 128934. [[CrossRef](#)]
8. Benettayeb, A.; Ghosh, S.; Usman, M.; Seihoub, F.Z.; Sohoo, I.; Chia, C.H.; Sillanpää, M. Some well-known alginate and chitosan modifications used in adsorption: A review. *Water* **2022**, *14*, 1353. [[CrossRef](#)]
9. Li, P.-W.; Wang, G.; Yang, Z.-M.; Duan, W.; Peng, Z.; Kong, L.-X.; Wang, Q.-H. Development of drug-loaded chitosan–vanillin nanoparticles and its cytotoxicity against HT-29 cells. *Drug Deliv.* **2014**, *23*, 30–35. [[CrossRef](#)]
10. Huang, Y.; Cai, Y.; Lapitsky, Y. Factors affecting the stability of chitosan/tripolyphosphate micro- and nanogels: Resolving the opposing findings. *J. Mater. Chem. B* **2015**, *3*, 5957–5970. [[CrossRef](#)]
11. Samani, S.; Bonakdar, S.; Farzin, A.; Hadjati, J.; Azami, M. A facile way to synthesize a photocrosslinkable methacrylated chitosan hydrogel for biomedical applications. *Int. J. Polym. Mater. Polym. Biomater.* **2020**, *70*, 730–741. [[CrossRef](#)]
12. Gruppuso, M.; Iorio, F.; Turco, G.; Marsich, E.; Porrelli, D. Hyaluronic acid/lactose-modified chitosan electrospun wound dressings—Crosslinking and stability criticalities. *Carbohydr. Polym.* **2022**, *288*, 119375. [[CrossRef](#)]
13. D’Amora, U.; Ronca, A.; Raucci, M.G.; Lin, H.; Soriente, A.; Fan, Y.; Zhang, X.; Ambrosio, L. Bioactive composites based on double network approach with tailored mechanical, physico-chemical, and biological features. *J. Biomed. Mater. Res. Part A* **2018**, *106*, 3079–3089. [[CrossRef](#)]
14. Yu, L.M.Y.; Kazazian, K.; Shoichet, M.S. Peptide surface modification of methacrylamide chitosan for neural tissue engineering applications. *J. Biomed. Mater. Res. Part A* **2007**, *82A*, 243–255. [[CrossRef](#)]
15. Machado, T.O.; Beckers, S.J.; Fischer, J.; Müller, B.; Sayer, C.; de Araújo, P.H.H.; Landfester, K.; Wurm, F.R. Bio-based lignin nanocarriers loaded with fungicides as a versatile platform for drug delivery in plants. *Biomacromolecules* **2020**, *21*, 2755–2763. [[CrossRef](#)]
16. Sánchez-Hernández, E.; Langa-Lomba, N.; González-García, V.; Casanova-Gascón, J.; Martín-Gil, J.; Santiago-Aliste, A.; Torres-Sánchez, S.; Martín-Ramos, P. Lignin–chitosan nanocarriers for the delivery of bioactive natural products against wood-decay phytopathogens. *Agronomy* **2022**, *12*, 461. [[CrossRef](#)]
17. Rajabzadeh-Khosroshahi, M.; Pourmadadi, M.; Yazdian, F.; Rashedi, H.; Navaei-Nigjeh, M.; Rasekh, B. Chitosan/agarose/graphitic carbon nitride nanocomposite as an efficient pH-sensitive drug delivery system for anticancer curcumin releasing. *J. Drug Deliv. Sci. Technol.* **2022**, *74*, 103443. [[CrossRef](#)]
18. Yang, X.; Ye, Y.; Sun, J.; Li, Z.; Ping, J.; Sun, X. Recent advances in g-C₃N₄-based photocatalysts for pollutant degradation and bacterial disinfection: Design strategies, mechanisms, and applications. *Small* **2021**, *18*, 2105089. [[CrossRef](#)]
19. Liu, X.; Ma, R.; Zhuang, L.; Hu, B.; Chen, J.; Liu, X.; Wang, X. Recent developments of doped g-C₃N₄ photocatalysts for the degradation of organic pollutants. *Crit. Rev. Environ. Sci. Technol.* **2020**, *51*, 751–790. [[CrossRef](#)]
20. Gupta, B.; Gupta, A.K. Photocatalytic performance of 3D engineered chitosan hydrogels embedded with sulfur-doped C₃N₄/ZnO nanoparticles for Ciprofloxacin removal: Degradation and mechanistic pathways. *Int. J. Biol. Macromol.* **2022**, *198*, 87–100. [[CrossRef](#)]
21. Ni, Y.; Nie, H.; Wang, J.; Lin, J.; Wang, Q.; Sun, J.; Zhang, W.; Wang, J. Enhanced functional properties of chitosan films incorporated with curcumin-loaded hollow graphitic carbon nitride nanoparticles for bananas preservation. *Food Chem.* **2022**, *366*, 130539. [[CrossRef](#)] [[PubMed](#)]
22. Yılmaz Baran, N.; Baran, T.; Çalışkan, M. Production of Pd nanoparticles embedded on micro-sized chitosan/graphitic carbon nitride hybrid spheres for treatment of environmental pollutants in aqueous medium. *Ceram. Int.* **2021**, *47*, 27736–27747. [[CrossRef](#)]

23. Santos-Moriano, P.; Fernandez-Arrojo, L.; Mengibar, M.; Belmonte-Reche, E.; Peñalver, P.; Acosta, F.N.; Ballesteros, A.O.; Morales, J.C.; Kidibule, P.; Fernandez-Lobato, M.; et al. Enzymatic production of fully deacetylated chitoooligosaccharides and their neuroprotective and anti-inflammatory properties. *Biocatal. Biotransform.* **2017**, *36*, 57–67. [[CrossRef](#)]
24. Tian, M.; Tan, H.; Li, H.; You, C. Molecular weight dependence of structure and properties of chitosan oligomers. *RSC Adv.* **2015**, *5*, 69445–69452. [[CrossRef](#)]
25. Dante, R.C.; Martín-Ramos, P.; Sánchez-Arévalo, F.M.; Huerta, L.; Bizarro, M.; Navas-Gracia, L.M.; Martín-Gil, J. Synthesis of crumpled nanosheets of polymeric carbon nitride from melamine cyanurate. *J. Solid State Chem.* **2013**, *201*, 153–163. [[CrossRef](#)]
26. Langa-Lomba, N.; Sánchez-Hernández, E.; Buzón-Durán, L.; González-García, V.; Casanova-Gascón, J.; Martín-Gil, J.; Martín-Ramos, P. Activity of anthracenediones and flavoring phenols in hydromethanolic extracts of *Rubia tinctorum* against grapevine phytopathogenic fungi. *Plants* **2021**, *10*, 1527. [[CrossRef](#)]
27. Sánchez-Hernández, E.; Santiago-Aliste, A.; Martín-Gil, J.; Martín-Ramos, P. Nanomaterial Basado en el Autoensamblaje de g-C₃N₄ y Oligómeros de Quitosano, Proceso de Obtención y Usos. Patent P202230668, 20 July 2022.
28. Fischer, J.; Beckers, S.J.; Yiamsawas, D.; Thines, E.; Landfester, K.; Wurm, F.R. Targeted drug delivery in plants: Enzyme-responsive lignin nanocarriers for the curative treatment of the worldwide grapevine trunk disease Esca. *Adv. Sci.* **2019**, *6*, 1802315. [[CrossRef](#)]
29. Krizsán, K.; Szókán, G.; Toth, Z.A.; Hollósy, F.; László, M.; Khlafulla, A. HPLC analysis of anthraquinone derivatives in madder root (*Rubia tinctorum*) and its cell cultures. *J. Liq. Chromatogr. Relat. Technol.* **2006**, *19*, 2295–2314. [[CrossRef](#)]
30. Tiunov, I.A.; Gorbachevskyy, M.V.; Kopitsyn, D.S.; Kotelev, M.S.; Ivanov, E.V.; Vinokurov, V.A.; Novikov, A.A. Synthesis of large uniform gold and core-shell gold-silver nanoparticles: Effect of temperature control. *Russ. J. Phys. Chem. A* **2016**, *90*, 152–157. [[CrossRef](#)]
31. Dong, G.; Zhang, L. Porous structure dependent photoreactivity of graphitic carbon nitride under visible light. *J. Mater. Chem.* **2012**, *22*, 1160–1166. [[CrossRef](#)]
32. Wang, J.; Wang, Y.; Wang, W.; Ding, Z.; Geng, R.; Li, P.; Pan, D.; Liang, J.; Qin, H.; Fan, Q. Tunable mesoporous g-C₃N₄ nanosheets as a metal-free catalyst for enhanced visible-light-driven photocatalytic reduction of U(VI). *Chem. Eng. J.* **2020**, *383*, 123193. [[CrossRef](#)]
33. *CLSI Standard M07*; Methods for Dilution Antimicrobial Susceptibility Tests for Bacteria that Grow Aerobically. 11th ed. Clinical and Laboratory Standards Institute: Wayne, PA, USA, 2018; 112p.
34. Arendrup, M.C.; Cuenca-Estrella, M.; Lass-Flörl, C.; Hope, W. EUCAST technical note on the EUCAST definitive document EDef 7.2: Method for the determination of broth dilution minimum inhibitory concentrations of antifungal agents for yeasts EDef 7.2 (EUCAST-AFST). *Clin. Microbiol. Infect.* **2012**, *18*, E246–E247. [[CrossRef](#)]
35. R Core Team. *R: A Language and Environment for Statistical Computing*; R Foundation for Statistical Computing: Vienna, Austria, 2022.
36. Cankaya, N. Grafting of chitosan: Structural, thermal and antimicrobial properties. *J. Chem. Soc. Pak.* **2019**, *41*, 240. [[CrossRef](#)]
37. Alwin, E.; Kočí, K.; Wojcieszak, R.; Zieliński, M.; Edelmánová, M.; Pietrowski, M. Influence of high temperature synthesis on the structure of graphitic carbon nitride and its hydrogen generation ability. *Materials* **2020**, *13*, 2756. [[CrossRef](#)]
38. Kolawole, O.M.; Lau, W.M.; Khutoryanskiy, V.V. Methacrylated chitosan as a polymer with enhanced mucoadhesive properties for transmucosal drug delivery. *Int. J. Pharm.* **2018**, *550*, 123–129. [[CrossRef](#)]
39. Shcherban, N.D.; Mäki-Arvela, P.; Aho, A.; Sergiienko, S.A.; Yaremov, P.S.; Eränen, K.; Murzin, D.Y. Melamine-derived graphitic carbon nitride as a new effective metal-free catalyst for Knoevenagel condensation of benzaldehyde with ethylcyanoacetate. *Catal. Sci. Technol.* **2018**, *8*, 2928–2937. [[CrossRef](#)]
40. Xu, R.; Peng, Y. Preparation of magnetic g-C₃N₄/Fe₃O₄ composite and its application in the separation of catechol from water. *Materials* **2019**, *12*, 2844. [[CrossRef](#)]
41. Guo, Q.; Xie, Y.; Wang, X.; Lv, S.; Hou, T.; Liu, X. Characterization of well-crystallized graphitic carbon nitride nanocrystallites via a benzene-thermal route at low temperatures. *Chem. Phys. Lett.* **2003**, *380*, 84–87. [[CrossRef](#)]
42. Sadeghi, R.; Etemad, S.G.; Keshavarzi, E.; Haghshenasfard, M. Investigation of alumina nanofluid stability by UV-vis spectrum. *Microfluid. Nanofluidics* **2015**, *18*, 1023–1030. [[CrossRef](#)]
43. Nisticò, R.; Lavagna, L.; Versaci, D.; Ivanchenko, P.; Benzi, P. Chitosan and its char as fillers in cement-base composites: A case study. *Bol. Soc. Española Cerám. Vidr.* **2020**, *59*, 186–192. [[CrossRef](#)]
44. Esmaeili, A.; Asgari, A. In vitro release and biological activities of *Carum copticum* essential oil (CEO) loaded chitosan nanoparticles. *Int. J. Biol. Macromol.* **2015**, *81*, 283–290. [[CrossRef](#)] [[PubMed](#)]
45. Shetta, A.; Kegere, J.; Mamdouh, W. Comparative study of encapsulated peppermint and green tea essential oils in chitosan nanoparticles: Encapsulation, thermal stability, in-vitro release, antioxidant and antibacterial activities. *Int. J. Biol. Macromol.* **2019**, *126*, 731–742. [[CrossRef](#)]
46. Soltanzadeh, M.; Peighambaroust, S.H.; Ghanbarzadeh, B.; Mohammadi, M.; Lorenzo, J.M. Chitosan nanoparticles as a promising nanomaterial for encapsulation of pomegranate (*Punica granatum* L.) peel extract as a natural source of antioxidants. *Nanomaterials* **2021**, *11*, 1439. [[CrossRef](#)] [[PubMed](#)]
47. Pan, H.; Gu, J.; Hou, K.; Li, J.; Wang, Y.; Yue, Y. High-efficiency, compressible, and recyclable reduced graphene oxide/chitosan composite aerogels supported g-C₃N₄/BiOBr photocatalyst for adsorption and degradation of rhodamine B. *J. Environ. Chem. Eng.* **2022**, *10*, 107157. [[CrossRef](#)]

48. Xu, S.; Xiao, G.; Wang, Z.; Wang, Y.; Liu, Z.; Su, H. A reusable chitosan/TiO₂@g-C₃N₄ nanocomposite membrane for photocatalytic removal of multiple toxic water pollutants under visible light. *Water Sci. Technol.* **2021**, *83*, 3063–3074. [[CrossRef](#)]
49. Shi, W.; Fang, W.-X.; Wang, J.-C.; Qiao, X.; Wang, B.; Guo, X. pH-controlled mechanism of photocatalytic RhB degradation over g-C₃N₄ under sunlight irradiation. *Photochem. Photobiol. Sci.* **2021**, *20*, 303–313. [[CrossRef](#)]
50. Gong, J.; Xie, Z.; Wang, B.; Li, Z.; Zhu, Y.; Xue, J.; Le, Z. Fabrication of g-C₃N₄-based conjugated copolymers for efficient photocatalytic reduction of U(VI). *J. Environ. Chem. Eng.* **2021**, *9*, 104638. [[CrossRef](#)]
51. Zhang, W.; Li, L.; Gao, Y.; Zhang, D. Graphitic carbon nitride-based materials for photocatalytic reduction of U(VI). *New J. Chem.* **2020**, *44*, 19961–19976. [[CrossRef](#)]
52. Sánchez-Hernández, E.; Buzón-Durán, L.; Andrés-Juan, C.; Lorenzo-Vidal, B.; Martín-Gil, J.; Martín-Ramos, P. Physicochemical characterization of *Crithmum maritimum* L. and *Daucus carota* subsp. *gummifer* (Syme) Hook.fil. and their antimicrobial activity against apple tree and grapevine phytopathogens. *Agronomy* **2021**, *11*, 886. [[CrossRef](#)]
53. Sánchez-Hernández, E.; Buzón-Durán, L.; Langa-Lomba, N.; Casanova-Gascón, J.; Lorenzo-Vidal, B.; Martín-Gil, J.; Martín-Ramos, P. Characterization and antimicrobial activity of a halophyte from the Asturian coast (Spain): *Limonium binervosum* (G.E.Sm.) C.E.Salmon. *Plants* **2021**, *10*, 1852. [[CrossRef](#)]
54. Sánchez-Hernández, E.; Buzón-Durán, L.; Lorenzo-Vidal, B.; Martín-Gil, J.; Martín-Ramos, P. Physicochemical characterization and antimicrobial activity against *Erwinia amylovora*, *Erwinia vitivora*, and *Diplodia seriata* of a light purple *Hibiscus syriacus* L. cultivar. *Plants* **2021**, *10*, 1876. [[CrossRef](#)]
55. Sánchez-Hernández, E.; Buzón-Durán, L.; Cuchi-Oterino, J.A.; Martín-Gil, J.; Lorenzo-Vidal, B.; Martín-Ramos, P. Dwarf pomegranate (*Punica granatum* L. var. *nana*): Source of 5-HMF and bioactive compounds with applications in the protection of woody crops. *Plants* **2022**, *11*, 550. [[CrossRef](#)]
56. Langa-Lomba, N.; Buzón-Durán, L.; Martín-Ramos, P.; Casanova-Gascón, J.; Martín-Gil, J.; Sánchez-Hernández, E.; González-García, V. Assessment of conjugate complexes of chitosan and *Urtica dioica* or *Equisetum arvense* extracts for the control of grapevine trunk pathogens. *Agronomy* **2021**, *11*, 976. [[CrossRef](#)]
57. Tran, D.A.; Nguyen Pham, C.T.; Nguyen Ngoc, T.; Nguyen Phi, H.; Hoai Ta, Q.T.; Truong, D.H.; Nguyen, V.T.; Luc, H.H.; Nguyen, L.T.; Dao, N.N.; et al. One-step synthesis of oxygen doped g-C₃N₄ for enhanced visible-light photodegradation of Rhodamine B. *J. Phys. Chem. Solids* **2021**, *151*, 109900. [[CrossRef](#)]
58. Yan, S.C.; Li, Z.S.; Zou, Z.G. Photodegradation of rhodamine B and methyl orange over boron-doped g-C₃N₄ under visible light irradiation. *Langmuir* **2010**, *26*, 3894–3901. [[CrossRef](#)]
59. Kong, X.; Liu, X.; Zheng, Y.; Chu, P.K.; Zhang, Y.; Wu, S. Graphitic carbon nitride-based materials for photocatalytic antibacterial application. *Mater. Sci. Eng. R Rep.* **2021**, *145*, 100610. [[CrossRef](#)]
60. Ma, Z.; Garrido-Maestu, A.; Jeong, K.C. Application, mode of action, and in vivo activity of chitosan and its micro- and nanoparticles as antimicrobial agents: A review. *Carbohydr. Polym.* **2017**, *176*, 257–265. [[CrossRef](#)]
61. Nazar Pour, F.; Pedrosa, B.; Oliveira, M.; Fidalgo, C.; Devreese, B.; Driessche, G.V.; Félix, C.; Rosa, N.; Alves, A.; Duarte, A.S.; et al. Unveiling the secretome of the fungal plant pathogen *Neofusicoccum parvum* induced by in vitro host mimicry. *J. Fungi* **2022**, *8*, 971. [[CrossRef](#)]
62. Xia, W.; Liu, P.; Liu, J. Advance in chitosan hydrolysis by non-specific cellulases. *Bioresour. Technol.* **2008**, *99*, 6751–6762. [[CrossRef](#)]
63. Labois, C.; Stempien, E.; Schneider, J.; Schaeffer-Reiss, C.; Bertsch, C.; Goddard, M.-L.; Chong, J. Comparative study of secreted proteins, enzymatic activities of wood degradation and stilbene metabolization in grapevine botryosphaeria dieback fungi. *J. Fungi* **2021**, *7*, 568. [[CrossRef](#)]
64. An, C.; Sun, C.; Li, N.; Huang, B.; Jiang, J.; Shen, Y.; Wang, C.; Zhao, X.; Cui, B.; Wang, C.; et al. Nanomaterials and nanotechnology for the delivery of agrochemicals: Strategies towards sustainable agriculture. *J. Nanobiotechnology* **2022**, *20*, 11. [[CrossRef](#)] [[PubMed](#)]

ARTÍCULO 8: “Potential of native *Trichoderma* strains as antagonists for the control of fungal wood pathologies in young grapevine plants” *Agronomy*, 2022, 12(2), 336; <https://doi.org/10.3390/agronomy12020336>; Q1 (JCR, Science Edition – AGRONOMY). JIF₂₀₂₂ = 3,7. 6 citas recibidas (CrossRef).



agronomy

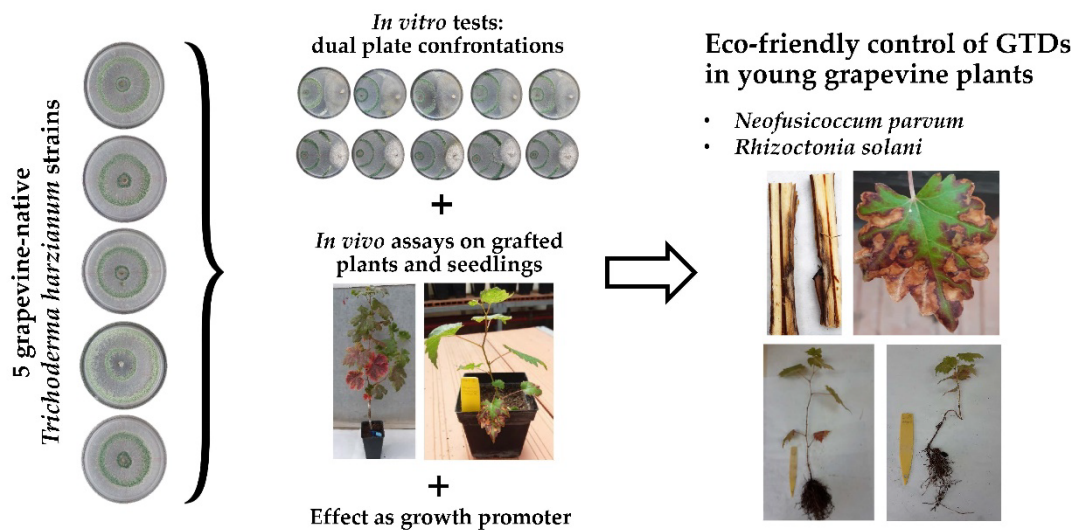
an Open Access Journal by MDPI



Potential of Native *Trichoderma* Strains as Antagonists for the Control of Fungal Wood Pathologies in Young Grapevine Plants

Natalia Langa-Lomba; Pablo Martín-Ramos; José Casanova-Gascón; Carmen Julián-Lagunas; Vicente González-García

Agronomy 2022, Volume 12, Issue 2, 336



Article

Potential of Native *Trichoderma* Strains as Antagonists for the Control of Fungal Wood Pathologies in Young Grapevine Plants

Natalia Langa-Lomba ^{1,2}, Pablo Martín-Ramos ¹, José Casanova-Gascón ¹, Carmen Julián-Lagunas ²
and Vicente González-García ^{2,*}

¹ Instituto Universitario de Investigación en Ciencias Ambientales de Aragón (IUCA), EPS, Universidad de Zaragoza, Carretera de Cuarte s/n, 22071 Huesca, Spain; natalialangalomba@gmail.com (N.L.-L.); pmr@unizar.es (P.M.-R.); jcasan@unizar.es (J.C.-G.)

² Unidad de Protección Vegetal, Centro de Investigación y Tecnología Agroalimentaria de Aragón, Instituto Agroalimentario de Aragón-IA2, CITA-Universidad de Zaragoza, Avda. Montañana 930, 50059 Zaragoza, Spain; cjulian@aragon.es

* Correspondence: vgonzalezg@aragon.es

Abstract: *Neofusicoccum parvum* and *Rhizoctonia solani* are fungal pathogens with an increasing incidence in young grapevine plants. In this study, the antagonistic potential of some strains of the genus *Trichoderma* isolated from grapevine against these pathogens was investigated at the laboratory and greenhouse levels. In-plate confrontation assays showed that the selected *Trichoderma* strains could inhibit the mycelial growth of both taxa, being more effective against *N. parvum*. In the in vivo assays, the biocontrol activity of the mentioned strains against the pathogens, when applied either simultaneously or successively, was tested on both grafted plants and seedlings germinated from seed. The effectiveness of the treatments was evaluated by comparing biomass weight and vascular rot lengths data. In seedling trials, successive treatments resulted in higher root development and a lower colonization rate of the pathogens, especially against *R. solani*. In grafted plants, some disparity was observed against *N. parvum*: simultaneous treatments resulted in higher aerial biomass, but successive treatments resulted in higher root biomass and lower necrosis. Against *R. solani*, simultaneous treatments were clearly more effective, with higher root and aerial length values and lower necrosis. The obtained data suggest that the use of *Trichoderma* spp. isolates can constitute an alternative to conventional fungicides to control certain grapevine wood diseases.

Keywords: biological control; *Neofusicoccum parvum*; *Rhizoctonia solani*; *Trichoderma harzianum*; *Vitis vinifera*; wood diseases



Citation: Langa-Lomba, N.; Martín-Ramos, P.; Casanova-Gascón, J.; Julián-Lagunas, C.; González-García, V. Potential of Native *Trichoderma* Strains as Antagonists for the Control of Fungal Wood Pathologies in Young Grapevine Plants. *Agronomy* **2022**, *12*, 336. <https://doi.org/10.3390/agronomy12020336>

Academic Editor: Noam Alkan

Received: 29 December 2021

Accepted: 27 January 2022

Published: 28 January 2022

Publisher's Note: MDPI stays neutral with regard to jurisdictional claims in published maps and institutional affiliations.



Copyright: © 2022 by the authors. Licensee MDPI, Basel, Switzerland. This article is an open access article distributed under the terms and conditions of the Creative Commons Attribution (CC BY) license (<https://creativecommons.org/licenses/by/4.0/>).

1. Introduction

One of the main challenges that modern viticulture faces is the control of fungal pathogens that cause grapevine trunk diseases (GTDs) [1]. These diseases decrease crop yields, limit grape and wine qualities, and reduce plant lifespan in many growing areas worldwide [2]. Moreover, they have a significant economic impact on the establishment of new plantations, as it has been estimated that the annual cost of replanting dead plants due to GTDs globally is 1132 M EUR [3]. The present study focuses on two pathogens associated with GTDs with a high incidence on young grapevine plants from nursery stock: *Neofusicoccum parvum* (Pennycook & Samuels) Crous, Slippers & A.J.L. Phillips and *Rhizoctonia solani* J.G. Kühn.

Neofusicoccum parvum is currently considered one of the most frequent and aggressive agents associated with the “black dead arm” or “Botryosphaeria dieback” disease, colonizing the woody tissue through wounds, being able to remain for a long time as a latent endophyte in these tissues, and eventually causing internal cankers, leaf chlorosis, and necrosis [4]. *Rhizoctonia solani*, a well-known polyphagous soil-borne pathogen, usually

appears as an increasing problem in grapevine nurseries, mainly associated with basal root and stem base rots, either in rootstocks or grafted plants produced in these facilities [5,6].

Currently, there are no completely effective measures for the elimination and/or control of fungi associated with GTDs [3]. With the withdrawal from official registers of numerous active materials of chemical origin, usually effective against these etiological agents, the current context of Integrated Pest Management (IPM) requires joining research efforts in aspects such as improving the sanitary quality of the propagation material, the reduction of practices that favor the spread and extension of infections of these fungi in the vineyard through improvements in management techniques, and the development and increased use of biological control agents (BCAs) [7].

Some of the best known and commercialized BCAs, also used to control GTDs, are species of the genus *Trichoderma* Pers. (Hypocreales, Ascomycetes), widely cited as an antagonist of numerous plant pathogens [8]. Their biocontrol mechanism is considered to be mixed, and it is mainly based on an active hyperparasitism behavior, together with the production of lytic enzymes, antimicrobial substances, and other secondary metabolites with germicidal action [9]. However, it has been shown that the different species of *Trichoderma* also present other positive effects on their host, improving growth rates and inducing plant defense responses, being considered a very effective biofertilizer [10]. In this sense, it has been demonstrated that the enzymes produced by the species of this genus, cause the release of oligosaccharides of low molecular weight that induce resistance [11].

In the case of GTDs, most products made up of *Trichoderma*-based formulations for the control of wood diseases are usually applied—by spraying—for wound protection shortly after pruning, at the time of the vegetative arrest of the vine or bleeding. The major obstacle for the extension and massive adoption of this type of treatment has been its variable effectiveness in field conditions, attributable to various factors, such as the phenological stage at which the treatment is carried out, the mode of application, the time interval between pruning and treatment, the climatic conditions during and after application, the level of incidence of GTDs in the treated vineyard, or the geographical origin of the grapevine used [12]. In this sense, many authors have pointed out that it is essential to complement the use of *Trichoderma* spp. with good management practices in the vineyard (less invasive pruning methods, restriction and elimination of potential inoculum sources, good nutritional balance of the vine, etc.) [13]. Different *Trichoderma* species have been evaluated against grapevine wood pathogens such as *Eutypa lata* (Pers.) Tul. & C. Tul., *Phaeoconiella chlamydospora* (W. Gams, Crous, M.J. Wingf. & Mugnai) Crous & W. Gams, *Phomopsis viticola* (Sacc.) Sacc., and different species of the family *Botryosphaeriaceae* [11,14,15]. However, independently of the level of protection against these species, a variable control with *Trichoderma* spp. was demonstrated, which was notably increased when the pathogens were inoculated shortly after applying the biocontrol agent [16].

This work has aimed to evaluate the antagonistic potential of different isolates of the genus *Trichoderma* previously isolated as endophytes from grapevine plants against *Neofusicoccum parvum* and *Rhizoctonia solani* through in vitro and in vivo assays on young plants in the greenhouse, in order to provide an alternative, benign, and environmentally safe control method.

2. Materials and Methods

2.1. Fungal Isolates

The selected pathogens used in the study were *Neofusicoccum parvum* and *Rhizoctonia solani*, while the antagonistic microorganisms were five different strains of the species *Trichoderma harzianum* Rifai, all of them conserved at the mycotheca of the Mycology Lab of the Plant Protection Unit at Centro de Investigación y Tecnología Agroalimentaria de Aragón (CITA), previously isolated as endophytes and/or pathogens of grapevine plants coming from both healthy and diseased samples of vineyards of Aragón (NE Spain) and identified at the morphological and molecular level. They were recovered from $-85\text{ }^{\circ}\text{C}$

cryovials and refreshed in Petri dishes with potato dextrose agar (PDA) for subsequent use in the bioassays.

2.2. In Vitro Assays of Mycelial Growth Inhibition

To evaluate the antagonistic effects of the selected *Trichoderma* strains, confrontation assays in plates were carried out, determining the percentage of inhibition of the fungal growth exerted by the protective isolates against the aforementioned grapevine pathogens.

The confrontations of antagonistic isolates and pathogens were performed using the dual culture technique in 9 cm diameter Petri dishes containing PDA as a nutrient medium. A 4 mm diameter agar block with mycelium coming from the margin of a fresh colony (4–5 days) of each pathogen was placed at one end of the plate (at 1 cm from its margin), and at the opposite end, the same operation was performed with the *Trichoderma* antagonists under the same conditions. Three replicates were made for each confrontation. For the controls, 4 mm diameter discs of pathogens and antagonists were individually sowed in the center of plates with the mentioned PDA medium. They were incubated for ten days at 25 °C in the dark, measuring the growth radius of pathogens and biocontrol agents every 24 h with a precision digital caliper.

The evaluation of the in vitro antagonistic effect was calculated using the formula of the Percentage of Inhibition of Radial Growth (PIRG) [17]: $PIRG = ((R_1 - R_2)/R_1) \times 100$, where R_1 = radius of the pathogen in control plate and R_2 = radius of the pathogen in confrontation plate.

2.3. Maintenance, Preservation, and Production of Fungal Inocula

Pure cultures of *N. parvum*, *R. solani*, and several strains of *T. harzianum* were maintained in Petri dishes of 12 cm diameter with PDA in a bacteriological oven at 25 °C in the dark, performing periodic replicates of each of the isolates to maintain fresh colonies.

Fungal inocula of both *R. solani* isolates employed in grafted plants and seedlings and *N. parvum* inocula in seedlings were made on a formulation based on cereal grains previously colonized by the aforementioned fungal taxa. For this purpose, organic wheat grains were used. Briefly, for pre-sterilization of the wheat grains, they were washed in a flask several times with sterilized bi-distilled water, then covered with the same type of water, incorporating streptomycin sulfate ($0.3 \text{ g} \cdot \text{L}^{-1}$) to prevent the development of bacterial contaminants, and left overnight in a refrigerator at 4 °C. Then, water was removed, and the flask was autoclaved (120 °C, 20 min). Afterwards, it was rewashed and drained. The grains were autoclaved two more times before use. Finally, sterilized grains were placed on 12 cm diameter Petri dishes and inoculated with 10–15 agar plugs from a fresh culture of each fungus. The plates were incubated for 5–7 days at 25 °C in the darkness. After this period, the fungi could colonize the whole grain content uniformly.

On the other hand, to obtain conidial solutions of the different strains of *T. harzianum* employed, each of them was inoculated in quintuplicate (4 mm diameter agar plugs) in 12 cm diameter PDA plates and incubated at 25 °C in the darkness until a profuse production of conidia was observed on the surface of the colonies. To obtain the conidial solution, the propagules were harvested. For this, sterile bi-distilled water was poured into each plate, completely covering each colony, and plates were sealed with Parafilm™. After this, the plates were shaken to detach the conidia, and the aqueous solution containing the spores was recovered with a syringe. Subsequently, the titration and adjustment of the different conidial solutions were carried out using a hemacytometer at a final concentration of $4.5 \times 10^6 \text{ conidia} \cdot \text{mL}^{-1}$ for each isolate.

2.4. Greenhouse Bioassays with Plants

To scale up the results of the in vitro tests, in vivo trials were carried out on two types of plant material: seedlings produced from germinated seeds and grafted grapevine plants from a commercial nursery. Inoculation was performed on 105 one-year-old grafted plants of the variety ‘Tempranillo’ (Clone 151) grafted on rootstock 110-R, and on 102 seedlings

of the same variety, obtained from an organic vineyard in Bospén (Huesca, Spain). The method used for seed germination consisted in soaking the seeds in commercial sodium hypochlorite diluted at 50% for 24 h, then rinsing them with sterile water and discarding those that floated. Then, the seeds were treated with gibberellic acid (1000 ppm), mixing it with 1 mL of 95% ethanol and distilled water for 24 h. The seeds were then rinsed with sterile water and allowed to dry on filter paper. After this, a seedbed was arranged.

The grafted plants and seedlings were planted in plastic pots of 3.5 and 0.3 L, respectively, containing a substrate of commercial peat and sterilized natural soil from a vineyard in Bospén (Huesca, Spain) in a 2:1 ratio.

For five months, plants were kept in the greenhouse with manual irrigation when needed (2–3 times per week). Three inoculation modalities were used according to the type of pathogen and/or the type of action of the biocontrol agent used, carrying out both successive (inoculating first the antagonist and five days later the pathogen) and simultaneous treatments (inoculating both types of fungi at the same time). Six replicates were arranged for each pathogen/antagonist combination, three of them being of the successive inoculation type and the other three of the simultaneous inoculation one, together with three positive controls inoculated only with pathogens, three negative controls that incorporated only the propagation material of the fungus according to the type of inoculation (agar block, wheat grain, and/or distilled water), and other three negative controls of each strain of *Trichoderma* (15 pots in total), as shown in Table 1.

Table 1. Summary of the experimental assays carried out for each pathogen and *T. harzianum* strain.

Test Conditions	Pathogen	Pathogen and <i>T. harzianum</i> Inoculation	Replicates
In vitro	<i>N. parvum</i>	-	15 (3 per <i>T. harzianum</i> strain)
	<i>R. solani</i>	-	15 (3 per <i>T. harzianum</i> strain)
	<i>T. harzianum</i> control	-	30 (15 per assay, 3 per <i>T. harzianum</i> strain)
	<i>N. parvum</i> control	-	3
	<i>R. solani</i> control	-	3
seedlings produced from germinated seeds	<i>N. parvum</i>	Simultaneous	15 (3 per <i>T. harzianum</i> strain)
		Successive	15 (3 per <i>T. harzianum</i> strain)
	<i>R. solani</i>	Simultaneous	15 (3 per <i>T. harzianum</i> strain)
		Successive	15 (3 per <i>T. harzianum</i> strain)
	<i>T. harzianum</i> control	-	30 (15 per assay, 3 per <i>T. harzianum</i> strain)
	<i>N. parvum</i> control	-	3
In vivo	<i>N. parvum</i>	Simultaneous	15 (3 per <i>T. harzianum</i> strain)
		Successive	15 (3 per <i>T. harzianum</i> strain)
	<i>R. solani</i>	Simultaneous	15 (3 per <i>T. harzianum</i> strain)
		Successive	15 (3 per <i>T. harzianum</i> strain)
	<i>T. harzianum</i> control	-	30 (15 per assay, 3 per <i>T. harzianum</i> strain)
	<i>N. parvum</i> control	-	3
	<i>R. solani</i> control	-	3
	Agar control	-	3
	Wheat control	-	3
	dH ₂ O control	-	3
grafted grapevine plants from a commercial nursery	<i>N. parvum</i>	Simultaneous	15 (3 per <i>T. harzianum</i> strain)
		Successive	15 (3 per <i>T. harzianum</i> strain)
	<i>R. solani</i>	Simultaneous	15 (3 per <i>T. harzianum</i> strain)
		Successive	15 (3 per <i>T. harzianum</i> strain)
	<i>T. harzianum</i> control	-	30 (15 per assay, 3 per <i>T. harzianum</i> strain)
	<i>N. parvum</i> control	-	3
	<i>R. solani</i> control	-	3
	Agar control	-	3
	Wheat control	-	3
	dH ₂ O control	-	3

2.4.1. Inoculation of *Trichoderma harzianum* against *Neofusicoccum parvum* in Grafted Grapevine Plants

Inoculations were performed on the stem at two separate points below the graft union. Agar plugs from fresh PDA cultures of each fungus were used as fungal inoculum. At the defined points of each grafted plant (2 per individual), slits were made (with a scalpel) about 5 mm in diameter and 5 mm deep. After this, 4 mm diameter agar discs previously colonized by each fungus were inoculated and placed in such a way that the mycelium was in contact with the incision of the stem. The discs were covered with sterile cotton wool moistened in sterile bi-distilled water and sealed with Parafilm™.

2.4.2. Inoculation of *Trichoderma harzianum* against *Rhizoctonia solani* in Grafted Grapevine Plants

The inoculations were carried out at root level, in a different way according to the incorporated strain: (1) the treatment of the grafted plants with *Trichoderma* strains was carried out by root immersion, and (2) the artificial infection with *R. solani* was carried out inoculating the culture substrate of the grafted plants with the pathogen previously propagated in solid medium (colonized wheat grains). For the different strains of *T. harzianum*, the roots of the tested plants were immersed in a series of conidial solutions of the mentioned antagonistic fungi previously adjusted to 4.5×10^6 conidia·mL⁻¹ for 2–2.5 h, before being transplanted to the pot. For the pathogen (*R. solani*), the grafted plants were infected upon contact with the potting substrate containing mixed wheat grains previously colonized by the fungus, at a dose of 15 g of colonized wheat per 2 L of the growing substrate.

2.4.3. Inoculation of *Trichoderma harzianum* against *Neofusicoccum parvum* and *Rhizoctonia solani* in Grapevine Seedlings Germinated from Seeds

The inoculations with the different strains of *Trichoderma* were carried out through root immersion of the seedlings in a conidial suspension of *Trichoderma* previously adjusted to 4.5×10^6 conidia·mL⁻¹ for 3–5 min. In the case of the pathogens (*R. solani* and *N. parvum*), they infected the seedlings (previously protected or not with *Trichoderma*, depending on whether they were inoculated successively or simultaneously) by contact with the culture substrate containing wheat grains previously colonized by each pathogen strain in question, at a dose of 2.5 g per pot (330 mL) (grams of colonized wheat per liter of growth substrate).

Five months after inoculation, both types of grapevine plants were removed, and, in the case of grafted plants, each one was measured longitudinally (root, aerial, and total biomass). After this, sections of them were cut longitudinally, and the length of the lesions caused by the pathogens (tracheomyces) was evaluated. For this purpose, the extent of the vascular lesions was measured longitudinally at both sides of the inoculation point in the case of artificial infection with *N. parvum* (analyzing lower, upper, and total necrosis). In contrast, in the *R. solani* trial, only the length of the basal necrosis (coming up from the root crown) was measured since this pathogen was inoculated by root infection. In this way, the extension of the different vascular lesions was analyzed and statistically compared as a function of if the grafted plants had been protected with *Trichoderma* in successive or simultaneous inoculation. All necrosis measurements were compared with those obtained for the controls. In the case of bioassays on seedlings, in addition to the longitudinal measurements of the root, aerial, and total biomass, the total fresh/dry weight of aerial and root biomass were analyzed. Finally, in grafted plants, after carrying out the above-mentioned measurements, pathogens previously inoculated were isolated (from over 87% of the inoculated plants) from the decayed vascular tissues in order to fulfill Koch's postulates.

2.5. Statistical Analysis

When the requirements of homogeneity and homoscedasticity were met, the results of the in vitro mycelial growth inhibition tests were statistically analyzed using ANOVA analysis, followed by comparisons of the measurements by Tukey's test ($p < 0.05$). For greenhouse bioassay results in which the requirements of normality and homoscedasticity were not met, the Kruskal–Wallis non-parametric test was used instead, accompanied by pairwise comparison using Dunn's and Conover–Iman's methods, applying the Bonferroni correction. IBM SPSS STATISTICS software was used for all statistical analyses.

3. Results

3.1. In Vitro Mycelial Growth Inhibition Tests

In general terms, the presence of high PIRG values (Table 2) was correlated with the ability of a given isolate to inhibit the development of a pathogen. The results showed that the different *T. harzianum* isolates used were more effective in inhibiting the mycelial

growth of *N. parvum* (with PIRG values between 44.65 and 51.32%) than that of *R. solani*, for which PIRG values between 20.57 and 28.04% were recorded, and even negative PIRG percentages (−3.47%) were obtained in some cases (*T. harzianum* isolate 1).

Table 2. PIRG values (mean \pm standard deviation) obtained in each dual plate confrontation, for the two pathogens (*N. parvum* and *R. solani*) against 5 *T. harzianum* isolates, after 7 days of culture.

Isolate	<i>Neofusicoccum parvum</i>	<i>Rhizoctonia solani</i>
<i>T. harzianum</i> 1	51.32 \pm 0.37 a	−3.47 \pm 24.04 a
<i>T. harzianum</i> 2	50.76 \pm 4.46 a	27.95 \pm 5.30 ab
<i>T. harzianum</i> 3	45.98 \pm 2.58 a	20.57 \pm 2.09 b
<i>T. harzianum</i> 4	47.94 \pm 2.23 a	28.04 \pm 4.48 b
<i>T. harzianum</i> 5	44.65 \pm 0.50 a	23.12 \pm 3.83 b

Means followed by different letters are significantly different ($p < 0.05$).

The data obtained for both pathogens suggest that the isolate with the best antagonistic behavior in plate assays against both pathogens would be the strain *T. harzianum* 2.

Along with the observed mycelial growth inhibition values, the presence of hyphal structures related to the presence of active hyperparasitism was verified. As a result of this, different types of interactions usually described in the confrontation of species of the genus *Trichoderma* against other fungal taxa were observed. Some of these included the formation of penetration structures, papilla-like bodies, appressoria, lysis of pathogen hyphae, profuse sporulation, intracellular growth, or the presence of typical coil hyphae (Figures 1 and 2).

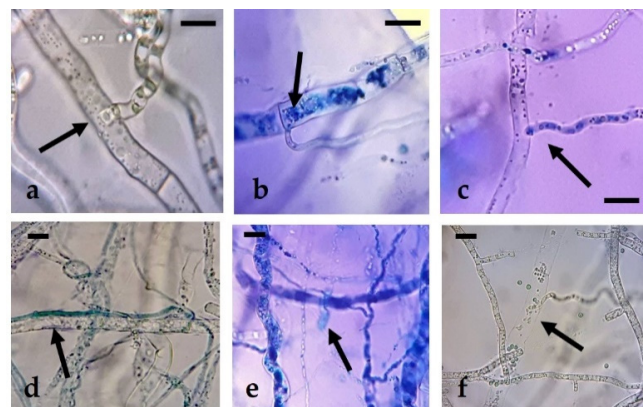


Figure 1. Hyphal interactions of *T. harzianum* with *N. parvum* in dual plate confrontations: (a–c): penetration structures; (d) appressorium; (e) papilla-like structures; (f) hyphal lysis. Bars = 10 μ m.

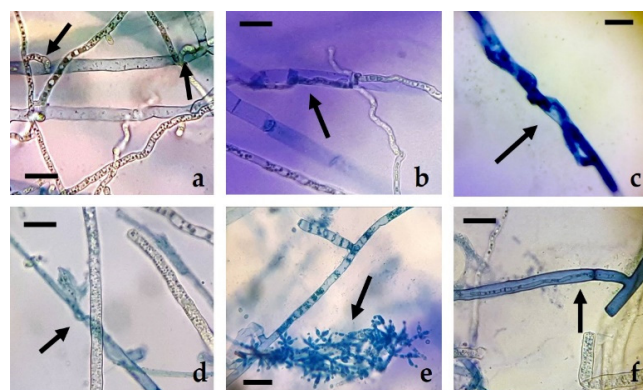


Figure 2. Hyphal interactions of *T. harzianum* with *R. solani* in dual plate confrontations: (a) penetration structures; (b) appressorium; (c,d) coiling hyphae; (e) sporulation; (f) intracellular growth. Bars = 10 μ m.

3.2. In Planta Bioassays

3.2.1. Control of *Neofusicoccum parvum* and *Rhizoctonia solani* with *Trichoderma harzianum* Isolates in Grapevine Seedlings Germinated from Seed

In biocontrol trials with seedlings, the protective effect of successive treatments with the *T. harzianum* antagonist strains resulted in higher root development and dry weight (compared to controls) and a lower colonization rate of the pathogen, especially against *R. solani*. The results suggest the convenience of incorporating the antagonist a few days before inoculation of the pathogen.

For *N. parvum*, in general, and regardless of the statistical significance, the highest dry weight values were obtained in all successive treatments with *T. harzianum* strains, except in the case of *T. harzianum* isolate 4 (which obtained better values in simultaneous inoculation). In the case of *R. solani*, it was also observed that the dry weight values of the successive treatments based on the different isolates of *T. harzianum* were higher than the rest, except for the controls (i.e., plants without inoculation of any microorganism) (Table 3).

Table 3. Total dry weight of seedlings in grams (mean \pm standard deviation) for each type of treatment (successive, simultaneous, and controls with *T. harzianum*, *N. parvum*, *R. solani*, and uninoculated wheat) obtained for each *T. harzianum* strain.

Pathogen	Treatment	Th1	Th2	Th3	Th4	Th5
<i>N. parvum</i>	Successive	3.64 \pm 0.18 d	3.93 \pm 1.96 a	2.92 \pm 1.12 a	2.95 \pm 0.99 a	3.72 \pm 0.14 c
	Simultaneous	3.30 \pm 0.17 cd	1.83 \pm 0.73 a	2.31 \pm 0.95 a	3.85 \pm 1.52 a	2.26 \pm 0.11 b
	Th control	2.49 \pm 0.12 bc	2.85 \pm 1.34 a	2.84 \pm 0.51 a	1.29 \pm 0.69 a	1.55 \pm 0.26 ab
	<i>N. parvum</i> control	1.92 \pm 0.49 ab	1.92 \pm 0.49 a	1.92 \pm 0.49 a	1.92 \pm 0.49 a	1.92 \pm 0.49 ab
	Wheat control	1.06 \pm 0.44 a	1.06 \pm 0.44 a	1.06 \pm 0.44 a	1.06 \pm 0.44 a	1.06 \pm 0.44 a
<i>R. solani</i>	Successive	2.85 \pm 0.48 b	3.93 \pm 0.68 b	1.91 \pm 0.75 ab	2.81 \pm 0.49 ab	2.89 \pm 0.20 bc
	Simultaneous	2.14 \pm 0.38 ab	1.52 \pm 0.08 a	1.59 \pm 0.08 ab	1.76 \pm 0.27 ab	1.45 \pm 0.45 ab
	Th control	2.49 \pm 0.12 ab	1.35 \pm 0.38 a	1.29 \pm 0.16 a	2.42 \pm 0.95 ab	1.46 \pm 0.35 ab
	<i>R. solani</i> control	1.09 \pm 0.05 a	1.09 \pm 0.05 a	1.09 \pm 0.055 a	1.09 \pm 0.05 a	1.09 \pm 0.05 a
	Wheat control	3.09 \pm 1.04 b	3.09 \pm 1.04 b	3.09 \pm 1.04 b	3.09 \pm 1.04 b	3.09 \pm 1.04 c

Means followed by different letters are significantly different ($p < 0.05$). Th = *T. harzianum*.

3.2.2. Control of *Neofusicoccum parvum* with *Trichoderma harzianum* in Grafted Grapevine Plants

The results of the biological control tests in grafted plants against *N. parvum* were shown to be heterogeneous, provided that—contrary to what was expected—no correlation was found between the increase (comparing with controls) of aerial biomass and the decrease of necrosis lengths in successive treatments versus simultaneous inoculations.

In this sense, it should also be noted that, regarding the length of the aerial biomass, in general, the simultaneous treatments led to higher aerial tissues lengths than the successive treatments, although none of the interactions was statistically significant (Table 4).

It was found that the only statistically significant differences in total necrosis values corresponded to those bioassays in which *T. harzianum* isolate 4 was employed. Nonetheless, when lower necrosis lengths were separately analyzed, statistically significant differences were also detected for *T. harzianum* isolate 2. The necrosis measurements (Table 5) obtained for the simultaneous treatments were higher than those of the successive treatments (except for the treatment with *T. harzianum* 3 in the lower necrosis), with a higher incidence of necrosis occurring when the antagonists were inoculated at the same time as *N. parvum*. As expected, thus validating the inoculation method, the highest necrosis length was found in the *N. parvum* pathogen control.

Table 4. Aerial and root biomass lengths of grafted plants in cm (mean \pm standard deviation) for each type of treatment (successive or simultaneous inoculation with *N. parvum* and *T. harzianum*, and controls with plant inoculated only with agar) as a function of the *T. harzianum* isolate used.

Length	Treatment	Th1	Th2	Th3	Th4	Th5
Aerial	Successive	69.75 \pm 2.25 a	75.67 \pm 20.23 a	77.00 \pm 4.00 a	86.00 \pm 12.76 a	88.83 \pm 7.32 a
	Simultaneous	72.17 \pm 3.33 a	78.40 \pm 18.15 a	82.50 \pm 8.05 a	88.83 \pm 0.76 a	71.67 \pm 2.89 a
	Th control	94.00 \pm 4.70 a	80.00 \pm 4.00 a	87.00 \pm 4.35 a	83.00 \pm 4.15 a	99.00 \pm 4.95 a
	<i>N. parvum</i> control	80.33 \pm 19.55 a	80.33 \pm 19.55 a	80.33 \pm 19.55 a	80.33 \pm 19.55 a	80.33 \pm 19.55 a
	Agar control	77.00 \pm 7.81 a	77.00 \pm 7.81 a	77.00 \pm 7.81 a	77.00 \pm 7.81 a	77.00 \pm 7.81 a
Radicular	Successive	57.00 \pm 6.50 ab	49.83 \pm 13.51 a	44.17 \pm 14.00 a	36.67 \pm 7.51 a	44.83 \pm 6.64 ab
	Simultaneous	47.83 \pm 11.36 ab	38.00 \pm 7.94 a	51.33 \pm 7.15 a	43.83 \pm 9.41 a	33.17 \pm 4.86 a
	Th control	60.00 \pm 3.00 b	35.00 \pm 1.75 a	51.00 \pm 2.55 a	58.00 \pm 2.90 a	57.00 \pm 2.85 b
	<i>N. parvum</i> control	40.50 \pm 11.30 ab	40.50 \pm 11.30 a	40.55 \pm 11.30 a	40.50 \pm 11.30 a	40.50 \pm 11.30 ab
	Agar control	35.33 \pm 10.41 a	35.33 \pm 10.41 a	35.33 \pm 10.41 a	35.33 \pm 10.41 a	35.33 \pm 10.41 a

Means followed by different letters are significantly different ($p < 0.05$). Th = *T. harzianum*.

Table 5. Total necrosis and lower necrosis of grafted plants in cm (mean \pm standard deviation) for each type of treatment (successive or simultaneous inoculation with *N. parvum* and *T. harzianum*, and controls with plant inoculated only with agar) for each *T. harzianum* strain.

Necrosis Length	Treatment	Th1	Th2	Th3	Th4	Th5
Total	Successive	2.95 \pm 0.85 a	2.31 \pm 0.34 a	2.78 \pm 0.84 a	3.30 \pm 0.52 ab	2.38 \pm 0.66 a
	Simultaneous	3.45 \pm 0.49 a	3.27 \pm 0.65 a	3.25 \pm 0.35 a	3.72 \pm 0.47 b	3.16 \pm 0.51 a
	Th control	2.40 \pm 0.12 a	1.95 \pm 0.10 a	1.85 \pm 0.09 a	2.03 \pm 0.10 a	1.83 \pm 0.09 a
	<i>N. parvum</i> control	2.73 \pm 0.51 a	2.73 \pm 0.51 a	2.73 \pm 0.51 a	2.73 \pm 0.51 ab	2.73 \pm 0.51 a
	Agar control	2.53 \pm 0.85 a	2.53 \pm 0.85 a	2.53 \pm 0.85 a	2.53 \pm 0.85 ab	2.53 \pm 0.85 a
Lower	Successive	3.09 \pm 1.18 a	2.06 \pm 0.17 ab	3.19 \pm 0.66 a	3.26 \pm 0.18 b	2.47 \pm 0.72 a
	Simultaneous	3.28 \pm 0.71 a	3.18 \pm 0.53 c	2.53 \pm 1.58 a	3.54 \pm 0.22 b	2.96 \pm 0.63 a
	Th control	2.39 \pm 0.12 a	1.90 \pm 0.10 a	2.08 \pm 0.10 a	1.76 \pm 0.09 a	2.20 \pm 0.11 a
	<i>N. parvum</i> control	3.05 \pm 0.47 a	3.05 \pm 0.47 bc	3.05 \pm 0.47 a	3.05 \pm 0.47 b	3.05 \pm 0.47 a
	Agar control	1.91 \pm 0.44 a	1.91 \pm 0.44 a	1.91 \pm 0.44 a	1.91 \pm 0.44 a	1.91 \pm 0.44 a

Means followed by different letters are significantly different ($p < 0.05$). Th = *T. harzianum*.

3.2.3. Control of *Rhizoctonia solani* with *Trichoderma harzianum* in Grafted Grapevine Plants

In these trials, it was found that the simultaneous treatments of both pathogen and protective isolates led to higher root and aerial biomass lengths than those of the controls, although these were not statistically significant (Table 6). Furthermore, in the aerial tissues length values, the treatments with *T. harzianum* isolates 3 and 4—both in simultaneous and successive inoculation—resulted in higher lengths than those observed for the *R. solani* control, slightly promoting the growth of the grafted plants.

When comparing internal vascular necrosis length measurements, simultaneous treatments seemed to work better against *R. solani*. In this sense, the best tracheomycosis inhibition data corresponded to *T. harzianum* isolate 4 (Table 7).

3.2.4. *Trichoderma harzianum* as a Growth Promoter

To evaluate the capacity as plant growth promoters of the *T. harzianum* isolates under study, the controls of these isolates (both in seedlings and in grafted plants inoculated with the five protective strains) were compared with the control plants without any treatment. This type of comparison was carried out because the potential of certain species of the genus *Trichoderma* as plant growth promoters has been widely demonstrated and documented, resulting in an increase in the size of the plants even in the absence of any pathogen [18].

In the case of seedlings, only *T. harzianum* isolate 5 significantly promoted root growth of treated plants compared to non-inoculated controls (Figure 3).

Table 6. Total aerial and root biomass length of grafted plants in cm (mean ± standard deviation) for each type of treatment (successive or simultaneous inoculation with *R. solani* and *T. harzianum*, and controls with plants inoculated only with wheat and dipped in distilled water) as a function of the *T. harzianum* isolate used.

Length	Treatment	Th1	Th2	Th3	Th4	Th5
Aerial	Successive	87.17 ± 15.61 a	81.33 ± 14.57 a	92.33 ± 30.02 a	87.33 ± 24.01 a	93.50 ± 15.60 a
	Simultaneous	77.30 ± 6.06 a	87.00 ± 20.54 a	86.00 ± 4.50 a	94.17 ± 17.96 a	70.17 ± 17.92 a
	Th control	84.00 ± 4.20 a	64.00 ± 3.20 a	74.00 ± 6.47 a	68.00 ± 3.40 a	72.20 ± 3.61 a
	<i>R. solani</i> control	85.90 ± 18.95 a				
	Wheat control	89.33 ± 3.06 a				
	Wheat control	89.33 ± 3.06 a				
	dH ₂ O control	89.77 ± 7.51 a				
Radicular	Successive	36.67 ± 16.07 a	34.67 ± 6.43 a	35.00 ± 3.61 a	35.17 ± 2.57 a	38.00 ± 11.79 a
	Simultaneous	44.83 ± 12.33 a	35.50 ± 7.37 a	38.80 ± 10.20 a	42.50 ± 7.40 a	26.83 ± 5.06 a
	Th control	43.50 ± 2.18 a	55.50 ± 2.78 a	36.00 ± 1.80 a	41.00 ± 2.05 a	52.00 ± 2.60 a
	<i>R. solani</i> control	40.10 ± 14.29 a				
	Wheat control	37.00 ± 9.54 a				
	Wheat control	37.00 ± 9.54 a				
	dH ₂ O control	32.17 ± 5.01 a				

Means followed by different letters are significantly different ($p < 0.05$). Th = *T. harzianum*.

Table 7. Basal vascular necrosis length of grafted plants in cm (mean ± standard deviation) for each type of treatment (successive or simultaneous inoculation with *R. solani* and *T. harzianum*, and controls with plants inoculated only with wheat and submerged in distilled water) as a function of the *T. harzianum* isolate used.

Treatments	Th1	Th2	Th3	Th4	Th5
Successive	8.06 ± 3.67 bc	6.96 ± 4.72 ab	6.10 ± 1.66 ab	6.68 ± 1.88 abc	5.58 ± 2.57 abc
Simultaneous	5.79 ± 2.50 abc	5.14 ± 1.24 ab	7.03 ± 1.20 ab	4.57 ± 2.71 ab	4.77 ± 2.77 ab
Th control	1.93 ± 1.17 a	5.75 ± 0.31 ab	6.78 ± 1.03 ab	5.08 ± 2.68 ab	7.40 ± 2.35 abc
<i>R. solani</i> control	9.70 ± 6.43 c	9.70 ± 6.43 b	9.70 ± 6.43 b	9.70 ± 6.43 c	9.70 ± 6.43 c
Wheat control	3.65 ± 3.65 ab	3.65 ± 3.65 a	3.65 ± 3.65 a	3.65 ± 3.65 a	3.65 ± 3.65 a
dH ₂ O control	8.69 ± 3.39 c	8.69 ± 3.39 b	8.69 ± 3.39 b	8.69 ± 3.39 bc	8.69 ± 3.39 bc

Means followed by different letters are significantly different ($p < 0.05$). Th = *T. harzianum*.

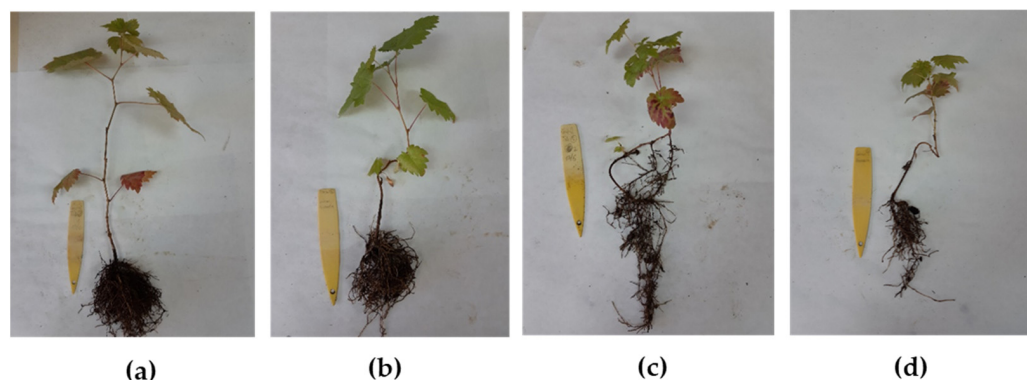


Figure 3. Growth promotion effects of *Trichoderma* strains: (a) control seedling inoculated with *T. harzianum* 2; (b) control seedling inoculated with *T. harzianum* 1; (c) control seedling inoculated with *T. harzianum* 5; (d) control seedling not inoculated.

In grafted plants, an increase in plant growth rates was detected in the controls inoculated with *T. harzianum*, especially in the roots, regardless of the statistical significance (Table 8). Thus, the different isolates of *T. harzianum* employed promoted and increased growth (in biometric terms) compared with the control plants. In the case of total biomass length measurements, *T. harzianum* isolates 1 and 5 obtained the best values, which were also statistically significant. Regarding root length, *T. harzianum* isolates 1 and 4 (whose

interaction was also statistically significant) stood out, followed by the values obtained with the application of *T. harzianum* isolate 5.

Table 8. Growth promotion effects of *Trichoderma* strains. Total, aerial, and root biomass lengths in cm (mean \pm standard deviation) of grafted plant controls treated with *T. harzianum* and untreated (agar only). Data are referred to the experiment of protection against *N. parvum*.

Treatment	Total Length	Aerial Length	Root Length
Th1 control	154.00 \pm 7.70 c	94.00 \pm 4.70 bc	60.00 \pm 3.00 b
Th2 control	115.00 \pm 5.75 ab	80.00 \pm 4.00 ab	35.00 \pm 1.75 a
Th3 control	138.00 \pm 6.90 abc	87.00 \pm 4.35 abc	51.00 \pm 2.55 b
Th4 control	141.00 \pm 7.05 bc	83.00 \pm 4.15 ab	58.00 \pm 2.90 b
Th5 control	156.00 \pm 7.80 c	99.00 \pm 4.95 c	57.00 \pm 2.85 b
Agar control	112.33 \pm 18.01 a	77.00 \pm 7.81 a	35.33 \pm 10.40 a

Columns followed by the same letter are not significantly different ($p > 0.05$).

4. Discussion

4.1. In Vitro Mycelial Growth Inhibition

Plate confrontation assays demonstrated the ability of *T. harzianum* strains to inhibit the mycelial growth of the two selected grapevine pathogens. In general terms, the highest inhibition values were recorded against *N. parvum*, representing almost twice those recorded against *R. solani*. Numerous studies have evaluated in vitro the antagonistic potential of several *Trichoderma* species, a well-known group of hyperparasitic mitosporic fungi [19,20]. In this sense, the values obtained in the present study seem to be relatively discrete in comparison with PIRG data obtained from the confrontations of species of the mentioned genus against other plant pathogens [21–23], in which the average rates of inhibition of microbial growth in dual confrontations with *T. harzianum* were usually higher than 50%, sometimes reaching PIRG values above 99%.

One possible explanation is that both *N. parvum* and *R. solani* species have simple nutritional requirements and usually show high-speed growth rates. This is especially true for isolates of the genus *Rhizoctonia*, a polyphagous basidiomycete with great colonizing capacity and very high vegetative growth rates (with practically absent reproductive mechanisms) [24]. This would hinder its inhibition by other antagonists, especially by those that, like *Trichoderma*, base their mode of action mainly on the colonization and parasitism of the mycelium of the pathogen to be controlled, always accompanied by an effective occupation of the culture medium. Thus, in the case of *R. solani*, the presence of hyperparasitism phenomena (enzymatic lysis of the mycelium of *R. solani*) and sporulation of the different isolates of *Trichoderma* on the mycelium of the pathogen can be observed, but not beyond half of the Petri dish (Figure 4), due to the rapid growth and colonization capacity of *R. solani*, with rates similar to those of *Trichoderma*. Siameto et al. [25], in a study on the growth inhibition of selected soil pathogens in Africa, found that *T. harzianum* inhibited the growth of *R. solani* with the highest PIRG being 61.55%, while the lowest was 25.88%; and, according to Guedez et al. [26], in a study on the in vitro growth-inhibitory activity of different strains of *T. harzianum* against *R. solani* and two other tomato pathogens, rates between 62 and 72% were recorded for inhibition against this fungus, well above those obtained here. However, the aggressiveness, virulence, or speed of colonization of isolates of a species as biologically complex as *R. solani* largely depends on the type of anastomosis group and/or subgroup in question [24,26].

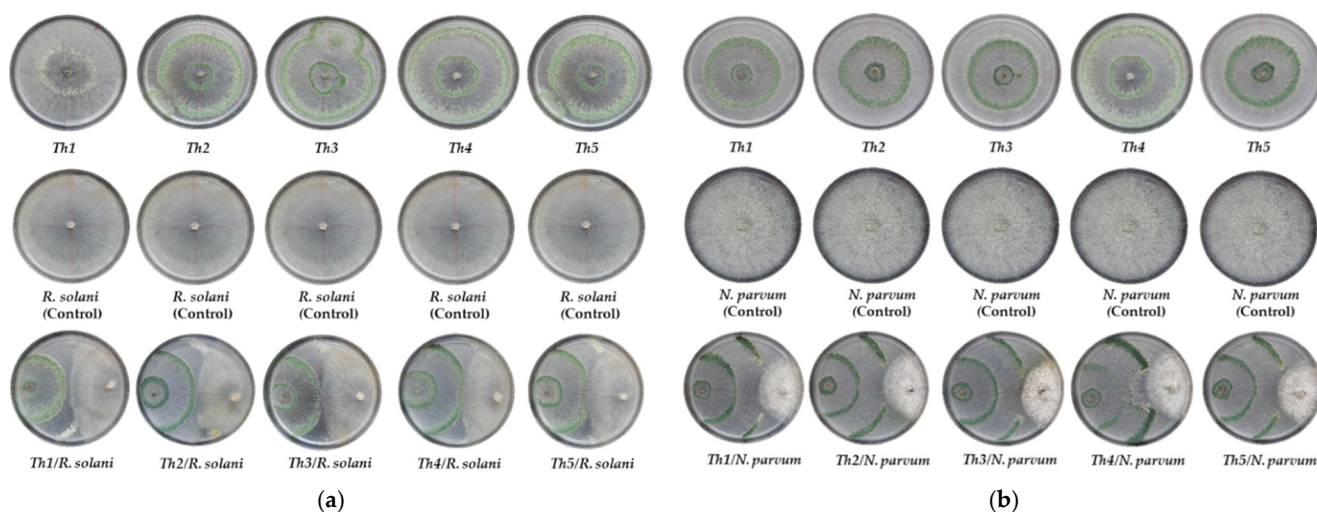


Figure 4. Dual plate confrontations of *Trichoderma harzianum* strains against the selected pathogens. (a) *Rhizoctonia solani*. Top row: control plates of the different strains of *T. harzianum*; middle row; control plates of *R. solani*; bottom row: dual confrontations with each of the protective strains; (b) *Neofusicoccum parvum*. Top row: control plates of the different strains of *T. harzianum*; middle row; control plates of *N. parvum*; bottom row: dual confrontations with each of the isolates of *T. harzianum*.

In the case of *N. parvum*, as indicated above, PIRG values were shown to be clearly higher (Figure 4). These values seem to be in line with the mycelial growth inhibition rates observed in certain species of the grapevine pathogenic *Botryosphaeriaceae* family in plate confrontations with different isolates of the genus *Trichoderma*. Marraschi et al. [27] evaluated the potential of different BCAs and determined that the tested *Trichoderma* species and commercial formulations could inhibit the growth of a member of the mentioned ascomycetous family such as *Lasiodiplodia theobromae* (Pat.) Griffon & Maubl. at rates above 75%. Urbez-Torres et al. [28] studied different isolates of *Trichoderma* spp. that inhibited the growth of several species of *Botryosphaeriaceae* in a range from 44.5 to 74.3%, with *T. atroviride* being the most effective, close to *T. harzianum*. Plata-Caudillo [29] obtained mycelial growth inhibition values of *N. parvum* around 50% in direct plate confrontations with several isolates and formulations based on *T. harzianum*, in line with the values obtained in the present work. Mutawila et al. [30] observed mycelial growth inhibition rates against *N. parvum* of 45–50%, although using extracts containing a metabolite of interest previously extracted from different *Trichoderma* strains. Finally, Kotze et al. [31], in an in vitro and in vivo evaluation of the antagonistic activity of different microorganisms and formulations, reported, in the case of plate confrontations with *T. harzianum* versus *N. parvum*, the existence of hyperparasitism of the former towards the latter, based on the presence of hyphal interactions, enzymatic lysis, and occupation of space and nutrients in Petri dish. These hyphal interactions were also observed in the confrontations of the present study, although they were not particularly abundant along the whole contact surface between the colonies.

4.2. Bioassays of *Trichoderma harzianum* against *Neofusicoccum parvum* in Plants

Neofusicoccum parvum has been repeatedly isolated from nurseries throughout the world's wine-growing areas in the last two decades and has been the subject of numerous investigations related to its epidemiology and characterization, as well as its control, including biological methods [12,32,33]. Most of the approaches related to the biocontrol of *N. parvum* and related *Botryosphaeriaceae* species have been based either on the protection of pruning wounds with antagonist-based formulations or other alternative methods to chemical fungicides [31,34,35], or with the application of these biocontrol agents in the different stages of production of grafted plants in nurseries [9,12,36].

In this sense, most of the investigations on the control of this and other pathologies of young grapevine plants, have been focused on grafted plants in the nursery and/or adult plants in the field, so the methodology and biometric results obtained after the treatment of grapevine plants germinated from seeds with different isolates of *T. harzianum* in the present study represents a novelty in this type of research. Nevertheless, the biometric data did not provide conclusive results regarding the protective effect of the different antagonistic strains used, given that a disparate behavior was observed among isolates, type of application, or measured parameter. Nevertheless, the reported data indicate, in agreement with the majority of studies based on the application of microbial antagonists at the root level, that the parameters most related to the development and activity of this type of tissue (root length and total weight) were the ones that offered better values compared to control plants inoculated with the pathogen.

Regarding the protection tests on grafted plants, successive treatments showed good root biomass lengths and lower necrosis (compared to controls). Several researchers claim that successive treatments with antagonists reduce the incidence of *N. parvum*. In this sense, Pintos et al. [37] concluded that inoculating *Trichoderma* in plants three days before the pathogen reduced more than twice the length of necrosis caused by the latter, being more effective than inoculating three days after the pathogen. Similarly, Kotze et al. [31] demonstrated a reduction of *N. parvum* damage in pruning wounds by applying *Trichoderma* products seven days before exposure, when the plant was healthy.

4.3. Bioassays of *Trichoderma harzianum* against *Rhizoctonia solani* in Plants

Members of the so-called *Rhizoctonia* species complex are considered a mixture of filamentous fungi, having in common the possession of a non-spored imperfect state, usually referred to as the *Rhizoctonia* anamorph [5,6,38–40]. Among them, *Rhizoctonia solani* is considered a very destructive plant pathogen, having a broad host range and causing diseases in a great variety of crops. Although *R. solani* has long been known as one of the main pathogens associated with grapevine wood in young plants in greenhouses [5,6,38–40], to date, there have been few studies on the biological protection of grapevine plants with microbial antagonists or other alternative methods against it. Crous et al. [39] examined the effects of thermotherapy treatments on the prevalence and incidence of a number of pathogens associated with apparently healthy grapevine seedlings in nurseries, including *R. solani*, concluding that hot water treatments did not significantly reduce its presence and the presence of other associated fungal pathogens. On the other hand, Ziedan et al. [41] tested the efficacy of a series of bacterial and fungal antagonistic strains such as *T. harzianum* against infection by *Fusarium oxysporum* E.F.Sm. & Swingle and *R. solani* in grapevine plants of the variety ‘Thompson Seedless’, concluding that both the application of these antagonists by immersion of the root system of the plants and the incorporation of the same to the culture substrate managed to reduce the incidence of root rot or the colonization of the roots by the pathogens. The results obtained in the present study on seedlings from germinated seed, although they cannot be compared with those reported in the studies mentioned above based on grafted plants, seem to agree with those previously cited on the fact that the protective effects of the antagonistic strains of *T. harzianum* are basically associated to the root system of the treated plants, where successive treatments with the different strains of *T. harzianum* reflected higher root development associated to lower colonization rates by the pathogen, compared to control plants artificially infected only with *R. solani*.

Regarding biological control trials on grafted plants, it was shown that simultaneous applications of certain strains of *T. harzianum* obtained higher values of root and aerial biomass length than controls with *R. solani*. This is consistent with the findings of authors such as Marais [38], Walker [42], and Hemida et al. [43], who stated that *R. solani* infections in young grapevine plants are associated with a reduction in root biomass and the existence of active root rot, in addition to general retardation of plant growth.

4.4. *Trichoderma harzianum* as a Growth Promoter

Along with the protective effects against specific plant pathogens, another important aspect related to biocontrol trials with *Trichoderma* is the ability of the different species of this genus to promote and stimulate plant growth, widely studied in different plant species [19], including grapevine [44–47].

In the present study, the inoculation of *Trichoderma* protective strains was carried out at two levels: (1) on grapevine seedlings germinated from seed and (2) on grafted plants coming from the protection experiments against *N. parvum* and *R. solani*.

In the case of seedlings, the results obtained suggested that the different strains of *T. harzianum* were not able to increase the different biometric parameters analyzed compared to control plants without any microbial inoculant, except for *T. harzianum* 5, which promoted root development. A possible explanation for this could be the scarce development of the root systems of this type of plant, where the culture system based on a small container with inert substrate could be a limitation for the incorporation and colonization of the plant by the mentioned isolates of *T. harzianum*.

Regarding *T. harzianum* growth promotion assays on grafted grapevine plants, biometric increases were recorded in plants from *T. harzianum* control experiments with the two mentioned pathogens. This increase was especially significant in root biomass, regardless of the statistical significance of this type of interaction. This type of beneficial effects, especially at the root system level, has been previously reported for this antagonistic genus in numerous plant hosts, including grapevine, where some authors (e.g., Di Marco and Osti [44]) observed significant increases in root biomass in grapevine plants treated with *Trichoderma*, especially at the time of rooting, suggesting another relevant feature of this genus from the biotechnological point of view: its potential use as a microbial fertilizer [48,49]. In this sense, in the study of Di Marco et al. [12], it was observed that grapevine roots developed four times more compared to controls when treated with *Trichoderma*. The mentioned authors concluded that the grapevines treated with the mentioned genus presented a more developed root system, which improved the absorption of water and nutrients and endowed them with a greater tolerance to stress-related diseases. Similarly, Fourie et al. [47] observed that the early shoot growth of *Trichoderma* treated grapevine plants was visibly better than that of untreated control plants. Regarding the effect of *Trichoderma* on rooting, these authors found that the fresh root weight of grapevine increased by 41.7% after monthly treatments with *Trichoderma* in the greenhouse soil.

5. Conclusions

In dual plate confrontations, it was found that the selected native *T. harzianum* strains were able to inhibit the mycelial growth of two grapevine pathogens, although the inhibition of *N. parvum* was much more effective than that of *R. solani*. In trials conducted on seedlings, the protective effects of successive treatments with the *T. harzianum* antagonist strains resulted in higher root development and dry weight, and a lower colonization rate of the pathogen, especially against *R. solani*. Concerning the tests carried out on grafted plants, in the case of *N. parvum*, the results were disparate, while simultaneous treatments led to higher aerial biomass lengths and higher necrosis than successive treatments, root lengths showed the opposite behavior. In the protection against *R. solani* tests, simultaneous treatments were more effective in several cases, resulting in higher values of root and aerial biomass length and lower rates of vascular necrosis. The *T. harzianum* strains tested herein offer a promising alternative as BCAs to traditional chemical fungicides, in addition to their ability to promote the growth of grafted plants, especially root biomass.

Author Contributions: Conceptualization, V.G.-G. and N.L.-L.; methodology, V.G.-G., N.L.-L., J.C.-G. and C.J.-L.; software, P.M.-R.; data curation, N.L.-L. and C.J.-L.; validation, V.G.-G., N.L.-L., J.C.-G. and P.M.-R.; investigation, V.G.-G., N.L.-L. and C.J.-L.; writing—original draft preparation, V.G.-G., N.L.-L., J.C.-G. and P.M.-R.; writing—review and editing, V.G.-G., N.L.-L. and P.M.-R.; supervision, V.G.-G. and P.M.-R. All authors have read and agreed to the published version of the manuscript.

Funding: This research received no external funding.

Institutional Review Board Statement: Not applicable.

Informed Consent Statement: Not applicable.

Data Availability Statement: The data presented in this study are available on request from the corresponding author. The data are not publicly available due to their relevance to be part of an ongoing Ph.D. Thesis.

Conflicts of Interest: The authors declare no conflict of interest.

References

- Mondello, V.; Songy, A.; Battiston, E.; Pinto, C.; Coppin, C.; Trotel-Aziz, P.; Clement, C.; Mugnai, L.; Fontaine, F. Grapevine trunk diseases: A review of fifteen years of trials for their control with chemicals and biocontrol agents. *Plant Dis.* **2018**, *102*, 1189–1217. [[CrossRef](#)] [[PubMed](#)]
- Rezgui, A.; Vallance, J.; Ben Ghnaya-Chakroun, A.; Bruez, E.; Dridi, M.; Demasse, R.D.; Rey, P.; Sadfi-Zouaoui, N. Study of *Lasiodiplodia pseudotheobromae*, *Neofusicoccum parvum* and *Schizophyllum commune*, three pathogenic fungi associated with the grapevine trunk diseases in the North of Tunisia. *Eur. J. Plant Pathol.* **2018**, *152*, 127–142. [[CrossRef](#)]
- Gramaje, D. Enfermedades de la madera de la vid: Situación actual y estrategias de control. In Proceedings of the Jornadas Vitivinícolas, Logroño, Spain, 1 December 2017; pp. 1–54.
- Massonnet, M.; Figueroa-Balderas, R.; Galarneau, E.R.; Miki, S.; Lawrence, D.P.; Sun, Q.; Wallis, C.M.; Baumgartner, K.; Cantu, D. *Neofusicoccum parvum* colonization of the grapevine woody stem triggers asynchronous host responses at the site of infection and in the leaves. *Front. Plant Sci.* **2017**, *8*, 1117. [[CrossRef](#)] [[PubMed](#)]
- Walker, G.E. Root rot of grapevine rootlings in South Australia caused by *Rhizoctonia solani*. *Australas. Plant Pathol.* **1992**, *21*, 58–60. [[CrossRef](#)]
- Halleen, F.; Crous, R.W.; Petrin, O. Fungi associated with healthy grapevine cuttings in nurseries, with special reference to pathogens involved in the decline of young vines. *Australas. Plant Pathol.* **2003**, *32*, 47–52. [[CrossRef](#)]
- Gramaje, D.; Urbez-Torres, J.R.; Sosnowski, M.R. Managing grapevine trunk diseases with respect to etiology and epidemiology: Current strategies and future prospects. *Plant Dis.* **2018**, *102*, 12–39. [[CrossRef](#)]
- Benítez, T.; Rincón, A.M.; Limón, M.C.; Codon, A.C. Biocontrol mechanisms of *Trichoderma* strains. *Int. Microbiol.* **2004**, *7*, 249–260.
- Pertot, I.; Prodorutti, D.; Colombini, A.; Pasini, L. *Trichoderma atroviride* SC1 prevents *Phaeoconiella chlamydospora* and *Phaeoacremonium aleophilum* infection of grapevine plants during the grafting process in nurseries. *BioControl* **2016**, *61*, 257–267. [[CrossRef](#)]
- Monte, E.; Liobell, A. *Trichoderma* in organic agriculture. In Proceedings of the V World Avocado Congress (Actas V Congreso Mundial del Aguacate), Granada-Málaga, Spain, 19–24 October 2003; pp. 725–733.
- Compant, S.; Mathieu, F. *Biocontrol of Major Grapevine Diseases: Leading Research*; CABI International: Wallingford, UK, 2016; p. 256.
- Di Marco, S.; Osti, F.; Cesari, A. Experiments on the control of esca by *Trichoderma*. *Phytopathol. Mediterr.* **2004**, *43*, 108–115.
- Fanjul, M.J. *Use of Trichoderma spp. in the Management of Grapevine Trunk Diseases in Europe*; Winetwork European Knowledge Transfer: Lisle-sur-Tarn, France, 2017; pp. 1–5.
- Wallis, C.M. Nutritional niche overlap analysis as a method to identify potential biocontrol fungi against trunk pathogens. *Biocontrol* **2021**, *66*, 559–571. [[CrossRef](#)]
- Silva-Valderrama, I.; Toapanta, D.; Miccono, M.D.; Lolos, M.; Diaz, G.A.; Cantu, D.; Castro, A. Biocontrol potential of grapevine endophytic and rhizospheric fungi against trunk pathogens. *Front. Microbiol.* **2021**, *11*, 13. [[CrossRef](#)] [[PubMed](#)]
- Mutawila, C. *Improving Pruning Wound Protection Against Grapevine Trunk Disease Pathogens*; Stellenbosch University: Stellenbosch, South Africa, 2014.
- Ezziyyani, M.; Sánchez, C.P.; Ahmed, A.S.; Requena, M.E.; Castillo, M.E.C. *Trichoderma harzianum* como biofungicida para el biocontrol de *Phytophthora capsici* en plantas de pimiento (*Capsicum annuum* L.). *An. Biol.* **2004**, *26*, 35–45.
- Monte, E. Understanding *Trichoderma*: Between biotechnology and microbial ecology. *Int. Microbiol.* **2001**, *4*, 1–4. [[PubMed](#)]
- Gupta, V.G.; Schmoll, M.; Herrera-Estrella, A.; Upadhyay, R.; Druzhinina, I.; Tuohy, M. *Biotechnology and Biology of Trichoderma*; Elsevier: Amsterdam, The Netherlands, 2014.
- Bastakoti, S.; Belbase, S.; Manandhar, S.; Arjyal, C. *Trichoderma* species as biocontrol agent against soil borne fungal pathogens. *Nepal J. Biotechnol.* **2017**, *5*, 39–45. [[CrossRef](#)]
- Aly, A.; Abdel-Sattar, M.; Omar, M.; Abd-Elsalam, K. Differential antagonism of *Trichoderma* sp. against *Macrophomina phaseolina*. *J. Plant Prot. Res.* **2007**, *47*, 91–102.
- Boughalleb, N.; Ben-Salem, I.; M’Hamdi, M. Evaluation of the efficiency of *Trichoderma*, *Penicillium*, and *Aspergillus* species as biological control agents against four soil-borne fungi of melon and watermelon. *Egypt. J. Biol. Pest Control* **2018**, *28*, 25. [[CrossRef](#)]
- Fernández, R.J.; Suárez, C.L. Antagonismo in vitro de *Trichoderma harzianum* Rifai sobre *Fusarium oxysporum* Schlecht f. sp. *passiflorae* en maracuyá (*Passiflora edulis* Sims var. *flavicarpa*) del municipio zona bananera colombiana. *Rev. Fac. Nac. Agron.-Medellín* **2009**, *62*, 4743–4748.
- González, V.; Portal, M.; Rubio, V. Biology and systematics of the form genus *Rhizoctonia*. *Span. J. Agric. Res.* **2006**, *4*, 55–79. [[CrossRef](#)]

25. Siameto, E.; Okoth, S.; Amugune, N.; Chege, N. Antagonism of *Trichoderma harzianum* isolates on soil borne plant pathogenic fungi from Embu District, Kenya. *J. Yeast Fungal Res.* **2010**, *1*, 47–54.
26. Guedez, C.; Cañizalez, L.; Castillo, C.; Olivar, R. Evaluación in vitro de aislamientos de *Trichoderma harzianum* para el control de *Rhizoctonia solani*, *Sclerotium rolfsii* y *Fusarium oxysporum* en plantas de tomate. *Rev. Soc. Venez. Microbiol.* **2012**, *32*, 44–49.
27. Marraschi, R.; Ferreira, A.; da Silva Bueno, R.N.; Leite, J.; Lucon, C.M.; Harakava, R.; Leite, L.G.; Padovani, C.R.; Bueno, C.J. A protocol for selection of *Trichoderma* spp. to protect grapevine pruning wounds against *Lasiodiplodia theobromae*. *Braz. J. Microbiol.* **2019**, *50*, 213–221. [[CrossRef](#)] [[PubMed](#)]
28. Urbez-Torres, J.R.; Tomaselli, E.; Pollard-Flamand, J.; Boule, J.; Gerin, D.; Pollastro, S. Characterization of *Trichoderma* isolates from southern Italy, and their potential biocontrol activity against grapevine trunk disease fungi. *Phytopathol. Mediterr.* **2020**, *59*, 425–439. [[CrossRef](#)]
29. Plata-Caudillo, J.A. *Aislamiento y Evaluación In Vitro del Efecto de Trichoderma spp. Nativas Sobre los Hongos Patógenos de la Madera de Vid Aislados en la Región Vitivinícola de Ensenada, Baja California*; Centro de Investigación Científica y de Educación Superior de Ensenada: Ensenada, Mexico, 2010.
30. Mutawila, C.; Vinale, F.; Halleen, F.; Lorito, M.; Mostert, L. Isolation, production and in vitro effects of the major secondary metabolite produced by *Trichoderma* species used for the control of grapevine trunk diseases. *Plant Pathol.* **2016**, *65*, 104–113. [[CrossRef](#)]
31. Kotze, C.; Van Niekerk, J.; Mostert, L.; Halleen, F.; Fourie, P.H. Evaluation of biocontrol agents for grapevine pruning wound protection against trunk pathogen infection. *Phytopathol. Mediterr.* **2011**, *50*, S247–S263.
32. D'Enjoy, G.; Nesler, A.; Frati, S. *Trichoderma atroviride* SC1 is a tool for life-long protection of grape against trunk diseases. *Nat. Prod. Biotechnol.* **2016**, *61*, 257–267. [[CrossRef](#)]
33. Hunt, J.S.; Gale, D.S.J.; Harvey, I.C. Evaluation of *Trichoderma* as bio-control for protection against wood-invading fungi implicated in grapevine trunk diseases. *Phytopathol. Mediterr.* **2001**, *40*, 485–486.
34. Halleen, F.; Fourie, P.H.; Lombard, P.J. Protection of grapevine pruning wounds against *Eutypa lata* by biological and chemical methods. *Enol. Vitic.* **2010**, *31*, 125–132. [[CrossRef](#)]
35. Harvey, I.; Hunt, J. Penetration of *Trichoderma harzianum* into grapevine wood from treated pruning wounds. *N. Z. Plant Prot.* **2006**, *59*, 343–347. [[CrossRef](#)]
36. Halleen, F.; Fourie, P.H. An integrated strategy for the proactive management of grapevine trunk disease pathogen infections in grapevine nurseries. *S. Afr. J. Enol.* **2016**, *37*, 104–114. [[CrossRef](#)]
37. Pintos, C.; Redondo, V.; Aguín, O.; Chaves, M.; Rial, C.; Mansilla, J. Evaluation of *Trichoderma atroviride* as biocontrol agent against five *Botryosphaeriaceae* grapevine trunk pathogens. *Phytopathol. Mediterr.* **2012**, *51*, 450.
38. Marais, P. Fungi associated with root rot in vineyards in the Western Cape. *Phytophylactica* **1979**, *11*, 65–68.
39. Crous, P.W.; Swart, L.; Coertze, S. The effect of hot-water treatment on fungi occurring in apparently healthy grapevine cuttings. *Phytopathol. Mediterr.* **2001**, *40*, S464–S466.
40. Mahrous, H. Reaction of different grapevine cultivars to infection with root rotting fungi and its control. *Phytopathol. Mediterr.* **2001**, *40*, S479–S486.
41. Ziedan, E.; Moataza, M.; Eman, S. Biological control of grapevine root-rot by antagonistic microorganisms. *Afr. J. Mycol. Biotechnol.* **2005**, *13*, 19–36.
42. Walker, G.E. Effects of *Meloidogyne* spp. and *Rhizoctonia solani* on the growth of grapevine rootings. *J. Nematol.* **1997**, *29*, 190. [[PubMed](#)]
43. Hemida, K.; Ziedan, E.H.; El-Saman, M.; El-Naggar, M.; Mostafa, H. Etiology of fungi associated with grapevine decline and their pathological potential. *Arab. Univ. J. Agric. Sci.* **2017**, *25*, 355–365. [[CrossRef](#)]
44. Di Marco, S.; Osti, F. Applications of *Trichoderma* to prevent *Phaeoemoniella chlamydospora* infections in organic nurseries. *Phytopathol. Mediterr.* **2007**, *46*, 73–83.
45. Ahmed, M. Evaluation of some biocontrol agents to control Thompson seedless grapevine powdery mildew disease. *Egypt. J. Biol. Pest Control* **2018**, *28*, 93. [[CrossRef](#)]
46. Fourie, P.H.; Halleen, F. Proactive control of Petri disease of grapevine through treatment of propagation material. *Plant Dis.* **2004**, *88*, 1241–1245. [[CrossRef](#)]
47. Fourie, P.H.; Halleen, F.; Vyver, J.; Schreuder, W. Effect of *Trichoderma* treatments on the occurrence of decline pathogens in the roots and rootstocks of nursery grapevines. *Phytopathol. Mediterr.* **2001**, *40*, 473–478. [[CrossRef](#)]
48. Kamal, R.K.; Athisayam, V.; Gusain, Y.S.; Kumar, V. *Trichoderma*: A most common biofertilizer with multiple roles in agriculture. *Biomed. J. Sci. Tech. Res.* **2018**, *4*, 4136–4137. [[CrossRef](#)]
49. Hermosa, R.; Viterbo, A.; Chet, I.; Monte, E. Plant-beneficial effects of *Trichoderma* and its genes. *Microbiology* **2012**, *158*, 17–25. [[CrossRef](#)] [[PubMed](#)]

ARTÍCULO 9: “Comparison of the efficacy of *Trichoderma* and *Bacillus* strains and commercial biocontrol products against grapevine *Botryosphaeria dieback* pathogens” *Agronomy*, 2023, 13(2), 533; <https://doi.org/10.3390/agronomy13020533>; Q1 (JCR, Science Edition – AGRONOMY). JIF₂₀₂₂ = 3,7. 1 cita recibida (WOS).



agronomy

an Open Access Journal by MDPI



Comparison of the Efficacy of *Trichoderma* and *Bacillus* Strains and Commercial Biocontrol Products against Grapevine *Botryosphaeria* Dieback Pathogens

Natalia Langa-Lomba; Vicente González-García; M. Eugenia Venturini-Crespo; José Casanova-Gascón; Juan J. Barriuso-Vargas; Pablo Martín-Ramos

Agronomy 2023, Volume 13, Issue 2, 533

Novel Biological Control Agents (BCAs) for grapevine pruning wound protection

2 research-grade strains, aligned with Conservation Biological Control strategies:

- *Trichoderma harzianum*
- *Bacillus velezensis* (BUZ-14)

vs. 3 commercial products:

- *Trichoderma harzianum* (strain T-22)
- *Trichoderma atroviride* (strain I-1237)
- *Bacillus subtilis* (BS03)



Control of fungi responsible for *Botryosphaeria dieback*:

- *Diplodia seriata*
- *Neofusicoccum parvum*

→ **Reduced vascular necroses**



Brief Report

Comparison of the Efficacy of *Trichoderma* and *Bacillus* Strains and Commercial Biocontrol Products against Grapevine *Botryosphaeria* Dieback Pathogens

Natalia Langa-Lomba^{1,2}, Vicente González-García¹, M. Eugenia Venturini-Crespo³ , José Casanova-Gascón⁴ , Juan J. Barriuso-Vargas⁴ and Pablo Martín-Ramos^{2,5,*} 

¹ Department of Agricultural, Forest and Environmental Systems, Agrifood Research and Technology Centre of Aragón, Instituto Agroalimentario de Aragón—IA2 (Universidad de Zaragoza-CITA), Avda. Montañana 930, 50059 Zaragoza, Spain

² Instituto Universitario de Investigación en Ciencias Ambientales de Aragón (IUCA), EPS, University of Zaragoza, Carretera de Cuarte s/n, 22071 Huesca, Spain

³ Plant Food Research Group, Instituto Agroalimentario de Aragón—IA2 (Universidad de Zaragoza-CITA), Miguel Servet 177, 50013 Zaragoza, Spain

⁴ Instituto Agroalimentario de Aragón-IA2 (Universidad de Zaragoza-CITA), Avda. Montañana 930, 50059 Zaragoza, Spain

⁵ Department of Agricultural and Forestry Engineering, ETSIIAA, University of Valladolid, Avenida de Madrid 44, 34004 Palencia, Spain

* Correspondence: pmr@unizar.es



Citation: Langa-Lomba, N.; González-García, V.; Venturini-Crespo, M.E.; Casanova-Gascón, J.; Barriuso-Vargas, J.J.; Martín-Ramos, P. Comparison of the Efficacy of *Trichoderma* and *Bacillus* Strains and Commercial Biocontrol Products against Grapevine *Botryosphaeria* Dieback Pathogens. *Agronomy* **2023**, *13*, 533. <https://doi.org/10.3390/agronomy13020533>

Academic Editors: Rita B. Santos and Andrea Figueiredo

Received: 29 December 2022

Revised: 6 February 2023

Accepted: 9 February 2023

Published: 13 February 2023



Copyright: © 2023 by the authors. Licensee MDPI, Basel, Switzerland. This article is an open access article distributed under the terms and conditions of the Creative Commons Attribution (CC BY) license (<https://creativecommons.org/licenses/by/4.0/>).

Abstract: Grapevine trunk diseases (GTDs) cause significant yield losses worldwide and limit the lifespan of vineyards. In the last few years, using biological control agents (BCAs) for pruning wound protection has become a promising management strategy for the control of these pathologies. This study aimed to compare the antifungal activities of a grapevine-native *Trichoderma harzianum* isolate and a high-potential *Bacillus velezensis* strain against two pathogenic *Botryosphaeriaceae* species in artificially inoculated, potted, grafted plants under controlled greenhouse conditions, taking three commercial biocontrol products (based on *T. atroviride* I-1237, *T. harzianum* T-22, and *Bacillus subtilis* BS03 strains) as a reference. To reproduce certain field conditions more realistically, inoculation of the protective agents and the pathogens was conducted simultaneously immediately after pruning instead of allowing the BCAs to colonize the wounds before pathogen inoculation. Significant differences in necrosis lengths were detected for both *Neofusicoccum parvum*- and *Diplodia seriata*-infected plants, and a remarkable protective effect of *Bacillus velezensis* BUZ-14 was observed in all cases. *Trichoderma*-based treatments showed different efficacies against the two pathogenic fungi. While the three tested BCAs resulted in significant reductions in vascular necrosis caused by *N. parvum*, they did not significantly reduce *D. seriata* infection compared to the untreated inoculated control. The *B. subtilis* strain was not effective. The reported results provide support for the potential *Bacillus velezensis* may have for pruning wound protection against *Botryosphaeriaceae* fungi, encouraging its evaluation under natural field conditions.

Keywords: *Bacillus subtilis*; *Bacillus velezensis*; BCAs; *Diplodia seriata*; GTDs; *Neofusicoccum parvum*; *Trichoderma harzianum*; *Trichoderma atroviride*; *Vitis vinifera*; wound protection

1. Introduction

Grapevine trunk diseases (GTDs) are diseases caused by several fungal genera and species that alter wood, causing general decay of the plant and leading to yield reductions and reduced lifespan [1]. Black-foot (mainly caused by species of the genera *Ilyonectria*, *Dactylonectria*, *Campylocarpon*, and *Cylindrocarpon*), Petri, and *Botryosphaeriaceae* dieback (caused by members of the genera *Botryosphaeria*, *Diplodia*, *Lasiodyplodia*, *Neofusicoccum*, and *Dothiorella*) diseases are most commonly associated with young vineyards, while Esca

(caused by species of the genera *Fomitiporia*, *Stereum*, *Inonotus*, *Phaeomoniella*, and *Phaeoacremonium*), eutypiosis (with the genus *Eutypa* as the main causal agent), and black dead arm diseases stand out for adult plants. In the last three decades, these fungal pathologies have become a major concern among winegrowers as they are causing important economic losses worldwide, with an annual cost associated with the replacement of grapevine plants estimated at more than EUR 1.1 billion in 2017 [2].

Interest in the development of new control methods to manage these diseases has increased for a variety of reasons, including the absence of curative crop protection products, the higher impact of these diseases as a result of more intensive vineyard management, and the banning of numerous fungicides of chemical origin. Hence, the lack of options for the control and management of these diseases makes the use of preventive measures, such as pruning wound-protectant biological control agents (BCAs), a key and environmentally friendly strategy [3].

Previous studies exploring the suitability and potential of biological control methods for GTDs have covered both bacterial antagonists (belonging to the genera *Bacillus*, *Pseudomonas*, *Streptomyces*, and *Enterobacter*) [4] and fungal BCAs (including several species of *Fusarium*, *Trichoderma*, and *Epicoccum*, among others) [1], but *Trichoderma* spp. and *Bacillus* spp. are by far the most widely tested and effective microorganisms against wood diseases in grapevines.

Trichoderma spp., one of the most widely used microorganisms in integrated pest management [5,6] and extensively licensed and employed as commercial preparations, exhibits complex mechanisms of interest for disease control, such as its hyperparasitic behavior and the production of lytic enzymes, antimicrobial substances, and other secondary metabolites with germicidal action [7], and it has also been reported to be a plant growth promoter [8]. In turn, the antibiosis mechanism based on *Bacillus* species functions through beneficial molecules (including hydrosoluble and volatile metabolites) that induce or trigger plant defense pathways (phytohormone precursors, lipopolysaccharides, siderophores, etc.) [4].

Concerning their efficacy against *Botryosphaeriaceae* dieback (one of the most significant emergent GTDs caused by fungal species belonging to the genera *Botryosphaeria*, *Diplodia*, *Neofusicoccum*, *Lasiodiplodia*, *Dothiorella*, and *Spencermartinsia* [9])—and, in particular, against two of the most frequently isolated species of the group (viz. *Neofusicoccum parvum* (Pennycook & Samuels) Crous, Slippers & A.J.L. Phillips and *Diplodia seriata* De Not)—several *Trichoderma atroviride* P. Karst. and *Trichoderma harzianum* Rifai strains have been reported to reduce these infections [4,8,10–13], albeit with variable results in terms of efficacy, as is also the case for *Bacillus subtilis* (Ehrenberg 1835) Cohn 1872 [4,10,14]. However, with a few exceptions [8,15], many of these BCAs are not native to grapevine plants, and commercial products were developed to control different pathogens in crops other than grapevines. As noted by Pollard-Flamand et al. [8], adopting a BCA product from another climate or ecosystem may present problems as the effectiveness of BCA-based formulations can vary between in vitro and in situ studies performed in different hosts and under different environmental conditions. Consequently, in recent years, there has been a growing interest in conservation biological control (CBC) [16] and the evaluation of the potential of locally isolated endophytic BCAs against GTD fungi, given that they could be better adapted.

Accordingly, a native grapevine strain of *T. harzianum* was chosen from among a set of isolates of this species tested in a previous study [15] due to the good protective results obtained. Thus, the work presented herein aimed to evaluate the efficacy of this microorganism in potted, grafted plants artificially inoculated with *N. parvum* and *D. seriata*, comparing it with that of the promising research-grade strain of *Bacillus velezensis* Ruiz-Garcia et al. 2005 (formerly named *B. amyloliquefaciens* BUZ-14, native to another plant host in the same geographical area) and three commercial biocontrol products (based on *T. atroviride* I-1237, *T. harzianum* T-22, and *Bacillus subtilis* BS03).

2. Material and Methods

2.1. Plant Material

The two-year-old grafted plants used in the bioassays were supplied by VCR Vivai Cooperativi Rauscedo (Italy) with supplier ID IT-06-1031. The chosen clone was “Tempranillo RJ 43” and the rootstock was “110R VCR114”.

2.2. Fungal Isolates

The *Botryosphaeriaceae* fungi selected for the assays were a *Neofusicoccum parvum* strain (isolate MYC-1270) and a *Diplodia seriata* strain (isolate MYC-1569) isolated from diseased young (5–7 years old) Aragonese grapevine plants preserved in the fungal living collection of the Mycology Laboratory at the Department of Agricultural, Forestry and Environmental Systems of the Centro de Investigación y Tecnología Agroalimentaria de Aragón (CITA, Zaragoza, Spain). The two pathogenic species were isolated from diseased grapevine plants sampled in wine-producing areas of Aragon (northeast Spain) and characterized using both morphological and molecular methods. In this way, ribosomal ITS sequences of both strains were obtained, and their taxonomical assignment was confirmed by comparison with public databases with the BLASTn tool. The isolates were recovered from cryovials with 20% glycerol at a temperature of $-80\text{ }^{\circ}\text{C}$ as potato dextrose agar (PDA, purchased from Becton, Dickinson, and Company; Franklin Lakes, NJ, USA) subcultures, performing periodic replicates to maintain optimal colonies. These two taxa were selected because they are among the more virulent, polyphagous, and faster-growing *Botryosphaeriaceae*, utilizing larger carbon and nitrogen sources than other species [17].

2.3. Treatments

Five biocontrol agents were tested against both pathogens: a native *Trichoderma harzianum* (isolate MYC-V102) strain isolated as an endophyte of grapevine plants originating from healthy samples from vineyards in Aragon and identified at the morphological and molecular level (through BLASTn comparison of its ribosomal ITS sequence) in previous work [15]; a *Bacillus velezensis* strain (BUZ-14) obtained from the Plant Food Research Group Collection at the University of Zaragoza, isolated from the surface of peach fruit from an orchard in Zaragoza, that had been successfully tested for antifungal potential against other phytopathogens [18,19]; the commercial wound protectant Trianum-P[®] based on *T. harzianum* (strain T-22), developed by Koppert BV (Berkel en Rodenrijs, the Netherlands) and commercialized by Koppert España (La Mojonera, Almería); the commercial wound protectant product Esquive[®] based on *Trichoderma atroviride* (strain I-1237), developed by Agrauxine S.A. (Quimper, France) and commercialized by Idai Nature S.L. (Valencia, Spain); and the commercial formulation FUNGISEI[®] based on *Bacillus subtilis* (strain BS03), developed by Seipasa (Valencia, Spain). The *Bacillus velezensis* (strain BUZ-14) had been previously characterized and its evolutionary relationships were elucidated through a phylogenetic reconstruction using Bayesian inference from a comparison of its ribosomal 16S sequence (Figure A1).

2.4. Production of *T. harzianum* and *B. velezensis* Treatments

To obtain conidial solutions of the native *T. harzianum* strain employed, it was inoculated in sextuplicate (4 mm diameter agar plugs) on PDA plates (12 cm in diameter) and incubated at $25\text{ }^{\circ}\text{C}$ in the dark. To harvest the conidia, sterile bidistilled water was poured into each plate, completely covering the colony, and the plates were sealed with ParafilmTM. The plates were then shaken to detach the conidia, and the aqueous solution containing the spores was recovered. Subsequently, the conidial solutions were titrated and adjusted using a hemacytometer to obtain a final concentration of 1×10^7 conidia·mL⁻¹. The inoculum was stored in cold storage until subsequent use.

To prepare a fresh cell suspension of the *B. velezensis* BUZ-14 strain, a 24 h old culture on tryptose soy agar (TSA, purchased from Becton, Dickinson, and Company) was transferred to 7 mL of tryptose soy broth (TSB, also supplied by Becton, Dickinson, and Company),

the suspension was incubated at 30 °C for 24 h on a rotary shaker at 150 rpm, and the concentration was finally adjusted to 1×10^7 CFU·mL⁻¹.

2.5. Greenhouse Bioassays on Grafted Plants

For the in vivo tests, 232 grafted grapevine plants were used: 100 were infected with *N. parvum* (20 plants/treatment), 100 were infected with *D. seriata* (20 plants/treatment), 20 were used as negative controls (4 plants/treatment), and 12 were used as positive controls (6 plants/pathogen) (Table 1).

Table 1. Treatments, concentrations, and replicates used in the bioassays.

Treatment	Concentration	Pathogen	Number of Replicates
Native <i>Trichoderma harzianum</i>	1×10^7 conidia·mL ⁻¹	<i>D. seriata</i>	20
		<i>N. parvum</i>	20
		Negative control	4
<i>Trichoderma harzianum</i> T-22 (Trianum-P®)	1×10^7 conidia·mL ⁻¹	<i>D. seriata</i>	20
		<i>N. parvum</i>	20
		Negative control	4
<i>Trichoderma atroviride</i> I-1237 (Esquire®)	1×10^7 conidia·mL ⁻¹	<i>D. seriata</i>	20
		<i>N. parvum</i>	20
		Negative control	4
<i>Bacillus velezensis</i> BUZ-14	1×10^7 CFU·mL ⁻¹	<i>D. seriata</i>	20
		<i>N. parvum</i>	20
		Negative control	4
<i>Bacillus subtilis</i> BS03 (FUNGISEI®)	1×10^7 CFU·mL ⁻¹	<i>D. seriata</i>	20
		<i>N. parvum</i>	20
		Negative control	4
-	-	<i>D. seriata</i> positive control	6
		<i>N. parvum</i> positive control	6

Each grafted plant was grown in a 3.5 L plastic pot with a mixed substrate of peat and natural grapevine soil (75:25) with a loamy texture from an experimental vineyard in the natural region “Hoya de Huesca” (Huesca, NE Spain) and treated in an autoclave, incorporating a slow-release fertilizer when necessary throughout the study period. Grapevine plants were kept in a greenhouse with drip irrigation and an anti-weed net at the Escuela Politécnica Superior, Universidad de Zaragoza, for six months (from May to November 2022). The cooling system installed in the greenhouse controlled parameters such as ventilation, humidity, and temperature. The mean temperature during the experiment ranged from 10 to 29 °C (day/night), while the relative humidity (RH) varied over the interval of 30–45%.

Rootstocks were simultaneously inoculated in May 2022 with the five BCAs and the two pathogens (*N. parvum* and *D. seriata*). Inoculations were performed on the rootstock trunk at two points below the grafting point. Slits (15 mm in diameter and 5 mm deep) were made with a scalpel. The protective treatments were applied in different ways on the slits. For native and commercial *T. harzianum* strains, the inocula were applied using alginate beads as a carrier, prepared by dispersing fungal propagule solutions in a 3% sodium alginate solution in a 1:4 ratio (i.e., 20 mL treatment/80 mL sodium alginate). Once the mixture was homogenized, the solution was dispensed dropwise over a 3% calcium carbonate solution to produce the ionic exchange and spherify the resulting solution. As a result, beads with $\varnothing = 0.4$ – 0.6 cm containing the different treatments were obtained. Two beads, one on each side of the agar plug with the pathogen, were placed on each wound (Figure 1a). The commercial *T. atroviride* I-1237 treatment was applied as a spray to the wound and allowed to dry (Figure 1b). The treatment with *Bacillus velezensis* BUZ-14 was amended with 1% ALKIR® wetting agent (De Sangosse Ibérica, Valencia, Spain),

applied to each wound using a pipette (1.5 mL per wound), and allowed to dry (Figure 1c). The same procedure was followed for the commercial formulation of *Bacillus subtilis* (BS03). Agar plugs (5 mm in diameter) from fresh pathogen PDA cultures were placed on the center of the slit, and the wound was covered with absorbent sterile cotton moistened with sterile bidistilled water and sealed with Parafilm™.

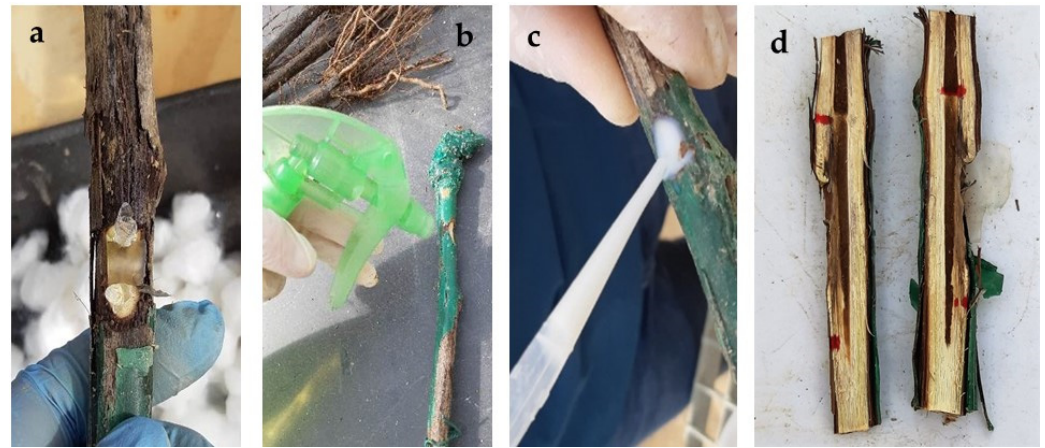


Figure 1. BCA application procedures. (a) Treatment with *T. harzianum* inocula dispersed in alginate beds placed at both sides of the agar plug together with the pathogen; (b) spraying of *T. atroviride* inocula; (c) application of *Bacillus* spp.-based treatments using a pipette; (d) longitudinally opened plant showing vascular necroses from the inoculation points.

In November 2022, the grafted plants were cut into sections and opened longitudinally, and the lengths of the vascular necroses were evaluated (Figure 1d). Lesions were measured longitudinally on both sides of each inoculation point in the upper and lower directions, taking the average of the four measurements as the necrosis length for each inoculation point. Finally, the two mentioned pathogens were re-isolated directly from the vascular lesions and morphologically identified to fulfill Koch's postulates.

2.6. Statistical Analyses

Since the normality and homoscedasticity requirements were not met, the Kruskal–Wallis nonparametric test was used, with the Conover–Iman test employed for post hoc multiple pairwise comparisons. R statistical software was used for all of the statistical analyses [20].

3. Results

3.1. Comparison of Efficacies against *N. parvum*

None of the biocontrol agents tested fully inhibited the vascular symptoms of *N. parvum* (Figure 2). However, some of the treatments were effective in reducing the length of the necrosis produced—with statistically significant differences (p -value < 0.0001)—in comparison to the controls inoculated only with the pathogen. As shown in Table 2, *B. velezensis* (BUZ-14) was found to be the most effective treatment, with an efficacy comparable to that of the commercial *T. atroviride* formulation. The native strain of *T. harzianum* showed an intermediate efficacy, comparable to that of the commercial T-22 strain, with vascular necrosis lengths that were also significantly different from those of the positive (pathogen) control. Concerning the *B. subtilis*-based product, the necrosis lengths were comparable to those of the positive control.

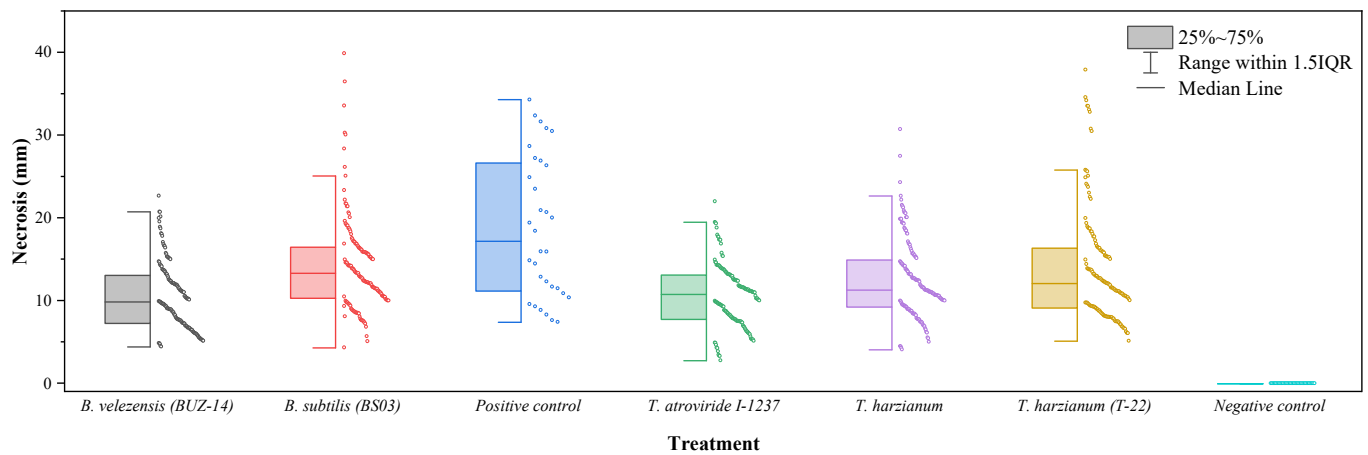


Figure 2. Box-plot of vascular necrosis lengths for *N. parvum*.

Table 2. Kruskal–Wallis test and multiple pairwise comparisons using the Conover–Iman procedure for the lengths of the vascular necroses for *N. parvum*.

Treatment	Mean of Ranks	Groups
Negative control	17.000	A
<i>B. velezensis</i> (BUZ-14)	360.994	B
<i>T. atroviride</i> (I-1237)	372.791	B
<i>T. harzianum</i> (native)	458.920	C
<i>T. harzianum</i> (T-22)	487.763	C
<i>B. subtilis</i> (BS03)	533.659	C
<i>N. parvum</i> positive control	623.578	D

3.2. Comparison of Efficacies against *D. seriata*

Concerning the efficacy of the treatments against *D. seriata* (Figure 3), statistically significant differences (p -value < 0.0001) were also detected depending on the treatment considered (Table 3). *Bacillus velezensis* (BUZ-14) was again the treatment with the highest efficacy and the only one for which necrosis lengths significantly differed from those of the positive (pathogen) control. The three *Trichoderma* strains did not control the growth of *D. seriata* in a significant manner, and necrosis lengths larger than those of the positive control were observed for the *B. subtilis* treatment.

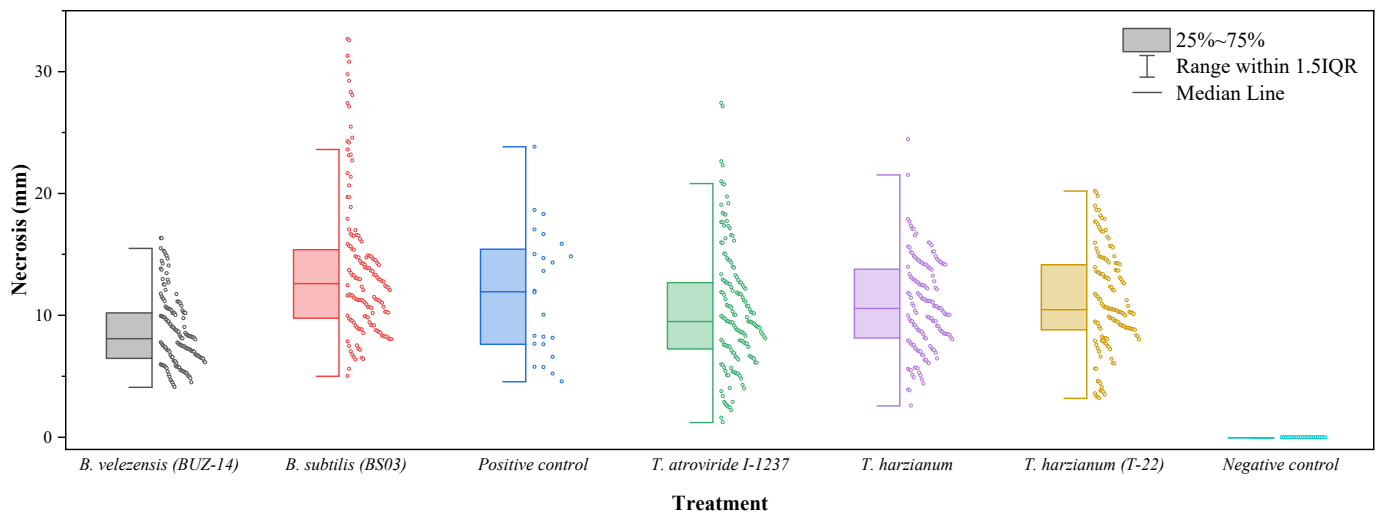


Figure 3. Box-plot of vascular necrosis lengths for *D. seriata*.

Table 3. Kruskal–Wallis test and multiple pairwise comparisons using the Conover–Iman procedure for the lengths of the vascular necroses for *D. seriata*.

Treatment	Mean of Ranks	Groups		
Negative control	12.500	A		
<i>B. velezensis</i> (BUZ-14)	297.784		B	
<i>T. atroviride</i> (I-1237)	399.234			C
<i>T. harzianum</i> (native)	438.197			C
<i>T. harzianum</i> (T-22)	457.480			C
<i>D. seriata</i> positive control	470.813		C	D
<i>B. subtilis</i> (BS03)	548.569			D

4. Discussion

The present work explored the potential of several native fungal and bacterial microorganisms as microbial antagonists against two of the most important pathogens associated with the “*Botryosphaeria dieback*” disease in grapevine. Their potential was tested in comparison to other commercial preparations based on similar microorganisms. When comparing our results with other BCA-based studies with similar GTD fungi—given that the application methods, product concentrations, testing conditions, durations of the assays, etc. differed from one study to another—the efficacy comparisons presented below should be treated with caution.

The strong and remarkable antifungal activity observed for *B. velezensis* BUZ-14 against both pathogens was consistent with previous findings reported by Calvo et al. [18,19] with other important pathogens, such as *Botrytis cinerea* Pers.; *Monilinia fructicola* (G. Winter) Honey; and *Monilinia laxa* (Aderh. & Ruhland) Honey. In these studies, the authors observed the antifungal activity of *B. velezensis* in direct applications on grape and peach fruits, and it was significantly increased when these treatments consisted of culture cell-free supernatant containing hydrosoluble and volatile metabolites. Other *B. amyloliquefaciens* strains have also been reported to be effective against grapevine fungal pathogens. For instance, Alfonzo et al. [21] reported that the crude protein extract obtained from the culture supernatant of a grapevine-native strain of *B. amyloliquefaciens* was effective in vitro against certain grapevine-associated fungi, including GTD pathogens, such as *Fomitiporia mediterranea* M. Fisch., *Lasiodiplodia theobromae* (Pat.) Griffon & Maubl., *Phaeoacremonium aleophilum* W. Gams, Crous, M.J. Wingf. & Mugnai, and *Phaeoconiella chlamydospora* (W. Gams, Crous, M.J. Wingf. & L. Mugnai) Crous & W. Gams. On the other hand, Brown et al. [22] reported a low in vivo efficacy for *B. amyloliquefaciens* against a set of GTD-related fungi that included *N. parvum*, suggesting that this BCA should be applied before the pathogenic infection as a protective strategy to allow the BCA to establish itself and be active in pruning wounds before being challenged by the pathogen. It should be noted that these authors used a formulation based on a wettable powder consisting of CFUs of the antagonist, the activation dynamics (and effectiveness) of which should have been slower than if a solution directly containing secondary metabolites was applied.

Concerning the low activity observed for the *B. subtilis*-based formulation, it should be taken into account that RADISEI® is not commercialized as a wound protectant but as a biostimulant. Nonetheless, it should be noted that there are mixed results about its efficacy in the literature. For instance, Halleen et al. [23] referred to the fact that it was not effective at all against *Eutypa lata* (Pers.) Tul. & C. Tul., and Kotze et al. [10] reported low efficacies against both *Diaporthe ampelina* (Berk. & M.A. Curtis) R.R. Gomes, C. Glienke & Crous and *N. parvum*. On the other hand, *B. subtilis* PTA-271—alone [24] or in combination with *T. atroviride* SC1 [4]—has been shown to be effective against *N. parvum* Bt67. According to Rezgui et al. [14], *B. subtilis* B6 had a positive effect on young vines of the “Muscat d’Italie” cultivar, reducing the size of the wood necrosis caused by *N. parvum*. Rusin et al. [25] also found that *B. subtilis* reduced the severity of *L. theobromae* after winter pruning in cv. “Syrah” grapevines. Alfonzo et al. [26] confirmed—in vitro—that *B. subtilis* AG1 showed antagonistic behavior against *P. aleophilum*, *P. chlamydospora*, and *Botryosphaeria rhodina* (Berk. & M.

A. Curtis) Arx, a result consistent with those reported by Sebestyén et al. [27] for *B. subtilis* (and *T. atroviride*)—also in vitro—against *E. lata*, *P. minimum*, and *P. chlamydospora*. In all these studies, regardless of whether *B. subtilis* was applied as a cell suspension of known concentration or as a crude extract of metabolites (CME), the designs of the treatments usually had in common that they were all employed as pruning wound protectors, where the existence of a protective effect depends on the early colonization by the antagonist prior to pathogenic infection. Thus, a possible explanation for the results obtained here is that *B. subtilis* reduces the incidence of GTD pathogens compared to untreated controls when applied in wounds several days before infection [10].

In the case of fungal BCAs, studies also report varying results on the efficacy of *Trichoderma* spp. against GTD fungi. *T. harzianum* has been reported to reduce the growth of *E. lata* in vitro [28]. In vivo, Rusin et al. [25] indicated that it was effective against *L. theobromae* in “Syrah” grapevines in terms of decreasing its re-isolation rates after treatments. Di Marco et al. [29] assayed *T. harzianum* T39 (Trichodex®) against *P. chlamydospora* in grafted, potted vines, observing that its application prevented black goo and necrosis in the wood below the wound. John et al. [30] found that *T. harzianum* applied to grapevine pruning wounds as a spore suspension reduced the recovery of *E. lata* both in the glasshouse and in the field but noted that—in field experiments—the incorporation of the *Trichoderma* formulate before the pathogen reduced the recovery of the latter. Other *Trichoderma harzianum*-based products also protected pruning wounds in “Cabernet Sauvignon”, “Sauvignon blanc”, “Red Globe”, and “Bonheur” grapevine cultivars, reducing the incidence of *E. lata* and other GTD pathogens [31].

Regarding previous results for *T. atroviride*, in an in vitro screening of *Trichoderma* isolates for the biocontrol of black foot disease pathogens, van Jaarsveld et al. [32] found that two isolates of *T. atroviride* showed the highest overall mycelium growth inhibition (although the efficacy was isolate-dependent, both for *Trichoderma* spp. and the pathogen). Commercial products based on *Trichoderma atroviride* significantly reduced pruning wound infection by GTD fungi, including *N. parvum* (by 80%) and *D. seriata* (by 85%), in studies conducted in South Africa [10]. Pintos et al. [33] also showed that the treatment of pruning wounds with a commercial product based on *T. atroviride* resulted in reductions in the recovery and necrosis lengths of *Botryosphaeriaceae* spp. by 65.7% to 91.9%. Urbez-Torres et al. [11], in a study that evaluated the potential of a collection of strains of different Italian *Trichoderma* species for use as pruning wound protectors, found that a *T. atroviride* isolate effectively protected pruning wounds in detached cane assays against *D. seriata* and *N. parvum* for at least 21 days after treatment. In another work conducted with native grapevine *Trichoderma* isolates from British Columbia (Canada) [8], it was reported that—in in planta detached cane assays under controlled greenhouse conditions—one isolate of *T. atroviride* provided 93% to 100% pruning wound protection against *D. seriata* and *N. parvum* for up to 21 days after treatment, respectively, provided that these two *Botryosphaeriaceae* fungi were inoculated at least 24 h after the protective treatment. Strong protection of pruning wounds against *E. lata* and *N. parvum* was reported by Blundell et al. [12], employing the biofungicide Vintec® based on *T. atroviride*. The same commercial product tested here (Esquive®) was effective in the control of *L. theobromae* on greenhouse-kept grapevines of cv. “Cabernet Sauvignon” and cv. “Touriga Nacional” [34] alone and in combination with LC2017, which is a low-copper-based product with an elicitor effect. Other studies based on *T. atroviride* SC1 (the microorganism formulated in the commercial product Vintec®) showed promise in both reducing infections during the grafting process [7] and protecting pruning wounds in field experiments [35]. Conversely, *T. atroviride*-based formulations did not reduce infection by *D. seriata* or *P. chlamydospora* compared to the untreated inoculated control in field trials conducted in Spain, even though the pathogens were artificially inoculated on the grapevine plants [13]. A tentative explanation for these inconsistencies found in the literature could be the non-optimized application time, given that, for *T. atroviride* or *T. harzianum* in vines at the breaking of dormancy, colonization has been shown [36] to be highest at 6 and 24 h after application.

Additionally, the effect of the plant genotype cannot be excluded, and some authors have reported that the wound protection effect of *Trichoderma* spp. is dependent on the grapevine cultivar [37]. As a rule, most studies evaluating *Trichoderma*-based products typically delay inoculation of pruning wounds with GTD fungi for up to 7 days after treatment to give the product a certain advantage in establishing itself and colonizing exposed wood surfaces after pruning. However, this approach could be controversial, as pruning wounds can be infected immediately after pruning if spores are present in the environment, especially in grapevine management systems or bioclimatic situations where the pruning season may coincide with the production of infective primary inoculum (both sexual and asexual propagules) [3], which supports the procedure chosen for the assays presented here.

Taking a look at the mode of action of the assayed BCAs, the efficacy of *B. velezensis* (BUZ-14) should be attributed to the production of iturin A (a cyclic lipopeptide) [19]. However, Calvo et al. [38] reported that certain volatile organic compounds (VOCs) could also be involved in the fungal growth inhibition mechanism observed for *B. velezensis*. Given the type of experimental design presented here, where the antagonist was formulated with an adjuvant agent and, subsequently, sealed inside the wound, the action of some compounds of the volatilome cannot be ruled out. In turn, the mode of action of *Trichoderma* spp. should be attributed to 6-pentyl-a-pyrone (a major secondary metabolite by quantity that accumulates in the culture filtrates of *T. harzianum* and *T. atroviride*), which has been shown to inhibit mycelial growth and ascospore/conidia germination in *E. lata*, *Neofusicoccum australe* (Slippers, Crous & M.J. Wingfield) Crous, Slippers & A.J.L. Phillips, *N. parvum*, and *P. chlamydospora* [39], together with the widely known mechanisms based on hyperparasitism that are habitually exhibited by members of the genus and a high rate of colonization of the plant surface thanks to their rapid growth.

5. Conclusions

In the bioassays conducted on grafted grapevine plants in controlled conditions presented herein, significant differences in the control of vascular necrosis lengths with different BCA-based products (including native microorganisms and those under experimental development) were found both for *N. parvum*- and *D. seriata*-infected plants. While treatments with *T. harzianum* and *T. atroviride* only resulted in significant reductions in necrosis caused by *N. parvum*, a remarkable protective effect from *Bacillus velezensis* BUZ-14 was detected against the two etiological agents. Therefore, the reported results call for further research on this promising iturin A-producing biocontrol agent.

Author Contributions: Conceptualization, V.G.-G., J.C.-G. and P.M.-R.; methodology, V.G.-G. and J.C.-G.; validation, M.E.V.-C. and J.J.B.-V.; formal analysis, J.C.-G. and P.M.-R.; investigation, N.L.-L., V.G.-G., M.E.V.-C., J.C.-G., J.J.B.-V. and P.M.-R.; resources, J.C.-G.; writing—original draft preparation, N.L.-L., V.G.-G., M.E.V.-C., J.C.-G., J.J.B.-V. and P.M.-R.; writing—review and editing, N.L.-L., V.G.-G., J.C.-G. and P.M.-R.; supervision, V.G.-G. and P.M.-R. All authors have read and agreed to the published version of the manuscript.

Funding: This research was co-financed by the European Union's Connecting Europe Facility (CEF), grant no. INEA/CEF/ICT/A2018/1837816 GRAPEVINE (hiGh peRformAnce comPUting sERVICES for preVenTion and coNtrol of pEsts in fruit crops) project.

Data Availability Statement: The data presented in this study are available upon request from the corresponding author. The data are not publicly available due to their relevance to an ongoing Ph.D. thesis.

Acknowledgments: The authors thank Seipasa for kindly providing the FUNGESEI® product used in the study.

Conflicts of Interest: The authors declare no conflict of interest. The funders had no role in the design of the study; in the collection, analyses, or interpretation of data; in the writing of the manuscript; or in the decision to publish the results.

Appendix A

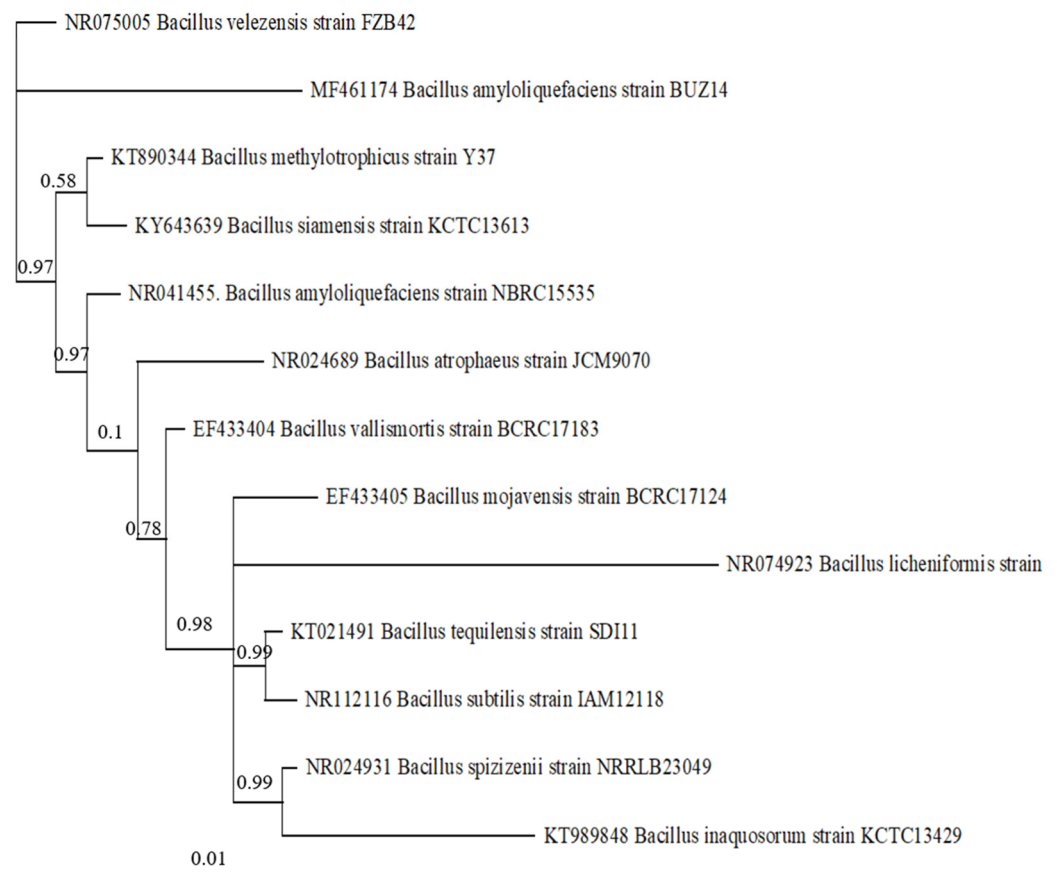


Figure A1. The Bayesian 50% majority-rule consensus tree obtained after 2,000,000 generations, inferred from the ribosomal 16S sequence of *B. velezensis* strain BUZ14 and allied *Bacillus* species. The numbers above nodes represent Bayesian posterior probabilities. Only nodes significantly supported bear values. GenBank accession numbers are indicated next to the specific epithets.

References

- Mondello, V.; Songy, A.; Battison, E.; Pinto, C.; Coppin, C.; Trozel-Aziz, P.; Clement, C.; Mugnai, L.; Fontaine, F. Grapevine trunk diseases: A review of fifteen years of trials for their control with chemicals and biocontrol agents. *Plant Dis.* **2018**, *102*, 1189–1217. [[CrossRef](#)]
- Gramaje, D. Enfermedades de la madera de la vid: Situación actual y estrategias de control. In *Proceedings of the Jornadas Vitivinícolas*; Instituto de Ciencias de la Vid y del Vino (ICVV): La Rioja, Spain, 2017.
- Gramaje, D.; Urbez-Torres, J.R.; Sosnowski, M.R. Managing grapevine trunk diseases with respect to etiology and epidemiology: Current strategies and future prospects. *Plant Dis.* **2018**, *102*, 12–39. [[CrossRef](#)] [[PubMed](#)]
- Leal, C.; Richet, N.; Guise, J.F.; Gramaje, D.; Armengol, J.; Fontaine, F.; Trotel-Aziz, P. Cultivar contributes to the beneficial effects of *Bacillus subtilis* PTA-271 and *Trichoderma atroviride* SC1 to protect grapevine against *Neofusicoccum parvum*. *Front. Microbiol.* **2021**, *12*, 726132. [[CrossRef](#)] [[PubMed](#)]
- Benítez, T.; Rincón, A.M.; Limón, M.C.; Codón, A.C. Biocontrol mechanisms of *Trichoderma* strains. *Int. Microbiol.* **2004**, *7*, 249–260. [[PubMed](#)]
- TariqJaveed, M.; Farooq, T.; Al-Hazmi, A.S.; Hussain, M.D.; Rehman, A.U. Role of *Trichoderma* as a biocontrol agent (BCA) of phytoparasitic nematodes and plant growth inducer. *J. Invertebr. Pathol.* **2021**, *183*, 107626. [[CrossRef](#)]
- Pertot, I.; Prodorutti, D.; Colombini, A.; Pasini, L. *Trichoderma atroviride* SC1 prevents *Phaeoconiella chlamydospora* and *Phaeoacremonium aleophilum* infection of grapevine plants during the grafting process in nurseries. *BioControl* **2016**, *61*, 257–267. [[CrossRef](#)]
- Pollard-Flamand, J.; Boule, J.; Hart, M.; Urbez-Torres, J.R. Biocontrol activity of *Trichoderma* species isolated from grapevines in British Columbia against *Botryosphaeria dieback* fungal pathogens. *J. Fungi* **2022**, *8*, 409. [[CrossRef](#)]
- Gramaje, D.; Armengol, J.; Barajas, E.; Berbegal, M.; Chacón, J.L.; Cibrián Sabalza, J.F.; Díaz-Losada, E.; López-Manzanares, B.; Muñoz Gómez, R.; Martínez-Diz, M. *Guía Sobre las Enfermedades Fúngicas de la Madera de la Vid*; Ministerio de Agricultura, Pesca y Alimentación: Madrid, Spain, 2020.

10. Kotze, C.; Van Niekerk, J.; Mostert, L.; Halleen, F.; Fourie, P.H. Evaluation of biocontrol agents for grapevine pruning wound protection against trunk pathogen infection. *Phytopathol. Mediterr.* **2011**, *50*, S247–S263.
11. Urbez-Torres, J.R.; Tomaselli, E.; Pollard-Flamand, J.; Boule, J.; Gerin, D.; Pollastro, S. Characterization of *Trichoderma* isolates from southern Italy, and their potential biocontrol activity against grapevine trunk disease fungi. *Phytopathol. Mediterr.* **2020**, *59*, 425–439. [[CrossRef](#)]
12. Blundell, R.; Eskalen, A. Biological and chemical pruning wound protectants reduce infection of grapevine trunk disease pathogens. *Calif. Agric.* **2021**, *75*, 128–134. [[CrossRef](#)]
13. Martínez-Diz, M.D.; Diaz-Losada, E.; Diaz-Fernandez, A.; Bouzas-Cid, Y.; Gramaje, D. Protection of grapevine pruning wounds against *Phaeomoniella chlamydospora* and *Diplodia seriata* by commercial biological and chemical methods. *Crop Prot.* **2021**, *143*, 105465. [[CrossRef](#)]
14. Rezgui, A.; Ben Ghnaya-Chakroun, A.; Vallance, J.; Bruez, E.; Hajlaoui, M.R.; Sadfi-Zouaoui, N.; Rey, P. Endophytic bacteria with antagonistic traits inhabit the wood tissues of grapevines from Tunisian vineyards. *Biol. Control* **2016**, *99*, 28–37. [[CrossRef](#)]
15. Langa-Lomba, N.; Martín-Ramos, P.; Casanova-Gascón, J.; Julián-Lagunas, C.; González-García, V. Potential of native *Trichoderma* strains as antagonists for the control of fungal wood pathologies in young grapevine plants. *Agronomy* **2022**, *12*, 336. [[CrossRef](#)]
16. van Lenteren, J.C.; Bolckmans, K.; Köhl, J.; Ravensberg, W.J.; Urbaneja, A. Biological control using invertebrates and microorganisms: Plenty of new opportunities. *Biocontrol* **2017**, *63*, 39–59. [[CrossRef](#)]
17. Wallis, C.M. Nutritional niche overlap analysis as a method to identify potential biocontrol fungi against trunk pathogens. *Biocontrol* **2021**, *66*, 559–571. [[CrossRef](#)]
18. Calvo, H.; Roudet, J.; Gracia, A.P.; Venturini, M.E.; Novello, V.; Fermaud, M. Comparison of efficacy and modes of action of two high-potential biocontrol *Bacillus* strains and commercial biocontrol products against *Botrytis cinerea* in table grapes. *Oeno One* **2021**, *55*, 228–243. [[CrossRef](#)]
19. Calvo, H.; Mendiara, I.; Arias, E.; Blanco, D.; Venturini, M.E. The role of iturin A from *B. amyloliquefaciens* BUZ-14 in the inhibition of the most common postharvest fruit rots. *Food Microbiol.* **2019**, *82*, 62–69. [[CrossRef](#)]
20. R Core Team. *R: A Language and Environment for Statistical Computing*; R Foundation for Statistical Computing: Vienna, Austria, 2022.
21. Alfonzo, A.; Lo Piccolo, S.; Conigliaro, G.; Ventorino, V.; Burruano, S.; Moschetti, G. Antifungal peptides produced by *Bacillus amyloliquefaciens* AG1 active against grapevine fungal pathogens. *Ann. Microbiol.* **2012**, *62*, 1593–1599. [[CrossRef](#)]
22. Brown, A.A.; Travadon, R.; Lawrence, D.P.; Torres, G.; Zhuang, G.; Baumgartner, K. Pruning-wound protectants for trunk-disease management in California table grapes. *Crop Prot.* **2021**, *141*, 105490. [[CrossRef](#)]
23. Halleen, F.; Fourie, P.H.; Lombard, P.J. Protection of grapevine pruning wounds against *Eutypa lata* by biological and chemical methods. *Enol. Vitic.* **2010**, *31*, 125–132. [[CrossRef](#)]
24. Trotel-Aziz, P.; Abou-Mansour, E.; Courteaux, B.; Rabenoelina, F.; Clement, C.; Fontaine, F.; Aziz, A. *Bacillus subtilis* PTA-271 counteracts *Botryosphaeria dieback* in grapevine, triggering immune responses and detoxification of fungal phytotoxins. *Front. Plant Sci.* **2019**, *10*, 25. [[CrossRef](#)] [[PubMed](#)]
25. Rusin, C.; Cavalcanti, F.R.; de Lima, P.C.G.; Faria, C.; Almanca, M.A.K.; Botelho, R.V. Control of the fungi *Lasiodiplodia theobromae*, the causal agent of dieback, in cv. Syrah grapevines. *Acta Sci.-Agron.* **2021**, *43*, e44785. [[CrossRef](#)]
26. Alfonzo, A.; Conigliaro, G.; Torta, L.; Burruano, S.; Moschetti, G. Antagonism of *Bacillus subtilis* strain AG1 against vine wood fungal pathogens. *Phytopathol. Mediterr.* **2009**, *48*, 155–158.
27. Sebestyen, D.; Perez-Gonzalez, G.; Goodell, B. Antioxidants and iron chelators inhibit oxygen radical generation in fungal cultures of plant pathogenic fungi. *Fungal Biol.* **2022**, *126*, 480–487. [[CrossRef](#)]
28. John, S.; Scott, E.S.; Wicks, T.J.; Hunt, J.S. Interactions between *Eutypa lata* and *Trichoderma harzianum*. *Phytopathol. Mediterr.* **2004**, *43*, 95–104.
29. Di Marco, S.; Osti, F.; Cesari, A. Experiments on the control of esca by *Trichoderma*. *Phytopathol. Mediterr.* **2004**, *43*, 108–115.
30. John, S.; Wicks, T.J.; Hunt, J.S.; Lorimer, M.F.; Oakey, H.; Scott, E.S. Protection of grapevine pruning wounds from infection by *Eutypa lata* using *Trichoderma harzianum* and *Fusarium lateritium*. *Australas. Plant Pathol.* **2005**, *34*, 569–575. [[CrossRef](#)]
31. Halleen, F.; Fourie, P.H. An integrated strategy for the proactive management of grapevine trunk disease pathogen infections in grapevine nurseries. *S. Afr. J. Enol. Vitic.* **2016**, *37*, 104–114. [[CrossRef](#)]
32. van Jaarsveld, W.J.; Halleen, F.; Bester, M.C.; Pierron, R.J.; Stempien, E.; Mostert, L. Investigation of *Trichoderma* species colonization of nursery grapevines for improved management of black foot disease. *Pest Manag. Sci.* **2020**, *77*, 397–405. [[CrossRef](#)]
33. Pintos, C.; Redondo, V.; Aguín, O.; Chaves, M.; Rial, C.; Mansilla, J. Evaluation of *Trichoderma atroviride* as biocontrol agent against five *Botryosphaeriaceae* grapevine trunk pathogens. *Phytopathol. Mediterr.* **2012**, *51*, 450.
34. Reis, P.; Mondello, V.; Diniz, I.; Alves, A.; Rego, C.; Fontaine, F. Effect of the combined treatments with LC2017 and *Trichoderma atroviride* strain I-1237 on disease development and defense responses in vines infected by *Lasiodiplodia theobromae*. *Agronomy* **2022**, *12*, 996. [[CrossRef](#)]
35. Berbegal, M.; Ramon-Albalat, A.; Leon, M.; Armengol, J. Evaluation of long-term protection from nursery to vineyard provided by *Trichoderma atroviride* SC1 against fungal grapevine trunk pathogens. *Pest Manag. Sci.* **2020**, *76*, 967–977. [[CrossRef](#)] [[PubMed](#)]
36. Mutawila, C.; Halleen, F.; Mostert, L. Optimisation of time of application of *Trichoderma* biocontrol agents for protection of grapevine pruning wounds. *Aust. J. Grape Wine Res.* **2016**, *22*, 279–287. [[CrossRef](#)]

37. Mutawila, C.; Fourie, P.H.; Halleen, F.; Mostert, L. Grapevine cultivar variation to pruning wound protection by *Trichoderma* species against trunk pathogens. *Phytopathol. Mediterr.* **2011**, *50*, S264–S276.
38. Calvo, H.; Mendiara, I.; Arias, E.; Gracia, A.P.; Blanco, D.; Venturini, M.E. Antifungal activity of the volatile organic compounds produced by *Bacillus velezensis* strains against postharvest fungal pathogens. *Postharvest Biol. Technol.* **2020**, *166*, 111208. [[CrossRef](#)]
39. Mutawila, C.; Vinale, F.; Halleen, F.; Lorito, M.; Mostert, L. Isolation, production and in vitro effects of the major secondary metabolite produced by *Trichoderma* species used for the control of grapevine trunk diseases. *Plant Pathol.* **2016**, *65*, 104–113. [[CrossRef](#)]

Disclaimer/Publisher’s Note: The statements, opinions and data contained in all publications are solely those of the individual author(s) and contributor(s) and not of MDPI and/or the editor(s). MDPI and/or the editor(s) disclaim responsibility for any injury to people or property resulting from any ideas, methods, instructions or products referred to in the content.

ARTÍCULO 10: "Screening of *Vitis vinifera* cultivars from the Grapevine Germplasm Bank of Aragon for susceptibility to *Botryosphaeria dieback* fungi" *Journal of Plant Diseases and Protection*, 2023, 130, 999-1006; <https://doi.org/10.1007/s41348-023-00741-9>; Q2 (JCR, Science Edition – AGRICULTURE, MULTIDISCIPLINARY). JIF₂₀₂₂ = 2,0.

[Home](#) > [Journal of Plant Diseases and Protection](#) > [Article](#)

Screening of *Vitis vinifera* cultivars from the Grapevine Germplasm Bank of Aragon for susceptibility to *Botryosphaeria dieback* fungi

[Original Article](#) | [Open Access](#) | [Published: 07 April 2023](#) | 130, 999–1006 (2023)

[Download PDF](#) 

 You have full access to this [open access](#) article



[Journal of Plant Diseases and Protection](#)

[Aims and scope](#) →

[Submit manuscript](#) →

[Natalia Langa-Lomba](#), [Vicente González-García](#), [Pablo Martín-Ramos](#)  & [José Casanova-Gascón](#)

912 Accesses 5 Altmetric [Metrics](#) [Cite this article](#)

Working on a manuscript?

[Avoid the common mistakes](#) →



ARTÍCULO 11: “Metagenomic study of fungal microbial communities in two PDO Somontano vineyards (Huesca, Spain): Effects of age, plant genotype, and initial phytosanitary status on the priming and selection of their associated microorganisms” *Plants*, 2023, 12(12), 2251; <https://doi.org/10.3390/plants12122251>. Q1 (JCR, Science Edition – PLANT SCIENCES). JIF₂₀₂₂ = 4,5.



plants

an Open Access Journal by MDPI



Metagenomic Study of Fungal Microbial Communities in Two PDO Somontano Vineyards (Huesca, Spain): Effects of Age, Plant Genotype, and Initial Phytosanitary Status on the Priming and Selection of their Associated Microorganisms

Natalia Langa-Lomba; Jerome Grimplet; Eva Sánchez-Hernández; Pablo Martín-Ramos; José Casanova-Gascón; Carmen Julián-Lagunas; Vicente González-García

Plants 2023, Volume 12, Issue 12, 2251

Article

Metagenomic Study of Fungal Microbial Communities in Two PDO Somontano Vineyards (Huesca, Spain): Effects of Age, Plant Genotype, and Initial Phytosanitary Status on the Priming and Selection of their Associated Microorganisms

Natalia Langa-Lomba ^{1,2}, Jerome Grimplet ^{3,4}, Eva Sánchez-Hernández ^{5,*}, Pablo Martín-Ramos ⁵, José Casanova-Gascón ⁶, Carmen Julián-Lagunas ^{2,3} and Vicente González-García ^{2,3,*}

- ¹ Instituto Universitario de Investigación en Ciencias Ambientales de Aragón (IUCA), EPS, University of Zaragoza, Carretera de Cuarte s/n, 22071 Huesca, Spain; natalialangalomba@gmail.com
 - ² Departamento de Sistemas Agrícolas, Forestales y Medio Ambiente, Centro de Investigación y Tecnología Agroalimentaria de Aragón (CITA), Avda. Montañana 930, 50059 Zaragoza, Spain; cjulian@aragon.es
 - ³ Instituto Agroalimentario de Aragón-IA2 (Universidad de Zaragoza-CITA), 50059 Zaragoza, Spain; jgrimplet@cita-aragon.es
 - ⁴ Departamento de Ciencia Vegetal, Centro de Investigación y Tecnología Agroalimentaria de Aragón (CITA), Avda. Montañana 930, 50059 Zaragoza, Spain
 - ⁵ Department of Agricultural and Forestry Engineering, ETSIIAA, Universidad de Valladolid, Avenida de Madrid 44, 34004 Palencia, Spain; pmr@uva.es
 - ⁶ Instituto Agroalimentario de Aragón-IA2 (Universidad de Zaragoza-CITA), EPS, University of Zaragoza, Carretera de Cuarte s/n, 22071 Huesca, Spain; jcasan@unizar.es
- * Correspondence: eva.sanchez.hernandez@uva.es (E.S.-H.); vgonzalezg@aragon.es (V.G.-G.)



Citation: Langa-Lomba, N.; Grimplet, J.; Sánchez-Hernández, E.; Martín-Ramos, P.; Casanova-Gascón, J.; Julián-Lagunas, C.; González-García, V. Metagenomic Study of Fungal Microbial Communities in Two PDO Somontano Vineyards (Huesca, Spain): Effects of Age, Plant Genotype, and Initial Phytosanitary Status on the Priming and Selection of their Associated Microorganisms. *Plants* **2023**, *12*, 2251. <https://doi.org/10.3390/plants12122251>

Academic Editors: Cecilia Rego and Pedro Reis

Received: 14 May 2023

Revised: 29 May 2023

Accepted: 6 June 2023

Published: 8 June 2023



Copyright: © 2023 by the authors. Licensee MDPI, Basel, Switzerland. This article is an open access article distributed under the terms and conditions of the Creative Commons Attribution (CC BY) license (<https://creativecommons.org/licenses/by/4.0/>).

Abstract: The study of microbial communities associated with different plants of agronomic interest has allowed, in recent years, to answer a number of questions related to the role and influence of certain microbes in key aspects of their autoecology, such as improving the adaptability of the plant host to different abiotic or biotic stresses. In this study, we present the results of the characterization, through both high-throughput sequencing and classical microbiological methods, of the fungal microbial communities associated with grapevine plants in two vineyards of different ages and plant genotypes located in the same biogeographical unit. The study is configured as an approximation to the empirical demonstration of the concept of “microbial priming” by analyzing the alpha- and beta-diversity present in plants from two plots subjected to the same bioclimatic regime to detect differences in the structure and taxonomic composition of the populations. The results were compared with the inventories of fungal diversity obtained by culture-dependent methods to establish, where appropriate, correlations between both microbial communities. Metagenomic data showed a differential enrichment of the microbial communities in the two vineyards studied, including the populations of plant pathogens. This is tentatively explained due to factors such as the different time of exposure to microbial infection, different plant genotype, and different starting phytosanitary situation. Thus, results suggest that each plant genotype recruits differential fungal communities and presents different profiles of associated potential microbial antagonists or communities of pathogenic species.

Keywords: NGS sequencing; endophytic mycobiota; GTDs; fungal diversity

1. Introduction

Grapevine crops are frequently threatened by a range of phytosanitary problems. Among these, grapevine trunk diseases (GTDs) have stood out, particularly in the last 2–3 decades [1], due to various factors. These include the gradual withdrawal of chemical substances that allow their control, the increase in newly planted areas (resulting in more

production of starting plant material), and the intensity of current crop management (such as pruning, planting densities, irrigation, fertilization, driving, etc.) [2,3].

GTDs are characterized by great complexity in terms of their etiology. Syndromes attributable to GTDs are typically multifaceted, with the existence of symptoms common to several diseases, several etiological agents acting simultaneously or sequentially, or the continuous appearance of new pathologies and species associated with them [1]. The etiological agents responsible for these types of pathologies are usually ubiquitous and polyphagous fungal pathogens, often living in alternative crops and refuge plant species or colonizing the inner parts of the woody tissues of the grapevine as endophytes or latent parasites (part of the usual endophytic microbiota of the plant) [4]. Their attack and symptoms appear randomly in time and space, generally as a result of imbalance phenomena in the plant's immune system, and are typically due to the generation of management stresses [5].

Until barely a decade ago, approaches to characterize and understand the role played by microbial communities associated with different agroecosystems, such as grapevines [6], employed classical microbiological methodologies dependent on the use of a limited number of axenic culture media available for the isolation of microorganisms. This procedure has limited the characterization only to cultivable microbial diversity, which represents a small fraction of the total number of microbes associated with the soil, rhizospheres, or host tissues of plants that they colonize [7,8]. Nowadays, with the generalization of different massive sequencing techniques, high-throughput sequencing analyses have made it possible to reveal aspects such as the total microbial diversity existing in agricultural soil, the relationships between communities, the biological potential of the agroecosystem, or the key microorganisms associated with the different types of phenotypic response observed against exposure and infection by different pathogens [9]. In this last approach, the plant genotype is considered as a part of a whole that must also integrate all the microbial communities that live connectedly with it. The role of these communities in the biology and behavior of the host has only begun to be elucidated in the last 10–15 years. In this way, the next-generation sequencing (NGS) analyses of microorganisms associated with grapevine crops have suggested that these microbial communities and numerous specific pathogens of each plant host can evolve and be different depending not only on the different agroecological and management conditions but also on the genetic profile of each variety, largely due to the processes of interaction and selection (“priming”) of certain microbial diversity promoted by the host plant, which would have been selected to confer adaptive advantages against all kinds of stresses, including diseases [10–12].

The importance and the role played by the different communities of microorganisms associated with agroecosystems have recently been focused on with a phytopathological viewpoint. This offers a new paradigm where plants are considered not only as an individual genotype but also as a larger genetic entity that includes their associated microorganisms (microgenome), which has given rise to the new concept of “holobiont” [13]. Under this perspective, a holobiont must be considered as a genetic set comprised of the individual plant and its symbionts, as well as other associated microbes, acting as a single unit of biological organization. The microbiome is compartmentalized into the rhizosphere, endosphere, phyllosphere, carposphere, and other non-specific endophytic microbiota, according to the different plant tissues colonized by microorganisms [14]. In addition, aspects such as the metabolism and morphology of a given plant species and its microbiota are closely related to each other to maintain the ecological fitness of the holobiont [15].

The use of high-throughput sequencing techniques has allowed for the characterization of microbial communities associated with the grapevine crop and has led to several studies focused on its ecological functionalities, management, breeding, and disease control [16]. Some of these studies have focused on the relationships between the plant microbiome and its phytosanitary status [6] or the influence of different vineyard management practices on the composition of microbial communities [17]. Other studies compared the microbiomes associated with crops of different ages [18], plant genotypes, phenological stages [19],

or plant tissues [20,21]. Metagenomic studies in microbial diversity have also identified potential biocontrol methods of GTDs using microbial antagonists of fungal or bacterial origin [22,23]. Finally, several works revealed that plant health is overall a direct consequence of the composition and balance of its associated microbial communities [6]. Therefore, the ecological fitness of the grapevine holobiont, including its behavior and resilience against a series of biotic and abiotic stresses, is modulated by the composition of its microbiome, which could serve as a biological marker [24]. Furthermore, metagenomic studies analyzing different compartments of the soil–plant interface in grapevine plants have identified several niches that have the potential for colonization and infection by certain soil-borne fungi associated with GTDs [20]. This finding demonstrates the preeminent role of the different compartments of the rhizosphere and its surrounding soil in the dispersal and spread of certain plant pathogens.

The objective of this study was, in the first step, to characterize the fungal microbial communities associated with two conventional vineyards of different ages that belong to the same biogeographical unit. This was accomplished by comparing both culture-dependent (direct isolation on synthetic media and characterization of endophytic fungal strains) and high-throughput sequencing methods. The aim was to detect dissimilarities between the composition of fungal communities and the factors that influenced them. Both culture-dependent techniques and high-throughput sequencing methods were utilized to compare the existing diversity between the two agroecosystems of different ages and plant genotypes. This approach allowed for the experimental examination of the concept of microbial priming by the plant host, revealing and explaining differences in the structure and composition of the microbial communities. These differences could be attributed to various factors, including the functional activity of the different genotypes present in each vineyard, the duration of exposure to infection and microbial colonization, the origin of the plant material, and the initial phytosanitary situation. Collectively, these factors influence and shape the selection of microorganisms observed in each of the analyzed plots. The experimental verification of these hypotheses highlights the significance and relevance of the holobiont concept and its functionality. It underscores how plant genotypes interact directly with the microbial genome to selectively include or exclude microorganisms that contribute, positively or negatively, to the maintenance of overall ecological fitness.

2. Results

2.1. Isolation of Endophytic Fungi from Grapevine Plants

Fungal communities present in the sampled grapevine individuals were characterized using culture-dependent microbiological methods. In the two vineyards sampled, a total of 240 endophytic fungal isolates were obtained (136 belonging to the plants surveyed in the “Clau” plot and 104 obtained from the “Almendros” vineyard). After taxonomic characterization of the different fungal operational taxonomic units (OTUs) employing both classical and molecular methods, it was found that the “Clau” vineyard yielded a higher number of endophytic isolates than the “Almendros” vineyard, with 44 and 35 fungal strains identified, respectively (Tables S1 and S2). Despite these differences in the number of characterized isolates, both surveyed plots had similar proportions between pathogenic grapevine-associated taxa and saprophytic ubiquitous endophytic species found. This ratio was found to be about 70/30% in the “Clau” vineyard and 60/40% in the “Almendros” vineyard. However, the composition of fungal genera and species exhibited some interesting differences between them. Putting aside some common grapevine pathogens associated with adult plants, which were isolated from both vineyards and represented by fungi responsible for the so-called ‘Botryosphaeria dieback’ (i.e., *Neofusicoccum parvum* (Pennycook and Samuels) Crous, Slippers and A.J.L. Phillips, and *Diplodia seriata* De Not.) and ‘eutypiose’ (*Eutypa lata* (Pers.) Tul. and C. Tul.), there were remarkable differences in other GTD-related pathogens. In this sense, some species and genera were isolated exclusively in one of the two vineyards analyzed. Thus, a conventional microbiological survey of the “Clau” plot revealed the presence of some species associated with the so-

called ‘Petri disease’, such as *Phaeoacremonium aleophilum* W. Gams, Crous and M.J. Wingf. or *Phaeomoniella chlamydospora* (W. Gams, Crous, M. J. Wingf. and L. Mugnai) Crous and W. Gams, which were not isolated in the sampling of plants in the “Almendros” vineyard. Interestingly, analyses of this latter plot revealed the presence of several isolates of *Cylindrocarpon macrodidymum* Schroers, Halleen and Crous, a member of the so-called ‘black foot’ disease, which is mostly associated with young grapevine plants, together with the presence of one of the etiological agents responsible for grapevine excoiiose, *Phomopsis viticola* Sacc.) Sacc.

Concerning other types of plant pathogenic endophytes obtained in both plots, it is worth noting the presence of other polyphagous species such as *Discostroma fuscillum* (Berk. and Broome) Huhndorf and *Didymella glomerata* (Corda) Qian Chen and L. Cai (the latter also present in the “Almendros” vineyard) in the “Clau” plot or *Didymosphaeria variabile* (Riccioni, Damm, Verkley and Crous) Ariyawansa and K.D. Hyde and *Phoma conidiogena* Schnegg in the “Almendros” plot. In addition, other ubiquitous endophytes, either saprophytic or facultative pathogens belonging to genera such as *Fusarium*, *Gibberella*, *Aspergillus*, *Rhizopus*, etc., were also repeatedly isolated. Finally, the presence of isolates belonging to genera commonly reported in the literature as microbial antagonists with the potential for use as biological control agents (BCAs) (genera *Trichoderma* and *Aureobasidium*) was also observed in both plots.

2.2. NGS Analyses of Fungal Communities

Together with analyzing the fungal diversity in grapevine plants using classical microbiological methods, the microbial diversity of internal wood samples coming from the same plant stands in two vineyards of different ages and phytosanitary status of the PDO ‘Somontano’ was characterized using high-throughput sequencing techniques. A metagenomic taxonomical analysis based on sequences of the ITS2 fragment from the ribosomal ITS (Internal Transcribed Spacer) region was conducted, resulting in ITS sequences from a total of 1300 OTUs (Table S3), with 635 binomials representing 318 taxa. Of the total OTUs identified, 632 were exclusive to the “Clau” vineyard and 412 were only found in the younger plot (the “Almendros” vineyard). Therefore, 25% more taxa were identified in the older plot (23 vs. 8 years). In addition, 256 OTUs (approximately 20% of the total) were common to both plots (Figure 1).

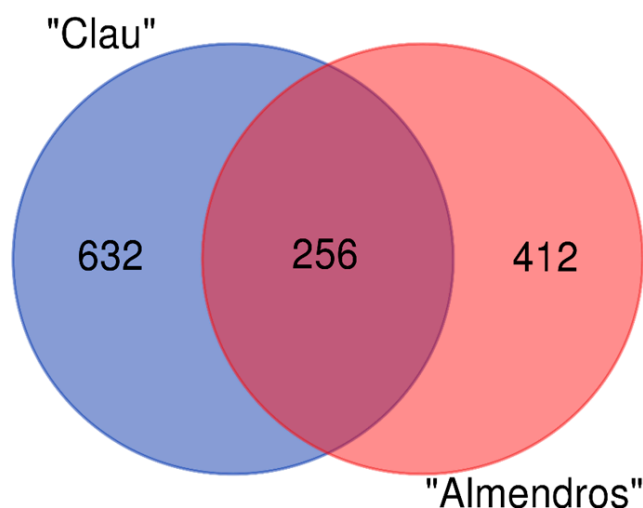


Figure 1. Venn Diagram showing the number of unique OTUs identified in each of the vineyards analyzed and those shared by both.

Regarding the common and exclusive taxa present in each of the analyzed plots (Figure 2), it was observed that the number of taxa common to all plants analyzed was

higher (75 OTUs) in the older “Clau” plot compared to the younger “Almendros” vineyard, where only 46 common OTUs were detected, representing almost 40% fewer.

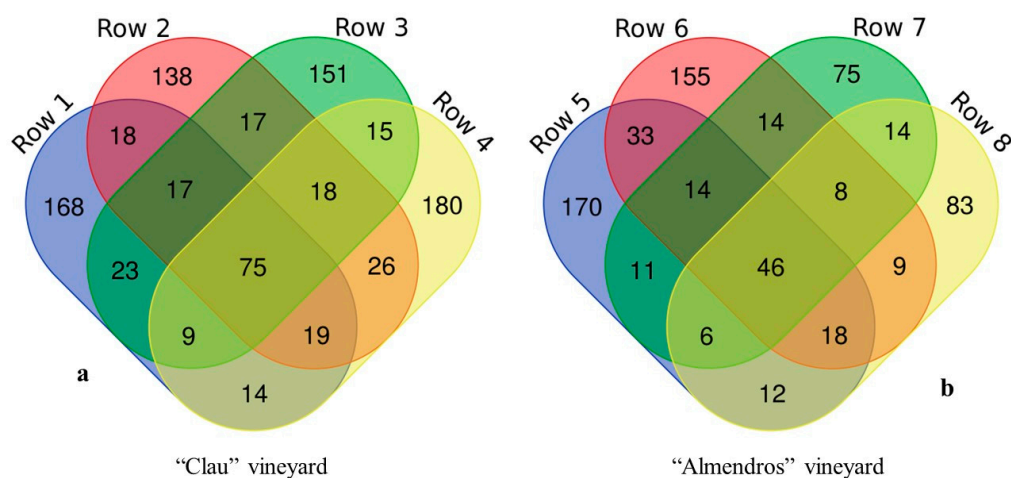


Figure 2. Venn Diagram showing the different common and unique OTUs present in the different rows sampled per plot for the two vineyards analyzed: (a) the “Clau” vineyard, rows 1–4; (b) the “Almendros” vineyard, rows 5–8.

When comparing all the sampled plant stands, including the two experimental plots, a total of 30 OTUs that were common to all the surveyed rows were identified (Table 1). Sixteen of these OTUs were grapevine-associated taxa, with varying degrees of specificity, which mainly consisted of specific pathogens (e.g., *Phaeoconiella chlamydospora*, *Cladosporium cladosporioides* (Fresen.) G.A. de Vries, *Seimatosporium vitis* Y.P. Xiao, Camporesi and K.D. Hyde, and *Neosetophoma lunariae* Crous and R.K. Schumach), ubiquitous or cosmopolitan endophytic species (e.g., *Aureobasidium pullulans* (de Bary) G. Arnaud, *Epicoccum nigrum* Link, *Alternaria alternata* (Fr.) Keissl., Beih., etc.), or miscellaneous taxa (e.g., *Cystofilobasidium macerans* Samp., *Vishniacozyma victoriae* (M.J. Montes, Belloch, Galiana, M.D. Garca, C. Andrs, S. Ferrer, and Torr.-Rodr. and J. Guinea) X.Z. Liu, F.Y. Bai, M. Groenew. and Boekhout, *Filobasidium stepposum* (Golubev and J.P. Samp.) Xin Zhan Liu, F.Y. Bai, M. Groenew. and Boekhout, etc.), which were somehow associated with the crop and cited in previous studies of a similar nature [11,25–27]. Taking into account the range of frequency values obtained and the fact that some of the OTUs common to all sampled rows were taxa usually associated with fruits (grapes), leaves, or even flowers (without being specifically associated with the interior of the woody tissues of the plant), and that others represented cosmopolitan fungal endophytes frequent in all types of plant hosts, the analysis of the grapevine’s inner wood microbiome did not allow the recognition of a true “core” population or essential microbiome in the two investigated vineyards. Among the OTUs common to all the samplings specifically associated with grapevine, only *Phaeoconiella chlamydospora*, a well-known specific pathogen associated with the vascular rot of grapevine wood, showed reading frequencies above 10,000. In this sense, the most frequent common taxa associated with vines (although with significantly lower values than those reported for *P. chlamydospora*) were essentially pathogenic species such as *Cladosporium cladosporioides*, responsible for grape rot [28], or *Seimatosporium vitis*, associated with GTD pathologies [29]. In summary, the essential microbial core inhabiting the inner wood and characterized for the two investigated vineyards seemed to be dominated, according to the present analysis, by pathogenic species present to a lesser or greater degree and frequency of appearance, followed by generalist or ubiquitous endophytic taxa, together with a series of species associated with the host, although not specifically with the type of tissue or organ analyzed.

Table 1. Fungal OTUs common to all grapevine plant rows analyzed (including both vineyards). Taxa followed by a “V” in parentheses indicate those specifically associated with *Vitis vinifera* L. Data on the relative frequency and fungal guild are provided.

Taxonomy	Frequency	Fungal Guild
<i>Cladosporium allacinum</i>	4601.6	Pathotroph
<i>Epicoccum nigrum</i> (V)	5101	Pathotroph–Saprotroph–Symbiotroph
<i>Stemphylium majusculum</i>	148.1	Pathotroph–Saprotroph
<i>Cystofilobasidium macerans</i> (V)	138	Saprotroph
<i>Seimatosporium vitis</i> (V)	1414.3	Pathotroph
<i>Phaeoconiella chlamydospora</i> (V)	12,741.1	Pathotroph
<i>Filobasidium stepposum</i> (V)	1028.8	Saprotroph
<i>Knufia perforans</i>	308.9	Pathotroph–Saprotroph
<i>Aureobasidium pullulans</i> (V)	683	Pathotroph–Saprotroph–Symbiotroph
<i>Filobasidium magnum</i> (V)	69.2	Saprotroph
<i>Rhinochadiella</i> sp. (V)	175	Pathotroph
<i>Cladosporium grevilleae</i> (V)	358.1	Saprotroph
<i>Cyphellophora</i> sp.	174.9	Pathotroph–Saprotroph
<i>Cladosporium cladosporioides</i> (V)	8257.4	Saprotroph
<i>Angustimassarina acerina</i> (V)	954.7	Saprotroph
<i>Myrmecridium banksiae</i>	65.3	Saprotroph
<i>Vishniacozyma victoriae</i> (V)	122.4	Saprotroph
<i>Aspergillus undulatus</i>	643.2	Pathotroph–Saprotroph
<i>Populocrescentia forlicesenensis</i>	1198.2	Pathotroph–Saprotroph
Ord. <i>Malasseziales</i>	23.2	Pathotroph–Saprotroph
<i>Acericola italica</i>	410.6	Pathotroph–Saprotroph
<i>Sporobolomyces roseus</i>	128.8	Pathotroph–Saprotroph
<i>Neoscytalidium</i> sp. (V)	43.8	Pathotroph–Saprotroph
<i>Alternaria infectoria</i>	359.2	Pathotroph–Saprotroph–Symbiotroph
<i>Neosetophoma lunariae</i> (V)	289.2	Pathotroph
<i>Vishniacozyma carnescens</i> (V)	751.5	Saprotroph
<i>Cladosporium exasperatum</i>	1392.3	Saprotroph
<i>Alternaria alternata</i> (V)	2608.3	Pathotroph–Saprotroph–Symbiotroph
<i>Cyphellophora oxyspora</i>	14.4	Pathotroph–Saprotroph
<i>Knufia mediterranea</i>	221.7	Pathotroph–Saprotroph

As expected, and in accordance with what has been reported in most inventories on endophytic fungal diversity [6], the majority presence of identified OTUs belonging to Div. Ascomycota (871) was detected in both plots, revealing a lower number (354) of OTUs from Basidiomycota. In addition, Div. Mortierellomycota was barely represented in the analysis, with the detection of only three OTUs, and no representative of the Oomycetes group (Kingdom Chromista) was found. Finally, a small number of OTUs (11) representing taxa from Div. Chytridiomycota were also identified.

The analysis of the metagenomic results revealed that almost 80% of the total identified taxa consisted of rare and/or infrequent taxa (with relative frequencies below 2%). The microbiota of the younger plot turned out to be less diverse, dominated by relatively few species that were highly represented in the plants sampled.

Regarding the pathogenic component of the fungal microbial communities analyzed, the results showed that *Phaeoconiella chlamydospora*, one of the etiological agents of the so-called Petri disease, was the most represented species in the metagenomic analysis, with a slightly higher frequency in the older “Clau” vineyard (16% of the reads) compared to the younger “Almendros” vineyard (13% of the reads). However, other members of the Petri complex, such as taxa from genera *Phaeoacremonium* (e.g., *P. aleophilum* and *P. minimum* (Tul. and C. Tul.) Gramaje, L. Mostert and Crous) and *Cadophora* (e.g., *C. luteo-olivacea* (J.F.H. Beyma) T.C. Harr. and McNew and *C. malorum* (Kidd and Beaumont) W. Gams), were scarcely represented. The genus *Eutypa* and other Xylariales were the second most frequent group of species associated with GTDs in both vineyards. Another group of taxa associated with ‘Botryosphaeria dieback’, including genera *Neofusicoccum*, *Dothiorella*, and

Diplodia, were more abundant in the older plants (“Clau” vineyard). However, despite the age of the oldest vineyard analyzed (23 years for the “Clau” plot), the analysis did not reveal the presence of OTUs representing any of the lignicolous basidiomycete taxa commonly associated with GTD syndromes such as grapevine esca in our latitudes (e.g., *Fomitiporia mediterranea* M. Fisch., *Inonotus hispidus* (Bull.) P. Karst., or *Stereum hirsutum* (Willd.) Pers.). Instead, the analysis characterized the presence of sequences belonging to some other genera of *Hymenochaetaceae* such as *Fuscoporia* (*F. ferruginosa* (Schrad.) Murrill), *Fomitiporella*, or *Phellinus* (*P. rhamni* (Bondartseva) H. Jahn), which have been related to esca symptoms in vine-producing areas such as Chile or South Africa [30] or cited in the metagenomic fungal inventories of grapevine [9].

2.2.1. Alpha-Diversity of Fungal Microbiome

The metagenomic analyses conducted on the two vineyards showed that the percentages of species associated with different lifestyles, guilds, and nutritional modes (Table S4) were equivalent regardless of the age of the experimental fields (Figure 3). The percentage of OTUs representing pathogenic lifestyles was similar in both plots, representing 16% and 18% in “Almendros” and “Clau”, respectively. The percentage of saprophytic taxa was slightly higher in the older plot, with 48% of the OTUs compared to 36% in the youngest vineyard. As expected, and depending on the type of sample and plant organ surveyed, the number of symbiont taxa was low in both plots, representing 5% and 4% in “Almendros” and “Clau”, respectively, and was dominated by lichenizing species, which were probably associated with DNA contamination coming from grapevine barks during sampling. When considering OTUs with a wider range of trophic modes, including combinations between types of nutrition (according to the available literature), the percentages between vineyards were also similar.

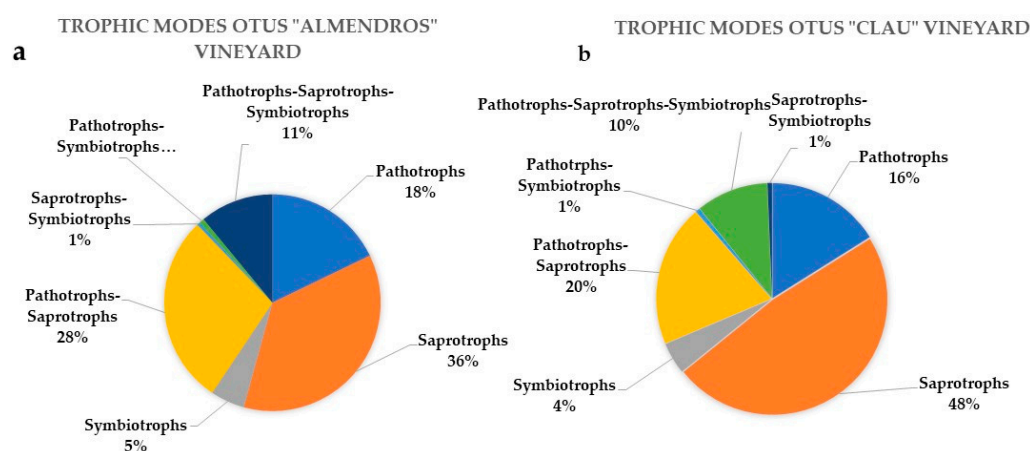


Figure 3. Circle charts showing the type and percentage of different trophic modes associated with the OTUs characterized for the two vineyards analyzed: (a) “Almendros” vineyard; (b) “Clau” vineyard.

As previously mentioned, *Phaemoniella chlamydospora*, a vascular pathogen associated with Petri disease, was the most abundant taxon in the entire metagenomic analysis; it was also the most abundant considering the two vineyards separately. Along with the aforementioned species, some of the most frequent OTUs in the analysis (Figure 4) were pathogens associated with the grapevine plant, including *Eutypa* sp., *Diplodia seriata*, and *Seimatosporium vitis*, the first two being specifically associated with GTDs. The analysis also identified two taxa commonly reported as microbial antagonists, namely the cosmopolitan endophyte *Epicoccum dendrobii* Q. Chen, Crous and L. Cai, and the yeast *Wickerhamomyces anomalus* (E.C. Hansen) Kurtzman, Robnett and Basehoar-Powers, among the 10 most frequent OTUs in the analysis, along with saprophytic or facultative parasitic taxa of the genus *Cladosporium*. *Mycosphaerella tassiana* (De Not.) Johanson, an ascomycete commonly reported as part of the fungal component of the microbial communities of the crops in nu-

merous previous studies [11,31], which was also among the most frequent OTUs identified in the analysis.

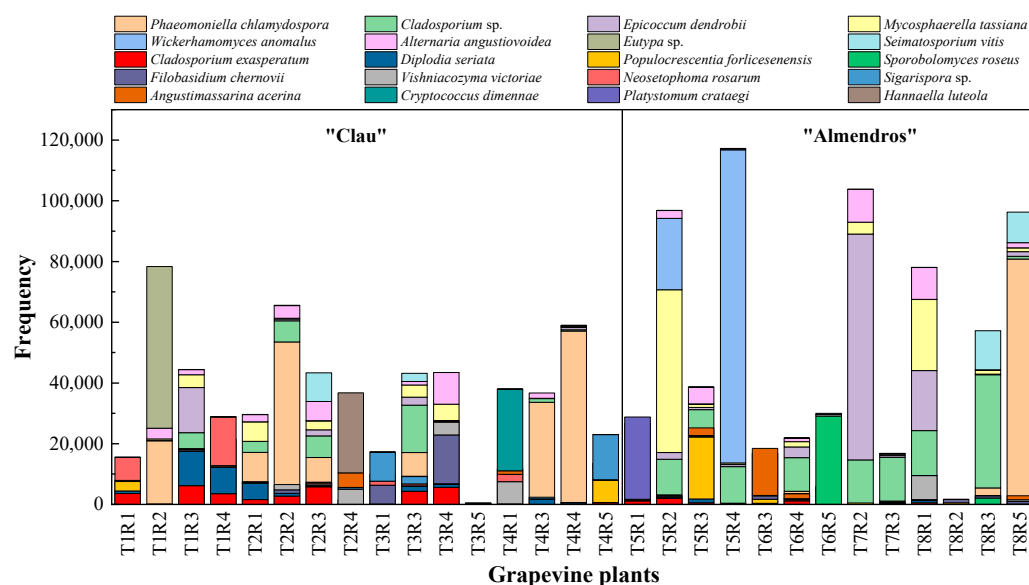


Figure 4. Stacked column histogram showing the twenty most frequent OTUs, ranked by abundance, in the two vineyards. The red line separates the plants from the two plots: (left) “Clau” vineyard, (right) “Almendros” vineyard.

When the ranking of the most frequent OTUs was analyzed in each plot separately, notable differences were observed in their distribution and abundance according to the age of the vineyard. The distribution of high frequencies of appearance was quite irregular. *Phaeomoniella chlamydospora*, the most abundant taxon in the study, was uniformly distributed in all the plants sampled from the oldest plot (“Clau”) (Figure 5), being present in most of the plants analyzed, although with higher frequency in individuals belonging to row 4. However, *P. chlamydospora* was only detected in five plants of the youngest vineyard (“Almendros”) (Figure 6), with generally low values, except for the case of a specific plant in row 8. *Eutypa*, another pathogen associated with GTDs, only appeared in two individuals, one in each vineyard. However, it appeared with different frequencies, being very abundant in a plant from row 1 of the oldest plot and appearing in an almost testimonial way in a plant from row 7 in the youngest vineyard. *Diplodia seriata*, one of the etiological agents related to ‘Botryosphaeria dieback’, was more abundant and homogeneously represented in the older plot, appearing in almost all the plants sampled from the “Clau” vineyard, while it was detected in the younger vineyard only in five plants, with low values of appearance frequency.

As expected, the most frequent species representing common and cosmopolitan endophytic taxa such as *Epicoccum dendrobii*, *Cladosporium* spp., or *Alternaria angustiovoidea* E.G. Simmons were present in almost all the plants analyzed with different frequency rates, regardless of the location and age of the plots.

An alpha-diversity analysis did not reveal significant differences in diversity and richness indexes (Figure 7) at the OTU level between the fungal communities of both vineyards. The Chao1 and ACE indices, which reflect the abundance of OTUs in the different samples (plants analyzed), had high ranges of values (48 to 175) for both vineyards, indicating a varying richness of species in each individual analyzed within the same plot or even the same row. The Shannon and Simpson indexes, which reflect the diversity of the OTUs in the samples, indicated that the fungal microbial communities associated with the inner grapevine wood in both vineyards have normal to low diversity values. The majority of values for the Shannon index (H) ranged between two and three, with only a few plants per plot presenting H values greater than three. For the Simpson index, in which higher

values denote a lower diversity of the microbiome associated with each sample, most of the plants sampled in both plots had values between 0.8 and 1.0, suggesting discrete rates of microbial diversity.

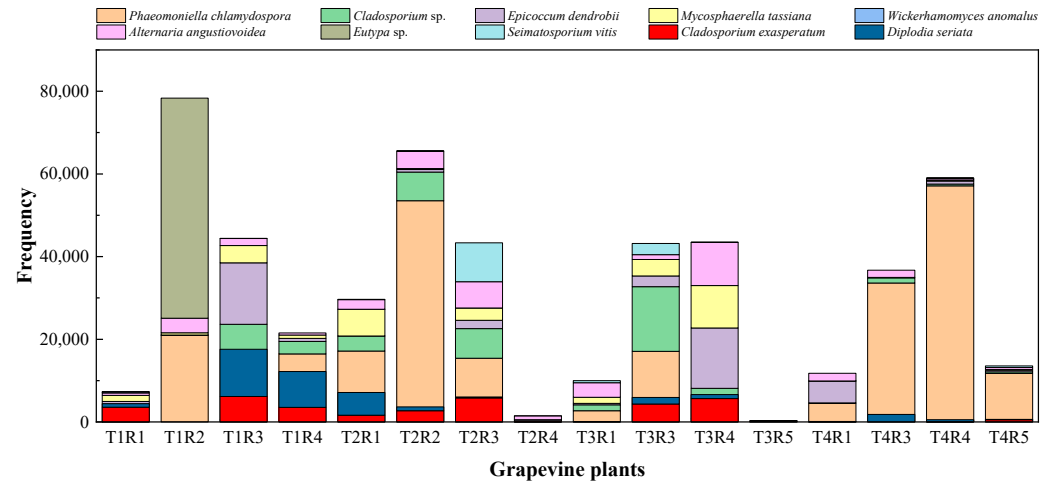


Figure 5. Stacked column histogram showing the ten most frequent OTUs, ranked by abundance, identified in the “Clau” vineyard.

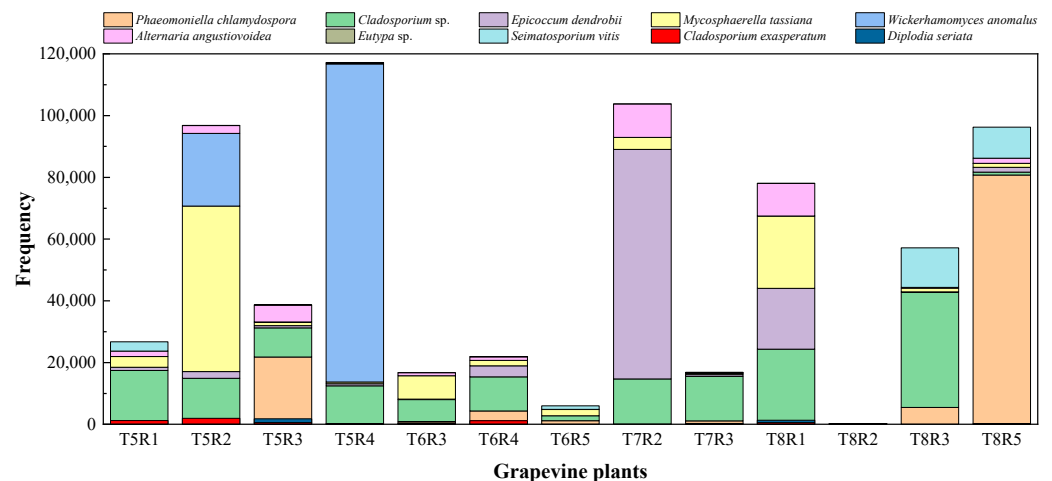


Figure 6. Stacked column histogram showing the ten most frequent OTUs, ranked by abundance, identified in the “Almendros” vineyard.

2.2.2. Comparison between Vineyards: Beta-Diversity

The difference in the composition of fungal communities between the analyzed vineyards was reflected in the beta-diversity analysis. Thus, a non-metric multidimensional scaling (NMDS) plot (Figure 8) revealed that the fungal microbial communities of the two vineyards sampled were not essentially different when considering each row of plants analyzed per plot, where an overlap was observed between the different groups. However, the communities associated with most of the rows and plants of the youngest vineyard (“Almendros” plot) exhibited a certain degree of differentiation from the rest of the samples analyzed, including all the rows sampled in the “Clau” plot, the oldest one.

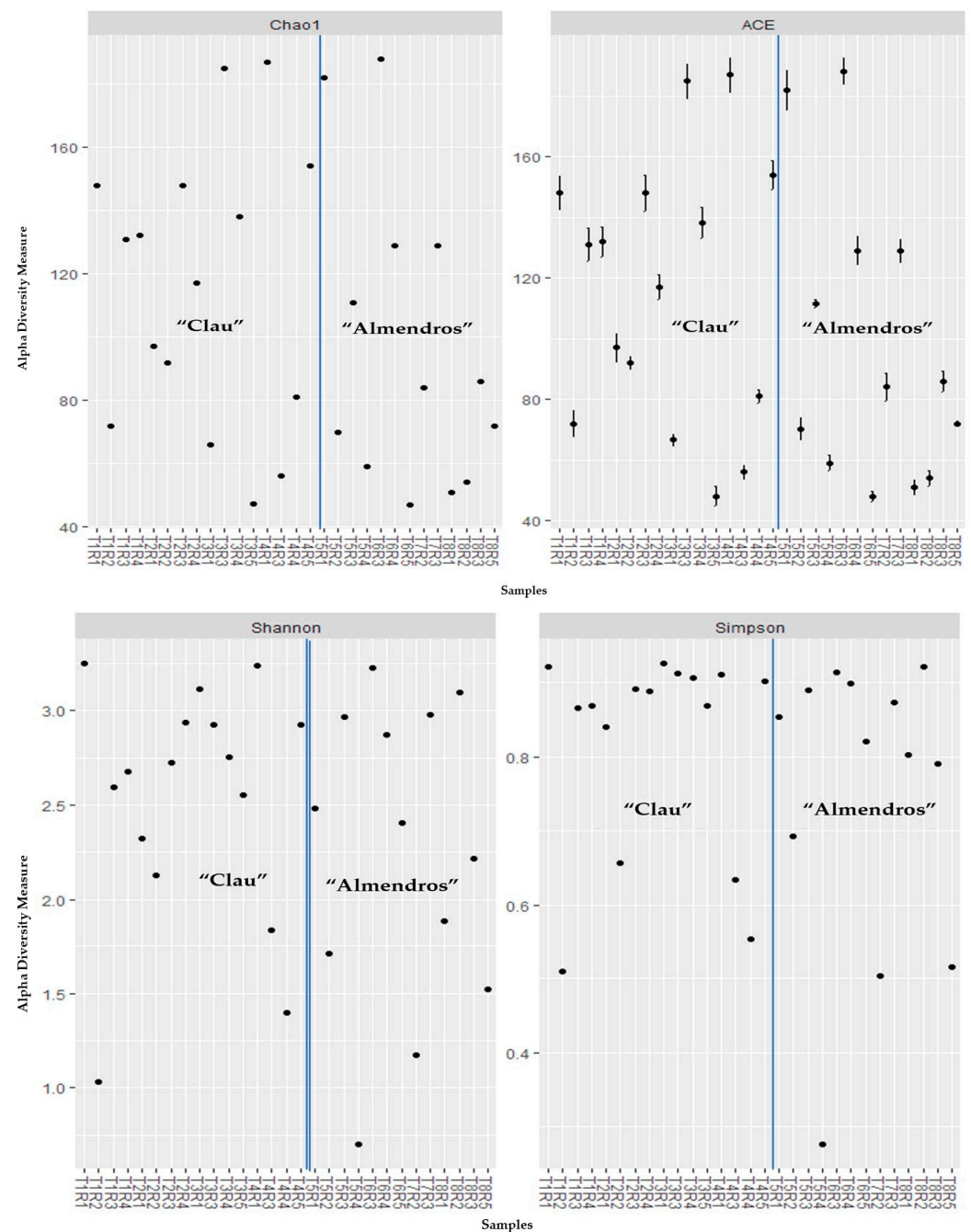


Figure 7. Alpha diversity and richness indexes for the fungal communities present in each sample: (top) Chao1 and ACE; (bottom) Shannon and Simpson. Blue lines separate plants from the two plots analyzed; T1–4 come from the “Clau” vineyard; T5–8 come from the “Almendros” vineyard.

When a principal coordinate analysis was carried out to assess beta-diversity based on the Jaccard’s index, the resulting PCoA plot (Figure 9) revealed some dissimilarity between the samples from both vineyards. The plot showed that 8.21% of the data variability was explained by axis 1, reasonably separating the different communities associated with the sampled plants into two distinct groups with overlap, suggesting a differential fungal microbiome composition in grapevine inner wood tissues depending on the plot analyzed.

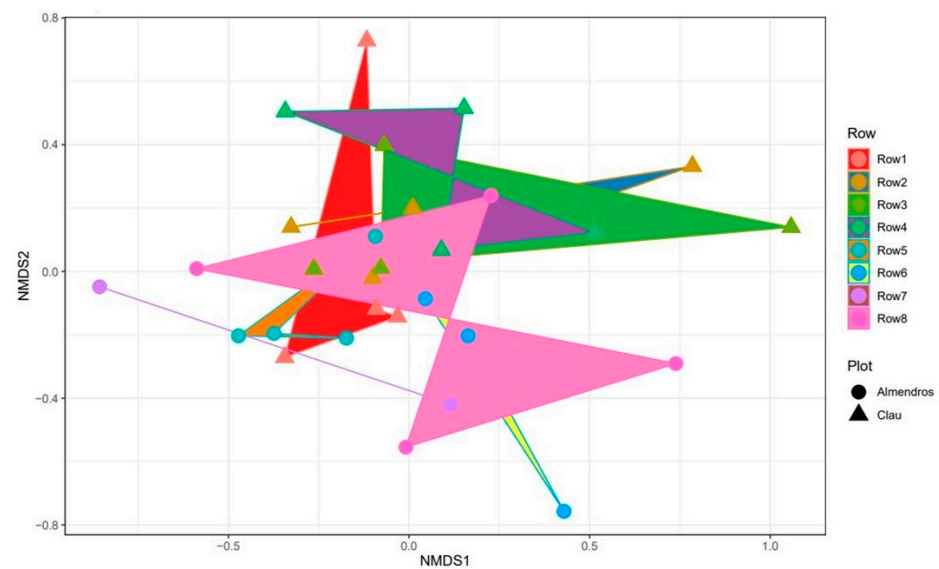


Figure 8. Non-metric multidimensional scaling (NMDS) plot of the metagenome of wood samples from the two surveyed vineyards. Samples in the different groups are represented by the symbols given in the legend, and colors represent the rows in the vineyard plots. Rows 1–4 come from the “Clau” vineyard; rows 5–8 come from the “Almendros” vineyard.

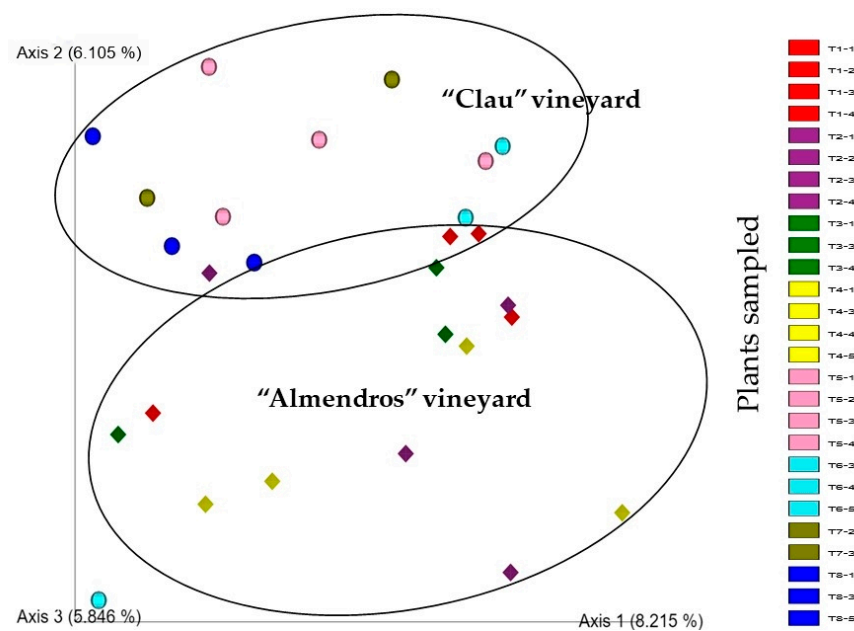


Figure 9. Emperor PCoA plot using Jaccard's index of the metagenomes of the wood samples analyzed. The T1–4 (spheres) are samples from the “Clau” vineyard; the T5–8 (diamonds) are samples from the “Almendros” vineyard. Different colors represent different rows.

A detailed out-level base pairwise comparison between the “Clau” and “Almendros” vineyards was conducted, and it revealed 21 differences in the abundance of OTUs (Figure 10), with 15 in the “Clau” vineyard and 6 in the “Almendros” plot. The analysis identified several genera belonging to the phylum Ascomycota, such as *Orbilia*, *Constantinomyces*, *Patellaria*, and *Nigrograna*, as well as GTD pathogens *Diplodia* or *Phaeomoniella*, and genera of the phylum Basidiomycota, such as *Kurtzmanomyces*, *Vishniacozyma*, or *Dioszegia* that were dominant in the oldest plot. In contrast, the genera of ascomycetes such as *Wickerhamomyces*, *Sigarispora*, or *Penicillium*, and basidiomycetes such as *Cryptococcus* or *Naganishia* were enriched in the samples of the youngest vineyard. This type of analysis

indicated that some genera related to GTDs such as *Diplodia* and *Phaeomoniella*, which are associated with Botryosphaeria dieback and Petri disease, respectively, were more abundant in the older plot, along with a series of basidiomycete yeast-like genera such as *Kurtzmanomyces*, *Dioszegia*, or *Vishniacozyma* (the most abundant yeast associated with the mentioned vineyard). On the other hand, yeast-like genera such as *Cryptococcus* and *Naganishia*, both basidiomycetes, or *Wickerhamomyces*, an ascomycete, were more abundant in the younger plot.

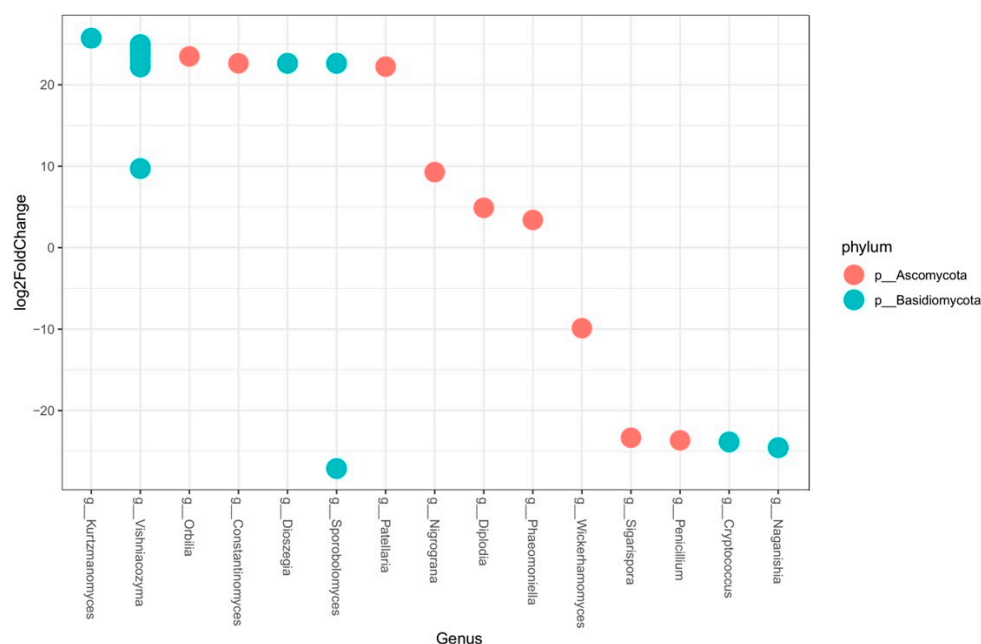


Figure 10. Pairwise comparison (DeSeq analysis). Differential abundance of OTUs ($p < 0.05$) in wood samples from the “Clau” and “Almendros” vineyards. OTUs were assigned to the genus level (x-axis) and phylum level (colors). For OTUs not defined at the genus level, the most specific taxonomic level available was used. Positive values indicate a higher abundance in the “Clau” vineyard and negative values indicate a greater abundance in the “Almendros” vineyard.

2.3. Correlation between NGS and Culture-Dependent Methods

During the analysis of taxonomic data obtained through culture-dependent microbiological methods in the same grapevine plants that were later analyzed by massive sequencing techniques, a low correlation rate was observed between the most frequent taxa that comprised the entire fungal microbiome of the woody tissues of the plants analyzed in both vineyards and the lists of endophytic species isolated and characterized using classical microbiological techniques. This suggests an important bias in the results obtained through classical microbiological techniques, where the microbial diversity revealed appears to be much lower and limited compared to the metagenomic results. Many endophytic taxa isolated and identified from both the “Clau” vineyard (Table S1) and the “Almendros” plot (Table S2) were part of the lists of OTUs obtained by high-throughput sequencing in the two plots, except for species such as *Rhizoctonia solani* J.G. Kühn, *Discostroma fuscillum*, *Didymella glomerata*, *Didymosphaeria variabile*, *Phomopsis viticola*, or *Phoma conidiogena*. However, the frequencies of appearance of the taxa common to the two approaches were found to be comparable only in certain cases. Among the ranked list of the 10 most frequent OTUs in the “Clau” vineyard (Figure 5), only the GTD pathogen *Diplodia seriata* was found to be frequent in the culture-dependent analyses (representing approximately 33% of the isolates from the plot), together with moderately frequent taxa such as *Epicoccum* sp. and *Eutypa lata* (representing approximately 9% and 4.5% of the isolates, respectively, in the microbiological survey). Despite being the most abundant taxon in the metagenomic analysis, the pathogenic species *Phaeomoniella chlamydospora* (representing 4.5% of the total number

of isolates) was scarcely represented in the list of isolates from the older plot. Another surprising result was that *Neofusicoccum parvum*, one of the species frequently associated with GTDs and isolated in axenic cultivation of the “Clau” vineyard (representing 20% of the total isolates), was not among the most frequent OTUs defining the microbiome of the aforementioned plot. A similar situation was observed for another species associated with the early stages of grapevine esca, *Phaeoacremonium aleophilum*, which represented 4.4% of the total isolates but was not among the most frequent OTUs in the inner wood microbiome of the plants analyzed in the oldest vineyard.

When this type of comparison was established in the youngest vineyard (“Almendros” plot), the data turned out to be similar, although the percentage of strains representing the taxa isolated in cultivation common to the ranking of the 10 most frequent OTUs in the microbiome of the “Almendros” vineyard was, in general, lower than for the older plot, suggesting a replacement of the dominant strains in the microbiological analysis. Thus, *Epicoccum* sp. represented 25.7% of the total isolates, followed by *D. seriata* (11.5% of the total), together with *N. parvum* and *E. lata* with percentages of the total isolates of 5.7% and 2.8%, respectively. Interestingly, *P. chlamydospora* was not isolated by microbiological methods from the youngest plot. As expected, another phytopathogen associated with GTDs in young grapevine plants such as *Cylindrocarpon* spp. (etiological agent of the so-called ‘black foot’ disease), although present in 4.4% of the isolates obtained in the “Almendros” plot (and absent from the oldest vineyard), did not appear as part of the microbiome of this last vineyard.

3. Discussion

3.1. Grapevine Inner Wood Microbiome

The grapevine crop is one of the many agroecosystems that has been analyzed for its associated microbial diversity in the past decade using high-throughput sequencing techniques. While these analyses have primarily focused on the microbial communities inhabiting above-ground plant tissues [26,32–34], there has been some examination of the microbial diversity present in both the rootstock and root tissues [35,36]. In the production area under study, as well as in all Spanish viticultural areas, GTDs pose a serious and growing problem that threatens the profitability of farms [1]. With new pathologies emerging [37] and previously known syndromes persisting [38], there is a risk to both established plantations and new ones. The implementation of more precise and extensive diagnostic and epidemiology techniques has allowed for the characterization of the global panorama of GTDs in recent years, identifying entry routes, management alternatives, control possibilities, and other factors of these pathologies [39]. In terms of NGS techniques, these have primarily contributed to broadening our knowledge of the microbial diversity associated with the grapevine plant, greatly increasing the taxonomic inventories of microorganisms (fungi and bacteria) that can be found living inside the various tissues, organs, and compartments of the vine. NGS techniques have also aided in clarifying and resolving key questions related to the etiology and population dynamics of the etiological agents involved in GTDs, including the relationships between pathogen populations and the expression of foliar symptoms in plants [26], the underestimation of the pathogenic species present in a certain vineyard, and the precise detection of latent infections in crops [40].

The metagenomic analysis of the vineyards considered in this study assigned a total number of 1300 OTUs to 318 different fungal species. The number of characterized taxa in our study falls within the range of those obtained in previous works that focused on the microbiome of different organs of the grapevine plant. For instance, in the study by Wei et al. [21], 569 species of fungi were characterized on leaves, 376 in the case of rootstock-associated fungal diversity in the work by Gramaje et al. [35], 289 in the study carried out by Del Frari et al. [26] on the internal wood microbiome of plants affected by esca, and 732 OTUs were detected in the study by Lade et al. [41], where the fungal communities associated with graft unions and root collars were characterized in propagation plant material from nurseries. As expected, the fungal microbiome in the two plots considered in this

study was dominated by Ascomycota, while Basidiomycota represented a minor fraction (less than half of the above), as previously reported in numerous studies on grapevine employing similar approaches [26,32,42]. It is important to highlight that, although the plants analyzed were chosen based on the presence of foliar symptoms, decay, and wood rot, the metagenomic analyses did not detect any of the lignicolous basidiomycete taxa that are traditionally associated with the advanced stages of complex syndromes such as esca, even in the oldest vineyard (23 years old). However, this finding aligns with the results of Bekris et al. [9] who found an increase in the distribution and abundance of this type of taxa (mainly *Fomitiporia mediterranea*) in the symptomatic plants they analyzed. Paolinelli et al. [43] and Del Frari et al. [44] also observed this increase in the presence of lignicolous basidiomycetes in symptomatic plants, suggesting that an increase in this type of species can serve as an early indicator of the extension of this type of GTD. Regarding other taxa associated with GTDs, numerous species were identified, with some being extremely frequent (as in the case of *Phaeoconiella chlamydospora*) and others being less represented, such as species associated with the so-called Petri disease, including *Phaeoacremonium aleophilum*, *P. minimum*, or *Cadophora luteo-olivacea*; etiological agents associated with ‘*Botryosphaeria dieback*’ (including representatives of the genera *Neofusicoccum*, *Dothiorella*, or *Diplodia*); or the causal agent of eutypiose (*Eutypa lata*). This finding is consistent with the results of authors such as Del Frari et al. [26] who found a similar profile of ascomycete species associated with the internal wood of the vine.

In our study, approximately 80% of the characterized taxa turned out to be rare species, with a relative abundance of less than 2%. This is similar to what was observed by Del Frari et al. [26] who reported that in their analysis of the internal wood microbiome of grapevine plants affected by esca, 80% of the characterized taxa exhibited a relative abundance of less than 0.1%. In both our study and that of Del Frari et al., many of these rare or occasional species were well characterized from the point of view of their ecology, but an important contingent of them is either not specifically associated with the host or its role in the plant has yet to be elucidated. This observation suggests the hypothesis of the existence of a reservoir of rare and occasional diversity that, under the presence of certain drivers such as the triggering of specific environmental conditions (both biotic and abiotic), can play a more relevant role in the well-being and ecological fitness of the plant. This hypothesis aligns with the principles and functioning of the holobiont concept [6].

Many metagenomic studies on grapevines have aimed to identify “core” microbial populations driven by factors such as biotic or abiotic stress [45], plant genotype [46], or crop age [18]. In this study, we identified a core fungal community shared between the two vineyards analyzed, consisting mostly of pathogenic taxa and other generalist or ubiquitous endophytic species, as well as several OTUs associated with the plant host. In this sense, and when considering the phytosanitary status or age of the hosts analyzed, some studies were equally capable of characterizing essential and common microbial communities in plants of different geographical locations and ages. For example, Berlanas et al. [18] reported the existence of a core population that was common to the rootstocks of two vineyards geographically separated and of very different ages, 25 and 7 years old, respectively, with planting ages very similar to those of our case study. Similarly, Del Frari et al. [26] reported in a study on the microbiome associated with inner wood and canes of grapevine plants affected by esca that the fungal core community common to both types of woody tissues was dominated, as in the present study, by the same spectrum of pathogenic taxa associated with GTDs, together with a series of cosmopolitan and ubiquitous endophytic OTUs. Among this core community, the study highlights, as in our metagenomic analysis, the presence of *Phaeoconiella chlamydospora* as the most abundant component in this essential population. Likewise, Niem et al. [22] reported in a metagenomic study on symptomatic and asymptomatic grapevine plants in two vineyards in Australia that *Phaeoconiella chlamydospora* was the most abundant species, being even more frequent in asymptomatic plants. These authors found, as in our analysis, that the microbiome was dominated to a lesser extent by *Botryosphaeriaceae* species, certain lignicolous basidiomycetes, cosmopolitan endophytes,

or species with potential as BCAs. Bekris et al. [9], in a study on the wood microbiome of grapevines from three Greek cultivars located in three geographically distinct viticultural zones, reported that both geographical location and plant genotype were the determinants of fungal diversity composition, not phytosanitary status, unlike what is reported in other studies. Despite this, these authors also identified *P. chlamydospora* as one of the main agents responsible for the GTDs present in the study. Finally, Patanita et al. [31], in a metagenomic approach to fungal microbial communities associated with healthy grapevine plants and common symptoms of GTDs, found that taxa such as *Diplodia* sp., *Mycosphaerella tassiana*, *Alternaria* sp., or *Cladosporium* sp. were the most abundant in the study, similar to what was reported in our analysis.

3.2. Comparison of Microbial Communities: Beta-Diversity

A key aspect of this study is comparing the microbial diversity associated with two vineyards of different ages and locations with a high prevalence of plants with symptoms compatible with the presence of GTDs. Our results suggest that the age of the plantation is the main factor that could explain the differences detected between both microbiomes. In general terms, the fungal microbiome in the older plot was found to be more diverse and complex than in the eight-year-old vineyard. Thus, a differential composition of OTUs was found in both communities, where some GTD-genera such as *Diplodia* and *Phaeoconiella* were more abundant in the older plot, along with a series of basidiomycete yeast-like genera such as *Kurtzmanomyces*, *Dioszegia*, or *Vishniacozyma*. On the other hand, yeast-like genera such as *Cryptococcus* and *Naganishia*, both basidiomycetes, or *Wickerhamomyces*, an ascomycete, were more abundant in the younger plot, as well as certain taxa associated with GTDs mainly found in young plants, such as those related to the so-called 'black foot' disease. Several studies, such as the one by Dissanayake et al. [47], have revealed a positive correlation between grapevine age and fungal endophytic diversity, suggesting an increase in the diversity and complexity of these populations with an increase in the exposure time to these microorganisms. In addition, Berlanas et al. [18], although focused on the fungal rhizosphere microbiome, also reported that the diversity of rhizospheric microorganisms could be affected by plant age, although this was not the most important factor when it came to differentially modeling the microbiome associated with the rootstocks of young and mature plants.

3.3. Comparative Microbial Diversity According to Methodology: NGS vs. Culture-Dependent Techniques

The present study compared the diversity of endophytic fungi (including those that are GTD pathogens) associated with the interior of vine plant wood through culture-dependent methods and NGS techniques. The results showed that the diversity of cultivable species inside the plant was significantly lower than that characterized by metagenomics, as expected and as shown in numerous previous studies [47,48]. Furthermore, no clear correlation was found between the composition of isolated endophyte communities in the pure culture and the most frequent OTUs characterized in the metagenomic analysis, suggesting a bias when using classical microbiological methods. These methods are only capable of characterizing the cultivable mycobiota, which represents a very minor portion of the total number of fungi associated with the host plant. Despite this, some taxa (especially those with pathogenic behavior) isolated by microbiological methods had a comparable abundance between methods since they were part of the most frequent OTU rankings in the NGS analysis. In this sense, in an analysis of the fungal diversity of the aerial parts of grapevine plants of the 'Furmint' variety in Hungary, Knapp et al. [32] found a notable difference between the number of species resolved by both methods (being clearly higher in the metagenomic analysis). However, as in the present study, the core communities of microorganisms shared species in both taxonomic inventories. Similar results have been reported when employing other types of massive, indirect high-throughput analyses. In the work of Morales-Cruz et al. [40], the authors analyzed the microbial diversity of

grapevine plants affected by GTD at various locations in California using the sequencing of ribosomal DNA transcripts (rRNA) in a metatranscriptomic approach. They also reported that metagenomic and metatranscriptomics approaches revealed much greater species complexity than that obtained by direct fungal isolations.

4. Materials and Methods

4.1. Grapevine Plots

The samplings were carried out in two commercial vineyards located in the Huesca province in Northeastern Spain. The vineyards, “Clau” (at 41°59′39.2″ N; 0°08′04.5″ E) and “Almendros” (at 41°59′01.7″ N; 0°07′33.9″ E) belong to the PDO “Somontano” and represent two plots that differ in their year of plantation. Both vineyards have phytosanitary problems associated with varied symptoms attributable to GTDs, such as interveinal “striping”, inner wood rotting, or entire branch collapse (Figure 11). Additional information on cultivar type, bioclimate parameters, management practices, and other relevant data can be found in Table 2.



Figure 11. Commercial vineyards studied in this work. Photographs on the left show general views of the plots in May 2021 and photographs on the right show details of GTD foliar symptoms. (a,b): “Clau” vineyard; (c,d): “Almendros” vineyard.

Table 2. Soil, bioclimatic, and agronomic data of the two vineyards surveyed.

Plot Name	“Clau”	“Almendros”
Var./Rootstock	“Cabernet Sauvignon” clone 170/SO4	“Sauvignon Blanc”/376 and R140
Year Established	2000	2015
Management/ Plantation frame	Cover crop, trellis formation system, and double cordon/3 × 1 m	Cover crop, trellis formation system, and double cordon/3 × 1.2 m
Soil Type	Loam texture; calcisol (accumulation of calcium carbonate at a certain depth, basic pH)	Loam texture; calcisol
Height (m.a.s.l)	375	401
Temperature, Rainfall, and Climate	14.23 °C, 486 mm, and continental Mediterranean climate	13.00 °C, 486 mm, and continental Mediterranean climate
Average Yield (last 3 years)	6000 kg/ha	9000 kg/ha

4.2. Wood Samples

In each of the two vineyards studied, a total of 20 grapevine plants were sampled. Specifically, five plants per row were chosen for sampling, with four rows sampled in total. The chosen plants had previously been marked as diseased due to the presence of GTD symptoms, such as foliar chlorosis, stunted growth, and wood rot. To characterize the fungal microbiome of the inner wood, each marked plant was sampled at the point of separation of both arms. This was achieved by drilling a hole approximately 4 mm in diameter and 8 cm deep and collecting all the plant material extracted (approximately 2 g) into plastic envelopes while trying to discard the bark. Finally, the inner wood samples were refrigerated at 4–6 °C before being taken to the laboratory, where they were stored at –20 °C until subsequent DNA extraction.

4.3. Isolation of Grapevine Endophytic Fungi

Grapevine plants were sampled for their aerial tissues (vine shoots and arms) to isolate and characterize the different fungal species associated with them (including GTD-associated fungi) using microbiological culture-dependent methods. To do this, plant material (either shoot discs or inner wood blocks) was cut into 0.5 cm fragments and surface sterilized with a 70% EtOH solution (1 min), followed by a 5% commercial sodium hypochlorite solution (3 min), and then rinsed with sterile bi-distilled water 3–5 times. The fragments were then placed in PDA plates (CULTIMED, Barcelona, Spain) amended with streptomycin sulfate (0.3 g/L) to avoid bacterial contamination and incubated in the dark at 25 °C for 3–5 days to obtain emerging fungal colonies. The resulting colonies were transferred to new PDA plates to obtain pure cultures of each endophytic strain. Finally, these isolates were taxonomically identified by applying both morphometrical and molecular methods, including comparing their ribosomal ITS fragment sequences in public databases using the BLASTn tool [49].

4.4. DNA Extraction and Sequencing

Prior to performing total genomic DNA extraction, the wood samples were deep-frozen for 30 min at –85 °C, then crushed in a mortar and pestle with liquid nitrogen, and subsequently lyophilized for 72 h in a Cryodos-80 device (Telstar, Barcelona, Spain). Then, approximately 250 mg of dried powdered wood per plant sample was used to extract total genomic DNA with the DNeasy® Plant Mini Kit (Qiagen, Germany), following the manufacturer's instructions. The concentration of extracted DNA was measured using a NanoDrop® ND-1000 spectrophotometer device (Waltham, Thermo Scientific, MA, USA). The integrity of DNA was assessed through 1.5% agarose gel electrophoresis. Samples were then sent to Stab Vida, Lda. (Caparica, Portugal) for NGS analysis. The ITS (ITS2 fragment) region was selected as the target amplicon for the metagenomic study of the fungal community. Due to the existence of suboptimal total DNA concentrations in some samples, the genomic libraries and subsequent massive sequencing analyzes were performed on 16 of the 20 plants in the “Clau” plot and on 13 of the 20 samples from the “Almendros” plot. In both cases, all the sampled rows were analyzed in at least one of their repetitions. The Illumina metagenomic sequencing library preparation protocol was used to construct the library, and the resulting DNA fragments were sequenced on the Illumina MiSeq platform using 300 bp paired-end reads.

4.5. Bioinformatics Procedure

After sequencing, the generated raw data (6,498,688 reads total, 105,964 to 361,014 raw sequence reads per sample) were downloaded and processed through a galaxy workflow using DADA2 (Galaxy Version 1.20+galaxy0) [50]. The sequences were trimmed and quality filtered, the error rate was denoised, and bimeras were removed. The reads were then grouped into OTUs and classified by taxon using the DADA2 modules assignTaxonomy and addSpecies and the 8.3 version of the general fasta release of the UNITE database [51]. The processed OTU table was composed of 2,386,482 reads from 1300 OTUs.

4.6. Statistical Data Analysis

Statistical analysis was performed in Rstudio using the phyloseq package [52]. Alpha-diversity was determined using four diversity indexes (Chao, Shannon, Fisher, and Simpson). For beta-diversity analysis purposes, principal coordinate analysis (PCoA) and ordination plots of OTU data were constructed using the Phyloseq program for R. The DESeq2 package was used to detect differentially abundant OTU between rows and plots with default parameters (Wald test). To delve deeper into the effects of alternate mycobiota communities in the different plots, FUNGuild annotation tools were utilized for functional predictions [53]. The different Venn diagrams showing the intersections between OTUs belonging to different vineyards and rows within each plot were generated with the 'Venn Diagrams' tool [54].

5. Conclusions

High-throughput sequencing enabled the characterization of the fungal microbiota associated with the grapevine internal plant wood tissues in two experimental vineyards, selected based on their planting age, phytosanitary status, and cultivated variety. In addition, an analysis of the fungal diversity existing in the same woody tissues was conducted using culture-dependent microbiological techniques. The metagenomic analysis revealed a high fungal diversity compared to classical taxonomic methods in terms of the number of characterized OTUs, abundance, and frequency of occurrence. The taxonomic results from classical microbiological methods did not reflect the true diversity of the endophytes associated with internal plant wood or the composition and population structure of this microbial diversity. The study of the microbiome demonstrated that the symptoms associated with GTDs could be attributable to the dominant presence of *Phaeomoniella chlamydospora* and, to a lesser extent, *Diplodia seriata*. However, culture-dependent methods did not yield the same view in terms of the abundance of isolates belonging to both taxa. In general, the microbiota of the older plot was more diverse and complex, being dominated at the level of pathogenic taxa by those associated with wood pathologies characteristic of mature plants, while in the young vineyard, elements associated with GTDs that preferentially affect young plants dominated. The results suggest a differential replacement and enrichment of fungal microbial communities based on age and exposure to endophytic infection, where the dominant species in each type of microbiota could have been prioritized by plant individuals based on the age, anatomy, and structure of their tissues. In general terms, the results of the metagenomic analysis revealed a characteristic mycobiota of the internal wood (and, to a lesser extent, of other plant organs) consisting of microorganisms repeatedly cited in previous studies of a similar nature, suggesting a priming effect promoted by the grapevine plant that is modulable according to each genotype in question, management modality, or the age of the crop.

Supplementary Materials: The following supporting information can be downloaded at: <https://www.mdpi.com/article/10.3390/plants12122251/s1>, Table S1: Fungal OTUs isolated by microbiological methods and identified from surveyed plants in the "Clau" vineyard; Table S2: Fungal OTUs isolated by microbiological methods and identified from surveyed plants in the "Almendros" vineyard; Table S3: Taxonomy table generated from NGS analyses. Total OTUs resolved indicating the appearance frequency per plant stand; Table S4: Ecology traits of the different OTUs characterized. For each taxon, indications about their trophic mode, guild, lifestyle, or growth form are given.

Author Contributions: Conceptualization, V.G.-G., P.M.-R. and N.L.-L.; methodology, V.G.-G., C.J.-L., P.M.-R., N.L.-L. and J.G.; software, J.G.; validation, V.G.-G., J.C.-G., P.M.-R., N.L.-L. and J.G.; formal analysis, V.G.-G., J.G., E.S.-H. and N.L.-L.; investigation, V.G.-G., P.M.-R., E.S.-H. and N.L.-L.; resources, V.G.-G., P.M.-R. and J.C.-G.; data curation, J.C.-G., J.G., N.L.-L., V.G.-G. and C.J.-L.; writing—original draft preparation, V.G.-G., P.M.-R., E.S.-H. and N.L.-L.; writing—review and editing, V.G.-G., J.G., P.M.-R. and N.L.-L.; supervision, V.G.-G. and P.M.-R.; project administration, V.G.-G., P.M.-R. and J.C.-G.; funding acquisition, P.M.-R. and J.C.-G. All authors have read and agreed to the published version of the manuscript.

Funding: This research was funded by Cátedra Agrobank under the “IV Convocatoria de Ayudas de la Cátedra AgroBank para la transferencia del conocimiento al sector agroalimentario” program.

Data Availability Statement: The data presented in this study are available on request from the corresponding author. The data are not publicly available due to their relevance to an ongoing Ph.D. Thesis.

Acknowledgments: To Sergio Torres-Sánchez, José M. Ayuso-Rodríguez, and Adrián Jarné-Casasús, from Viñas del Vero S.A. winery.

Conflicts of Interest: The authors declare no conflict of interest.

References

1. Gramaje, D.; Urbez-Torres, J.R.; Sosnowski, M.R. Managing grapevine trunk diseases with respect to etiology and epidemiology: Current strategies and future prospects. *Plant Dis.* **2018**, *102*, 12–39. [[CrossRef](#)] [[PubMed](#)]
2. Mondello, V.; Songy, A.; Battiston, E.; Pinto, C.; Coppin, C.; Trotel-Aziz, P.; Clement, C.; Mugnai, L.; Fontaine, F. Grapevine trunk diseases: A review of fifteen years of trials for their control with chemicals and biocontrol agents. *Plant Dis.* **2018**, *102*, 1189–1217. [[CrossRef](#)] [[PubMed](#)]
3. Bertsch, C.; Ramírez-Suero, M.; Magnin-Robert, M.; Larignon, P.; Chong, J.; Abou-Mansour, E.; Spagnolo, A.; Clément, C.; Fontaine, F. Grapevine trunk diseases: Complex and still poorly understood. *Plant Pathol.* **2013**, *62*, 243–265. [[CrossRef](#)]
4. Hrycan, J.; Hart, M.; Bowen, P.; Forge, T.; Úrbez-Torres, J.R. Grapevine trunk disease fungi: Their roles as latent pathogens and stress factors that favour disease development and symptom expression. *Phytopathol. Mediterr.* **2020**, *59*, 395–424. [[CrossRef](#)]
5. Fontaine, F.; Gramaje, D.; Armengol, J.; Smart, R.; Nagy, Z.A.; Borgo, M.; Rego, C.; Corio-Costet, M.-F. *Grapevine Trunk Diseases. A Review*; De la Fuente, M., Ed.; OIV Publications: Paris, France, 2016; p. 25.
6. Bettenfeld, P.; Cadena i Canals, J.; Jacquens, L.; Fernandez, O.; Fontaine, F.; van Schaik, E.; Courty, P.-E.; Trouvelot, S. The microbiota of the grapevine holobiont: A key component of plant health. *J. Adv. Res.* **2022**, *40*, 1–15. [[CrossRef](#)] [[PubMed](#)]
7. Forbes, J.D.; Knox, N.C.; Ronholm, J.; Pagotto, F.; Reimer, A. Metagenomics: The Next Culture-Independent Game Changer. *Front. Microbiol.* **2017**, *8*, 1069. [[CrossRef](#)]
8. Hinsu, A.; Dumadiya, A.; Joshi, A.; Kotadiya, R.; Andharia, K.; Koringa, P.; Kothari, R. To culture or not to culture: A snapshot of culture-dependent and culture-independent bacterial diversity from peanut rhizosphere. *PeerJ* **2021**, *9*, e12035. [[CrossRef](#)]
9. Bekris, F.; Vasileiadis, S.; Papadopoulou, E.; Samaras, A.; Testempasis, S.; Gkizi, D.; Tavlaki, G.; Tzima, A.; Paplomatas, E.; Markakis, E.; et al. Grapevine wood microbiome analysis identifies key fungal pathogens and potential interactions with the bacterial community implicated in grapevine trunk disease appearance. *Environ. Microbiome* **2021**, *16*, 23. [[CrossRef](#)]
10. Tiwari, M.; Pati, D.; Mohapatra, R.; Sahu, B.B.; Singh, P. The Impact of Microbes in Plant Immunity and Priming Induced Inheritance: A Sustainable Approach for Crop protection. *Plant Stress* **2022**, *4*, 100072. [[CrossRef](#)]
11. Liu, D.; Howell, K. Community succession of the grapevine fungal microbiome in the annual growth cycle. *Environ. Microbiol.* **2021**, *23*, 1842–1857. [[CrossRef](#)]
12. Liu, H.; Brettell, L.E. Plant Defense by VOC-Induced Microbial Priming. *Trends Plant Sci.* **2019**, *24*, 187–189. [[CrossRef](#)] [[PubMed](#)]
13. Rosenberg, E.; Zilber-Rosenberg, I.; Collier, R.J. Microbes Drive Evolution of Animals and Plants: The Hologenome Concept. *mBio* **2016**, *7*, e01395-15. [[CrossRef](#)] [[PubMed](#)]
14. Gopal, M.; Gupta, A. Microbiome Selection Could Spur Next-Generation Plant Breeding Strategies. *Front. Microbiol.* **2016**, *7*, 1971. [[CrossRef](#)] [[PubMed](#)]
15. Berg, G.; Rybakova, D.; Grube, M.; Köberl, M. The plant microbiome explored: Implications for experimental botany. *J. Exp. Bot.* **2016**, *67*, 995–1002. [[CrossRef](#)] [[PubMed](#)]
16. Fournier, P.; Pellan, L.; Barroso-Bergadà, D.; Bohan, D.A.; Candresse, T.; Delmotte, F.; Dufour, M.-C.; Lauvergeat, V.; Le Marrec, C.; Marais, A.; et al. The functional microbiome of grapevine throughout plant evolutionary history and lifetime. *Adv. Ecol. Res.* **2022**, *67*, 27–99. [[CrossRef](#)]
17. Morgan, H.H.; du Toit, M.; Setati, M.E. The Grapevine and Wine Microbiome: Insights from High-Throughput Amplicon Sequencing. *Front. Microbiol.* **2017**, *8*, 820. [[CrossRef](#)]
18. Berlanas, C.; Berbegal, M.; Elena, G.; Laidani, M.; Cibriain, J.F.; Sagües, A.; Gramaje, D. The fungal and bacterial rhizosphere microbiome associated with grapevine rootstock genotypes in mature and young vineyards. *Front. Microbiol.* **2019**, *10*, 1142. [[CrossRef](#)]
19. Hamaoka, K.; Aoki, Y.; Takahashi, S.; Enoki, S.; Yamamoto, K.; Tanaka, K.; Suzuki, S. Diversity of endophytic bacterial microbiota in grapevine shoot xylems varies depending on wine grape-growing region, cultivar, and shoot growth stage. *Sci. Rep.* **2022**, *12*, 15772. [[CrossRef](#)]
20. Martínez-Diz, M.d.P.; Andrés-Sodupe, M.; Bujanda, R.; Díaz-Losada, E.; Eichmeier, A.; Gramaje, D. Soil-plant compartments affect fungal microbiome diversity and composition in grapevine. *Fungal Ecol.* **2019**, *41*, 234–244. [[CrossRef](#)]
21. Wei, Y.-J.; Wu, Y.; Yan, Y.-Z.; Zou, W.; Xue, J.; Ma, W.-R.; Wang, W.; Tian, G.; Wang, L.-Y. High-throughput sequencing of microbial community diversity in soil, grapes, leaves, grape juice and wine of grapevine from China. *PLoS ONE* **2018**, *13*, e0193097. [[CrossRef](#)]

22. Niem, J.M.; Billones-Baaijens, R.; Stodart, B.; Savocchia, S. Diversity Profiling of Grapevine Microbial Endosphere and Antagonistic Potential of Endophytic *Pseudomonas* Against Grapevine Trunk Diseases. *Front. Microbiol.* **2020**, *11*, 477. [[CrossRef](#)] [[PubMed](#)]
23. Cobos, R.; Ibañez, A.; Díez-Galán, A.; Calvo-Peña, C.; Ghorehshizadeh, S.; Coque, J.J.R. The Grapevine Microbiome to the Rescue: Implications for the Biocontrol of Trunk Diseases. *Plants* **2022**, *11*, 840. [[CrossRef](#)] [[PubMed](#)]
24. Darriaut, R.; Lailheugue, V.; Masneuf-Pomarède, I.; Marguerit, E.; Martins, G.; Compant, S.; Ballestra, P.; Upton, S.; Ollat, N.; Lauvergeat, V. Grapevine rootstock and soil microbiome interactions: Keys for a resilient viticulture. *Hortic. Res.* **2022**, *9*, uhac019. [[CrossRef](#)] [[PubMed](#)]
25. Pauvert, C.; Fort, T.; Calonnec, A.; Faivre d'Arcier, J.; Chancerel, E.; Massot, M.; Chiquet, J.; Robin, S.; Bohan, D.A.; Vallance, J.; et al. Microbial association networks give relevant insights into plant pathobiomes. *bioRxiv* **2020**. [[CrossRef](#)]
26. Del Frari, G.; Gobbi, A.; Aggerbeck, M.R.; Oliveira, H.; Hansen, L.H.; Ferreira, R.B. Characterization of the Wood Mycobiome of *Vitis vinifera* in a Vineyard Affected by Esca. Spatial Distribution of Fungal Communities and Their Putative Relation With Leaf Symptoms. *Front. Plant Sci.* **2019**, *10*, 910. [[CrossRef](#)]
27. Cordero-Bueso, G.; Mangieri, N.; Maghradze, D.; Foschino, R.; Valdetara, F.; Cantoral, J.M.; Vigentini, I. Wild Grape-Associated Yeasts as Promising Biocontrol Agents against *Vitis vinifera* Fungal Pathogens. *Front. Microbiol.* **2017**, *8*, 2025. [[CrossRef](#)]
28. Liu, Z.; Jiao, R.; Chen, S.; Ren, Y.; Zhang, L.; Zhang, D.; Chen, J.; Li, G. First Report of Fruit Rot of Grapes (*Vitis vinifera*) Caused by *Cladosporium cladosporioides* in Xinjiang, China. *Plant Dis.* **2022**, *106*, 315. [[CrossRef](#)]
29. Lawrence, D.P.; Travadon, R.; Baumgartner, K. Novel Seimatosporium Species from Grapevine in Northern California and Their Interactions with Fungal Pathogens Involved in the Trunk-Disease Complex. *Plant Dis.* **2018**, *102*, 1081–1092. [[CrossRef](#)]
30. Cloete, M.; Fischer, M.; Mostert, L.; Halleen, F. Hymenochaetales associated with esca-related wood rots on grapevine with a special emphasis on the status of esca in South African vineyards. *Phytopathol. Mediterr.* **2015**, *54*, 299–312. [[CrossRef](#)]
31. Patanita, M.; Albuquerque, A.; Campos, M.D.; Materatski, P.; Varanda, C.M.R.; Ribeiro, J.A.; Félix, M.D.R. Metagenomic assessment unravels fungal microbiota associated to grapevine trunk diseases. *Horticultrae* **2022**, *8*, 288. [[CrossRef](#)]
32. Knapp, D.G.; Lázár, A.; Molnár, A.; Vajna, B.; Karácsony, Z.; Váczy, K.Z.; Kovács, G.M. Above-ground parts of white grapevine *Vitis vinifera* cv. Furmint share core members of the fungal microbiome. *Environ. Microbiol. Rep.* **2021**, *13*, 509–520. [[CrossRef](#)] [[PubMed](#)]
33. Singh, P.; Santoni, S.; Weber, A.; This, P.; Péros, J.-P. Understanding the phyllosphere microbiome assemblage in grape species (*Vitaceae*) with amplicon sequence data structures. *Sci. Rep.* **2019**, *9*, 14294. [[CrossRef](#)] [[PubMed](#)]
34. Wicaksono, W.A.; Morauf, C.; Müller, H.; Abdelfattah, A.; Donat, C.; Berg, G. The mature phyllosphere microbiome of grapevine is associated with resistance against *Plasmopara viticola*. *Front. Microbiol.* **2023**, *14*, 1149307. [[CrossRef](#)] [[PubMed](#)]
35. Gramaje, D.; Eichmeier, A.; Spetik, M.; Carbone, M.J.; Bujanda, R.; Vallance, J.; Rey, P. Exploring the temporal dynamics of the fungal microbiome in rootstocks, the lesser-known half of the grapevine crop. *J. Fungi* **2022**, *8*, 421. [[CrossRef](#)]
36. Carbone, M.J.; Alaniz, S.; Mondino, P.; Gelabert, M.; Eichmeier, A.; Tekielska, D.; Bujanda, R.; Gramaje, D. Drought influences fungal community dynamics in the grapevine rhizosphere and root microbiome. *J. Fungi* **2021**, *7*, 686. [[CrossRef](#)]
37. Claverie, M.; Notaro, M.; Fontaine, F.; Wery, J. Current knowledge on grapevine trunk diseases with complex etiology: A systemic approach. *Phytopathol. Mediterr.* **2020**, *59*, 29–53. [[CrossRef](#)]
38. Kenfaoui, J.; Radouane, N.; Mennani, M.; Tahiri, A.; El Ghadraoui, L.; Belabess, Z.; Fontaine, F.; El Hamss, H.; Amiri, S.; Lahlali, R.; et al. A panoramic view on grapevine trunk diseases threats: Case of *Eutypa dieback*, *Botryosphaeria dieback*, and esca disease. *J. Fungi* **2022**, *8*, 595. [[CrossRef](#)]
39. Azevedo-Nogueira, F.; Rego, C.; Gonçalves, H.M.R.; Fortes, A.M.; Gramaje, D.; Martins-Lopes, P. The road to molecular identification and detection of fungal grapevine trunk diseases. *Front. Plant Sci.* **2022**, *13*, 960289. [[CrossRef](#)]
40. Morales-Cruz, A.; Figueroa-Balderas, R.; García, J.F.; Tran, E.; Rolshausen, P.E.; Baumgartner, K.; Cantu, D. Profiling grapevine trunk pathogens in planta: A case for community-targeted DNA metabarcoding. *BMC Microbiol.* **2018**, *18*, 214. [[CrossRef](#)]
41. Lade, S.B.; Štraus, D.; Oliva, J. Variation in fungal community in grapevine (*Vitis vinifera*) nursery stock depends on nursery, variety and rootstock. *J. Fungi* **2022**, *8*, 47. [[CrossRef](#)]
42. Bruez, E.; Vallance, J.; Gautier, A.; Laval, V.; Compant, S.; Maurer, W.; Sessitsch, A.; Lebrun, M.H.; Rey, P. Major changes in grapevine wood microbiota are associated with the onset of esca, a devastating trunk disease. *Environ. Microbiol.* **2020**, *22*, 5189–5206. [[CrossRef](#)] [[PubMed](#)]
43. Paolinelli, M.; Escoriaza, G.; Cesari, C.; Garcia-Lampasona, S.; Hernandez-Martinez, R. Metatranscriptomic approach for microbiome characterization and host gene expression evaluation for “Hoja de malvón” disease in *Vitis vinifera* cv. Malbec (preprint). *Res. Sq.* **2020**, 1–20. [[CrossRef](#)]
44. Del Frari, G.; Oliveira, H.; Ferreira, R.B. White rot fungi (*Hymenochaetales*) and esca of grapevine: Insights from recent microbiome studies. *J. Fungi* **2021**, *7*, 770. [[CrossRef](#)] [[PubMed](#)]
45. Vacher, C.; Francioni, C.; Michel, M.; Fort, T.; Faivre d'Arcier, J.; Chancerel, E.; Delmotte, F.; Delmas, C.E.L. Fungal metabarcoding data for two grapevine varieties (Regent and *Vitis vinifera* ‘Cabernet-Sauvignon’) inoculated with powdery mildew (*Erysiphe necator*) under drought conditions. *Phytobiomes J.* **2022**, *6*, 358–367. [[CrossRef](#)]
46. Awad, M.; Giannopoulos, G.; Mylona, P.V.; Polidoros, A.N. Genotype may influence bacterial diversity in bark and bud of *Vitis vinifera* cultivars grown under the same environment. *Appl. Sci.* **2020**, *10*, 8405. [[CrossRef](#)]

47. Dissanayake, A.J.; Purahong, W.; Wubet, T.; Hyde, K.D.; Zhang, W.; Xu, H.; Zhang, G.; Fu, C.; Liu, M.; Xing, Q.; et al. Direct comparison of culture-dependent and culture-independent molecular approaches reveal the diversity of fungal endophytic communities in stems of grapevine (*Vitis vinifera*). *Fungal Divers.* **2018**, *90*, 85–107. [[CrossRef](#)]
48. Jayawardena, R.S.; Purahong, W.; Zhang, W.; Wubet, T.; Li, X.; Liu, M.; Zhao, W.; Hyde, K.D.; Liu, J.; Yan, J. Biodiversity of fungi on *Vitis vinifera* L. revealed by traditional and high-resolution culture-independent approaches. *Fungal Divers.* **2018**, *90*, 1–84. [[CrossRef](#)]
49. Johnson, M.; Zaretskaya, I.; Raytselis, Y.; Merezuk, Y.; McGinnis, S.; Madden, T.L. NCBI BLAST: A better web interface. *Nucleic Acids Res.* **2008**, *36*, W5–W9. [[CrossRef](#)]
50. Callahan, B.J.; McMurdie, P.J.; Rosen, M.J.; Han, A.W.; Johnson, A.J.A.; Holmes, S.P. DADA2: High-resolution sample inference from Illumina amplicon data. *Nat. Methods* **2016**, *13*, 581–583. [[CrossRef](#)]
51. Abarenkov, K.; Zirk, A.; Piirmann, T.; Pöhönen, R.; Ivanov, F.; Nilsson, R.H.; Kõljalg, U. UNITE General FASTA Release for Fungi 2; Version 10.05.2021; UNITE Community. 2021. Available online: <https://doi.plutof.ut.ee/doi/10.15156/BIO/1280089> (accessed on 5 June 2023).
52. Watson, M.; McMurdie, P.J.; Holmes, S. phyloseq: An R Package for Reproducible Interactive Analysis and Graphics of Microbiome Census Data. *PLoS ONE* **2013**, *8*, e61217. [[CrossRef](#)]
53. Nguyen, N.H.; Song, Z.; Bates, S.T.; Branco, S.; Tedersoo, L.; Menke, J.; Schilling, J.S.; Kennedy, P.G. FUNGuild: An open annotation tool for parsing fungal community datasets by ecological guild. *Fungal Ecol.* **2016**, *20*, 241–248. [[CrossRef](#)]
54. Bioinformatics & Evolutionary Genomics. Calculate and Draw Custom Venn Diagrams. Available online: <http://bioinformatics.psb.ugent.be/webtools/Venn/> (accessed on 2 May 2023).

Disclaimer/Publisher’s Note: The statements, opinions and data contained in all publications are solely those of the individual author(s) and contributor(s) and not of MDPI and/or the editor(s). MDPI and/or the editor(s) disclaim responsibility for any injury to people or property resulting from any ideas, methods, instructions or products referred to in the content.

3. DISCUSIÓN GLOBAL

3.1. Productos naturales

La Tabla 2 recoge una comparativa de todos los productos ensayados en la Tesis Doctoral contra patógenos asociados a las EMV.

Aunque las dosis inhibitorias efectivas muestran una clara dependencia del patógeno contra el que se ensaya el producto, la conjugación con oligómeros de quitosano o con esteviósido se tradujo en una mejora de la eficacia antifúngica de los productos naturales en todos los casos, con un claro efecto sinérgico resultado de la mejora de la solubilidad y biodisponibilidad.

En un análisis más pormenorizado, se aprecia que los resultados de inhibición del crecimiento de los patógenos empleando extractos de plantas (mezclas complejas) fueron mejores que los obtenidos empleando productos puros. Por ejemplo, el complejo conjugado de COS con aminoácidos con la eficacia más alta fue COS-tirosina, con valores de concentración efectiva CE_{90} de 1021 $\mu\text{g}\cdot\text{mL}^{-1}$ para *N. parvum*, 672 $\mu\text{g}\cdot\text{mL}^{-1}$ para *D. seriata*, y 708 $\mu\text{g}\cdot\text{mL}^{-1}$ para *B. dothidea*. Los resultados para COS-*E. arvense* y COS-*U. dioica* fueron mejores, con valores de CE_{90} de 637–650, 429–483 y 267–334 $\mu\text{g}\cdot\text{mL}^{-1}$, respectivamente. Esto debe atribuirse a la presencia de múltiples compuestos bioactivos en cada extracto en cuestión, con distintos mecanismos de actuación que interactúan a la hora de controlar el patógeno, con un comportamiento sinérgico.

Por otra parte, no todos los extractos de plantas presentan la misma eficacia frente a cada patógeno ensayado. Si se comparan los resultados arriba indicados para COS-*E. arvense* y COS-*U. dioica* frente a *N. parvum* y *D. seriata* con los obtenidos para el complejo conjugado COS-*R. tinctorum* (con valores de CE_{90} de 66 y 73 $\mu\text{g}\cdot\text{mL}^{-1}$, respectivamente), resulta evidente que la planta de la familia *Rubiaceae* es mucho más eficaz, aunque las primeras figuren en la lista de sustancias básicas de la UE y la rubia no.

Respecto a la elección entre COS y esteviósido para la formación de los complejos conjugados (abordada en el artículo #5), si bien ambos son buenas opciones, el COS arroja valores de CE menores, por lo que debería ser la opción preferente cara a futuros estudios.

También resulta llamativa la mejora de eficacia alcanzada por los extractos de *R. tinctorum*, *S. marianum*, *U. dioica*, y *E. arvense* al ser encapsulados en *nanocarriers*, con valores de CE_{90} en el rango de 66–113 $\mu\text{g}\cdot\text{mL}^{-1}$ frente a *N. parvum*, más bajos que los de los complejos conjugados. Tal mejora debe atribuirse a las propiedades de liberación controlada del contenido de los NCs en el lugar de la infección, que permiten optimizar la dosis de producto bioactivo utilizado, en línea con lo referido por otros autores para la encapsulación de distintos tipos de agroquímicos.

Tabla 2. Comparativa de resultados de los artículos 1-7 sobre la eficacia de productos naturales frente a patógenos responsables de EMV, solos, conjugados con oligómeros de quitosano (COS) o esteviósido, y encapsulados en nanotransportadores (NCs).

Artículo	Tratamiento	CE ($\mu\text{g}\cdot\text{mL}^{-1}$)	<i>N. parvum</i>	<i>D. seriata</i>	<i>B. dothidea</i>	<i>D. viticola</i>	<i>D. iberica</i>	<i>D. coryli</i>	<i>D. sarmentorum</i>	
1	COS	50	320.9	448.1	425.8					
		90	957.4	1360.6	1339.2					
	COS–tirosina	50	258.9	254.6	255.1					
		90	1021.4	672.1	707.7					
	COS–cisteína	50	280.8	297.8	306.2					
		90	1347.0	774.6	897.9					
	COS–prolina	50	402.9	398.7	316.0					
		90	1439.0	1086.5	907.4					
	COS–glicina	50	417.8	448.5	291.1					
		90	1498.5	1286.7	887.9					
	2	COS	50	680.2	744.4	362.8	554.3	706.6	472.2	398.7
			90	1326.6	1179.9	1191.6	1138.7	1196.4	972.4	1075.9
COS– <i>Equisetum arvense</i>		50	214.1	173.9	109.4	148.2	304.1	155.3	198.2	
		90	637.1	429.0	267.1	351.1	817.3	999.0	669.0	
COS– <i>Urtica dioica</i>		50	215.2	211.5	72.6	175.3	253.0	162.9	203.0	
		90	650.2	483.5	334.4	379.7	625.8	411.6	533.0	
3	Esteviósido	50	152.2	230.1		271.4				
		90	824.1	840.5		1017.0				
	<i>Silybum marianum</i>	50	677.2	703.0		1088.4				
		90	2938.3	1461.1		9943.2				
	Alcohol coniferílico	50	214.3	370.3		361.1				
		90	1005.3	913.2		988.5				
	Ácido ferúlico	50	1394.5	433.0		1387.2				
		90	2948.6	903.4		3921.3				
	Esteviósido– <i>S. marianum</i>	50	89.2	127.1		148.3				
		90	262.1	355.4		360.7				
	Esteviósido–alcohol coniferílico	50	157.8	191.6		156.5				
		90	384.9	360.5		368.2				
	Esteviósido–ácido ferúlico	50	465.9	209.0		544.5				
		90	1132.7	465.9		1183.2				

Artículo	Tratamiento	CE ($\mu\text{g}\cdot\text{mL}^{-1}$)	<i>N. parvum</i>	<i>D. seriata</i>	<i>B. dothidea</i>	<i>D. viticola</i>	<i>D. iberica</i>	<i>D. coryli</i>	<i>D. sarmentorum</i>	
4	Esteviósido	50	154.9			309.6				
		90	923.8			1007.1				
	Rutina	50	656.9				575.1			
		90	1156.5				981.1			
	Ácido ferúlico	50	1394.4				1287.2			
		90	4121.3				2948.6			
	Esteviósido–rutina	50	306.0				241.6			
		90	714.9				457.8			
	Esteviósido–ácido ferúlico	50	435.6				574.4			
		90	1032.2				921.8			
	5	COS	50	680.2	744.4		554.3			
			90	1326.6	1179.9		1138.7			
Esteviósido		50	194.8	288.1		306.9				
		90	723.8	840.5		917.0				
<i>Rubia tinctorum</i>		50	92.3	78.0		66.2				
		90	184.0	87.8		90.2				
COS– <i>R. tinctorum</i>		50	38.2	63.1		22.1				
		90	66.3	73.4		55.5				
Esteviósido– <i>R. tinctorum</i>		50	75.1	73.6		80.0				
		90	89.2	82.4		90.7				
6		ML–COS	50	82.7						
			90	243.2						
	<i>S. marianum</i>	50	557.0							
		90	2938.0							
	<i>R. tinctorum</i>	50	92.3	78.0						
		90	184.0	87.8						
	ML–COS– <i>R. tinctorum</i> (NC)	50	41.2	59.3						
		90	65.8	91.0						
	ML–COS– <i>S. marianum</i> (NC)	50	60.9							
		90	90.6							
	ML–COS– <i>U. dioica</i> (NC)	50	50.2							
		90	113.0							
ML–COS– <i>E. arvense</i> (NC)	50	66.5								
	90	105.2								

Artículo	Tratamiento	CE ($\mu\text{g}\cdot\text{mL}^{-1}$)	<i>N. parvum</i>	<i>D. seriata</i>	<i>B. dothidea</i>	<i>D. viticola</i>	<i>D. iberica</i>	<i>D. coryli</i>	<i>D. sarmentorum</i>
7	<i>R. tinctorum</i>	50	92.3	78.0					
		90	184.0	87.8					
	<i>R. tinctorum</i> encapsulado en g-C ₃ N ₄ -MA-COS NCs	50	50.8	27.0					
		90	88.4	33.7					

COS = oligómeros de quitosano; ML = lignina metacrilada; NC = extracto encapsulado en nanotransportador. Los extractos con baja eficacia ($\text{CE}_{90} > 1500 \mu\text{g}\cdot\text{mL}^{-1}$) no se han incluido en la tabla.

3.2. Agentes de biocontrol

Respecto a los resultados obtenidos en la Tesis Doctoral referidos al potencial de microorganismos fúngicos y bacterianos como antagonistas microbianos frente a los patógenos asociados a las EMV, y concretamente en relación con los hongos del género *Trichoderma*, en las dos investigaciones se observó la capacidad de *T. harzianum* aislada de vides aragonesas para inhibir el crecimiento de *N. parvum*, y para uno de los aislados (MYC-V102) también se encontró inhibición frente a *R. solani*. Estos resultados coinciden con otros artículos que también han demostrado que *T. harzianum* puede reducir el desarrollo de *R. solani*, como el de Siameto *et al.* [133], y de *N. parvum*, según Mutawila *et al.* [134] y Kotze *et al.* [135]. Además, la literatura científica respalda la capacidad de *T. harzianum* para inhibir el crecimiento de otros hongos como *E. lata* y *P. chlamydospora* [85,136,137]. Resulta destacable que la efectividad de la cepa endófito seleccionada ha sido comparable a la de formulaciones comerciales basadas en *T. harzianum* (T22) frente a *N. parvum*, o comparable también a la de formulaciones comerciales basadas en *T. atroviride* (I-1237) frente a *D. seriata*.

En cuanto a los agentes de biocontrol bacterianos ensayados, destaca la efectividad del tratamiento con *Bacillus velezensis* (BUZ-14). Pese a que esta bacteria no es nativa de la vid (se aisló de la piel de un melocotón en la provincia de Zaragoza), su adaptación a las condiciones agroclimáticas de la zona puede haber contribuido a su alta eficacia. De hecho, la excelente actividad antifúngica de esta cepa concuerda con los resultados de investigaciones previas de Calvo *et al.* frente a otros patógenos como *Botrytis cinerea* Pers.; *Monilinia fructicola* (G. Winter) Honey, y *Monilinia laxa* (Aderh. & Ruhland) Honey [138,139].

Respecto al otro bacilo, *Bacillus subtilis* (BS03), se observó una baja actividad antifúngica. Sin embargo, es importante tener en cuenta que el producto utilizado, RADISEI®, no se comercializa actualmente como protector de heridas, sino como un bioestimulante para vid y otros cultivos. Además, los resultados de eficacia de *B. subtilis* frente a las EMV son dispares: en algunos artículos se ha referido baja actividad frente a *Diaporthe ampelina*, *E. lata*, y *N. parvum* [135,140], mientras que otros autores informan de un buen comportamiento frente a hongos como *N. parvum*, *E. lata*, *Phaeoacremonium minimum*, *P. aleophilum*, *Phaeomoniella chlamydospora* y *Botryosphaeria rhodina* [96,97,141,142]. Tal variabilidad puede atribuirse al uso de distintas cepas de *B. subtilis* y a diferencias en el procedimiento de aplicación, por ejemplo.

3.3. Resistencias

En relación con los ensayos de resistencia/tolerancia realizados con variedades del Banco de Germoplasma de Vid de Aragón, ninguna de las variedades y genotipos ensayados mostró resistencia a la infección por los dos patógenos de la familia de *Botryosphaeriaceae* estudiados (*N. parvum* y *D. seriata*). Este resultado es coherente con los referidos por otros autores. Por ejemplo, Ramirez *et al.* [124], en un estudio de sensibilidad de cinco variedades de vid frente a la infección artificial por *Diplodia seriata* y *D. mutila*, encontraron (como en nuestro caso) que todos los cultivares eran sensibles a la acción del patógeno. En otro estudio de Martínez-Diz *et al.* [13] frente a *Phaeomoniella chlamydospora*, también se concluyó que todas las variedades son potencialmente susceptibles de ser infectadas, mostrando no obstante, un gradiente de sensibilidad/tolerancia y expresión de síntomas.

En cuanto a las variedades más o menos tolerantes identificadas en el artículo #10, 'Macabeo' y uno de los ecotipos de 'Garnacha Tinta' (procedente de Villanueva de Huerva, Zaragoza) fueron los cultivares de uva blanca y tinta menos susceptibles, respectivamente, mientras que 'Monegrina', 'Grumel', y 'Torcijón' serían los menos tolerantes a la infección fúngica. A efectos comparativos, en el

mencionado estudio de Martínez-Diz *et al.* [13], la longitud de las lesiones en 'Garnacha Tintorera' fue alta, en línea con el comportamiento observado aquí para el ecotipo 'Garnacha Tinta' de Borja (Zaragoza). Además, 'Moscatel de Grano Menudo' se encontraba entre los cultivares menos susceptibles a *P. chlamydospora* en el citado estudio, lo que coincide con nuestros resultados. En un ensayo realizado por Chacon-Vozmediano *et al.* [29], basado únicamente en los síntomas externos observados en el viñedo, los autores referían que 'Garnacha Tinta' y 'Garnacha Tintorera' no mostraron ningún síntoma, mientras que en nuestro estudio uno de los ecotipos de 'Garnacha Tinta' se clasificó entre los mejores cultivares, aunque mostrando sintomatología. En este estudio de campo, 'Macabeo' estuvo entre los cultivares que presentaron síntomas, pero menos severos (resultado compatible con lo aquí reportado). Otros de los cultivares ensayados, 'Moscatel de Alejandría', fue identificado como sensible en ambos estudios; 'Moscatel de Grano Menudo' mostró poca sensibilidad a *D. seriata* en nuestros ensayos y no mostró sintomatología en las pruebas realizadas en la DO La Mancha; finalmente, 'Mazuela', el segundo cultivar menos susceptible a *D. seriata* en nuestro estudio, no presentó sintomatología en el realizado en La Mancha.

Respecto a las diferencias arriba referidas para 'Garnacha Tinta', reportada tanto como un cultivar muy sensible o muy tolerante dependiendo del estudio, en otro trabajo de Chacón *et al.* [28] se observó que 'Garnacha Tinta' mostró una susceptibilidad intermedia a *N. parvum*, pero se identificaron diferencias notables entre las poblaciones de este cultivar. A este respecto, una conclusión importante del artículo #10 es que, en las variedades antiguas, que no han sido sometidas a presión de selección y en las que no se han llevado a cabo programas de mejora vegetal, pueden existir muchos clones circulantes, la mayoría de los cuales representan variantes poblacionales. En otras palabras, el concepto ampelográfico de estos cultivares se basa en la existencia de una amplia diversidad intravarietal en estos ecotipos, que, manteniendo la identidad del cultivar, aportan variabilidad genética en términos de caracteres agronómicos, rendimiento, aptitudes enológicas y tolerancia a enfermedades.

También cabe destacar que, pese a la ausencia de variedades resistentes, la identificación de variedades menos sensibles realizada en el estudio puede ser de utilidad para los viticultores aragoneses, sirviendo de orientación cara a la selección del material vegetal a utilizar en futuras plantaciones.

3.4. Análisis de comunidades microbianas

En el estudio recogido en el artículo #11, el análisis metagenómico de dos viñedos de la D.O.P. Somontano permitió identificar un total de 1300 unidades taxonómicas operativas (OTUs) correspondientes a 318 especies de hongos diferentes. Estos datos se encuentran dentro del rango de los obtenidos en trabajos previos [121,143-145]. El microbioma fúngico en las dos parcelas analizadas estuvo dominado por táxones de la clase *Ascomycota*, mientras que aquellos pertenecientes al grupo de los *Basidiomycota* representaron una fracción menor, en torno a menos de la mitad de los anteriores. Estos resultados también concuerdan con los de otros estudios *in vivo* que emplearon enfoques similares [144,146,147].

Se identificaron numerosas especies, algunas muy frecuentes (como *Phaeoconiella chlamydospora*) y otras menos representadas, como especies asociadas a la enfermedad de Petri, (*Phaeoacremonium aleophilum*, *P. minimum*, o *Cadophora luteo-olivacea*); agentes etiológicos asociados con el decaimiento por *Botryosphaeria* (con representantes de los géneros *Neofusicoccum*, *Dothiorella*, o *Diplodia*); o el agente causal de la eutipiosis (*Eutypa lata*). Estos resultados son similares a los obtenidos por Del Frari *et al.* [144]. También es coherente con dicho estudio el hecho de que aproximadamente el 80% de los taxones caracterizados resultaron ser especies raras (con una abundancia relativa inferior al 2%). Este reservorio de diversidad microbiana rara o poco

frecuente puesta de manifiesto bajo ciertas condiciones ambientales específicas, puede desempeñar un papel más relevante en el bienestar y aptitud ecológica de la planta [116].

Los resultados de nuestro estudio indican que la edad de la plantación es el principal factor que podría explicar las diferencias detectadas entre ambos microbiomas, siendo la parcela más antigua la más diversa y compleja. Esto sugiere una sustitución y enriquecimiento diferencial de las comunidades microbianas fúngicas en función de la edad y la exposición a la infección endofítica, donde las especies dominantes en cada tipo de microbiota podrían haber sido priorizadas por los individuos vegetales en función de la edad, anatomía y estructura de sus tejidos (“*priming*”). Estos hallazgos son consistentes con otros estudios que han establecido una relación entre la diversidad de los microorganismos y la edad de la planta [118,148], lo que, a efectos prácticos de control de las EMV, conlleva la necesidad de adaptar los tratamientos a la edad de la planta, pues la efectividad de estos depende de la especie patógena presente a tratar.

Respecto a la influencia de la metodología aplicada (NGS frente a métodos clásicos de cultivo de microorganismos) en la diversidad de los hongos endófitos (incluidos los patógenos EMV), los resultados revelaron que la diversidad de especies obtenida con métodos dependientes de cultivo fue considerablemente menor que con métodos metagenómicos, lo que concuerda con numerosos estudios previos [148,149]. Además, no se encontró una correlación clara entre la composición de las comunidades endófitas aisladas en el cultivo puro y las OTUs más frecuentes caracterizadas en el análisis metagenómico, lo que sugiere un sesgo al utilizar métodos microbiológicos clásicos. No obstante, pese a que estos últimos métodos solo permitan caracterizar una fracción reducida de la diversidad microbiana total de una planta y no arrojen, como en nuestro análisis, los mismos resultados en cuanto a la abundancia de aislados de interés pertenecientes a taxones como *P. chlamydospora* y *D. seriata*, su menor coste y rapidez para la obtención de resultados (en comparación con NGS) no los descarta totalmente como una opción válida desde un punto de vista práctico.

4. CONCLUSIONES

Las principales conclusiones de esta Tesis Doctoral son:

1. El uso directo de extractos naturales de plantas (como extractos hidrometanólicos de cola de caballo, ortiga, cardo mariano, y rubia) como tratamientos para el control de algunas de las especies responsables de EMV, resulta preferible al uso de materias activas naturales puras (como aminoácidos, polifenoles, o flavonoides). Además de un menor coste asociado, presentan una mayor eficacia, atribuible a que, al tratarse de mezclas complejas, se producen sinergias entre los distintos componentes con múltiples modos de acción simultáneos. Tal variedad de mecanismos de actuación debería contribuir además a una mayor eficacia a largo plazo de los extractos, a prevenir el desarrollo de resistencias, y a un espectro de actividad más amplio. Respecto a la elección del extracto, los de cola de caballo y ortiga cuentan con la ventaja de estar aprobados como sustancias básicas conforme al Artículo 23 del Reglamento (CE) nº 1107/2009 del Parlamento Europeo y del Consejo, pero la eficacia del extracto de raíces de *Rubia tinctorum* ha resultado ser el más eficaz (concentración mínima inhibitoria inferior a 200 ppm).
2. La formación de complejos conjugados de los extractos con oligómeros de quitosano o con esteviósido se traduce en una mejora sustancial de la eficacia de los tratamientos, lográndose concentraciones mínimas inhibitorias inferiores a 1000 ppm en todos los casos (independientemente del extracto y los patógenos ensayados). Tal mejora es atribuible no sólo a un comportamiento sinérgico (pues tanto los oligómeros de quitosano como el esteviósido tienen propiedades antimicrobianas) sino también a una mejora de la solubilidad y la biodisponibilidad de los principios activos contenidos en los extractos. Además, en el caso de los complejos de oligómeros de quitosano, su mayor eficacia y su menor coste les convierte en la opción preferente.
3. La encapsulación de los extractos bioactivos en nanotransportadores basados en oligómeros de quitosano facilita no sólo su vehiculización y aplicación (ensayada vía endoterapia), sino que conlleva un importante ahorro de producto activo: la liberación *ad-hoc* de forma controlada, por exposición del encapsulado al secretoma de los microorganismos responsables de las EMV, se traduce en una alta inhibición para dosis notablemente más bajas del agente terapéutico, lográndose la inhibición completa para concentraciones inferiores a 150 ppm. El tratamiento con nanotransportadores cargados con extracto de *R. tinctorum* en vides de 20 años con síntomas de EMV no ha mostrado fitotoxicidad ni alteración del contenido de azúcar del jugo de uva, observándose una disminución notable de los síntomas foliares, diferencias estadísticamente significativas en el número de racimos por brazo y un rendimiento superior en los brazos tratados.
4. El uso de aislados de *Trichoderma harzianum* nativos de vides aragonesas ha conducido a la inhibición del crecimiento micelial de *Neofusicoccum parvum* y *Rhizoctonia solani*. En ensayos con plántulas, los tratamientos sucesivos con las cepas antagonistas han demostrado efectos protectores, promoviendo el desarrollo de raíces, mayor peso seco de la planta y menor colonización del patógeno, destacando los resultados frente a *R. solani*. No obstante, en ensayos posteriores para la protección de heridas de poda, su eficacia ha sido comparable a la de formulaciones comerciales de *T. harzianum* y *T. atroviride* (no nativas). Diferente ha sido el caso de una cepa de *Bacillus velezensis* (BUZ-14), nativa de otro cultivo aragonés, que se ha convertido en el tratamiento con mayor eficacia frente a *N. parvum* y *D. seriata*, y sería la opción preferente para futuros estudios en campo.
5. Los tratamientos ensayados, basados en extractos naturales de plantas o en antagonistas microbianos, pueden ser una alternativa prometedora a los fungicidas de síntesis, con menores impactos medioambientales y de salud. No obstante, su eficacia es limitada y, aunque

son capaces de ralentizar el avance de las EMV o disminuir sus síntomas, no son capaces de erradicar los patógenos (son tratamientos paliativos, no curativos). Su uso debería combinarse con otras medidas de control para asegurar la efectividad de los tratamientos (por ejemplo, en viveros, con la aplicación de termoterapia).

6. Los ensayos realizados en variedades comerciales, locales y minoritarias del Banco de Germoplasma de Vid de Aragón no han permitido identificar cultivares resistentes a *N. parvum* o *D. seriata*. No obstante, la información sobre el gradiente de sensibilidad puede ser de utilidad para la selección de variedades en futuras plantaciones, aprovechando, por ejemplo, su mayor tolerancia. Es el caso observado para “*Macabeo*” y uno de los ecotipos de “*Garnacha Tinta*”, en el caso de uva blanca y tinta, respectivamente, con beneficios asociados para los viticultores en términos de menor uso de fitosanitarios o menores costes de arranque y reposición.
7. En relación con el análisis de las comunidades microbianas en vides de distinta edad de la D.O.P. Somontano, el análisis metagenómico ha mostrado una mayor diversidad fúngica que la identificada por los métodos taxonómicos clásicos. El microbioma de las plantas de más edad ha resultado ser más diverso y complejo (tanto en términos de microorganismos patógenos, saprofitos o con potencial como BCAs), lo que sugiere una sustitución y enriquecimiento diferencial de las comunidades microbianas fúngicas en función de la edad y la exposición a la infección endofítica (“*priming*”). El estudio de dicho microbioma ha orientado a considerar que los síntomas asociados a las enfermedades de la madera pueden atribuirse a la presencia dominante de *Phaeoconiella chlamydospora* y, en menor medida, de *Diplodia seriata*.

APÉNDICE

Factor de impacto de las revistas:

Revista	Factor de impacto	Cuartil
<i>Agronomy</i>	3,949 (2021); 3,7 (2022)	Q1
<i>Plants</i>	4,658 (2021); 4,5 (2022)	Q1
<i>Materials</i>	3,4 (2022)	Q2
<i>Phytopathologia Mediterranea</i>	2,4 (2022)	Q2
<i>Journal of Plant Diseases and Protection</i>	2,0 (2022)	Q2

Áreas temáticas de las publicaciones que se recogen en la Tesis Doctoral:

1. "On the applicability of chitosan oligomers-amino acid conjugate complexes as ecofriendly fungicides against grapevine trunk pathogens" *Agronomy*, 2021, 11(2), 324; <https://doi.org/10.3390/agronomy11020324>. **Área temática: Science Edition – AGRONOMY**
2. "Assessment of conjugate complexes of chitosan and *Urtica dioica* or *Equisetum arvense* extracts for the control of grapevine trunk pathogens" *Agronomy*, 2021, 11(5), 976; <https://doi.org/10.3390/agronomy11050976>. **Área temática: Science Edition – AGRONOMY**
3. "Antifungal activity against *Botryosphaeriaceae* fungi of the hydro-methanolic extract of *Silybum marianum* capitula conjugated with stevioside" *Plants*, 2021, 10(7), 1363; <https://doi.org/10.3390/plants10071363>. **Área temática: Science Edition – PLANT SCIENCES**
4. "Rutin-stevioside and related conjugates for potential control of grapevine trunk diseases" *Phytopathologia Mediterranea*, 2022, 61 (1), 65; <https://doi.org/10.36253/phyto-13108>. **Área temáticas: Science Edition – AGRONOMY; Science Edition – PLANT SCIENCES**
5. "Activity of anthracenediones and flavoring phenols in hydromethanolic extracts of *Rubia tinctorum* against grapevine phytopathogenic fungi" *Plants*, 2021, 10(8), 1527; <https://doi.org/10.3390/plants10081527>. **Área temática: Science Edition – PLANT SCIENCES**
6. "Lignin-chitosan nanocarriers for the delivery of bioactive natural products against wood-decay phytopathogens" *Agronomy*, 2022, 12(2), 461; <https://doi.org/10.3390/agronomy12020461>. **Área temática: Science Edition – AGRONOMY**
7. "Multifunctional nanocarriers based on chitosan oligomers and graphitic carbon nitride assembly". *Materials* 2022; 15(24), 8981; <https://doi.org/10.3390/ma15248981>. **Área temática: Science Edition – METALLURGY & METALLURGICAL ENGINEERING**
8. "Potential of native *Trichoderma* strains as antagonists for the control of fungal wood pathologies in young grapevine plants" *Agronomy*, 2022, 12(2), 336; <https://doi.org/10.3390/agronomy12020336>. **Área temática: Science Edition – AGRONOMY**
9. "Comparison of the efficacy of *Trichoderma* and *Bacillus* strains and commercial biocontrol products against grapevine *Botryosphaeria dieback* pathogens" *Agronomy*, 2023, 13(2), 533; <https://doi.org/10.3390/agronomy13020533>. **Área temática: Science Edition – AGRONOMY**
10. "Screening of *Vitis vinifera* cultivars from the Grapevine Germplasm Bank of Aragon for susceptibility to *Botryosphaeria dieback* fungi" *Journal of Plant Diseases and Protection*, 2023, 130, 999-1006; <https://doi.org/10.1007/s41348-023-00741-9>. **Área temática: Science Edition – AGRICULTURE, MULTIDISCIPLINARY**
11. "Metagenomic study of fungal microbial communities in two PDO Somontano vineyards (Huesca, Spain): Effects of age, plant genotype, and initial phytosanitary status on the priming and selection of their associated microorganisms" *Plants*, 2023, 12(12), 2251; <https://doi.org/10.3390/plants12122251>. **Área temática: Science Edition – PLANT SCIENCES**

Justificación de la contribución de la Doctoranda en los trabajos realizados en coautoría (conforme a taxonomía de roles de colaboración académica, CRediT):

1. "On the applicability of chitosan oligomers-amino acid conjugate complexes as ecofriendly fungicides against grapevine trunk pathogens" *Agronomy*, 2021, 11(2), 324; <https://doi.org/10.3390/agronomy11020324>. **Roles: investigación, redacción – borrador original, visualización.**
2. "Assessment of conjugate complexes of chitosan and *Urtica dioica* or *Equisetum arvense* extracts for the control of grapevine trunk pathogens" *Agronomy*, 2021, 11(5), 976; <https://doi.org/10.3390/agronomy11050976>. **Roles: investigación, redacción – borrador original, visualización.**
3. "Antifungal activity against *Botryosphaeriaceae* fungi of the hydro-methanolic extract of *Silybum marianum* capitula conjugated with stevioside" *Plants*, 2021, 10(7), 1363; <https://doi.org/10.3390/plants10071363>. **Roles: investigación, redacción – borrador original, visualización.**
4. "Rutin-stevioside and related conjugates for potential control of grapevine trunk diseases" *Phytopathologia Mediterranea*, 2022, 61 (1), 65; <https://doi.org/10.36253/phyto-13108>. **Roles: investigación, redacción – borrador original, visualización.**
5. "Activity of anthracenediones and flavoring phenols in hydromethanolic extracts of *Rubia tinctorum* against grapevine phytopathogenic fungi" *Plants*, 2021, 10(8), 1527; <https://doi.org/10.3390/plants10081527>. **Roles: investigación, redacción – borrador original, visualización.**
6. "Lignin-chitosan nanocarriers for the delivery of bioactive natural products against wood-decay phytopathogens" *Agronomy*, 2022, 12(2), 461; <https://doi.org/10.3390/agronomy12020461>. **Roles: investigación, redacción – borrador original, visualización.**
7. "Multifunctional nanocarriers based on chitosan oligomers and graphitic carbon nitride assembly". *Materials* 2022; 15(24), 8981; <https://doi.org/10.3390/ma15248981>. **Roles: investigación, redacción – borrador original.**
8. "Potential of native *Trichoderma* strains as antagonists for the control of fungal Wood pathologies in young grapevine plants" *Agronomy*, 2022, 12(2), 336; <https://doi.org/10.3390/agronomy12020336>. **Roles: conceptualización, metodología, curación de datos, validación, investigación, redacción – borrador original, redacción – revisión y edición.**
9. "Comparison of the efficacy of *Trichoderma* and *Bacillus* strains and commercial biocontrol products against grapevine *Botryosphaeria dieback* pathogens" *Agronomy*, 2023, 13(2), 533; <https://doi.org/10.3390/agronomy13020533>. **Roles: investigación, redacción – borrador original, redacción – revisión y edición.**
10. "Screening of *Vitis vinifera* cultivars from the Grapevine Germplasm Bank of Aragon for susceptibility to *Botryosphaeria dieback* fungi" *Journal of Plant Diseases and Protection*, 2023, 130, 999-1006; <https://doi.org/10.1007/s41348-023-00741-9>. **Roles: investigación, redacción – borrador original.**
11. "Metagenomic study of fungal microbial communities in two PDO Somontano vineyards (Huesca, Spain): Effects of age, plant genotype, and initial phytosanitary status on the priming and selection of their associated microorganisms" *Plants*, 2023, 12(12), 2251; <https://doi.org/10.3390/plants12122251>. **Roles: conceptualización, metodología, curación de datos, análisis formal, validación, investigación, redacción – borrador original, redacción – revisión y edición.**